ABSTRACT

Title of Document: LIGAND-ENABLED PLATINUM—CARBON BOND FUNCTIONALIZATION UTILIZING DIOXYGEN AS THE TERMINAL OXIDANT

Julia Khusnutdinova, Doctor of Philosophy, 2009

Directed By: Assistant Professor Andrei N. Vedernikov, Department of Chemistry and Biochemistry

The use of organotransition metal complexes for selective functionalization of hydrocarbons is of great importance. Dioxygen is the most practical oxidant for large-scale applications in the petroleum industry. The focus of this work is the development of ligand-modulated platinum-based systems that can utilize O_2 or air for selective transformation of organoplatinum(II) derivatives into alcohols, diols, aminoalcohols and epoxides in aqueous media.

We found that the hemilabile tripod ligand dipyridylmethanesulfonate (dpms) enables facile aerobic functionalization of various $Pt^{II}Me$ complexes and some olefin hydroxo Pt^{II} complexes in hydroxylic solvents such as water and alcohols.

Complexes $LPt^{II}(R)(HX)$ (L = dpms; R = Me, Ph; HX = H_2O, MeOH, $PhNH_2$) are oxidized by O_2 to yield virtually quantitatively $LPt^{IV}(R)(X)(OH)$. Some of the derived Pt^{IV} alkyls $LPt^{IV}(Alk)(X)(OH)$ (X = OH, OMe) can reductively eliminate methanol in high yield. The mechanism of C-O elimination from $LPt^{IV}(Me)(X)(OH)$ (X = OH,

OMe) in acidic aqueous media involves two concurrent pathways: an S_N2 attack by water and an S_N2 attack by a hydroxo or methoxo ligand of another Pt^{IV} species. In the latter case dimethyl ether is produced.

The complex (dpms)Pt(ethylene)(OH) is oxidized by O_2 in water to give a Pt^{IV} hydroxyethyl derivative that reductively eliminates ethylene oxide and ethylene glycol in aqueous solutions.

The complexes derived from cyclic alkenes, *cis*-cyclooctene, norbornene, benzonorbornadiene, (dpms)Pt^{II}(*cy*-alkene)(OH), undergo olefin oxoplatination to give 1,2-oxaplatinacyclobutanes (Pt^{II} oxetanes). The derived Pt^{II} oxetanes are easily oxidized by O_2 to produce Pt^{IV} oxetanes. The latter eliminate cleanly the corresponding epoxides by the mechanism of direct C(sp^3)-O reductive eliminations, unprecedented in organoplatinum chemistry.

The 1,2-azaplatinacyclobutanes (Pt^{II} azetidines) LPt^{II}(CH_2CH_2NHR-$\kappa C,\kappa N$) (R = *t*-Bu, Me) are oxidized by O_2 in the presence of acids to give Pt^{IV} azetidine complexes, [LPt(CH_2CH_2NHR-$\kappa C,\kappa N$)(OH)]$^+$. The latter undergo reductive elimination of *N*-alkyl ethanolammonium salts, $HOCH_2CH_2NH_2R^+$, in acidic aqueous solutions at elevated temperatures.

Efficient catalytic systems based on palladium acetate, di(6-pyridyl)ketone and 6-methyldi(2-pyridyl)methanesulfonate ligands, suitable for selective oxidation of ethylene with H_2O_2 to glycol acetates were developed. Glycol acetates were obtained in high selectivity and high yield on H_2O_2 under mild reaction conditions.

LIGAND-ENABLED PLATINUM—CARBON BOND FUNCTIONALIZATION UTILIZING DIOXYGEN AS THE TERMINAL OXIDANT

By

Julia Khusnutdinova

Dissertation submitted to the Faculty of the Graduate School of the
University of Maryland, College Park, in partial fulfillment
of the requirements for the degree of
Doctor of Philosophy
2009

Advisory Committee:
Assistant Professor Andrei Vedernikov, Chair
Professor Michael P. Doyle
Professor Philip DeShong
Professor Lawrence R. Sita
Associate Professor Gregory Jackson

Dedication

Dedicated to my mother,

and to the memory of my father.

"The time has come", the Walrus said,
"To talk of many things:
Of shoes – and ships – and sealing wax –
Of cabbages – and kings."

-"The Walrus and the Carpenter" (Lewis Carroll)

The White Rabbit put on his spectacles. "Where shall I begin, please your Majesty?" he asked.
"Begin at the beginning," the King said very gravely, "and go on till you come to the end: then stop."

-"Alice's Adventures in Wonderland" (Lewis Carroll)

Acknowledgements

I would like to express my sincere gratitude to my supervisor, Professor Andrei Vedernikov for his excellent advice and support throughout my research and without whom I wouldn't be where I am now.

I'd like to thank former and current members of the Vedernikov group for their friendship and inspiration: Eugene Khaskin, Jing Zhang, Williamson Oloo, Fabian Mohr, Greg Downs and Pratheep Khanthapura. Special thanks to Eugene Khaskin for interesting discussions and for being my friend through these years. I would also like to thank my undergraduate students at the University of Maryland, especially Laura Newman, Anthony Maiorana and Seth Binfield.

My sincere thanks to my friends and colleagues Krupa Shukla, Sofya Berezin, Regan Nally, Yomi Okunola, Wei Zhang and Xia Bai.

This work would not be possible without the help of our X-ray crystallographer Peter Y. Zavalij, NMR staff Yiu-Fai Lam and Yinde Wang and mass spectrometry staff Noel Whittaker and Yue Li.

My warmest thanks belong to my mother and sister for their great love, care and support.

Table of Contents

List of Tables

List of Figures

List of Schemes

Chapter 1

Chapter 2

Chapter 3

Chapter 4

Chapter 5

Chapter 6

Chapter 7

List of Abbreviations

Ac	acetyl
Alk	alkyl
Ar	aryl
aq.	aqueous
atm	atmosphere
BHT	2,6-di-*tert*-butyl-*p*-cresol
bpy	2,2'-bipyridyl
bpym	bipyrimidine
calcd	calculated
CH	carbon-hydrogen bond
CI	chemical ionization
COSY	NMR Correlation Spectroscopy
Cp	cyclopentadienyl
Cp*	pentamethylcyclopentadienyl
Cy	cyclohexyl
DCE	1,2-dichloroethane
DFT	Density Functional Theory
DMF	*N,N*-dimethylformamide
DMSO	dimethylsulfoxide
dpk	di-2-pyridyl ketone
dpm	di-2-pyridylmethane
dpms	di-2-pyridylmethanesulfonate
DβH	dopamine β-mooxygenase
EI	electron ionization
equiv.	equivalent(s)
ESI-MS	electrospray ionization mass spectrometry
eV	electron volt
EXSY	NMR Exchange Spectroscopy
Fp	cyclopentadienyliron dicarbonyl
g	grams
GC/MS	gas chromatography-mass spectrometry
h	hour(s)
HMDS	hexamethyldisiloxane
HOMO	Highest Occupied Molecular Orbital
HSQC	NMR Heteronuclear Single Quantum Coherence spectroscopy
Hz	Hertz
i-Pr	isopropyl
IR	infrared
J	coupling constant
kcal/mol	kilocalorie(s) per mole
LUMO	Lowest Unoccupied Molecular Orbital
M	moles per liter
*m*CPBA	*meta*-chloroperoxybenzoic acid

Me	methyl
Medpms	6-methylpyridyl pyridyl methanesulfonate
MeOH	methanol
mg	milligrams
MHz	megahertz
min	minute(s)
mL	milliliter(s)
mM	millimoles per liter
mmol	millimole(s)
mol	mole(s)
MMO	methane monooxygenase
m/z	mass-to-charge ratio
NADH	nicotinamide adenine dinucleotide
NBS	N-bromosuccinimide
NHC	N-heterocyclic carbene
NMR	nuclear magnetic resonance
NOE	Nuclear Overhauser Effect
o	ortho
OAc	acetate
ORTEP	Oak Ridge Thermal Ellipsoid Plot
Ph	phenyl
PHM	peptidylglycine α-hydroxylating monooxygenase
psi	pounds per square inch
py	pyridine
rt	room temperature
s	second(s)
sec-	secondary
$t_{1/2}$	half-life
tach	1,3,5-triaminocyclohexane
tacn	1,4,7-triazacyclononane
TBHP	*tert*-butyl hydroperoxide
t-Bu	tertiary butyl
t-Bu-dpms	4-tert-butyl-pyridyl pyridyl methanesulfonate
TFE	2,2,2-trifluoroethanol
THF	tetrahydrofuran
TMEDA	*N,N,N′,N′*-tetramethylethylene diamine
Tol	tolyl
Tp	trispyrazolylborate
v/v	volume to volume ratio
wt.%	weight percent
XRD	X-ray diffraction
µL	microliter(s)
µM	micromoles per liter
µmol	micromole(s)

Chapter 1: Functionalization of Hydrocarbons Utilizing Molecular Oxygen as the Terminal Oxidant

1.1 Introduction

Hydrocarbons, alkanes, arenes and alkenes, serve as a primary feedstock for production of a number of valuable organic products and commodity chemicals. Selective oxidation of these substrates is an important problem faced by chemical industry. The most practically advantageous oxidant for large scale applications is molecular oxygen since it is abundant, cheap and environmentally benign oxidant. Unlike other commonly used oxidants, dioxygen potentially can produce no hazardous wastes; water is a typical by-product of oxidation. However, the reactions between dioxygen and hydrocarbons are often unselective. They are difficult to control and can ultimately lead to combustion of substrate yielding water and carbon dioxide thus limiting practical application of dioxygen for production of oxygenated products. It is therefore important to explore pathways for more selective and efficient use of dioxygen for oxidation of hydrocarbon substrates. Homogeneous catalysis by transition metal complexes can provide novel selective pathways for hydrocarbon functionalization under mild conditions. The focus of this work is to explore possible pathways for selective hydrocarbon functionalization that involve organoplatinum intermediates that are able to activate O_2 and allow for its use as the terminal oxidant in these reactions. These

transformations can be valuable for development of novel homogeneous platinum-catalyzed aerobic oxidation processes.

1.2 Utilization of O_2 for Oxidation of CH Bonds of Alkanes and Alkylarenes

Alkanes are major constituents of the natural gas and petroleum and serve as an important feedstock for the chemical industry. Despite this, the majority of saturated hydrocarbons extracted today are currently burned to produce energy. Most reactions of alkanes are unselective and require harsh conditions. Alkanes serve as a source of unsaturated hydrocarbons, such as alkylarenes and alkenes that can be obtained by catalytic reforming process, steam cracking or dehydrogenation under harsh conditions.

Reactions of alkanes with O_2 typically proceed via an "autoxidation" free radical chain mechanism and are characterized by the following selectivity with respect to CH bonds involved, $3^o > 2^o >> 1^o$.[1, 2] Therefore, molecular oxygen (or air) is typically used for oxidation of hydrocarbon substrates containing tertiary alkane or benzylic CH bonds; the latter are even more reactive in homolytic processes compared to tertiary alkane CH bonds.[2] For example, *tert*-butylhydroperoxide (TBHP) is produced by the oxidation of isobutane with molecular oxygen in the presence of a radical initiator at 124-155 ^oC (eq. 1.1) and can be obtained in 70% yield at 80% conversion of isobutane.[3, 4]

$$(CH_3)_3CH + O_2 \xrightarrow[24\text{-}55\ atm]{125\text{-}155^oC} (CH_3)_3C\text{-}OOH \qquad (1.1)$$

The mechanism of autoxidation of isobutane is given in Scheme 1.1.[1, 2]

Scheme 1.1. The radical chain mechanism for autoxidation of isobutane in the presence of a radical initiator.

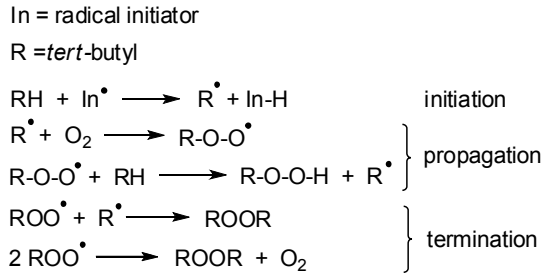

The homolytic oxidation of the reactive benzylic CH bonds of alkylarenes is utilized for the manufacture of phthalic anhydride, terephthalic acid,[5] and benzoic acid.[6, 7]

Oxidation of CH bonds other than tertiary, allylic and benzylic ones is typically much less selective. For instance, manufacture of cyclohexanol and cyclohexanone by autoxidation of cyclohexane with air over cobalt-manganese catalysts requires low conversions of cyclohexane, 10-12%, in order to achieve 80-85% selectivity for cyclohexanol/cyclohexanone and to avoid formation of overoxidation products.[8]

The catalytic "Gif-systems" were developed by Barton for more selective oxidation of secondary CH bonds using iron salts as catalysts and Zn as a sacrificial reductant. However, the "Gif-systems" are not effective for oxidation of primary CH bonds of alkanes as they involve formation of free substrate-centered radicals.[9, 10]

Selective oxidation of primary CH bonds of alkanes is a very important practical target for the chemical industry. For example, direct partial oxidation of methane, a main component of a natural gas, to methanol (eq. 1.2) would be a highly attractive alternative for the current production of methanol from synthesis gas (CO + H_2, "syngas") (Scheme 1.2).

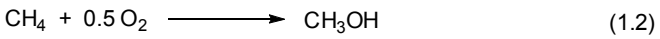

(1.2)

Methanol is a valuable feedstock for organic synthesis and an efficient and a readily transportable liquid fuel alternative to gasoline and methane. Currently methanol is produced in a multistage process involving steam-reforming of methane to a synthesis gas (eq. 1.3, Scheme 1.2) and synthesis of methanol from syngas (eq. 1.4) under harsh reaction conditions in the presence of various heterogeneous catalysts. As the H_2 to CO ratio in syngas is approximately 3 : 1, which is different from 2 : 1 ratio required by stoichiometry for synthesis of methanol, the amount of H_2 is reduced by reacting with CO_2 gas (eq. 1.5).[5]

Scheme 1.2. The synthesis of methanol from methane using the ICI (Imperial Chemical Industries) Cu-Zn-Al-oxide catalyst.

$$CH_4 + H_2O \xrightarrow[700\text{-}830^oC,\ 15\text{-}40\ bar]{Ni\ /Al_2O_3\ cat.} CO + 3H_2 \qquad (1.3)$$

$$CO + 2H_2 \xrightarrow[240\text{-}260^oC,\ 50\text{-}100\ bar]{Cu/Zn\ cat.} CH_3OH \qquad (1.4)$$

$$CO_2 + H_2 \xrightarrow{Cu/Zn\ cat.} CO + H_2O \qquad (1.5)$$

A direct, one-step partial oxidation of methane to methanol (eq. 1.2) cannot be achieved via traditional autoxidation route as it leads to unselective overoxidation and combustion into carbon dioxide and water. The CH bonds of methane are the strongest among alkanes; the bond dissociation energy of a single CH bond in CH_4 is 104 kcal/mol. Hence, under harsh reaction conditions required for methane autoxidation the reaction products, methanol or formaldehyde, are not stable toward further oxidation and thermal decomposition. A few examples of direct oxidation of methane to methanol using O_2 or

air as an oxidant have been reported, however, most of them require harsh reaction conditions and suffer from low selectivity.[11-14]

Interestingly, methanotrophic bacteria are capable of mild and selective aerobic conversion of methane to methanol. The multicomponent enzyme, methanemonooxygenase (MMO), catalyzes oxidation of methane under mild conditions (4-72 ^{o}C) using a reduced form of nicotineamide adenine dinucleotide (NADH) as a source of electrons. In this process, only one oxygen atom of O_2 is incorporated into methanol (monooxygenase-type behavior), and another oxygen atom of O_2 is reduced to one equivalent of water (eq. 1.6).[15] However, as oxygenases are multicomponent and cofactor-dependent enzymes, practical application of enzymatic oxidation of hydrocarbon substrates is limited.[15, 16]

$$CH_4 + O_2 + NADH + H^+ \xrightarrow{MMO} CH_3OH + H_2O + NAD^+ \qquad (1.6)$$

In contrast to the above mentioned processes involving free-radical aerobic oxidation, many late transition metals may allow for selective and mild activation of primary CH bonds of alkanes via non-radical pathways. Hence, application of homogeneous transition metal-based catalysis for selective oxidation of primary CH bonds of alkanes seems to be a promising approach. Activation of terminal, primary CH bonds of linear hydrocarbons by late transition metals occurs preferentially, in contrast to the selectivity observed in homolytic CH cleavage.[17]

In 1970's Shilov[18] and coworkers developed a catalytic system for selective alkane oxidation in the presence of Pt^{II} chloro complex as a catalyst in acidic aqueous solution using H_2PtCl_6 as an oxidant under mild reaction conditions (eq. 1.7).[19]

$$CH_4 + [PtCl_6]^{2-} + H_2O\ (Cl^-) \xrightarrow[H_2O,\ 120^oC]{[PtCl_4]^{2-}\ cat.} CH_3OH\ (CH_3Cl) + [PtCl_4]^{2-} + 2\ HCl \qquad (1.7)$$

The proposed mechanism of this reaction consists of three major steps: (i) CH activation of the alkane to form Pt^{II}-alkyl intermediate **1.1**; (ii) the oxidation of the Pt^{II}-alkyl intermediate **1.1** to generate a Pt^{IV}-alkyl species **1.2**, and (iii) reductive elimination of ROH or RCl to produce functionalized product and the Pt^{II} catalytically active species (Scheme 1.3).[19, 20]

Scheme 1.3. Proposed mechanism for Pt^{II}-catalyzed oxidation of alkanes in aqueous solution.

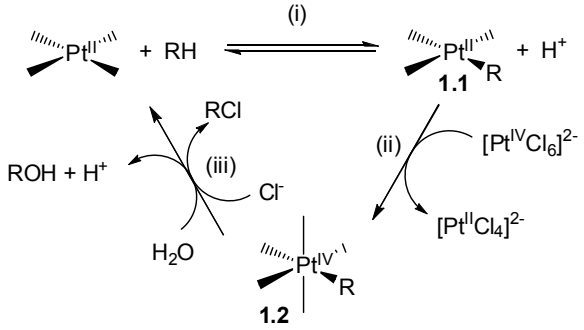

The major drawback of the "Shilov system" is the use of a stoichiometric amount of expensive H_2PtCl_6 as an oxidant to produce methanol, thus making the catalytic system impractical. Hexachloroplatinic acid H_2PtCl_6 could not be replaced in this system by more available and cheap oxidants without significant loss of catalytic activity.[20]

A similar catalytic cycle operates in the "Catalytica" system for methane oxidation to methyl bisulfate (CH_3OSO_3H), catalyzed by Pt^{II} bipyrimidine (bpym) complex (bpym)$Pt^{II}Cl_2$ in fuming sulfuric acid, developed by Periana (eq. 1.8).[21] In this system, SO_3 acts as an oxidant to generate Pt^{IV} methyl species by reacting with Pt^{II} methyl intermediate resulting from the CH activation of methane. The major drawbacks of the "Catalytica" system are that an additional step is necessary for conversion of methyl

bisulfate into methanol and the use of corrosive reaction media as well as inhibition of the catalyst by the water byproduct.[22]

$$CH_4 + 2H_2SO_4 \xrightarrow[220^oC]{(bpym)PtCl_2} CH_3OSO_3H + 2\,H_2O + SO_2 \quad (1.8)$$

~ 81% selectivity

Although SO_2 formed via reduction of the SO_3 oxidant in the "Catalytica" system can be potentially oxidized to SO_3 using O_2 or air, the direct use of O_2 for selective and mild oxidation of methane to methanol has not been achieved.

1.3 Utilization of O_2 for Functionalization of Alkenes C=C Bonds

Molecular oxygen is currently used by the chemical industry the for manufacture of ethylene oxide via direct oxidation over a silver catalyst (eq. 1.9).[5] The reaction is ~70% selective, and careful temperature control is necessary to avoid combustion into carbon dioxide and water. Ethylene oxide is used for production of ethylene glycol, the latter being utilized for manufacture of polyethylene terephtalate used in production of polyester fibers, in antifreeze and for production of ethanolamines.[5, 23]

$$CH_2{=}CH_2 + 0.5\,O_2 \xrightarrow[270\text{-}290^oC,\ 120\text{-}300\ psi]{Ag/\alpha\text{-}Al_2O_3\ cat.} \underset{H_2C-CH_2}{\overset{O}{\triangle}} \quad (1.9)$$

However, a direct oxidation route could not be used for olefins that contained allylic CH bonds. Attempts to directly oxidize propylene and butenes with O_2 over heterogeneous catalysts lead predominantly to allylic oxidation and combustion into carbon dioxide and water.[5, 24] For production of propylene oxide, two major routes are currently used: the chlorohydrin and hydroperoxide processes.[5]

The chlorohydrine process involves reaction of an olefin with HOCl formed in aqueous solution in the presence of Cl_2 to give a mixture of chlorohydrins followed by their dehydrochlorination with $Ca(OH)_2$ or sodium hydroxide solution to yield propylene oxide (Scheme 1.4).[5] The disadvantage of the chlorohydrine process is formation of significant amounts of waste. For example, 2.01 ton of NaCl and 0.102 ton of 1,2-dichloropropane are produced per ton of propylene oxide.[25] Significant efforts are devoted toward replacing the chlorohydrin process with a less waste-producing, "greener" epoxidation route.[25]

Scheme 1.4. Chlorohydrin process for propylene oxide manufacture.

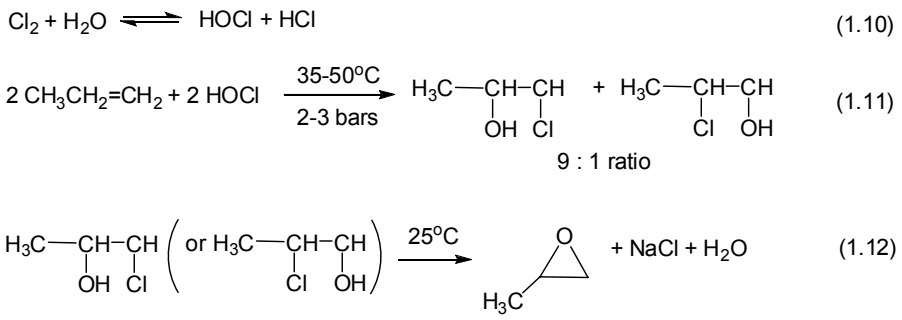

An alternative route to manufacture of propylene oxide involves oxidation of propylene with organic hydroperoxides, the so called "hydroperoxide process" (Scheme 1.5).[5] Molecular oxygen is utilized in this process for oxidation of hydrocarbons, ethylbenzene or isobutane, into the corresponding hydroperoxides, **1.3a** and **1.3b**, respectively (eq. 1.13, Scheme 1.5). Propylene is then oxidized with the hydroperoxide **1.3** to produce propylene oxide and an alcohol **1.4a** or **1.4b** (eq. 1.14); the reaction is accompanied by partial spontaneous decomposition of **1.3**.

Scheme 1.5. Hydroperoxide process for propylene oxide manufacture.

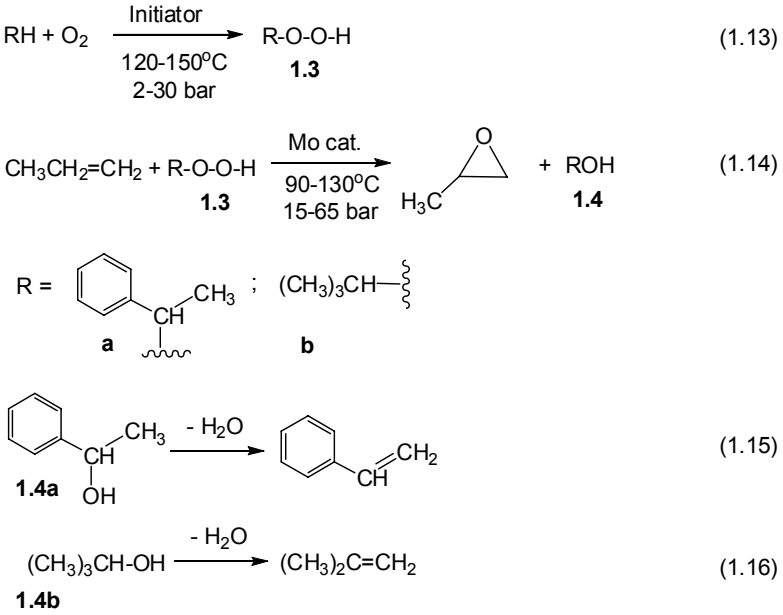

The important feature of the hydroperoxide process for production of propylene oxide is that a co-product **1.4a** or **1.4b** is formed in a fixed ratio relative to propylene oxide produced, usually 2-4 moles of **1.4** to 1 mole of propylene oxide, due to spontaneous decomposition of **1.3**. The co-product **1.4a** or **1.4b** is then converted into styrene (eq. 1.15) or isobutene (eq. 1.16) respectively by dehydration. The disadvantage of the hydroperoxide process is that production of propylene oxide is always combined with a manufacture of a co-product, styrene or isobutene, in amounts larger than the amount of propylene oxide.

Selective direct epoxidation of propylene with O_2 has not yet been realized. Hydrogen peroxide can be considered as a viable alternative to organic hydroperoxides, as it produces water as the only by-product during oxidation. However the use of commercially available H_2O_2 for propylene oxide production is not practical due to its high cost and instability of its concentrated (>30 wt.%) aqueous solutions. An indirect route is currently being developed using production of hydrogen peroxide from H_2 and

O_2 via anthrahydroquinone autooxidation process (eq. 1.17-1.18, Scheme 1.6)[26] and epoxidation of propylene with H_2O_2 over zeolite titanium silicate-1 (TS-1) (eq. 1.19).[27, 28]

Scheme 1.6. Hydrogen peroxide combination process for production of propylene oxide.

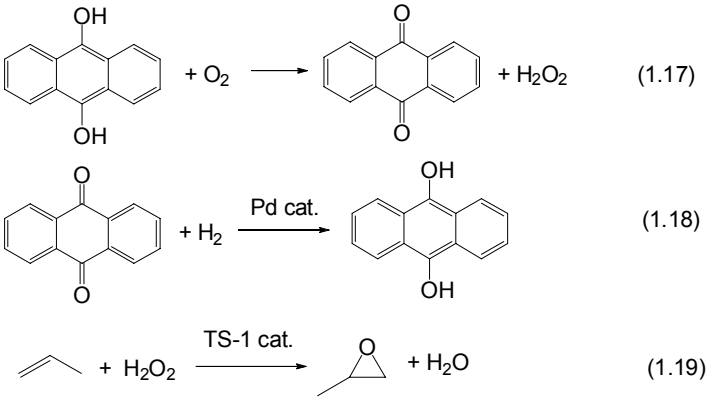

1.4 Our Approach and Goal

Inspired by the work of Shilov and coworkers on mild Pt^{II}-catalyzed alkane oxidation, we sought to investigate the possibility of using O_2 as the terminal oxidant for direct (mediatorless) functionalization of Pt^{II}-alkyl intermediates into oxygenated organic products in water solvent. We proposed that the key to the mediatorless aerobic functionalization of organoplatinum(II) intermediates is through careful control over the redox-properties of the Pt^{II} center that can be accomplished through rational ligand design.

A new hemilabile hydrophilic *fac*-coordinating ligand, di(2-pyridyl)methanesulfonate (dpms, **1.5a**, Scheme 1.7) and its *ortho*-methyl substituted analogue, Me-dpms (**1.5b**), have been developed in our group.[29] According to the results obtained previously, the ability of the dpms-type ligands to coordinate in both dicoordinate (η^2) and tricoordinate (η^3) fashion to a square planar Pt^{II} and an octahedral Pt^{IV} center respectively allows for

the observation of relatively stable Pt^{IV} hydrides $LPt^{IV}Me_2H$, **1.7**, (L – dpms, Me-dpms) that form in aqueous solutions of $K[LPt^{II}Me_2]$ (**1.6**) (eq. 1.20).[29]

Scheme 1.7. A new family of dipyridylmethanesulfonate ligands and reactivity of the derived complexes

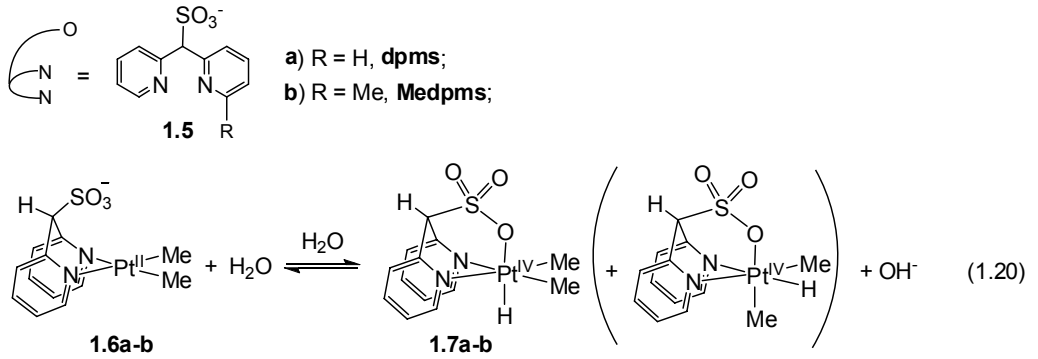

The resulting Pt^{IV} hydrides **1.7a-b** reductively eliminate methane in water and some less polar solvents.[29] The resulting highly reactive LPtMe(solvent) (L = dpms, Me-dpms) complexes are capable of activating the C-H bonds of benzene and methane or the Si-H bond of Et_3SiH in weakly coordinating dichloromethane to form the corresponding Pt^{IV} hydrides (Scheme 1.8).[29]

Scheme 1.8. The C-H and Si-H bond activation by $LptMe_2H$ complexes (L = dpms, Medpms), **1.7a-b**.

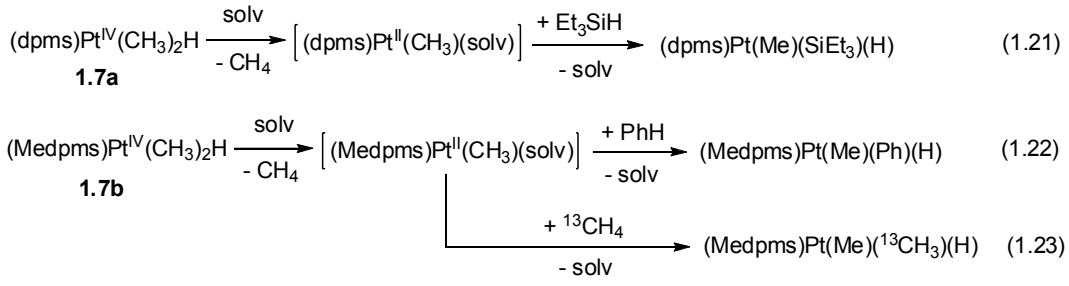

Importantly, the ability of *fac*-chelating ligands to facilitate oxidation of the Pt^{II} center to Pt^{IV} by various oxidants, including O_2, has been previously described and will be discussed in more detail in Chapter 2.[30] We proposed that the hemilabile *fac*-chelating dpms ligand could facilitate oxidation of the relatively electron-poor monohydrocarbyl

Pt^{II} intermediates such as (dpms)PtR(solv) (R – alkyl, aryl) by direct reaction with O_2 in protic solvents (water or alcohols) (step **a**, Scheme 1.9). At the same time, hemilabile nature of the sulfonate group would allow for facile reductive elimination of a functionalized organic product (step **b**) (see Chapter 2 for more detailed discussion). The realization of the reaction sequence given in Scheme 1.9 can be valuable for development of novel Pt^{II}-catalyzed hydrocarbon oxidation processes.

Scheme 1.9

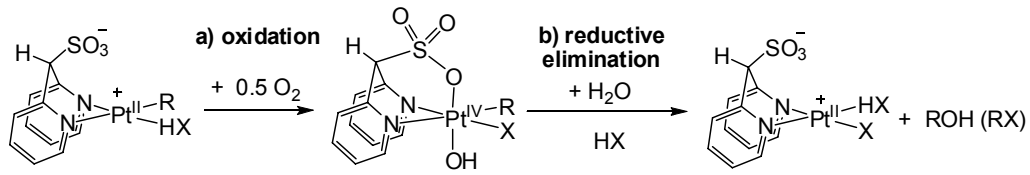

We thought it might also be interesting to extend the substrates scope of Pt- or Pd-mediated oxidative functionalization processes to olefins. In this case the formation of an alkyl M^{II} complex might result from the nucleophilic attack on a coordinated olefin.[31, 32] The subsequent oxidative functionalization of a M^{II}-C bond as opposed to the β-hydride elimination pathway operative in Wacker-type chemistry,[33, 34] could lead to 1,2-functionalized alkenes and catalytically active M^{II} species (Scheme 1.10).[35, 36]

Scheme 1.10. Possible catalytic cycle for Pt^{II}- or Pd^{II}-catalyzed olefin 1,2-functionalization.

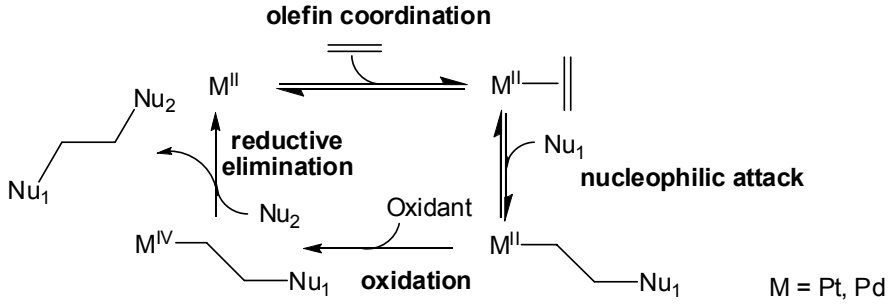

The goal of the present work is to explore ligand-enabled oxidative functionalization of organoplatinum(II) compounds, such as alkyl, aryl and olefin complexes utilizing O_2 as the terminal oxidant. We sought to use water as a solvent in these reactions. An important goal of this work is to study mechanisms of these transformations since such knowledge can efficiently serve as a foundation for future discoveries.

Chapter 2: Oxidative Functionalization of (dpms)Pt^{II} Methyl Complexes Utilizing Dioxygen

2.1 Oxidation of (dpms)Pt^{II} Methyl Complexes with Dioxygen

2.1.1 Introduction: Oxidation of Transition Metal Complexes with O_2

There has been long-standing interest in studying interactions of dioxygen with transition metal complexes since the pioneering works of Vaska,[37, 38] Basolo,[39] Collman[40] and others, due to their relevance to metalloenzymatic and synthetic catalysis.

Some properties of molecular oxygen and its derivatives relevant to the discussion of the reactions of O_2 with transition metal complexes are summarized below. The ground state of molecular dioxygen is a triplet, $^3\Sigma_g^-$, and its electronic configuration is given by eq. 2.1.[39]

$$O_2: [KK](2s\sigma_g)^2(2s\sigma_u^*)^2(2p\sigma_g)^2(2p\pi_u)^4(2p\pi_g^*)^1(2p\pi_g^*)^1 \qquad (2.1)$$

The lowest excited state of dioxygen, the singlet O_2, lies 23.4 kcal/mol above the ground state. The triplet ground state of O_2 is mainly responsible for its kinetic inertness. Although thermodynamically O_2 is a potentially powerful oxidant, dioxygen in its ground state is a relatively kinetically inert molecule if the reactants and the products are ground state singlets, due to the constraint imposed by the overall spin conservation rule.[41]

Four-electron reduction of O_2 to water in acidic media under standard conditions ($[H^+]$=1.0 M) (eq. 2.2) is characterized by the reduction potential of +1.23 V in acidic solutions ($[H^+]$=1.0 M) under standard conditions.[41]

$$O_2 + 4H^+ + 2e \longrightarrow 2H_2O \qquad E^o = 1.23\ V \qquad (2.2)$$

However, redox potentials of O_2 are dependent on the pathway and are additionally pH-dependent. Values of the standard oxidation potentials in acidic solution ($[H^+]$=1.0 M, O_2 = 1 atm) are summarized below (Fig. 2.2).[41]

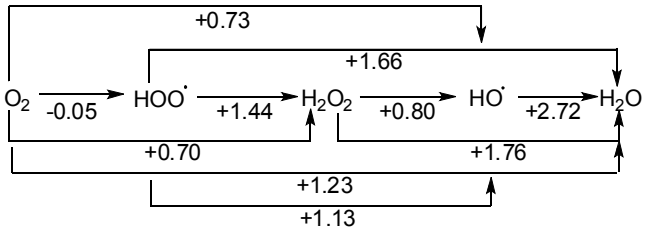

Figure 2.1. Standard potentials for oxygen reduction (in V; $[H^+]$=1.0 M, O_2 1 atm).

Some properties of O_2 and its derivatives are shown in Scheme 2.1. It is worth to note that reduction of O_2 places electron on partially occupied antibonding π^* orbitals thus decreasing the bond order and the interatomic O-O distance and increasing vibrational frequency ν_{O2} (Scheme 2.1).[39, 41]

Scheme 2.1. Some properties of O_2 and its ionic derivatives.

	O_2^+	$\xrightarrow{-e^-}$ O_2	$\xrightarrow{+e^-}$ O_2^-	$\xrightarrow{+e^-}$ O_2^{2-}	$\xrightarrow{+2e^-}$ $2O^{2-}$
Bond order	2.5	2.0	1.5	1.0	0
O-O distance, A^o	1.12	1.21	1.28	1.49	
ν_{O2}, cm^{-1}	1858	1555	1145	842	
Example cmpd	$O_2[AsF_6]$	O_2	KO_2	Na_2O_2	

Accordingly, there are several types of transition metal complexes typically produced by reaction of the transition metal center with molecular O_2, which can be classified according to the oxidation states of oxygen that vary from 0 to -2.[38]

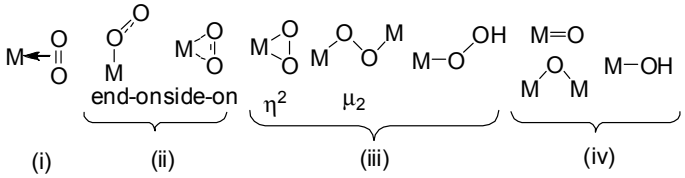

Figure 2.2. Principal types of transition metal complexes formed by oxidation with O_2.

(i) Adducts with O_2 might form without the change in the oxidation state of both O_2 and a metal.

(ii) Superoxo complexes involve coordination to O_2^-, the product of one electron reduction of O_2. Both end-on and side-on coordination modes of the superoxo ligand are known.

(iii) Peroxo complexes incorporate the two electron-reduced form of dioxygen, O_2^{2-} containing O in formal oxidation state -1. Typical coordination modes involve side-on coordination or end-on μ_2 bridging mode in dinuclear complexes. Protonation of the peroxo ligand could lead to the formation of a hydroperoxo complex M-OOH.

(iv) Four-electron oxidation of dioxygen produces metal oxo complexes with oxygen in the oxidation state -2, or hydroxo complexes as their protonated analogues.

Although complexes of type (i) are currently unknown for platinum, an isoelectronic d^8 Rh^I complex with a bulky N-heterocyclic carbene (NHC) ligand was reported to react with O_2 without change in the oxidation state of both metal center and coordinated O_2 to give a diamagnetic complex that was assigned to type (i), $(IPr)_2RhCl(O_2)$ (eq. 2.3). Based on spectroscopic and structural data and DFT-analysis, Kennepohl and co-workers proposed that the complex is best described as a Rh^I complex with a singlet O_2, rather than a Rh^{III}-peroxo compound.[42] The O-O distance is relatively short, 1.267 Å, that is only slightly longer than in free O_2 (1.21 Å).

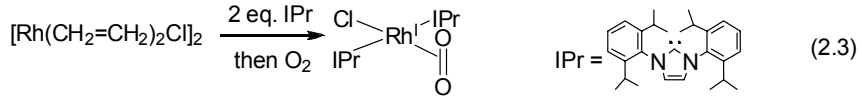

(2.3)

Formation of a superoxo complex by O_2 oxidation formally involves transfer of one electron from a metal center to the O_2 ligand; it is therefore more likely to be observed in transition metals that tend to undergo one-electron oxidations. Considering that the most

stable oxidation states of platinum are 0, +2 and +4, it is not surprising that no stable platinum superoxo-complexes are currently known,[41] although superoxo-Pt species have been invoked as intermediates in an overall two-electron aerobic oxidation of platinum.[43] Examples of characterized superoxo complexes reported in the literature mostly involve 3d-transition metals of groups 8-11: iron,[40, 44] cobalt,[45] nickel,[46] and copper.[47, 48] Copper superoxides are commonly proposed as active intermediates in oxidation processes involving mononuclear copper enzymes, such as peptidylglycine α-hydroxylating monooxygenase (PHM) or dopamine β-monoxygenase (DβH).[49, 50] Sundemeyer *et al.* reported reversible oxygen binding by copper(I) complexes with tetradentate nitrogen-donor ligands to form an end-on superoxo Cu^{II} complex (eq. 2.4).[51, 52] According to X-ray diffraction analysis, the O-O bond distance in the superoxo Cu^{II} complex is 1.280 Å.[52]

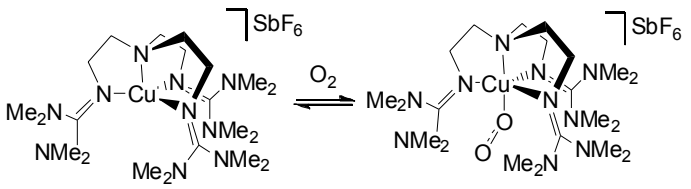

(2.4)

The bonding situation in trigonal bipyramidal copper superoxo complexes with tetradentate ligands can be described as a σ-overlap between the π_σ* orbital of the superoxide with the d_{z2} orbital of the Cu^{II} ion (Fig. 2.3).[47]

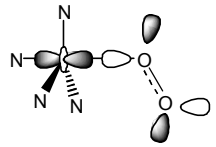

Figure 2.3. Overlap between the π_σ* orbital of the superoxide and the d_{z2} orbital of the Cu for a trigonal-bypiramidal geometry.

Experimental characterization of superoxo-complexes is often complicated due to their low stability and tendency to undergo further reduction of the O_2 moiety to produce peroxo complexes.[47]

A number of peroxo- and hydroperoxo-complexes of platinum has been reported in the literature. For example, some phosphine Pt^0 (eq. 2.5)[53, 54] and other low valent late transition metal complexes (Rh^I,[55, 56] Ir^I,[37] Pd^0 [57]) can react with O_2 to produce mononuclear diamagnetic η^2-peroxo complexes in aprotic solvents.

$$Pt^0(PPh_3)_4 + 2O_2 \longrightarrow Pt^{II}(PPh_3)_2(\eta^2\text{-}O_2) + 2Ph_3PO \qquad (2.5)$$

The O-O bond distance in $(PPh_3)Pt(O_2)$ complex is 1.45 Å, and a vibrational frequency ν_{O_2} is 830 cm^{-1}, typical for peroxo-complexes.[58] Peroxo compounds of Pt^{II}, Rh^{III} and Ir^{III} can act as oxidants toward a range of organic an inorganic substrates such as phosphines or SO_2.[59] Protonation of these complexes with acid generates free H_2O_2.[54]

It is important to remember that the ground state of molecular O_2 is a triplet, and therefore its conversion into a close-shell peroxo complex by reaction with a close-shell d^{10} metal center should involve spin crossover. Based on the computational analysis of palladium(0) oxidation by O_2, Stahl proposed that the spin crossover in palladium-O_2 complex is facilitated by formation of an intermediate triplet diradical Pd^I-superoxide with spin density delocalized onto the Pd^I center and O_2^- ligand.[57]

The oxidation of dimethyl Pt^{II} complexes with bidentate N-donor ligands $(NN)PtMe_2$ (NN = tmeda, 2,2'-bipyridyl, 1,10-phenanthroline) with O_2 has been studied by Bercaw *et al.* It has been noted that only neutral complexes with two strong σ-donor Me ligands $(NN)PtMe_2$ (NN = tmeda, 2,2'-bipyridyl, 1,10-phenanthroline) are oxidized by air,

whereas no oxidation was observed for complexes (NN)PtMeCl, (NN)$PtCl_2$, (NN)$PtPh_2$.[43, 60]

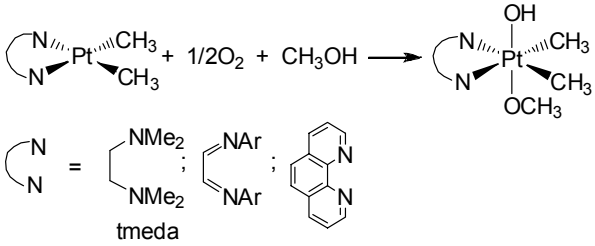

Bercaw and other authors proposed that the oxidation of Pt^{II} complexes involves initial formation of a superoxo-Pt^{III} complex, followed by its conversion to hydroperoxo $HOOPt^{IV}$ in protic solvents (eq. 2.7). The resulting hydroperoxo complex in turn can act as an oxidant and react with another molecule of Pt^{II} to produce two molecules of Pt^{IV}-hydroxo complex (eq. 2.8).[43]

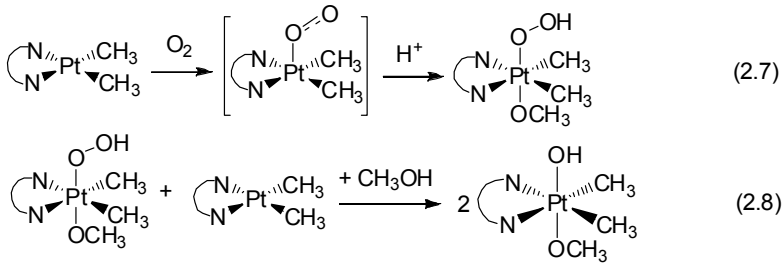

The X-ray structure of (tmeda)$PtMe_2$(OOH)(OMe) reveals the O-O distance of 1.48 Å, typical for hydroperoxo complexes. Since formation of the hydroperoxo complex involves proton transfer, but no dependence of the reaction rate on $[H^+]$ was observed, authors concluded that formation of a superoxo intermediate is a rate determining step.[43]

One might expect that the hydroperoxo Pt^{IV} species will be even stronger oxidant for Pt^{II} complexes than molecular O_2. For comparison, standard reduciton potential of conversion of hydrogen peroxide H_2O_2 to H_2O in neutral solution is +1.35 V, whereas standard potential of reduction of O_2 to H_2O is only +0.82 V at pH 7.[41] Indeed, Bercaw *et*

al.[43] demonstrated that the reaction of (tmeda)$Pt^{IV}Me_2$(OOH)(OMe) complex with (tmeda)$Pt^{II}Me_2$ is very fast even at low temperatures, with a half-life of 5 minutes at -80 ^oC, at sufficient Pt concentrations. An alternative pathway for the hydroxo complex formation, disproportionation of a hydroperoxo complex (eq. 2.9), presumably via homolysis of a O-O bond, was found to be much slower under the same reaction conditions.[43]

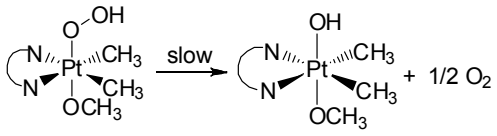

(2.9)

From a practical standpoint, it is important to achieve the oxidation of mono-hydrocarbyl Pt^{II} species, since in most cases the substrate (arene, alkane, olefin) activation by Pt^{II} center results in the formation of mono-hydrocarbyl complexes. However, examples of aerobic oxidation of Pt^{II} compounds other than electron-rich dimethyl complexes are very rare. Importantly, potentially tridentate *fac*-chelating ligands, capable of changing the coordination mode from dicoordinate ("dihapto", η^2) to tricoordinate ("trihapto", η^3) bonding, such as 1,3,5-triaminocyclohexane (tach),[61] or 1,4,7-triazacyclononane (tacn),[30] significantly facilitate the susceptibility of a species to aerobic oxidation, so that even Pt^{II} complexes that do not bear strongly σ-donating alkyl groups are oxidized by air. For example, Sarneski[61] described facile oxidation of $[(bpy)Pt(\eta^2\text{-tach})]^{2+}$ (bpy = 2,2'-bipyridyl), formed *in situ*, into $[(bpy)Pt((\eta^3\text{-tach})(OH_2)]^{2+}$ under air (Scheme 2.2) and Wieghardt[30] reported the aerobic oxidation of a cationic complex $[(\eta^2\text{-tacn})_2Pt]^{2+}$ to $[(\eta^3\text{-tacn})_2Pt]^{4+}$ in water at 90 ^oC (Scheme 2.3).

Scheme 2.2

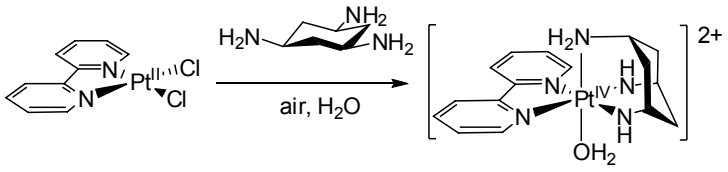

Scheme 2.3

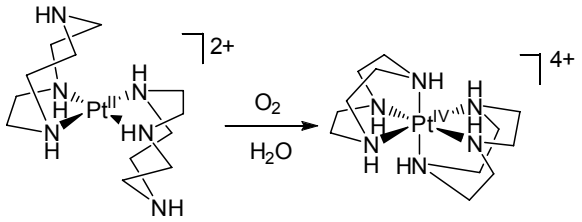

However, tridentate amino-donor ligands such as tach or tacn are not suitable for utilization in catalytic aerobic oxidation of hydrocarbons due to the overstabilization of the octahedral Pt^{IV} center that prevents further reductive elimination reactions.[62-64] Moreover, in the envisioned catalytic cycle the oxidant must be selective toward Pt^{II}-monohydrocarbyl species only. The Pt^{II} disolvento precursor responsible for substrate activation must remain in unoxidized form.[65] As can be seen from the examples above, such selectivity cannot be achieved by the use of triamino ligands such as tach or tacn.

Our approach to the problem of selective aerobic oxidation of Pt^{II} complexes is based on the utilization of a hemilabile di(pyridyl)methanesulfonate ligand (dpms)[29] bearing two pyridyl donors that can chelate to a square planar Pt^{II} center in a η^2 mode, and a labile sulfonate group.

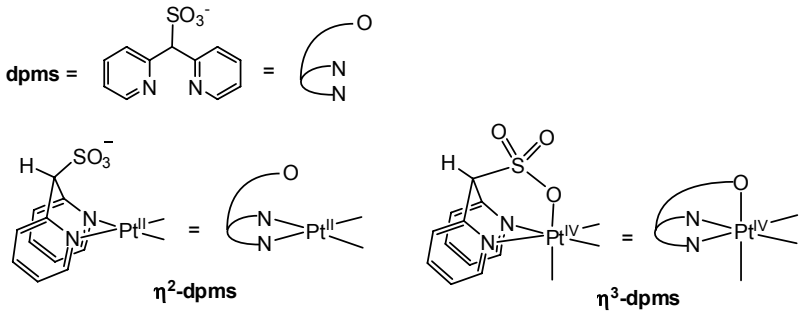

Figure 2.4. Coordination modes of the dpms ligand in platinum complexes.

We expected that the dpms ligand will enable aerobic oxidation of a Pt^{II} complexes by stabilizing the emerging octahedral Pt^{IV} center via coordination of the sulfonate oxygen. However, the relatively weak donor ability and lability of the sulfonate group prevents overstablization of the Pt^{IV} complex thus allowing for a further reductive elimination after scorpionate arm decoordination and formation of a transient penta-coordinate Pt^{IV} species.

2.1.2 Preparation and Oxidation of (dpms)$PtMe^{II}$(HX) Complexes with O_2

The synthesis of monomethyl complexes of type (dpms)Pt^{II}Me(ROH) (R = H, Me) was accomplished by protonolysis of K(dpms)$Pt^{II}Me_2$ precursor, prepared according to the literature procedure[29] with 1 equivalent of HBF_4 or H_2SO_4 using ROH as a solvent. Complex (dpms)PtMe($PhNH_2$) was obtained by ligand exchange from (dpms)PtMe(MeOH) in the presence of aniline in methanolic solution.

Scheme 2.4. Preparation of monomethyl Pt^{II} complexes

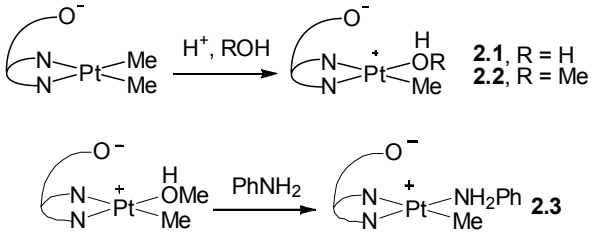

Methylplatinum(II) complexes **2.1** and **2.2** containing coordinated water or methanol are readily oxidized under O_2 (1 atmosphere) at room temperature upon stirring: formation of corresponding (dpms)PtMe(OH)(OR) (R=H, **2.5**; R = Me, **2.6**) products is complete in less than 3 hours; no other product were detected in significant amounts. The half-life of oxidation of **2.1** in H_2O solution under 1 atm of O_2 was determined to be ~15 minutes at 20 ^oC. The products of oxidation, **2.4** and **2.5**, were isolated in an analytically pure form in high yields and characterized by ^1H and ^{13}C NMR spectroscopy, ESI-MS, elemental analysis and single crystal X-ray diffraction.

Scheme 2.5. Oxidation of (dpms)PtMe(ROH) complexes by O_2.

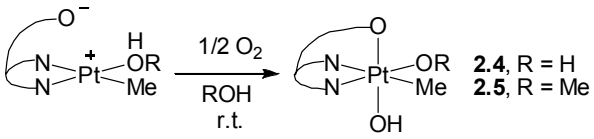

NMR spectra of **2.4** reveal low C_1 symmetry of the complex: two inequivalent pyridyl fragments of the dpms ligands give rise to eight multiplets in the aromatic region of ^1H NMR spectrum, and ten aromatic carbons peaks of pyridyl are seen in ^{13}C NMR spectrum of **2.4**. Methyl group bound to platinum gives rise to a singlet in ^1H NMR spectrum accompanied by platinum satellites with a H-^{195}Pt coupling constant $^2J_{PtH}$ = 66 Hz; in ^{13}C NMR spectrum it appears as a characteristically upfield shifted peak at 4.5 ppm with platinum satellites and a large coupling constant value of $^1J_{PtC}$ = 547 Hz. Low C_1 symmetry of dihydroxo complex **2.4** implies that Me group is located in an equatorial plane formed by platinum and two pyridyl ligands, and two inequivalent hydroxo ligands are present in an equatorial and an axial positions. The structure was also confirmed by an X-ray analysis of a single crystal obtained by Vedernikov from methanolic solution (Figure 2.5).

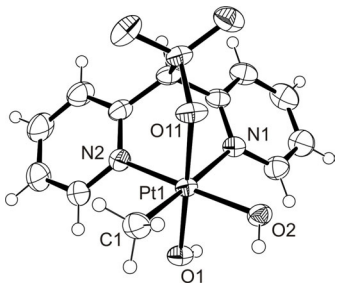

Figure 2.5. ORTEP drawings of complex **2.4**, 50% probability ellipsoids. Selected bond distances, Å: Pt1-O1, 1.963(3); Pt1-O2, 1.977(3); Pt1-O11, 2.057(3); Pt1-N1, 2.171(3); Pt1-N2, 2.022(3); Pt1-C1, 2.048(4).

We established in this work that one of the hydroxo ligands in **2.4** comes from dioxygen, and another OH group originates from the solvent, by reacting isotopically labeled complex (dpms)PtMe($^{18}OH_2$) with O_2 in $H_2{}^{18}O$ solution. Complex (dpms)PtMe($^{18}OH_2$) was obtained by protonolysis of (dpms)$PtMe_2H$ in isotopically labeled $H_2{}^{18}O$ solvent; subsequent oxidation with O_2 (natural abundance of ^{16}O-^{16}O in O_2 is 99.5%) gave a singly labeled product, (dpms)PtMe(^{18}OH)(^{16}OH), as determined by ESI-MS analysis.

In order to find out if solvento ligand ROH, initially present in the plane formed by Pt and two nitrogens of dpms ligand in complexes (dpms)Pt^{II}Me(ROH), changes its position during aerobic oxidation, we determined the crystal structure of (dpms)PtMe(OMe)(OH) (**2.5**), obtained by aerobic oxidation of (dpms)PtMe(MeOH) (Figure 2.6).

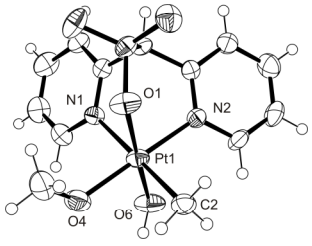

Figure 2.6. ORTEP drawings of complex **2.5**, 50% probability ellipsoids. Selected bond distances, Å: Pt1-O1, 2.100(5); Pt1-O4, 1.978(5); Pt1-O6, 1.952(5); Pt1-N1(6), 2.156; Pt1-N2(6), 2.052; Pt1-C2, 2.099(7).

As can be seen from Fig. 2.6, both methyl and methoxo ligand in **2.5** retained their positions in the equatorial plane formed by platinum and two nitrogen atoms of dpms.

Therefore, we can conclude that dioxygen attack on (dpms)Pt^{II} complex occurs from one of the axial sites.

A conclusion can therefore be made, that HX ligands – O-donors (X = OH, MeO) favor the aerobic oxidation of $MePt^{II}(HX)$ to $MePt^{IV}(OH)X$ complexes.

Oxidation of $MePt^{II}$ complex with aniline, (dpms)$Pt^{II}Me(NH_2Ph)$, proceeds slower than for O-donors; the reaction half-life time is 8-10 hours at 20 ^{o}C under an O_2 atmosphere. According to NMR and ESI analysis, the product of the oxidation by dioxygen was identical to that obtained in the reaction with H_2O_2 and was identified as an amido complex (dpms)PtMe(NHPh)(OH) (**2.6**). Complex **2.6** was obtained in an analytically pure form by oxidation of **2.3** with H_2O_2 and characterized by ^{1}H and ^{13}C NMR spectroscopy, ESI-MS, elemental analysis and single crystal X-ray diffraction.

Scheme 2.6. Oxidation of aniline complex with O_2 or H_2O_2.

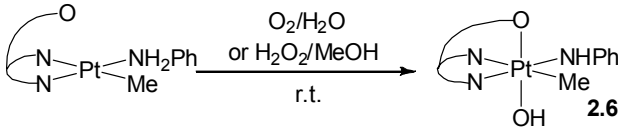

X-ray analysis revealed that Me and aniline ligands retained their position in an equatorial plane formed by Pt and two nitrogens of pyridyls in the oxidation product **2.6**, consistent with our earlier observation of retention of stereochemistry in the equatorial Pt-N1-N2 plane (Fig. 2.7). According to X-ray, deprotonation of the bound aniline to phenylamido ligand occurred upon oxidation to Pt^{IV} in complex **2.6**, similar to deprotonation of two amino groups of 1,3,5-triaminocyclohexane in Pt^{IV} complex formed by aerobic oxidation observed by Sarneski (Scheme 2.2).[61]

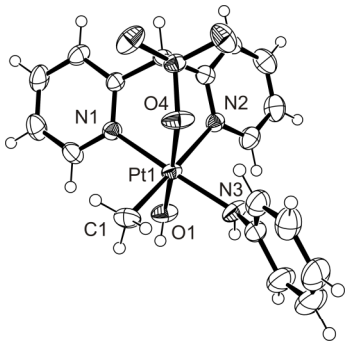

Figure 2.7. ORTEP drawings of complex **2.6**, 50% probability ellipsoids. Selected bond distances, Å: Pt1-O1, 1.946(3); Pt1-N3, 2.018(3); Pt1-C1, 2.036(4); Pt1-N1, 2.089(3); Pt1-O4, 2.102(3); Pt1-N2, 2.189(3).

To prove that the pendant sulfonate group in the dpms ligand enabled aerobic transformations of (dpms)PtMe(HX), we compared their reactivity with that of analogous $LPtMe(OH_2)$ complexes derived from the structurally similar bidentate dipyridylmethane ligand (dpm), Py_2CH_2.[66] Dipyridylmethane contains a CH_2 bridging two pyridyl fragments; it can coordinate by two nitrogens of pyridyls to a Pt^{II} square planar center in a η^2-fashion, however, unlike dpms, it has no third donor group and it is therefore unable to achieve the η^3-coordination mode necessary for stabilizing an octahedral Pt^{IV} center. The methyl aqua complex $[(dpm)PtMe(OH_2)]BF_4$ was shown to be inert toward dioxygen in protic solvents (Scheme 2.7).[79]

Scheme 2.7

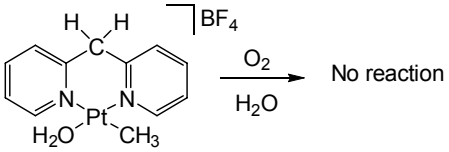

We can conclude therefore that the presence of the oxygen of a sulfonate group in proximity to Pt center was sufficient to raise the energy of the highest occupied molecular orbital (HOMO) so that even monomethyl complexes are oxidized with O_2.

It is noteworthy that disolvento complexes such as $[(dpms)Pt(OH_2)_2]^+BF_4^-$ or even anionic $Na^+[(dpms)Pt(OH)_2]^-$ are inert toward O_2 under the same conditions. Therefore, the presence of at least one strong σ-donor,[43] Me group, is necessary in $(dpms)Pt^{II}$ complexes in order to raise the energy of HOMO to a sufficient level for aerobic oxidation.[43] Such selectivity toward Pt^{II}-alkyl species can be beneficial for possible catalytic applications in the aerobic oxidation of hydrocarbons. This reactivity stands in contrast to other potentially tridentate ligands with three amino-donors such as 1,4,7-triazacyclononane[30] or 1,3,5-triaminocyclohexane,[61] which are known to oxidize even cationic Pt^{II} complexes with weaker σ-donor ligands, such as amines or 2,2'-bipyridyl.

We can conclude that presence of the pendant sulfonate donor enhances reactivity of the derived complexes toward aerobic oxidation and provides beneficial selectivity toward complexes with at least one Pt-C bond.

Oxidation of dimethyl anionic complex $K[(dpms)PtMe_2]$ (**2.7**) was reported earlier by Vedernikov.[29] The product of oxidation was identified as *sym*-$(dpms)PtMe_2(OH)$, and its structure was established by X-ray diffraction.[29] Similar to our observations for monomethyl complexes, two methyl groups in *sym*-$(dpms)PtMe_2(OH)$ retain their positions in Pt-N-N plane, and the OH group is located in the axial position. Complex $K[(dpms)PtMe_2]$ is even more reactive than monomethyl complexes and its half-life was estimated to be ~5 minutes under 1 atm of O_2 at 20 ^oC in an aqueous solution.[29] The order of increasing ease of aerobic oxidation of (dpms)PtMe(HX) complexes can therefore be summarized as follows:

$$(dpms)Pt(OH_2)_2^+, (dpms)Pt(OH)_2^- << (dpms)PtMe(PhNH_2) <$$

$$(dpms)PtMe(MeOH) \sim (dpms)PtMe(OH_2) < (dpms)PtMe_2^-$$

Based on the above trend in reactivity, we suggest that the ease of oxidation is not solely determined by σ-donor strength of the HX ligands in our system, and that other factors might be responsible for susceptibility to oxidation. We propose that deprotonation of zwitterionic neutral $LPt^{II}Me(HX)$ might be necessary prior to oxidation to form an anionic and more reactive $[LPt^{II}Me(X)]^-$ (Scheme 2.8). The ease of oxidation would then correlate with the acidity of coordinated HX ligand and would account for the slow oxidation of much less acidic amine complexes compared to LPtMe(ROH).

Scheme 2.8

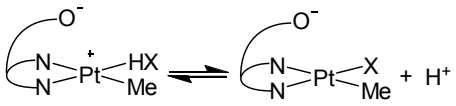

We then decided to explore the effect of solution pH on the ease of oxidation of (dpms)PtMe(OH_2) in aqueous solutions. The NMR yields of oxidation products and the remaining starting material were determined after 60 min of stirring under 1 atm of O_2 at 20 °C in aqueous solutions at variable concentrations of added NaOH; the results of three runs were averaged (Table 2.1). It was not possible to follow the reaction in acidic solution due to fast protonolysis of methyl Pt complexes in the presence of acids.

Table 2.1. Results of oxidation of 19 mM $LPt^{II}Me(OH_2)$ in water as a function of concentration of additives of NaOH after 60 min of reaction at 20 °C and 1 atm O_2.

NaOH, equiv. ([NaOH], mM)	Yield of *unsym*-**2.4**, %[a]	Unreacted **2.1**, %[a,b]
0 (0)	88±1	6±1
0.10 (1.9)	99±1	0
0.54 (10)	82±1	17±1
1.1 (21)	53±1	45±1
2.2 (42)	22±1	73±1

[a] Average of 3 runs
[b] Another oxidation product, *unsym*-$LPt^{IV}Me_2(OH)$, formed in the amount of 3-5%.

Surprisingly, we found that the yield of oxidation product goes through the maximum in the presence of 0.1 equivalents of added NaOH, and then decreases at higher concentrations of NaOH (from 0.1 to 2.2 equivalents relative to **2.1**).

We explained the observed pH dependence by the combined action of two opposing effects. As mentioned earlier, in alkaline solutions complex **2.1** can reversibly deprotonate to form an anionic $[(dpms)PtMe(OH)]^-$ (**2.8**), which is expected to be more reactive toward aerobic oxidation. However, if the oxidation of the latter is inhibited by NaOH, this will result in the presence of a maximum on the plot of the oxidation product yield *vs.* [NaOH]. Similar results were observed in case of $(dpms)Pt(C_2H_4)(OH)$ and the detailed kinetic analysis of this reaction will be discussed in Chapter 2.

The observed inhibition of oxidation with O_2 at high NaOH concentrations implies that the proton transfer step should be involved in the oxidation before or at the rate limiting step. Based on our observations and analysis of the literature data, we proposed two possible mechanistic scenarios of oxidation that allow us to account for these results:

(i) a proton-coupled electron transfer to a Pt^{II} coordinated dioxygen ligand (eq 2.10, 2.11; L = dpms):

$$\underset{\textbf{2.8}}{LPt^{II}(Me)OH^-} + O_2 \rightarrow \underset{\textbf{2.9}}{(\eta^2\text{-}L)Pt^{II}(\eta^1\text{-}O_2)(Me)OH^-} \qquad (2.10)$$

$$\underset{\textbf{2.9}}{(\eta^2\text{-}L)LPt^{II}(\eta^1\text{-}O_2)(Me)OH^-} + H^+ \rightarrow \underset{\textbf{2.10}}{(\eta^3\text{-}L)LPt^{IV}(O_2H)(Me)OH} \qquad (2.11)$$

The first step involves initial axial attack of dioxygen on the platinum(II) center of an anionic **2.8** to generate a transient intermediate **2.9** that can be represented in extreme

cases as a Pt^{III}-superoxo complex or as a Pt^{II} complex with η^1-coordinated O_2 ligand (eq. 2.10). Subsequent proton-coupled electron transfer leads to the formation of a transient hydroperoxo Pt^{IV} complex **2.10**, stabilized by η^3 coordination to a dpms ligand (eq. 2.11). A transient hydroperoxo platinum(IV) complex **2.10** could then react with another Pt(II) species (eq. 2.12) to afford two equivalents of the observed (dpms)PtMe$(OH)_2$ product.

$$\underset{\textbf{2.10}}{LPt^{IV}(O_2H)(Me)OH} + \underset{\textbf{2.8}}{LPt^{II}(Me)OH^-} + H_2O \rightarrow 2\underset{\textbf{2.4}}{LPt^{IV}(Me)(OH)_2} + OH^- \qquad (2.12)$$

This mechanism is similar to that proposed by Bercaw[67] and Puddephatt[63] for oxidation of Pt^{II} complexes with O_2. The important difference between the two mechanisms is that in mechanism (i) initial deprotonation of (dpms)PtMe(OH_2) is required to produce more reactive [(dpms)PtMe(OH)]$^-$, and that the formation of **2.9** is a reversible step before rate-determining step (2.11), as will be discussed below.

Volumetric measurements of oxidation of (dpms)Pt(CH_2CH_2)(OH) with O_2, which likely proceeds via the same mechanism and involves formation of the alkyl complex [(dpms)Pt(C_2H_4OH)(OH)]$^-$ as will be discussed in more detail in Chapter 2, indicate that 0.5 moles of O_2 are consumed per oxidation of 1 mole of Pt^{II} complex, consistent with the proposed mechanism.

(ii) An alternative mechanism could involve protonation of the Pt^{II} center leading to a transient Pt^{IV} hydride and subsequent oxidation of the Pt^{IV} hydride (eq 2.13, 2.14):

$$(\eta^2\text{-L})LPt^{II}(Alk)OH^- + H^+ \rightarrow (\eta^3\text{-L})Pt^{IV}H(Alk)OH \qquad (2.13)$$

$$(\eta^3\text{-L})Pt^{IV}H(Alk)OH + O_2 \rightarrow (\eta^3\text{-L})Pt^{IV}(O_2H)(Alk)OH \qquad (2.14)$$

Photochemical insertion of O_2 into of Pt^{IV}-H bond has been observed previously by Karen Goldberg in $(Tp^{Me2})PtMe_2H$ complexes (Tp^{Me2} = hydridotris(3,5-dimethylpyrazolyl)borate) and the mechanistic studies of this reaction showed that it follows radical chain mechanism and is sensitive to radical inhibitors.[68]

Scheme 2.9

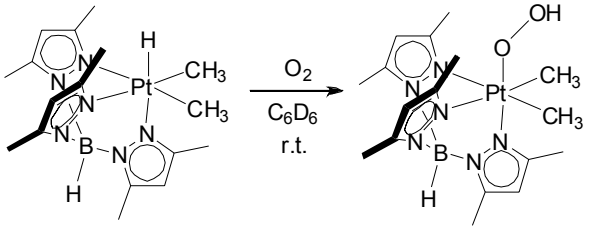

The $(dpms)Pt^{IV}$ hydride $(dpms)PtMe_2H$ was isolated and characterized by Vedernikov[29] previously, however, the aerobic oxidation of aqueous solutions containing $(dpms)PtMe_2H$ was found to be slower than in aqueous solutions containing $(dpms)PtMe(OH_2)$ (**2.1**).[29] We also established in this work that the oxidation rate of (dpms)PtPh(MeOH), which presumably occurs via the same mechanism as oxidation of methyl complexes and will be discussed in Chapter 6, is not affected by the presence of a radical inhibitor. We postulate that platinum(IV) hydrides are not viable intermediates of aerobic oxidation of **2.1**, and that a mechanism (i), a proton-coupled electron transfer to η^1-coordinated dioxygen ligand involving a triplet-singlet spin interconversion, might be operative here.

Importantly, a paramagnetic intermediate **2.9** was never observed by NMR even in strongly alkaline solutions, when the proton-coupled electron transfer (eq. 2.10) might be very slow, implying that the formation of an intermediate **2.9** is a reversible step. If the formation of **2.9** were irreversible, noticeable accumulation of an intermediate **2.9** would be observed in strongly basic solution, when its subsequent transformation to **2.10** is

slow. Accumulation of a paramagnetic **2.9** should be reflected in NMR spectra as line broadening or disappearance of the fraction of the starting material **2.1**, not compensated by the formation of **2.5**. Since this was not observed experimentally, we suggest that formation of **2.9** is a reversible reaction, and the equilibrium (2.10), is shifted to the left.

The intermediate **2.10** was never observed experimentally as well; we believe that formation of **2.10** occurs at a rate determining step (eq. 2.11) thus causing observed inhibition at high [NaOH], followed by fast conversion of **2.10** into the product (dpms)PtMe(OH)$_2$ (eq. 2.12).

2.1.3 DFT-Modeling of a Proton-Coupled Electron Transfer from Pt^{II} to a Coordinated Dioxygen Ligand

The viability of the proposed mechanism of oxidaiton of (dpms)PtMe(OH)$_2$ (eq. 2.10-2.12) was supported by Density Functional Theory (DFT) calculations. All DFT calculations in this work were done by Andrei N. Vedernikov. A full geometry optimization and Gibbs energy calculation was performed for **2.8**, LPt^{II}Me(OH)$^-$, and two proposed reaction intermediates, (η^2-L)Pt^{II}(η^1-O$_2$)(Me)(OH)$^-$, **2.9**, and (η^3-L)LPt^{IV}(O$_2$H)(Me)(OH), **2.10**, in both the triplet and the singlet ground state configurations. The optimized structures of ^{3}**[2.9]**, ^{1}**[2.9]**, ^{3}**[2.10]**, and ^{1}**[2.10]** along with spin densities for the triplet species, selected bond lengths and the relative standard Gibbs energies are given in Fig. 2.8.

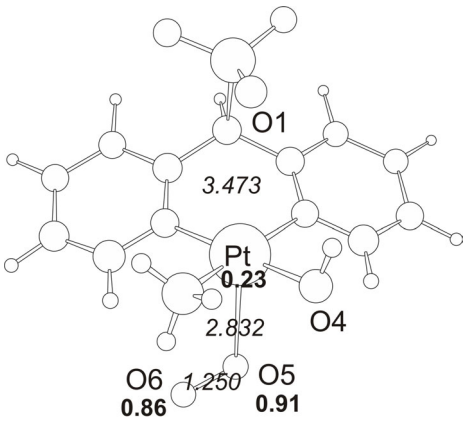

a) ^{3}**[2.9]** (0 kcal/mol)

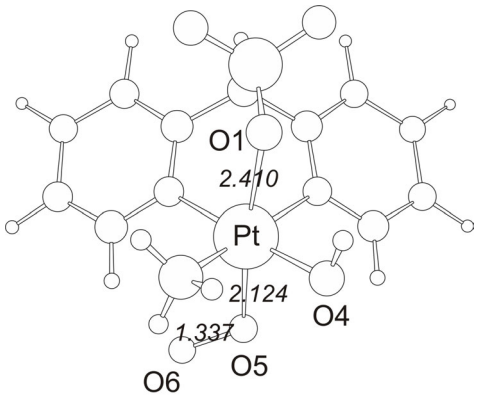

b) ^{1}**[2.9]** (19.1 kcal/mol)

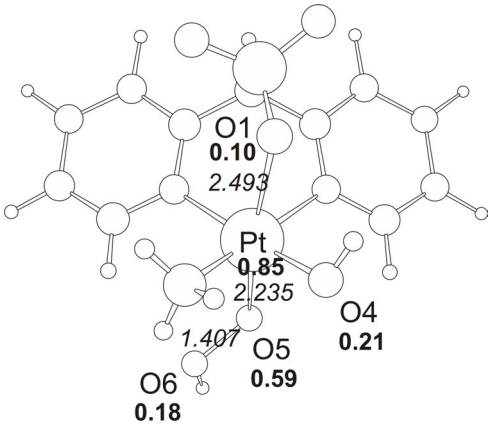

c) ^{3}**[2.10]** (0 kcal/mol)

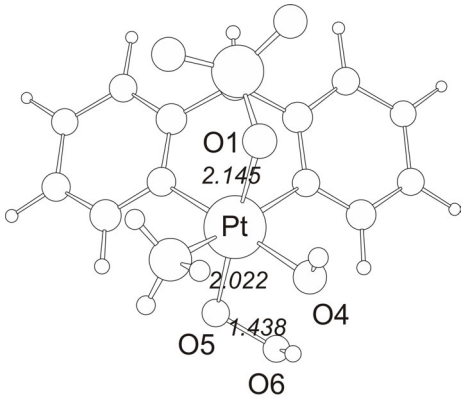

d) ^{1}**[2.10]** (-37.5 kcal/mol)

Figure 2.8. The DFT optimized structures of: a) (η^2-L)Pt^{II}(η^1-O_2)$MeOH^-$ in the triplet state, ^{3}**[2.9]**; b) (η^2-L)Pt^{II}(η^1-O_2)$MeOH^-$ in the singlet state, ^{1}**[2.9]**; c) (η^3-L)LPt^{IV}(O_2H)Me(OH) in the triplet state, ^{3}**[2.10]**, d) c) (η^3-L)LPt^{IV}(O_2H)Me(OH) in the singlet state, ^{1}**[2.10]**. Selected bond lengths are given in italics, spin densities are in bold, and the relative standard Gibbs energies of species of different multiplicity are given in parentheses.

The DFT calculated Gibbs energy of reaction between **2.8** and O_2 leading to ^{3}**[2.9]** was found to be 3.5 kcal/mol suggesting that reaction (2.10) may be a slightly uphill process only. The spin density on the platinum atom in ^{3}**[2.9]**, 0.23, is not very high, and the distance between Pt and oxygen of sulfonate, Pt-O1, is very long, 3.473 Å, implying that ^{3}**[2.9]** is essentially a Pt^{II} complex. The O5-O6 distance on O2 ligand is 1.250 Å, only slightly longer than O-O distance in free O_2, 1.21 Å.[38]

In the singlet species **^{1}[2.9]** the O5-O6 distance is more significantly elongated, 1.337 Å, indicating greater degree of electrons transfer from platinum to the antibonding orbital of the coordinated O_2 ligand. Accordingly, Pt-O5 (2.124 Å) and Pt-O1 (2.410 Å) distances are much shorter compared to **^{3}[2.9]**. Notably, the energy difference between the singlet adduct **^{1}[2.9]** and more stable triplet adduct is very high, 19.1 kcal/mol, comparable to the energy difference between a singlet and a triplet states of free O_2 (23.4 kcal/mol), thus making a possible spin interconversion too unfavorable.

However, since terminal oxygen of O_2 ligand, O6, bears a greater negative charge in a singlet complex **^{1}[2.9]** (-0.38), compared to the triplet state **^{3}[2.9]**, -0.14, one could expect that protonation on the terminal oxygen will affect significantly the relative stabilities of a triplet and a singlet states of the resulting hydroperoxo product **[10]**. Our calculations showed that the singlet hydroperoxo complex **^{1}[2.10]** is 37.1 kcal/mol more stable than the triplet **^{3}[2.10]**. As a result, the energy difference between the singlet and the triplet potential energy surfaces will be rapidly decreasing as we move along the reaction coordinate corresponding to the proton transfer to O6. When the energy difference between two potential energy surfaces becomes sufficiently small, a rapid spin interconversion can occur leading ultimately to **^{1}[2.10]**. Therefore, we can expect that a higher acidity of a reaction medium will favor a faster electron transfer from the Pt^{II} center to the coordinated oxygen ligand in complexes such as $(\eta^2\text{-L})LPt^{II}(Alk)OH^-$.

The DFT-optimized structure of complex **^{1}[2.10]** shown in Fig.2.8d is consistent with its formulation as a Pt^{IV} hydroperoxo complex. The distance between Pt and

oxygen of sulfonate is 2.145 Å, close to that observed experimentally in (dpms)Pt^{IV} complexes (~2.1-2.2 Å), and Pt-O5 distance is also similar, 2.022 A. The O5-O6 bond length in hydroperoxo ligand is 1.438 Å, typical for hydroperoxo complexes.[43] Therefore, our DFT results support the mechanism (i), which involves initial reversible formation of **[2.9]** followed by proton transfer/spin interconversion to form a hydroperoxo complex **[2.10]**.

2.1.4 Conclusions

Monomethyl complexes (dpms)PtMe(HX) where HX = H_2O, MeOH undergo facile oxidation with O_2 in protic solvents at room temperature to cleanly give (dpms)PtMe(X)(OH) product.

The monomethyl complex with aniline, (dpms)PtMe(NH_2Ph), reacts with O_2 much slower compared to complexes, where HX = H_2O, MeOH, under the same conditions. Low reactivity of monomethyl complexes with amines correlates the low acidity of the $PhNH_2$ ligands compared to ROH (R = Me, OH_2) and can be explained by low concentration of the anionic species (dpms)PtMe$(X)^-$, resulting from acidic dissociation of the coordinated HX, which are more reactive toward oxidation.

High reactivity of the dpms derivatives toward O_2 can be attributed to the presence of the third sulfonate donor group in proximity to Pt center and the ability of the dpms ligand to adopt either the η^2 or η^3 cooridnation modes. At the same time, unlike in complexes with tridentate amino-donor ligands (1,4,7-triazacyclononane, 1,3,5-triaminocyclohexane), the oxidation selectively occurs in complexes activated by the presence of at least one Pt-Me group, whereas disolvento complexes,

(dpms)Pt$(OH_2)_2^+$ and (dpms)Pt$(OH)_2^-$, are inert toward O_2. This fulfills an important criterion on the road to possible catalytic aerobic alkane functionalization.

2.2 Mechanistic Studies of C-O Reductive Elimination from (dpms)Pt^{IV}Me Complexes in Aqueous Solutions

2.2.1 Introduction: Mechanisms of C-X Reductive Elimination

Having found that (dpms)Pt^{II} methyl complexes are easily oxidized with O_2, we next sought to investigate (dpms)Pt^{IV} reactivity toward reductive elimination of functionalized organic products.

Reductive elimination is a key product-release step in various homogeneous processes catalyzed by transition metal complexes. For example, reductive elimination of MeOH and MeCl from Pt^{IV}-Me complexes is involved in Shilov-type chemistry related to catalytic conversion of methane into methanol.[65] Understanding of the mechanism of this step is therefore important for designing efficient catalytic systems for hydrocarbon oxidation.

Reductive elimination can be considered as the microscopic reverse of the oxidative addition reaction. By analogy with the mechanisms of oxidation addition of alkyl halides to d^8 metal centers, which in the case of platinum complexes typically proceeds via two-electron non-radical pathways, two fundamentally different mechanisms for the reductive elimination of C(sp^3)-heteroatom bond could be envisioned: an S_N2 mechanism involving external attack of the nucleophile on metal-bound carbon atom C(sp^3)-Pt^{IV} (Scheme 2.10a) and direct (concerted) reductive elimination involving a three-center transition state (Scheme 2.10b).[69]

Scheme 2.10. Mechanism of C(sp^3)-heteroatom reductive elimination

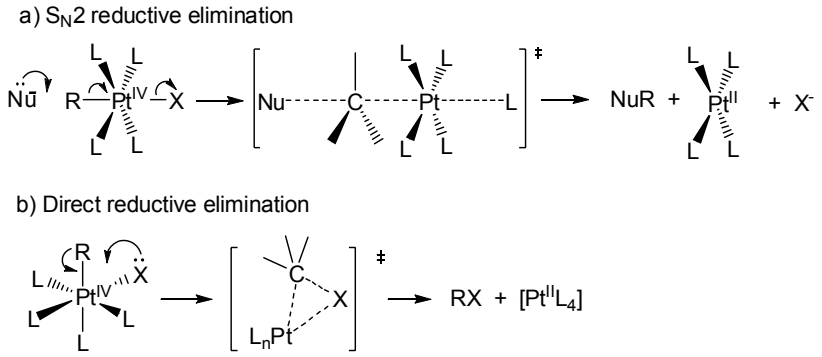

The kinetics of reductive elimination from $[Cl_5Pt^{IV}Me]^{2-}$ complexes to produce methanol and methyl chloride and $[Cl_4Pt]^{2-}$ as products (eq. 2.15) has been studied independently by Bercaw[62, 70] and Zamashchikov.[71-73]

$$[Cl_5PtCH_3]^{2-} \xrightarrow[20\text{-}45^oC]{Cl^-/H_2O} CH_3Cl + CH_3OH\ [PtCl_4]^{2-} \qquad (2.15)$$

It was shown that the kinetics of reductive elimination were consistent with an S_N2 mechanism involving external nucleophilic attack of chloride or water on the Me-Pt^{IV} of a five-coordinate intermediate $[Cl_4PtMe]^-$ or, alternatively, an intermediate $[Cl_4(H_2O)PtMe]^-$ having an aqua ligand *trans* to the Me group, formed by dissociation of the chloro-ligand *trans* to Pt-Me (Scheme 2.11).[62]

Scheme 2.11

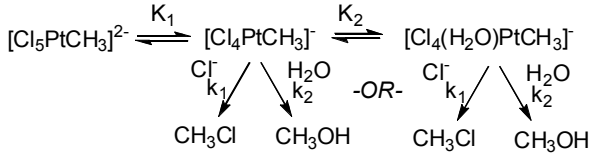

The authors concluded that a six-coordinate pentachloro complex $[Cl_5PtMe]^{2-}$ with a chloro ligand *trans* to Me group is unreactive. An S_N2 reductive elimination of MeCl from a five-coordinate intermediate with a vacant coordination site *trans* to Pt-Me is consistent with the commonly accepted mechanism of the microscopic reverse reaction,

oxidation addition of methyl halides to square planar d^8 metal complexes, which presumably involves formation of an analogous five-coordinate intermediate.[62, 69] Therefore, the nature of the ligand *trans* to the Pt^{IV} methyl group is important in determining reactivity towards reductive elimination.

Another argument in favor of an S_N2 pathway would be inversion of stereochemistry at the platinum-bound carbon in the elimination product. The evidence in support of an S_N2 mechanism of reductive elimination was obtained by Bercaw[62] and co-workers from studying stereochemistry of the C(sp^3)-Cl reductive elimination from deuterium-labeled hydroxyethyl Pt^{IV}CHDCHDOH complexes, obtained by oxidation of Zeise's salt K[Cl_3Pt(CHD=CHD)] prepared from *cis*- or *trans*-1,2-dideuterioethylene. The authors established that oxidation of Zeise's salt obtained from *trans*-CHD=CHD with H_2PtCl_6 as an oxidant produced primarily *erythro*-[Cl_5Pt^{IV}CHDCHDOH]$^{2-}$ product with 85-90% selectivity, resulting mostly from external nucleophilic attack of water on coordinated *trans*-CHD=CHD. Complex *erythro*-[Cl_5Pt^{IV}CHDCHDOH]$^{2-}$ undergoes reductive elimination of chloroethanol in aqueous solutions in the presence of Cl^- ions to give *threo*-ClCHDCHDOH with 100% inversion of configuration (Scheme 2.12).

Scheme 2.12

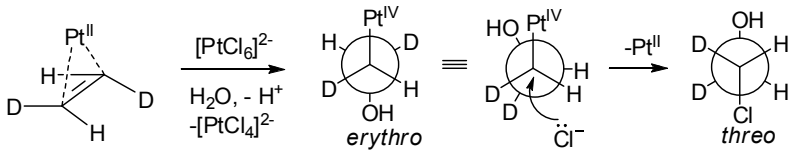

The mechanism of C(sp^3)-O elimination from Pt^{IV} complexes with diphosphine ligands (PP)$PtMe_3$(OR) (RO = AcO, ArO; PP = dppe, dppbz) was studied by Goldberg *et al.* [64, 74] Authors proposed that C-O elimination involves S_N2 attack of RO^- on the Pt-Me group of a five-coordinate intermediate (Scheme 2.13).[64, 74]

Scheme 2.13

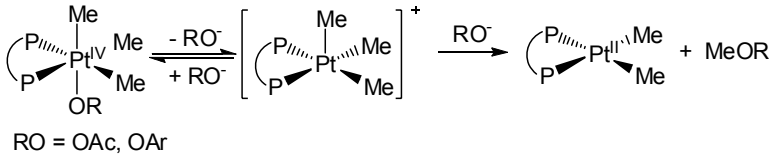

RO = OAc, OAr

An interesting example of methanol elimination from d^6 Ir^{III} center was originally reported by Atwood and the mechanism of this reaction was later revisited by Hartwig. In the original report Atwood *et al.*[75] suggested that reductive elimination from Ir^{III} complex $[Ir^{III}(CO)(OH)(I)(Me)(L)_2]$ (L = P(*p*-tolyl)$_3$) leads to the formation of methanol and Ir^{I} complex, which then reacts with excess of MeI present in solution to give $[Ir^{III}(CO)(I)_2(Me)(L)_2]$ as a final product observed in the reaction mixtures. However, Hartwig[76] has recently established that the isolated complex $[Ir^{III}(CO)(OH)(I)(Me)(L)_2]$ (L = PPh_3) did not eliminate methanol in the absence of MeI; however, upon addition of CD_3I an isotopically labeled CD_3OH formed. This result suggests that methanol resulted from methylation of Ir-OH with MeI, presumably via an S_N2 attack of a nucleophilic hydroxo ligand of $[Ir^{III}(CO)(OH)(I)(Me)(L)_2]$ on a carbon atom of MeI.

Scheme 2.14

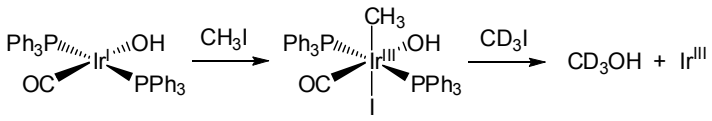

By contrast, examples of direct (concerted) C(sp^3)-heteroatom reductive elimination from d^6 metals are exceedingly rare. The Milstein group has recently demonstrated that reductive elimination of MeI from d^6 Rh^{III} complex with a bulky pincer PCP ligand is unlikely to occur via a conventional S_N2 mechanism (Scheme 2.15).[77]

Scheme 2.15

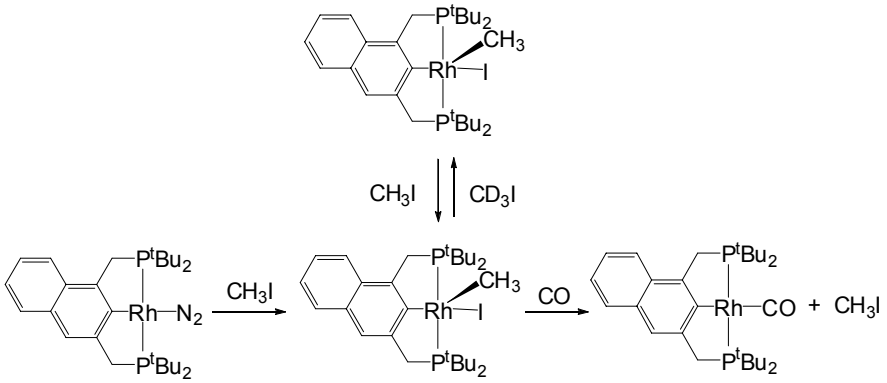

The Pd-catalyzed tetrahydrofurane formation was shown by the Sanford group to involve direct intramolecular C(sp^3)-O reductive elimination from a Pd^{IV} center with retention of configuration at carbon.[78]

As discussed in Section 2.1 of this chapter, di(2-pyridyl)methanesulfonate ligand (dpms) promotes facile clean aerobic oxidation of the associated methyl aqua Pt^{II} complexes, (dpms)PtMe(XH) (**2.1**-**2.3**), leading to dihydroxo methyl platinum(IV) compounds, (dpms)PtMe(OH)(X) (**2.4**-**2.6**).

Our group has recently found that methanol elimination occurs cleanly from (dpms)PtMe$(OH)_2$ complex, obtained by aerobic oxidation of (dpms)PtMe(OH_2), **2.1**, in aqueous acidic or alkaline solutions (eq. 2.16-2.17; L = dpms).[79]

$$LPt^{IV}Me(OH)_2 + H^+ + H_2O \rightarrow MeOH + LPt^{II}(OH_2)_2^+ \quad (2.16)$$

$$LPt^{IV}Me(OH)_2 + OH^- \rightarrow MeOH + LPt^{II}(OH)_2^- \quad (2.17)$$

Vedernikov[79] has earlier demonstrated that reductive elimination of methanol was preceded by isomerization of *unsym*-(dpms)PtMe$(OH)_2$, **2.4**, with Me group trans to pyridyls into a more thermodynamically stable symmetrical isomers *sym*-(dpms)PtMe$(OH)_2$, **2.11**, with methyl group trans to the sulfonate. The synthesis of the

symmetrical isomer via thermal isomerization of *unsym*-(dpms)PtMe(OH)$_2$, **2.4**, in neutral aqueous solution at 80-90 ^{o}C and its characterization was previously reported by Vedernikov.[79] The complex is stable in neutral solution, and reductive elimination of methanol from *sym*-(dpms)PtMe(OH)$_2$ (**2.11**) could be performed in either acidic or basic conditions. The platinum-containing product formed in acidic or basic solutions is a cationic complex (dpms)Pt(OH$_2$)$_2^+$, **2.12**, or an anionic dihydroxo complex (dpms)Pt(OH)$_2^-$, **2.13**, respectively.[79]

Scheme 2.16. Reductive elimination from *sym*-(dpms)PtMe(OH)$_2$ in acidic solutions.

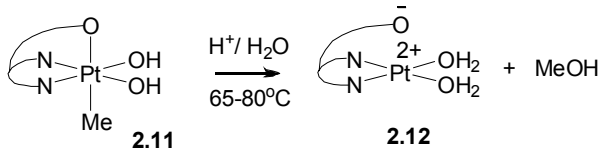

Scheme 2.17. Reductive elimination from *sym*-(dpms)PtMe(OH)$_2$ in basic solutions.

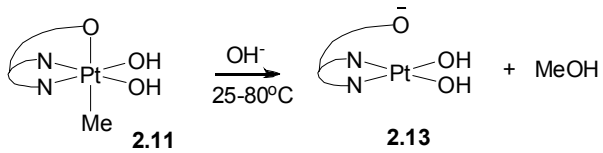

Vedernikov[79] has previously established that only symmetrical isomer **2.11** is reactive towards reductive elimination, whereas the unsymmetrical isomer **2.4** did not eliminate methanol. We assume that different reactivities of Pt^{IV}Me in **2.11** and **2.4** were determined by the quality of the leaving group *trans* to Pt^{IV}Me. Since formation of five-coordinate Pt^{IV} intermediates is viewed as a key step of the fast C(sp^3)-O elimination from the Pt^{IV} center,[64] only *sym*-LPtMe(OH)$_2$ **2.11** with Me ligand *trans* to a sulfonate, which is a good leaving group, was reactive toward reductive elimination, whereas *unsym*-LPtMe(OH)$_2$ **2.4** with Me trans to pyridyl, which is not a good leaving group, did not exhibit reactivity in reductive elimination.

Earlier kinetic studies by Vedernikov of reductive elimination of MeOH in basic solutions have shown the reaction to be 1st order in hydroxide, consistent with S_N2 attack of strongly nucleophilic OH^-.[79]

At the same time, it may be important to explore mechanisms of C-O coupling in *acidic* media that are widely used in the Shilov-type chemistry.[18, 21, 62, 72] In the case of the simplest scenario water or another suitable solvent might be the major nucleophile involved in an acid-catalyzed S_N2 – type reaction with an electrophilic substrate **2.11a** produced upon protonation of **2.11** (eq 2.18).

$$\underset{\textbf{2.11}}{LPt^{IV}Me(OH)_2} + H^+ \overset{K_1}{\rightleftharpoons} \underset{\textbf{2.11a}}{LPt^{IV}Me(OH)_2 \cdot H^+} \qquad (2.18)$$

In aqueous solutions a nucleophilic attack by water at a Pt-bound Me group of an electrophilic **2.11a** would lead to the formation of methanol (Scheme 2.18, eq 2.16):[79]

Scheme 2.18

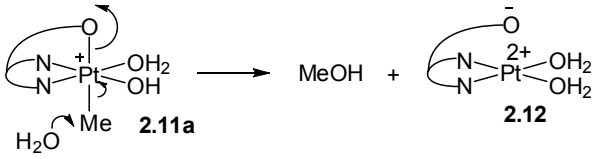

An alternative mechanism could involve a direct intramolecular C-O reductive elimination of methanol (Scheme 2.19).

Scheme 2.19

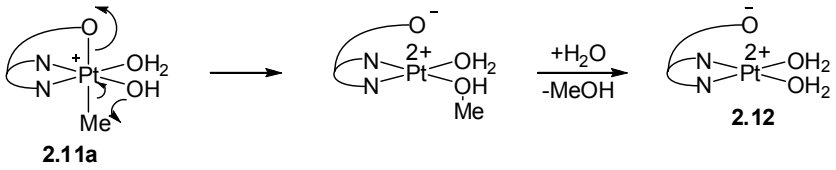

A possible way to distinguish between two mechanisms presented in Schemes 2.18 and 2.19 is by using an isotopically labeled solvent such as $H_2{}^{18}O$. The reaction in Scheme 2.18, which involves the solvent as a nucleophile, would produce an ^{18}O-

labeled methanol, $Me^{18}OH$, whereas the reaction in Scheme 2.19, which does not involve the solvent as a nucleophile, would give an unlabeled product, $Me^{16}OH$.

Remarkably, we found in this work that when reaction (2.16) was set up in a 98% enriched $H_2{}^{18}O$ two isotopologous methanols, $Me^{18}OH$ and $Me^{16}OH$, were formed in comparable amounts suggesting that at least two different mechanisms of methanol elimination were operative. In addition to methanol, noticeable amounts of dimethyl ether were found (up to 7%, depending on concentration of **2.11**) (eq. 2.19):

$$\underset{\textbf{2.11}}{2LPt^{IV}Me(OH)_2} + 2H^+ + H_2O \rightarrow Me_2O + \underset{\textbf{2.12}}{2LPt^{II}(OH_2)_2{}^+} \qquad (2.19)$$

Interestingly, reductive elimination from the product of isomerization of methoxo complex (dpms)PtMe(OMe)(OH) (**2.5)**, obtained by aerobic oxidation of (dpms)PtMe(MeOH), **2.2**, and bearing Pt-Me trans to sulfonate, leads to the formation of two products: MeOH and Me_2O in comparable amounts.

In this chapter the results of our studies of the mechanisms of C-O reductive elimination from monomethyl $(dpms)Pt^{IV}$ complexes in acidic solutions in $H_2{}^{18}O$ or $H_2{}^{16}O$ as a solvent will be discussed. Importantly, methyl Pt complexes used in this study, were obtained by aerobic oxidation of the corresponding $(dpms)Pt^{II}Me$ complexes and therefore can be considered as model compounds for aerobic functionalization of methane.

2.2.2 Results and Discussion

2.2.2.1 Synthesis of Isotopically Labeled Complexes ***2.11****-*^{18}*O and* ***2.11****-d*$_3$*.*

The method of preparation of the parent methyl dihydroxo platinum(IV) complex was reported earlier by Vedernikov.[79] The same method was applied in this work in the synthesis of isotopically labeled analogues, **2.11-^{18}O** and **2.11-*d*$_3$**.

Scheme 2.20

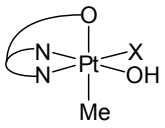

2.11 (Me = CH_3; X = OH)
2.11-^{18}O (Me = CH_3; X = ^{18}OH)
2.11-*d*$_3$ (Me = CD_3; X = OH)

The preparation of a complex (dpms)PtCH_3(^{18}OH)(OH), **2.4-**^{18}O, containing a methyl group in the equatorial position was described in the previous section. Complex **2.4-**^{18}O was then isomerized to the target **2.11-^{18}O** containing an axial methyl group and two equatorial hydroxo ligands at 90 ^{o}C in a dilute aqueous solution and isolated in 96% yield, pure according to ^{1}H NMR spectroscopy.

Scheme 2.21

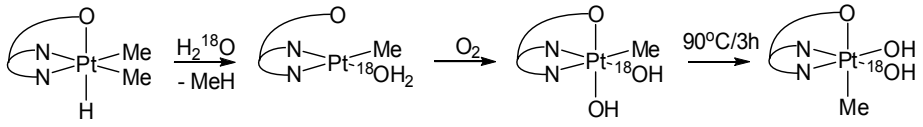

2.1-^{18}O **2.4-^{18}O** **2.11-^{18}O**

The complex **2.11-*d*$_3$** containing a deuterated methyl ligand was prepared using similar procedure (Scheme 2.22).

Scheme 2.22

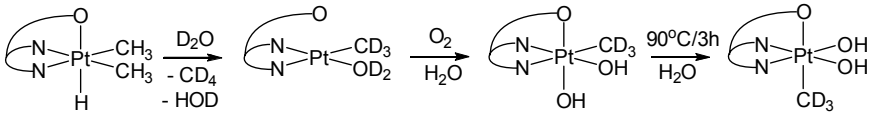

2.1-*d*$_5$ **2.4-*d*$_3$** **2.11-*d*$_3$**

The d_5-labeled aqua methyl platinum(II) complex **2.1-*d*$_5$**, $LPt^{II}CD_3(OD_2)$, was prepared in virtually quantitative yield by dissolving the dimethyl hydride (dpms)$PtMe_2H$[29] in D_2O at 40-45 ^oC (eq 2.20):

$$\underset{}{LPt^{IV}(CH_3)_2H} + 8D_2O \rightarrow CD_4 + \underset{\textbf{2.1-}\boldsymbol{d}_5}{LPt^{II}CD_3(OD_2)} + 7HOD \qquad (2.20)$$

An aerobic oxidation of the resulting **2.1-*d*$_5$** was performed in regular water to produce cleanly, the *unsym*-(dpms)$Pt(CD_3)(OH)_2$. **2.4-*d*$_3$**, according to ^1H NMR spectroscopy, (eq 2.21):

$$\underset{\textbf{2.1-}\boldsymbol{d}_3}{2LPt^{II}CD_3(OH_2)} + O_2 \rightarrow 2\ \underset{\textbf{2.4-}\boldsymbol{d}_3}{\textit{unsym}\text{-}LPt^{IV}CD_3(OH)_2} \qquad (2.21)$$

The target complex **2.11-*d*$_3$**, containing CD_3 group in the axial position, *trans* to the sulfonate group, was obtained by thermal isomerization at 90 ^oC and isolated in 87% yield, pure according to ^1H NMR spectroscopy.

*2.2.2.2 Acidity of Complexes **2.12** and **2.11a**.*

The platinum-containig product of the reductive elimination was identified as a cationic diaqua complex (dpms)$Pt(OH_2)_2^+$, **2.12**.[79] In order to establish the position of equilibrium (23) under the reaction conditions employed in reductive elimination of MeOH, we determined the pK'_{a1} of **2.12**. To estimate pK'_{a1}, solutions of $LPt^{II}(OH_2)_2(NO_3)$ were prepared by protonolysis of a $K[(L)Pt^{II}Me_2]$[29] with an excess of standardized solution of HNO_3. The pK'_{a1} of $LPt^{II}(OH_2)_2^+$ determined by potentiometric titration, was found to be 4.76±0.07. Therefore, at $[H^+] \sim 0.1$ M, typically used in this work, most part of Pt^{II} should be present in the form of diaqua complex **2.12**.

$$\underset{\textbf{2.12}}{LPt^{II}(OH_2)_2^+} \overset{K'_{a1}}{\rightleftharpoons} \underset{\textbf{2.12a}}{LPt^{II}(OH)(OH_2)} + H^+ \qquad (2.22)$$

Although reactivity under acidic conditions and low basicity of **2.11** did not allow for direct potentiometric determination of the equilibrium constant K_1, the available estimate of the protonation constant[79] of the dimethyl hydroxo complex, *sym*-$LPt^{IV}Me_2(OH)$, a *di*methyl analogue of **2.11**, was found to be $K \sim 46\pm5$ at 97 °C in water.[79] Assuming that *sym*-$LPt^{IV}Me_2(OH)$ is more basic than *sym*-$LPt^{IV}Me(OH)_2$, we can estimate $K_1 < 46$. Therefore, at $[H^+]$ = 60-120 mM, typically used in this work, equilibrium concentrations of **2.11** and **2.11a** are expected to be of the same order of magnitude.

2.2.2.3 Isotopic Labeling Experiments.

i) Reaction of Complexes 2.11 and 2.11-d_3 with $H_2{}^{18}O$; Reaction of 2.11-^{18}O with $H_2{}^{16}O$. A reaction between 38 mM **2.11** and 63 mM HBF_4 in 98% enriched $H_2{}^{18}O$ at 80 °C resulted in the formation of two isotopologous alcohols, $Me^{18}OH$ (eq. 2.23) and $Me^{16}OH$ (eq 2.24):

$$\underset{\textbf{2.11}}{LPt^{IV}Me(^{16}OH)_2} + H^+ + 3H_2{}^{18}O \rightarrow \underset{\textbf{2.12-}^{18}\textbf{O}_2}{LPt^{II}(^{18}OH_2)_2^+} + Me^{18}OH + 2H_2{}^{16}O \qquad (2.23)$$

$$\underset{\textbf{2.11}}{LPt^{IV}Me(^{16}OH)_2} + H^+ + 2H_2{}^{18}O \rightarrow \underset{\textbf{2.12-}^{18}\textbf{O}_2}{LPt^{II}(^{18}OH_2)_2^+} + Me^{16}OH + H_2{}^{16}O \qquad (2.24)$$

The ratio of the major products, $Me^{18}OH/Me^{16}OH$, as established by ESI mass spectrometry, was 1.7/1 in the beginning of the reaction (12 min, 13% conversion of **2.11**; see Table 2.2) and steadily increased over time reaching 2.4/1 when the reaction was almost complete (70 min, 95% conversion).

Table 2.2. The ratio of isotopologous alcohols, $CH_3{}^{18}OH/CH_3{}^{16}OH$, established by ESI mass-spectrometry as a function of reaction time; 63 mM HBF_4 and 38 mM **2.11** in 98% enriched $H_2{}^{18}O$ at 80 °C.

Time, min	12	25	40	70
$CH_3{}^{18}OH/CH_3{}^{16}OH$	1.7	2.1	2.4	2.4

For further experiments a partially deuterated complex $LPt(CD_3)(OH)_2$ (**2.11-*d*$_3$**) and 120 mM HBF_4 in $H_2{}^{18}O$ were used since the ratio of isotopologous $CD_3{}^{18}OH_2{}^+$ and $CD_3{}^{16}OH_2{}^+$ can be determined more accurately by ESI technique than $CH_3{}^{18}OH_2{}^+/CH_3{}^{16}OH_2{}^+$ due to the presence of adventitious O_2H^+ peak overlapping with $CH_3{}^{16}OH_2{}^+$ signal. Concentration of **2.11-*d*$_3$** was varied from 29 to 120 mM. Peaks derived from isotopologous methanols, $CD_3OH_2{}^+$ with m/z = 36.05256 $CD_3{}^{16}OH_2{}^+$ and $CD_3{}^{18}OH_2{}^+$ with m/z = 38.05686 did not interfere with a peak of adventitious O_2H^+ (calc m/z = 32.99765), so that the ratio of the alcohols could be determined more reliably compared to analogous non-deuterated isotopologous species CH_3X (X = ^{16}OH and ^{18}OH).

Interestingly, the ratio of isotopologous methanols was found to be a function of the concentration of the (dpms)$Pt^{IV}Me$ complex. The ratio of isotopologous methanols, $CD_3{}^{18}OH/CD_3{}^{16}OH$, formed by reductive eliminatin from **2.11-*d*$_3$**, measured at low conversions of **2.11-*d*$_3$** (~10%) is given in Table 2.3. The fraction of $Me^{16}OH$ increases as **2.11-*d*$_3$** concentration increases: the $CD_3{}^{18}OH/CD_3{}^{16}OH$ ratio measured decreased approximately linearly with 1/[Pt], so that the product $[Pt]\cdot(CD_3{}^{18}OH/CD_3{}^{16}OH)$ remained approximately constant, 130±10.

Table 2.3. The $CD_3{}^{18}OH/CD_3{}^{16}OH$ ratio at the early stages of reaction between **2.11-*d*$_3$** and 120 mM [HBF_4] in $H_2{}^{18}O$ solution at 80 °C, as established by ESI mass-spectrometry at various concentration of complex **2.11-*d*$_3$**.

[Pt], mM	29	39	60	120
$CD_3{}^{18}OH/CD_3{}^{16}OH$	4.8	2.7	2.2	1.2
[Pt]·($CD_3{}^{18}OH/CD_3{}^{16}OH$)	140	110	130	140

Formation of two isotopologous methanols in these reactions suggests that at least two different mechanisms of methanol elimination are operative here. While the heavier isotopologue, $Me^{18}OH$, could result from an S_N2 attack of $H_2{}^{18}O$ at the carbon of Pt^{IV}-Me of electrophilic complex **2.11a**,[79] (Scheme 2.18), the unlabeled, ^{16}O-methanol formed in a coupling reaction not involving solvent as a nucleophile.

To further confirm our observations, a 26 mM solution of ^{18}O-labeled complex **2.11-^{18}O**, $LPt^{IV}Me(^{18}OH)(OH)$ in $H_2{}^{16}O$ as a solvent, was reacted with a 63 mM HBF_4 in $H_2{}^{16}O$ at 80 °C. Formation of the 17/83 mixture of the ^{18}O-labeled and a non-labeled methanol was observed at ~83% conversion of **2.11-^{18}O**.

$$\underset{\textbf{2.11-}^{18}\textbf{O}}{LPt^{IV}Me(^{16}OH)(^{18}OH)} + H^+ + H_2{}^{16}O \rightarrow \underset{\textbf{2.12}}{LPt^{II}(^{16}OH_2)_2{}^+} + Me^{18}OH \qquad (2.25)$$

Similarly, the ^{18}O-labeled methanol, $Me^{18}OH$, could not form via an external S_N2 attack of the solvent, $H_2{}^{16}O$, at **2.11-^{18}O**.

Therefore, in both reactions a noticeable fraction of an appropriate isotopologous methanol formed, which did not incorporate oxygen from the solvent.

ii) An Attempted $^{16}O/^{18}O$ Exchange between CH_3OH and $H_2{}^{18}O$, an $^{16}O/^{18}O$ Exchange between 2.11 and $H_2{}^{18}O$, and an Attempted Pt^{IV}-to-Pt^{II} Methyl Group Transfer.

As mentioned in the previous section, the ratio of methanol isotopologues was not constant over time during the course of the reaction. In order to analyze what factors might be responsible for this observation, we decided to study stability of the reaction product, $Me^{16}OH$, and the starting material, **2.11**, toward isotopic exchange in $H_2{}^{18}O$. In particular, the following possibilities were considered: (i) the $^{16}O/^{18}O$ exchange between the reaction product, $Me^{16}OH$, and bulk $H_2{}^{18}O$ (eq. 2.26); (ii) acid-catalyzed $^{16}O/^{18}O$ exchange between complex **2.11** and $H_2{}^{18}O$, leading to **2.11-^{18}O** and **2.11-$^{18}O_2$** (Scheme 2.23, eq. 2.28-2.29), and (iii) a methyl group transfer between an electrophilic $MePt^{IV}$ complex **2.11a** and a potentially nucleophilic Pt^{II} complex **2.12a-$^{18}O_2$** leading to **2.12** and **2.11a-$^{18}O_2$** (eq. 2.29), similar to the Pt^{IV}/Pt^{II} methyl exchange reactions reported by Puddephatt.[80, 81]

$$Me^{16}OH + H_2{}^{18}O \rightarrow Me^{18}OH + H_2{}^{16}O \qquad (2.26)$$

Scheme 2.23. Acid-catalyzed $^{16}O/^{18}O$ exchange in **2.11**

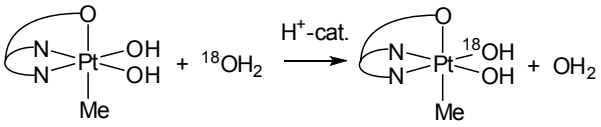

(2.27)

2.11 **2.11-^{18}O**

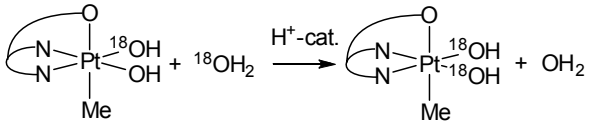

(2.28)

2.11-^{18}O **2.11-$^{18}O_2$**

Scheme 2.24. Pt^{IV}/Pt^{II} methyl exchange

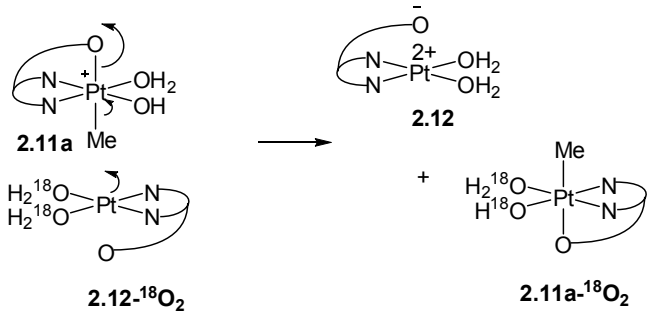

(2.29)

According to ESI mass-spectrometry, no $^{16}O/^{18}O$ exchange between 44 mM $CH_3{}^{16}OH$ and 60 mM HBF_4 in $H_2{}^{18}O$ (eq. 2.26) occurred after 3 hours at 80 ^oC.

In contrast, ESI-MS monitoring of 38 mM solution of **2.11** and 63 mM HBF_4 in $H_2{}^{18}O$ showed that a slow $^{16}O/^{18}O$ exchange took place at 80 ^oC and both **2.11-^{18}O** (eq. 2.27) and **2.11-$^{18}O_2$** (eq. 2.28) formed (Scheme 2.23, Fig. 2.9). At a 75% conversion of $LPt^{IV}Me(OH)_2$, *ca* 40% of complex **2.11** contained either one or two ^{18}O-labels. Isotopologues with more than two ^{18}O labels were not detected. Therefore, acid-catalyzed exchange of hydroxo ligand of **2.11** with a solvent (eq. 2.27-2.28) might be responsible for the increase of $Me^{18}OH/Me^{16}OH$ ratio over time (Table 2.2).

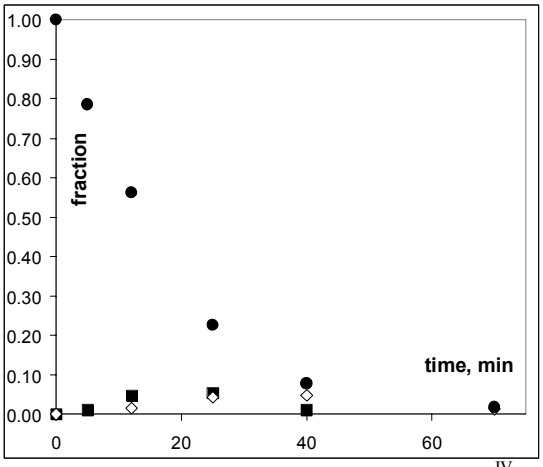

Figure 2.9. Relative concentrations of isotopologous complexes $LPt^{IV}Me(^{18}OH)_n(^{16}OH)_{2-n}$, n = 0 (filled circles), 1 (filled squares), 2 (empty rhombs), given as a fraction of the initial concentration of complex **2.11** (38 mM), determined by ESI-MS as a function of the reaction time at 80 ^oC and $[H^+]$=63 mM.

Importantly, even up to 75% conversion of **2.11**, the fraction of the mono-labeled isotopologue **2.11-^{18}O** exceeded that of the doubly labeled **1-$^{18}O_2$**. In contrast to slow exchange in Pt^{IV} complex **2.11**, the exchange of aqua ligands in Pt^{II} complex **2.12** is fast even at room temperature, and **2.12-$^{18}O_2$** was the only aqua platinum(II) complex present in $H_2{}^{18}O$ solutions, according to ESI-MS. Therefore, if reaction (2.29) was competitive to reactions (2.27-2.28), this would lead to the greater fraction of the doubly labeled **1-$^{18}O_2$**, resulting from Me group transfer to **2.12-$^{18}O_2$** complex, than the fraction of mono-labeled **1-^{18}O**, Since this is not observed experimentally, we can conclude that the doubly labeled **1-$^{18}O_2$**, forms predominantly via stepwise hydrolysis (eq. 2.27-2.28), rather than Me-group transfer (eq. 2.29). Additional evidence against the Pt^{IV}-to-Pt^{II} methyl group transfer, based on the analysis of the isotopologous methanols ratio in experiments between **2.11-*d*$_3$** and **2.12-$^{18}O_2$**, will be discussed below.

Therefore, to eliminate the effect of reactions 2.27-2.28 on the observed $Me^{18}OH/Me^{16}OH$ ratio in a maximum possible extent, the ratio should be measured at early stages of reaction when conversion of complex **2.11** is low.

*2.2.2.4 Plausible Mechanisms of Reaction between **2.11** and H_2O in Acidic Solutions.*

The following mechanisms were considered in order to explain formation of isotopologous methanols.

(i) The S_N2 reaction of non-labeled $LPtMe(OH)_2$ with $H_2{}^{18}O$ used as a solvent could lead to the formation of labeled $Me^{18}OH$ (reaction 2.30, Scheme 2.25).

Scheme 2.25

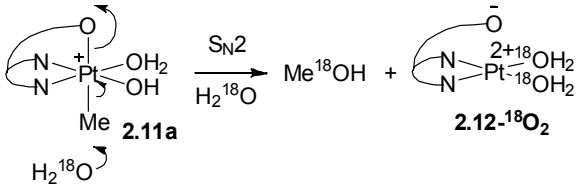

The reaction is very slow in neutral aqueous solutions but is accelerated in the presence of acid, due to the formation of more electrophilic cationic $LPtMe(OH)(OH_2)^+$ (eq. 2.18). Our observations of labeled methanol formation in reaction of **2.11-*d*$_3$** in $H_2{}^{18}O$ are consistent with this mechanism.

The following two possible reaction scenarios were proposed to explain formation of the non-labeled methanol in reactions of **2.11** in $H_2{}^{18}O$:

(ii) An *intramolecular* Me-OH elimination could lead to the formation of $Me^{16}OH$ (reaction 2.31, Scheme 2.26).

Scheme 2.26

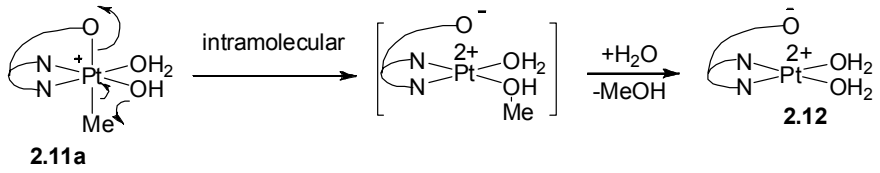

The mechanism for the CH_3-O elimination from Pt^{IV} reported in Scheme 2.26 is unprecedented in the literature. Accordingly, the DFT calculated reaction barrier of the reductive elimination via a direct intramolecular mechanism is very high, 37.2 kcal/mol. Notably, no reductive elimination of methanol was observed upon heating complex **2.11** in other solvents such as DMSO, or in dilute *neutral* aqueous solutions, providing another argument against the direct reductive elimination mechanism.

(iii) We also suggested that in acidic reaction mixture a hydroxo ligand of $LPtMe(OH)_2$ can be more nucleophilic than water, and proposed an *intermolecular* nucleophilic pathway shown in Scheme 2.27.

Scheme 2.27

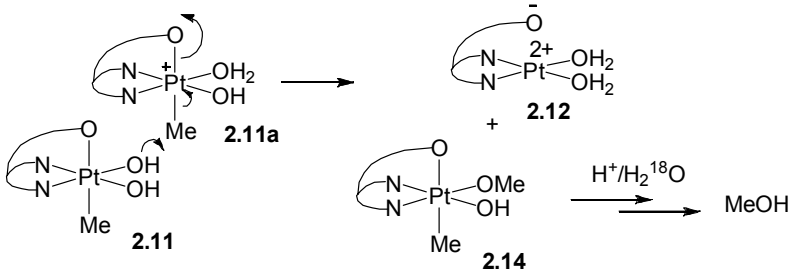

In the case of the mechanism (iii) **2.11a** could serve as an electrophilic component whereas one of the hydroxo ligands of a non-protonated **2.11** could play the role of a nucleophile, reacting via an S_N2 mechanism to produce an intermediate methoxo complex **2.14** that subsequently reacts to produce non-labeled methanol (for example, via acid-catalyzed hydrolysis of the methoxo ligand in **2.14**, eq. 2.30).

$$\underset{\textbf{2.14}}{LPt^{IV}Me(OH)(OMe)} + H_2{}^{18}O \rightarrow \underset{\textbf{2.11-}^{\textbf{18}}\textbf{O}}{LPt^{IV}Me(OH)(^{18}OH)} + MeOH \qquad (2.30)$$

The nucleophilic reactivity of late transition metal hydroxides or alkoxides has literature precedents.[82] For example, Hartwig established that hydroxo ligands of the complex $[Ir^{III}(CO)(OH)(I)(Me)(L)_2]$ (L = PPh_3) is easily methylated by reacting $[Ir^{III}(CO)(OH)(I)(Me)(PPh_3)_2]$ with CD_3I to give free CD_3OH (Scheme 2.14).[76] Bergman[83] suggested that a nucleophilic attack by the hydroxo ligand of $(Cp^*)Ir^{III}(PPh_3)(OH)(Ph)$ on a double bond of a coordinated ethylene of $[(Cp^*)Ir^{III}(PMe_3)(Ph)(CH_2{=}CH_2)]^+$ was responsible for the formal ethylene insertion into Ir^{III}-OH bond to give $(Cp^*)Ir^{III}(PMe_3)(Ph)(CH_2CH_2OH)$.

While pathway (i) is a plausible explanation of formation of $Me^{18}OH$, the pathways (ii) and (iii) of $Me^{16}OH$ elimination should be considered in more detail in order to distinguish between these mechanisms. The analysis of the reaction orders in complex **2.11** might help to elucidate the mechanistic pathway.

Mechanisms (i) and (ii) are both expected to be the 1st order in **2.11**. Therefore, if reductive elimination of methanol occurred via pathways (i) and (ii) predominantly, the ratio of isotopologues would be independent of the concentration of **2.11**, since both patways (i) and (ii) have the same order in **2.11**. In contrast, our observations show that this is not the case, and the ratio of isotopologous methanols observed in the initial period of reaction, when acid-catalyzed $^{16}O/^{18}O$ in complex **2.11** can be neglected, was found to be inversely proportional to the initial concentration of **2.11**.

If, however, non-labeled $Me^{16}OH$ forms in a bimolecular reaction (iii), which is 2nd order in complex **2.11**, one should also expect that the ratio of MeOH isotopologues must be a function of the initial concentration of **2.11**. In other words, since the formation of $Me^{16}OH$ is 2nd order in Pt, whereas the formation of $Me^{18}OH$ via mechanism (i) is 1st order in Pt, the contribution from the 2nd order reaction can be increased by the increasing the initial concentration of the reagent.[84] We have experimentally observed a linear dependence of the ratio of isotopologous $CD_3{}^{16}OH/CD_3{}^{18}OH$ upon the concentration of complex **2.11-*d*$_3$**. Considering that the pathway (i) is expected to be 1st order in **2.11**, this result implies that the formation of the unlabeled methanol follows 2nd order in complex **2.11,** consistent with mechanism (iii).

Therefore, pathways (i) and (iii) allow to account for the formation of $Me^{16}OH$ and $Me^{18}OH$ in $H_2{}^{18}O$ solutions of **2.11** and are consistent with the observed dependence of $CD_3{}^{16}OH/CD_3{}^{18}OH$ on the concentration of **2.11-*d*$_3$**.

Though the results obtained strongly support the viability of the intermolecular path (iii) of the C-O coupling of complex **2.11** (Scheme 2.27), the precision of data presented in Table 2.3 does not allow us to completely rule out a possible minor (few percent) contribution arising from the intramolecular mechanism (ii) to the C-O elimination from **2.11** (Scheme 2.26).

The viability of mechanism (iii) was further confirmed by kinetic studies and characterization of reaction intermediates, discussed in the following sections.

2.2.2.5 Synthesis and Reactivity of Methoxo Complexes LPtMe(OMe)(OH), ***2.14****, and LPtMe(OMe)$_2$,* ***2.15***

i) Synthesis and Reactivity of 2.14. The mechanism (iii) involves the formation of intermediate complex **2.14**; therefore, detection of this intermediate in the reaction mixtures could prove or disprove the viability of the pathway (iii). The NMR and ESI analysis of acidic reaction mixtures of reductive elimination from concentrated solutions of **2.11** allowed us to detect several new Pt-Me species which formed at the beginning of reaction, whose fraction reached maximum in 15-25 minutes and which eventually disappeared by the end of the reaction. Identification and characterization of these intermediates will be discussed below.

Indeed, one of the reaction intermediates was further identified as LPtMe(OMe)(OH), **2.14,** based on its spectral characteristics and independent synthesis.

The independent synthesis of LPtMe(OMe)(OH) (**2.14**) was achieved through thermal isomerization of LPtMe(OMe)(OH), **2.5**, obtained by oxidation of (dpms)PtMe(MeOH) (**2.2**) with O_2. The complex was isolated in 66% yield in an analytically pure form and characterized by NMR spectroscopy, ESI mass spectrometry, elemental analysis and single crystal X-ray diffraction.

Scheme 2.28

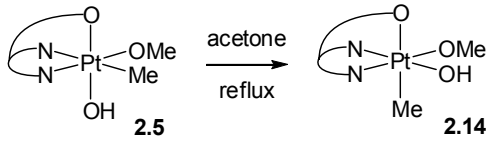

2.5 **2.14**

Complexes **2.5** and **2.14** were found to be hydrolytically unstable even in neutral aqueous solution: slow formation of methanol and **2.11** was observed in aqueous solution already at room temperature (eq. 2.31).

$$\underset{\textbf{2.14}}{LPt^{IV}Me(OH)(OMe)} + H_2O \rightarrow \underset{\textbf{2.11}}{LPt^{IV}Me(OH)(OH)} + MeOH \qquad (2.31)$$

X-Ray quality crystals of the salt $\mathbf{2.14}_2 \cdot HBF_4$ were produced by layering saturated methanolic solution of **2.14** containing 0.5 equivalent of HBF_4 with an equal volume of benzene (Fig. 2.10).

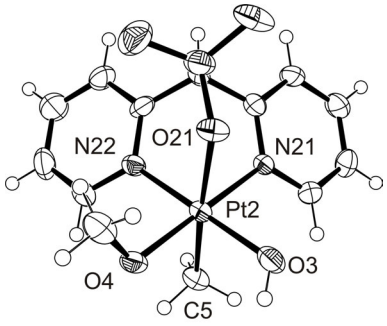

Figure 2.10. ORTEP drawings of complex **2.14** present in $\mathbf{2.14_2 \cdot HBF_4}$, 50% probability ellipsoids. Selected bond distances, Å, and angles, °, for moiety **2.14** in $\mathbf{2.14_2 \cdot HBF_4}$: Pt2-O3, 1.982(5); Pt2-O4, 1.990(4); Pt2-O21, 2.220(5); Pt2-N21, 2.040(5); Pt2-N22, 2.020(5); Pt2-C5, 2.025(7); O21-Pt2-N22, 91.8(2); O21-Pt2-N21, 84.56(19); O21-Pt2-O4, 96.17(18); O21-Pt2-O3, 87.6(2); N21-Pt2-N22, 90.0(2); N21-Pt2-O3, 90.3(2); N22-Pt2-O4, 90.1(2); O21-Pt2-C5, 176.5(2).

However an alternative path of formation of the methoxo complex can be suggested. The fast exchange between MeOH, the product of C-O elimination, and hydroxo ligands of $LPtMe(OH)_2$ in the acidic solutions could also lead to the formation of methoxo complex (eq. 2.32).

$$\underset{\textbf{2.11}}{LPt^{IV}Me(OH)_2} + MeOH \rightarrow \underset{\textbf{2.14}}{LPt^{IV}Me(OH)(OMe)} + H_2O \qquad (2.32)$$

In order to check if free MeOH can react with $LPtMe(OH)_2$ (**2.11**) in the acidic solutions to form LPtMe(OMe)(OH) (**2.14**), an experiment was set up in the presence of a more than 5 fold excess of MeOH that significantly exceeded the maximum concentration of MeOH that could be produced in our reaction mixtures. The kinetics of formation of LPtMe(OMe)(OH) (**2.14**) and disappearance of $LPtMe(OH)_2$ (**2.11**) in acidic solutions were monitored and compared to the control experiment without MeOH additive. Neither fraction of LPtMe(OMe)(OH) (less than 4.5% both in the presence and in the absence of MeOH additive; Fig. 2.11), nor the rate of disappearance of $LPtMe(OH)_2$, changed in the presence of extra MeOH as compared to the control mixture. The rate of disappearance of **2.11** of $(4.55\pm0.23)\cdot10^{-4}$ s^{-1} in the presence of added MeOH was virtually the same as in the absence of methanol additives $(4.60\pm0.15)\cdot10^{-4}$ s^{-1}. We can therefore conclude that free MeOH is not involved in the formation of LPtMe(OMe)(OH) (**2.14**), and complex **2.14** was a reaction intermediate and not a secondary product of the OH/MeO ligand exchange in **2.11**.

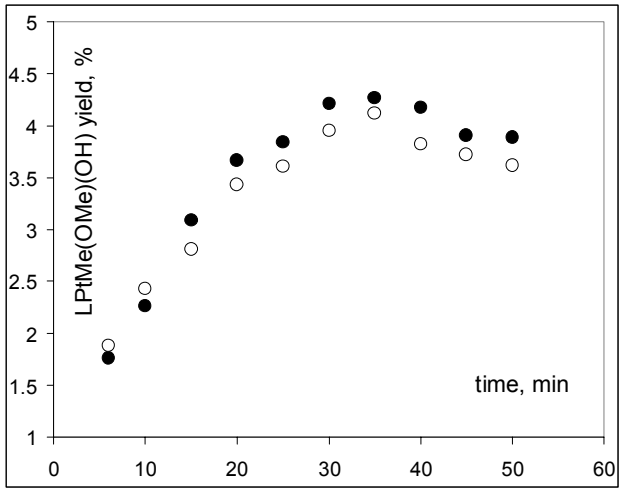

Figure 2.11. Formation of intermediate **2.14** in 8.8 mM solution of **2.11** in D_2O in the absence (filled circles) and in the presence of 50 mM of MeOH (empty circles) at 80 °C; $[HBF_4]$ = 60 mM.

Importantly, according to ESI, the intermediate LPtMe(OMe)(OH) formed in a $H_2{}^{18}O$ reaction mixture, was identified as an unlabeled complex LPtMe(^{16}OMe)(^{16}OH); no peaks of comparable intensity were observed that could correspond to ^{18}O-isotopologues such as LPt^{IV}Me(OMe)(^{18}OH)*H^+ up to at least 80% conversion of **2.11**. Formation of the unlabeled methanol Me^{16}OH from LPtMe(^{16}OMe)(^{16}OH) could be then explained by the subsequent acid-catalysed hydrolysis of the methoxo-ligand in **2.14**. However, one might envision that two possible pathways of hydrolysis of the methoxo ligand leading to two different products: if Pt^{IV}-^{16}OMe bond cleavage occurs, formation of Me^{16}OH is expected (eq. 2.30). Alternatively, if Pt^{16}O-Me bond is cleaved by $H_2{}^{18}O$, this would lead to the formation of Me^{18}OH (eq. 2.33).

$$\underset{\textbf{2.14}}{LPt^{IV}Me(OH)(OMe)} + H_2{}^{18}O \rightarrow \underset{\textbf{2.11}}{LPt^{IV}Me(OH)_2} + Me^{18}OH \qquad (2.33)$$

In order to establish whether the Pt^{IV}-OMe or the Pt^{IV}O-Me bond is cleaved by water, an experiment was set up with an isomeric methoxo hydroxo methylplatinum(IV) complex **2.5** and acidified $H_2{}^{18}O$. Isomeric complex **2.5** was used in place of **2.14**, since **2.5**, similar to **2.14**, undergoes hydrolysis of the MeO ligand;

however, unlike **2.14**, it is stable toward methanol formation via reductive elimination, which in the case of **2.4** would compete with hydrolysis and affect isotopic composition of MeOH.

According to ESI-MS, a room temperature hydrolysis of methoxo complex **2.5** in 129 mM HBF_4 in $H_2{}^{18}O$ solution showed clean formation of *unsym*-LPtMe(OH)(^{18}OH) **2.4-^{18}O** and Me^{16}OH exclusively (23% conversion of **2.5** after 3.5 days, eq. 2.30). No Me^{18}OH isotopologue was found in the reaction mixture. Therefore, hydrolysis of **2.14**, formed via mechanism (iii), could produce unlabeled methanol in the solutions of **2.11** in $H_2{}^{18}O$.

ii) Formation of Dimethyl Ether and Dimethoxo Complex 2.15. In addition, if pathway (iii) is viable, one might expect that methoxo complex **2.14**, although present in relatively low concentrations, could be involved in further bimolecular reactions with **2.11**. In this case formation of other two products could be envisioned: dimethyl ether, resulting from the methylation of the methoxo ligand in **2.14** by electrophilic **2.11a** (Scheme 2.29), and the dimethoxy complex LPtMe(OMe)$_2$ (**2.15**), which could result from the methylation of the hydroxo ligand of **2.14** by complex **2.11a** (Scheme 2.30).

Scheme 2.29

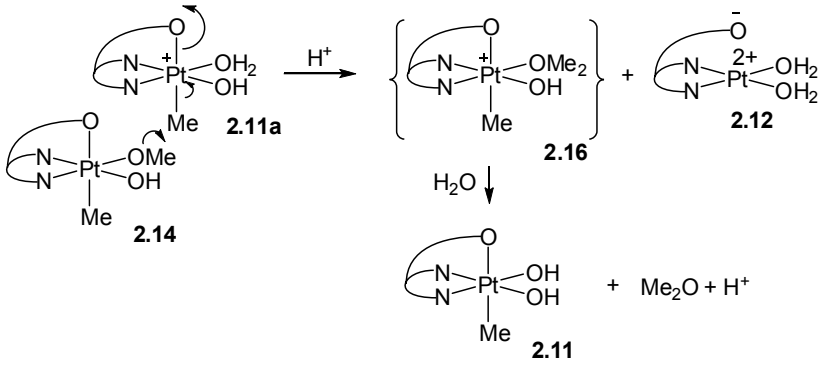

Scheme 2.30

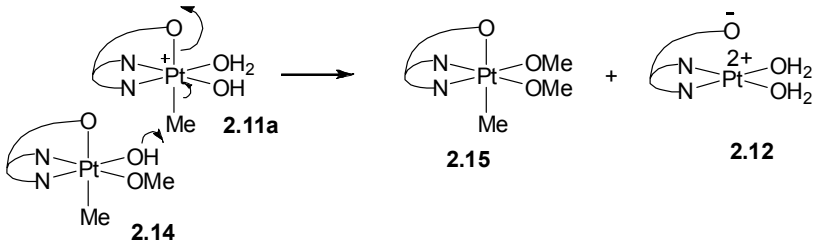

Remarkably, formation of small amounts of dimethyl ether (up to 7% yield) was confirmed by ^{1}H NMR spectroscopy and ESI mass spectrometry in concentrated acidic solutions of **2.11**. The formation of the dimethyl ether could involve hydrolysis cationic dimethyl ether Pt^{IV} intermediates such as **2.16**. Complex **2.16** was not detected by ^{1}H NMR spectroscopy presumably because of its high reactivity and low concentration; ESI mass spectrometry could not be used for detection of **2.16**, since it would give the same signal as **2.15**.

The identity of *sym*-(dpms)PtMe(OMe)$_2$ (**2.15**) as one of the intermediates observed by ^{1}H NMR spectroscopy and ESI-MS in small amounts in acidic reaction mixtures containing **2.11** was confirmed by its independent synthesis (Scheme 2.31) and characterization.

Scheme 2.31

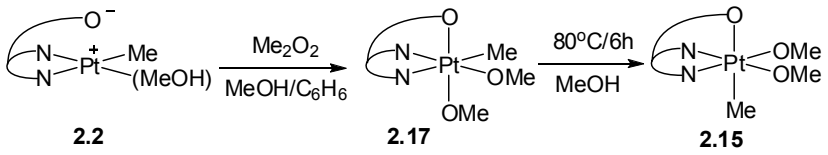

The unsymmetrical isomer of dimethoxo complex *unsym*-(dpms)PtMe(OMe)$_2$, **2.17**, was prepared by oxidation of (dpms)PtMe(MeOH) by dimethyl peroxide in methanol/benzene solution.

$$\underset{\textbf{2.2}}{LPt^{II}Me(MeOH)} + Me_2O_2 \rightarrow \underset{\textbf{2.17}}{LPt^{IV}Me(OMe)_2} + MeOH \qquad (2.34)$$

The resulting *unsym*-(dpms)PtMe(OMe)$_2$ (**2.17**) was characterized by ^{1}H and ^{13}C NMR spectroscopy and used for thermal isomerization to *sym*-(dpms)PtMe(OMe)$_2$ (**2.15**) in methanol solution without isolation. The thermal isomerization of *unsym*-(dpms)PtMe(OMe)$_2$ to *sym*-(dpms)PtMe(OMe)$_2$ was achieved by heating a solution of **2.17** in methanol at 80 ^{o}C for 6h. The isolated yield of an analytically pure complex **2.15** was 46%.

Therefore, formation of dimethyl ether and dimethoxo complex *sym*-(dpms)PtMe(OMe)$_2$ further confirms the viability of bimolecular reactions involving Pt-OH or Pt-OMe as nucleophiles and another Pt^{IV}-Me species (in a protonated form) acting as an electrophile.

*2.2.2.6 Synthesis of Dinuclear Heterovalent Isomeric Complexes $LPt^{IV}Me(\mu\text{-}OH)_2Pt^{II}L$, cis- and trans-**2.18**.*

We decided to check whether any of the reaction products are involved in certain secondary transformations. As confirmed by a previous experiment, MeOH did not affect reaction kinetics. In order to check whether $LPt^{II}(OH_2)_2^+$ (**2.12**) participates in secondary transformations involving LPtMe(OH)$_2$ (**2.11**), the equimolar amount of $LPt(OH_2)_2^+$ was added to a reaction mixture containing acidic aqueous solution of LPtMe(OH)$_2$ and the kinetics of the reaction were compared to the control. Interestingly, in the presence of $LPt(OH_2)_2^+$ additive, rapid consumption of LPtMe(OH)$_2$ (**2.11**) was observed during the first 5 minutes, after which the reaction followed first order kinetics, albeit the rate was faster than in the absence of added $LPt(OH_2)_2^+$ (Fig. 2.12). The plot of $\ln(C_0/C)$ versus time was practically linear after 5 min (Fig. 2.12, upper line) with the observed pseudo-first order rate constant $k_{obs} = (5.82\pm0.30)\cdot10^{-4}$ s^{-1}. In the control experiment

in the absence of added (dpms)Pt$(OH_2)_2^+$ (**2.12**) the disappearance of **2.11** followed clean first-order kinetics during the entire reaction period with the observed rate constant $k_{obs} = (4.53\pm0.05)\cdot10^{-4}$ s^{-1} (Fig. 2.12, lower line).

Moreover, formation of MeOH was also accelerated in the presence of LPt$(OH_2)_2^+$ (**2.12**) (Fig. 2.13). The formation of MeOH followed 1st order kinetics during the whole reaction period; pseudo-1st order observed rate constants of formation of MeOH (eq. 2.35) were found to be $k_{obs,\ MeOH} = (2.74\pm0.09)\cdot10^{-4}$ s^{-1} in the absence of LPt$(OH_2)_2^+$ additive ([**2.11**]=7.5 mM; $[H^+]$=60 mM) and $(3.70\pm0.27)\cdot10^{-4}$ s^{-1} in the mixture of **2.11** and **2.12** ([**2.11**]=7.6 mM; [**2.12**]=7.5 mM; $[H^+]$=60 mM).

$$\frac{d[MeOH]}{dt} = k_{obs,MeOH}[Pt^{IV}] \qquad (2.35)$$

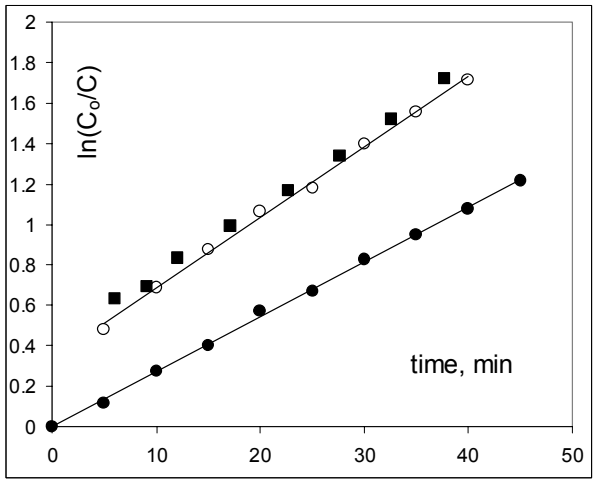

Figure 2.12. First-order kinetic plot of: i) a reaction of 7.5 mM **2.11** in D_2O (filled circles), ii) a reaction of 7.6 mM **2.11** in D_2O in the presence of 7.5 mM **2.12** (empty circles); iii) a reaction of 7.4 mM **2.18** in D_2O (filled squares). In all experiments $[HBF_4]$=60 mM and temperature is 80 °C. C_0 is initial concentration of **2.11** measured before addition of **2.12** (experiment i or ii) or initial concentration of **1** expected as a result of complete dissociation of **2.18** used instead of **2.11** and **2.12** in experiment iii. *C* is current concentration of **2.11** as determined by ^1H NMR integration of PtMe signal of **2.11**.

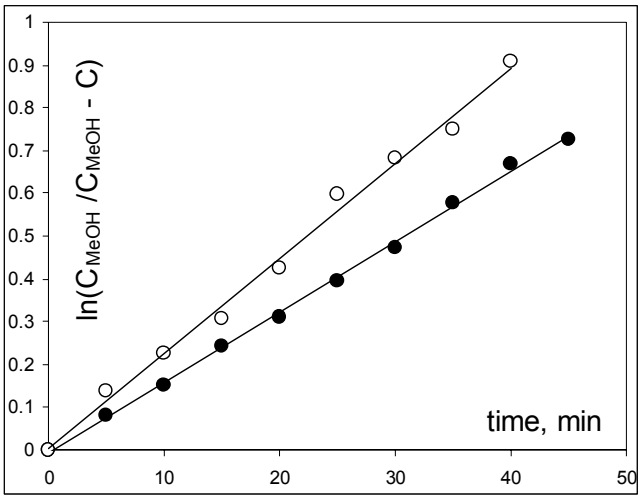

Figure 2.13. Kinetic plot of formation of methanol in a reaction between 7.5 mM solution of **2.11** and D_2O (filled circles) and a reaction between 7.6 mM solution of **2.11** and D_2O in the presence of 7.5 mM **2.12** (empty circles); $[HBF_4]$=60 mM and 80 ^oC; C_{MeOH} and C are the final and current concentrations of MeOH.

ESI analysis of reaction mixtures containing $LPtMe(OH)_2$ and $LPt(OH_2)_2^+$ allowed us to detect new species (**2.18**) with m/z 937.02124, which was identified as a dinuclear cationic heterovalent $[LPt^{IV}Me(\mu\text{-}OH)_2Pt^{II}L]^+BF_4^-$ (**2.18**) complex (eq. 2.36).

$$\underset{\textbf{2.11}}{LPt^{IV}Me(OH)_2} + \underset{\textbf{2.12}}{LPt^{II}(OH_2)_2^+} \rightleftharpoons \underset{\textit{cis}\text{- and }\textit{trans}\text{-}\textbf{2.18}}{LPt^{IV}Me(\mu\text{-}OH)_2Pt^{II}L^+} + 2H_2O \qquad (2.36)$$

This new species crystallized slowly upon cooling from highly acidic reaction mixtures; it was isolated as a mixture of two isomers, *cis*- and *trans*-, and characterized by NMR spectroscopy and ESI mass spectrometry. The predominant isomer was also characterized by X-ray diffraction.

Scheme 2.32

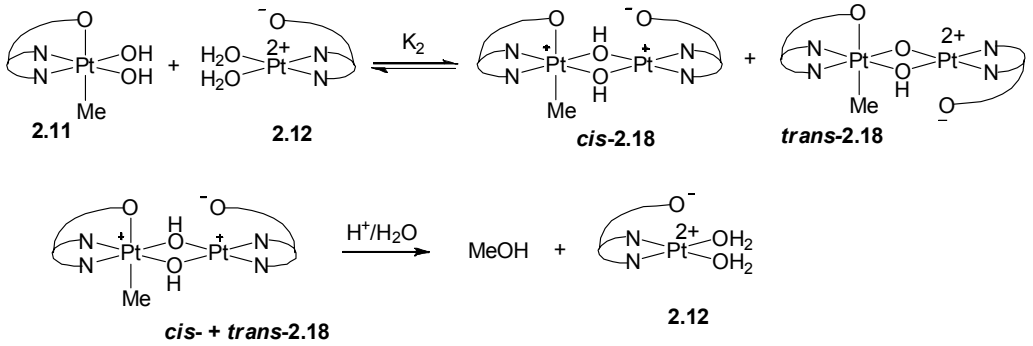

The isolated yield of an analytically pure product containing *cis*- and *trans*-**2.18** in a ratio of 3:1 was 41%. The X-ray crystal structure of *cis*-**2.18** (Fig. 2.14) was shown to have two platinum atoms at a distance of 3.076 Å, one platinum atom in a square planar and another platinum atom in an octahedral environment. Both platinum atoms, two bridging oxygens and four nitrogen atoms of two dpms ligands are located in one plane. Two sulfonate groups are above the plane, hence, the term "*cis*-" was used to designate this isomer. Lengths of Pt-O, Pt-N and Pt-C bonds around the Pt^{IV} center are almost the same as in complex **2.14**, for instance, the Pt-sulfonate oxygen bond was 2.221 Å long.

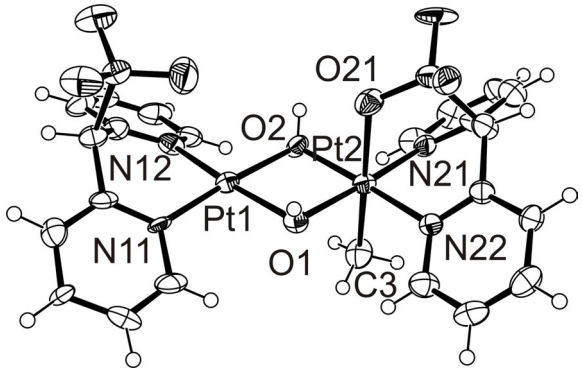

Figure 2.14. ORTEP drawings of cationic complex ***cis*-2.18**, 50% probability ellipsoids. Selected bond distances, Å: Pt1-O1, 2.059(9); Pt1-O2, 2.041(9); Pt2-O1, 2.019(9); Pt2-O2, 2.030(9); Pt2-C3, 2.032(12); Pt2-O21, 2.220(8).

Interestingly, when a 7.44 mM solution of isomeric complexes **2.18** was heated at 80 ^{o}C, the kinetics plot (Fig. 2.12, upper line, filled squares) was undistinguishable from that of the reaction mixture containing equimolar mixture of **2.11** and **2.12** (Fig. 2.12, upper line, empty circles). Therefore, the rate of establishing equilibrium between **2.11**, **2.12** and **2.18** (eq. 2.35) was much faster than the rate of subsequent nucleophilic reactions of complex **2.18** (eq. 2.36-2.37).

The accelerating effect of Pt^{II} additive on MeOH formation indicates that dinuclear complex **2.18** is not inert and undergoes reductive elimination of MeOH via either an S_N2 attack of water or an S_N2 attack of Pt^{IV}-OH. The isolated complex (**2.18**) is not stable in acidic aqueous solutions and produced $LPtMe(OH)_2$, $LPt(OH_2)_2^+$ and MeOH (eq. 2.37).

$$\underset{\textit{cis}\text{- and }\textit{trans}\textbf{-2.18}}{LPt^{IV}Me(\mu\text{-}OH)_2Pt^{II}L^+} + 3H_2O + H^+ \rightarrow \underset{\textbf{2.12}}{2LPt^{II}(OH_2)_2^+} + MeOH \qquad (2.37)$$

Formation of a cationic dinuclear complex **2.18** can be considered as another way to activate the $Pt^{IV}Me$ group toward nucleophilic attack as an alternative to protonation. Methanol elimination from $LPtMe(OH)_2$ is facilitated by the presence of acid due to formation of electrophilic cationic $LPtMe(OH)(OH_2)^+$, **2.11a**.[79] Similarly, Pt^{IV}-Me group in a cationic dinuclear complex **2.18** is expected to be more electrophilic than in neutral $LPtMe(OH)_2$ **2.11**. The reactivity of this cationic complex toward subsequent nucleophilic attack of water or the hydroxo ligand of $LPtMe(OH)_2$ may be similar to that of protonated cationic species $LPtMe(OH)(OH_2)^+$, **2.11a**, considering that the accelerating effect of the formation of $[LPt^{IV}Me(\mu\text{-}OH)_2Pt^{II}L]^+$ is not very significant.

We propose that formation of a dinuclear compex **2.18** occurs via an aqua ligand substitution in the coordination sphere of a platinum(II) atom in a relatively labile complex **2.12**. The attacking nucleophilic groups originate from a dihydroxo platinum(IV) complex **2.11**, as confirmed in the following experiment.

$$\underset{\textbf{2.11}}{LPt^{IV}Me(OH)_2} + \underset{\textbf{2.12}}{LPt^{II}(^{18}OH_2)_2^+} \rightleftharpoons \underset{\textit{cis}\text{- and }\textit{trans}\textbf{-2.18}}{LPt^{IV}Me(\mu\text{-}OH)_2Pt^{II}L^+} + 2H_2{}^{18}O \qquad (2.38)$$

A 39 mM solution of **2.12-$^{18}O_2$** in 98% $H_2{}^{18}O$, acidified with HBF_4 (120 mM), was combined with complex **2.11-*d*$_3$**. The ESI analysis of the resulting reaction mixture, containing complex **2.12-$^{18}O_2$** (39 mM), **2.11-*d*$_3$** (39 mM) and HBF_4 (120 mM) in

$H_2{}^{18}O$, after heating at 80 ^oC for 5 minutes, showed formation of $[LPt^{IV}CD_3(\mu\text{-}{}^{16}OH)_2Pt^{II}L]^+$, containing no ^{18}O labels in it.

Similarly, formation of a mixed-valence Pt complex containing one Pt^{IV} center bridged by six hydroxo groups to three Pt^{II} centers $[\{(Me_3P)_2Pt^{II}\}_3Pt^{IV}(OH)_6](NO_3)_4$ by reacting $H_2Pt^{IV}(OH)_6$ with $(Me_3P)_2Pt^{II}(NO_3)_2$ in aqueous solution was reported by Ozawa and Yagasaki.[85]

*2.2.2.7 Test on Viability of the Pt^{IV}-to-O Methyl group Transfer between Complexes **2.11a** and **2.12a***

Since Pt^{IV}-to-O methyl group transfer between **2.11a** and **2.11** was proven to be viable (Scheme 2.27), one might expect that a similar methyl group transfer would be possible between **2.11a** and (dpms)Pt(OH)(OH_2) **2.12a**, formed by deprotonation of **2.12**, possessing a nucleophilic hydroxo ligand. Although our potentiometric studies showed that complex **2.12** is present mostly in a protonated form as (dpms)Pt$(OH_2)_2{}^+$, its conjugated base, (dpms)Pt(OH)(OH_2) **2.12a**, could be still present in low concentration in the acidic mixtures. The Pt^{IV}-to-O methyl group transfer between an electrophilic complex **2.11a** and **2.12a** then might lead to the formation of easily hydrolysable methoxo Pt^{II} complex, which could then release free methanol into solution.

$$\underset{\textbf{2.12-}{}^{\textbf{18}}\textbf{O}_{\textbf{2}}}{LPt^{IV}Me({}^{16}OH)_2{\cdot}H^+} + \underset{\textbf{2.12a-}{}^{\textbf{18}}\textbf{O}_{\textbf{2}}}{LPt^{II}({}^{18}OH_2)({}^{18}OH)} \rightarrow \rightarrow \underset{\textbf{2.12}}{LPt^{II}({}^{16}OH_2)_2{}^+} + \underset{\textbf{2.19-}{}^{\textbf{18}}\textbf{O}_{\textbf{2}}}{LPt^{II}({}^{18}OH_2)({}^{18}OMe)} \qquad (2.39)$$

Scheme 2.33

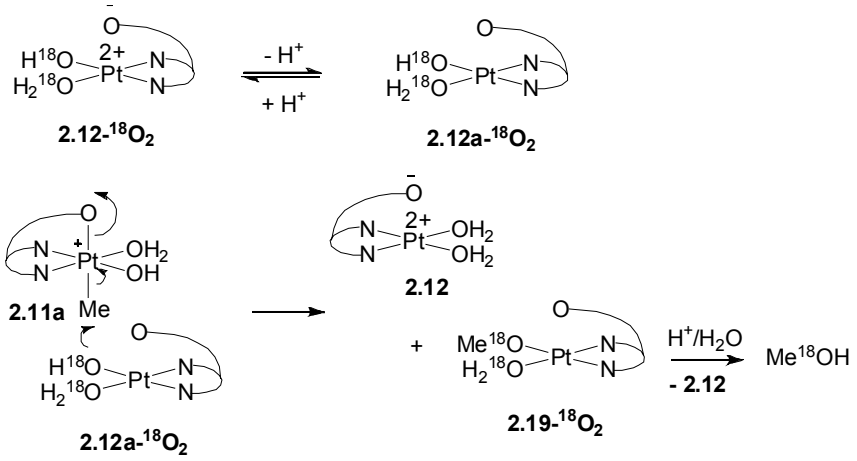

To obtain evidence in favor or against viability of the path (2.39), an isotope labeling experiment was performed, in which complex **2.12-$^{18}O_2$** was allowed to react with **2.11-*d*$_3$** and 120 mM HBF_4 in $H_2{}^{18}O$ at 80 ^oC. After five minutes the $CD_3{}^{18}OH$: $CD_3{}^{16}OH$ ratio was 2.7 : 1, which matched the ratio of isotopologues found in experiments performed under the same conditions but with no additive of **2.12** (2.7 : 1) (Table 2.3). Therefore, we can conclude that reaction (2.39) did not contribute noticeably to the C-O elimination from **2.11**. Moreover, this result is evidence against the Pt^{IV}-to-Pt^{II} methyl group transfer between **2.11** and **2.12** discussed above (Scheme 2.24, eq. 2.29). If such a transfer occurred, one could expect the $CD_3{}^{18}OH$: $CD_3{}^{16}OH$ ratio to be higher than the observed 2.7 : 1.

*2.2.2.8 Kinetic Studies of Reaction between **2.11** and H_2O in Acidic Solutions.*

After having established identities of all detectable reaction intermediates, **2.14**, **2.15** and **2.18** and products, MeOH, Me_2O and **2.12**, we next set out to study kinetics of the reductive elimination from complex **2.11** in acidic solutions, which could

provide additional evidence in favor or against proposed mechanisms (i) and (iii) as the two main contributors to reductive elimination from **2.11**.

i) Reaction Balance. Complex **2.11** reacted in clear acidic aqueous solutions at 25-80 ^{o}C to ultimately produce methanol, complex **2.12**, (eq. 2.16) and dimethyl ether (eq. 2.19) as the only detectable products. The fraction of dimethyl ether depends on the concentration of **2.11** and the acidity of a reaction mixture, and did not exceed 5-7%. By the end of reaction methanol (93-95% yield) and dimethyl ether (5-7%) were the only organic products formed in virtually quantitative combined yield. Besides reactions (2.16) and (2.19) products, formation of intermediates **2.14**, **2.15** and isomeric complexes **2.18** was observed in the beginning of a reaction. These intermediates persisted at middle stages of reaction and disappeared completely by the end of the reaction. Figure 2.15 shows the dependence of concentrations of complexes **2.11**, **2.12**, **2.14**, **2.15**, **2.18**, methanol and Me_2O on reaction time for 41 mM solution of **2.11** in 60 mM HBF_4 at 80 ^{o}C. Assuming that equilibrium (2.18) was very fast in the NMR time scale, the concentration of complex **2.11** determined by NMR integration represented the total concentration of free **2.11** and its protonated form, complex **2.11a**.

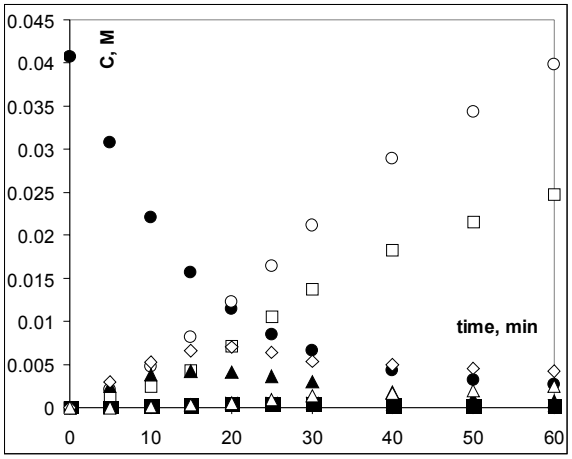

Figure 2.15. Concentration of components of a reaction mixture composed by 41 mM complex **2.11** and D_2O in the presence of 60 mM of HBF_4, 80 ^oC as a function of reaction time: **2.11** (filled circles), MeOH (empty circles), Me_2O (empty triangles), **2.12** (empty squares), **2.14** (filled triangles), two isomeric complexes **2.18** (rhombs), and **2.15** (filled squares).

Considering methanol, dimethyl ether, **2.11**, **2.12**, **2.14**, **2.15** and **2.18** as the major species involved in the reaction of complex **2.11** in acidic aqueous solutions (Fig. 2.15), the balance of all methyl groups originating from the $MePt^{IV}$ fragment of **2.11** and all dpms ligands also having their origin in complex **2.11** was calculated. The combined concentrations of methanol, complex **2.11**, isomeric complexes **2.18**, doubled concentrations of dimethyl ether and complex **2.14**, each bearing two methyl groups, and a tripled concentration of **2.15** incorporating three methyls remained constant, 41±2 mM, up to a 95% conversion of **2.11.** Similarly, the combined concentration of complexes **2.11**, **2.12**, **2.14**, **2.15** and a doubled concentration of isomeric dinuclear complexes **2.18** remained constant, 41±2 mM, for the same period of time.

ii) Effect of Reactants Concentration, $[H^+]$ and $[Pt^{IV}]$, on the Rate of Disappearance of Complex 2.11. A kinetic study of reaction (2.16) was carried out in 60 mM and 120

mM HBF_4 solutions in D_2O at 80 ^oC with the initial concentration of complex **2.11**, C_0, ranging from 4.6 to 41 mM.

Good linear plots of $\ln(C_0/C)$ versus time were obtained for $[HBF_4]$ = 60 mM and 120 mM (Fig. 2.16) suggesting that reaction (2.16) was formally first order in **2.11**. However, corresponding pseudo-first order rate constants, k_{obs}, were found to be dependent on the *initial* concentration of complex **2.11**, $[Pt]_0$ (Table 2.4). This result is evident of complex reaction mechanism, which cannot be described in terms of a simple 1st order reaction, as would be expected in the case of mechanisms (i) and/or (ii) only.

Table 2.4. Observed pseudo-first order rate constants of disappearance of complex **2.11**, k_{obs}, measured at various initial concentrations, $[Pt]_0$, and HBF_4 additive; 80 ^oC.

$[H^+]$ = 60 mM		$[H^+]$ = 120 mM	
$[Pt]_0$, mM	$k_{obs}\cdot10^4$, s^{-1}	$[Pt]_0$, mM	$k_{obs}\cdot10^4$, s^{-1}
4.6	4.10±0.15	5.0	7.69±0.31
7.5	4.53±0.15	9.9	8.18±0.36
9.9	4.92±0.07	21	9.67±0.49
20	6.99±0.19	2	10.57±0.38
29	8.52±0.37	40	12.31±0.79
41	10.63±0.23		

An empirical linear relationship between k_{obs} and *initial* concentrations of complex **2.11**, $[Pt]_0$, can be described by equation 2.37 (Fig. 2.17):

$$k_{obs} = k_0 + k_{Pt}\cdot[Pt]_0 \qquad (2.37)$$

$[H^+]$ = 60 mM $\quad k_0 = (3.20\pm0.04)\cdot10^{-4}$ s^{-1} and $k_{Pt} = (18.2\pm0.2)\cdot10^{-3}$ $s^{-1}\cdot M^{-1}$;

$[H^+]$ = 120 mM $\quad k_0 = (6.94\pm0.08)\cdot10^{-4}$ s^{-1} and $k_{Pt} = (13.2\pm0.3)\cdot10^{-3}$ $s^{-1}\cdot M^{-1}$

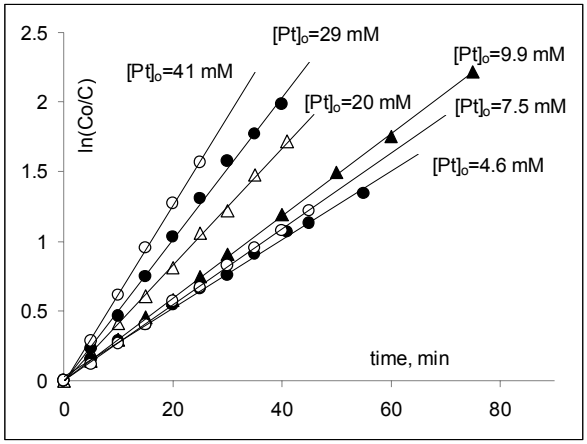

Figure 2.16. First order kinetic plots of reaction between complex **2.11** and D_2O at $[HBF_4]$=60 mM and 80 ^oC; C_0 and C are initial and current concentrations of **2.11**.

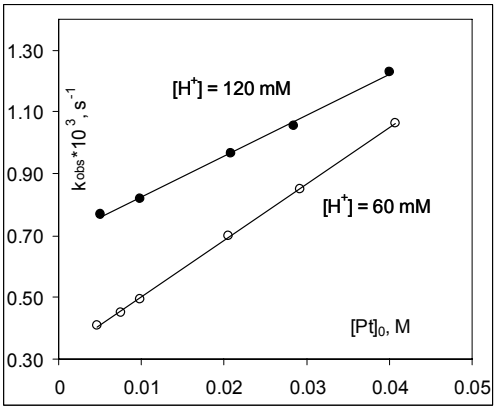

Figure 2.17. Relationship between the observed pseudo-first order rate constants of reaction between complex **2.11** and D_2O, k_{obs}, at 80 ^oC and *initial* concentration of complex **2.11**, $[Pt]_0$; $[HBF_4]$=60 (empty circles) and 120 mM (filled circles).

The pseudo-first order rate constants for the formation of methanol, $k_{obs,MeOH}$, were independent on $[Pt]_0$, $(6.0\pm0.2)\cdot10^{-4}$ s^{-1} for $[H^+]$=120 mM and $(3.7\pm0.1)\cdot10^{-4}$ s^{-1} for $[H^+]$=60 mM, and were smaller than k_{obs}, close to k_0 values given by equation 2.37.

iii) Modeling on the Rate of Disappearance of Complex 2.11. Our analysis of reaction (2.16) kinetics was based on the following assumptions: i) protonation constant for **2.11**, K_1 (eq. 2.18), is low enough to allow for co-existence of **2.11** and **2.11a** in comparable amounts at $[H^+]$ = 60-120 mM and 80 ^oC. This hypothesis is consistent

with the available estimate of the protonation constant for a presumably more basic dimethyl hydroxo analogue of **2.11**, *sym*-LPt^{IV}Me$_2$(OH),[79] $K \sim 46\pm5$ at 97 ^{o}C in D_2O; ii) weakly acidic complex **2.12** did not produce its conjugated base **2.12a** in noticeable amounts (eq. 2.22). Indeed, the pK_{a1} of **2.12** was found to be 4.76±0.07 at 22 ^{o}C; iii) concentration of complex **2.14** was low enough to neglect its bimolecular reactions with **2.11a** and with itself (Schemes 2.29 and 2.30); formation of complex **2.15** can be neglected. Indeed, plot in Fig. 2.15 shows that the fraction of **2.14** never exceeded few percent of the initial concentration of **2.11** and the fraction of **2.15** was close to zero at all times; iv) the rate constants for C-O elimination from **2.11** (Scheme 2.34, eq. 2.40) and **2.14** in acidic solutions leading to MeOH and **2.12** are essentially the same. This assumption is based on the measured observed pseudo-first order rate constants of **2.11** and **2.14** with water at 80 ^{o}C and [HBF_4] = 60 mM, $(10.6\pm0.2)\cdot10^{-4}$ s^{-1} for **2.11** at [Pt^{IV}] = 41 mM (Table 2.4) and $(7.1\pm0.1)\cdot10^{-4}$ s^{-1} for **2.14** at [Pt^{IV}] = 39 mM as will be discussed below; v) complexes **2.18** formed from **2.11** and **2.12** reversibly at a rate much faster than they reacted with water (Scheme 2.34, eq. 2.43) or with other nucleophiles. In particular, reaction plot in Fig. 2.12 provides evidence for that. While the subsequent reaction of **2.18** with water (Scheme 2.34, eq. 2.43) should be taken into consideration here, we could neglect second-order reactions between **2.18** and **2.11** (eq. 2.37) since concentration of **2.18** is low (see Fig. 2.15).

Scheme 2.34

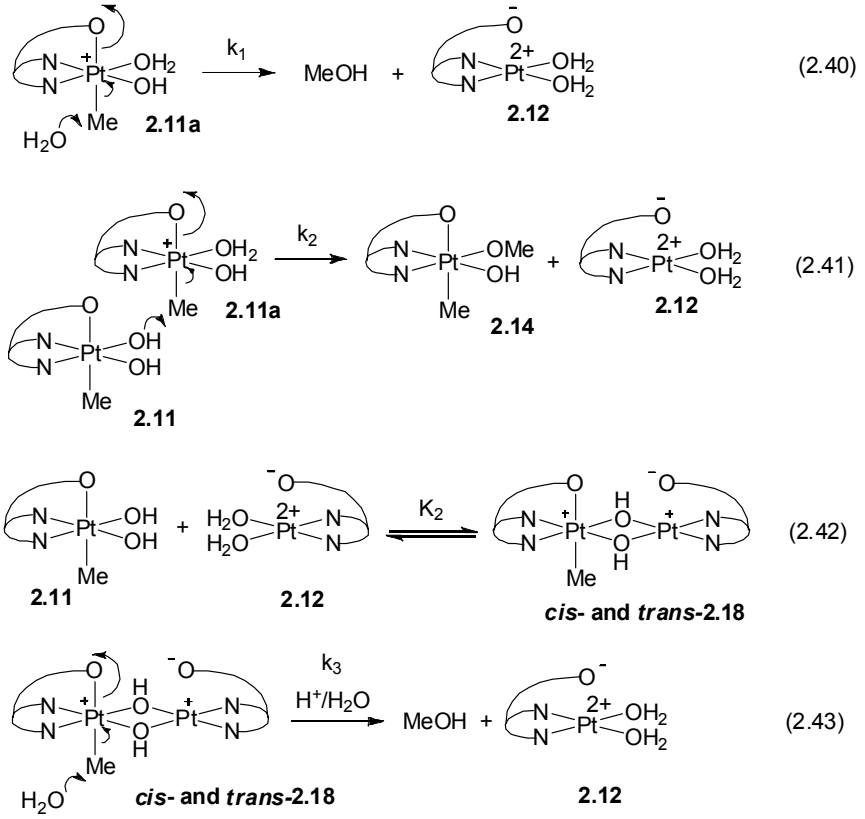

First of all, let us derive an expression describing the rate of disappearance of complex **2.11** measured in our NMR experiments. If C is a combined concentration of complexes **2.11** and **2.11a** in a solution as determined by ^{1}H NMR spectroscopy, then using the expression for the equilibrium constant K_1 (eq. 2.18) we can get equation 2.44:

$$[2.11a] = \frac{K_1[H^+]}{1+K_1[H^+]}C \quad \text{and} \quad [2.11] = \frac{C}{1+K_1[H^+]} \tag{2.44}$$

Using steady-state approximation for complex **2.18** and considering major reaction paths given in Scheme 2.34 (eq. 2.40-2.43) contributing to the rate of disappearance of **2.11**+**2.11a**, we can get an equation 2.45 for the total rate of disappearance of **2.11**+**2.11a**:

$$-\frac{dC}{dt} = k_1[2.11a] + k_2[2.11][2.11a] + k_3[2.18] \quad (2.45)$$

Here the first term corresponds to the pseudo-first order reaction of **2.11a** with water (Scheme 2.34, eq. 2.40), the second term accounts for the bimolecular reaction of **2.11a** with **2.11** (Scheme 2.34, eq. 2.41), the third term corresponds to a reaction between water and complexes **2.18** that exist in fast equilibrium with **2.11** and **2.12** and are present at a steady concentration (Scheme 2.34, eq. 2.43). At the early stages of reaction, the steady state approximation for **2.18** may be not correct and the fourth term corresponding to the change of the concentration of [**2.18**] over time, *d*[**2.18**]/*dt*, should be added (Scheme 2.34, eq. 2.42). Therefore, from equation 2.45 we can get a four-term equation 2.46:

$$-\frac{dC}{dt} = k_1[2.11a] + k_2[2.11][2.11a] + k_3[2.18] + \frac{d[2.18]}{dt} \quad (2.46)$$

Using numerical integration of eq. 2.46 to calculate *C* after consecutive short periods of time and calculating concentrations of **2.11**, **2.11a**, **2.12**, **2.14**, $[H^+]$ and **2.18** after each step using eq. 2.45 and eq 2.47-2.49 given below, one can describe dependence of *C* on time if all necessary constants, k_1, k_2, k_3, K_1 and K_2 are known.

$$[2.18] = K_2[2.11][2.12] \quad (2.47)$$

$$\frac{d([2.12]+[2.18])}{dt} = k_1[2.11a] + \frac{1}{2}k_2[2.11][2.11a] + k_3[2.18] + k_1[2.14] \quad (2.48)$$

$$\frac{d[2.14]}{dt} = \frac{1}{2}k_2[2.11][2.11a] - k_1\frac{K_1[H^+]}{1+K_1[H^+]}[2.14] \quad (2.49)$$

Vice versa, by performing the fitting of the twelve experimentally obtained kinetic curves of dependences between *C* and reaction time to the proposed mechanistic scheme, one can extract all necessary set of constants. The following optimized

values of rate constants and equilibrium constants were extracted by the fitting of the experimental data to the mechanistic scheme described above using a macros on a Visual Basic for Excel written by Andrei Vedernikov: K_1 = 4.5±0.1, K_2 = 90±1, k_1 = (1.50±0.01)·10^{-3} s^{-1}, k_2 = (5.8±0.1)·10^{-2} M^{-1} s^{-1}, k_3 = (7.9±0.1)·10^{-4} s^{-1} (Fig. 2.18).

The model allows to describe satisfactorily the dependence of concentrations of complexes **2.12**, **2.18** and methanol on reaction time. Four calculated and experimental kinetic curves of disappearance of complex [**2.11**]+[**2.11a**] are shown in Fig 2.18.

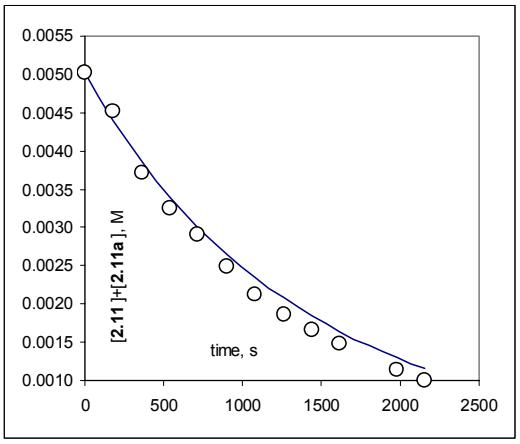

a) $[Pt]_0$ = 5.0 mM, $[HBF_4]$ = 120 mM; standard deviation = 1.03·10^{-4}

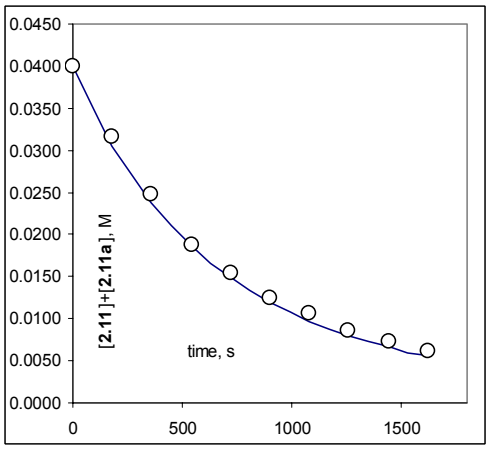

b) $[Pt]_0$ = 40 mM, $[HBF_4]$ = 120 mM; standard deviation = 3.83·10^{-4}

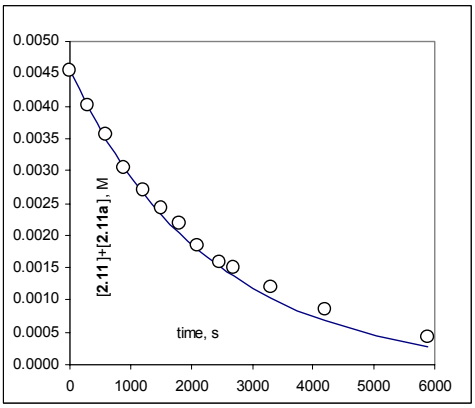

c) $[Pt]_0$ = 4.6 mM, $[HBF_4]$ = 60 mM; standard deviation = 5.9·10^{-5}

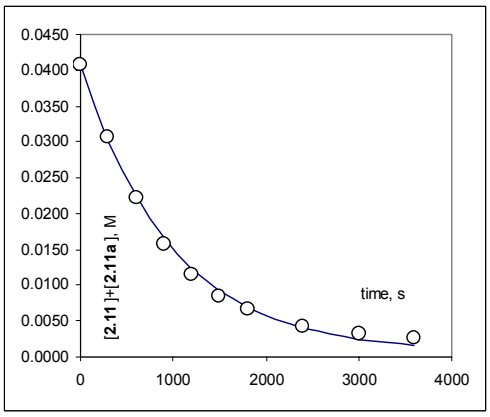

d) $[Pt]_0$ = 41 mM, $[HBF_4]$ = 60 mM; standard deviation = 1.23·10^{-3}

Figure 2.18. Modeling of kinetics data on disappearance of complexes **2.11**+**2.11a** (combined concentration) in acidic solutions in D_2O at 80 °C (calculated values are represented by solid line; experimentally determined concentrations are shown with empty circles).

Therefore, we can conclude that our kinetic model proposed for reductive elimination from **2.11** adequately describes experimentally observed reaction kinetics.

2.2.2.9 C-O reductive elimination from Methoxo Platinum(IV) Complex 2.14 at Various [H^+]

In an effort to further investigate the nucleophilic reactivity of Pt^{IV}-O bond, we performed C-O elimination studies from LPtMe(OMe)(OH) (**2.14**) in acidic and neutral aqueous solutions. Two organic products were detected in the reaction mixtures, MeOH and Me_2O, as well as an intermediate dimethoxy complex *sym*-$LPtMe(OMe)_2$ (**2.15**).

In contrast to **2.11**, which was stable in neutral solutions, a slow reaction of ~40 mM **2.14** was observed in the absence of HBF_4 at 80 ^oC (Fig. 2.19). After 6 hours, the conversion of **2.14** was 80%. Main reaction products were methanol (24% yield), Me_2O (20% yield), and **2.15** (13% yield), along with ~30% of water-insoluble complex **2.20**, identified as $L_2Pt^{II}{}_2(\mu\text{-}OMe)_2$ (eq. 2.50-2.52). Thus, MeOH and Me_2O formed in the 1.2/1 ratio.

$$\underset{\textbf{2.14}}{4LPt^{IV}Me(OH)(OMe)} \rightarrow \underset{\textbf{2.20}}{L_2Pt^{II}{}_2(\mu\text{-}OMe)_2} + \underset{\textbf{2.15}}{2LPt^{IV}Me(OMe)_2} + 2H_2O \qquad (2.50)$$

$$\underset{\textbf{2.14}}{4LPt^{IV}Me(OMe)(OH)} \rightarrow \underset{\textbf{2.20}}{2L_2Pt^{II}{}_2(\mu\text{-}OMe)_2} + 2Me_2O + 2H_2O \qquad (2.51)$$

$$\underset{\textbf{2.14}}{2LPt^{IV}Me(OMe)(OH)} \rightarrow \underset{\textbf{2.20}}{L_2Pt^{II}{}_2(\mu\text{-}OMe)_2} + 2MeOH \qquad (2.52)$$

In the presence of 60 mM HBF_4 ~40 mM solution of **2.14** produced Me_2O and MeOH in a 5/1 molar ratio, which is higher than in the absence of the acid; formation of small anounts (up to 5%) of an intermediate dimethoxo complex **2.15** and product **2.12** was also observed in the reaction mixtures (Fig. 2.20). The observed pseudo-first

order rate constant of disappearance of **2.14** with 39 mM **2.14** 60 mM HBF_4 in D_2O solution was found to be $(7.1\pm0.1)\cdot10^{-4}$ s^{-1} at 80 ^oC.

We propose that formation of dimethoxo complex **2.15** and dimethyl ether occurs via bimolecular reactions similar to those shown in Scheme 2.29 and 2.30. An S_N2 attack by nucleophilic MeO ligand of **2.14** on a Pt-Me group (which could belong to the protonated from of **2.14**, **2.15** or **2.11a**) would lead to the formation of Me_2O. Similarly, methylation of the hydroxo-ligand of **2.14** would produce dimethoxo complex **2.15**. Methanol could form via hydrolysis of **2.14**, nucleophilic attack by water or bimolecular pathways similar to those shown in Scheme 2.27.

Since dimethyl ether can form via a bimolecular pathway (Scheme 2.29) only, the ratio MeOH/Me_2O can be controlled by varying [Pt^{IV}] and [H^+]. The contribution of bimolecular reactions shown in Scheme 2.29-2.30 and therefore the fraction of Me_2O are diminished at lower Pt concentrations or higher [H^+]. Indeed, in dilute 10.0 mM solution of the ratio of MeOH / Me_2O formed by the end of the reaction was found to be 21/1, much higher compared to a 5/1 MeOH / Me_2O ratio observed in concentrated 40 mM solutions of **2.14**, and a 1.2/1 MeOH / Me_2O ratio, observed in neutral 40 mM solutions of **2.14**.

Hence, higher concentration of acid and lower concentration of complex **2.14** allowed for a decrease in the fraction of the C-O coupling products not involving solvent as a nucleophile, such as Me_2O and **2.15**. A similar behavior was observed for complex **2.11**. This information may be valuable for designing aqueous Pt-based systems for selective methane functionalization.

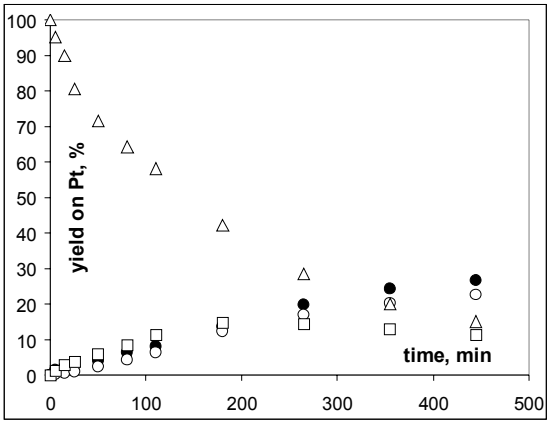

Figure 2.19. Yield of water-soluble products of reaction of 42 mM **2.14** (triangles) in neutral D_2O solution at 80 °C, MeOH (filled circles), Me_2O (empty circles), and *sym*-$LPt^{IV}Me(OMe)_2$, **2.15** (squares).

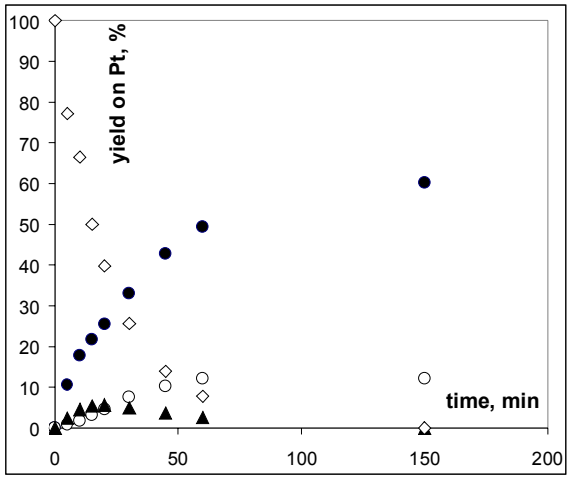

Figure 2.20. Yield of water-soluble products of reaction of 39 mM **2.14** (rhombs) with 60 mM HBF_4 in D_2O at 80 °C: MeOH (filled circles), Me_2O (empty circles), *sym*-$LPt^{IV}Me(OMe)_2$, **2.15** (triangles).

2.2.3 Conclusions

The C-O reductive elimination from $LPt^{IV}Me(X)(Y)$ (X, Y = OH, ^{18}OH, OMe; L = dpms) is achieved in aqueous acidic or neutral solutions and leads to the formation functionalized products: MeOH and dimethyl ether. The reaction of $LPtMe(OH)_2$ in acidic $H_2{}^{18}O$ solution lead to the formation of two isotopologous methanols, $Me^{18}OH$ and $Me^{16}OH$.

The mechanism of C-O elimination from $LPt^{IV}Me(X)(Y)$ (X, Y = OH, ^{18}OH, OMe) in weakly nucleophilic acidic aqueous media involves two concurrent pathways: S_N2 attack by water and bimolecular nucleophilic attack by a hydroxo or methoxo ligand of another species. Competition between these two mechanisms affects the ratio of products formed, $Me^{18}OH/Me^{16}OH$, in the case of reaction between **2.11** and $H_2{}^{18}O$ solvent, or $MeOH/Me_2O$ in the case of reaction of **2.14** with water, and can be controlled by varying Pt^{IV} concentration and acidity of the solution. The nucleophilic attack of hydroxo or methoxo ligand is suppressed at lower concentrations of $LPt^{IV}Me(X)(Y)$ complex or higher acidity of the solution, leading to greater amounts of methanol as opposed to dimethyl ether, or greater fraction of $Me^{18}OH$ in the case of reaction of **2.11** in $H_2{}^{18}O$.

One of the products of reductive elimination, $LPt^{II}(OH_2)_2{}^+$ (**2.12**), was responsible for accelerating the rate of C-O coupling. This effect might be explained by an electrophilic activation of $LPt^{IV}Me(OH)_2$ via formation of cationic dinuclear μ-hydroxo bridged heterovalent $Pt^{II} – Pt^{IV}$ complexes (**2.18**).

2.3 Experimental Section

Preparation of (dpms)PtMe(OH_2), 2.1. In an argon-filled glove box a 50 mL Schlenk flask was charged with 200 mg of isomeric dimethyl hydrides (dpms)$PtMe_2H$ (420 μmol), 15 mL of air-free water and a stirring bar. The flask was placed in a 45 ^oC water bath and the mixture was vigorously stirred under argon for 6 h to produce a clear colorless solution of (dpms)$PtMe(OH_2)$. A sample of the solution was diluted by D_2O and characterized by ^1H NMR spectroscopy as

(dpms)PtMe(OH_2). Complex **2.1** is air sensitive; upon addition of the acid protonolysis of Me group occurs to produce methane.

^{1}H NMR (D_2O/H_2O, 22 ^oC), δ: 0.92 (s, $^2J_{PtH}$ = 70 Hz, 3H), 5.88 (s, 1H, $CHSO_3$), 7.37 (m, 1H), 7.61 (m, 1H), 7.77 (vd, *J*=7.9 Hz, 1H), 7.87 (vd, *J*=8.0 Hz, 1H), 8.08 (dt, *J*=1.4, 7.8 Hz, 1H), 8.11 (dt, *J*=1.4, 7.9 Hz, 1H), 8.73 (m, 1H), 8.77 (m, 1H).

^{13}C NMR (D_2O/H_2O, 22 ^oC): -16.2 (s, $^1J_{PtC}$ = 596 Hz), 75.9, 125.6, 126.2, 128.4, 129.6, 138.9, 139.3, 148.8, 148.6, 152.1, 154.2.

The solution of complex with ^{18}O-labeled water as a ligand was prepared by analogous procedure using $H_2{}^{18}O$ as a solvent.

Preparation of *unsym*-(dpms)PtMe(OH)$_2$ (*unsym*-2.4). An aqueous solution of (dpms)PtMe(OH_2) was prepared from 200 mg of (dpms)$PtMe_2H$ (420 μmol) as described above and used in the next step without isolation. A solution of (dpms)PtMe(OH_2) in 15 mL of water was placed into a 250 mL round bottom flask equipped with a magnetic stirring bar. The flask was filled with dioxygen (1 atm) and vigorous stirring continued for 3-4 h. After that time, according to ^{1}H NMR spectroscopy, the transformation of the methyl aqua platinum(II) complex to *unsym*-**2.4** was complete. The solvent was removed under high vacuum at room temperature and the residue was dried at 0.2 Torr at room temperature for 1 h to produce a pale yellow solid. Yield 205 mg (99%). Perfectly soluble in water, methanol, and DMSO, scarcely soluble in acetonitrile and acetone. Insoluble in chloroform and dichloromethane.

^{1}H NMR (D_2O, 22 ^{o}C), δ: 2.44 (s, $^{2}J_{195PtH}$ = 66 Hz, 3H), 6.67 (s, 1H), 7.79 (ddd, *J*=1.0, 6.1, 7.6 Hz, 1H), 7.89 (ddd, *J*=1.0, 5.4, 7.6 Hz, 1H), 8.04 (vd, *J*=7.9 Hz, 1H), 8.07 (vd, *J*=8.0 Hz, 1H), 8.27 (m, 2H), 8.55 (m, 1H), 8.88 (m, 1H).

^{13}C NMR (D_2O, 22 ^{o}C), δ: 4.5 ($^{1}J_{195PtC}$ = 547 Hz), 71.8, 127.4, 127.8, 128.0, 129.1, 142.5, 143.5, 147.6, 148.0, 150.4, 150.8. **ESI-MS** of solution of **2.4** in H_2O acidified with 1 eq of HBF_4, m/z = 494.035. Calculated for (**2.4**·H^+), $C_{12}H_{15}O_5N_2PtS$, 494.03495. **Anal.** Found: H, 2.89; C, 29.69; N, 6.00. Calculated for $C_{12}H_{14}O_5N_2PtS$, H, 2.86; C, 29.21; N, 5.68.

Preparation of (dpms)Pt^{II}CH$_3$(^{18}OH$_2$) (2.1-^{18}O) and its oxidation to *unsym*-(dpms)Pt^{IV}CH$_3$(^{18}OH)(OH), 2.4-^{18}O. Thermal isomerization into *sym*-(dpms)Pt^{IV}CH$_3$(^{18}OH)(OH), 2.11-^{18}O. In an argon-filled glove box a 5 mL Schlenk flask was charged with 40 mg of dimethyl hydride LPtMe$_2$H (84 μmol), 1.0 g of air-free water $H_2{}^{18}O$ and a stirring bar. The flask was placed in a 45 ^{o}C water bath and the mixture was vigorously stirred under argon for 1h to produce a clear, colorless solution of LPtCH$_3$(^{18}OH$_2$). Air was then admitted into the flask and vigorous stirring continued for a further 5h. After that time, according to the ESI-MS analysis of a slightly acidified sample of the reaction mixture, all LPtCH$_3$(^{18}OH$_2$) complex had reacted and a singly labeled complex LPtMe(^{18}OH)(OH) had formed. ESI-MS of solution of 2.4-^{18}O in H_2O acidified with HBF_4, m/z = 496.074. Calculated for (2.4-^{18}O*H^+), $C_{12}H_{15}{}^{16}O_4{}^{18}ON_2{}^{195}Pt{}^{32}S$, 496.03924.

Isomerization into *sym*-(dpms)Pt^{IV}CH$_3$(^{18}OH)(OH), 2.11-^{18}O. The reaction mixture was diluted with distilled water (5 mL) and heated at 93 ^{o}C for 3h. After that

time, all the starting complex isomerized to the "symmetrical" isomer of LPtMe(^{18}OH)(OH), according to ^{1}H NMR spectroscopy. The mixture was filtered through Celite and the solvent was removed under vacuum at room temperature to produce **2.11-^{18}O**, 40 mg (96%). The product was pure according to ^{1}H NMR spectroscopy. It was re-dissolved in regular water (960 mg) and stored at 5 ^{o}C in a sealed vial. ESI-MS of solution of **2.11-^{18}O** in H_2O acidified with HBF_4, m/z = 496.074. Calculated for (**2.11-^{18}O***H^+), $C_{12}H_{15}{}^{16}O_4{}^{18}ON_2{}^{195}Pt{}^{32}S$, 496.03924.

Preparation of (dpms)Pt^{II}Me(MeOH), 2.2 and its oxidation to (dpms)Pt^{IV}Me$_{eq}$(MeO)(OH), 2.5. Thermal isomerization to (dpms)Pt^{IV}Me$_{ax}$(MeO)(OH), 2.14.

(dpms)Pt^{II}Me(MeOH), 2.2. In an argon-filled glove box a 25 mL Schlenk flask was charged with 95 mg of dimethyl hydride LPt^{IV}Me$_2$H[17] (200 μmol), 10.0 mL of air-free methanol and a stirring bar. The flask was placed in a 45 ^{o}C water bath and the mixture was stirred under argon for 1h to produce a clear colorless solution of LPt^{II}Me(HOMe), pure according to ^{1}H NMR spectroscopy:

^{1}H NMR (CD_3OD, 22 ^{o}C), δ: 0.94 ($^2J_{195PtH}$ = 75 Hz, 3H), 5.89 (s, 1H), 7.27 (ddd, *J*=2.0, 6.1, 7.6 Hz, 1H), 7.55 (ddd, *J*=1.4, 5.4, 7.1 Hz, 1H), 7.74 (vd, *J*=7.9 Hz, 1H), 7.86 (vd, *J*=8.0 Hz, 1H), 8.01 (dt, *J*=1.6, 8.0 Hz, 1H), 8.05 (dt, *J*=2.0, 8.0 Hz, 1H), 8.70 (m, 2H).

(dpms)Pt^{IV}Me$_{eq}$(MeO)(OH), 2.5. The methanolic solution containing **2.2** prepared as described above was stirred vigorously under an O_2 atmosphere for 5h. After that time according to ^{1}H NMR all LPt^{II}Me(HOMe) complex had reacted and pale yellow

precipitate of the poorly soluble product, $LPt^{IV}Me(OMe)(OH)$, **2.2**, with an equatorial Me ligand, formed. The mixture was filtered; the precipitate was washed with 1 mL of methanol and dried. Yellowish powder, yield 76 mg (75%).

^{1}H NMR (D_2O, 22 ^oC), δ: 2.44 ($^2J_{195PtH}$ = 67 Hz, 3H), 2.96 ($^3J_{195PtH}$ = 23 Hz, 3H), 6.67 (s, 1H), 7.80 (ddd, *J*=1.4, 6.0, 7.5 Hz, 1H), 7.80 (ddd, *J*=1.0, 5.0, 7.7 Hz, 1H), 8.06 (vd, *J*=7.8 Hz, 1H), 8.08 (vd, *J*=8.0 Hz, 1H), 8.29 (vt, *J*=7.8 Hz, 2H), 8.52 (vd, *J*=6.0 Hz, $^3J_{PtH}$ = 25 Hz, 1H), 8.90 (vd, *J*=5.3 Hz, 1H). **^{13}C NMR** (D_2O, 22 ^oC), δ: 5.7, 55.0, 71.8, 127.4, 127.8, 128.0, 129.2, 142.6, 143.5, 147.8, 148.1, 150.6, 150.7. Due to the limited solubility of **2.5** in water and weak NMR signals platinum satellites for the PtMe and PtOMe groups were not observed. **ESI-MS** of solution of **2.5** in methanol acidified with one drop of HBF_4, m/z = 508.034. Calculated for (**2.5**·H^+), $C_{13}H_{17}O_5N_2{}^{195}Pt^{32}S$, 508.0506. **Anal.** Found: H, 3.31; C, 31.0; N, 5.68; S, 6.15. Calculated for $C_{13}H_{16}O_5N_2PtS$, H, 3.18; C, 30.8; N, 5.52; S, 6.32.

(dpms)$Pt^{IV}Me_{ax}$(MeO)(OH), 2.14. Subsequent isomerization of complex **2.5** with an equatorial PtMe group to **2.14** featuring the axial PtMe was performed in refluxing acetone. Complex **2.5** (120 mg) was placed in a Teflon-sealed Schlenk flask with 5 mL of dry acetone and heated in an oil bath at 80 ^oC for 48h. After cooling the mixture was filtered and the precipitate washed with hot acetone. It was dried to yield pure target complex. Yellowish powder, 80 mg (66%).

^{1}H NMR (D_2O, 22^oC), δ: 2.58 ($^2J_{195PtH}$ = 77 Hz, 3H), 3.08 ($^3J_{195PtH}$ = 28 Hz, 3H), 6.53 (s, 1H), 7.83 (m, 2H), 8.09 (m, 2H), 8.33 (m, 2H), 8.56 (vd, *J*=6.0 Hz, $^3J_{PtH}$ = 28 Hz, 1H), 8.65 (vd, *J*=6.0 Hz, $^3J_{PtH}$ = 29 Hz, 1H). **^{13}C NMR** (D_2O, 22 ^oC), δ: 12.5 ($^1J_{PtC}$=641 Hz), 56.0 ($^2J_{PtC}$=14 Hz), 72.7 ($^3J_{PtC}$=34 Hz), 127.6 (J_{PtC}=28 Hz), 127.7

(J_{PtC}=29 Hz), 128.9 (J_{PtC}=15 Hz), 129.1 (J_{PtC}=14 Hz), 143.3 (2C), 148.9, 149.2, 149.3, 149.5. **ESI-MS** of solution of **2.14** in methanol acidified with one drop of HBF_4, m/z = 508.034. Calculated for (**2.14**·H^+), $C_{13}H_{17}O_5N_2{}^{195}Pt^{32}S$, 508.0506.

Preparation of (dpms)Pt^{II}Me(NH_2Ph), 2.3. Solution of (dpms)PtMe(MeOH) (192 μmol) in deaerated methanol (10 mL), prepared from isomeric hydrides (dpms)$PtMe_2H$ (91.4 mg, 192 μmol) (5) was placed in a 50 mL Schlenk tube and combined with distilled aniline (18.1 mg; 194 μmol, 1.01 equ). The mixture was stirred at room temperature. According to ^{1}H NMR, the ligand exchange was complete after 15 minutes. The reaction mixture was evaporated to dryness; the resulting colorless solid was washed with ether and dried under vacuum for 6h. Yield 92.9 mg, 87%. White solid, soluble in methanol and water, slowly oxidizes in air. **^{1}H NMR** (D_2O, 22 ^{o}C), δ: 0.79 ($^2J_{195PtH}$ = 72 Hz, 3H), 5.91 (s, 1H), 7.05-7.33 (m, 6H), 7.38 (m, 1H), 7.74 (vd, J = 7.8 Hz, 2H), 7.88 (vt, J = 7.8 Hz, 1H), 8.03 (vt, J = 7.8 Hz, 1H), 8.14 (d, J = 5.5 Hz, 1H), 8.73 (d, J = 5.9 Hz, $^3J_{195PtH}$ = 56 Hz, 1H). **ESI-MS** of aqueous solution of (dpms)PtMe(NH_2Ph), m/z observed: 553.1. Calcd. for (dpms)PtMe(NH_2Ph)·H^+, $C_{18}H_{20}N_3SO_3{}^{195}Pt$, 553.1.

Preparation of (dpms)Pt^{IV}Me(NHPh)(OH), 2.6. Distilled aniline (33.3 mg, 358 μmol, 1.2 equiv.) was added to a solution of (dpms)PtMe(MeOH) prepared from 140.1 mg (295 μmol) isomeric hydrides (dpms)$PtMe_2H$ and 15 mL MeOH (5). According to ^{1}H NMR, the ligand exchange was complete in 15 minutes to give (dpms)PtMe(NH_2Ph) which was used in the next step without isolation. The mixture

was placed into an ice bath; 35 mg of 30% H_2O_2 (~308 μmol) were slowly added to the stirred reaction mixture. Mixture turned yellow immediately after addition of H_2O_2. According to ^{1}H NMR, oxidation was complete in less than 15 minutes to give (dpms)PtMe(NHPh)(OH) quantitatively. The resulting solution was reduced in volume to 2 mL; the product was precipitated with 6 mL of ether, filtered off and dried under vacuum for 3 hours. Yield 106.2 mg, 63%. Red crystalline solid, soluble in methanol, DMSO and water; aqueous solutions have weakly basic reaction (pH ~9).

^{1}H NMR (dmso-d_6, 22 ^{o}C), δ: 2.22 (br s, 1H), 4.17 (br s, 1H), 6.40-6.87 (m, 5H), 7.26 (s, 1H), 7.68-7.77 (m, 1H), 7.80 (ddd, J = 7.9, 5.7, 1.2 Hz, 1H), 8.02 (d, J = 7.9 Hz, 1H), 8.06 (d, J = 7.9 Hz, 1H), 8.23 (td, J = 7.9, 1.9 Hz, 1H), 8.30 (td, J = 7.9, 1.2 Hz, 1H), 8.63 (dd, J = 5.7, 1.2 Hz, 1H), 8.67-8.77 (m, 1H). **^{13}C NMR** (dmso-d_6, 22 ^{o}C), δ: 2.2 ($^1J_{195PtC}$ = 606 Hz), 70.4, 116.0, 119.4, 125.8, 126.7, 126.9, 128.0, 128.2, 141.5, 142.4, 148.3, 149.7, 150.0, 152.2, 155.8. **IR** (KBr), ν: 3548 (w, br), 3087 (w), 2973 (w), 1592 (w), 1489 (w), 1448 (w), 1296 (m), 1212 (m), 1154 (s), 980 (m), 750 (m), 688 (m) cm^{-1}. **ESI-MS** of aqueous solution of (dpms)PtMe(NHPh)(OH), m/z observed: 569.1. Calcd. for (dpms)PtMe(NHPh)(OH)·H$^+$, $C_{18}H_{20}N_3SO_4{}^{195}Pt$, 569.1. **Anal.** Found: H, 3.24; C, 38.18; N, 6.97; S, 5.50. Calcd for $C_{18}H_{19}O_4N_3PtS$, H, 3.37; C, 38.03; N, 7.39; S, 5.64.

Oxidation of (dpms)Pt^{II}Me(NH$_2$Ph), 2.3 with O$_2$. (dpms)Pt^{II}Me(PhNH$_2$) (40 mg, 72 μmol) and 10 mL of water were placed into a 50 mL round bottom flask equipped with a magnetic stirring bar. The flask was filled with O_2 and the solution was stirred

vigorously under an O_2 atmosphere at room temperature. According to ^{1}H NMR spectroscopy, slow oxidation occurred to give (dpms)PtMe(NHPh)(OH) (**2.6**) as the only Pt^{IV} product. The reaction half-life is ~30 hours at 20 ^oC. Signals corresponding to protonated starting material (m/z 553.1) and oxidation product (dpms)Pt^{IV}Me(NHPh)(OH) (m/z 569.1) were detected by ESI MS.

Preparation of $LPt^{IV}CD_3(OH)_2$, 2.11-*d*$_3$. In an argon-filled glove box a 25 mL Schlenk flask was charged with 100 mg of dimethyl hydride $LPt^{IV}Me_2H$ (210 μmol), 3.0 mL of air-free D_2O and a stirring bar. The flask was placed in a 45 ^oC water bath and the mixture was vigorously stirred under argon for 1h to produce a clear colorless solution of $LPt^{II}CD_3(OD_2)$. The air was then admitted to the flask and vigorous stirring continued for 5h. After that time, according to the ESI-MS analysis, all $LPt^{II}CD_3(OD_2)$ complex has reacted and a labeled complex $LPt^{IV}CD_3(OH)_2$ formed. The solvent was removed under vacuum at room temperature. The residue was dissolved in distilled water (10.0 mL) and heated at 93 ^oC for 3h. After that time, according to ^{1}H NMR spectroscopy, all the dihydroxo Pt^{IV} complex isomerized to the "symmetrical" isomer $LPt^{IV}CD_3(OH)_2$.

The mixture was filtered through Celite, the solvent was removed under vacuum at room temperature to produce **2.11-*d*$_3$**, 91 mg (87%), pure according to ^{1}H NMR spectroscopy. The product was re-dissolved in regular water (5.91 g) and kept in refrigerator in a sealed vial at 5 ^oC.

^{1}H NMR spectrum of **2.11-*d*$_3$** is identical to that of **2.11** with the exception that there are only weak residual resonances for the PtMe group. In the ^{13}C NMR spectrum of

2.11-d_3 the signal of the PtMe group was not observed either due to the high multiplicity of the signal leading to a set of short lines masked by noise. ESI-MS of solution of **2.11-d_3** in H_2O acidified with one drop of HBF_4, m/z = 497.081. Calculated for (**2.11-d_3·H$^+$**), $C_{12}H_{12}D_3O_5N_2{}^{195}Pt^{32}S$, 497.05348.

Preparation of *unsym*-LPt^{IV}Me(OMe)$_2$ and *sym*-LPt^{IV}Me(OMe)$_2$ (2.15).

***unsym*-LPt^{IV}Me(OMe)$_2$ (2.17).** Solution of 55.2 mg (112 μmol) LPt^{II}Me(HOMe) in 5 mL of air-free methanol was placed in a 50 mL Schlenk flask. 3.7 mL of 0.6 M solution of Me_2O_2 in benzene (2.2 mmol) prepared according to reference[86] was added. The mixture was stirred overnight under argon and then heated at 45^{0}C for 3h to produce unsymmetrical LPt^{IV}Me(OMe)$_2$ along with ca 14% of the isomeric *sym*-LPt^{IV}Me(OMe)$_2$.

Caution: Me_2O_2 can explode during preparation. The explosion can be caused even by friction between glass joints if a drop of the reaction mixture is present on their surface. We therefore recommend using a reaction flask without attached devices such as dropping funnel, condenser or stoppers. In addition, we scaled the synthesis of Me_2O_2 [86] down to 2.5 mL of Me_2SO_4 and used extraction of the reaction mixture with benzene instead of distillation. Concentration of Me_2O_2 in the extract was determined by solvent suppression ^{1}H NMR spectroscopy (after dilution with C_6D_6) using CH_2Cl_2 as an internal standard.

unsym-LPt^{IV}Me(OMe)$_2$, **^{1}H NMR** (CD_3OD, 22 ^{o}C), δ: 2.40 ($^2J_{195PtH}$ = 70 Hz, 3H), 2.65 ($^3J_{195PtH}$ = 55 Hz, 3H), 2.89 ($^3J_{195PtH}$ = 25 Hz, 3H), 6.51 (s, 1H), 7.76-7.81 (m, 1H), 7.89 (ddd, *J*=1.2, 5.2, 7.9 Hz, 1H), 8.00-8.07 (m, 2H), 8.22-8.30 (m, 2H), 8.59-

8.71 (m, 1H), 8.95-9.00 (m, $^{3}J_{PtH}$ = 26 Hz, 1H). **^{13}C NMR** (CD_3OD, 22 ^{o}C), δ: 8.4, 57.6, 73.2, 127.8, 128.3, 128.7, 129.8, 143.1, 144.0, 149.6, 151.1, 151.6, 153.7. Due to the limited solubility of *unsym*-$LPt^{IV}Me(OMe)_2$ in methanol and weak NMR signals platinum satellites for the PtMe and PtOMe groups were not observed.

***sym*-$LPt^{IV}Me(OMe)_2$ (2.15).** *unsym*-$LPt^{IV}Me(OMe)_2$ prepared as above was used without isolation for isomerization to the symmetrical isomer. Solvent was removed by evaporation under vacuum. The solid residue was re-dissolved in 50 mL methanol and heated in a sealed Schlenk tube at 80 ^{0}C for 6h. The mixture was cooled down, its volume was reduced to 2 mL and resulting white precipitate was filtered and washed with 1 mL of methanol, then with 1 mL of CH_2Cl_2 and dried under vacuum for 5 h. Yield 26.8 mg, 46%. **2.15** reacted slowly in water to produce methanol and **2.14**.

^{1}H NMR (D_2O, 22 ^{o}C), δ: 2.50 ($^{2}J_{195PtH}$ = 77 Hz, 3H), 3.08 ($^{3}J_{195PtH}$ = 27 Hz, 6H), 6.50 (s, 1H), 7.84 (ddd, *J*= 1.4, 6.1, 7.6 Hz, 2H), 8.08 (vd, *J*=8.0 Hz, 2H), 8.31 (dt, *J*= 1.3, 7.8 Hz; 2H), 8.63 (vd, *J*=5.8 Hz, $^{3}J_{PtH}$= 28 Hz, 2H). **ESI-MS** of solution of **2.15** in water, m/z = 522.076. Calculated for (**2.15**·H^+), $C_{14}H_{19}O_5N_2{}^{195}Pt^{32}S$, 522.06625. **Anal.** Found: H, 3.22; C, 31.81; N, 5.59; S, 5.88. Calculated for $C_{14}H_{18}O_5N_2PtS$, H, 3.48; C, 32.25; N, 5.37; S, 6.15.

Preparation of Isomeric $[LPt^{IV}Me(\mu\text{-}OH)_2Pt^{II}L]BF_4$, *cis*- and *trans*- 2.18.

Complex *sym*-$LPt^{IV}Me(OH)_2$ (102.5 mg, 208 μmol) was dissolved in 4 mL of 120 mM HBF_4 solution in D_2O containing $[LPt^{II}(OH_2)_2]BF_4$ (36.6 mg, 64.5 μmol). The mixture was kept at 95^{0}C for 5 min, cooled down slowly to room temperature and left for one week. Isomeric complexes $[LPt^{IV}Me(\mu\text{-}OH)_2Pt^{II}L]BF_4$ crystallized slowly

from the mixture as colorless crystals that were collected and washed with water until the filtrate was neutral to give 27.3 mg of a colorless crystalline solid (3:1 *cis*- : *trans*-**2.18**, yield 41%). The product is poorly soluble in water and aqueous solutions of HBF_4.

^{1}H NMR (D_2O, 22^{0}C), δ: *cis*-Isomer: 3.56 ($^2J_{195PtH}$=64 Hz, 3H), 6.16 (s, 1H), 6.71 (s, 1H), 7.58 (m, 2H), 7.83-7.93 (m, 4H), 8.08-8.18 (m, 4H), 8.38 (vt, *J*=7.7 Hz, 2H), 8.64 (vd, *J*=6.1 Hz, 2H), 8.74 (vd, *J*=6.0 Hz, 2H). *trans*-Isomer: 3.38 (3H), 6.21 (s, 1H), 6.83 (s, 1H), 7.52 (m, 2H), 8.47 (vd, *J*=6.1 Hz, 2H), 8.54 (vd, *J*=6.1 Hz, 2H); other signals of the pyridyls overlap with signals of the *cis*-isomer.

ESI-MS: m/z 937.02124 (calc. for $[LPt^{IV}Me(\mu\text{-}OH)_2Pt^{II}L]^+$ 937.024292). **^{19}F NMR** (D_2O, 22^{0}C), δ: -150.8. **Anal.** Found: H, 2.75; C, 24.73; N, 5.00; S, 6.08. Calculated for $C_{23}H_{35}O_{14}N_4Pt_2S_2BF_4$ ($L_2Pt_2Me(\mu\text{-}OH)_2\cdot 6H_2O$), H, 3.11; C, 24.39; N, 4.95; S, 5.66.

Chapter 3: Aerobic Functionalization of (dpms)Pt^{II} Ethylene Complexes

3.1 Introduction

The aerobic functionalization chemistry described in Chapter 2 could also be applied to oxidative transformations of alkenes. Transition metal catalysts are widely used in the oxidative functionalization of olefins. Compared to alkanes, alkenes are much better ligands for transition metals, and coordination of a double bond to a metal center enhances the reactivity of an olefin toward nucleophilic attack; free alkenes are typically more prone towards electrophilic attack.[32] Since nucleophilic attack leads to the formation of a metal-alkyl species,[87] we expected that similar aerobic oxidation/reductive elimination sequence enabled by the dpms ligand could also be used for aerobic functionalization of Pt(alkene) complexes, as an alternative to Wacker-type oxidation (Scheme 1.10).

Oxidation of Pt^{II}(alkene) complexes typically requires the use of strong oxidants, and no examples of oxidation of Pt^{II}(alkene) species with O_2 directly has been reported prior to our work.[88]

Halpern[88] observed oxidation of Zeise's salt $K[Cl_3Pt(CH_2{=}CH_2)]$ in aqueous solution containing HCl with Cl_2 to initially produce $[Cl_5PtCH_2CH_2Cl]^{2+}$, which is subsequently hydrolyzed to form $[Cl_5PtCH_2CH_2OH]^{2+}$. The latter undergoes reductive elimination, presumably via an S_N2 mechanism, to produce chloroethanol, ethylene glycol (or ethylene oxide in the presence of NaOH) and $[Pt^{II}Cl_4]^{2-}$ (Scheme 3.1).[88]

Scheme 3.1

$$[Cl_3Pt^{II}(CH_2{=}CH_2)]^- \xrightarrow{Cl_2,\ Cl^-} [Cl_5Pt^{IV}(CH_2CH_2Cl]^{2-} \xrightarrow{H_2O\ (-HCl)}$$

$$\longrightarrow [Cl_5Pt^{IV}(CH_2CH_2OH)]^{2-} \longrightarrow [Pt^{II}Cl_4]^{2-} + ClCH_2CH_2OH$$

Bercaw and co-workers have studied the mechanism of Zeise's salt oxidation with $[PtCl_6]^{2-}$.[62] Noteworthy, the oxidation is inhibited by acid additives; the rate of the oxidation was found to be inversely proportional to $[H^+]$. The authors concluded that a reaction with water is required prior to oxidation to produce a hydroxyethyl Pt^{II} complex (eq. 3.1), which is expected to be more reactive toward oxidation compared to Zeise's salt due to the presence of a strongly σ-donating hydroxyethyl group. Since at low *pH*'s the equilibrium in eq. 3.1 is shifted toward the ethylene complex, inhibition of the oxidation rate with increasing $[H^+]$ is observed.[62]

$$[Cl_3Pt^{II}(CH_2{=}CH_2)]^- + H_2O \rightleftharpoons [Cl_3Pt^{II}(CH_2CH_2OH]^{2-} + H^+ \qquad (3.1)$$

$$[Cl_3Pt^{II}(CH_2CH_2OH]^{2-} + [PtCl_6]^{2-} \longrightarrow [Cl_5Pt^{IV}(CH_2CH_2OH]^{2-} + [PtCl_4]^{2-} \qquad (3.2)$$

Although an oxidation state of 3 is not common for platinum, a number of bridged Pt^{III} dinuclear diamagnetic complexes containing a Pt-Pt bond are known. In some cases such complexes can display reactivity patterns typical for both Pt^{+2} and Pt^{+4} oxidation states. This property was exploited by Kazuko Matsumoto[89, 90] in developing a catalytic aerobic epoxidation of olefins using amidate-bridged Pt^{III} dinuclear complexes (Scheme 3.2). The reaction is catalyzed by "platinum tan" pyrrolidonate-bridged complex $[Pt_4(NH_3)_8(C_4H_6NO)_2](NO_3)_6{*}2H_2O$ and by pivalamidate-bridged "platinum blue" compound $[Pt_4(NH_3)_8(t\text{-}BuCCONH)_2](NO_3)_5$ in biphasic acidic $H_2O/ClCH_2CH_2Cl$ system under an O_2 atmosphere. Cyclohexene and norbornene are converted to epoxides with 76-92% selectivity. Turnover numbers vary from 5 to 22, and the reaction is

accompanied by the formation of cyclic ketones. The proposed mechanism of epoxidation is shown in Scheme 3.2.[89]

Scheme 3.2

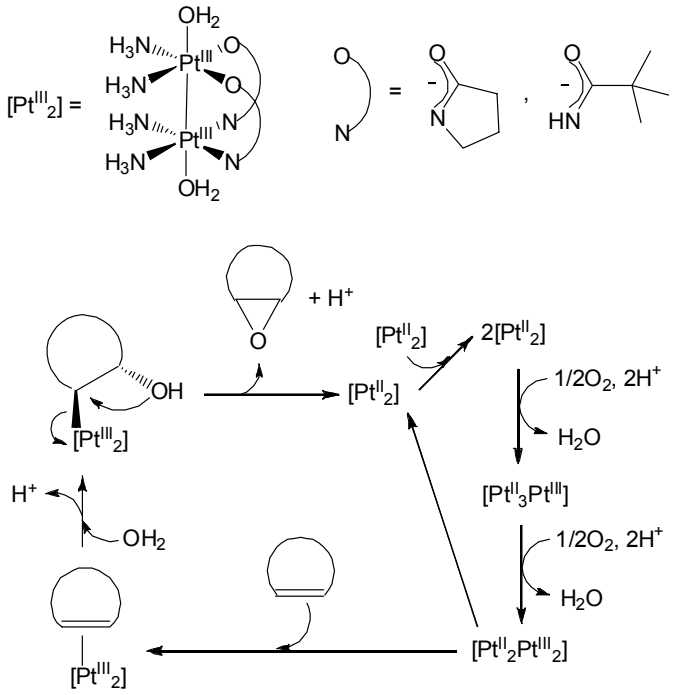

Similar to other platinum-based systems, described above, the reaction sequence involves initial *trans*-nucleophilic attack of water on a double bond of coordinated olefin in Pt^{III} dimer complex, followed by the reductive elimination step, which involves an intramolecular S_N2 attack of a β-hydroxyl group on a platinum-bound α-carbon to produce an epoxide and a Pt^{II} dimer.[91]

As we have shown in Chapter 2, the dpms scaffold allows for facile aerobic oxidation of the (dpms)Pt^{II} methyl complexes to (dpms)Pt^{IV}Me and promotes subsequent C-O reductive elimination. We next decided to examine if the same approach could be used for aerobic functionalization of (dpms)Pt^{II} complexes with alkenes. In this chapter oxidative functionalization of (dpms)Pt^{II}(ethylene) complexes with O_2 leading to the

ethylene oxide and ethylene glycol will be discussed. Chapter 4 will focus on the aerobic transformations of (dpms)Pt^{II} complexes with cyclic alkenes.

3.2 Results and Discussion

3.2.1 Synthesis of Pt^{II} Ethylene Complexes $LPt(CH_2CH_2)X$ (X = OH, Cl)

Preparation of chloro ethylene LPt^{II} complex **3.1** (L = dpms) was achieved by reacting equivalent amounts of Zeise's salt $K[PtCl_3(CH_2{=}CH_2)]{*}H_2O$[92] and potassium salt of the dpms ligand K(L) in aqueous solution at room temperature (eq. 3.3, Scheme 3.3)

$$K[Pt^{II}Cl_3(\eta^2\text{-}C_2H_4)] + K(L) \rightarrow \underset{\mathbf{3.1}}{LPt^{II}(\eta^2\text{-}C_2H_4)Cl} + 2\ KCl \qquad (3.3)$$

Scheme 3.3. Preparation of ethylene Pt^{II} complexes

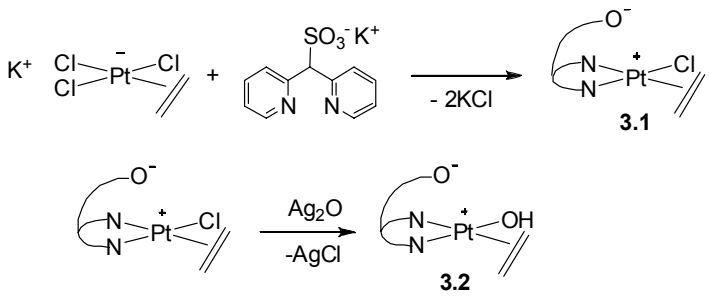

The poorly soluble **3.2** was isolated in analytically pure form in 80% yield and was characterized by NMR spectroscpy, ESI mass spectrometry, X-ray diffraction and elemental analysis. Platinum-coordinated ethylene exhibited two multiplets with the platinum-195 satellites at 4.9 ppm and 5.1 ppm ($^2J_{PtH}$ = 55 Hz) integrating as 2H each per one dpms ligand. The ethylene resonances were downfield shifted as compared to the 4.6 ppm signal ($^2J_{PtH}$ = 67 Hz) observed for Zeise's salt[92] and upfield shifted compared to free ethylene (5.4 ppm).[32]

The X-ray structure of **3.1** in shown in Fig. 3.1. The platinum atom in **3.1** is four-coordinate and has a square planar environment with the angle between the platinum coordination plane and the mean plane of the ethylene ligand of 89.9° (Fig. 3.1). The length of the C-C bond in the coordinated olefin, 1.378 Å, is greater than in free ethylene (1.337 Å) and is almost the same as in Zeise's salt, 1.375 Å.[32]

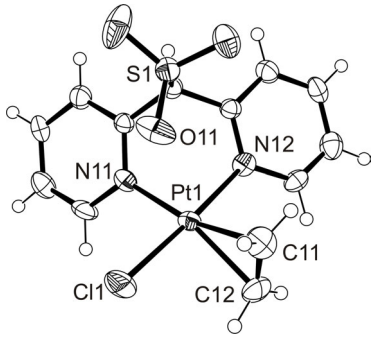

Figure 3.1. ORTEP drawings of complex **3.1**, 50% probability ellipsoids. Selected bond distances, Å: Pt1-O11, 2.890(9); Pt1-C12, 2.180(8); Pt1-C11, 2.156(9); Pt1-N11, 2.062(7); Pt1-N12, 2.013(6); Pt1-Cl1, 2.295(3); C11-C12, 1.379(11).

The Pt^{II}-alkene bond is generally described using the Dewar-Chatt-Duncanson model.[32, 33] This model involves a σ-component resulting from donation of π-electrons of the C=C bond to the d_σ orbital of a metal and π-back donation from d_π orbital of a metal to an alkene lowest unoccupied molecular orbital (LUMO), π^* of C=C (Fig. 3.2a). The olefin-to-metal σ-donation makes the olefin susceptible to nucleophilic attacks. The π-back donation is considered as a main factor contributing to the lengthening of the C=C bond and to the upfield shift of coordinated alkene protons and carbons in ^1H spectra compared to the free alkene. As a results, in ethylene complexes with transition metals the CH_2 planes are usually distorted from the ideal planar geometry of free ethylene, to some extent approaching to the limiting metallacyclopropane structure, depending on the degree of π-back donation (Fig. 3.2b).[33] The strength of π-back donation also affects the

susceptibility of coordinated alkene toward nucleophilic attack: the coordinated alkene becomes less electrophilic with increasing π-back donation.[32]

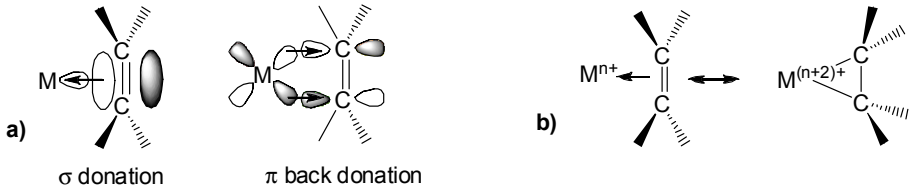

Figure 3.2. Dewar-Chatt-Duncanson model of alkene bonding in transition metal complexes.

The geometry of the coordinated ethylene in complex **3.1** is not significantly distorted from the planar geometry of free alkene and hydrogen atoms of ethylene are only slightly bent away from the metal center, indicative of weak π-back donation to ethylene. Therefore, we expected the (dpms)PtCl(CH_2CH_2) and similar complexes to be susceptible to nucleophilic attack.

The analogous hydroxo ethylene complex $LPt^{II}(CH_2CH_2)OH$ (**3.2**) was prepared by chloride abstraction from **3.1** with 1.3 equivalent of silver(I) oxide Ag_2O under an argon atmosphere in deaerated water at room temperature (eq. 3.4, Scheme 3.3) in virtually quantitative NMR yield.

$$\underset{\textbf{3.1}}{2LPt^{II}(\eta^2\text{-}C_2H_4)Cl} + Ag_2O + H_2O \rightarrow \underset{\textbf{3.2}}{2LPt^{II}(\eta^2\text{-}C_2H_4)OH} + 2AgCl \qquad (3.4)$$

Analytically pure **3.2** was isolated from a pale yellow solution, obtained upon centrifugation of silver compounds, in 76% yield, and was characterized by NMR spectroscopy, ESI mass spectrometry and elemental analysis.

In ^1H NMR spectrum of **3.2**, the platinum-coordinated ethylene exhibited two multiplets centered at 4.7 and 5.0 ppm with each multiplet integrating as 2H per one dpms ligand. Since chemical shifts of bound ethylene are upfield shifted in hydroxo complex **3.2**, compared to the chloro complex **3.1**, indicative of a greater degree of π-

back donation, one might expect that **3.2** would be less reactive toward nucleophilic attack than complex **3.1**. Ethylene carbon gave rise to a peak at 78.6 ppm in ^{13}C NMR spectrum of **3.2** accompanied by platinum-195 satellites, $^{1}J_{PtC}$ = 180 Hz. Aqueous solutions of analytically pure complex **3.2** are slightly alkaline (pH ~ 8), due to the weakly basic nature of the $Pt^{II}(OH)$ fragment. The equilibrium constant for the basic hydrolysis K_b (eq. 3.5) in aqueous solution was determined by potentiometric titration and was found to be $1.0 \cdot 10^{-11}$; accordingly, the *pH* of 50 mM solution of **3.2** in water should be equal to 7.8, matching our observations.

$$\underset{\mathbf{3.2}}{LPt^{II}(\eta^2\text{-}C_2H_4)(OH)} + H_2O \overset{K_b}{\rightleftharpoons} \underset{\mathbf{3.2*H^+}}{LPt^{II}(\eta^2\text{-}C_2H_4)(OH_2)^+} + OH^- \qquad (3.5)$$

Upon acidification of an aqueous neutral solution of **3.2** with HBF_4, an upfield shift is observed in ^{1}H NMR spectrum for the ethylene protons, due to the protonation of the Pt-OH group to form a cationic aqua complex $[(dpms)Pt(C_2H_4)(OH_2)]^+$, **3.2***$H^+$.

3.2.2 Nucleophilic Addition of OH^- to $LPt^{II}(C_2H_4)X$ Complexes to Produce $[LPt^{II}(C_2H_4OH)X]^-$ (X = Cl, OH)

Nucleophilic addition of hydroxide to $LPt^{II}(CH_2CH_2)Cl$ was achieved by reacting complex **3.1** with 4 equivalents of NaOH in deaerated D_2O under an argon atmosphere at room temperature. According to ^{1}H NMR, all starting material **3.1** had disappeared by 10 minutes of reaction time, and two new products were detected in the resulting clear colorless solution. The major product, obtained in 96% yield after 10 minutes, was identified as 2-hydroxyethyl chloro complex $Na[LPt^{II}(CH_2CH_2OH)Cl]$, **3.3**, and resulted from a nucleophilic attack of OH^- at the ethylene ligand in **3.1** (eq. 3.6). The minor product, produced in 4% yield after 10

minutes, was identified as 2-hydroxyethyl hydroxo complex $Na[LPt^{II}(CH_2CH_2OH)(OH)]$, **3.4**, and resulted from Cl/OH ligand exchange in complex **3.3** (eq. 3.7).

$$\underset{\mathbf{3.1}}{LPt^{II}(\eta^2\text{-}C_2H_4)Cl} + NaOH \rightleftharpoons \underset{\mathbf{3.3}}{Na[LPt^{II}(CH_2CH_2OH)Cl]} \qquad (3.6)$$

$$\underset{\mathbf{3.3}}{Na[LPt^{II}(C_2H_4OH)Cl]} + NaOH \rightarrow \underset{\mathbf{3.4}}{Na[LPt^{II}(C_2H_4OH)OH]} + NaCl \qquad (3.7)$$

The ratio of **3.4**/**3.3** increased over time due to a slow Cl/OH ligand exchange (eq. 3.7) in the presence of excess NaOH with a half-life of 16 hours for complex **3.3** under the above conditions. The ligand exchange was complete after 8 days to produce complex **3.4** as the sole water-soluble product.

Nucleophilic attack of hydroxide at the ethylene ligand in **3.1** leading to **3.3** is a reversible reaction, as confirmed in the following experiment.

A 4.0 mM solution of complex **3.1** was allowed to react with approximately 1 equivalent of NaOD in D_2O solution. According to ^1H NMR, the resulting solution contained a mixture of complexes **3.1**, **3.3** and **3.2** in a 6 : 87 : 7 molar ratio after 10-15 minutes after its preparation. Complex **3.2** could result from the reverse reaction given by eq. 3.6 and subsequent Cl/OH ligand exchange in **3.1** to produce complex **3.2** (eq. 3.8).

$$\underset{\mathbf{3.1}}{LPt^{II}(\eta^2\text{-}C_2H_4)Cl} + NaOH \rightarrow \underset{\mathbf{3.2}}{LPt^{II}(\eta^2\text{-}CH_2CH_2)OH} + NaCl \qquad (3.8)$$

After 1 hour the molar ratio of **3.1**, **3.3** and **3.2** in products in the reaction mixture was found to be 6 : 84 : 10. The addition of 1 equivalent of HBF_4 to the resulting solution produced complexes **3.1** and **3.2** in an 85 : 15 ratio (eq. 3.9). The ratio did

not change after one day. Hence, we can conclude that the nucleophilic addition of hydroxide to **3.1** (eq. 3.6) is fully reversible.

$$\underset{\textbf{3.3}}{Na[LPt^{II}(CH_2CH_2OH)Cl]} + HBF_4 \rightarrow \underset{\textbf{3.1}}{LPt^{II}(CH_2CH_2)Cl} + NaBF_4 + H_2O \quad (3.9)$$

Similarly, nucleophilic attack of hydroxide at a double bond of ethylene on hydroxo complex $LPt(CH_2CH_2)(OH)$ was achieved by reacting chloride-free 4 mM solution of **3.2** with 1.4-fold excess of NaOH under as argon atmosphere to give clear yellowish solution of **3.4** (eq. 3.10).

$$\underset{\textbf{3.2}}{LPt^{II}(\eta^2\text{-}C_2H_4)OH} + OH^- \overset{K}{\rightleftharpoons} \underset{\textbf{3.4}}{[LPt^{II}(CH_2CH_2OH)OH]^-} \quad (3.10)$$

According to ^{1}H NMR, complex **3.4** formed quantitatively as the sole product. The identity of anionic **3.4** was confirmed by ESI mass spectrometry of the alkaline solutions prepared in deaerated H_2O. The complex decomposed slowly in strongly alkaline solutions (pH > 10) with a half-life *ca* 28 hours at room temperature leading to formation of an unidentified dark precipitate.

The reversibility of the nucleophilic addition of hydroxide to the ethylene ligands in **3.2** was demonstrated in the following experiment. A solution of $LPt^{II}(CH_2CH_2)OH$, **3.2**, in deaerated D_2O was combined with one equivalent of NaOH under an argon atmosphere. According to ^{1}H NMR spectroscopy, in 10 minutes after its preparation the reaction mixture contained **3.4** and **3.2** in a 77 : 23 ratio. This ratio remained unchanged during the course of 10 hours, thereby suggesting that a dynamic equilibrium had been reached (eq. 3.10). When this mixture was combined with one equivalent of HBF_4 in D_2O, $LPt^{II}(CH_2CH_2)OH$ formed as the sole product quantitatively in less than 10 minutes (eq. 3.11):

$$\underset{\textbf{3.4}}{Na[LPt^{II}(CH_2CH_2OH)OH]} + HBF_4 \rightarrow \underset{\textbf{3.2}}{LPt^{II}(C_2H_4)OH} + NaBF_4 + H_2O \qquad (3.11)$$

Having established reversibility of the addition of OH^- to **3.2**, we were able to estimate the equilibrium constant *K* for reaction given by equation 3.10. A potentiometric determination of $[D^+]$[93, 94] combined with ^1H NMR measurements of the [**5b**]/[**4b**] ratio in alkaline D_2O solutions of **4b** at several *pD* values gave the equilibrium constant *K* value of $(3\pm1)\cdot10^6$ at 20 °C.

It was of note that the ratio 77 : 23 of 2-hydroxyethyl : ethylene hydroxo complexes **3.4** : **3.2**, formed by reacting **3.2** with 1 equivalent of NaOH, was lower than the 87 : 6 ratio of the chloro-analogues **3.3** : **3.1**, obtained by reacting **3.1** with 1 equivalent of NaOH under analogous reaction conditions. This result implies that the chloro ethylene complex **3.1** was more electrophilic than the hydroxo complex **3.2**.

The higher electrophilicity of complex **3.1** compared to **3.2** was also confirmed by another experiment. Complex **3.1** was combined wiht 1 equivalent of NaOD in deaerated D_2O under an argon atmosphere, and the composition of the reaction mixture was monitored by ^1H NMR spectroscopy at room temperature.

Complexes **3.1**, **3.2** and **3.3** were present in solution, with complex **3.3** being the major product in the beginning of reaction (>90%). Complex **3.4** was not detected during the course of the experiment. The plot of concentrations of complexes **3.1**, **3.2** and **3.1** *vs.* time is given in Fig. 3.3.

The concentration of **3.3** decreased over time due to reversible elimination of OH^- to give **3.1** (eq. 3.6, reverse reaction). The reaction was driven by an irreversible Cl/OH ligand exchange in complex **3.1** (eq. 3.7), which consumed NaOH released by **3.3** (Scheme 3.4).

An alternative pathway could involve the Cl/OH ligand exchange in **3.3** leading to **3.4**, which could subsequently produce **3.2**. However, one might expect that the Cl/OH ligand exchange occurs faster in a neutral complex **3.1** to give **3.2**, compared to the Cl/OH ligand exchange in anionic and therefore less electrophilic complex **3.3** leading to **3.4**.

Scheme 3.4

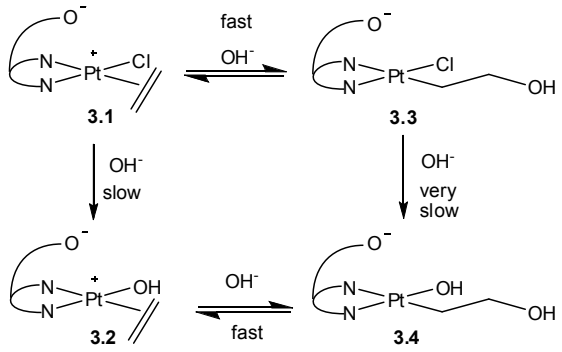

Notably, no 2-hydroxyethyl complex **3.4** was observed by ^{1}H NMR spectroscopy in a solution containg **3.1**, **3.2** and **3.3**. Therefore, under identical reaction conditions and *pH* the hydroxo complex **3.2** was less electrophilic than the chloro analogue **3.1** and was not able to compete with **3.1** for nucleophilic hydroxide anion. Trace amounts (< 1 mM) of free ethylene were seen in the reaction mixture after 5 hours due to slow decomposition of platinum complexes.

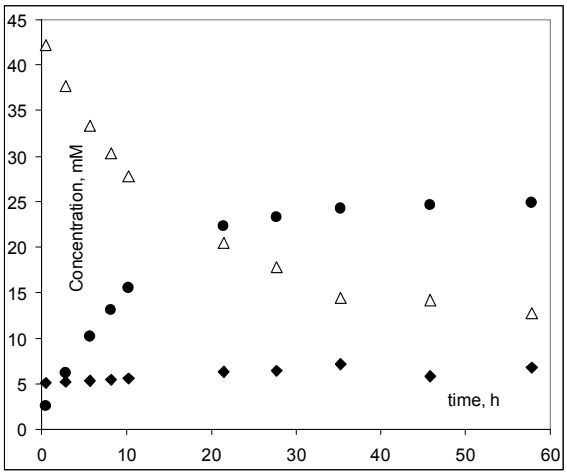

Figure 3.3. Transformations of a mixture of $LPt^{II}(CH_2CH_2OH)Cl^-$, **3.3** (empty triangles), $LPt^{II}(CH_2CH_2)Cl$, **3.1** (rhombs) and $LPt^{II}(CH_2CH_2)OH$, **3.2** (filled circles), prepared from equimolar amounts of **3.1** and NaOH in D_2O under an argon atmosphere; $[Pt]_0 = 50$ mM, $[NaOH]_0 = 50$ mM.

3.2.3 Oxidation of $LPt^{II}(CH_2CH_2)(X)$ (X=OH, Cl) in Aqueous Solution

3.2.3.1 Oxidation of $LPt^{II}(CH_2CH_2)X$ (X = OH, Cl) by Molecular Oxygen or H_2O_2.

Our next goal was to explore reactivity of (dpms)Pt$(CH_2CH_2)(X)$ toward aerobic oxidation in neutral aqueous solutions. The oxidation of hydroxo Pt^{II} ethylene complex **3.2**, LPt$(CH_2CH_2)(OH)$, in neutral solutions under an ambient atmosphere of O_2 is facile at room temperature and is accompanied by nucleophilic attack at the olefin to cleanly produce unsymmetrical hydroxyethyl Pt^{IV} complex *unsym*-LPt$(CH_2CH_2OH)(OH)_2$, **3.5** (eq. 3.12, Scheme 3.5).

$$\underset{\textbf{3.2}}{2LPt^{II}(\eta^2\text{-}C_2H_4)OH} + 2H_2O + O_2 \rightarrow \underset{\textbf{3.5}}{2LPt^{IV}(CH_2CH_2OH)(OH)_2} \qquad (3.12)$$

According to ^{1}H NMR, the oxidation was complete after 5 days at 20 ^{o}C to give **3.5** in virtually quantitative yield; no intermediate platinum complexes were detected. A similar reaction under air was approximately five times slower. Complex *unsym*-$LPt^{IV}(CH_2CH_2OH)(OH)_2$, **3.5**, was isolated in high yield in an analytically pure form and characterized by NMR spectroscopy, ESI mass spectrometry and elemental analysis.

Scheme 3.5. Oxidation of LPt(ethylene) complexes with O_2.

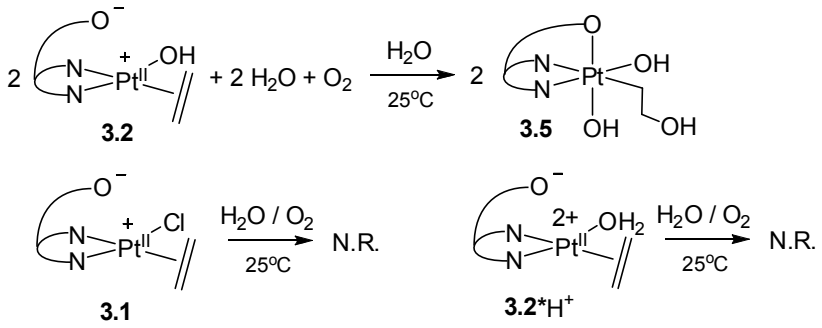

The observed pseudo-order rate constant of the reaction (3.12) performed under 1 atmosphere of O_2 was $(8.2\pm0.2)\cdot10^{-6}$ s^{-1} at 20 °C in D_2O solution (half-life 23.5 hours). Volumetric studies of the oxidation of an aqueous solution of **3.2** with O_2 confirmed the stoichiometry of the reaction shown in eq. 3.12 and showed that on average 0.54±0.02 mole of O_2 is consumed per 1 mole of **3.2**.

Interestingly, attempted oxidation of the aqueous solution of cationic aqua complex $LPt(CH_2CH_2)(OH_2)^+BF_4^-$ (**3.2***H^+), obtained by reacting **3.2** with 1.5 equivalent of HBF_4, gave no oxidation products after 4 days at room temperature. The slow displacement of ethylene by water took place in acidic solution of **3.2***H^+ to give $[LPt(OH_2)_2]^+BF_4^-$ and free ethylene with a half-life of **3.2***H^+ of *ca* 65 hours at 20 °C.

$$LPt^{II}(\eta^2\text{-}C_2H_4)OH \;+\; HBF_4 \;\rightarrow\; [LPt^{II}(CH_2CH_2)(OH_2)]BF_4 \qquad (3.13)$$

There are several factors that could be responsible for the lack of oxidation activity of **3.2** in low *pH* environments. Due to the net positive charge of $[LPt(CH_2CH_2)(OH_2)]^+$, the energy of the HOMO is expected to be lower in **3.2***H^+, compared to neutral **3.2**, thus preventing **3.2***H^+ from oxidation. Similarly, Bercaw *et al.* observed significantly higher irreversible one-electron oxidation potentials for cationic $[(NN)PtMe(MeCN)]^+$ complexes with α-diimine ligand NN, compared to neutral species $[(NN)PtMe_2]$,

[(NN)PtMeCl] or even [(NN)$PtCl_2$] (NN = ArN=CR′-CR′=NAr; Ar = 2,6-(*i*-Pr)$_2C_6H_3$, R′ = Me).[95]

Additionally, transformation of a zwitterionic olefinic **3.2** into more electron rich anionic hydroxyethyl **3.4** may be required prior to oxidation with O_2 in neutral solutions (Scheme 3.6).

Scheme 3.6

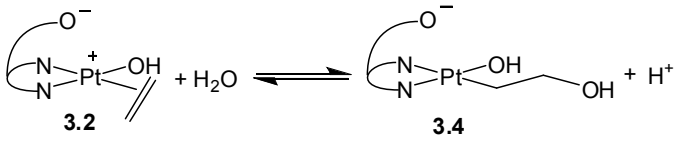

Although the hydroxyethyl anionic complex **3.4** is present only in trace amounts that can be detected by ^{1}H NMR spectroscopy in neutral solutions, it can be responsible for the reactivity toward oxidation due to better σ-donating ability of the 2-hydroxyethyl ligand compared to **3.2** containing π-acceptor ethylene ligand. In acidic solutions, the equilibrium is shifted toward the olefinic complex **3.2**, thus suppressing aerobic oxidation.[62]

In contrast to a neutral solution of **3.2**, the chloro complex LPtCl(CH_2CH_2) **3.1** was found to be stable toward O_2 for several days at room temperature. However, in the presence of a stronger oxidant, an excess of aqueous H_2O_2, complex **3.1** is oxidized towards the corresponding 2-hydroxyethyl chloro hydroxo platinum(IV) complex $LPt^{IV}(OH)(CH_2CH_2OH)(Cl)$, **3.6** (eq. 3.14), quantitatively by ^{1}H NMR. The product was obtained in an analytically pure form in 82% isolated yield and was charactrerized by NMR spectroscopy, ESI mass spectrometry and elemental analysis.

$$\underset{\textbf{3.1}}{LPt^{II}(\eta^2\text{-}CH_2CH_2)Cl} + H_2O_2 \rightarrow \underset{\textbf{3.6}}{LPt^{IV}(OH)(CH_2CH_2OH)(Cl)} \qquad (3.14)$$

3.2.3.2 Oxidation of $LPt^{II}(CH_2CH_2)Cl$ by O_2 in the Presence of 1 Equivalent of NaOH.

Interestingly, when complex **3.2** was allowed to react with O_2 in the presence of approximately one equivalent of NaOH in aqueous solution, the product *unsym*-$LPt^{IV}(CH_2CH_2OH)(OH)$, **3.5**, was obtained cleanly, whereas no traces of **3.6** were detected by ^1H NMR spectroscopy and ESI mass spectrometry when the oxidation was complete after 3 days.

The oxidation of **3.1** with O_2 in the presence of 1 equivalent of hydroxide was monitored by ^1H NMR spectroscopy. A fresh solution of $Na[LPt^{II}(CH_2CH_2OD)Cl]$ prepared from **3.1** and one equivalent of NaOD in D_2O and characterized by the total concentration of platinum of 50 mM was stirred under 1 atmosphere of oxygen at room temperature for several days. The presence of complexes **3.1**, **3.2**, **3.3** and **3.5** was detected in the reaction mixture by ^1H NMR spectroscopy and ESI mass spectrometry. Small amounts of $LPt^{II}(OH)_2^-$ (<5%)[79] resulting from the loss of ethylene ligand were seen by the end of reaction. Since the chloro complex **3.6** was not detected after the reaction was complete, we can conclude that the chloro complexes **3.1** and **3.3** were inert toward O_2, and the formation of **3.5** was due to the Cl/OH ligand exchange in **3.1** or **3.3**.

The plot of concentrations of $LPt^{II}(CH_2CH_2OH)Cl^-$, $LPt^{II}(CH_2CH_2)Cl$, $LPt^{II}(CH_2CH_2)OH$ and *unsym*-$LPt^{IV}(OH)_2(CH_2CH_2OH)$ *vs.* time is given in Fig. 3.4.

Complex **3.3** persisted as the major component of the reaction mixture during first 10-15 minutes and disappeared with a half-life of 10 hours to give **3.5**. Complex **3.2**, resulting from the Cl/OH ligand exchange in **3.1** (eq. 3.8), was detected in low concentrations (≤1 mM) and disappeared when the reaction was complete. The

concentration of another ethylene complex, **3.1**, decreased rapidly in the course of the reaction.

The formation of **3.2** resulting from the Cl/OH exchange in **3.1** in the presence of 1 equivalent of NaOH was also observed in the absence of O_2, under an argon atmosphere, as described above (Scheme 3.5, Fig. 3.3). However, in the absence of O_2 the fraction of the hydroxo complex **3.2** in the reaction mixture was much greater, compared to the experiment performed under O_2. Therefore, we can propose that the oxidation of **3.1** in the presence of 1 equivalent of NaOH proceeds via inial Cl/OH ligand exchange to form **3.2** (eq. 3.8), which is subsequently oxidized with O_2 as discussed above (Scheme 3.7).

Scheme 3.7

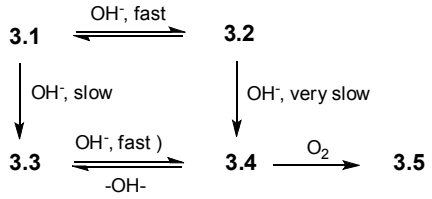

The rate of disappearance of **3.3** in the experiment performed under oxygen atmosphere was not significantly different from that in analogous experiment under argon. The half-life was about 15 hours in both cases, consistent with inertness of **3.3** toward O_2. The rate limiting step of the indirect aerobic oxidation of **3.3** might be its irreversible transformation to **3.2** via **3.1**.

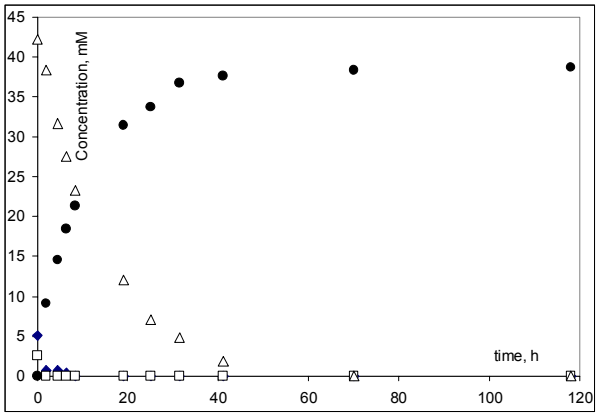

Figure 3.4. Transformations of $LPt^{II}(CH_2CH_2OH)Cl$ (empty triangles), $LPt^{II}(CH_2CH_2)Cl$ (empty squares), $LPt^{II}(CH_2CH_2)OH$ (rhombs) and *unsym*-$LPt^{IV}(OH)_2(CH_2CH_2OH)$ (filled circles) prepared from equimolar amounts of **3.1** and NaOH in D_2O under an O_2 atmosphere; $[Pt]_0 = 50$ mM.

Therefore, the presence of chloro ligand is detrimental for aerobic oxidation of neutral olefinic and anionic hydroxyethyl complexes. This result is consistent with observations of Bercaw and Rostovtsev who showed that, unlike easily oxidizable $(tmeda)PtMe_2$ complexes, more electron deficient $(tmeda)Pt^{II}MeCl$ and $(tmeda)Pt^{II}Cl_2$ species do not react with O_2.[43] This effect was explained by the chloro complexes possessing a lower energy HOMO when compared to the more electron rich $(tmeda)PtMe_2$.[43]

To get an estimate of the effects of the ligand X and the formal charge on the platinum atom on the energy of the HOMO in ethylene and hydroxyethyl $(dpms)Pt^{II}$ complexes, we carried out DFT calculations on neutral $LPt(CH_2CH_2)X$ and anionic complexes $[LPt(CH_2CH_2OH)X]^-$ **3.1-3.4** and a cationic complex $[LPt(C_2H_4)(OH_2)]^+$ (gas phase values, Table 3.1). All DFT calculations discussed in this work were done by Dr. Vedernikov.

According to our results, if oxidation reaction operates by the same mechanism involving an electron transfer between the Pt^{II} atom and an oxidant, the reactivity of Pt^{II} complexes towards the oxidant would increase in the series: $LPt^{II}(C_2H_4)OH_2^+$ <

$LPt^{II}(C_2H_4)Cl$ < $LPt^{II}(C_2H_4)OH$ < $[LPt^{II}(C_2H_4OH)Cl]^-$ < $[LPt^{II}(C_2H_4OH)OH]^-$. Therefore, the DFT-predicted trend was consistent with the experimentally observed inertness of the cationic complex **3.2***H^+ and chloro-complexes **3.3** and **3.1** and explains higher reactivity of the hydroxo complex **3.4**.

Table 3.1. DFT calculated energy of the HOMO of cationic, neutral and anionic Pt^{II} dpms complexes in the gas phase, eV.

Complex	DFT calculated energy of HOMO, eV
$[LPt^{II}(CH_2CH_2)OH_2]^+$	-9.08
$LPt^{II}(CH_2CH_2)Cl$	-5.51
$LPt^{II}(CH_2CH_2)OH$	-5.26
$[LPt^{II}(C_2H_4OH)Cl]^-$	-1.95
$[LPt^{II}(C_2H_4OH)OH]^-$	-1.51

3.2.3.3 Oxidation of $LPt^{II}(CH_2CH_2)OH$ by O_2 in the Presence of Variable Amounts of NaOH.

To find out whether or not complex **3.5** resulted from the direct oxidation of the anionic hydroxyethyl complex **3.4** rather than oxidation of the neutral hydroxo ethylene complex **3.2** we determined the NMR yield of complex **3.5** formed in a reaction between mixtures of **3.2** + **3.4** and dioxygen (1 atmosphere) as a function of concentration of NaOH. ^1H NMR analysis of the reaction mixtures before oxidation showed that, as the concentration of NaOH increased, the fraction of the anionic Pt^{II} complex **3.4** increased from 4% to 100% due to the equilibrium shift (eq. 3.10) to the right (Table 3.2, second column). The yield of the oxidation product, **3.5**, was measured after 60 minutes of stirring the reaction mixture under O_2 (Table 3.2). Notably, the yield of **3.5** increased more than tenfold in the presence NaOH additives (0.12-0.35 equiv. NaOH) as compared to an NaOH–free solution. The yield passed

through a maximum at approximately 0.23 equivalents of NaOH (4.0 mM) and then decreased slowly as the amount of NaOH increased to 1.4 equivalents (26 mM). The significant acceleration of the reaction at low [NaOH] can be considered as evidence of a direct oxidation of the anionic complex **3.4** by O_2. Similarly, Bercaw and Labinger found that the oxidation of Zeise's salt $[Pt^{II}Cl_3(\eta^2\text{-}CH_2CH_2)]^-$ with $[Pt^{IV}Cl_6]^{2-}$ was preceded by the nucleophilic addition of hydroxide at the ethylene to form hydroxyethyl complex $[Pt^{II}Cl_3(CH_2CH_2OH)]^{2-}$, which was more reactive toward oxidation compared to the ethylene adduct $[Pt^{II}Cl_3(\eta^2\text{-}CH_2CH_2)]^-$.[62]

Table 3.2. Results of oxidation of 18 mM $LPt^{II}(CH_2CH_2)OH$, **3.2**, in water as a function of concentration of additives of NaOH after 60 min of reaction at 20 °C and 1 atm O_2.

NaOH, equiv. ([NaOH], mM)	**3.4** before oxidation, %	Yield of **3.5**, %[a]	**3.2** + **3.4**, %[a,b]
0 (0)	<4	7±2	93±2
0.06 (1.1)	6	47±2	54±2
0.12 (2.1)	9	72±1	29±2
0.23 (4.0)	19	78±1	21±2
0.35 (6.2)	29	71±1	24±2
0.57 (10.0)	55	56±1	42±1
0.85 (15.0)	82	37±1	58±2
1.4 (25)	100	20±2	80±2

[a] Average of 3 runs
[b] Unreacted $LPt^{II}(CH_2CH_2)(OH)$, **3.2**, and $LPt^{II}(CH_2CH_2OH)OH^-$, **3.4**, combined.

A partial inhibition of oxidation reaction (3.12) at higher concentrations of NaOH is similar to the inhibition of the oxidation of methyl platinum complex at high NaOH concentration described in Chapter 2. We propose that the mechanism of the oxidation of hydroxyethyl complex **3.4** is similar to the mechanism of the aerobic oxidation of methyl complex $[LPtMe(OH)]^-$ (eq. 3.15-3.17, R = CH_2CH_2OH, L = dpms; Scheme 3.6). Inhibition of the oxidation of Pt^{II} complexes $[LPt^{II}R(OH)]^-$ (R =

CH_2CH_2OH; L = dpms) at high OH^- concentration can be explained by the involvement of a proton-coupled electron transfer between Pt center and a coordinated O_2 ligand in paramagnetic dioxygen adduct $[LPt(R)(OH)(O_2)]^-$, **3.7** (which can also be represented as a Pt^{III} superoxide in the limiting case), at the rate-limiting step of the formation of the diamagnetic hydroperoxo intermediate $[LPt^{IV}(R)(OOH)(OH)]$, **3.8**. The subsequent fast reaction between the hydroperoxo complex $[LPt^{IV}(R)(OOH)(OH)]$ and another molecule of $[LPt^{II}(R)(OH)]^-$ then produced two equivalents of $LPt^{IV}(R)(OH)_2$, consistent with our volumetric measurements, which showed the uptake up of 0.54±0.2 equivalents of O_2 per mole of $LPt^{IV}(CH_2CH_2OH)(OH)_2$ formed.

$$\underset{\textbf{3.4}}{LPt^{II}(R)OH^-} + O_2 \rightarrow \underset{\textbf{3.7}}{(\eta^2\text{-}L)Pt^{II}(\eta^1\text{-}O_2)(R)OH^-} \quad (3.15)$$

$$\underset{\textbf{3.7}}{(\eta^2\text{-}L)LPt^{II}(\eta^1\text{-}O_2)(R)OH^-} + H^+ \rightarrow \underset{\textbf{3.8}}{(\eta^3\text{-}L)LPt^{IV}(O_2H)(R)OH} \quad (3.16)$$

$$\underset{\textbf{3.8}}{LPt^{IV}(O_2H)(R)OH} + \underset{\textbf{3.4}}{LPt^{II}(R)OH^-} + H_2O \rightarrow 2\underset{\textbf{3.5}}{LPt^{IV}(R)(OH)_2} + OH^- \quad (3.17)$$

The proposed mechanism should be inhibited by electron-withdrawing ligands X in hydroxyethyl complex $[LPt(CH_2CH_2OH)X]^-$, which would decrease the energy of the metal complex HOMO. Accordingly, unlike hydroxo complex **3.4**, the chloro complex **3.3** was found to be unreactive toward O_2.

*3.2.3.4 Qualitative Analysis of the Observed pH-Dependence of the Rate of Oxidation of **3.2** in Alkaline Solutions.*

Based on the observations above we suggested a qualitative kinetic scheme that allows to account for the observed *pH*-dependence of rate of oxidation of **3.2** in

alkaline solutions (Table 3.2). The analysis was based on the following established facts and/or assumptions: (i) formation of **3.4** from **3.2** and OH^- is reversible (rate constants k_1 and k_{-1}; $K=k_1/k_{-1}$); (ii) oxidation of **3.4** proceeds via a triplet η^1-dioxygen adduct **3.7**, $[LPt^{II}(\eta^1\text{-}O_2)(C_2H_4OH)OH]^-$ (eq. 3.15), formation of which is reversible (rate constants k_2 and k_{-2}); (iii) a rate-determining protonation of an anionic triplet adduct **3.7** to form a diamagnetic Pt^{IV} hydroperoxo complex **3.8**, $LPt^{IV}(O_2H)(C_2H_4OH)OH$, (eq. 3.16) is irreversible.[43] The protonation of **3.7** is coupled to a spin interconversion in triplet **3.7** and oxidation to Pt^{IV} (rate constant k_3); (iv) subsequent reaction of **3.8** with Pt^{II} complex **3.4** leading to **3.5** is fast (Scheme 3.8).[43]

Scheme 3.8

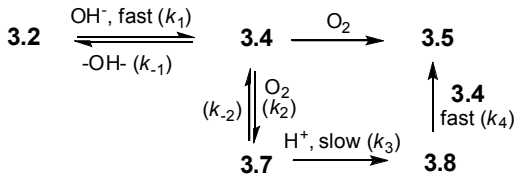

Using steady-state approximation for intermediates **3.4**, **3.7** and **3.8** and assuming that formation of **3.7** from **3.4** occurs much slower than addition of OH^- to **3.2**, the following rate law was obtained (eq. 3.18):

$$\frac{dC}{dt} = k_2 \frac{k_3[H^+]}{(k_{-2} + k_3[H^+])} \frac{KK_w}{(KK_w + [H^+])}[O_2]C \qquad (3.18)$$

where K_w is the ionization constant for water and C is combined concentration of **3.2** and **3.4**.

No sign of mass misbalance was observed by ^1H NMR spectroscopy even in strongly alkaline solutions of **3.4** under an O_2 atmosphere, when oxidation of **3.4** is inhibited by hydroxide anions and is very slow. Hence, formation of a paramagnetic

NMR-silent intermediate **3.7** is thermodynamically unfavorable and reversible. In the opposite case, if formation of **3.7** were irreversible ($k_{-2} = 0$), noticeable amounts of paramagnetic **3.7** should be accumulated leading to a mass misbalance, which was not observed in our experiments. Similar conclusion was made in the case of aerobic oxidation of $[LPtMe(OH)]^-$ complexes discussed in Chapter 2.

The rate law given by eq. 3.18 allows to account for the observed *pH*-dependence of the oxidation rate (Table 3.2). The factor $[H^+]$ in numerator of eq. 3.18 might cancel out in the following two limiting cases that would lead to the disappearance of the maximum for the pH dependence: i) in the case of weak binding of hydroxide by complex **3.2** (eq. 3.10), so that $KK_w << [H^+]$. In fact, $KK_w = 3 \cdot 10^{-9}$, whereas $[D^+] \leq 1 \cdot 10^{-12}$ M for all our experiments performed in alkaline D_2O solutions (Table 3.2); ii) if $k_{-2} << k_3[H^+]$, which corresponds to the case of a fast proton-coupled electron transfer in **3.7** to give **3.8** (eq. 3.16).

To account for the presence of the maximum we must assume that transformation of **3.7** to **3.8** was the rate limiting *pH*-dependent step, $k_{-2} \geq k_3[H^+]$; the formation of **3.8** according to eq. 3.16 is inhibited by OH^-. However, the formation of complex **3.4** from **3.2** is also *pH* dependent (eq. 3.10), but with the dependence of the opposite character, so that the formation of **3.4** is accelerated at higher $[OH]^-$. Since formation of **3.4** from **3.2** occurs before the rate-limiting step (eq. 3.16) and therefore affects the rate of the overall reaction, this leads to the observed maximum on the plot of reaction (3.12) rate versus *pH*.

3.2.4 Thermal Isomerization and C-O Reductive Elimination from $LPt^{IV}(CH_2CH_2OH)(OH)(X)$ (X = OH, Cl)

It was previously established by Vedernikov[79] that C-O reductive elimination from methyl complexes *unsym*-$LPtMe(OH)_2$ (L = dpms), formed by aerobic oxidation of $LPtMe(OH_2)$ is preceded by thermal isomerization into a corresponding C_s-symmetrical isomer *sym*-$LPtMe(OH)_2$, which then undergoes C-O reductive elimination. Only symmetrical isomer was found to be reactive in the reductive elimination, whereas the *unsym*-$LPtMe(OH)_2$ was practically inert. Higher reactivity of the symmetrical isomer was explained by the position of the methyl group of *sym*-$LPtMe(OH)_2$ *trans* to sulfonate, a good leaving group, as compared to *unsym*-$LPtMe(OH)_2$, which contains Me group *trans* to pyridyl.

Similarly, thermal isomerization was observed for *unsym*-$LPt(CH_2CH_2OH)(OH)_2$ **3.5** in neutral aqueous solution with a half-life of 1 hour at 80 ^oC to produce a corresponding symmetrical isomer *sym*-$LPt(CH_2CH_2OH)(OH)_2$ **3.9** (eq. 3.19). However, subsequent C-O elimination of ethylene oxide and ethylene glycol occurred at a very fast competitive rate (eq. 3.19-3.20, Scheme 3.9). The plot of concentrations of **3.5**, **3.9**, ethylene oxide and ethylene glycol observed by ^1H NMR spectroscopy upon heating of D_2O solution of **3.5** at 80 ^oC is given in Fig. 3.5. A platinum-containing product of reductive elimination was identified as a hydroxo-bridged dimer $L_2Pt^{II}{}_2(\mu\text{-}OH)_2$, **3.10**, characterized previously.[79]

$$\underset{\textbf{3.5}}{\textit{unsym}\text{-}LPt^{IV}(CH_2CH_2OH)(OH)_2} \rightarrow \underset{\textbf{3.9}}{\textit{sym}\text{-}LPt^{IV}(CH_2CH_2OH)(OH)_2} \qquad (3.19)$$

$$2\ \underset{\textbf{3.10}}{\textit{sym}\text{-}LPt^{IV}(C_2H_4OH)(OH)_2} \rightarrow \underset{\textbf{3.10}}{L_2Pt^{II}{}_2(\mu\text{-}OH)_2} + C_2H_4O + HOC_2H_4OH + H_2O \qquad (3.20)$$

Complex **3.9** was characterized in aqueous solution by ^{1}H NMR spectroscopy without isolation. The C_s symmetry of **3.9** was evident from ^{1}H NMR spectrum: a set of four multiplets were present in the aromatic region typical for a mirror-symmetrical dpms-complex. The hydroxyethyl ligand gave rise to two sharp triplets of methylene groups with platinum satellites at 3.16 ppm (^3J = 5.8 Hz, $^3J_{195PtH}$ = 40 Hz) and 3.51 ppm (^3J = 5.8 Hz, $^3J_{195PtH}$ = 80 Hz). The organic products were identified by ^{1}H NMR spectroscopy and ESI mass spectroscopy.

Scheme 3.9

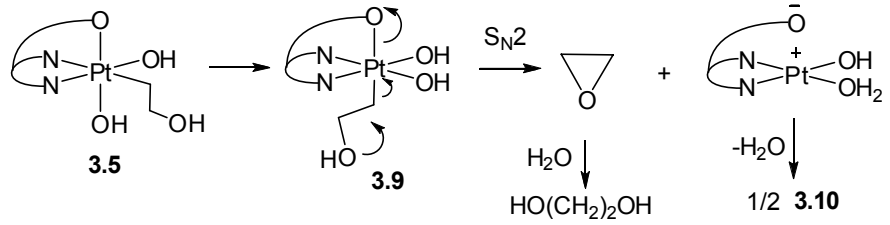

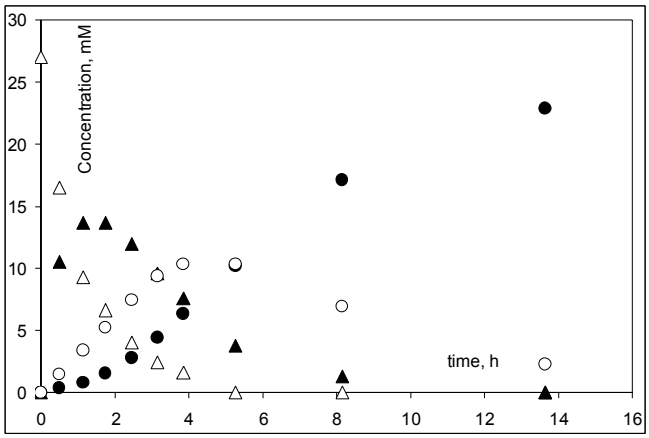

Figure 3.5. Transformations of *unsym*-LPt^{IV}(OH)$_2$(CH$_2$CH$_2$OH) (empty triangles) to *sym*-LPt^{IV}(OH)$_2$(CH$_2$CH$_2$OH) (filled triangles), ethylene oxide (empty circles) and ethylene glycol (filled circles) in neutral D_2O solution at 80 ^{o}C; $[Pt]_0$ = 27 mM.

After heating a solution of *unsym*-LPt(CH$_2$CH$_2$OH)(OH) for 5 hours at 80 ^{o}C all starting material **3.5** disappeared to give a mixture of the following water-soluble products: symmetrical isomer **3.9** (14% yield on Pt), ethylene glycol (38%) and ethylene oxide (38%). A white precipitate of insoluble dimeric **3.10** was also present.

Further heating of the reaction mixture for three more hours produced a solution containing 11% of **3.9**, 63% of ethylene glycol and 26% of ethylene oxide. The ratio of ethylene glycol to ethylene oxide changed over time due to partial hydrolysis of ethylene oxide to ethylene glycol in heated aqueous solution. Therefore, ethylene glycol could not form from ethylene glycol under these conditions and was a primary product of reductive elimination from **3.9**. The elimination of ethylene oxide can be explained by the intramolecular S_N2 attack of the OH group of CH_2CH_2OH ligand at its Pt-bound α-carbon (Scheme 3.9).[88, 89, 96] Ethylene glycol could form either via hydrolysis of ethylene oxide or by nucleophilic attack of water at the α-carbon of hydroxyethyl ligand. However, reductive elimination of ethylene oxide as via an intramolecular nucleophilic attack of the β-OH group of the hydroxyethyl ligand at its α-carbon as shown in Scheme 3.9 should be favored entropically over intermolecular reaction between water and **3.9** leading to ethylene glycol.

Interestingly, in contrast to reductive elimination from methyl complex $LPtMe(OH)_2$, no acid catalysis was required for the C-O reductive elimination from **3.9** (eq. 3.20) and fast reaction was observed even in neutral solution. The higher reactivity of *sym*-$LPt(CH_2CH_2OH)(OH)_2$, **3.9**, might be due to greater electrophilicity of the α-carbon atom of the 2-hydroxyethyl group due to the presence of the electron withdrawing hydroxy group at β-carbon. Another factor contributing to higher reactivity of **3.9** could be an entropic advantage of the intramolecular reaction: the close proximity of the β-hydroxo group to the platinum-bound carbon helps to increase the effective concentration of the nucleophile near the reactive center, thus making an S_N2 reductive elimination more entropically favorable.

Complex LPt(CH_2CH_2OH)(Cl)(OH), **3.6**, reacted in a similar way to give a mixture of ethylene glycol (yield 94%) and ethylene oxide (4%) in almost quantitative yield after 10 hours of heating at 80 ^oC in aqueous solution. The major Pt-containing product (> 80%) was identified as an unsymmetrical complex $LPt^{II}Cl(OH_2)$.

$$2LPt^{IV}(OH)(C_2H_4OH)Cl + H_2O \rightarrow 2LPt^{II}Cl(OH_2) + C_2H_4O + HOC_2H_4OH \quad (3.21)$$

No signs of isomerization of **3.6** were found in ^1H NMR spectra of the reaction mixture, presumably due to high reactivity of the isomer with 2-hydroxyethyl group *trans* to the sulfonate group of dpms. The absence of 1-chloroethanol, which is expected to be stable under these conditions, indicates that direct intramolecular C-Cl reductive elimination did not occur in complex **3.6**. This is consistent with the fact that intramolecular C(sp^3)-Cl elimination was never reported in similar complexes $[Cl_5Pt(CH_2CH_2OH)]^-$, which are more prone to an S_N2 reductive elimination in the presence of external nucleophiles.[62]

3.3 Conclusions

The dpms scaffold allows for facile aerobic oxidation of (dpms)Pt^{II}(ethylene) complexes LPt(CH_2CH_2)(OH) to hydroxyethyl Pt^{IV} species LPt(CH_2CH_2OH)$(OH)_2$ and promotes subsequent C-O reductive elimination of ethylene oxide and ethylene glycol.

The ease of oxidation of ethylene and hydroxyethyl complexes with O_2 depends on the complex net charge and nature of ligand X: chloro complexes $[LPt(CH_2CH_2OH)Cl]^-$ were unreactive toward O_2, whereas replacement of Cl with OH in the presence of 1 equivalent of NaOH led to facile oxidation that gave *unsym*-LPt(CH_2CH_2OH)$(OH)_2$.

The oxidation of $LPt(CH_2CH_2)(OH)$ by O_2 in water is facile. It occurs via initial nucleophilic attack at the ethylene ligand by hydroxide anion produced as a result of protonation of $LPt(CH_2CH_2)(OH)$ by water to give an anionic complex $[LPt(CH_2CH_2OH)(OH)]^-$. The latter is reactive toward O_2 due to the presence of a strong σ-donating 2-hydroxyethyl group and the pendant sulfonate tail of the dpms ligand.

The C-O reductive elimination from *unsym*-$LPt(CH_2CH_2OH)(OH)_2$ is facile in neutral aqueous solution upon heating at 80 ^oC and produces ethylene oxide, ethylene glycol and $L_2Pt^{II}{}_2(\mu\text{-}OH)_2$ and involves isomerization into *sym*-$LPt(CH_2CH_2OH)(OH)_2$. In conclusion, one pot stoichiometric aerobic oxidation of Pt^{II}-coordinated ethylene to ethylene oxide and ethylene glycol can be readily and efficiently performed in aqueous media, thus opening up pathways to development of the catalytic version of an aerobic oxidation of ethylene into ethylene glycol.

3.4 Experimental Section

$LPt^{II}(CH_2CH_2)Cl$, 3.1. Solution of K(L) (93.1 mg, 323 μmol) in 1 mL H_2O was added to a stirred solution of Zeise's salt $KPtCl_3(CH_2CH_2)\cdot H_2O$ (124.8 mg, 323 μmol) in 1 mL H_2O. White precipitate formed in several minutes and yellow color of Zeise's salt disappeared. The mixture was stirred for 3 h, filtered and dried under vacuum. White powder; yield 136.1 mg (80%). The complex is slightly soluble in water and methanol, stable in aqueous and methanolic solutions at room temperature under an O_2 atmosphere. It decomposes slowly upon heating with the concomitant loss of ethylene.

^{1}H NMR (D_2O, 22 ^oC), δ: 4.89 (m, 2H), 5.05 (m, $^2J_{195PtH}$=55 Hz, 2H) 6.32 (s, 1H), 7.57 (ddd, *J*=7.9, 5.9, 1.4 Hz, 1H), 7.70 (ddd, *J*=7.7, 5.9, 1.4 Hz, 1H), 7.92-8.03 (m, 2H), 8.17 (td, *J*=7.7, 1.4 Hz, 1H), 8.22 (td, *J*=7.9, 1.4 Hz, 1H), 8.54 (m, 1H), 9.04 (dd, *J*=5.9, 1.4 Hz, 1H). Coupling constant $^2J_{195PtH}$ for a multiplet at 4.89 ppm was not determined due to overlap with the HDO signal. **IR** (KBr), ν: 3122 (w), 3092 (w), 3034 (w), 2991 (w), 2953 (w), 1607 (w), 1482 (w), 1438 (w), 1377 (w), 1314 (w), 1252 (m), 1233 (s), 1175 (m), 1035 (s), 857 (w), 807 (w), 766 (s), 686 (m) cm^{-1}. **ESI-MS**, solution of **3.1** in water, m/z = 508.012. Calculated for **3.1**·H^+, $C_{13}H_{14}{}^{35}ClN_2O_3{}^{195}PtS$, 508.006. **Anal.** Found (Calcd for $C_{13}H_{13}ClN_2O_3PtS$): H, 2.38 (2.58); C, 30.49 (30.75); N, 5.41 (5.52). X-ray quality crystals of **3.1** were obtained by slow crystallization from a mixture prepared by addition of 0.1 M aqueous K(dpms) to an equal volume of 0.1 M aqueous solution of Zeise's salt placed in an NMR tube.

$LPt^{II}(CH_2CH_2)(OH)$, 3.2. Solid $LPt(CH_2CH_2)Cl$ (45.3 mg, 89.2 μmol), Ag_2O (13.7 mg, 59.1 μmol) and 2.6 mL of deaerated H_2O were placed into a 5 mL Schlenk tube, and the mixture was stirred in the dark for 1 day at room temperature under an argon atmosphere. According to ^{1}H NMR, the reaction was complete in 1 day. Yield was quantitative by NMR. The mixture was centrifuged for 30 min at 10,000 rpm, and the solution was carefully separated from the precipitate of AgCl and excess Ag_2O. The resulting pale yellow solution was evaporated to dryness under vacuum to give a yellow crystalline solid. Yield 33.3 mg (76%). The air-sensitive complex was perfectly soluble in water and moderately soluble in methanol. It slowly decomposed

in aqueous solution at room temperature, but was stable at 7-8 °C for several days under an argon atmosphere. In strongly alkaline solutions (pH > 10) formation of a black precipitate occurred.

^{1}H NMR (D_2O, 22 °C), δ: 4.69 (m, 2H, $^2J_{195PtH}$=54 Hz), 5.01 (m, $^2J_{195PtH}$=60 Hz, 2H), 6.30 (s, 1H), 7.55 (ddd, *J*=7.8, 5.8, 1.1 Hz, 1H), 7.82 (ddd, *J*=7.8, 5.8, 1.1 Hz, 1H), 7.96 (vd, *J*=7.8 Hz, 1H), 8.06 (vd, *J*=7.8 Hz, 1H), 8.15 (vt, *J*=7.8 Hz, 1H), 8.29 (vt, *J*=7.8 Hz, 1H), 8.44 (vd, *J*=5.8 Hz, 1H), 8.75 (vd, *J*=5.8 Hz, 1H). **^{13}C NMR** (D_2O, 22 °C), δ: 74.8, 78.6 (br s, $^1J_{PtC}$ 180 Hz), 126.0, 127.2, 128.9, 130.1, 141.2, 142.6, 148.3, 149.5, 149.6, 150.9. **IR** (KBr), ν: 3472 (w br), 3084 (w), 3059 (w), 2893 (w), 1605 (w), 1478 (w), 1435 (w), 1367 (w), 1314 (w), 1227 (m), 1159 (m), 1030 (s), 853 (w), 808 (w), 761 (m) cm^{-1}. **ESI-MS**, solution of **3.2** in water, m/z = 490.04173. Calculated for **3.2**·H^+, $C_{13}H_{15}N_2O_4{}^{195}PtS$, 490.040134. **Anal.** Found (Calcd for $C_{13}H_{14}O_4N_2PtS$): H, 2.62 (2.88); C, 31.94 (31.90); N, 5.40 (5.72); S, 6.71 (6.55).

Na[LPt^{II}(CH_2CH_2OH)Cl], 3.3. A sample of LPt(CH_2CH_2)Cl (27.3 mg, 54 μmol) and 1 mL of 0.2 M NaOH solution in deaerated D_2O were placed into a vial equipped with a magnetic stirring bar. The suspension was stirred under an argon atmosphere to produce a clear colorless solution in less than 10 minutes ([Pt] = 0.0538 M, [NaOH] = 0.2 M). The reaction mixture was transferred into an NMR Young tube under an argon atmosphere and the ^{1}H NMR spectrum was recorded in 10 minutes after its preparation; the ^{13}C NMR spectrum was recorded 1-3 hours after preparation. According to NMR, in 10 minutes after its preparation the solution contained 96% of **3.3** and 4% of **3.4**. The relative amounts of **3.3** and **3.4b** were calculated by

integration of multiplets of C(5)-H protons of **3.3** and **3.4** at 7.41 ppm and 7.51 ppm respectively. Slow Cl/OH exchange occurred so that in 2.3h the reaction mixture contained **3.3** and **3.4** in an 87 : 13 ratio (half-life 16.4h). The exchange was complete after 8 days to give complex **5b** as the only species detected by NMR. However, slight decomposition to form platinum black was observed.

^{1}H NMR (D_2O, 22 ^oC), δ: 1.69 (m, $^2J_{PtH}$=41 Hz, 1H), 1.98 (m, $^2J_{PtH}$=38 Hz, 1H), 3.46 (m, 2H), 5.89 (s, 1H), 7.36 (ddd, *J*=7.7, 5.8, 1.5 Hz, 1H), 7.41 (ddd, *J*=7.7, 5.5, 1.5 Hz, 1H), 7.66-7.74 (m, 2H), 7.94 (td, *J*=7.7, 1.5 Hz, 1H), 8.02 (td, *J*=7.8, 1.5 Hz, 1H), 8.75 (vd, *J*=5.8 Hz, 1H), 8.86 (vd, *J*=5.5 Hz, 1H). **^{13}C NMR** (D_2O, 22 ^oC), δ: 7.95 ($^1J_{PtC}$=728 Hz), 65.8, 76.8, 126.2, 127.2, 129.0, 130.4, 139.6, 139.8, 149.4, 151.4, 152.4, 153.6. **ESI-MS** (negative mode) of **3.3**, immediately after its preparation (pH ~ 10): m/z 524.1. Calculated for $LPt(CH_2CH_2OH)Cl^-$, $C_{13}H_{14}{}^{35}ClSO_4N_2{}^{195}Pt$, 524.0.

Na[LPt^{II}(CH_2CH_2OH)OH], 3.4

Procedure A, from 3.2. 8.8 mg (18 μmol) of $LPt(CH_2CH_2)OH$ (**3.2**) were dissolved in 1.0 mL of NaOH solution (25.2 mM) in deaerated D_2O under an argon atmosphere. The resulting yellowish solution was transferred into a NMR Young tube under argon. According to ^{1}H NMR, compound **3.4** was obtained in quantitative yield in less than 10 minutes. Complex **3.4** is air sensitive and produces **3.5** in the presence of oxygen.

Procedure B, from 3.1. A sample of $LPt(CH_2CH_2)Cl$ (27.3 mg, 54 μmol) and 1 mL of 0.2 M NaOH solution in deaerated D_2O were placed into a vial equipped with a

magnetic stirring bar. The suspension was stirred under argon to produce a clear yellowish solution in less than 10 minutes ([Pt] = 0.0538 M, [NaOH] = 0.2 M). The reaction mixture was transferred into an NMR Young tube. The Cl/OH ligand exchange was monitored by ^{1}H NMR at room temperature (half-life time 16.4h). The ligand exchange was complete in 8 days to give complex **3.4** in virtually quantitative yield. Trace amounts of a black precipitate were also observed.

^{1}H NMR (D_2O, 22 ^{o}C), δ: 1.76 (m, $^{2}J_{PtH}$=37 Hz, 1H), 1.87 (m, $^{2}J_{PtH}$=37 Hz, 1H), 3.42 (m, 1H), 3.55 (m, 1H), 7.28 (ddd, *J*=7.8, 5.5, 1.3 Hz, 1H), 7.51 (ddd, *J*=7.8, 5.5, 1.3 Hz, 1H), 7.64 (vd, *J*=7.7 Hz, 1H), 7.76 (vd, *J*=7.7 Hz, 1H), 7.98 (td, *J*=7.8, 1.5 Hz, 1H), 8.02 (td, *J*=7.8, 1.5 Hz, 1H), 8.71 (vd, *J*=5.5 Hz, 1H), 8.81 (vd, *J*=5.5 Hz, 1H) ($CHSO_3$ bridge peak was not seen due to complete H/D exchange in basic solution).

^{13}C NMR (D_2O, 22 ^{o}C), δ: 9.1, 64.8, 125.5, 126.3, 128.3, 129.5, 137.9, 139.0, 148.9, 151.8, 153.3 ($CDSO_3$ peak was not seen because of carbon - deuterium coupling and low intensity of resulting lines). **ESI-MS** (negative mode) of **3.4** (pH ~ 10-11): m/z 506.2. Calculated for $LPt(CH_2CH_2OH)OH^-$, $C_{13}H_{15}SO_5N_2{}^{195}Pt$, 506.0.

$LPt^{IV}(OH)(CH_2CH_2OH)Cl$, 3.6. $LPt^{II}(CH_2CH_2)Cl$ (**3.1**) (103.1 mg, 203 μmol) and 10 mL of water were placed into a 50 mL round bottom flask equipped with a stirring bar. To a stirred suspension 34.4 mg of 30% H_2O_2 (~303 μmol) were added. The mixture became cloudy and a white precipitate slowly formed. After 1 day the white solid was filtered off, washed with water (2 x 1 mL) and dried under vacuum. The yield was 90.7 mg (82%).

^{1}H NMR (D_2O, 22 ^oC), δ: 3.21-3.84 (m, 4H), 6.73 (s, 1H), 7.84-7.92 (m, 2H), 8.06 (vd, *J*=7.7 Hz, 1H), 8.08 (vd, *J*=7.8 Hz, 1H), 8.27 (td, *J*=7.8, 1.5 Hz, 1H), 8.34 (td, *J*=7.8, 1.2 Hz, 1H), 8.71 (vd, *J*=6.0 Hz, 1H), 8.99 (vd, *J*=5.4 Hz, 1H). Limited solubility of $LPt^{IV}Cl(OH)(CH_2CH_2OH)$ in water (< 2 mg/mL) and methanol prevented from obtaining a good quality ^{13}C NMR spectrum. **ESI-MS** of **3.6** in water: m/z = 542.029. Calculated for $LPt^{IV}(OH)(CH_2CH_2OH)Cl{\cdot}H^+$, $C_{13}H_{16}{}^{35}ClO_5N_2{}^{195}PtS$, 542.012. **Anal.** Found (Calcd for $C_{13}H_{15}ClO_5N_2PtS$): H, 2.49 (2.79); C, 28.41 (28.82); N, 5.07 (5.17); S, 5.68 (5.92); Cl, 6.58 (6.54).

***unsym*-$LPt^{IV}(CH_2CH_2OH)(OH)_2$, 3.5**

Procedure A, from 3.2. A sample of $LPt(CH_2CH_2)OH$ (106 mg, 216 μmol) was dissolved in 50 mL distilled water. The solution was placed into a 250 mL round bottom flask and stirred vigorously under an O_2 atmosphere at room temperature. According to ^1H NMR, the oxidation was complete in 5 days. The reaction mixture was filtered from a white precipitate of $L_2Pt^{II}{}_2(\mu\text{-}OH)_2$ that resulted from partial loss of ethylene. The precipitate was washed with 3 mL H_2O and the combined filtrate was evaporated to dryness under vacuum at room temperature to give a pale yellow solid. The yield was 82.2 mg (72%).

^{1}H NMR (D_2O, 22 ^oC), δ: 3.00-3.66 (m, 4H), 6.69 (s, 1H), 7.81 (ddd, *J*=7.7, 5.9, 1.5 Hz, 1H), 7.89 (ddd, *J*=7.9, 5.5, 1.3 Hz, 1H), 8.06 (dd, *J*=8.0, 1.3 Hz, 1H), 8.09 (vd, *J*=7.8 Hz, 1H), 8.24-8.31 (m, 2H), 8.63 (vd, *J*=5.9, 1H), 8.86 (vd, *J*=5.5, 1H).

^{13}C NMR (D_2O, 22 ^oC), δ: 25.2 ($^1J_{PtC}$=543 Hz), 61.8, 72.1, 127.9, 128.4, 128.6, 129.7, 143.1, 144.1, 148.1, 148.5, 150.7, 151.5. **ESI-MS** of **3.5** in water: m/z =

524.04528. Calculated for **3.5**·H^+, $C_{13}H_{17}O_6N_2{}^{195}PtS$, 524.04516. **Anal.** Found (Calcd for for $C_{13}H_{16}O_6N_2PtS$): H, 3.25 (3.08); C, 29.55 (29.83); N, 5.15 (5.35); S, 5.73 (6.13).

Procedure B, from 3.1. To a suspension of **3.1** (400 mg, 788 μmol) in 10 mL H_2O 1 equivalent of NaOH (31.8 mg, 790 μmol) was added. After a few minutes **3.1** dissolved completely. The solution was placed into 250 mL round bottom flask and stirred vigorously under an O_2 atmosphere. According to ^1H NMR, complex **3.5** was obtained after 4 days in 80-90% yield and contained admixtures of $LPt(OH)_2^-$ and $LPt^{II}(\mu\text{-}OH)_2$.[79] The reaction mixture was neutralized with dilute H_2SO_4 to pH 7 to precipitate anionic $LPt^{II}(OH)_2^-$ in the form of an insoluble $L_2Pt^{II}{}_2(\mu\text{-}OH)_2$, then filtered and washed with small amounts of water. The resulting solution was evaporated and dried under vacuum for 5-6h (0.3 Torr). The solid was separated from inorganic salts by extraction with anhydrous 2,2,2-trifluoroethanol (3 mL). After evaporation of trifluoroethanol a yellow solid was obtained, pure by NMR and elemental analysis. Yield 144.4 mg (35%). **Anal.** Found (Calcd for for $C_{13}H_{16}O_6N_2PtS$): H, 3.20 (3.08); C, 29.54 (29.83); N, 4.96 (5.35); S, 5.85 (6.13).

Chapter 4: Allylic CH Activation and Aerobic Oxidation of Some Cycloolefins to Olefin Oxides Mediated by (dpms)Pt^{II}(OH) Complexes

4.1 Pt^{IV} Oxetanes: Synthesis via *Aerobic Oxidation of Pt^{II} – Cycloolefins Complexes and Direct C-O Reductive Elimination of Epoxides*

4.1.1 Introduction: Metallaoxetanes as Intermediates in Olefin Oxidation Reactions

Having established that the dpms-platinum complexes with ethylene are easily converted to ethylene oxide and ethylene glycol using O_2 as an oxidant, we next prepared (dpms)Pt^{II} complexes with some cyclic alkenes and explored their reactivity toward O_2. Similar to the (dpms)Pt^{II}(OH)(olefin) complex where olefin is ethylene CH_2CH_2, complexes derived from olefin = *cis*-cyclooctene, norbornene of benzonorbornadiene (Scheme 4.1.) were found to react cleanly with O_2 in protic solvents. In contrast to (dpms)Pt^{II}(OH)(CH_2CH_2), the reaction products are metallacyclic platina(IV)oxetanes (platina(IV)oxacyclobutanes). Platina(IV)oxetanes are able to cleanly produce olefin oxides via direct C(sp^3)-O reductive elimination previously unprecedented in organoplatinum(IV) chemistry (Scheme 4.1).

Scheme 4.1

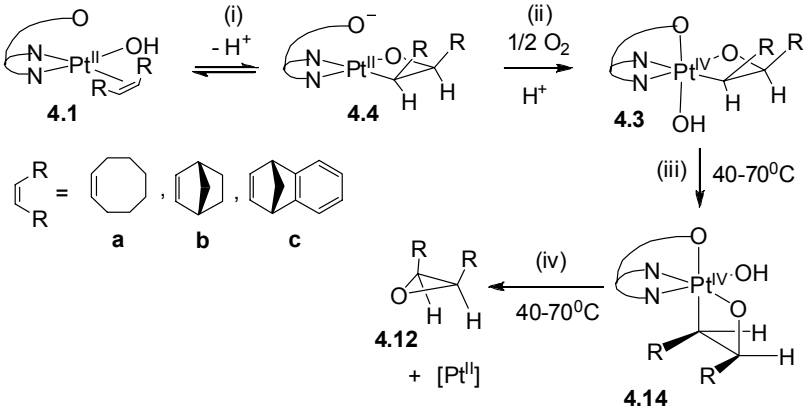

Metallaoxetanes (1-metalla-2-oxacyclobutanes) are often proposed as intermediates in homogeneous and heterogeneous olefin oxidation processes catalyzed by transition metals.[97] The study of the reactivity of metallaoxetanes is of great practical interest due to their relevance to commercialized olefin epoxidation processes. For instance, industrial production of ethylene oxide involves oxidation of ethylene with O_2 over heterogeneous silver catalyst supported by α-Al_2O_3 and promoted by alkali metal ions and halides.[5] The oxidation of ethylene into ethylene oxide is accompanied by exothermic combustion into CO_2 and water, presumably via formation of acetaldehyde, so that low conversions are necessary to achieve high selectivity toward ethylene oxide.[98] Another feature of the existing silver catalysts is their low selectivity in aerobic oxidation of olefins containing allylic C-H bonds.[24] Understanding mechanisms of olefin epoxidation is therefore of great importance as a tool for controlling reaction selectivity and designing new catalysts.

Two possible pathways of the epoxide formation in heterogeneous silver-catalyzed ethylene oxidation were considered: concerted addition of surface oxygen to a double bond of ethylene (Scheme 4.2, a) and sequential formation of two C-O bonds via an intermediate surface metallaoxetane (Scheme 4.2, b).[99-102]

Scheme 4.2. Possible intermediate in ethylene epoxidation on Ag catalyst

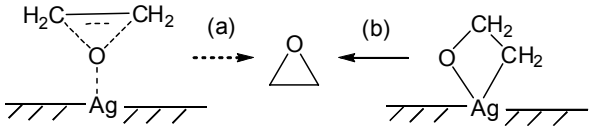

Recent studies by Barteau and co-workers provided evidence in favor of path (b): metallaoxetane on the Ag surface was identified and characterized spectroscopically, and was shown to eliminate ethylene oxide at 300-310 K.[101, 102]

According to the original proposal by Sharpless,[103] metallaoxetanes might also be involved in homogeneous oxygen-transfer reaction to alkenes. It was found that olefin oxidation with chromyl chloride CrO_2Cl_2 at low temperatures leads to the formation of products of *cis*-addition predominantly: epoxides, *cis*-chlorohydrins and *cis*-dichlorides as primary products. To explain the observed selectivity, the following mechanism was proposed (Scheme 4.3):[103]

Scheme 4.3

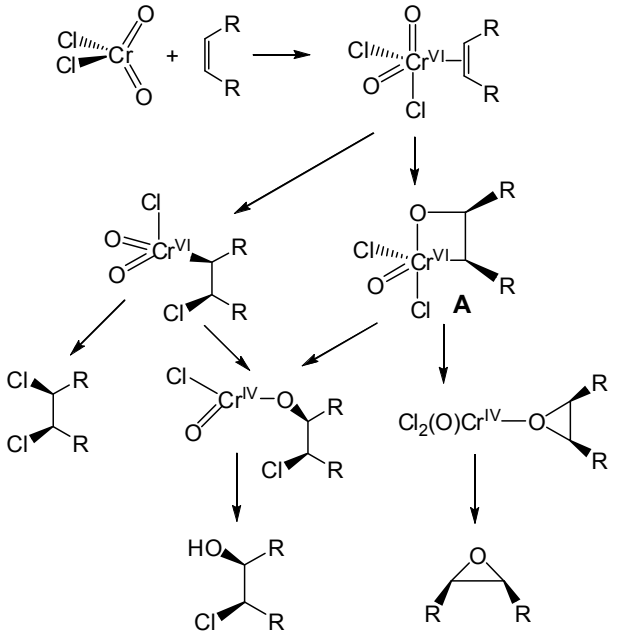

In this mechanism the intermediate chromaoxetane **A** (Scheme 4.3) is formed by the formal [2+2] cycloadditon of olefin to a metal-oxo bond, and the epoxide is formed by

reductive elimination from chromaoxetane. The mechanism proposed by Sharpless was in contrary to previously suggested direct oxygen atom transfer by electrophilic attack of the metal oxo-species at the olefin, not involving formation of organometallic intermediates (Scheme 4.4).[104-106]

Scheme 4.4

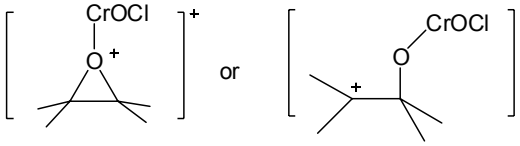

Having admitted the lack of direct experimental data to support metallaoxetane formation in mechanism shown in Scheme 4.3, Sharpless nevertheless suggested that similar metalloxetanes might play an important role in other transition-metal mediated oxidation processes such as olefin oxidation with OsO_4,[107] ReO_3Cl,[108] or biomimetic olefin oxidation.[109, 110]

Since then, metallaoxetanes have often been proposed as possible intermediates in various olefin epoxidation reactions, catalyzed by Ru[111], Mn,[112, 113] Fe[109] and other transition metal complexes, often without direct experimental evidence.[97] Only a few isolated metallaoxetanes have been reported in the literature and the reductive elimination of epoxides from isolated metallaoxetanes was not observed until recently.[114, 115]

A number of irida- and rhodaoxetanes have been prepared by oxidation with H_2O_2 or O_2 of alkene complexes of Rh^I and Ir^I, supported by tri- or tetradentate ligands (Scheme 4.5a, 4.6a).[116-125]

Scheme 4.5

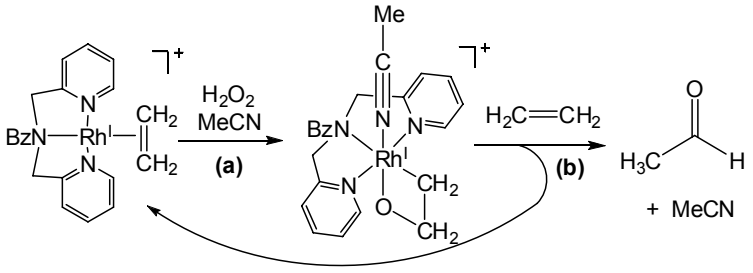

Scheme 4.6

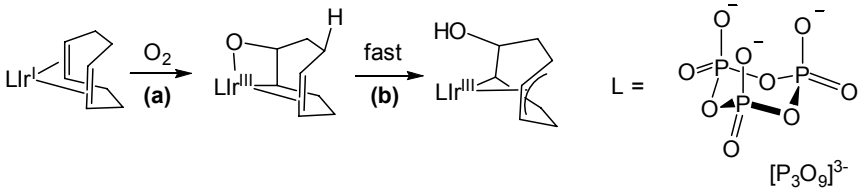

De Bruin and Budzelaar proposed that formation of rhodaoxetane by H_2O_2 oxidation of Rh^I-alkene complexes involves heterolytic cleavage of the peroxide O-O bond on approach to the metal center, leading to Rh^{III}-OH, followed by intramolecular nucleophilic attack by the Rh^{III}-bound OH group at the coordinated alkene.[122, 126]

It was suggested that the oxidation of $[(COD)Ir^I(P_3O_9)]^{2-}$ complex with O_2 (Scheme 4.6a) involves dinuclear activation of O_2 by two iridium centers, based on volumetric measurements, which indicated the uptake of 0.5 mole of O_2 per mole of Ir^I.[125] By contrast, acid-catalyzed oxidation of [(bpa)Rh(COD)] (bpa = *N*,*N*-bis(2-pyridylmethyl)amine; COD = 1,5-cyclooctadiene) complex with O_2 in CH_2Cl_2 requires consumption of 1 mole of O_2 per mole of Rh^I to form rhodaoxetane product, and is accompanied by the formation of paramagnetic products.[122]

Known rhoda-[117, 124, 127], ruthena-[128] and iridaoxetanes[117, 129] do not eliminate epoxides. At the same time, elimination of carbonyl-containing products, aldehydes and ketones, presumably via β-hydride shift to the unsaturated metal center, was found to be much

more accessible pathway of thermal decomposition of Rh^{III} and Ir^{III} oxetanes (Scheme 4.5b).[120, 124] In some cases allylic CH activation is observed (Scheme 4.6b).[116, 117, 125]

It was suggested that metallaoxetanes might be involved in palladium chemistry, related to the Wacker process.[117, 130, 131] Based on DFT-study of the mechanism of the Wacker process, Keith, Oxgaard and Goddard proposed that *syn*-hydroxypalladation in Wacker-process occurs via internal nucleophilic attack at the coordinated ethylene and initially produces a protonated palladaoxetane, which subsequently undergoes β-hydride elimination to yield acetaldehyde (Scheme 4.7).[130]

Scheme 4.7

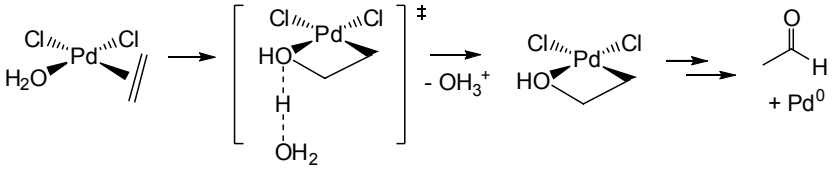

A number of platina(II)oxetanes were synthesized recently by the Paul Sharp group by reacting Pt^{II} oxo-bridged complex $[(1,5\text{-COD})_4Pt_4(\mu_3\text{-O})_2Cl_2](BF_4)_2$ with olefins.[132-134] Platinaoxetanes derived from strained bicyclic olefins, norbornene or substituted benzonorbornadienes, were stable enough to allow for isolation, X-ray analysis and reactivity studies.[135] Reaction of Pt^{II} oxo-bridged complexes with ethylene yielded a mixture of products, including acetaldehyde, which presumably formed via β-hydride elimination from a transient platinaoxetane.[134] Notably, none of these Pt^{II} oxetanes was reported to eliminate epoxides.

Scheme 4.8

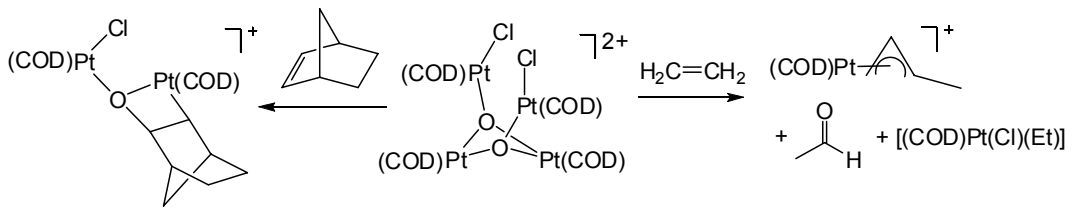

The microscopic reverse of reductive elimination, oxidative addition of epoxides, was observed experimentally for low-valent late transition complexes, Pt^0,[136, 137] Pt^{II},[138] and Rh^I.[127, 139] It was suggested that in many cases the reductive elimination of epoxides from metallaoxetanes is likely to be a thermodynamically unfavorable process due to the greater ring strain in epoxides compared to four-membered ring of oxetanes.[117, 127]

The oxidative addition of electron-poor epoxides such as tetracyanoethylene oxide, to Pt(0) complexes L_4Pt (L = PPh_3, P(*o*-Tol)$_3$, $AsPh_3$) in aprotic solvents yielding platina(II)oxetanes was reported by Ibers, Lenarda and Graziani.[136, 137] Several possible mechanisms were proposed for oxidative addition of tetracyanoethylene oxide. Ibers[137] suggested a step-wise mechanism that involves initial nucleophilic attack by L_2Pt^0 at the epoxide ring leading to the cleavage of one of the C-O bonds. The subsequent cyclization produces platinum oxetane (pathway **a**, Scheme 4.9). Alternatively, Jørgensen[97] proposed direct oxidative addition of the C-O bond of epoxide to a L_3Pt^0 center (pathway **b**, Scheme 4.9).

Scheme 4.9

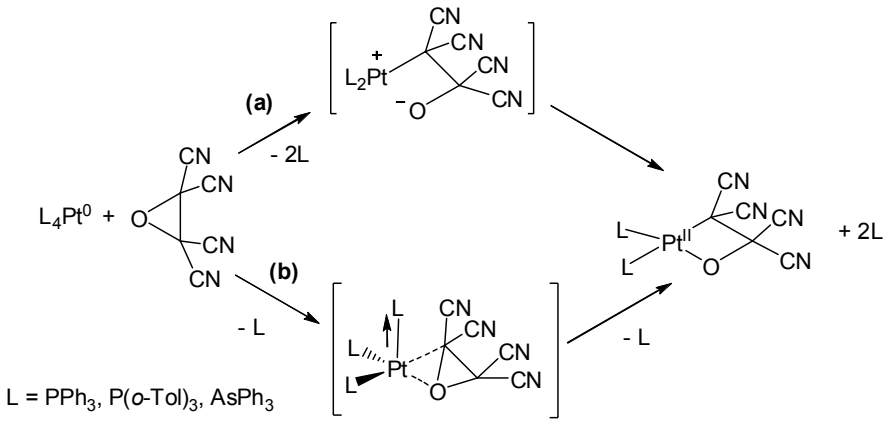

Oxidative addition of ethylene oxide to $K_2Pt^{II}Cl_4$ in aqueous solutions was studied by Zamashchikov.[138] Two products of the oxidative addition were observed, depending on

the chloride ion concentration. At high chloride concentrations when $[PtCl_4]^{2-}$ is the predominant Pt^{II} – containing species present in aqueous solutions of $K_2Pt^{II}Cl_4$, the major product was assigned as a platina(IV)oxetane $[PtCl_4(CH_2CH_2O\text{-}\kappa C,\kappa O)]^{2-}$ **I** (Scheme 4.10a).

At low Cl^- concentrations, when the fraction of an aqua complex $PtCl_2(OH_2)_2$ present in aqueous solutions of $K_2Pt^{II}Cl_4$ is significant, a mixture of platina(IV)oxetane and 2-hydroxyethyl complex $[Pt(CH_2CH_2OH)(Cl)_i(OH_2)_{5-i}]^{3-i}$ **II**, resulting from the ring-opening of epoxide, was detected (Scheme 4.10b).

The authors suggested that **I** results from concerted oxidative addition of the C-O bond of epoxide to $[PtCl_4]^{2-}$ via a three-center transition state (Scheme 4.10a). Formation of the acyclic hydroxyethyl complex **II** was suggested to proceed by an S_N2 oxidative addition of ethylene oxide to $PtCl_2(OH_2)_2$ (Scheme 4.10b).

Scheme 4.10. Proposed mechanisms of the oxidative addition of ethylene oxide to $[PtCl_4]^{2-}$ (a) and $[PtCl_2(OH_2)_2]$ (b).

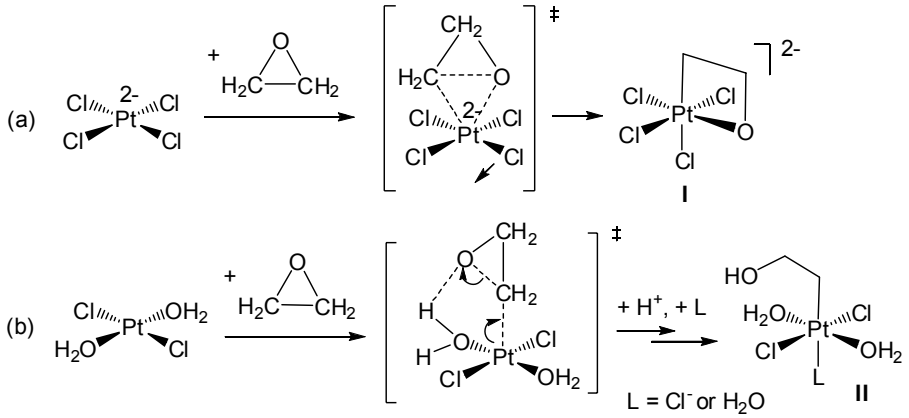

The first example of reductive elimination of epoxide from an isolated metallaoxetane complex in homogeneous system was reported in 2005 by Cinellu[115] and involved aura(III)oxetane, formed by reaction of gold(III) oxo-complexes with norbornene.

However, the reaction was not clean and was accompanied by the formation of aldehydes and other products.

Scheme 4.11

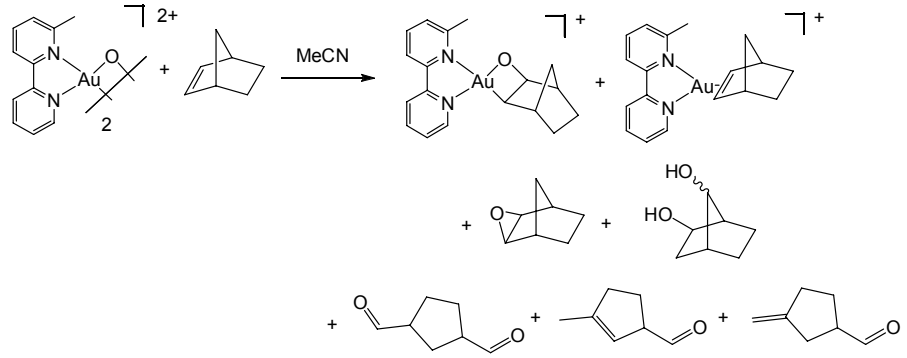

Interestingly, Kawashima and Okazaki reported that some main group element analogues of metallaoxetanes, 1,2-oxaselenetanes[140] and 1,2-oxastibetanes,[141-143] are capable of eliminating oxiranes at high temperatures (140-220 ^{o}C) with retention of configuration. They suggested a concerted mechanism of the epoxide elimination from isolated 1,2-oxaselenetanes, by contrast to an S_N2 type mechanism proposed for oxirane formation in Corey-Chaykovsky type reactions.[140] Similar concerted mechanism of oxirane elimination from isolated 1,2-oxastibetanes with retention of configuration was proposed by Kawashima.[143]

Scheme 4.12

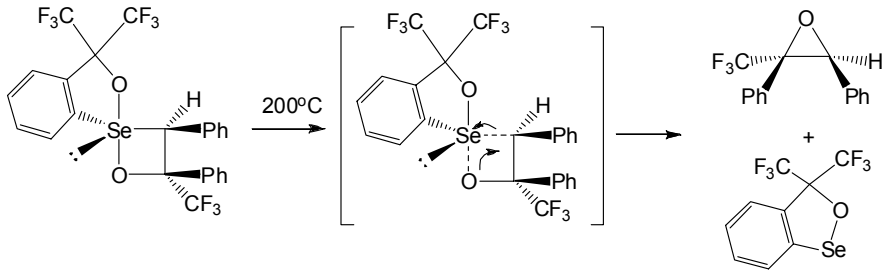

We have recently found that a number of Pt^{IV} oxetanes can be readily prepared by oxidation of (dpms)Pt^{II}(OH) complexes derived from cyclic alkenes. Importantly, the

resulting Pt^{IV} oxetanes were capable of clean and quantitative reductive elimination of epoxides under mild conditions (Scheme 4.1). The oxidation chemistry of dpms-supported platina(II)oxetanes, the reactivity of resulting platina(IV)oxetanes in C-O reductive elimination, and mechanistic studies will be discussed in this chapter.

4.1.2 Results and Discussion

4.1.2.1 Preparation of (dpms)Pt^{II} Oxetanes and Their Oxidation with O_2 and H_2O_2.

a) *cis*-Cyclooctene derivatives. The preparation of hydroxo (dpms)Pt complex with *cis*-cyclooctene, $LPt^{II}(\eta^2\text{-}cis\text{-}C_8H_{14})OH$ was accomplished through ethylene displacement in complex $LPt^{II}(\eta^2\text{-}CH_2CH_2)OH$ (L = dpms) (**3.2**, Chapter 3) under reduced pressure (eq. 4.1). Upon stirring biphasic system containing aqueous solution of **3.2** and *cis*-cyclooctene under reduced pressure (127 torr) for 2 days clean formation of complex $LPt^{II}(\eta^2\text{-}cis\text{-}C_8H_{14})OH$, **4.1a**, was observed. Small amounts of precipitate were filtered off, and analytically pure **4.1a** was isolated upon evaporation of the resulting yellow solution in 91% yield and was characterized by ^1H and ^{13}C NMR spectroscopy, ESI mass spectrometry and elemental analysis.

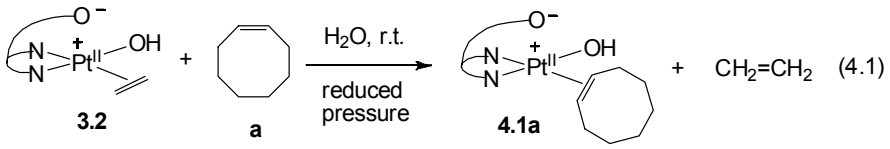

^1H and ^{13}C NMR spectra of complex **4.1a** in D_2O were consistent with low C_1 symmetry of **4.1a**, the presence of a coordinated olefin and an OH ligands. A broad singlet at -0.53 ppm integrating as 1H, diagnostic of a PtOH fragment, was observed in freshly prepared acetone-d_6 solutions. Two multiplets at 5.11 ppm ($^2J_{PtH}$=55 Hz) and 5.67 ppm ($^2J_{PtH}$=55 Hz) produced by the coordinated olefin CH groups were

observed in the "vinylic" region of ^{1}H NMR spectrum in water. The ^{13}C NMR chemical shifts and C-Pt coupling constants of the olefinic carbons of *cis*-cyclooctene at 97.6 ppm (J_{PtC}=172 Hz) and 99.5 ppm (J_{PtC}=163 Hz) are typical for η^2-coordinated alkenes in platinum(II) complexes.[32]

The crystal structure of the analogous chloro complex $LPt^{II}(\eta^2$-*cis*-$C_8H_{14})Cl$, **4.2a**, was determined by X-ray diffraction. Complex $LPt^{II}(\eta^2$-*cis*-$C_8H_{14})Cl$, **4.2a**, was obtained by reacting aqueous solution of potassium salt of the dpms ligands, K(L), with *cis*-cyclooctene analogue of Zeise's salt, $K[Pt^{II}Cl_3(\eta^2$-*cis*-$C_8H_{14})]$ (eq. 4.2). The poorly soluble complex **4.2a** was isolated in an analytically pure form in 71% yield and characterized by NMR spectroscopy, ESI mass spectrometry, elemental analysis and X-ray diffraction.

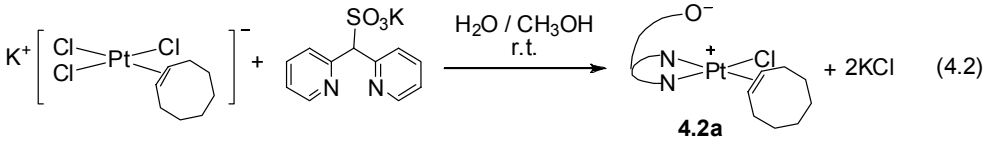

The X-ray crystal structure of complex **4.2a** in shown in Fig. 4.1.

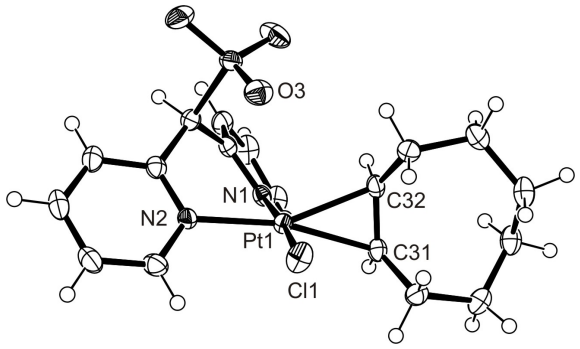

Figure 4.1. ORTEP plot for complex **4.2a**. Selected bond length (Å): Pt1-Cl1, 2.3034(6);Pt1-N1, 2.0305(18); Pt1-N2, 2.0707(18); Pt1-C31, 2.192(2);Pt1-C32, 2.183(2); C31-C21, 1.389(3).

No oxidation occurred when a neutral solution of **4.1a** in water was exposed to O_2. In contrast to neutral solutions, oxidation of **4.1a** with O_2 in water was clean in the

presence of 0.25 equivalents of NaOH (eq. 4.3) and was complete after 19 hours at room temperature. A single reaction product, identified as Pt^{IV} oxetane **4.3a** was isolated in an analytically pure form in 86% yield. The identical product can also be obtained by oxidation of **4.1a** with H_2O_2 in aqueous solution in an analytically pure form in 63% isolated yield.

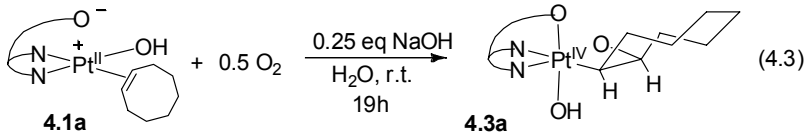

(4.3)

In the ^{1}H NMR spectrum of **4.3a** in DMSO-d_6, the platinum-bound CH group exhibits a doublet of doublets (J=11.8, 7.6 Hz) centered at 3.38 ppm with a characteristically large coupling constant $^2J_{PtH}$=70 Hz. The peak of the CHO group of the oxetane fragment appeared at 5.20 ppm as a doublet of doublets and was characterized by a smaller coupling constant $^3J_{PtH}$=34 Hz. The signal assignment for **4.3a** was confirmed by NOE experiments. The Pt-OH group gave rise to a broad singlet at 2.47 ppm integrating as 1H relative to peaks of the dpms ligand. ^{13}C NMR spectrum showed the signal of the platinum-bound carbon at 14.0 ppm with a coupling constant $^1J_{PtC}$=369 Hz and a downfield-shifted signal of the oxygen-bound carbon of the oxetane ring at 91.1 ppm ($^2J_{195PtC}$=82 Hz). Only one peak was present in an ESI mass-spectrum of acidified solution of **4.3a**, characterized by m/z 588.1, corresponding to the protonated oxetane **4.3a***H^+.

Consistent with the results of ^{1}H, NOE, ^{13}C NMR spectroscopy and ESI-MS characterization, a single crystal X-ray diffraction analysis of **4.3a** confirmed the presence of a Pt^{IV}-oxetane fragment (Fig. 4.2). The bond angles within the oxetane ring in **4.3a**, Pt1-C2-C1, 90.9(2), C2-C1-O1, 101.1(3), reveal its strained character.

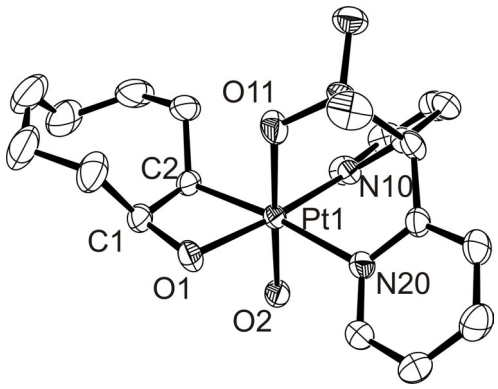

Figure 4.2. ORTEP plot (50% probability ellipsoids) for complex **4.3a**. Hydrogen atoms are omitted for clarity. Selected bond lengths (Å) and angles (°): Pt1-C2, 2.055(3); Pt1-O1, 1.971(2); Pt1-O2, 1.955(2); Pt1-N10, 2.046(3); Pt1-N20, 2.204(3); Pt1-O11, 2.086(2); Pt1-C2-C1, 90.9(2), C2-C1-O1, 101.1(3).

Formation of oxetane **4.3a** can be rationalized as follows. In contrast to the ethylene complex **3.2**, the secondary sp^2-carbons in **4.1a** are not electrophilic enough to accept an intermolecular nucleophilic attack[32] by an external OH^- and produce a 2-hydroxoalkyl Pt^{II} complex. A lower propensity of alkyl-substituted olefin ligands, compared to ethylene, toward external nucleophilic attack has been noted previously.[144] Instead, an entropy-favored intramolecular attack at one of the olefinic carbons by an adjacent $Pt^{II}(OH)$ occurs in the presence of a base leading to an anionic Pt^{II} oxetane **4.4a** (eq. 4.4; Scheme 4.1, step *i*).

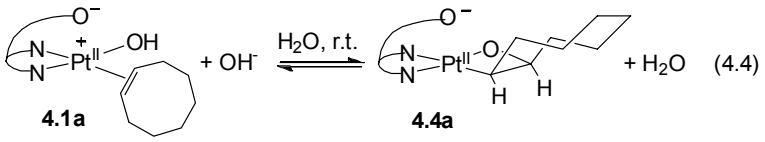

Some steric strain present in *cis*-cyclooctene is expected to diminish upon formation of the platinaoxetane ring because of rehybridization of the olefinic carbons from sp^2 to sp^3. This factor might favor formation of **4.4a** as well. The latter anionic complex contains a strongly σ-donating platinum-bound alkyl group and is expected to be reactive toward O_2, similar to anionic $[(dpms)Pt^{II}(OH)Me]^-$ (see

Chapter 2). Aerobic oxidation of **4.4a** then leads to Pt^{IV} oxetane **4.3a** (Scheme 4.1, step *ii*). The mechanism of the oxidation with O_2 can be similar to that discussed in Chapters 2 and 3 for oxidation of $[LPtMe(OH)]^-$ (eq. 2.10-2.12, Chapter 2) and $[LPt(CH_2CH_2OH)(OH)]^-$ (eq. 3.15-3.17, Chapter 3) and is consistent with our volumetric measurements, which indicated the uptake of 0.51±0.04 mole of O_2 per mole of **4.1a**.

Since aerobic oxidation was only possible in the presence of a base, we studied the reactivity of **4.1a** toward OH^- in the absence of dioxygen with the hope of detecting proposed reactive intermediate, Pt^{II} oxetane **4.4a**.

Upon addition of 4 equivalents of NaOD to a solution of **4.1a** in deaerated D_2O under an argon atmosphere a fast reversible reaction was observed leading to the formation of a mixture of **4.1a** and a new moderately unstable Pt^{II} complex ($t_{1/2}$=3 hours at 22 ^oC) in a 1 : 4 molar ratio respectively. Based on ESI mass spectrometry, ^1H, NOE and ^{13}C NMR spectroscopy data, the new species was identified as an anionic Pt^{II} oxetane **4.4a**.

The presence of an anionic species characterized by m/z 570.1 was consistent with the oxetane structure of **4.4a**. ^{13}C NMR spectrum revealed the presence of the characteristically upfield shifted signal of the platinum-bound carbon at -2.6 ppm. The chemical shift of the oxygen-bound carbon of the oxetane ring in ^{13}C NMR spectrum, 95.1 ppm, was similar to the chemical shift of the O-bound carbon in ^{13}C NMR spectrum of oxetane **4.3a** (91.1 ppm). The proton signal of the CHO group of the oxetane ring appeared at 5.20 ppm and was characterized by a coupling constant $^3J_{195PtH}$=38 Hz, similar to that in **4.3a**. The formation of **4.4a** is reversible: addition of

an equivalent amount of HBF_4 to the above solution allowed to convert **4.4a** back to **4.1a** quantitatively. No Pt^{II} oxetanes were observed by NMR spectroscopy in neutral aqueous solutions of **4.1a**.

b) Norbornene derivatives. Formation of Pt^{II} oxetanes from olefin complexes should be favored if a cycloolefin more strained than *cis*-cyclooctene is used. To explore this possibility, we attempted to prepare the Pt^{II} norbornene complex. Ligand exchange between **3.2** and norbornene led to a 6:4 mixture of two isomeric products characterized by elemental analysis, ESI mass spectrometry and NMR spectroscopy as *cis*- and *trans-exo*-Pt^{II} oxetanes **4.5b**, obtained in 82% isolated yield in an analytically pure form (eq. 4.5).

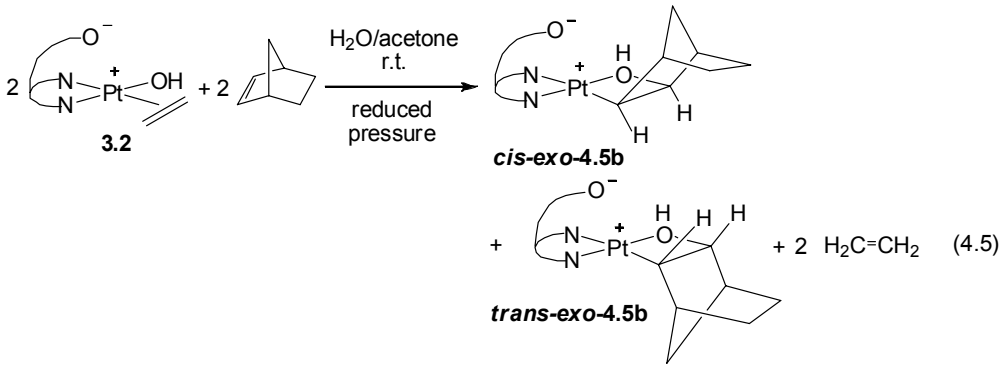

(4.5)

In contrast to the olefin complex **4.1a**, only one doublet at 6.21 ppm (J_{PtH}=31 Hz, CHO-group of the oxetane ring), integrating as 1H was observed in the "vinylic" region of ^1H NMR spectrum of **4.5b**, suggesting that the oxetane is the predominant species. The relative stability of the oxetane **4.5b** and the parent olefin complex is reversed in the presence of 10 equivalents of HBF_4 that allowed for the protonation of the Pt^{II}(OH) fragment in **4.5b** and conversion of **4.5b** to an unstable cationic olefin complex **4.6b**, $LPt^{II}(\eta^2$-norbornene$)(OH_2)^+$ (eq. 4.6).

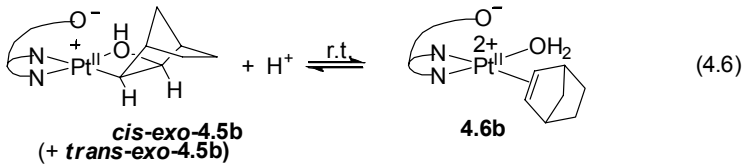

(4.6)

Typical for Pt^{II} complexes with η^2-coordinated alkenes, olefinic carbon atoms of norbornene gave rise to two peaks in ^{13}C NMR spectrum of **4.6a** at 109.4 ppm (J_{PtC}=153 Hz) and 112.3 ppm (J_{PtC}=157 Hz). Vinylic protons of the coordinated norbornene appeared as two broad singlets in the "vinylic" region of ^1H NMR spectrum at 5.68 ppm (J_{PtC}=21 Hz) and 6.18 ppm (J_{PtC}=23 Hz), each integrating as 1H.

Complex **4.6b** was not stable in acidic trifluoroethanol-H_2O solutions and slowly decomposed with the loss of norbornene to produce $[LPt(OH_2)_2]^+$, characterized previously (Chapter 2),[79] with a half-life of 17 hours at 20 ^oC (eq. 4.7).

$$LPt(\eta^2\text{-}C_7H_{10})(OH_2)^+ + H_2O \rightarrow (dpms)Pt(OH_2)_2^+ + C_7H_{10} \qquad (4.7)$$

Similar to the cyclooctene analogue **4.4a**, an anionic norbornene-derived Pt^{II} oxetane **4.4b** was produced as a 5.7:1 mixture of *cis*- and *trans*- isomers quantitatively upon combination of **4.5b** with 1.2 equivalents of NaOH (eq. 4.8).

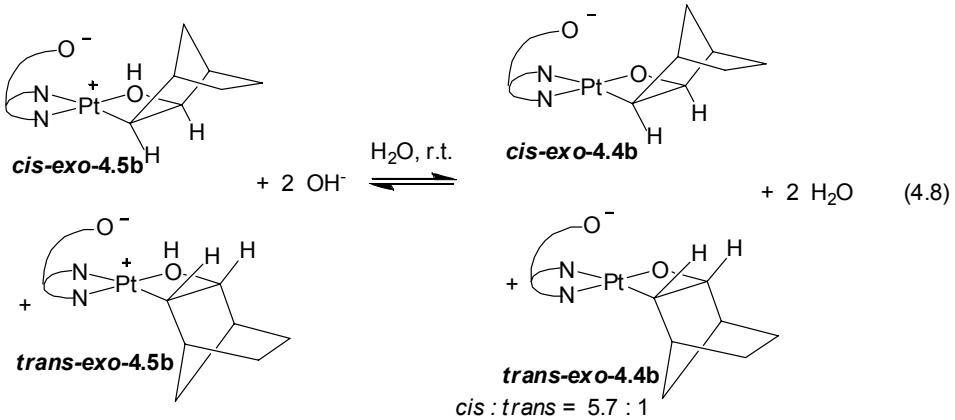

(4.8)

High stability of **4.4b** in aqueous solutions allowed for its detailed characterization by means of ESI mass spectrometry, ^{1}H and ^{13}C NMR spectroscopy. *Trans*- and *cis*-configurations were assigned from NOE experiments and refer arbitrarily to the position of the methylene bridge of the norbornane fragment with respect to the sulfonate group of the dpms ligand. *Exo*-positions of platinum and oxygen atoms were confirmed by NOE experiments. The major isomer was assigned a structure of ***cis*-4.5b**, based on the observed NOE between CHPt protons of the oxetane ring and *ortho*-protons of one of the pyridyls of the dpms ligand (Fig. 4.3).

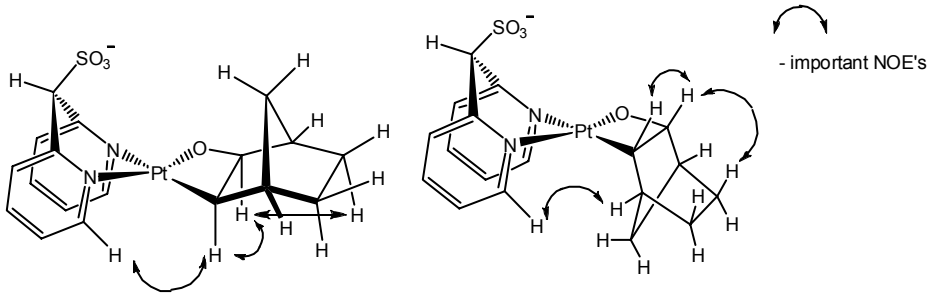

Figure 4.3. *Cis*- and *trans-exo*-configuration assignment of **4.4b**, based on NOE experiments.

Consistent with the oxetane structure, ^{1}H NMR spectrum of the major isomer, ***cis-exo*-4.4b**, reveals characteristic doublets of CHPt and CHO groups of the oxetane ring at 0.93 ppm (J_{HH}=5.8 Hz) and 5.59 ppm (J_{HH}=5.8 Hz) respectively, each integrating as 1H relative to the signals of the dpms ligand. In ^{13}C NMR spectrum of ***cis*-4.4b**, the platinum-bound α-carbon and the oxygen-bound β-carbon of the oxetane ring appear at -3.1 ppm ($^{1}J_{PtC}$=585 Hz) and 96.9 ppm ($^{2}J_{PtC}$=105 Hz) respectively.

An anionic compound characterized by m/z 554.1 corresponding to **4.4b** was detected by ESI mass spectrometry as the only Pt-containing species present in alkaline aqueous solution prepared by deprotonation of **4.5b** with NaOH.

Formation of η^2-coordinated norbornene complex from oxetanes is reversible: fast addition of an excess NaOH to a solution of **4.6b** allowed to cleanly convert **4.6b** to **4.4b**.

Importantly, **4.5b** is cleanly oxidized with O_2 in the absence of base additives in 2,2,2-trifluoroethanol (TFE) - H_2O solutions to produce a 30:1 mixture of *cis*- and *trans*- isomeric Pt^{IV} oxetanes **4.3b** after 22 hours at room temperature (the isomeric ratio was determined before isolation in the crude reaction mixture), and isolated in 85% yield (eq. 4.9) in an analytically pure form. Oxidation of a suspension of complex **4.5b** in H_2O with aqueous H_2O_2 produced an identical product, according to NMR spectroscopy and mass spectrometry data, which was isolated in 82% yield as a *cis-exo*-isomer predominantly (>99% after isolation).

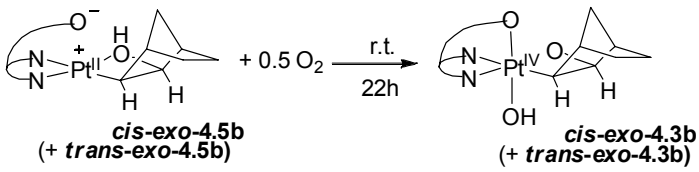

***cis-exo*-4.5b**
(+ ***trans-exo*-4.5b)**

***cis-exo*-4.3b**
(+ ***trans-exo*-4.3b)**

(4.9)

Complex ***cis*- 4.3b** was characterized by ^1H, NOE ^{13}C NMR spectroscopy, ESI mass spectrometry and elemental analysis. Solid-state structure of ***cis*-4.3b** determined by single crystal X-ray diffraction is given in Fig. 4.4.

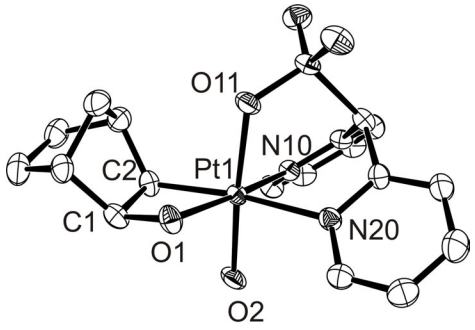

Figure 4.4. ORTEP plot (50% probability ellipsoids) for complex ***cis-exo*-4.3b**. Hydrogen atoms are omitted for clarity. Selected bond length (Å) and angles (°): Pt1-C2, 2.046(3); Pt1-O1, 1.9953(18); Pt1-N10, 2.056(2); Pt1-N20, 2.206(2); Pt1-O2, 1.9597(19); Pt1-O11, 2.0912(19); Pt1-C2-C1, 91.6(2), C2-C1-O1, 100.6(2).

The ^{1}H NMR spectrum of ***cis*-4.3b** in DMSO-d_6 shows the presence of two characteristic doublets of CHPt and CHO protons of the oxetane ring at 2.58 ppm (J_{HH}=5.0 Hz, $^{2}J_{PtH}$=72 Hz) and 5.27 ppm (J_{HH}=5.0 Hz, $^{3}J_{PtH}$=25 Hz) respectively, each integrating as 1H relative to the signals of the dpms ligand, and a broad singlet of the Pt-OH group at 2.63 ppm integrating as 1H. Similar to **4.3a**, in ^{13}C spectrum of ***cis*-4.3b**, the platinum-bound α-carbon and the O-bound β-carbon of the oxetane ring appear at 11.5 ppm ($^{1}J_{PtC}$=416 Hz) and 94.7 ppm ($^{2}J_{PtC}$=70 Hz) respectively. The *cis-exo* configuration of the major isomer of **4.3b** was confirmed by single crystal X-ray diffraction.

As noted above, **4.5b** is oxidized with O_2 in high yield in neutral solutions, in contrast to **4.1a**, for which the presence of NaOH was required in order to react with O_2. By analogy with our previous studies of mechanism of oxidation of (dpms)Pt^{II} alkyl complexes with O_2, discussed in Chapters 2 and 3, we propose that oxidation occurs via initial formation of an anionic oxetane **4.4b** (eq. 4.8), which then reacts with O_2 (Scheme 4.1, step *ii*). Accordingly, the reactivity of **4.5b** toward O_2 observed in neutral solution is consistent with higher acidity of an anionic oxetane **4.4b**, compared to a *cis*-cyclooctene derived oxetane **4.4a**. The higher acidity of **4.4b** is evident for the fact that this complex was obtained quantitatively upon addition of 1.3 equivalents of NaOH to complex **4.5b**, whereas in the presence of 1.3 equivalent of NaOH a neutral complex **4.1a** produced a mixture of an anionic **4.4a** and **4.1a** in a 1.1 : 1 ratio under analogous reaction conditions. Therefore, **4.4b**, reactive toward O_2, could be present in sufficient concentration already in neutral solutions.

Formation of *cis*-**4.3b** predominantly (*cis* : *trans*-**4.3b** is 30 : 1) from a 6:4 mixture of isomeric **4.5b** in neutral solution indicates that interconversion between *cis*- and *trans*-isomers of **4.5b** is faster than their reaction with O_2, with *cis*-isomer being more reactive toward O_2 than the corresponding *trans*-isomer. One of the reasons for the higher reactivity of *cis*-isomer of Pt^{II} oxetane could be the greater steric accessibility of the axial position *trans* to the sulfonate group of the dpms in *cis*-**4.4b**, required for the initial attack by O_2 at the Pt^{II} center (see Chapter 2), compared to *trans*-**4.4b**, in which an approach to the axial position might be partially blocked by the methylene bridge of the norbornane fragment (Fig. 4.3). High sensitivity of Pt^{II} and Rh^{I} complexes to sterics in O_2 oxidation reactions was previously noted by Bercaw[43] and de Bruin.[117]

Interconversion between *cis*- and *trans*-isomers of Pt^{II} oxetanes might involve intermediacy of an η^2-coordinated norbornene complex $LPt(\eta^2\text{-}C_7H_{10})(OH)$, **4.1b**, analogous to **4.1a**, in which case one might expect slower rate of interconversion in the presence of a base. Accordingly, oxidation of a strongly alkaline aqueous solution of **4.4b** (*cis* : *trans*-**4.4b** = 5.7:1), obtained by reacting **4.5b** with 1.5 equivalent of NaOH, with dioxygen produces a mixture of isomeric **4.3b**, in which the ratio of *cis*- and *trans*-isomers remains almost unchanged (*cis* : *trans*-**4.3b** is 6.1:1). This is consistent with the idea of slow *cis*/*trans* interconversion in the presence of excess NaOH.

c) Benzonorbornadiene derivatives. We next decided to test if replacement of the ethylene bridge of norbornene with *o*-phenylene in benzonorbornadiene would affect the reactivity of the derived complexes. Importantly, a great variety of substituted benzonorbornadienes can be prepared via Diels-Alder cycloaddition of benzynes and cyclopentadiene.

Similar to norbornene derivatives **4.5b**, analogous complexes with benzonorbornadiene (dpms)Pt^{II}($C_{11}H_{10}$OH-$\kappa C,\kappa O$), **4.5c**, was obtained by ethylene displacement in **3.2** under reduced pressure (eq. 4.10). The resulting complexes **4.5c** were identified as isomeric Pt^{II} oxetanes, based on NMR spectroscopy and mass spectrometry data.

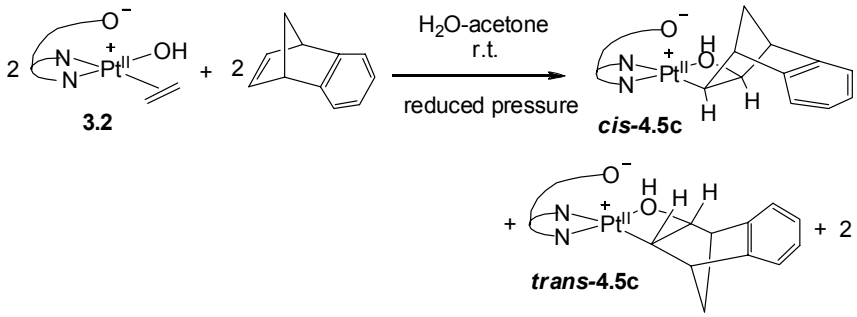

+ 2 CH_2=CH_2 (4.10)

Only one species was detected by ESI-MS characterized by m/z 604.0 in neutral aqueous solution of **4.5c**, corresponding to protonated **4.5c***H^+. The ^{1}H NMR spectrum in CD_3OD showed the presence of two species in a 3:1 ratio with similar NMR characteristics, presumably the two isomers ***cis*-4.5c** and ***trans*-4.5c**. The protons of CHPt and CHO groups of the oxetane fragments appeared in the ^{1}H NMR spectrum of the major isomer as two doublets at 1.43 ppm ($^3J_{HH}$ = 6.0 Hz, $^2J_{PtH}$ = 40 Hz) and 5.88 ppm ($^3J_{HH}$ = 6.0 Hz, $^3J_{PtH}$ = 17 Hz), each integrating as 1H, typical for Pt oxetanes.

The reactivity of **4.5c** was similar to the reactivity of the norbornene analogue **4.5b**. Deprotonation of **4.5c** with 1.2 equivalent of NaOH in aqueous solution produced a mixture of isomeric anionic oxetanes $[(dpms)Pt^{II}(C_{11}H_{10}O\text{-}\kappa C,\kappa O)]^-$, ***cis*-4.4c** and ***trans*-4.4c**, in an 8:1 ratio respectively (eq. 4.11). The major isomer was assigned a structure of ***cis*-4.5c**, based on the observed NOE between CHPt protons of the oxetane ring and *ortho*-protons of the pyridyls of dpms.

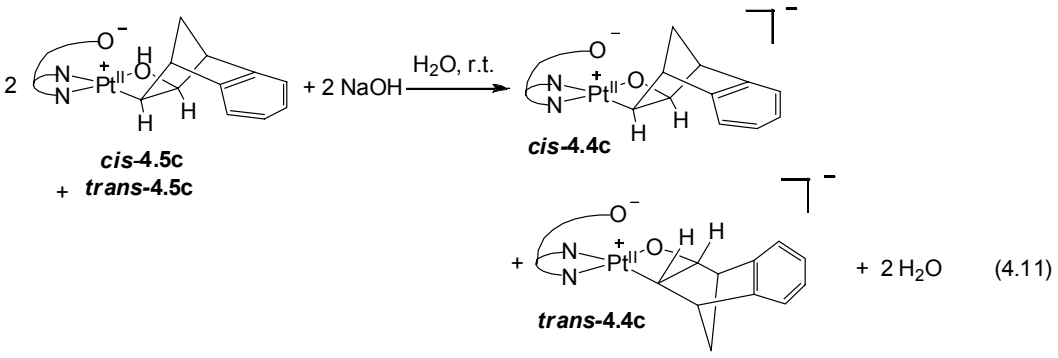

(4.11)

The ^{1}H NMR spectrum of ***cis*-4.4c** in D_2O showed characteristic doublets of the CHPt and CHO protons of the oxetane system at 0.89 ppm (J_{HH} = 5.6 Hz, $^2J_{PtH}$ = 44 Hz) and 5.51 ppm (J_{HH} = 5.6 Hz, $^3J_{PtH}$ ~25 Hz). The chemical shifts of the Pt-bound α-carbon and the O-bound β-carbon in ^{13}C NMR spectrum of ***cis*-4.4c** were similar to those observed for other anionic oxetanes, **4.4a** and **4.4b**, and appeared at -5.4 ppm and 96.0 ppm respectively.

The presence of the anionic species characterized by m/z 602.0, corresponding to **4.4c**, was detected by ESI mass spectrometry in aqueous solution containing **4.5c** and 1.5 equivalent of NaOH.

The oxidation of **4.5c** with O_2 was accomplished in solution in trifluoroethanol-water with a half-life of 2 hours at room temperature to produce ***cis*-4.3c**, which was

isolated in 70% yield (eq. 4.12). Complex ***cis*-4.3c** could also be obtained by oxidation of **4.5c** with H_2O_2 in aqueous solution in 85% isolated yield

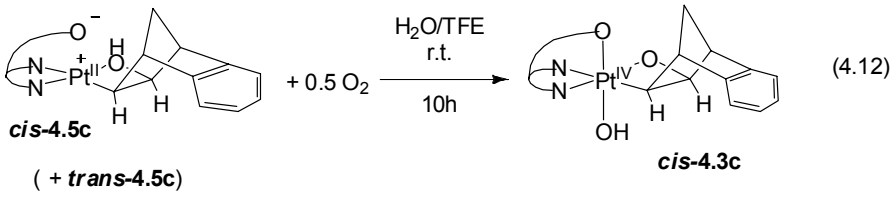

(4.12)

The structure of ***cis*-4.3c** was confirmed by ^{1}H, NOE, ^{13}C NMR spectroscopy and mass-spectrometry data. In ^{13}C NMR spectrum of ***cis*-4.3c**, the Pt-bound α-carbon and O-bound β-carbon appeared at 10.7 ppm ($^1J_{PtC}$ = 457 Hz) and 93.5 ppm respectively. ^{1}H NMR spectrum in DMSO-d_6 revealed two doublets of CHPt and CHO groups at 2.34 ppm (J_{HH} = 5.1, $^2J_{PtH}$ = 60 Hz) and 5.17 ppm (J_{HH} = 5.1 Hz, $^3J_{PtH}$ = 17 Hz) respectively and a broad singlet of Pt-OH at 2.61 ppm, integrating as 1H. The *cis*-configuration of **4.3c** was assigned based on NOE data.

Therefore, replacement of the ethylene bridge in norbornene structure with *o*-phenylene in benzonorbornadiene does not significantly affect the reactivity of the derived (dpms)Pt complexes toward deprotonation and oxidation by O_2 and H_2O_2.

d) 1,4-Epoxy-1,4-dihydronaphthalene derivatives. We next probed the effect of replacing the methylene bridge of benzonorbornadiene skeleton with the oxo-bridge on reactivity of the derived complexes. Such olefins can be produced via Diels-Alder cycloaddition of furan and substituted benzynes.

Complex **4.7d** was obtained by reaction of **3.2** with excess 1,4-epoxy-1,4-dihydronaphthalene, $C_{10}H_8O$, in H_2O-acetone solution under reduced pressure (eq. 4.13).

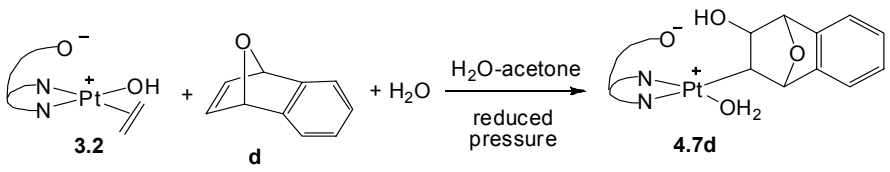

Surprisingly, a signal was detected by ESI mass spectrometry in neutral aqueous solution of **4.7d** characterized by m/z 624.0, which did not match the mass of the expected protonated oxetane and might correspond to the protonated hydroxoalkyl aqua complex (dpms)$Pt^{II}(C_{10}H_9O_2$-$\kappa C)(OH_2)$*H^+. Two platinum complexes in a 1.8:1 ratio were detected in D_2O solutions of **4.7d** by ^1H NMR spectroscopy with similar NMR characteristics, which could be assigned to the two diastereomeric species **4.7d'** and **4.7d"** (Scheme 4.13), presumably resulting from the nucleophilic attack of H_2O at the double bond of a coordinated 1,4-epoxy-1,4-dihydronaphthalene. Our attempts to grow single crystals of **4.7d** suitable for single crystal X-ray analysis were not successful due to its limited solubility, however, the reactivity studies of **4.7d**, described below, are consistent with the acyclic structure (dpms)$Pt^{II}(C_{10}H_9O_2$-$\kappa C)(OH_2)$ proposed above.

Scheme 4.13

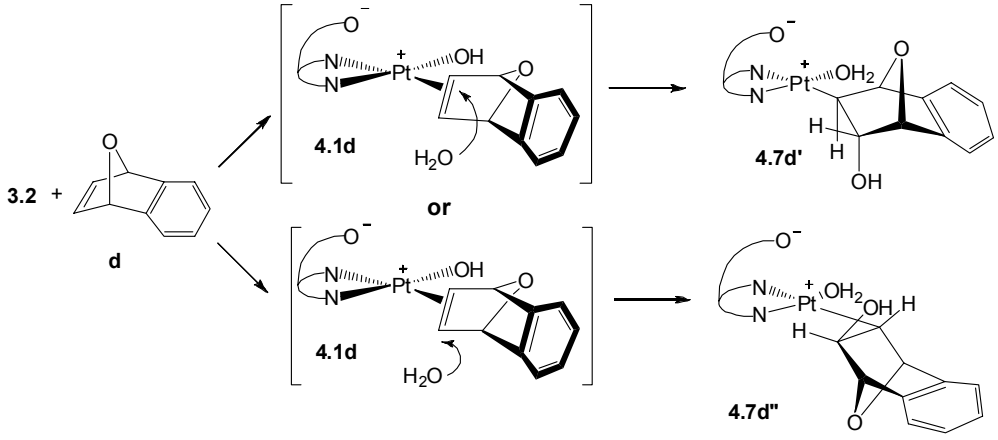

The structure shown in Scheme 4.13 was proposed based on the following considerations. Since steric factors are known to be important for reactivity of [2.2.1] bicyclic systems,[145] we propose that in a transient complex **4.1d** formed via ethylene substitution the platinum atom is coordinated to a double bond of 1,4-epoxy-1,4-dihydronaphthtalene from its less sterically crowded *exo*-face. If this assumption is correct, the *external* nucleophilic attack by H_2O, well-precedented in Pt^{II} chemistry (see examples in Chapter 3),[62] at the coordinated double bond in **4.1d** would lead to the formation of a *trans*-substituted product with an *endo*-OH group.

The propensity of 1,4-epoxy-1,4-dihydronaphthalene to react via external nucleohilic attack of water, by contrast to the intramolecular nucleophilic addition to the coordinated Pt-OH observed in oxetanes **4.4a-c**, could result from the presence of an electron-withdrawing bridging oxo-substituent in a β-position to the olefin carbons, which could increase the electrophilicity of the double bond of the coordinated alkene.[94]

Complex **4.7d** was found to react with strongly coordinating solvents such as DMSO to yield quantitatively $LPt^{II}(C_{10}H_9O_2\text{-}\kappa C)$(DMSO), resulting from an aqua ligand displacement by DMSO solvent (eq. 4.14), characterized by mass-spectrometry, ^1H and ^{13}C NMR spectroscopy.

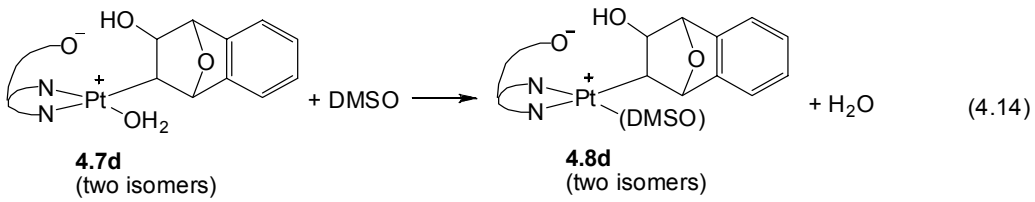

4.7d (two isomers) **4.8d** (two isomers) (4.14)

When solutions of **4.7d** were prepared in thoroughly dried DMSO-d_6, formation of one equivalent free H_2O was detected by ^1H NMR spectroscopy (eq. 4.14). In the ^1H

NMR spectrum of **4.8d** in DMSO-d_6, the OH groups of a major and a minor isomers appeared as a doublet at 5.28 ppm (J_{HH} = 2.4 Hz) and a singlet at 5.63 ppm respectively, each integrating as 1H relative to the corresponding PtCH resonances at 1.80 ppm and 2.19 ppm respectively. This observation is consistent with the proposed structure of **4.7d** as an aqua complex $LPt^{II}(C_{10}H_9O_2\text{-}\kappa C)(OH_2)$.

According to ^{1}H NMR, two complexes with similar NMR characteristics were present in DMSO-d_6 solution, presumably two diastereomers of **4.8d** in a molar ratio of 4.9:1. Only one species was detected by ESI-MS in acidified solution of **4.8d**, prepared by reaction **4.7d** with DMSO-h_6 characterized by m/z 683.9, corresponding to **4.8d***H^+. Accordingly, ESI-MS of the solution of product obtained by dissolving **4.7d** in DMSO-d_6 showed the presence of a peak with m/z 690.1, corresponding to protonated **4.8d-*d*$_6$***H^+.

Fast oxidation of **4.7d** with H_2O_2 in aqueous solution produced an acyclic complex $(dpms)Pt^{IV}(C_{10}H_9O_2\text{-}\kappa C)(OH)_2$, **4.9d**, isolated in 76% yield in an analytically pure form and characterized by ^{1}H and ^{13}C NMR spectroscopy, mass spectrometry and elemental analysis.

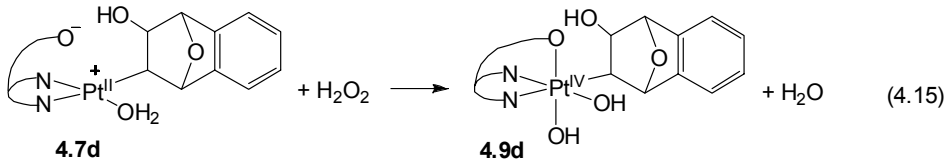

4.7d **4.9d** (4.15)

Only one isomer of **4.9d** was detected by ^{1}H and ^{13}C NMR spectroscopy. Although the diastereomeric configuration of **4.9d** was not established, assuming that geometry of the Pt-bound 1,4-epoxy-3-hydroxo-1,2,3,4-tetrahydro-naphthalyl does not change during oxidation, we can propose that OH group is present in *trans*-position to Pt, by analogy with **4.7d**.

The ^{1}H NMR spectrum of **4.9d** in DMSO-d_6 showed the presence of three inequivalent hydroxyl groups as broad singlets at 2.14 ppm, 3.42 ppm (two nonequivalent Pt-OH), and a downfield shifted singlet at 8.31 ppm (β-OH of 1,4-epoxy-3-hydroxo-1,2,3,4-tetrahydro-naphthalyl). The assignment of the signals of OH groups in ^{1}H NMR spectrum of **4.9d** was confirmed by ^{1}H-^{13}C HSQC NMR spectroscopy. In the ^{13}C NMR spectrum of **4.9d**, the Pt-bound α-C and O-bound β-C gave rise to peaks at 35.1 ppm and 76.9 ppm respectively. Notably, the chemical shifts of these peaks were very distinct form the chemical shifts of the Pt-bound and O-bound carbons of Pt^{IV} oxetane complexes **4.3a-c**, which typically appeared in the range of 11-14 ppm (for C-Pt) and 91-96 ppm (for C-O) respectively.

The ESI-MS of a dilute solution of **4.9d** showed a cationic species with m/z 640, corresponding to protonated **4.9d***H^{+}.

In the absence of oxidants in deaerated water the poorly soluble complex **4.7d** is deprotonated with 1.2 equivalent of NaOH to produce a clear, colorless solution of well-soluble anionic complex **4.10d**, detected by NMR spectroscopy and mass spectrometry (Scheme 4.14).

Scheme 4.14

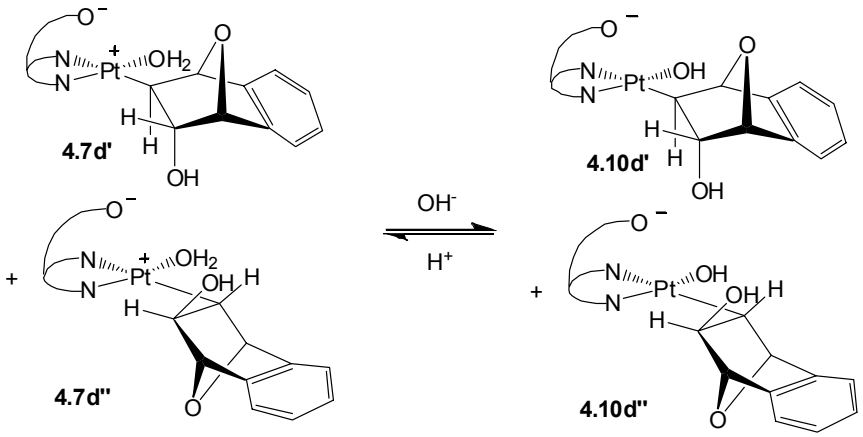

The only anionic species detected by ESI mass spectrometry in a freshly prepared (10-20 minutes) alkaline solution of **4.7d** was characterized by m/z 622.1 that corresponds to acyclic anionic $[(dpms)Pt^{II}(C_{10}H_9O_2\text{-}\kappa C)(OH)]^-$, **4.10d**.

According to NMR, two species were present in a freshly prepared alkaline D_2O solutions of **4.10d** in a 1.7:1 ratio, presumably the two diastereomeric complexes **4.10d'** and **4.10d"** (Scheme 4.14). In the ^{13}C NMR spectrum of **4.10d**, the OH-bound β-carbons of the two isomeric **4.10d** gave rise to peaks at 78.2 ppm (for major isomer) and 77.6 ppm (for minor isomer), close to the chemical shifts of β-C in acyclic Pt^{IV} complex **4.9d**.

Interestingly, a slow reaction took place in alkaline aqueous solution of **4.10d** with a half-life 53 hours at room temperature, which is effectively accelerated at elevated temperatures to cleanly and quantitatively produce an anionic oxetane $[(dpms)Pt^{II}(C_{10}H_8O_2\text{-}\kappa C,\kappa O)]^-$, **4.4d**, as a mixture of *cis*- and *trans*-isomers in a 2:1 ratio after heating at 60 ^oC for 20 hours (Scheme 4.15).

Scheme 4.15

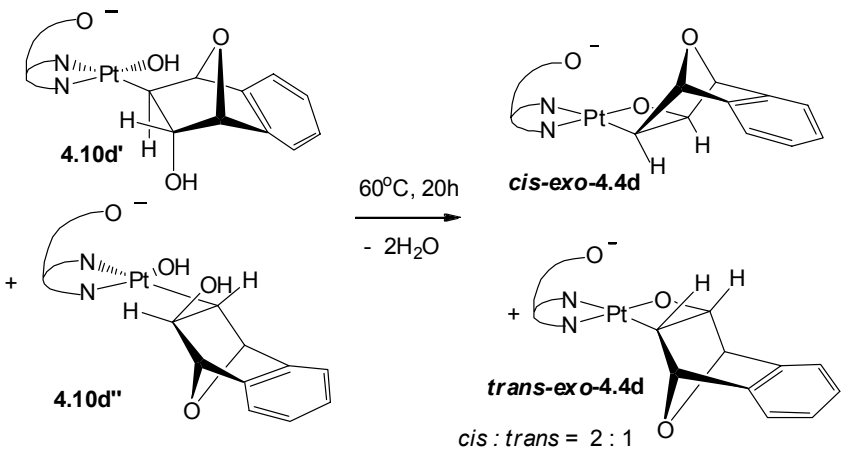

When conversion of **4.9d** into **4.4d** was complete according to ^1H NMR spectroscopy, the only Pt-containing anionic species detected by ESI mass

spectrometry had a m/z of 604.1, corresponding to an anionic oxetane **4.4d** $[LPt^{II}(C_{10}H_8O_2\text{-}\kappa C,\kappa O)]^-$. ^1H and ^{13}C NMR characteristics of **4.4d** were similar to those of anionic oxetanes **4.4a-c.** ^{13}C NMR spectrum of *cis*-**4.4d** showed the presence of the Pt-bound α-C and O-bound β-carbon of the oxetane ring at -7.9 ppm and 94.5 ppm respectively.

Formation of **4.4d** is reversible: upon neutralization of the alkaline aqueous solution of **4.4d** with an equivalent amount of acid the complex **4.7d** forms quantitatively after less than 15 minutes.

We propose that the interconversion between **4.4d** and **4.10d**, as well as interconversion between isomeric **4.4d** and **4.10d**, could occur via an intermediate **4.1d** bearing η^2-coordinated 1,4-epoxy-1,4-dihydronaphthalene $LPt^{II}(\eta^2\text{-}C_{10}H_8O)(OH)$ (Scheme 4.16), and subsequent reversible inter- and intramolecular nucleophilic additions at the double bond of **4.1d**.

Scheme 4.16

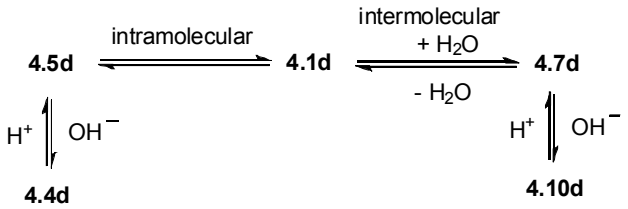

Unexpectedly, neutral solutions of **4.7d** in neat water or trifluoroethanol-water mixtures react with O_2 with a half-life of 18 hours at 20 ^oC to produce the Pt^{IV} oxetane ***cis*-4.3d** (eq. 4.16). The product was isolated in 86% yield in an analytically pure form and was characterized by NMR spectroscopy, ESI mass spectrometry and elemental analysis. No trace of the acyclic product **4.9d** was detected in the reaction

mixtures by ^{1}H NMR spectroscopy during oxidation and after completion of the reaction.

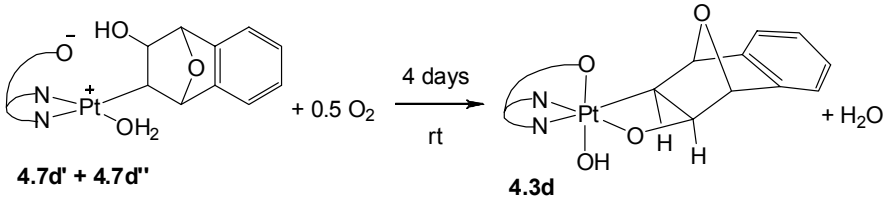

4.7d' + 4.7d'' **4.3d** (4.16)

The ^{1}H NMR spectrum of **4.3d** in DMSO-d_6 is indicative of the presence of only one OH group, which appeared as a broad singlet at 3.51 ppm. ^{13}C NMR spectrum of **4.3d** reveals the presence of the Pt-bound α-carbon at 2.5 ppm, characterized by a coupling constant $^1J_{PtC}$ = 463 Hz, and the O-bound β-carbon of the oxetane ring at 93.1 ppm, accompanied by Pt satellites with a smaller coupling constant $^2J_{PtC}$ = 80 Hz, which are similar to ^{13}C NMR characteristics of Pt^{IV} oxetanes **4.3a-c**. Consistent with the proposed structure, ESI-MS of acidified aqueous solution of ***cis*-4.3d** is evident of the presence of a protonated **4.3d***H^+, characterized by m/z 622.1. *Cis*-configuration of complex **4.3d** was assigned based on NOE experiments.

Formation of Pt^{IV} oxetane product from initially acyclic complex **4.7d** implies that the acyclic **4.7d** / **4.10d** and the oxetanes **4.5d** / **4.4d** are interconvertible in neutral aqueous solutions (Scheme 4.16). Although oxetanes **4.5d** or **4.4d** were not detected in neutral aqueous solutions of **4.7d** in noticeable amounts, they could be present at low concentrations undetectable by ^{1}H NMR spectroscopy, and in the presence of O_2 **4.4d** could be oxidatively "trapped" to irreversibly form **4.3d**, as one might expect from our earlier observations of facile aerobic oxidation of **4.4a-c**.

Although an acyclic anionic complex **4.10d** might also be present in a neutral aqueous solution of **4.7d**, no acyclic Pt^{IV} product **4.9d** was detected by ^{1}H NMR

spectroscopy among the reaction products in noticeable amounts. One possible explanation for this observation might be higher acidity of the Pt-bound OH group of oxetane **4.5d**, compared to an aqua ligand in **4.7d**, which would lead to higher concentrations of a reactive anionic species **4.4d**, compared to an anionic **4.10d**. Unfortunately, the low solubility of a neutral complex **4.7d** prevented us from obtaining experimental data on its acidity, so that the hypothesis stated above could not be tested experimentally.

By contrast to aerobic oxidation, which requires the presence of a reactive anionic species, a strong oxidant such as H_2O_2 oxidatively "traps" the predominant acyclic form of **4.7d** existing in solution, thus leading to the formation of the acyclic product **4.9d** exclusively.

Interestingly, heating solutions of **4.9d** in DMSO at 80 ^{o}C quantitatively produced another isomeric Pt^{IV} oxetane, **4.11d**, which was isolated in 80% yield in an analytically pure form and was characterized by NMR spectroscopy, mass spectrometry and elemental analysis. When the reaction was performed in thoroughly dried DMSO-d_6, formation of one equivalent of free water was detected by ^{1}H NMR spectroscopy (eq. 4.17). Based on NOE experiments, **4.11d** was assigned a structure with the Pt-bound alkyl *trans* to the sulfonate (Fig. 4.5).

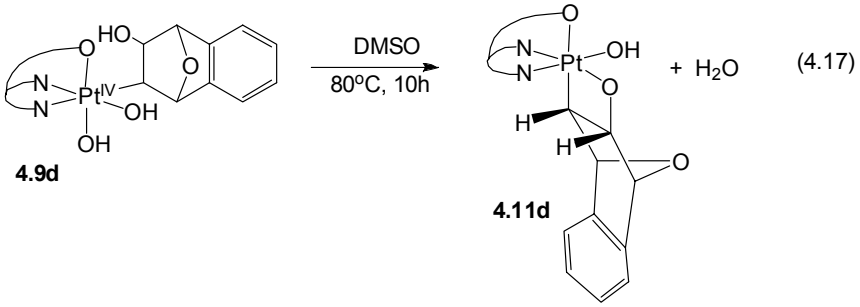

(4.17)

The ^{1}H NMR spectrum of the isolated **4.11d** in DMSO-d_6 had only one OH group appearing as a broad singlet at 3.90 ppm, characterized by platinum satellites ($^{2}J_{PtH}$ = 20 Hz). The assignment of this peak as the OH group was confirmed by the absence of cross-peaks in HSQC spectrum. The ^{13}C NMR the chemical shifts of the Pt-bound carbon, 6.8 ppm, ($^{1}J_{PtC}$ = 500 Hz) and O-bound carbon, 93.4 ppm, ($^{2}J_{PtC}$ = 82 Hz) observed for **4.11d** were notably different from those of the acyclic complex **4.9d**, and similar to ^{13}C characteristics of Pt^{IV} oxetanes **4.3a-c**.

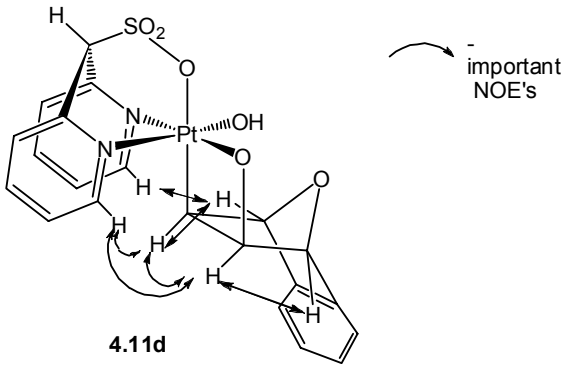

Figure 4.5. Structure assignment of complex **4.11d**, based on NOE experiments.

The complex **4.11d** could result from an intramolecular, entropy-favored nucleophilic substitution of the hydroxyl group of the 1,4-epoxy-3-hydroxynaphthalyl residue in **4.9d** with the oxygen atom of the Pt-OH group, to release water and a Pt^{IV} oxetane. Nucleophilic reactivity of transition-metal hydroxo groups is known and was discussed in more detail in Chapter 2.[76, 82, 83, 146] The nucleophilic substitution in **4.9d** proposed above could be followed, or preceded, by thermal isomerization of the acyclic or oxetane complex into an isomer with a Pt-bound carbon *trans* to the sulfonate, similar to thermal isomerization of (dpms)Pt alkyl complexes described in Chapters 2 and 3.

4.1.2.2. Reductive Elimination of Epoxides from Pt^{IV} Oxetanes

a) Reductive elimination of *cis*-cyclooctene oxide from 4.3a. The Pt^{IV} oxetane complex **4.3a** eliminates *cis*-cyclooctene oxide **4.12a** in DMSO solution at 60-80 ^{o}C and produces Pt^{II} complex **4.13** ($t_{1/2}$ = 132 min, $\Delta G^{\neq}$ = 25.7 kcal/mol at 60 ^{o}C), quantitatively by ^{1}H NMR (Scheme 4.17).

Scheme 4.17

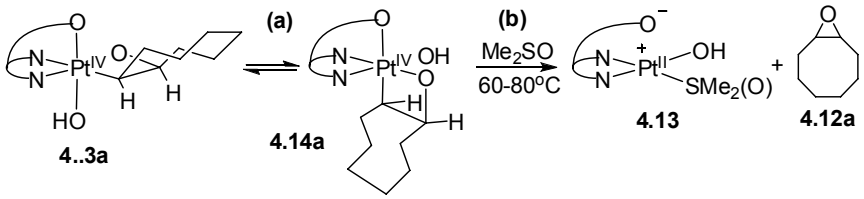

The epoxide **4.12a** was identified by GC/MS and NMR spectroscopy by comparison with an authentic sample. Complex **4.13**, isolated from the reaction mixture in 59% yield in an analytically pure form, was characterized by ^{1}H, ^{13}C NMR spectroscopy, ESI mass spectrometry and elemental analysis. The identity of **4.13** was confirmed by its independent synthesis from **4.1a** or **3.2** in DMSO solutions via olefin displacement. The IR spectrum of a solid sample **4.13** confirmed coordination of the DMSO ligand through sulfur atom: the ν(S=O) band of S-coordinated dimethylsulfoxide appeared at 1127 cm^{-1}, typical for dimethyl sulfoxide Me_2S=O coordinated to a metal through the sulfur atom, and was shifted to higher frequencies compared to free DMSO (1050 cm^{-1}).[147]

The reaction is 1st order in **4.3a**, with the reaction rate constant well reproducible to the extent of 2% in two runs at variable concentrations of **4.3a**. The activation parameters, $\Delta H^{\neq}$ = 23.7±0.3 kcal/mol and $\Delta S^{\neq}$ = -6.2±0.9 cal/(K·mol), determined from the Eyring plot given in Fig. 4.6, are very similar to those found for

isomerization of *unsym*-(dpms)$Pt^{IV}Me(OH)_2$ to *sym*-(dpms)$Pt^{IV}Me(OH)_2$ in water described previously by Vedernikov.[79] Hence, the rate-liming step might be the transformation of **4.3a** into the more reactive isomer with a Pt-bound carbon in the axial position, **4.13a** (Scheme 4.17, step **a**). By analogy with the methyl complexes *unsym*-(dpms)$Pt^{IV}Me(OH)_2$ and *sym*-(dpms)$Pt^{IV}Me(OH)_2$, one could expect that the isomer with the alkyl group *trans* to a better leaving group, the sulfonate, is more reactive toward reductive elimination than the isomer with an alkyl group *trans* to the pyridyl, a poorer leaving group.

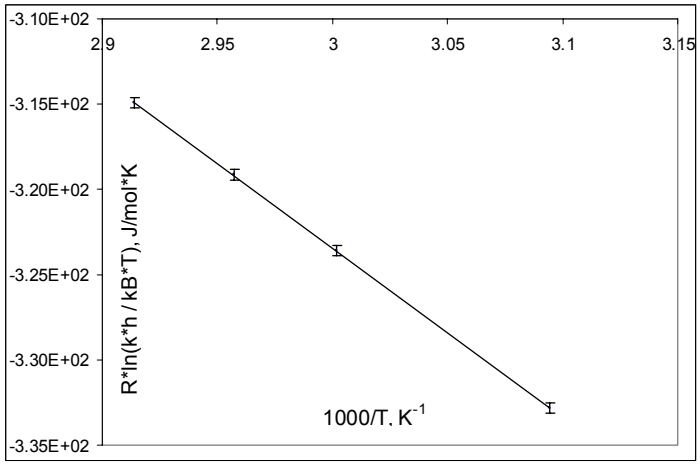

Figure 4.6. Eyring plot of reductive elimination from **4.3a** in DMSO-d_6.

The first order kinetic behavior and clean reductive elimination of **4.12a** from **4.3a** were also observed in MeOH ($t_{1/2}$= 388 min, 60 ^oC), water ($t_{1/2}$= 81 min, 60 ^oC) and CD_2Cl_2 ($t_{1/2}$= 526 min, 40 ^oC). In the latter two cases an insoluble complex, identified as a hydroxo-bridged dimer $L_2Pt^{II}{}_2(\mu\text{-}OH)_2$, **3.10** (Chapter 3), was produced along with **4.12a** (eq. 4.18). Interestingly, the epoxide elimination occurred even when solid **4.3a** was heated at 60-85 ^oC ($t_{1/2}$ = 6 hours at 85 ^oC).

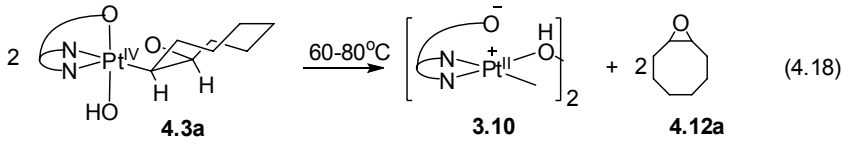

4.3a **3.10** **4.12a**

To get evidence in favor of the reaction mechanism given in eq. 4.16 we attempted to detect the proposed intermediate **4.14a** in DMSO, water or MeOH solutions, but without success. The result was different when less polar CD_2Cl_2 solvent was used. In this solvent, an intermediate was observed in concentrations not exceeding 13% of the initial concentration of **4.3a**, and was proven to be **4.14a** by ^1H NMR spectroscopy, COSY and NOE experiments (Scheme 4.18). The position of the cyclooctane ring pointing away from the Pt-OH ligand (Scheme 4.18) was determined from NOE experiments.

Scheme 4.18

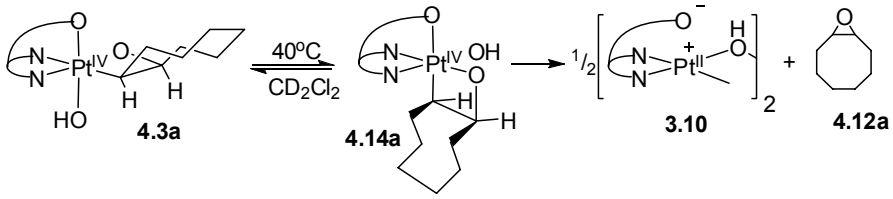

4.3a **4.14a** **3.10** **4.12a**

Modeling of the kinetic data obtained in CD_2Cl_2 at 40 °C (Fig. 4.7) allowed us to establish that the rate limiting step is the reversible isomerization of **4.3a** to **4.14a** ($\Delta G^{\neq}$ = 25.1 kcal/mol) followed by the epoxide elimination from **4.14a** ($\Delta G^{\neq}$ = 24.3 kcal/mol); with complex **4.3a** being 0.2 kcal/mol more stable than **4.14a**.

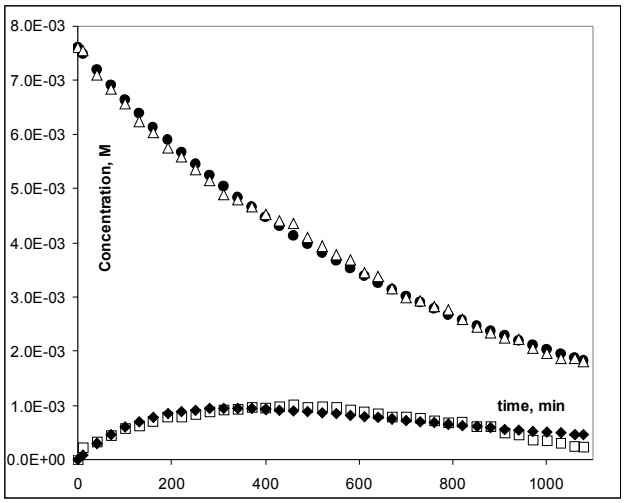

Figure 4.7. Modeling of kinetic data on isomerization of **4.3a** (measured: empty triangles, calculated: filled circles) to **4.14a** (measured: empty squares, calculated: diamonds) and epoxide **4.12a** elimination in CD_2Cl_2 solution at 40 °C.

Thus, the elimination of epoxide from **4.14a** is an intramolecular reaction which occurs readily in aprotic non-nucleophilic solvents such as dichloromethane. An intramolecular version of an S_N2 pathway, similar to that shown in Scheme 4.9a and involving dissociation of a negatively charged alkoxy tail of the oxetane, can be ruled out based on i) stereochemical considerations, since it requires inversion of the configuration at Pt-bound carbon, and ii) based on the fact that the reaction is facile even in weakly polar solvents such as dichloromethane.

We propose that the formation of epoxide from **4.14a** occurs via direct, concerted C(sp^3)-O reductive elimination from a Pt^{IV} center. The concerted mechanism of the alkyl-O reductive elimination from a Pt^{IV} center has, to the best of our knowledge, not been reported in the literature. Direct C(sp^3)-O reductive elimination from another d^6 metal center, Pd^{IV}, was proposed by Sanford, based on stereochemical studies.[78] An example of direct C(sp^3)-X elimination from a d^6 metal center involving a different heteroatom (X = I) was proposed by the Milstein group.[77] The latter reaction involves

intramolecular CH_3-I elimination from d^6 Rh^{III} complex, which was not consistent with an S_N2 pathway (Scheme 2.15, Chapter 2).[77]

b) Reductive elimination from 4.3b. Similar to the cyclooctene derivative **4.3a**, ***cis*-4.3b** eliminated *exo*-norbornene oxide **4.12b** and **4.13** in DMSO quantitatively by NMR (eq. 4.19).

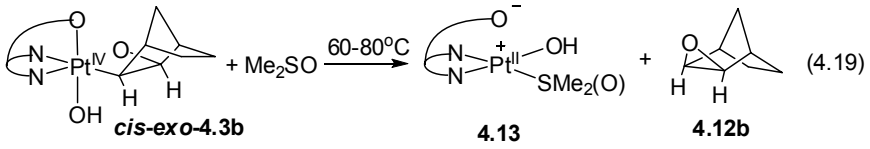

(4.19)

The reaction occurred at a faster rate ($t_{1/2}$=18 min at 60 °C) than for **4.3a** ($\Delta H^{\neq}$ = 22.1±0.7 kcal/mol and $\Delta S^{\neq}$ = -6.9±2.1 cal/(K·mol)). The Eyring plot for reaction 4.19 in DMSO is given in Fig. 4.8.

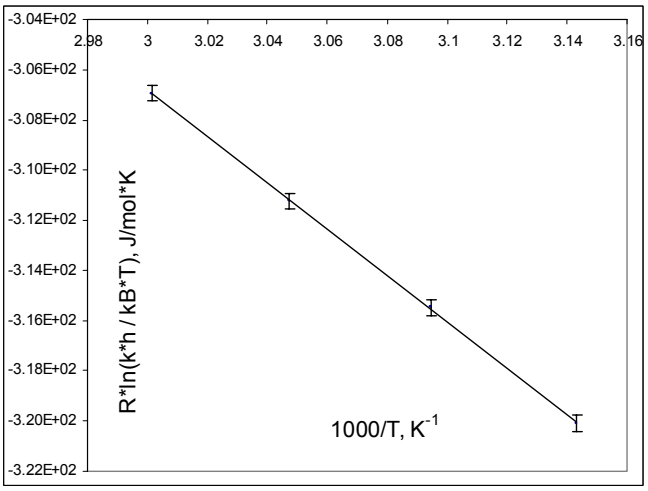

Figure 4.8. Eyring plot of reductive elimination from **4.3b** in DMSO-d_6.

The similarity of activation parameters observed in reactions (4.16) and (4.19) suggests that both reactions might have a similar rate determining step involving isomerization of **4.3** to **4.14**.

Elimination of *exo*-2,3-epoxynorbornane with a half-life of 58 minutes at 60 °C was also quantitative in CD_3OD solutions of **4.3b**.

With these results in hand, we attempted catalytic oxidation of norbornene with O_2 using **4.13** as a catalyst. The preliminary observations using methanol or 2,2,2-trifluoroethanol as solvents showed the complex decomposition via the loss of free DMSO and formation of $L_2Pt_2(\mu\text{-}OH)_2$ (**3.10**) and non-catalytic yields of epoxide **4.12b** (10-20% after 2-3 days based on **4.13**).

c) Reductive elimination from 4.3c. Complex **4.3c** reacted in DMSO-d_6 solution with a half-life of 18 minutes at 60 ^oC to produce a mixture of benzonorbornadiene-2,3-*exo*-oxide **4.12c** and **4.13**, which were identified by comparison with authentic samples. The reaction showed 1st order in **4.3c** and the rate constant was reproducible in two runs at 60 ^oC at variable concentrations of **4.3c** (k = (6.33±0.31)*10^{-4} s^{-1} at [**4.3c**] = 16 mM and k = (6.29±0.37)*10^{-4} s^{-1} at [**4.3c**] = 3.1 mM). However, the reaction was not clean. According to ^1H NMR spectroscopy, **4.12c** and **4.13** were produced in DMSO-d_6 solutions in low yields, 30-32% and 54-56% respectively. A mixture of unidentified products formed along with these products.

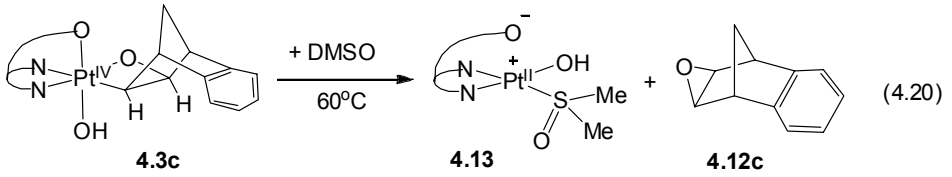

4.3c **4.13** **4.12c** (4.20)

The selectivity toward epoxide elimination was *ca* 30% and could not be improved by varying temperature, reaction time, concentration of **4.3c** and water content in DMSO-d_6 solvent. The reaction was unselective in other aprotic and protic solvents such as dichloromethane, methanol, acetone and acetonitrile.

The low selectivity of reaction (4.20) could not be explained by certain secondary transformations of the reaction products. Heating the epoxide **4.12c** together with

complex **4.13** in DMSO-d_6 solution at 60 ^{o}C did not show noticeable changes in concentrations of both **4.12c** and **4.13**.

Therefore, although the elimination of epoxide **4.12c** was observed in DMSO-d_6 solutions at as low as 60 ^{o}C, complex **4.3c** was prone to concurrent and yet undetermined decomposition pathways occurring at comparable reaction rates.

d) Attempted reductive elimination from 4.3d and 4.9d. By contrast to **4.3a-c**, complex **4.3d** was found to be more stable in DMSO-d_6 solution and decomposed with a half-life of *ca* 15 hours at 60 ^{o}C. However, neither *exo*-2,3-epoxide **4.12d** nor Pt^{II} complex **4.13** was detected after prolonged heating in DMSO or other solvents (dichloromethane, methanol, trifluoroethanol) by ^{1}H NMR and GC/MS. The absence of **4.12d** could not be explained by the low stability of epoxide **4.12d**. Heating **4.12d** together with **4.13** under the same conditions showed no significant changes to **4.12d** or **4.13** after 2 days at 60 ^{o}C. Their concentrations remained practically constant (±2%) by ^{1}H NMR. We can therefore conclude that the $\Delta G^{\neq}$ of the reductive elimination of epoxide from complex **4.3d** exceeds 30 kcal/mol. Therefore, the major process involved in reaction of **4.3d** involved some as yet undetermined side reactions.

A mixture of unidentified products and a dark precipitate formed eventually upon further heating of **4.3d** at 60 ^{o}C for several days. Trace amounts (<5%) of naphtol-1, naphtol-2 and naphthalenediols were detected after 160 hours of heating at 60 ^{o}C. These products were identified by ^{1}H NMR spectroscopy and GC/MS by comparison with authentic samples.

The isomeric oxetane complex **4.9d** was found to be extremely stable in DMSO-d_6 solutions. It decomposed slowly with a half-life of ~13.5 days at 80 ^{o}C and ~99 hours at 100 ^{o}C. No epoxide **4.12d** or **4.13** were found in reaction mixtures heated at 60-100 ^{o}C by ^{1}H NMR spectroscopy and GC/MS. Eventually, a mixture of unidentified soluble products and a dark precipitate formed after prolonged heating times; naphthalene, naphtol-1 and naphtol-2 were detected among the reaction products in 15%, 15% and 1% yield respectively. Formation of naphtols and naphthalene in reaction mixtures containing **4.9d** or **4.3d** could not be explained by decomposition of epoxide **4.12d**, as heating authentic samples of **4.12d** in the presence of Pt complex **4.13** under analogous reaction conditions did not produce any of these products.

Therefore, we can assume that the barrier of the epoxide reductive elimination from **4.9d** is very high, $\Delta G^{\neq}$ exceeding 30 kcal/mol.

4.1.2.3. DFT Modeling of the Pt Oxetane Formation and Reductive Elimination of Epoxides.

To gain insight into the reaction mechanism and to explain our experimental observations, we performed a DFT study of the reaction profile of oxidation of complexes **4.1a-b** with O_2 and the reductive elimination of epoxides from **4.14a-d**. DFT geometry optimization of the starting materials and products and reaction path calculations were done by Andrei Vedernikov.

The transformation of the olefin complex **4.1a** to the Pt^{II} oxetane **4.5a** is thermodynamically uphill, whereas the oxidation of **4.1a** with O_2 to form **4.3a** is favored by 14.1 kcal/mol (Fig. 4.9). This is consistent with our experimental observations of the olefin complex **4.1a** as a main species present in neutral solutions.

By contrast, the norbornene-derived Pt^{II} oxetane **4.5b** is significantly more stable than an isomeric hydroxo olefin complex **4.1b** due to a noticeable bicycloolefin strain relief achieved in the oxetane form, in accordance with our observation of an oxetane form present exclusively in solutions of **4.5b**.

The reaction path calculations show that the C-O elimination from **4.14a** is a concerted reaction that can be viewed as a "carbocation"-like migration of an alkyl from the Pt^{IV} center to the oxetane oxygen. The calculated Gibbs activation energy $\Delta G^{\neq}$ of the epoxide elimination from **4.14a** is 23.4 kcal/mol. The DFT calculations of Mulliken[148] and Hirshfeld[149] atomic charges on reacting Pt, C and O atoms of **4.14a** during C-O reductive elimination (eq. 4.21) showed that a positive charge is being built up at the reacting carbon atom during the transformation of **4.14a** to **TS-4.14a**.

The reductive elimination of epoxide from **4.3a** to form initially a Pt^{II} complex with the coordinated epoxide $LPt(C_8H_{14}O\text{-}\kappa O)(OH)$ **4.15a**, as shown in eq. 4.21, is characterized by the calculated ΔG^{o}_{298} of +0.3 kcal/mol. However, in the presence of a coordinating solvent such as DMSO, formation of the solvento complex **4.13** (eq. 4.22) is thermodynamically favorable. For example, formation of epoxide **4.12a** and **4.13** from **4.14a** is characterized by calculated ΔG^{o}_{298} of -11.0 kcal/mol.

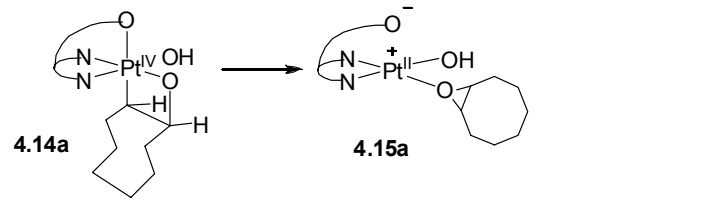

(4.21)

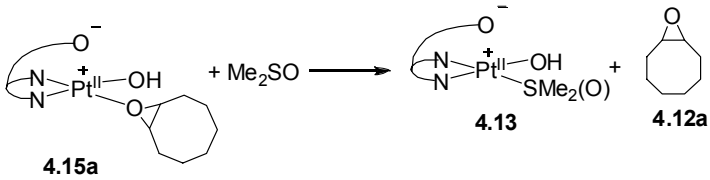

(4.22)

The transition state of the C-O epoxide elimination from **4.14a, TS-4.14a** (eq. 4.21), shown in Fig. 4.10a, is characterized by a significantly elongated distance between Pt and oxygen of the sulfonate group, Pt-O(SO_2) 2.932 Å , close to the Pt-O(SO_2) distance observed in (dpms)Pt^{II} complexes (3.0-3.1Å, determined by X-ray diffraction). The Pt-C5 distance in the transition state **TS-4.14a**, 2.665 Å, is considerably elongated compared to the Pt-C5 distance calculated for the ground state of **4.14a**, 2.095 Å. By contrast, the Pt-O2 distance changes only slightly during the transformation from **4.14a** (Pt-O2 2.009 Å, calculated by DFT) to **TS-4.14a** (Pt-O2 2.067 Å, Fig. 4.10).

Taking into account the polar character of the transition state, characterized by a significantly elongated Pt-O(S) bond (Fig. 4.10a), the activation barrier might diminish in polar solvents, consistent with our failure to detect the intermediate **4.14a** in DMSO, water, or MeOH.

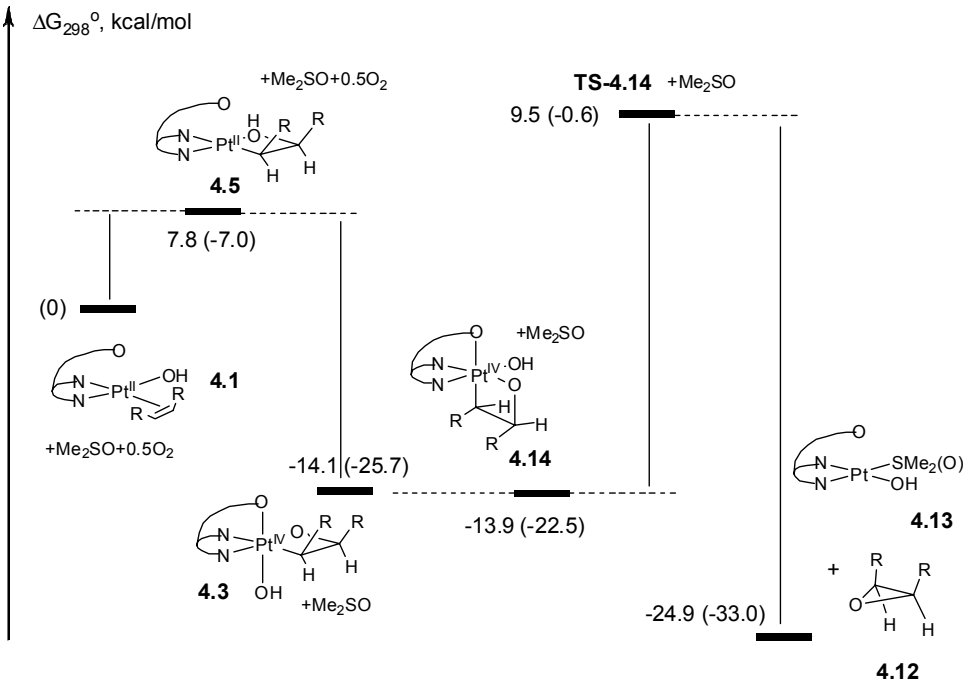

Figure 4.9. DFT-calculated Gibbs energy reaction profile for aerobic transformation of complexes **4.1a** and **4.1b** (numbers in parentheses) to corresponding olefin oxides.

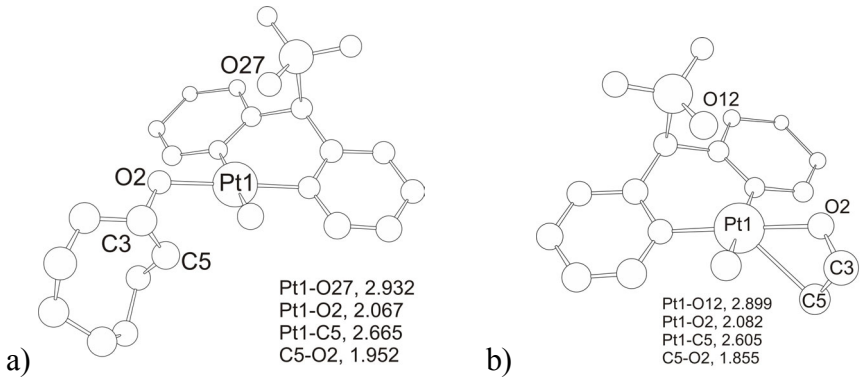

Figure 4.10. DFT-optimized geometry of transition states for direct C-O elimination from complexes TS-**4.14a** (a) and **4.14e** (b); bond lengths are in Å. Hydrogen atoms are omitted.

In turn, the Gibbs activation energy for the C-O elimination of *exo*-**4.14b**, 21.9 kcal/mol, is slightly lower than that for cyclooctene analogue **4.14a**. Consistent with this estimate, no trace of **4.14b** could be detected by NMR spectroscopy even in CD_2Cl_2 solutions during the course of C-O elimination from **4.3b**.

The geometry of the transition state for epoxide elimination from **4.14b**, **TS-4.14b**, was similar to the geometry of **TS-4.14a**, and characterized by the presence of a long Pt-C bond (2.722 Å) and a long Pt-O(SO_2) bond (2.914 Å).

The barrier $\Delta G^{\neq}$ for reductive elimination from **4.14c** was calculated to be 20.5 kcal/mol, suggesting that the reductive elimination from **4.14c** should be facile, as was indeed observed experimentally, despite observed low selectivity.

To understand the origin of the ability of Pt^{IV} oxetanes to react via a mechanism of a direct C(sp^3)-O reductive elimination, previously unprecedented in Pt^{IV} chemistry, we calculated the reaction barrier for concerted C-O reductive elimination of alcohols from a series of acyclic alkyl complexes *sym*-LPtR$(OH)_2$ (R = Me, Et, *i*-Pr) (Scheme 4.18).

Scheme 4.19

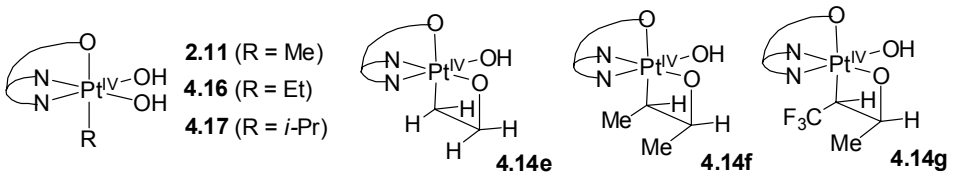

Notably, a very high reaction barrier was calculated for the direct C-O elimination from *sym*-LPtMe(OH)$_2$ **2.11**, 37.2 kcal/mol. Indeed, no reaction was observed for this complex in DMSO solution in the absence of strong nucleophiles after heating for several days at 80 ^{o}C. Interestingly, the DFT-calculated reaction barrier decreased in the order R = Me (37.2 kcal/mol) > R = Et (36.1 kcal/mol) > R = *i*-Pr (32.2 kcal/mol), implying that the substitution at the Pt-bound carbon affects the barrier of reductive elimination.

As compared to acyclic systems, even a lower barrier of 31.6 kcal/mol was calculated for the parent ethylene-derived Pt^{IV} oxetane **4.14e**, $LPt^{IV}(OH)(C_2H_4O$-*κC,κO*) (Scheme 4.18, Fig. 4b, Table 4.1), suggesting that the oxetane ring strain plays an important role in lowering the reaction barrier. The calculated barrier of 24.3 kcal/mol for the *cis*-2-butene-derived oxetane complex **4.14f** (Scheme 4.18, Table 4.1), containing a secondary alkyl at the platinum was lower than for **4.14e**.

The lower calculated reaction barrier in complexes containing secondary alkyls bound to platinum might be due to a weaker Pt-*sec*-alkyl bond, as compared to a Pt-primary alkyl bond.[150] As discussed above, the transition states of the epoxide reductive elimination from **4.14a-c** (Fig. 4.10) are characterized by significantly elongated Pt-C bonds, meaning that the energy of the Pt-alkyl bond is an important factor.

Although no experimental data are available for Pt^{IV}-*sec*-alkyl bond energies, the Bergman group established that in a d^6 Ir^{III} complex $(Cp^*)(PMe_3)Ir^{III}(H)(R)$ the Ir-(*n*-pentyl) (primary) bond is 5.5 kcal/mol stronger than the Ir-cyclohexyl (secondary) bond.[151] Similar trend of increasing bond strength in the order of $3^o > 2^o > 1^o$ was found in other metal-alkyl complexes and was explained by contributions of both steric and electronic factors.[150, 152-155]

The DFT calculations showed that the barrier for direct C-O reductive elimination from 1,4-epoxy-1,4-dihydronaphththalene derivative **4.14d** is very high, 30.5 kcal/mol, consistent with our observation that **4.3d** did not eliminate epoxide **4.12d** even after heating for prolonged reaction times in various aprotic and protic solvents.

We hypothesized that one of the reasons for that might be a stronger Pt-C bond in **4.14d**, which contains an electron-withdrawing oxo-substituent in the β-position to the Pt-bound carbon. It is often proposed that the electron-withdrawing ability of the alkyl ligand correlates with the metal-alkyl bond strength and bond length.[69, 150, 153, 154] Moreover, in ^1H NMR spectrum of the equatorial isomer **4.3d**, the value of a coupling constant $^2J_{PtH}$ of the CHPt signal of 82 Hz is greater than the value of $^2J_{PtH}$ in other Pt^{IV} oxetanes, **4.3a-c** (70-72 Hz), suggesting that a stronger Pt-alkyl bond is present in **4.3d**, as compared to **4.3a-c**. In addition, steric factors might also be important,[152, 153, 155] and greater stabilization of the ground state in less sterically crowded **4.14d** containing a more compact oxo-bridge as compared to the methylene in norbornene analogues **4.14b-4.14c** might play a role. Although we do not have X-ray data for **4.14a-d**, there is correlation between the calculated reaction barriers and the calculated bond lengths in the DFT-optimized structures of **4.14a-f**.

Table 4.1. Calculated reaction barriers for direct C-O reductive elimination and calculated bond lengths in DFT-optimized structures of **4.14** (Scheme 4.18).

Complex	DFT-calcd. $\Delta G^{\neq}$, kcal/mol, for direct C-O elimination	DFT-calcd. Pt-C bond length, Å, in optimized geometry of **4.14**
4.14c	20.5	2.091
4.14b	21.9	2.089
4.14a	23.4	2.085
4.14f	24.3	2.087
4.14d	30.6	2.078
4.14e	31.6	2.063
4.14g	33.7	2.070

Altogether, our experimental observations and computational study suggest that the C-O reductive elimination from oxetanes **4.14a-c** proceeds via a concerted mechanism which is different from an S_N2 process observed for alkyl Pt^{IV} complexes earlier.[146]

4.1.3 Conclusions

The isolated and fully characterized complexes **4.3a-d** are first Pt^{IV} oxetanes obtained by oxidation of the corresponding olefin precursors with dioxygen, enabled by the presence of the tripod dpms ligand. In the absence of oxidants formation of the corresponding Pt^{II} oxetanes involving an intramolecular nucleophilic addition of a Pt^{II}(OH) ligand to the coordinated olefin was observed.

The Pt^{IV} oxetanes **4.3a-c**, derived from *cis*-cyclooctene, norbornene and benzonorbornadiene reductively eliminate epoxides and Pt^{II} complex under mild conditions in various aprotic and protic solvents via a mechanism of direct C(sp^3)-O reductive elimination from a Pt^{IV} center, previously undocumented for this metal.

Importantly, **4.1a** derived from *cis*-cyclooctene containing reactive allylic hydrogens, could also be involved in these aerobic transformations, so that Pt^{IV} oxetane and epoxide were produced cleanly in aqueous solutions.

Nature of the olefin substrate affects strongly the ease of C-O reductive elimination: 1,4-epoxy-1,4-dihydronaphthalene derivatives do not eliminate corresponding epoxides.

Future directions of this works might involve development of a catalytic system for aerobic epoxidation of olefins by modification of the ligand system aiming at improving solubility, stability and activity of the Pt^{II} catalyst.

4.2 Allylic CH Activation in (dpms)Pt^{II}OH Complexes with cis-Cyclooctene, Cyclopentene and Propylene

4.2.1 Introduction

One of the limitations of the currently used heterogeneous silver catalyst of direct epoxidation of olefins with O_2 (air) is its low selectivity in oxidation of olefins containing allylic hydrogens, such as propylene and 1- and 2-butene. Activation of reactive allylic bonds precludes epoxidation route and results in complete combustion to CO_2 and H_2O.[24, 98] Similar allylic CH activation was noted in homogeneous chemistry of metallaoxetanes, proposed intermediates of olefin epoxidation (Scheme 4.6).[117, 125] According to Paul Sharp's results, Pt^{II} oxetane formation by the reaction of Pt^{II} oxo complexes with olefins is limited to derivatives of bicyclic [2.2.1] strained olefins such as norbornene and benzonorbornadiene, in which formation of η^3-allyl complexes is prohibited by Bredt's rule,[2] whereas the reaction of Pt^{II} oxo complex [(1,5-COD)$_4$Pt$_4$(μ^3-

$O)_2Cl_2](BF_4)_2$ with propylene gave the product of the allyl CH bond activation, the allyl complex $[(COD)Pt(\eta^3\text{-}CH_2CHCH_2)]^+$, along with acetone, $[(COD)PtCl_2]$, and $[(COD)Pt(Cl)(CH_2C(O)CH_3)]$.[133] As we have shown in Section 4.1 of Chapter 4, the *cis*-cyclooctene complex $LPt(\eta^2\text{-}cis\text{-cyclooctene})(OH)$ (L = dpms), **4.1a**, is involved in clean Pt^{IV} oxetane formation and epoxide elimination in aqueous solutions. However, we have found that the reactivity of **4.1a** depends dramatically on a solvent used and the allylic complex is readily produced in aprotic solvents or in methanol-water mixtures (eq. 4.23). However, the allylic CH activation proceeds in neat water at a very slow rate and does not compete with oxidation with O_2 in the presence of substoichiometric NaOH, thus explaining high selectivity of Pt^{IV} oxetane formation in aqueous solution. Interestingly, we observed slow H/D exchange in allylic positions of the coordinated *cis*-cyclooctene in D_2O in the absence of NaOH, in neutral solutions. The effect of solvents and acid additives on the reactivity of **4.1a** in allylic CH activation will be discussed in this section.

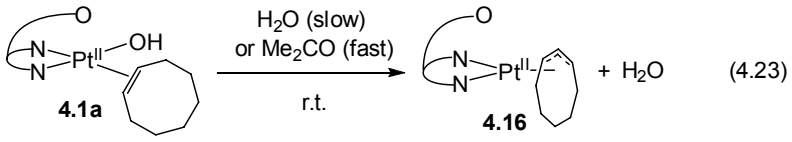

(4.23)

It is proposed that the double bond coordination to a metal center increases reactivity and acidity of the allylic hydrogens of the olefin ligand.[156, 157] For example, deprotonation of the allylic positions of the coordinated alkenes in Fe(II),[158-160] Re(II),[157] Rh(I) and Ir(I)[161] complexes in the presence of a base (trialkylamines, *t*-BuOK, NaOMe), leading to the formation of the corresponding η^3- or η^1-allyl complexes is known for many decades. Allylic CH activation is involved in a number of synthetically useful transformations catalyzed by Pd(II).[162] A few examples of the allylic CH activation both in the presence[163]

or in the absence of a base are known in Pt(II) chemistry, in the latter case involving complexes containing weakly bound ligands such as triflates[164] and trifluoroethanol CF_3CD_2OD[165] in weakly coordinating solvents (CH_2Cl_2, 2,2,2-trifluoroethanol). For example, Bercaw *et al.* reported an allylic activation of cyclohexene in trifluoroethanol by dicationic diimine bis(trifluoroethanol) complexes and proposed the mechanism involving dissociation of the two weakly bound trifluoroethanol ligands as shown in Scheme 4.20.[165]

Scheme 4.20

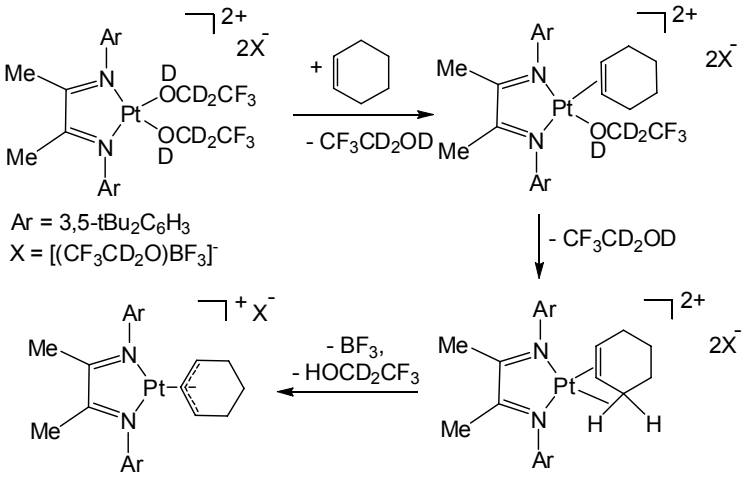

At the same time, examples of the allylic CH activation with Pt^{II} complexes bearing more strongly coordinating aqua or hydroxo ligands in the absence of an external base are much less common. A recent example involves an acid-catalyzed allylic CH activation of cyclohexene and indene by dihydroxo-bridged diimine Pt^{II} dimers in dichloroethane, reported by Bercaw *et al.* (Scheme 4.21),[166] however, the mechanism of the CH activation was not studied.

Scheme 4.21

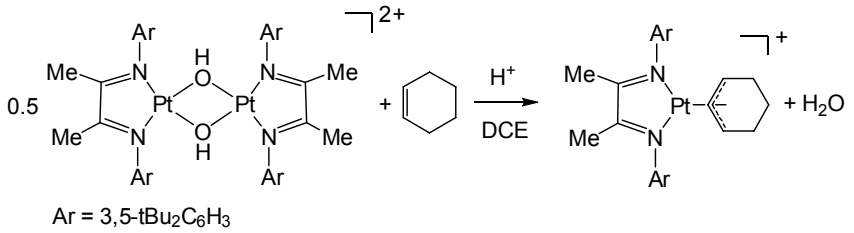

At the same time, it is especially important to know the mechanism of CH activation in hydroxo or aqua complexes since it is relevant to the CH activation of hydrocarbons in water, which is considered as the practically advantageous "green" solvent for possible catalytic applications. It is known that the presence of the basic hydroxo group can play an active role in some CH activation processes.[167]

Since allylic activation of the coordinated *cis*-cyclooctene in LPt(η^2-C_8H_{14})(OH) **4.1a** (eq. 4.23) is observed in the presence of large amounts of water and in the absence of strong bases, we thought it might be interesting to explore the mechanism of this transformation in order to gain insight into the reactivity of Pt hydroxo complexes in CH activation reactions.

4.2.2 Results and Discussion

*4.2.2.1 Preparation of LPt(η^3-C_8H_{13}) **4.16** and H/D Exchange in **4.1a** in D_2O Solution.*

Aqueous 19.5 mM solution of LPt(η^2-C_8H_{14})(OH), **4.1a**, reacts slowly at room temperature with a half-life of 40 days to produce a small amount of colorless prismatic crystals after two weeks that were identified by single crystal X-ray diffraction as an allylic complex **4.16** (eq. 4.23). The X-ray crystal structure of **4.16** is given in Fig. 4.11. White fine-crystalline powder that precipitated along with **4.16** was identified by ESI mass spectrometry as $L_2Pt^{II}_2(\mu\text{-}OH)_2$, **3.10**, characterized earlier.[79] Formation of

3.10 can be explained by the loss of the *cis*-cyclooctene ligand in **4.1a** to form unstable LPt(OH)(OH_2), which, according to the previous studies by Vedernikov,[79] tends to dimerize with the loss of water to give **3.10** (eq. 4.24).

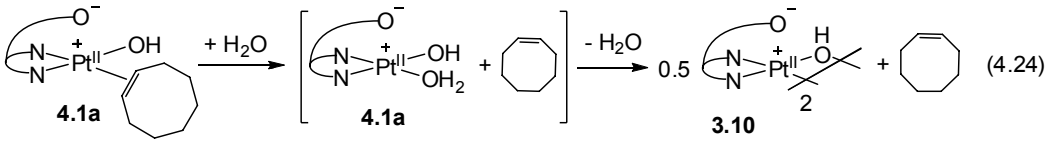

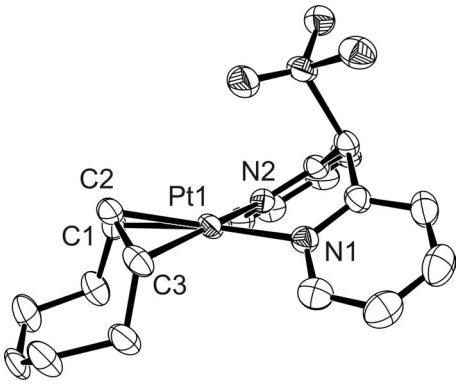

Figure 4.11. ORTEP plot for complex ***exo*-4.16**. Hydrogen atoms are omitted for clarity. Selected bond lengths (Å) and angles (°): Pt1-C1, 2.143(5); Pt1-C3, 2.132(5); Pt1-C2, 2.086(5); Pt1-N1, 2.102(4); Pt1-N2, 2.089(4); C1-C2, 1.440(7); C2-C3, 1.428(7); C1-C2-C3, 118.8(4).

According to X-ray diffraction data, complex **4.16** has a C_s symmetry with an orientation of a *meso*-proton C2-H pointing toward the sulfonate group and the cyclooctenyl ring pointing away from the sulfonate, which will be referred to as an *exo*-isomer. Only an *exo*-isomer was present in a single crystal analyzed by X-ray diffraction.

The reaction (4.24) can be accelerated at elevated temperatures: **4.1a** reacts at 70 °C with a half-life of 2 hours and produces a mixture of **4.16** and **3.10** in 30% and 70% yield respectively. Therefore, in neat water as a solvent the loss of cyclooctene ligand to produce **3.10** (eq. 4.24) occurs faster than the allylic activation to form **4.16** (eq. 4.23).

Notably, if a mixture of methanol and water was used, more facile and more selective transformation into allylic complex **4.16** (eq. 4.24) was accomplished. For example, **4.1a** in CD_3OD-D_2O mixture (8.2/1 ratio by volume, corresponding to $[CD_3OD]$=22 M and $[D_2O]$=6.0 M) reacted at 70 ^oC with a half-life of 12 minutes to give **4.16** in 85-90% yield after 3 hours.

Remarkably, fast and virtually quantitative formation of the allylic complex **4.16** as the sole product occurred readily even at room temperature in aprotic weakly coordinating solvents, such as acetone, dichloromethane and DMF (eq. 4.23). Upon dissolving **4.1a** in these solvents clean conversion into **4.16** was observed in dilute solutions with a half-life of 10-20 minutes at room temperature. When the reaction was performed in dry deuterated solvent, formation of one equivalent of free water was detected by ^{1}H NMR spectroscopy (eq. 4.23). Complex **4.16** was isolated in an analytically pure form in 67% yield from acetone solution of **4.1a** and characterized by NMR spectroscopy, ESI mass spectrometry and elemental analysis.

Two isomers were detected by ^{1}H NMR in solutions of **4.16**, assigned as *endo*-**4.16** and *exo*-**4.16**, with an *endo*- : *exo*- ratio being a function of a solvent. The configuration of the isomers was established by NOE experiments as shown in Fig. 4.12. The *endo*- : *exo*- ratio was found to be 3.3:1 in DMF-d_7, 3:1 in DMSO-d_6 and 1:1 in CD_3OD.

^{1}H NMR spectra of both *endo*- and *exo*-isomers were consistent with C_s symmetry of **4.16**. Each isomer gave rise to a set of four multiplets of the aromatic protons of two equivalent pyridyls of the dpms ligand, each multiplet integrating as 2H relative to a singlet of the bridging $CHSO_3$ group. Accordingly, each isomer was

characterized by a triplet of a *meso*-proton integrating as 1H and a multiplet of two equivalent *syn*-protons of mirror-symmetrical **4.16** integrating as 2H. *Meso*-protons of an *endo*- and *exo*-isomer appeared as downfield shifted triplets at 5.75 ppm and 5.39 ppm respectively, accompanied by platinum-195 satellites with J_{PtH} coupling constants of 93 Hz (*endo*-**4.16**) and 79 Hz (*exo*-**4.16**) in DMF-d_7 solution. *Syn*-protons of *cis*- and *trans*-**4.16** gave rise to multiplets at 4.40 ppm and 4.36 ppm respectively, with J_{PtH} coupling constants of 48 Hz in *endo*-isomer and 44 Hz in *exo*-isomer.

Observation of two separate sets of peaks for *endo*- and *exo*-isomers of **4.16** in various solvents (DMF-d_7, DMSO-d_6 and CD_3OD) suggests that the interconversion between isomers is slow on the NMR time scale. We can conclude, based on the frequency difference between singlets of the $CHSO_3$ groups of 28 Hz in DMF-d_7, that the half-life of the isomer interconversion is greater than 0.011 seconds at 20 ^oC.[2]

At the same time, the constant ratio of two isomers, characteristic for each solvent, establishes in less than 10-15 minutes at room temperature after dissolution of **4.16**. For example, when a 1:1 *endo*- : *exo*-isomeric mixture, obtained by evaporating solution of **4.16** in CD_3OD, was redissolved in DMSO-d_6, a 3:1 mixture of *endo*- : *exo*-isomers was seen by ^1H NMR in less than 10-15 minutes after addition of a DMSO-d_6 solvent and the ratio of two isomers remained unchanged after several days at ambient temperature, suggesting that the interconversion between *endo*- and *exo*-isomers was complete in less than 15 minutes at 20 ^oC.

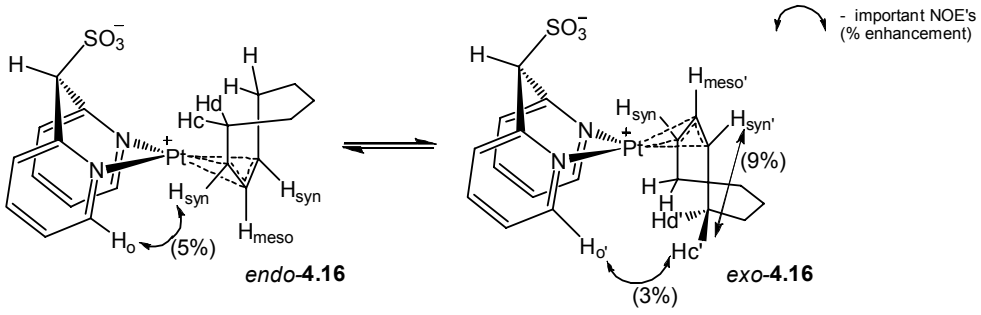

Figure 4.12. Structure assignment of *endo*- and *exo*-**4.16** from NOE experiments.

Allyl complexes of transition metals often show fluxional behavior that can be revealed by 2D exchange spectroscopy (EXSY) NMR.[2, 69] 2D EXSY spectrum of **4.16** in DMF-d_7 showed the exchange cross-peaks between the corresponding resonances of *endo*- and *exo*-isomers at a mixing time of 0.3 seconds. For example, an exchange cross-peak was seen between well-resolved *meso*-protons of *endo*- and *exo*-isomers isomers at 5.75 ppm and 5.39 ppm respectively. Exchange peaks were also observed between aromatic peaks of the pyridyl protons of the dpms ligand in two isomers, for example, multiplets of *ortho*-protons of pyridyls at 9.12 ppm and 9.23 ppm assigned to *endo*-**4.16** and *exo*-**4.16** respectively.

No intermediates were detected by ^{1}H NMR spectroscopy in solutions of **4.16** containing interconverting *endo*- and *exo*-isomers in various solvents. Although the mechanism of *endo*-**4.16**/*exo*-**4.16** interconversion was not studied in this work, several possible pathways of such interconversion could be suggested, for example, dissociation/recoordination of the pyridyl arm of the dpms ligand or η^3-η^1 interconversion of the allyl fragment.[69]

Interestingly, an *intermolecular* allylic CH activation was accomplished by reacting LPt(DMSO)(OH) **4.13** with excess *cis*-cyclooctene in water-methanol solutions (eq. 4.25). However, the yield of **4.16** in this reaction was low, 22-31%

based on **4.13** after heating at 60 ^{o}C for 1 day, due to the faster concurrent loss of DMSO ligand to produce insoluble dihydroxo-bridged dimer **3.10** (eq. 4.26). The presence of O_2 did not affect the outcome of this reaction and no epoxide was detected among the reaction products, meaning that the allylic CH activation may be an important side reaction in platinum-mediated aerobic epoxidation of olefins containing allylic CH bonds.

$$\underset{\textbf{4.13}}{LPt^{II}(DMSO)(OH)} + C_8H_{14} \rightarrow \underset{\textbf{4.16}}{LPt^{II}(\eta^3\text{-}C_8H_{13})} + H_2O + DMSO \qquad (4.25)$$

$$2\ \underset{\textbf{4.13}}{LPt^{II}(DMSO)(OH)} \rightarrow \underset{\textbf{3.10}}{L_2Pt^{II}_2(\mu\text{-}OH)_2} + 2\ DMSO \qquad (4.26)$$

Although neutral aqueous solutions of **4.1a** are relatively stable toward formation of **4.16** and **3.10** under ambient conditions (half-life of decomposition of **4.1a** is 40 days at 20 ^{o}C), selective H/D exchange was observed in D_2O solution in allylic positions. Approximately 50% of all allylic protons were exchanged by deuterium from D_2O after 6 days at 20 ^{o}C. At the same time, H/D exchange in vinylic and other aliphatic protons of the *cis*-cyclooctene ligand did not exceed 6% after 14 days. The absence of H/D exchange in vinylic positions implies that the mechanism of this H/D exchange does not involve the formation of the η^3-allyl complex and the position of the double bond does not change during the H/D exchange.

The allyl complex **4.16** did not undergo H/D exchange in neutral CD_3OD-D_2O solutions and in the presence of NaOH or HBF_4 at 60-80 ^{o}C. After heating the neutral or basic solution of **4.16** in CD_3OD/D_2O at 100 ^{o}C for 12 hours no deuterium incorporation into cyclooctenyl ligand was observed by NMR spectroscopy. Very

slow decomposition took place in basic and neutral solutions of **4.16** at 100 °C. After heating for 12 hours, 95% of unreacted **4.16** remained in solution and small amount of unidentified dark precipitate formed. This result suggests that the reaction barrier $\Delta G^{\neq}$ for the H/D exchange in **4.16** in neutral and basic solutions exceeds 30 kcal/mol. Similarly, no H/D exchange was observed in acidic solution after heating **4.16** for 12 hours at 80 °C, and 5% of the starting material decomposed to unidentified insoluble products. Hence, formation of the allyl complex **4.16** from **4.1a** is essentially an irreversible process and H/D exchange in **4.1a** occurs before formation of **4.16**.

4.2.2.2. Preparation of Allylic Complexes Derived from Propylene and Cyclopentene. Attempted Preparation of Complexes Derived from Cycloheptene, Cyclohexene and Some Disubstituted Acyclic Alkenes.

We next attempted preparation of olefin complexes, analogous to **4.1a**, with other cycloalkenes, *cis*-cycloheptene and cyclohexene, using the same method of ethylene displacement in LPt(CH_2=CH_2)(OH), **3.2**, successfully applied earlier for synthesis of **4.1a**. No ethylene displacement was observed in reaction between **3.2** and excess cyclohexene in water or acetone–water solutions under reduced pressure at 20-50 °C. The ethylene complex **3.2** remained unreacted after several days, and no trace of a product that might incorporate cyclohexene was detected.

A slow allylic CH activation occurred when **3.2** was stirred with excess *cis*-cycloheptene in acetone–water solution under reduced pressure at room temperature. The product detected after 2 days was identified as an allyl complex LPt(η^3-C_7H_{11}), **4.17**. However, *ca* 60% of the starting material remained unreacted, according to ^{1}H NMR spectroscopy. In the ESI mass spectrum of the acidified reaction mixture, a signal of

protonated allyl complex $LPt(\eta^3\text{-}C_7H_{11})^*H^+$ characterized by m/z 540.1 was observed. ^1H NMR spectrum of the reaction mixture showed the presence of a new signal at 5.27 ppm (triplet, $J = 5$ Hz), that was assigned to a *meso*-proton of $LPt(\eta^3\text{-}C_7H_{11})$, based on its characteristically downfield shifted position and multiplicity. Low yield and the presence of significant amounts of unreacted starting material prevented us from isolating $LPt(\eta^3\text{-}C_7H_{11})$ in a pure form. When the reaction was performed at higher temperatures (40-50 ^oC) significant decomposition of **3.2** was observed.

We propose that the low reactivity of cyclohexene and *cis*-cycloheptene in ethylene substitution reaction is due to their weak binding ability toward platinum center, compared to ethylene or *cis*-cyclooctene. It is known that strained olefins form stronger complexes with metals compared to unstrained olefins.[69, 168] The equilibrium constant of the complex formation of cycloalkenes with silver nitrate in ethylene glycol solution, determined by Muhs and Weiss, was found to increase in the following order: cyclohexene < cyclopentene < cycloheptene < *cis*-cyclooctene < norbornene, ethylene.[168] The trend observed in a series of cycloalkenes correlates with the net strain energy calculated from their heats of hydrogenation to the corresponding cycloalkanes: *cis*-cyclooctene > cycloheptene ~ cyclopentene > cyclohexene.[169] The correlation between the complex formation constants and the heats of hydrogenation can be explained by the partial relief of the ring strain upon sp^2 to sp^3 rehybridization resulting from either hydrogenation or coordination to a metal center.[168]

Interestingly, the reaction between **3.2** and cyclopentene in water-acetone mixture (1:1 by volume) under reduced pressure led to the formation of the allyl complex LPt(η^3-C_5H_7) **4.18** in 60-70% yield by NMR. No product, which could be identified as η^2-cyclopentene complex LPt(η^2-C_5H_8)(OH), **4.19**, was detected during the course of the reaction (Scheme 4.22). The absence of **4.19** could be explained by a very low kinetic barrier of the subsequent allylic CH activation in intermediate **4.19** to produce LPt(η^3-C_5H_7) **4.20** in water-acetone mixture (Scheme 4.22).

Scheme 4.22

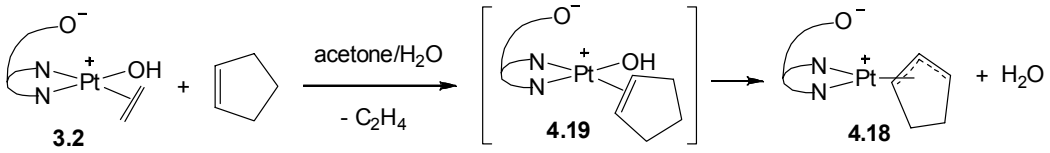

The low barrier for the allylic activation in LPt(η^2-C_5H_8)(OH), compared to **4.1a**, could be in part due the use of acetone-water mixture solvent during preparation of **4.18**. A shown above, allylic activation in **4.1a** is slow in neat water, but becomes more facile in neat acetone. Unfortunately, the reaction of **3.2** with cyclopentene in neat water was too slow, and mostly unreacted material was present in solution after stirring a biphasic water-cyclopentene mixture under reduced pressure for several days at 20-50 ^oC due to low solubility of cyclopentene in water.

Complex **4.18** was isolated in 30% yield after recrystallization from acetone and was characterized by NMR spectroscopy and ESI mass spectrometry. According to ^1H NMR, the two mirror-symmetrical isomers of **4.18** were present in D_2O solution in 1.1 : 1 ratio, presumably *endo*- and *exo*-**4.18**, resulting from different orientation of the allyl ligand relative to the sulfonate of the dpms ligand, similar to *endo*- and *exo*-isomers of **4.16**.

Hence, the ethylene displacement occurs more readily in reaction of **3.2** with cyclopentene, compared to cycloheptene, although the strain energies of cycloheptene and cyclopentene determined from their heats of hydrogenation[169] are almost the same. This result suggests that steric factor might play an important role in complexation of cycloolefin to a (dpms)Pt^{II}(OH) center, resulting in higher reactivity of less sterically demanding cyclopentene, compared to cycloheptene.

We next attempted to expand the scope of substrates to acyclic substituted alkenes. Not surprisingly, attempted ethylene displacement in **3.2** with acyclic 1,2- and 1,1-disubstitued olefins such as *cis*-stilbene, 1,1-diphenylethylene, and dimethyl maleate was unsuccessful, and these complexes could not be prepared by this method. This lack of reactivity could be attributed to steric bulkiness of these subtractes resulting in a weaker coordinating ability toward (dpms)Pt^{II}OH compared to ethylene.

A different strategy was used to prepare (dpms)Pt complex with gaseous olefins such as propylene and *cis*-2-butene. We first attempted to synthesize an olefinic complex LPt(η^2-C_3H_6)(OH) **4.20** via chloride abstraction from LPt(η^2-C_3H_6)Cl (**4.21**) with silver oxide Ag_2O in water. Complex LPt(η^2-C_3H_6)Cl was prepared by reacting potassium salt of the dpms with a propylene analogue of Zeise's salt, K[$PtCl_3$(η^2-C_3H_6)] (eq. 4.27).

$$K[PtCl_3(\eta^2\text{-}C_3H_6)] + KL \rightarrow \underset{\textbf{4.21}}{LPt(\eta^2\text{-}C_3H_6)Cl} + 2KCl \qquad (4.27)$$

$$\underset{\textbf{4.21}}{2LPt(\eta^2\text{-}C_3H_6)Cl} + Ag_2O \rightarrow \underset{\textbf{4.22}}{2LPt(\eta^3\text{-}C_3H_5)} + 2AgCl + H2O \qquad (4.28)$$

The allyl complex LPt(η^3-C_3H_5) **4.22** was detected by ^{1}H NMR spectroscopy and ESI mass spectrometry in the resulting reaction mixture (eq. 4.28). However, this

reaction was not clean and other unidentified byproducts were present along with **4.22**. The preparation of LPt(η^3-C_3H_5) **4.22** was achieved more cleanly by reacting LPt(η^2-C_3H_6)Cl with 1 equivalent of NaOH in water at 50 ^oC (Scheme 4.22).

Interestingly, the allyl complex **4.22** formed slowly already at room temperature. According to ^1H NMR spectroscopy the yield of **4.22** was 15% after 25 hours at 20 ^oC. At the same time, no trace of LPt(η^2-C_3H_6)(OH) **4.20** was detected in the reaction mixtures by ^1H NMR spectroscopy. By analogy with **4.18** (Scheme 4.22), we propose that formation of **4.22** occurs via initial rate-limiting Cl/OH ligand exchange in **4.21** to give **4.20**, followed by fast allylic activation to produce **4.22** (Scheme 4.23).

Scheme 4.23

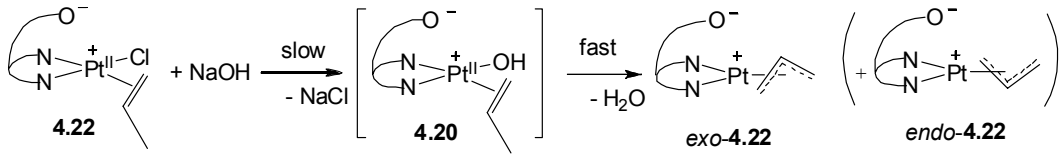

The reaction is accompanied by the formation of insoluble byproducts, presumably $L_2Pt_2(\mu\text{-}OH)_2$ or $L_2Pt_2(\mu\text{-}Cl)_2$, resulting from the loss of propylene. The product **4.22** was isolated in 47% yield after recrystallization from methanol, and characterized by ^1H, NOE, ^{13}C NMR spectroscopy and ESI mass spectrometry.

Complex **4.22** exists in D_2O solution as a mixture of two C_s-symmetrical isomers with similar ^1H and ^{13}C NMR characteristics, *exo*- and *endo*-**4.22** in 1.7 : 1 ratio respectively. Configuration of the isomers was determined by NOE experiments.

In the ^1H NMR spectrum of the major isomer, identified as *exo*-**4.21**, the *meso*-proton appeared as a multiplet centered at 5.06 ppm, accompanied by platinum-195 satellites (J_{PtH} = 84 Hz). Two doublets at 2.94 ppm ($^3J_{anti\text{-}meso}$ = 12 Hz) and 3.98 ppm ($^3J_{syn\text{-}meso}$ = 6.5 Hz), each integrating as 2H relative to the multiplet of the *meso*-

proton, were assigned as *anti*-protons H_a, and *syn*-protons H_s, respectively (Fig. 4.13). This assignment was based on the magnitudes of coupling constants and chemical shifts, which are expected to decrease in the order ${}^3J_{anti\text{-}meso} > {}^3J_{syn\text{-}meso}$; $\delta_{meso} > \delta_{syn} > \delta_{anti}$.[69]

Similar to **4.16**, both **4.22** and **4.18** were resistant to H/D exchange and stable in neutral and alkaline D_2O solutions after heating at 100 ^oC for 2-3 days.

In contrast to propylene complex **4.21**, the complex derived from *cis*-2-butene, LPt(η^2-*cis*-MeCH=CHMe)Cl (**4.23**), reacts with NaOH in water with liberation of *cis*-butene gas, and no allyl complex or LPt(η^2-*cis*-MeCH=CHMe)(OH) was detected. Therefore, *cis*-2-butene behaves as a better leaving group compared to chloride, and the displacement of the alkene rather than chloro ligand with hydroxide becomes more favorable process.

*4.2.2.3. Possible Mechanisms of the Allylic CH Activation in **4.1a**.*

Several possible mechanisms of the allylic CH activation in *cis*-cyclooctene involving complex **4.1a** were considered.

(i) As discussed in Chapter 3, the hydroxo ligand in the analogous ethylene complex LPt(η^2-CH_2CH_2)(OH), **3.2**, is a weakly basic group and its equilibrium constant for the basic hydrolysis K_b in water was determined to be $1.0*10^{-11}$. Although potentiometric determination of the basic properties of LPt(η^2-C_8H_{14})(OH), **4.1a**, was not possible due to low stability of **4.1a** in basic or acidic solutions, we propose that the basicity of Pt-OH in **4.1a** will be similar to that of **3.2**. Therefore, in 20 mM solution of **4.1a** in water a small fraction of a protonated complex **4.1a***H^+ [LPt(η^2-C_8H_{14})(OH_2)]$^+$ and OH^- could be present in low concentrations, $4.5*10^{-7}$ M,

corresponding to the *pH* 7.6. In turn, in aprotic solvents $[LPt(\eta^2\text{-}C_8H_{14})(OH_2)]^+$ might result from the protonation of **4.1a** with residual trace water that could be present in these solvents. Since an aqua ligand can serve as a better leaving group than the hydroxo ligand, one of the mechanistic possibilities might involve displacement of an aqua ligand of **4.1a***H^+ with a σ-CH bond of coordinated *cis*-cyclooctene to generate an intermediate **4.23** (Scheme 4.24, step *i-a*). Similar step was proposed by Bercaw for allylic CH activation in Pt complexes containing two weakly coordinating trifluoroethanol ligands (Scheme 4.20).[165]

Subsequent transformations might involve oxidative cleavage of the allylic CH bond to form platinum η^3-allyl hydride **4.24** (step *i-b*), which could undergo H/D exchange in D_2O or deprotonation to yield **4.16** (step *i-e*).

Scheme 4.24

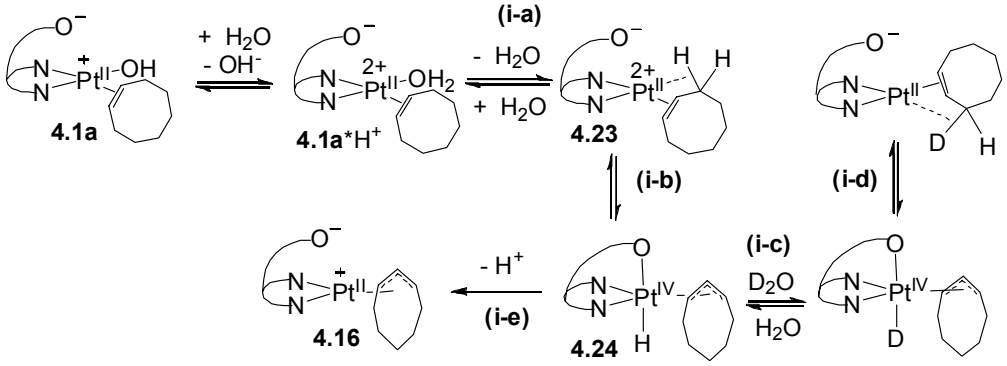

However, the mechanism shown in Scheme 4.24 (steps *i-b*, *i-c*, *i-d*) is not consistent with experimentally observed selectivity of deuterium incorporation: H/D exchange in vinylic positions of coordinated *cis*-cyclooctene should be expected, if mechanism (i) is operative, which is not observed experimentally.

A more important implication of this mechanism that can be checked experimentally is that formation of the allyl complex should be significantly

accelerated in the presence of acids due to higher concentrations of the aqua complex **4.1a***H^+, compared to a neutral solution.

(ii) Another possible mechanism might involve allylic CH cleavage in complex **4.25** which could result from a rearrangement of η^2-(π-C=C) coordinated *cis*-cyclooctene in **4.1a** to a less stable η^2-(σ-C-H) complex, as shown in Scheme 4.25 (step *ii-a*). Such σ-complexes of Pt^{II} are often proposed as intermediates in CH bond cleavage of alkanes.[170]

The cleavage of the allylic CH bond could involve oxidative addition to form Pt^{IV} η^1-allyl hydride **4.26** (step *ii-b*), which could subsequently undergo H/D exchange (step *ii-c*) or proton transfer isomerization to form an η^1-allyl complex **4.27** (step *ii-d*). Intermediate **4.27** can be transformed to **4.16** by displacement of an aqua ligand by a double bond of η^1-allyl to produce **4.16** (step *ii-e*).

The mechanism (ii) allows to account for selective H/D exchange in allylic position. At the same time, acid additives would accelerate prototropic isomerization of **4.26** to **4.27** and subsequently transformation of the latter to allylic complex **4.16**. This effect would be non-existent if steps *ii-d* and *ii-e* follow the rate-determining formation of **4.26**.

This mechanism does not allow to account for a very strong dependence of the rate of **4.16** formation on the polarity of the solvent used.

Scheme 4.25

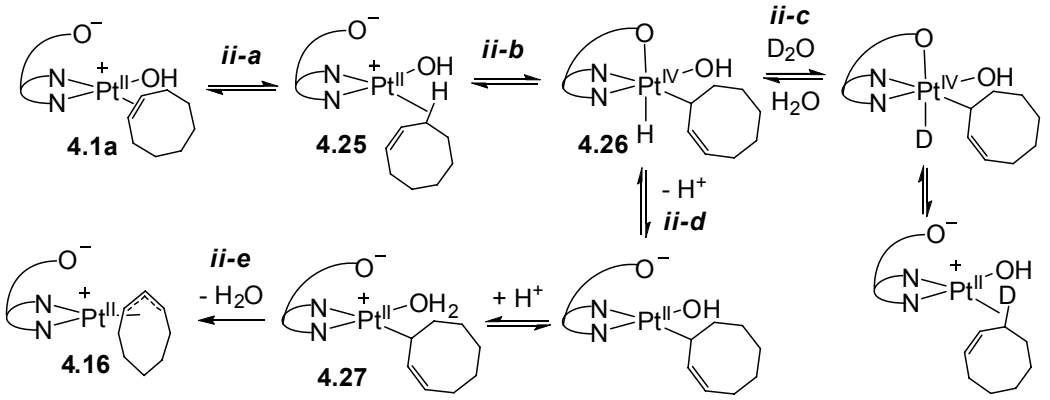

(iii) The third mechanism we analyzed is shown in Scheme 4.26. It involves *intramolecular* deprotonation of the allylic CH bond of the π-complex of *cis*-cyclooctene **4.1a** with a coordinated hydroxo ligand Pt-OH as a base, leading to an η^1-allyl complex **4.27** (step *iii-a*) as the first step.

Scheme 4.26

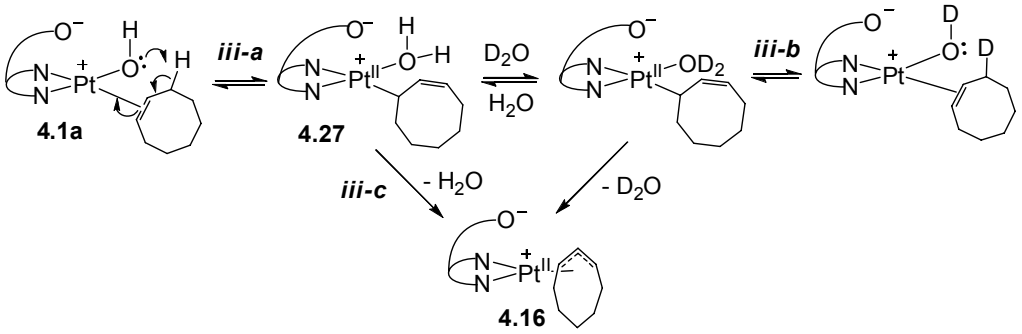

Intermolecular deprotonation of the allyl CH bonds of coordinated alkenes with external bases, such as Et_3N and *t*-BuOK, has been reported in the literature.[157, 159] For example, selective deprotonation of the allylic protons of alkene complexes of the iron Lewis acid $[CpFe(CO)_2]^+$ (Fp^+) with Et_3N in CH_2Cl_2 solution was demonstrated by Rosenblum (Scheme 4.27a).[159] The reverse reaction, protonation of Fe η^1-allyl complexes, is also known (Scheme 4.27b).[159]

Scheme 4.27

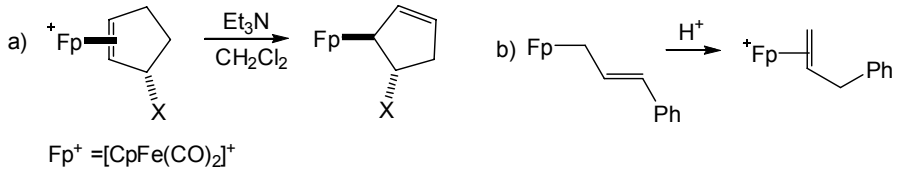

The deprotonation of Fp^+ alkene complexes reported by Rosenblum was highly stereospecific, and the mechanism was suggested resembling an E2 mechanism of elimination in organic chemistry (Scheme 4.28).[159]

Scheme 4.28. Mechanism for allylic deprotonation of alkene complexes of Fp^+ (cyclopropane resonance structure of the alkene complex was used to emphasize the similarity to E2 mechanism).

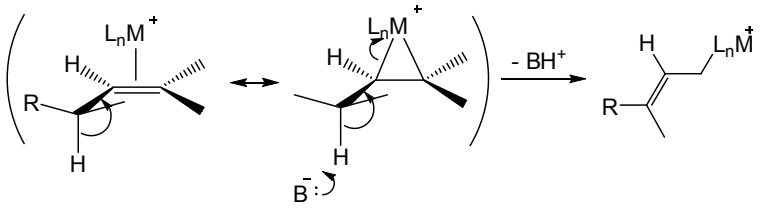

By contrast to a reaction in Scheme 4.27, the allylic deprotonation in our system might be intramolecular. The concentration of the hydroxide ion in aqueous 20 mM solution of **4.1a** is extremely low; $[OH^-]$ is estimated to be ~$4.5*10^{-7}$ M as described above. Assuming that the basicities of **4.1a** and **3.2** are similar, complex **4.1a** must be present in solution mostly (>99%) in its neutral form, with an intact Pt-OH group.

The ability of hydroxo complexes of late transition metals to act as bases has recently been reviewed by Fulton.[82] For instance, some Pt^{II} hydroxo complexes are known to react with acidic CH bonds of cyclopentadiene,[171] nitromethane, acetophenone,[172] acetone, phenylacetylene, 1,3-dibutadiyne[173] in aprotic solvents to form the corresponding organometallic complexes containing Pt-C bond.

Assuming that the mechanism (iii) is operative, one can account for selective H/D exchange at allylic positions of coordinated olefin in D_2O solutions of **4.1a** (Scheme 4.26, *iii-b*).

According to the mechanism (iii), both steps (*iii-a*) and (*iii-c*) are expected to accelerate in aprotic solvents and in methanol due to a greater basicity of the Pt-OH group in these solvents compared to water. The enhanced basicity is due to the absence of or weaker hydrogen bonding between the hydroxo ligand and a solvent. Methanol is known to be a weaker hydrogen bond donor than water.[174]

In addition, since the transformation of **4.27** into **4.16** (step *iii-c*) involves displacement of a coordinated water with a double bond of the η^1-allyl group, the formation of **4.16** is expected to be faster in poorly coordinating solvents. A faster water displacement in **4.27** might be anticipated in aqueous methanol due to lower concentrations of both water and methanol ([CD_3OD] = 25 M in neat CD_3OD, as compared to [D_2O] = 55 M in neat D_2O] and weaker coordination of methanol to Pt^{II} center.[175]

If mechanism (iii) is operative, acid additives are expected to weakly inhibit the formation of allyl complex **4.16**, due to protonation of the basic Pt-OH group required for step (*iii-a*) in Scheme 4.26. By contrast, just opposite effect is expected for mechanism (i), in which the protonated form **4.1a***H^+ is a reactive species in CH activation. Hence, a study of the effect of acid additives on the rate of formation of **4.16** might help rule out one of the mechanisms (i) or (iii). Unfortunately, the effect of the hydroxide ion on the kinetics of **4.16** formation could not be established

experimentally, since **4.1a** reacts rapidly with bases to produce a relatively unstable anionic oxetane **4.4a**.

*4.2.2.4. Kinetic Study of Formation of Allyl Complex **4.16** at Various Concentration of Acid in Methanol-Water Mixtures*

To establish the effect of acid additives on the rate of transformation of **4.1a** to **4.16**, the reaction was carried out in the presence of various amounts of HBF_4 in a $CD_3OD–D_2O$ mixture at 50 ^oC. The formation of **4.16** was monitored by ^1H NMR spectroscopy.

Methanol–water mixtures used in this study allowed for high selectivity of the transformation of **4.1a** to **4.16** *vs.* its concurrent hydrolysis to form **3.10**. The presence of methanol allowed also for sufficient solubility of both **4.1a** and **4.16** to monitor the reaction by ^1H NMR spectroscopy. The concentrations of **4.1a** and two isomeric complexes *exo*-**4.16** and *endo*-**4.16** were determined by integration of the resonances of the corresponding *ortho*-protons of pyridyls using 1,4-dioxane as an internal standard. Complex **3.10** and free *cis*-cyclooctene were only partially soluble in methanol-water mixture and their concentration could not be quantified by NMR spectroscopy. Both **4.16** and **3.10** were stable under the reaction conditions and no H/D exchange in **4.1a** was seen.

Since no other compounds except **4.1a**, **4.16**, free *cis*-cyclooctene, and $[LPt(OH_2)_2]^+(BF_4)^-$ **2.12** (in the presence of acid) were observed by ^1H NMR spectroscopy in the reaction mixtures, we assume that the disappearance of **4.1a** was solely due to two parallel pathways (4.23) and (4.24). The average selectivity toward

4.16 formation was 84% in 6:1 by volume CD_3OD : H_2O mixture in the absence of acid additives ([CD_3OD] = 21 M, [H_2O] = 7.9 M, [**4.1a**]=1.4 or 2.8 mM).

The observed pseudo-first order rate constant *k* for disappearance of **4.1a** (eq. 4.29) was determined at variable concentrations of water and acid additives and is given in Table 4.2. The reaction shows 1st order in **4.1a**: good linear graphs were obtained in coordinates $\ln(C_o/C)$ *vs.* time, and the rate constants *k* determined at two different initial concentrations of **4.1a**, 2.8 mM and 1.4 mM, were practically identical, $(7.0\pm0.2)*10^{-5}$ s^{-1} and $(7.1\pm0.2)*10^{-5}$ s^{-1} respectively (entries 1 and 2, Table 4.2). The disappearance of **4.1a** was slower in a more water-rich mixture (compare entry 1 and 3).

$$-\frac{d[4.1a]}{dt} = k \cdot [4.1a] \qquad (4.29)$$

Since two parallel pathways are responsible for disappearance of **4.1a**, we used initial rates of formation of **4.16** to determine the effect of acid on the kinetics of the allylic CH activation. The initial rates of formation of **4.16**, V_1, (eq. 4.30, Table 4.2) were calculated from the slope of the kinetic curve in coordinates **4.16** concentration *vs.* time during the initial period of the reaction, at low conversions of **4.1a**, using the reaction mixtures with identical initial concentrations of **4.1a** and various concentrations of added HBF_4.

$$V_1 = \frac{d[4.16]}{dt} \qquad (4.30)$$

Table 4.2. Observed pseudo-first order rate constants of disappearance of **4.1a** and initial rates of formation of **4.16** in CD_3OD-H_2O at 50 °C (CD_3OD/H_2O 6:1 by volume, $[CD_3OD]$ = 21 M, $[H_2O]$= 7.9 M, if not indicated otherwise).

Entry [a]	$[\mathbf{4.1a}]_{initial}$, mM	$[HBF_4]$, mM	$k*10^5$, s^{-1}	V_1*10^7, $mol*L^{-1}*s^{-1}$
1	2.8	none	7.0±0.2	1.9±0.1
2	1.4	none	7.1±0.2	1.0±0.1
3[a]	2.8	none	3.9±0.1	1.4±0.2
4	2.8	1.4	17.4±0.4	1.5±0.2
5	2.8	2.8	18.2±0.6	1.5±0.1

[a] CD_3OD : H_2O = 5:2 by volume, $[CD_3OD]$ = 18 M, $[H_2O]$ = 16 M.

From comparison of initial rates V_1 in entry 1 and entries 4-5 a conclusion can be made that the formation of **4.16** is not accelerated by acid additives. By contrast, slight inhibition occurs in the presence of 0.5 and 1 equivalents of acid (entries 4 and 5), compared to a neutral solution (entry 1).

At the same time, the observed rate constant k for disappearance of **4.1a** increases more than two-fold in the presence of HBF_4 (entries 1, 4-5). This acceleration can be attributed to a much faster loss of *cis*-cyclooctene to produce **3.10** according to eq. 4.24 in the presence of acid. Similar acceleration of the olefin loss was observed in acidic solutions of $LPt(CH_2{=}CH_2)(OH)$, described in Chapter 3, and could be explained by a weaker metal-olefin bonding in $[LPt(alkene)(OH_2)]^+$ complexes due to a weaker π-back donation from a cationic metal center.[32]

These observations are consistent with the reaction sequence shown in Scheme 4.29, where a neutral hydroxo complex **4.1a** is responsible for the allylic complex formation (k_1), and where the loss of *cis*-cyclooctene (k_2) takes place from a protonated **4.1a***H^+.

Scheme 4.29

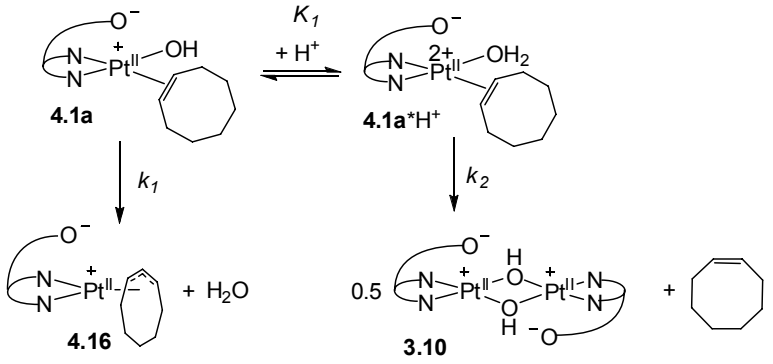

Since the equilibrium between **4.1a** and **4.1a***H^+ is fast in protic solvents, both **4.1a** and **4.1a***H^+ produce only one set of signals in an NMR spectrum, and the rate law for the disappearance of the starting material can be given by eq. 4.31, where *C* is the sum of concentrations of **4.1a** and **4.1a***H^+.

$$-\frac{dC}{dt} = k_1[4.1\text{a}] + k_2[4.1\text{a}*\text{H}^+] \tag{4.31}$$

Using the expression for equilibrium constant K_1 of protonation of **4.1a** (Scheme 4.28, eq. 4.32), the rate law can be rewritten as shown in eq. 4.33:

$$K_1 = \frac{[4.1\text{a}*\text{H}^+]}{[4.1\text{a}][\text{H}^+]} \tag{4.32}$$

$$-\frac{dC}{dt} = k_1 \frac{1}{1+K_1[H^+]} C + k_2 \frac{K_1[H^+]}{1+K_1[H^+]} C \tag{4.33}$$

The observed acceleration of the complex **3.10** formation (eq. 4.24) and slight inhibition of the allyl complex formation (eq. 4.23) could be explained by the rate law given in eq. 4.33, assuming that the protonation constant K_1 is not very large, $K_1 < 10^3$. If so, the fraction of **4.1a** would not decrease dramatically in the presence of dilute [HBF_4] (1.4-2.8 mM), whereas the fraction of **4.1a***H^+ would increase by several orders of magnitude compared to a neutral solution where it is expected to be

$<<10^{-3}$ M for aqueous solutions. Although our data are not sufficient to conclusively prove inhibition of the reaction (4.23) in the presence of acid, the use of higher concentrations of acid was prevented by low selectivity (~27%) of the reaction with respect to **4.16** and very fast hydrolysis of **4.1a** (eq. 4.24) already at $[HBF_4]$ = 2.8 mM.

Based in these data, we can rule out mechanism (i), which involves protonated **4.1a***H^+ as a reactive intermediate in the allylic CH activation and would lead to acceleration of both reactions (4.23) and (4.24) to the same extent in the presence of HBF_4, not observed experimentally. However, our current observations do not allow to distinguish between pathways (ii) and (iii), which both could involve a hydroxo complex **4.1a** as an intermediate in the allylic CH activation.

*4.2.2.5. DFT Modeling of the Allyl CH Bond Activation by Complex **4.1a**.*

In order to distinguish between mechanisms (ii) and (iii), a DFT study of these reaction pathways was done by Andrei Vedernikov. Reaction profiles for paths (ii) (Scheme 4.25) and (iii) (Scheme 4.26) are shown in Fig. 4.13.

A shown in Fig. 4.13, path (i**)** involves formation of a high energy CH-agostic Pt^{II} complex **4.25** and a high energy transition state $\mathbf{TS_{oa}}$ connecting **4.25** and η^1-allyl Pt^{IV} hydride **4.26**, so that the DFT-calculated reaction barriers for the allyl complex formation and H/D exchange can be estimated as $\Delta G^{\neq} \geq 33.6$ kcal/mol. Path (iii) involves a low lying transition state $\mathbf{TS_d}$ that was shown to be connected to **4.1a** and intermediate **4.27** by a single minimal-energy reaction path, responsible for the allylic H/D exchange in **4.1a**. The rate limiting step in path (iii) is the transformation of **4.27**

to **4.16** with a trasition state $\mathbf{TS_{LS}}$ that lies several kilocalories lower than $\mathbf{TS_{oa}}$ in path (ii). Based on these data, we suggest that the mechanism (iii) is operative in our systems. For the cyclopentene analogue, complex **4.18**, path (iii) is also preferred with even lower Gibbs energies of corresponding $\mathbf{TS_{oa}}$ and $\mathbf{TS_{d}}$, 26.2 and 13.1 kcal/mol respectively.

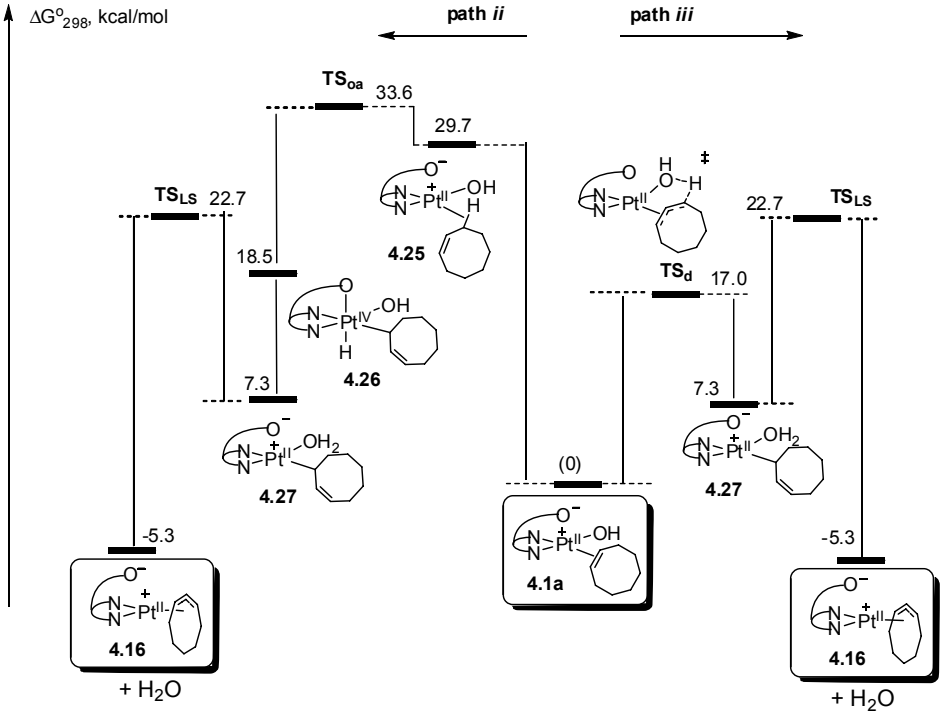

Figure 4.13. DFT-calculated Gibbs energy reaction profiles for aerobic transformation of complexes **4.1a** to **4.16** via paths (ii) (left) and (iii) (right). The reaction barriers for transformations of intermediate **4.1a** to **4.25** and **4.26** to **4.27** were not calculated.

4.2.3 Conclusions

The allylic CH activation may be an important side reaction in aerobic transformations of (dpms)Pt(OH) complexes with olefins containing allylic CH bonds. The nature of the solvent is an important factor determining reactivity of (dpms)Pt(*cis*-cyclooctene)(OH) **4.1a** in the allylic CH activation: aprotic solvents promote facile allylic complex formation.

The formation of an allylic complex (dpms)Pt(η^3-C_8H_{13}) **4.16** does not involve protonated complex **4.1a***H^+ [LPt(*cis*-cyclooctene)(OH_2)]$^+$ as a reactive intermediate, and presumably occurs from a neutral hydroxo complex **4.1a** without dissociation of the hydroxo or aqua ligand. Based on our DFT study, we propose a mechanism of the allyl CH activation by **4.1a** that involves intramolecular deprotonation of the CH bond with a Pt-bound hydroxo group.

The formation of complexes (dpms)Pt^{II}(alkene)(OH) by displacement of ethylene ligand in (dpms)Pt(CH_2=CH_2)(OH) is favored for strained olefins, such as *cis*-cyclooctene, bicyclo[2.2.1]heptene, cyclopentene, whereas less strained substrates, such as cyclohexene, did not react.

We can therefore conclude that the most suitable substrates for platinum-mediated aerobic epoxidation of olefins are strained bicyclic olefins, in which allylic deprotonation is disfavored, such as derivatives of bicyclo[2.2.1]heptene or benzonorbornadiene. A great variety of substrates of this type can be obtained by Diels-Alder reaction of cyclopentadiene with various dienophiles, alkenes, alkynes or benzynes.

4.3 Experimental Section

Preparation of (dpms)Pt^{II}(*cis*-cyclooctene)(OH), 4.1a. (dpms)Pt^{II}(CH_2CH_2)(OH) (104 mg, 212 μmol) was dissolved in 5 mL of deaerated water under an argon atmosphere, and 2 mL of degassed *cis*-cyclooctene were added. The reaction mixture was placed into a 30 mL Schlenk flask equipped with a magnetic stirring bar, and the emulsion was vigorously stirred under reduced pressure (127 Torr) in a vacuum desiccator at room temperature. After 2 days, according to ^{1}H NMR, all starting material has disappeared and **4.1a** formed as the only soluble product. The reaction mixture was filtered through Celite and washed with 1 mL of distilled water. The resulting yellow solution was evaporated to dryness under vacuum to give 111 mg of **4.1a** (194 μmol) as a pale yellow solid, 91% yield. The complex is soluble in water and methanol, does not oxidize under air in neutral solution. In D_2O undergoes slow multiple H/D exchange in cyclooctene ligand as evidenced by ESI-MS and ^{1}H and ^{13}C NMR spectroscopy. The compound **2a** is unstable in water, acetone, DMF or CH_2Cl_2. Complex **4.1a** undergoes fast ligand substitution in DMSO (half-life <2 minutes at 20 ^{o}C) to form (dpms)Pt^{II}(Me_2SO)(OH) and free *cis*-cyclooctene.

^{1}H NMR (H_2O/D_2O 3:1 v/v, 22 ^{o}C, 500 MHz), δ: 1.23-1.52 (m, 5H), 1.58-1.70 (m, 1H), 1.70-1.80 (m, 1H), 1.81-1.93 (m, 1H), 2.00-2.22 (m, 1H), 2.16-2.26 (m, 1H), 2.28-2.39 (m, 1H), 2.40-2.54 (m, 1H), 5.11 (ddd, *J*=11.1, 7.9, 4.6 Hz, $^2J_{195PtH}$=55 Hz, 1H), 5.67 (ddd, *J*=11.1, 8.4, 4.4 Hz, $^2J_{195PtH}$=60 Hz, 1H), 6.22 (s, 1H), 7.50 (ddd, *J*= 7.7, 5.7, 1.3 Hz, 1H), 7.73 (ddd, *J*= 7.7, 5.7, 1.3 Hz, 1H), 7.90 (dd, *J*= 7.7, 1.3 Hz, 1H), 7.98 (vd, *J*= 7.7 Hz, 1H), 8.10 (td, *J*= 7.7, 1.3 Hz, 1H), 8.20 (td, *J*= 7.7, 1.3 Hz, 1H), 8.50 (vd, *J*= 5.7 Hz, 1H), 8.73 (dd, *J*= 5.7, 1.3 Hz, 1H). **^{1}H NMR** (acetone-d_6,

22 °C, 400 MHz), δ: -0.53 (br s, 1H), 1.24-2.75 (m, 12H), 4.82 (m, $^{2}J_{195PtH}$=56 Hz, 1H), 5.48 (m, $^{2}J_{195PtH}$ =52 Hz, 1H), 5.97 (s, 1H), 7.50 (ddd, *J*=7.7, 5.8, 1.5 Hz, 1H), 7.69 (ddd, *J* =7.9, 5.8, 1.3 Hz, 1H), 7.91 (dd, *J* =7.9, 1.3 Hz, 1H), 7.95 (d, *J* =7.9 Hz, 1H), 8.10 (td, *J* =7.7, 1.5 Hz, 1H), 8.18 (td, *J* =7.9, 1.3 Hz, 1H), 8.50 (d, *J* =5.8 Hz, 1H), 9.21 (d, *J* =5.8 Hz, $^{3}J_{195PtH}$ =38 Hz, 1H). **^{13}C NMR** (H_2O/D_2O 3:1 v/v, 22 °C, 500 MHz), δ: 26.4, 26.7, 27.4, 28.8, 29.4, 76.2, 97.6 ($^{1}J_{195PtC}$=172 Hz), 99.5 ($^{1}J_{195PtC}$=163 Hz), 126.6, 127.6, 129.5, 131.0, 141.6, 142.8, 149.3, 150.9 (integrates as 2C), 151.2.

IR (KBr), ν: 3482 (w, br), 3097 (w), 2922 (w), 2854 (w), 1607 (w), 1479 (w), 1438 (w), 1230 (m), 1171 (m), 1033 (s), 856 (w), 809 (w), 764 (m), 688 (m) cm^{-1}. **ESI-MS** of solution of **4.1a** in water, m/z = 572.1. Calculated for **4.1a**·H^{+}, $C_{19}H_{25}N_2O_4{}^{195}PtS$, 572.1. **Anal.** Found: C, 39.55; H, 3.85; N, 4.92. Calculated for $C_{19}H_{24}N_2O_4PtS$, C, 39.93; H, 4.23; N, 4.90.

Selective 1D-difference NOE experiments (D_2O) (mixing time 0.5s, delay time 4s).

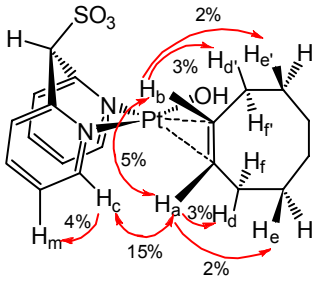

- important NOE's (% enhancement)

Selected ^{1}H NMR assignments:

H_a	5.67 ppm
H_b	5.11 ppm
H_c	8.50 ppm
H_d	2.28-2.39 ppm
$H_{d'}$	2.40-2.54 ppm
H_e	1.58-1.70 ppm
$H_{e'}$	1.31-1.51 ppm
H_f or $H_{f'}$	2.16-2.26 ppm
H_f or $H_{f'}$	2.00-2.22 ppm

Preparation of (dpms)Pt^{II}(*cis*-cyclooctene)Cl, 4.2a. KPt(*cis*-cyclooctene)Cl_3 was prepared according to the literature procedure.[176, 177] A solution of K(dpms) (168.5 mg, 584 μmol) in 3 mL of water was added to a stirred solution of KPt(*cis*-cyclooctene)Cl_3 (263.3 mg, 584 μmol) in 9 mL of methanol. The resulting solution

was allowed to evaporate slowly under air; white solid precipitated upon evaporation of methanol. After 1 day the volume of the reaction mixture was reduced to 3 mL by vacuum evaporation at room temperature; the white microcrystalline solid formed was filtered, washed with 5 mL of water and dried under vacuum for 1h. Yield 245 mg (415 μmol), 71%. White solid, stable under air, poorly soluble in water, methanol and acetone; dissolves in dmso with loss of coordinated cis-cyclooctene.

^{1}H NMR (CD_3OD/D_2O 1:1 v/v, 22 ^oC), δ:1.30-2.00 (m, 8H), 2.30-2.70 (m, 4H), 5.21 (m, 1H), 5.73 (m, 1H), 6.23 (s, 1H), 7.62 (ddd, *J*=7.9, 5.9, 1.4 Hz, 1H), 7.68 (ddd, *J*=7.9, 5.9, 1.4 Hz, 1H), 8.00 (vd, *J*=7.9 Hz, 1H), 8.03 (vd, *J*=7.9 Hz), 8.21 (td, *J*=7.9, 1.5 Hz, 2H), 8.67 (vd, *J*=5.9 Hz, 1H), 9.01 (dd, *J*=5.9, 1.5 Hz, 1H). Pt-H coupling constants could not be determined because of partial overlap with solvent signal and low intensity. **IR** (KBr), ν: 3090 (w), 2921 (w), 2844 (w), 1607 (w), 1477 (w), 1441 (w), 1248 (m), 1227 (s), 1168 (m), 1026 (s), 855 (w), 809 (m), 768 (m), 685 (m) cm^{-1}. **ESI-MS** of solution of **4.2a** in water/methanol (1:1 v/v) acidified with HBF_4, m/z = 590.1. Calculated for **4.2**·H^+, $C_{19}H_{24}N_2O_3{}^{195}Pt^{35}ClS$, 590.1. **Anal.** Found: H, 3.99; C, 38.75; N, 4.67; Cl, 6.37. Calculated for $C_{19}H_{23}ClN_2O_3PtS$, H, 3.93; C, 38.68; N, 4.75; Cl, 6.01.

Preparation of (dpms)Pt^{IV}($C_8H_{14}O$-*κC,κO*)(OH), 4.3a

Procedure A. Oxidation with O_2 in weakly alkaline solutions. 4.5 mL of 19.5 mM solution of **4.1a** (50.1 mg, 87.7 μmol) were placed into a 250 round bottom flask equipped with a magnetic stirring bar. 222 μL of a standardized 0.100 N NaOH solution were added (22.2 μmol, 0.25 eq.). The flask was filled with O_2 and stirred

vigorously at 20 ^{o}C for 19 hours; slow formation of a yellow precipitate was observed during the course of the reaction. After 19h, a yellow solid was filtered off through a sintered glass filter and washed with several milliliters of water until neutral reaction of the filtrate. Yellow solid was dried under vacuum; yield 25.2 mg. An additional fraction of the product was obtained by evaporation of the filtrate to a volume of 1-2 mL. The resulting suspension was cooled down to 0 °C, and a yellow precipitate was filtered off from cold solution, washed with ice-cold water to neutral reaction of the filtrate and dried under vacuum to give 19.1 mg of the product. Combined yield of two crops 44.3 mg (75 μmol), 86%.

The filtrate left after separation of the product was analyzed by ^{1}H and ESI-MS and found to contain a mixture of **4.3a** and (dpms)Pt(OH)$_2^-$ in 1 : 1.5 molar ratio (the latter complex has been characterized earlier. Only one isomer, **4.3a**, was detected in all reaction mixtures.

Procedure B. Oxidation with H_2O_2. A solution of **4.1a** was prepared from 115 mg (235 μmol) of (dpms)Pt^{II}(CH_2CH_2)(OH) in 10 mL H_2O and 2 mL of *cis*-cyclooctene according to the procedure described above for synthesis of **4.1a**. After filtration and separation of the organic phase from the aqueous phase, the resulting clear yellow aqueous solution of **4.1a** was used in the oxidation step.

0.25 mL (2.45 mmol) of 30% H_2O_2 (aq.) were added slowly to a stirred solution of **4.1a** at room temperature. Stirring continued for 5h during which poorly soluble **4.3a** precipitated slowly from solution as a yellow microcrystalline solid. After 5h the yellow precipitate was filtered off, washed with 3 mL of distilled water and dried under vacuum to give 57.9 mg of **4.3a**. An additional portion of pure **4.3a** was

obtained by reducing the volume of the filtrate to 2 mL by evaporation under vacuum at room temperature. The resulting yellow precipitate was filtered, washed with 1 mL of water and dried under vacuum to give additional 29.5 mg of the product. Combined yield 87.4 mg (149 μmol), 63%. Yellowish solid, moderately soluble in water, methanol and dichloromethane; scarcely soluble in chloroform; perfectly soluble in dmso; insoluble in benzene and alkanes; slowly eliminates cyclooctene oxide and forms Pt^{II} complexes in solutions.

^{1}H NMR (dmso-d_6, 22 ^{o}C, 500 MHz), δ: 0.83 (d, J= 14.2 Hz, 1H), 1.00-1.63 (m, 9H), 1.80-2.09 (m, 2H), 2.47 (br s, 1H), 3.38 (dd, J=11.8, 7.6 Hz, $^{2}J_{PtH}$=70 Hz, 1H), 5.20 (dd, J=11.6, 7.6 Hz, $^{3}J_{195PtH}$=34 Hz, 1H), 6.64 (s, 1H), 7.75 (ddd, J=7.9, 5.5, 1.2 Hz, 1H), 7.78 (ddd, J= 7.9, 5.2, 1.1 Hz, 1H), 7.99 (vd, J=7.9 Hz, 2H), 8.21 (td, J=7.9, 1.5 Hz, 1H), 8.23 (td, J=7.9, 1.4 Hz, 1H), 8.62 (vd, J=5.5 Hz, 1H), 8.81 (vd, J=5.2 Hz, 1H). **^{13}C NMR** (dmso-d_6, 22 ^{o}C, 500 MHz), δ: 14.0 ($^{1}J_{PtC}$=369 Hz), 25.6, 25.7, 26.9, 27.2, 28.4, 34.2, 70.1, 91.1 ($^{2}J_{195PtC}$=82 Hz), 126.1, 126.6, 127.2, 127.7, 141.3, 142.1, 148.4, 149.4, 149.8, 153.1. **IR** (KBr), ν: 3429 (w, br), 2923 (w), 2854 (w), 1605 (w), 1480 (w), 1444 (w), 1296 (m), 1201 (m), 1142 (s), 1037 (w), 981 (m), 948 (m), 767 (m), 696 (m) cm^{-1}. ESI-MS of solution of **4.3a** in water acidified with HBF_4, m/z = 588.1. Calculated for **4.3a**·H^{+}, $C_{19}H_{25}N_2O_5{}^{195}PtS$, 588.1. **Anal.** Found: C, 38.52; H, 4.42; N, 4.60. Calculated for $C_{19}H_{24}N_2O_5PtS$, C, 38.84; H, 4.12; N, 4.77.

Selective 1D-difference NOE experiments (dmso-d_6) (mixing time 0.5s, delay time 4s)

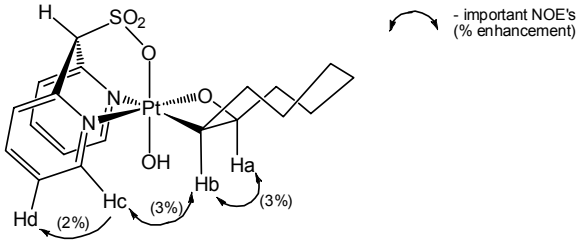

Generation of [(dpms)Pt^{II}($C_8H_{14}O$-*κC,κO*)]$^-$ (4.4a) in aqueous solution

1) 261 μL of 153 mM NaOD/D_2O solution (40 μmol, 1.3 eq.) was added to a stirred 28 mM solution of **4.1a** in H_2O (1.107 mL, 31 μmol) (a mixture of H_2O and D_2O was used to suppress H/D exchange in cyclooctene ligand). A yellow color of solution intensified upon addition of NaOD. A resulting solution was analyzed by ^1H NMR spectroscopy immediately after its preparation. According to ^1H NMR, complexes **4.4a** and **4.1a** were present in solution in 1.1:1 ratio. Decomposition into a complex mixture of products occurred with a half-life of 3.3 hours at 20 ^oC.

2) A 28 mM solution of **4.12a** in H_2O (767 μL, 21.5 μmol) was placed into 3 mL vial equipped with a magnetic stirring bar; 244 μL of 328 mM solution of NaOD in D_2O (80 μmol, 3.7 eq.) were added to a stirred mixture; the resulting solution was analyzed by ^1H and ^{13}C NMR spectroscopy immediately. According to ^1H NMR, complexes **4.4a** and **4.1a** were present in solution in 3.9:1 ratio. Complete decomposition occurred after 17 h to give a complex mixture of unidentified products. In all cases only one isomer of **4.4a** was detected by NMR spectroscopy.

Based on the results on two experiments above, the equilibrium constant for the title reaction is 63 M^{-1}.

4.4a: ^1H NMR (H_2O/D_2O, [OH^-]~0.1M, 22 ^oC, 500 MHz), δ: 1.06 (vd, *J*=13.5 Hz, 1H), 1.12-1.24 (m, 2H), 1.25-1.57 (m, 7H), 1.68 (dd, *J*=11.6, 7.6 Hz, 1H), 1.72-1.84 (m, 1H), 1.99-2.09 (m, 1H), 5.45 (ddd, *J*=11.5, 7.6, 2.0 Hz, $^3J_{195PtH}$=38 Hz, 1H), 5.79 (s, 1H), 7.25-7.29 (m, 1H), 7.49-7.53 (m, 1H), 7.62 (d, *J*=7.9 Hz, 1H), 7.75 (d, *J*=7.9 Hz, 1H), 8.01 (t, *J*=7.9 Hz, 1H), 8.03 (t, *J*=7.9 Hz, 1H), 8.51 (d, *J*=5.4 Hz, 1H), 8.82

(d, J=5.6 Hz). (Coupling constant $^{2}J_{PtH}$ of a CHPt peak at 1.68 ppm could not be determined due to overlapping of platinum satellites with other peaks in the aliphatic region). **^{13}C NMR** (H_2O/D_2O, [OH^-]~0.1M, 22 ^{o}C, 500 MHz), δ: -2.6, 26.4 (integrates as 2C), 27.8, 29.3, 32.5, 35.7, 76.3, 95.1, 126.2, 127.1, 129.3, 130.5, 138.1, 139.5, 149.0, 149.8, 151.9, 154.4 (Coupling constants $^{1}J_{195PtC}$ and $^{2}J_{195PtC}$ could not be determined due to low concentration and instability of the sample). **ESI** (negative mode) of the alkaline solution prepared by addition of 0.2 equivalents of NaOH to 20 mM aqueous solution of **4.1a**, m/z 570.1. Calculated for **4.4a**, $C_{19}H_{23}N_2O_4{}^{195}PtS$, 570.1. No signals were detected in neutral aqueous solution of **4.1a** (20 mM) in negative mode of ESI.

Selective 1D-difference NOE experiments (D_2O) (mixing time 0.5s, delay time 4s).

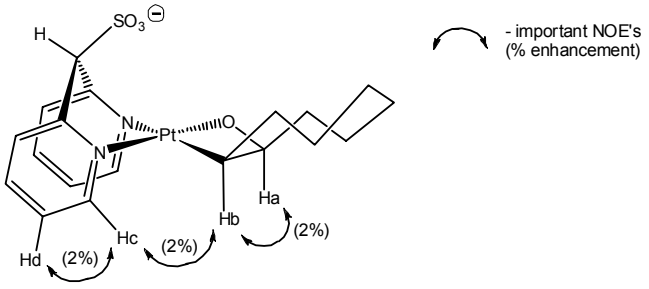

Preparation of (dpms)Pt^{II}(C_7H_{10}OH-κ*C*,κ*O*), 4.5b. A solution of (dpms)Pt^{II}(CH_2CH_2)(OH) (75 mg, 153 μmol) in 3.5 ml of deaerated water was placed into a 25 mL Schlenk tube equipped with a stirring bar; a solution of norbornene (375 mg, 3.98 mmol) in 3.5 mL of degassed acetone was added to the reaction mixture under an argon atmosphere. The resulting solution was degassed by three freeze-pump-thaw cycles, frozen in liquid nitrogen, and then the Schlenk flask was evacuated and Teflon-sealed under vacuum (0.3 Torr). The reaction mixture was

stirred at room temperature for 2 days; white solid precipitated slowly from solution. White microcrystalline solid was filtered and washed thoroughly with 1 mL of water, 50 mL of acetone and 50 mL of pentane; dried under vacuum. Yield 69.7 mg (125 μmol), 82%. White solid, insoluble in water, methanol, acetone, dichloromethane, DMF and DMSO, slightly soluble in trifluoroethanol; reacts with acidic and basic aqueous solutions to give well-soluble (dpms)$Pt^{II}(OH_2)$(norbornene)$^+$ and **4.4b** respectively.

According to ^{1}H NMR spectrum recorded in trifluoroethanol-d_3, two isomers were present in the solution in a 6:4 ratio. Peaks of *ortho*-protons of pyridyls of dpms ligands and some aliphatic resonances were broadened in ^{1}H NMR spectrum. Each isomer was characterized by eight multiplets of dpms ligand, each integrating as 1H, consistent with C_1 symmetric structure, and only one peak in the region 6.0-6.5 ppm integrating as one proton, consistent with an oxetane structure. At the same time, ^{1}H NMR characteristics of both of these isomers were not consistent with alternative structures containing η^2-coordinated norbornene. In the case of a structure with η^2-coordinated norbornene, two peaks of vinylic protons of norbornene (each integrating as 1H) would be expected in the region 5.0-6.5 ppm for each isomer (see ^{1}H NMR of complex **4.6b** (dpms)$Pt^{II}(OH_2)$(norbornene)$^+$).

^{1}H NMR (CF_3CD_2OD, 22 ^{o}C, 500 MHz), δ: **4.5b** (major isomer): 0.83-1.99 (m, 6H), 2.07 (s, 1H), 2.28 (s, 1H), 3.00 (d, *J*=8.9 Hz, 1H), 5.65 (s, 1H), 6.21 (d, *J*=5.2 Hz, $^3J_{195PtH}$=31 Hz, 1H), 7.19-7.27 (m, 1H), 7.41-7.49 (m, 1H), 7.65 (d, *J*=8.0 Hz, 1H), 7.71 (d, *J*=7.7 Hz, 1H), 7.87-8.01 (m, 2H), 8.39 (br d, *J*=4.2 Hz, 1H), 8.92 (br d, *J*=5.2 Hz, 1H). **4.5b** (minor isomer): 0.83-1.99 (m, 6H), 2.24 (br s, 1H), 2.44 (br s,

1H), 2.89-2.61 (m, 1H), 5.65 (s, 1H), 6.07 (br s, 1H), 7.19-7.27 (m, 1H), 7.41-7.49 (m, 1H), 7.65 (d, *J*=8.0 Hz, 1H), 7.71 (d, *J*=7.7 Hz, 1H), 7.87-8.01 (m, 2H), 8.43 (br s, 1H), 9.01 (br s, 1H). Selective COSY experiment conforms to the oxetane structure: upon irradiation of a doublet at 6.21 ppm of the major isomer of **4.5b**, assigned as CHO, a correlation is observed with a resonance at 1.58 ppm, assigned as CHPt. Selective NOE experiments were not satisfactory even after overnight acquisition due to low solubility. **IR** (KBr), ν: 3494 (vw, br), 2926 (w), 2859 (w), 1602 (w), 1479 (w), 1454 (w), 1432 (w), 1351 (w), 1312 (w), 1242 (s), 1170 (s), 1158 (s) 1036 (s), 761 (s), 686 (m) cm^{-1}. **ESI-MS** of solution of **4.5b** in methanol, m/z = 556.1. Calculated for **3b**·H^+, $C_{18}H_{21}N_2O_4{}^{195}PtS$, 556.1. **Anal.** Found: C, 38.90; H, 3.90; N, 4.95. Calculated for $C_{18}H_{20}N_2O_4PtS$, C, 38.92; H, 3.63; N, 5.04.

Preparation of (dpms)Pt^{II}(η^2-C_7H_{10})(OH_2)$^+BF_4^-$, 4.6b. 60 mg of 50% wt. aqueous HBF_4 (342 μmol) were added to a suspension of 20.2 mg (36 μmol) of **4.5b** in 0.7 mL of CF_3CD_2OD. Complex **4.5b** dissolved after 30-60 min of stirring at room temperature to form a clear yellowish solution, which was analyzed by NMR spectroscopy and ESI immediately after its preparation. According to NMR, a new complex **4.6b** formed quantitatively and no other dpms-containing species were present in solution. Complex **4.6b** is soluble in trifluoroethanol and trifluoroethanol-water mixtures.

^{1}H NMR (CF_3CD_2OD, 22 °C, 400 MHz), δ: 0.20 (d, *J*=10.5 Hz, 1H), 0.87 (d, *J*=10.5 Hz, 1H), 0.95-1.19 (m, 2H), 1.62-1.90 (m, 2H), 3.11 (s, 1H), 3.19 (s, 1H), 5.68 (br s, $^2J_{195PtH}$=21 Hz, 1H), 6.04 (s, 1H), 6.18 (br s, $^2J_{195PtH}$=23 Hz, 1H), 7.41-7.49 (m, 1H),

7.62-7.72 (m, 1H), 7.84 (d, *J*=7.7 Hz, 1H), 7.99 (d, *J*=7.7 Hz, 1H), 8.05 (t, *J*=7.7 Hz, 1H), 8.17 (t, *J*=7.7 Hz, 1H), 8.51 (d, *J*=5.7 Hz, 1H), 8.62 (d, *J*=5.6 Hz, 1H).

^{13}C NMR (CF_3CD_2OD, 22 ^{o}C, 400 MHz), δ: 24.0, 24.1, 39.3, 44.9, 45.4, 78.1, 109.4 ($^{1}J_{195PtC}$=153 Hz), 112.3 ($^{1}J_{195PtC}$=157 Hz), 128.1, 129.0, 130.9, 131.7, 144.4, 144.7, 150.6, 152.1, 153.7, 155.6. **ESI-MS** of a dilute acidified solution of **4.6b** in CF_3CH_2OH, m/z = 556.1. Calculated for cationic **4.6b**, $C_{18}H_{21}N_2O_4{}^{195}PtS$, 556.1.

Complex **4.6b** was unstable in solution: dissociation of coordinated norbornene occurred with a half-life 17 hours at 20 ^{o}C. Formation of free norbornene and diaqua complex (dpms)$Pt^{II}(OH_2)_2^{+}$, characterized previously,[79] was confirmed by ^{1}H NMR and ESI.

Selective 1D-differenceNOE experiments (CF_3CD_2OD) (mixing time 500 ms, delay time 5 s)

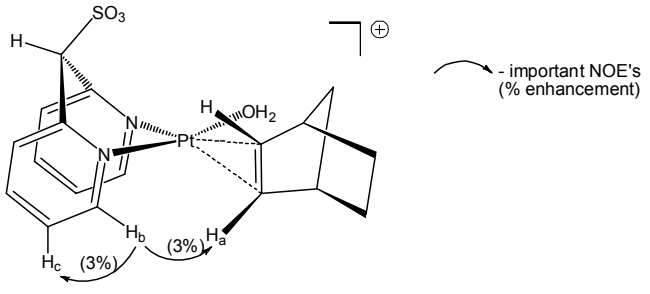

Preparation of [(dpms)Pt($C_7H_{10}O$-*κC,κO*)]$^{-}$, 4.4b. All operations were performed under argon in deaerated solvents. A sample of **4.5b** (33 mg, 59 μmol) and 200 μL of D_2O were combined in a 3 mL vial equipped with a magnetic stirring bar. 720 μL of 100 mM solution of NaOD/D_2O (72 μmol, 1.2 eq.) were added to a stirred suspension. The white solid (**4.5b**) dissolved after 30-40 minute of stirring at 20 ^{o}C to give a clear yellow solution. According to NMR, a quantitative formation of a

mixture of isomeric complexes **4.4b** occurred. *cis* : *trans* ratio was 5.7:1 based on integration of doublets at 2.73 ppm and 2.46 ppm respectively. No decomposition was observed after 1 day at 20 ^{o}C. The same ratio of isomers was observed when 7.2 equivalents of NaOD were used.

^{1}H NMR (NaOD/D_2O, 22 ^{o}C, 500 MHz), δ: ***cis-exo*-4b** (major isomer): 0.69-0.81 (m, 1H), 0.89 (d, *J*=9.0 Hz, 1H), 0.93 (d, *J*=5.8 Hz, 1H), 0.98 (vt, *J*=9.5 Hz, 1H), 1.17-1.41 (m, 2H), 1.89 (d, *J*=2.6 Hz, 1H), 1.90 (s, 1H), 2.73 (d, *J*=9.0 Hz, 1H), 5.59 (d, *J*=5.8 Hz, $^{3}J_{195PtH}$=22 Hz, 1H), 5.78 (s, 1H), 7.19 (ddd, *J*=7.8, 5.7, 1.3 Hz, 1H), 7.46 (ddd, *J*=8.0, 5.3, 1.3 Hz, 1H), 7.57 (d, *J*=7.8 Hz, 1H), 7.69 (d, *J*=8.0 Hz, 1H), 7.96 (td, *J*=7.8, 1.3 Hz, 1H), 7.99 (td, *J*=8.0, 1.3 Hz, 1H), 8.39 (d, *J*=5.3 Hz, 1H), 8.93 (d, *J*=5.7 Hz, 1H). (Coupling constant $^{2}J_{PtH}$ of CHPt peak at 0.93 ppm could not be determined due to overlapping with other peaks in this region). ***trans-exo*-4.4b** (minor isomer): 0.69-0.81 (m, 1H), 1.07 (vt, *J*=9.7 Hz, 1H), 1.10 (d, *J*=9.1 Hz, 1H), 1.23 (d, *J*=5.2 Hz, 1H), 1.3-1.41 (m, 1H), 1.43-1.55 (m, 1H), 1.96 (d, *J*=3.5 Hz, 1H), 2.30 (s, 1H), 2.46 (d, *J*=9.1 Hz, 1H), 5.29 (d, *J*=5.2 Hz, $^{3}J_{195PtH}$=23 Hz, 1H), 5.80 (s, 1H), 8.50 (d, *J*=5.3 Hz, 1H), 9.00 (d, *J*=5.7 Hz, 1H). (Other peaks of dpms ligand in the aromatic region overlapped with corresponding peaks of the major isomer ***cis-exo*-4.4b.** Coupling constant $^{2}J_{PtH}$ of CHPt peak at 1.23 ppm could not be determined due to overlapping with other peaks in the same region). **^{13}C NMR** ((NaOD/D_2O/H_2O, 22 ^{o}C, 500 MHz), δ: ***cis-exo*-4.4b** (major isomer): -3.1 ($^{1}J_{PtC}$=585 Hz), 23.4, 30.1, 36.0, 40.0, 43.6, 76.1, 96.9 ($^{2}J_{PtC}$=105 Hz), 126.0, 126.5, 129.2, 130.6, 138.0, 139.3, 148.4, 149.5, 151.6, 154.8. ***trans-exo*-4.4b** (minor isomer): -7.1, 23.2, 30.6, 35.5, 39.8, 44.6, 76.0, 97.1, 126.2, 129.1, 130.6, 138.3, 139.4, 149.0, 151.5, 155.7. (Two peaks of

pyridyls of dpms ligands overlapped with signals of the major isomer ***cis-exo*-4.4b**. Coupling constants $^{1}J_{PtC}$ and $^{2}J_{PtC}$ could not be determined due to low intensity of the peaks of minor isomer ***trans-exo*-4.4b**). **ESI-MS** (negative mode) of 4 mM solution of **4.4b** prepared by dissolving 2 mg of **4.5b** in 1 mL of 5 mM solution of NaOH in water, m/z 554.1. Calculated for **4.4b**, $C_{18}H_{19}N_2O_4{}^{195}PtS$, 554.1.

Selective 1D-difference NOE experiments (D_2O) (mixing time 0.5s, delay time 5s).

***cis-exo*-4.4b** (major isomer):

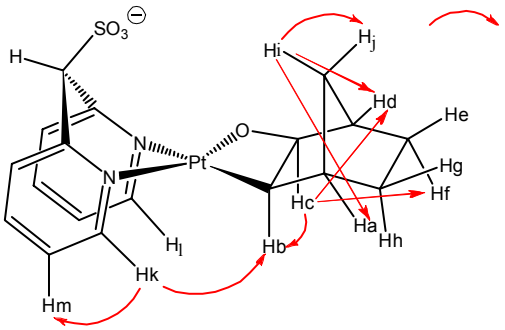

- important NOE's

Selected 1H NMR assignments (based on NOE; NaOD/D_2O, ppm):

Ha: 1.90 (s)
Hb: 0.93 (d, J=5.8 Hz)
Hc: 5.59 (d, J=5.8 Hz, $^{3}J_{PtH}$=22Hz)
Hd: 1.89 (d, J=2.6 Hz)
Hf: 0.69-0.81 (m)
Hi: 2.73 (d, J=9.0 Hz)
Hj: 0.89 (d, J=9.0 Hz)
Hk: 8.93 (d, J=5.7 Hz).
Hm: 7.19 (ddd, J=7.8, 5.7, 1.3 Hz)

***trans-exo*-4.4b** (minor isomer):

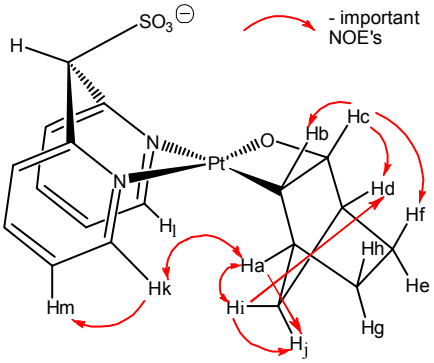

- important NOE's

Selected 1H NMR assigments (based on NOE; NaOD/D_2O, ppm):

Ha: 2.30 (s)
Hb: 1.23 (d, J=5.2 Hz)
Hc: 5.29 (d, J=5.2 Hz, $^{3}J_{PtH}$=23Hz)
Hd: 1.96 (d, J=3.5 Hz)
Hf: 0.69-0.81 (m)
Hi: 2.46 (d, J=9.1 Hz)
Hj: 1.10 (d, J=9.1 Hz)
Hk: 9.00 (d, J=5.7 Hz)

Preparation of (dpms)Pt^{IV}($C_7H_{10}O$-*κC,κO*)(OH), 4.3b

Procedure A. Oxidation of 4.5b with O_2 in neutral trifluoroethanol solution.

A suspension of **4.5b** (39.4 mg, 70.9 μmol) in 14 mL of trifluoroethanol and 3.4 mL of water was placed into 100 mL round bottom flask and stirred vigorously under an

O_2 atmosphere at 20 °C. After several hours white precipitate dissolved and a clear yellowish solution formed. After 22 h a sample of the reaction mixture was evaporated to dryness, re-dissolved in D_2O and analyzed by NMR spectroscopy; no insoluble products were found. According to NMR, no starting material was remaining in solution and two isomers ***cis-exo*-4.3b** and ***trans-exo*-4.3b** formed in 30 : 1 ratio, based on the integration of doublets at 2.33 and 2.49 ppm respectively. The reaction mixture was evaporated to dryness, and a yellowish solid was extracted with 50 mL of acetone. The solution was filtered; filtrate was evaporated to dryness under vacuum to give **4.3b** as a yellow solid that was dried under high vacuum for 6 hours. Yield 34.4 mg (60.1 μmol), 85%.

Procedure B. Oxidation of 4.5b with H_2O_2. A suspension of white poorly soluble **3b** (77.8 mg, 140 μmol) in 3 mL of water was placed in a vial equipped with a magnetic stirring bar. 0.15 mL (1.47 mmol) of 30% aqueous H_2O_2 were added to a stirred reaction mixture. The suspension was stirred for 1 hour at room temperature. The color of the mixture changed from white to yellow. A pale yellow precipitate was filtered off, washed with 1 mL of water and dried under vacuum. According to NMR, the product was isomerically pure (>99% of ***cis-exo*-5b**). Yellowish solid, 65.6 mg (115 μmol), 82%.

***cis-exo*-4.3b** (major isomer): **^{1}H NMR** (dmso-d_6, 22 °C, 400 MHz), δ: 0.70-0.89 (m, 1H), 1.00 (d, J=9.0 Hz, 1H), 1.19-1.43 (m, 3H), 1.82 (s, 1H), 1.98 (s, 1H), 2.47 (d, J=9.0 Hz, 1H), 2.58 (d, J=5.0 Hz, $^2J_{195PtH}$=72 Hz, 1H), 2.63 (br s, 1H), 5.27 (d, J=5.0 Hz, $^3J_{195PtH}$=25 Hz, 1H), 6.66 (s, 1H), 7.75 (ddd, J=7.8, 5.7, 1.3 Hz, 1H), 7.83 (ddd, J=7.8, 5.2, 1.1 Hz, 1H), 7.99 (vd, J=7.8 Hz, 2H), 8.24 (td, J=7.8, 1.8 Hz, 1H), 8.25

(td, *J*=7.8, 1.4 Hz, 1H), 8.65 (vd, *J*=5.7, 1H), 8.81 (vd, *J*=5.2 Hz, 1H). **^{13}C NMR** (dmso-d_6, 22 °C, 400 MHz), δ: 11.5 ($^{1}J_{195PtC}$=416 Hz), 21.8 (CH_2), 28.3 (CH_2), 33.5, 37.9, 42.3, 69.9, 94.7 ($^{2}J_{195PtC}$=70 Hz), 126.1, 126.5, 127.2, 127.8, 141.5, 142.3, 148.3, 149.4, 149.7 (C quat), 152.6 (C quat). **IR** (KBr), ν: 3406 (w, br), 2954 (w), 2874 (w), 1605 (w), 1477 (w), 1445 (w), 1294 (m), 1202 (m), 1143 (s), 1032 (m), 981 (s), 766 (m), 696 (m) cm^{-1}.

***trans-exo*-4.3b** (minor isomer): **^{1}H NMR** (D_2O, 22 °C, 400 MHz), δ: 2.49 (d, *J*=10.2 Hz, 1H), 2.62 (s, 1H), 3.15 (d, *J*=4.9 Hz, 1H), 5.20 (d, *J*=4.9 Hz, $^{3}J_{195PtH}$=22 Hz, 1H), 6.62 (s, 1H), 8.74 (d, *J*=5.2 Hz). (Other peaks overlapped with resonances of major isomer ***cis-exo*-4.3b**. Coupling constant $^{2}J_{195PtH}$ of CHPt peak at 3.15 ppm could not be determined because of overlapping of platinum satellites with other peaks.)

ESI-MS of solution of **4.3b** in methanol, m/z = 572.1. Calculated for **4.3b**·H^{+}, $C_{18}H_{21}N_2O_5{}^{195}PtS$, 572.1. **Anal.** Found: C, 37.44; H, 3.87; N, 4.68. Calculated for $C_{18}H_{20}N_2O_5PtS$, C, 37.83; H, 3.53; N, 4.90.

Selective 1D-difference NOE experiments (dmso-d_6) **(**mixing time 0.5s, delay time 5s)

***cis-exo*-4.3b** (major isomer):

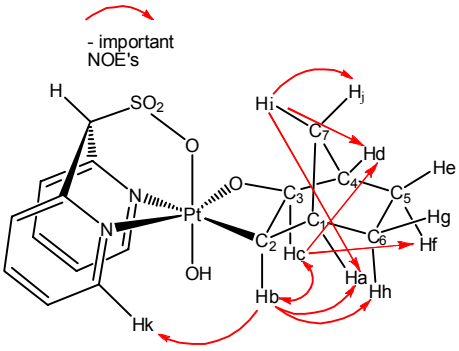

Selected 1H NMR assignments (based on NOE; dmso-d_6, ppm)

Ha:	1.98 (s)
Hb:	2.58 (d, J=5.0 Hz, $^{2}J_{PtH}$=72 Hz)
Hc:	5.27 (d, J=5.0 Hz, $^{3}J_{PtH}$=25 Hz)
Hd:	1.82 (s)
Hf:	0.70-0.89 (m)
Hi:	2.47 (d, J=9.0 Hz)
Hj:	1.00 (d, J=9.0 Hz)
Hk:	8.65 (vd, J=5.7)

Selected 13C NMR assignments (from HSQC and DEPT, dmso-d_6, ppm)

C1:	37.9
C2:	11.5 ($^{1}J_{PtC}$=416 Hz)
C3:	94.7 ($^{2}J_{PtC}$=70 Hz)
C4:	42.3
C5:	21.8
C6:	28.3
C7:	33.5
$CHSO_3$:	69.9

Preparation of (dpms)Pt^{II}(dmso)(OH), 4.13

Procedure A. Reductive elimination from 4.3a. Complex **4.3a** (30 mg, 51 μmol) and 5 mL of dry degassed DMSO were placed into 25 mL Schlenk tube under an argon atmosphere, and the resulting yellow solution was stirred at 65 °C for 16h. DMSO was removed from the reaction mixture by vacuum distillation at 60 °C and the resulting yellowish solid residues were dried under vacuum (0.2 Torr) for several hours at 65 °C. Organic products were removed from the solid residues by extraction with 10 mL of benzene; white insoluble complex **4.13** was filtered off, washed with pentane and dried under vacuum (0.2 Torr) at 70 °C for 1 day. Yield of complex **4.13** 16.2 mg (30 μmol), 59%; white microcrystalline solid; insoluble in acetone, slightly soluble in methanol, perfectly soluble in water.

Procedure B. *Cis*-cyclooctene displacement in 4.1a. A sample of **4.1a** (53.2 mg, 93 μmol) was placed into a 25 mL Schlenk tube and dissolved in 3 mL of dry degassed DMSO under an argon atmosphere. The solution was stirred at room temperature for 5 hours. DMSO was removed by vacuum distillation at 60 °C. The resulting white solid was dried under vacuum (0.2 Torr) at 70 °C for 1 day. Yield 49.2 mg (91 μmol), 98%.

^{1}H NMR (D_2O, 22 ^{o}C, 400 MHz), δ: 3.44 (s, $^{3}J_{PtH}$=14 Hz, 3H), 3.52 (s, $^{3}J_{PtH}$=15 Hz, 3H), 6.23 (s, 1H), 7.49 (ddd, *J*=7.8, 5.9, 1.5 Hz, 1H), 7.69 (ddd, *J*=7.7, 5.8, 1.5 Hz, 1H), 7.87 (dd, *J*=7.7, 1.5 Hz, 1H), 7.96 (dd, *J*=7.8, 1.5 Hz, 1H), 8.10 (td, *J*=7.7, 1.5 Hz, 1H), 8.20 (td, *J*=7.8, 1.5 Hz, 1H), 8.72 (dd, *J*=5.8, 1.5 Hz, 1H), 8.90 (dd, *J*=5.9, 1.5 Hz, 1H). **^{13}C NMR** (D_2O, 22 ^{o}C, 400 MHz), δ: 41.0, 43.6, 76.1, 126.5, 126.6, 129.5, 129.6, 141.8, 142.9, 150.5, 151.0, 151.1, 155.9. **IR** (KBr), ν: 3483 (w, br), 3094 (w), 3005 (w), 2917 (w), 1609 (w), 1489 (w), 1441 (w), 1319 (w), 1236 (s),

1182 (m), 1127 (m), 1036 (s), 855 (w), 809 (m), 763 (m), 690 (m) cm^{-1}. The ν(S=O) band of S-coordinated dimethylsulfoxide at 1127 cm^{-1} is missing in IR spectra other sulfonate complexes reported here. The frequency is typical for Me_2SO ligand coordinated to a metal through the sulfur atom. **Anal.** Found: C, 28.64; H, 3.09; N, 5.00. Calculated for $C_{13}H_{16}N_2O_5PtS_2$, C, 28.94; H, 2.99; N, 5.19.

Aqueous solutions of complex **4.13** are stable at room temperature for several days, but decompose at 60 °C. The decomposition of **4.13** (eq. 4.34) is accompanied by liberation of DMSO ligand and formation of dimeric **3.10**; half-life was found to be 350 min at 60 °C.

$$\underset{\textbf{4.13}}{2\ (dpms)Pt^{II}(dmso)(OH)} \rightarrow \underset{\textbf{3.10}}{(dpms)_2Pt^{II}_2(\mu\text{-}OH)_2} + 2\ dmso \qquad (4.34)$$

Preparation of (dpms)Pt^{II}($C_{11}H_{10}OH$-*κC,κO*), 4.5c. Benzonorbornadiene was prepared according to literature procedure.[178] A solution of (dpms)Pt(C_2H_4)(OH) (199.8 mg, 408 μmol) in 6 mL of degassed H_2O and a solution of benzonorbornadiene (340 mg, 2.39 mmol) in 6 mL of acetone were placed into a 50 mL Schlenk flask equipped with a magnetic stirring bar under argon. The resulting yellow solution was degassed by three freeze-pump-thaw cycles and Teflon-sealed under vacuum (100 mTorr). Stirring under reduced pressure continued at 20 ^oC; product partially precipitates as white solid. After 2 days acetone was removed by vacuum evaporation and the product precipitated from an aqueous solution as a white solid. The resulting suspension was cooled down in ice-bath for 30 minutes, vacuum-filtered, washed with water (1-2 mL), acetone (1-2 mL), ether (50 mL) and pentane (10 mL) and dried under vacuum (200 mTorr) for 1 day to give 141.1 mg of the

product as white solid. An additional fraction of product was obtained from the filtrate by evaporating to dryness and mixing with 1-2 mL dry acetone; the resulting suspension was cooled down in ice-bath, vacuum-filtered, washed with water, acetone, ether and pentane and dried under vacuum to give 70.2 mg of product. Yield of combined fractions 211.3 mg (350 μmol), 86%. White solid, slightly soluble in methanol, moderately soluble in trifluoroethanol and DMF, water-acetone mixture, insoluble in water; solutions in protic solvents are oxidized in air. According to ^{1}H NMR, two isomers are present in CD_3OD solution in 3:1 ratio. Ratio of isomers depends on solvent: in trifluoroethanol two isomers are detected in 1.3:1 ratio.

^{1}H NMR (CD_3OD, 22 ^{o}C), δ: **Major isomer:** 1.43 (d, J = 6.0 Hz, $^{2}J_{PtH}$ = 40 Hz, 1H), 1.69 (d, J = 9.2 Hz, 1H), 3.14 (s, 1H), 3.29 (s, 1H), 5.88 (d, J = 6.0 Hz, $^{3}J_{PtH}$ = 17 Hz, 1H), 5.92 (s, 1H), 6.92-7.22 (m, 4H), 7.38 (ddd, J = 7.7, 5.8, 1.2 Hz, 1H), 7.54 (ddd, J = 7.7, 5.5, 1.2 Hz, 1H), 7.81 (d, J = 7.7 Hz, 1H), 7.88 (d, J = 7.7 Hz, 1H), 8.04 (td, J = 7.7, 1.6 Hz, 1H), 8.11 (td, J = 7.7, 1.6 Hz, 1H), 8.52 (d, J = 5.5 Hz, 1H), 9.08 (d, J = 5.8 Hz, 1H). **Minor isomer:** 1.73 (dd, J = 6.0, 3.0 Hz, $^{2}J_{PtH}$ = 40 Hz, 1H), 1.89 (d, J = 8.7 Hz, 1H), 3.25 (d, J = 8.7 Hz, 1H), 3.62 (s, 1H), 5.73 (d, J = 6.0 Hz, $^{3}J_{PtH}$ = 18 Hz, 1H), 5.93 (s, 1H), 6.92-7.22 (m, 4H), 7.44 (ddd, J = 7.8, 6.0, 1.2 Hz, 1H), 7.57 (ddd, J = 7.8, 5.6, 1.2 Hz, 1H), 8.54 (d, J = 5.6 Hz, 1H), 9.18 (d, J = 6.0 Hz, 1H) (one of the bridgehead atoms is not seen due to overlap with a solvent peak; C(4)-H and C(3)-H peaks of pyridyls of dpms are not distinct due to overlap with peaks of major isomer.) **IR** (KBr), ν: 3371 (w br), 2979 (w), 2954 (w), 2931 (w), 1606 (w), 1474 (w), 1434 (w), 1270 (m), 1222 (m), 1187 (m), 1154 (m), 1026 (s), 918 (w), 808 (m), 759 (s), 689 (m) cm^{-1}. **ESI-MS** of the solution of **4.5c** in CH_3OH-H_2O solution, m/z

604.0; calculated for M^*H^+, $C_{22}H_{21}N_2O_4{}^{195}PtS$, 604.0. No peaks that could correspond to acyclic complex at $(M+18)^*H^+$, similar to **4.7d**, were observed. **Anal.** Found: C, 40.97; H, 3.35; N, 4.51. Calculated for $C_{22}H_{20}N_2O_4PtS$, C, 43.78; H, 3.34; N, 4.64.

Preparation of *cis*-(dpms)Pt^{IV}($C_{11}H_{10}O$-*κC,κO*)(OH), *cis*-4.3c

Procedure A. Oxidation with O_2. A sample of **4.5c** (40 mg, 76 μmol) was dissolved in a mixture of 6 mL of trifluoroethanol and 4 mL of H_2O. The resulting yellow solution was placed into 50 mL flask equipped with a magnetic stirring bar. The flask was filled with O_2, stoppered and stirred vigorously at 20 ^oC. Samples of the reaction mixture were periodically analyzed by ^1H NMR by evaporation and redissolving in CD_3OD. According to ^1H NMR, clean oxidation into Pt^{IV} occurs with a half-life of 2h at 20 ^oC. After 10 hours the reaction was complete by NMR; no starting material was detected. The resulting yellow solution was reduced in volume to 1 mL by vacuum evaporation. The resulting suspension in H_2O was cooled down in ice bath for 30 min, yellow precipitate was vacuum-filtered, washed with small amount of with ice-cold water and dried under vacuum (200 mTorr) for 2 days. Yield 28.8 mg (46 μmol), 70%. Yellow solid, soluble in DMSO, moderately soluble in methanol, acetonitrile, slightly soluble in acetone and CH_2Cl_2.

Procedure B. Oxidation with H_2O_2. A sample of **4.5c** (46.1 mg, 76 μmol) and 0.6 mL of water were placed into 10 ml vial, equipped with a magnetic stirring bar. 30% H_2O_2 (80 μL, 776 μmol, 10 equiv) was added to a stirred suspension at 20 ^oC. Stirring continued at 20 ^oC for 3 hours. Yellow precipitate forms in the reaction mixture. After

3 hours the reaction was complete, according to ^{1}H NMR analysis of the sample of the reaction mixture. The resulting suspension was cooled down in ice bath for 30 minutes, then vacuum-filtered, washed with 0.5-1 mL of cold water and dried under vacuum (200 mTorr) for 1 day. Yield of pale yellow microcrystalline product 40.3 mg (65 μmol), 85%. Major product of oxidation was assigned structure ***cis*-4.3c** based on NOE data. Trace amount of the minor complex with very similar characteristics was also detected, presumably *trans*-isomer of complex ***cis*-4.3c**, however detailed characterization was not possible due to low concentration. Major and minor isomers are present in 17:1 ratio. The minor isomer was removed by washing (dpms)Pt^{IV}($C_{11}H_{10}O$-*κC,κO*)(OH) with sufficient amount of water.

Major isomer, ***cis*-4.3c**: **^{1}H NMR** (dmso-d_6, 22 ^{o}C), δ: 1.57 (d, J = 8.8 Hz, 1H), 2.34 (d, J = 5.1, $^{2}J_{PtH}$ = 60 Hz, 1H), 2.61 (br s, OH), 2.79 (d, J = 8.8 Hz, 1H), 3.01 (s, 1H), 3.17 (s, 1H), 5.17 (d, J = 5.1 Hz, $^{3}J_{PtH}$ = 17 Hz, 1H), 6.72 (s, 1H). 7.02-7.10 (m, 2H), 7.17-7.24 (m, 2H), 7.78 (ddd, J = 7.7, 5.7, 1.3 Hz, 1H), 7.85 (ddd, J = 7.7, 5.2, 1.0 Hz, 1H), 8.00-8.05 (m, 2H), 8.27 (td, J = 7.7, 1.1 Hz, 1H), 8.29 (td, J = 7.7, 1.1 Hz, 1H), 8.64 (dd, J = 5.8, 1.1 Hz, 1H), 8.85 (d, J = 5.2 Hz, 1H). **^{13}C NMR** (dmso-d_6, 22 ^{o}C), δ: 10.7 (CH, $^{1}J_{PtC}$ = 457 Hz), 44.5 (CH2), 45.0, 50.0, 69.8, 93.5, 120.4, 122.7, 125.2, 125.7, 126.1, 126.6, 127.3, 127.8, 141.6, 142.3 (CH), 143.9 (C quat), 148.1 (C quat), 148.5, 149.4 (CH), 149.7 (C quat), 152.5 (C quat).

Minor product, ***trans*-4.3c**. ^{1}H NMR (dmso-d_6, 22 ^{o}C), δ: 1.69 (d, J = 9.0 Hz, 1H), 2.19 (d, J = 5.0 Hz, $^{2}J_{PtH}$ is not seen due to low concentration), 4.73 (d, J = 5.0 Hz, 1H), 6.75 (s, 1H), 8.78 (d, J = 5.5 Hz, 1H), 8.90 (d, J = 5.5 Hz, 1H); other peaks overlap with peaks of the major isomer and solvent and cannot be identified.

IR (KBr), ν: 3413 (w br), 3024 (w), 2956 (w), 2913 (w), 1607 (w), 1478 (w), 1446 (w), 1291 (m), 1275 (m), 1205 (m), 1145 (s), 1031 (w), 977 (s), 961 (s), 760 (s), 697 (m) cm^{-1}. **ESI-MS** of the solution of **4.3c** in CH_3OH-H_2O solution, m/z 620.0; calculated for M^*H^+, $C_{22}H_{21}N_2O_5{}^{195}PtS$, 620.0. **Anal.** Found: C, 40.80; H, 2.99; N, 4.30. Calculated for $C_{22}H_{20}N_2O_5PtS$, C, 42.65; H, 3.25; N, 4.52.

Selective 1D difference NOE experiments (dmso-d_6) (mixing time 0.5s, delay time 4s)

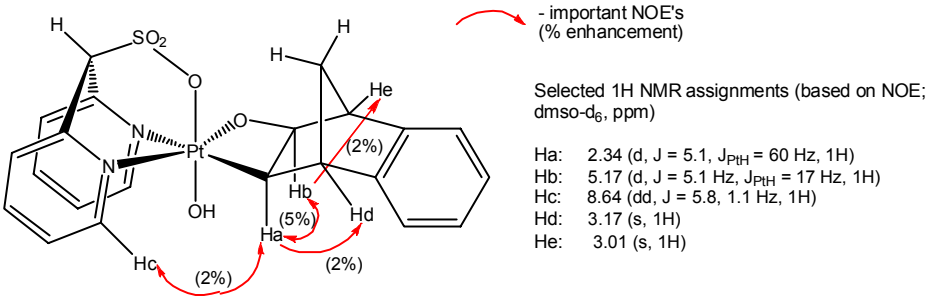

Generation of [(dpms)Pt^{II}($C_{11}H_{10}O$-*κC,κO*)]$^-$ in aqueous solution, 4.4c. A sample of **4.5c** (10.4 mg, 17 μmol) and 0.5 mL of degassed D_2O were placed into a 5 mL flask equipped with a magnetic stirring bar. 200 μL of 0.1N NaOD/D_2O solution (20 μmol, 1.2 equiv) was added to the stirred suspension of **4.5c**. Initially insoluble neutral complex **4.5c** dissolved after several minutes to give colorless solution of anionic form **4.4c** as a mixture of two isomers. The solution was stable at room temperature for several days in the absence of air.

Negative mode **ESI-MS** of the solution of **4.4c** in alkaline H_2O solution, m/z 602.1; calculated for [**4.4c**]$^-$, $C_{22}H_{191}N_2O_4{}^{195}PtS$, 602.1. No peaks that could correspond to acyclic complex, similar to **4.10d**, at $(M+18)^-$ were observed.

According to ^{1}H NMR, two isomers are present in 8 : 1 ratio; major isomer was assigned structure ***cis*-4.4c**, based on NOE experiments. The ratio of isomers does not change after 1 day at 20 ^{o}C.

***cis*-4.4c (major isomer). ^{1}H NMR** (NaOD/D_2O, 22 ^{o}C), δ: 0.89 (d, J = 5.6 Hz, $^{2}J_{PtH}$ = 44 Hz, 1H), 1.56 (d, J = 8.7 Hz, 1H), 3.11 (s, 1H), 3.13 (s, 1H), 3.29 (d, J = 8.7 Hz, 1H), 5.51 (d, J = 5.6 Hz, $^{3}J_{PtH}$ ~25 Hz, 1H), 5.85 (s, 1H; $CHSO_3$ peask can be seen in H_2O/D_2O mixtures but undergoes H/D exchange in neat D_2O alkaline solution), 7.02-7.20 (m, 3H), 7.21-7.38 (m, 2H), 7.48-7.55 (m, 1H), 7.67 (d, J = 7.7 Hz, 1H), 7.76 (d, J = 7.7 Hz, 1H), 8.00-8.10 (m, 2H), 8.50 (d, J = 5.3 Hz, 1H), 9.04 (d, J = 5.6 Hz, 1H). **^{13}C NMR** (NaOD/D_2O, 22 ^{o}C), δ: -5.4, 46.6, 46.9, 50.9, 75.7, 96.0, 119.7, 122.6, 124.8, 125.5, 125.9, 126.1, 128.7, 130.0, 137.7, 138.9, 144.8 (C quat), 148.2, 149.0 (Cquat), 151.0 (C quat), 152.1 (C quat), 154.0. ($^{1}J_{PtC}$ was not determined due to limited solubility and low intensity of satellites).

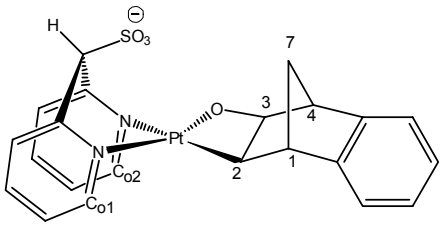

Selected ^{13}C NMR assignments
(based on HSQC , DEPT; dmso-d_6, ppm)

C2:	-5.4
C3:	96.0
C1 or C4:	46.0
C4 or C1:	50.9
C7:	46.9
C_{o1}:	154.0
C_{o2}:	148.2
$CHSO_3$:	75.7

***trans*-4.4c (minor isomer). ^{1}H NMR** (NaOD/D_2O, 22 ^{o}C), δ: 1.17 (d, J = 5.4 Hz, 1H; $^{2}J_{PtH}$ was not determined due to low intensity of satellites and low concentration), 1.71 (d, J = 8.5 Hz, 1H), 2.99 (d, J = 8.5 Hz, 1H), 3.21 (s, 1H), 3.57 (s, 1H), 5.25 (d, J = 5.4 Hz, 1H), 8.62 (d, J = 5.1 Hz, 1H), 9.19 (d, J = 5.8 Hz, 1H); other peaks of the minor isomer overlap with peaks of major species and cannot be identified.

Selective 1D difference NOE experiments (D_2O) (mixing time 0.5s, delay time 4 s).

Major isomer, *cis*-4.4c:

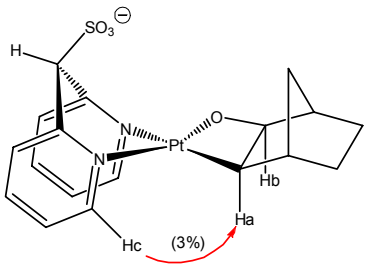

Preparation of (dpms)Pt^{II}($C_{10}H_9O_2$-*κC*)(OH_2), 4.7d. A 25 mL Schlenk tube equipped with a magnetic stirring bar was charged with a solution of (dpms)Pt(C_2H_4)(OH) (102.0 mg, 208 μmol) in water (2 mL) and a solution of 1,4-epoxy-1,4-dihydronapthalene (124 mg, 860 μmol) in acetone (2 mL); the Schlenk tube was sealed under argon. The resulting solution was degassed by three freeze-pump-thaw cycles and Teflon-sealed under vacuum (100 mTorr). White precipitate formed slowly after evacuation, and the reaction continued under reduced pressure upon stirring for 2 days at 20 ^{o}C. After 2 days precipitated product was filtered, washed with 2 mL of acetone and 10 mL of pentane and dried under vacuum (100 mTorr, 1 day) to give 68.4 mg of the product. The filtrate was evaporated to dryness and the resulting solid was washed with 10 mL of ether to remove excess of 1,4-epoxy-1,4-dihydronapthalene, which thus can be recovered and reused, and then washed with 1 mL of water to remove traces of unreacted (dpms)Pt(C_2H_4)(OH). The resulting white solid was dried under vacuum (100 mTorr, 1 day) to give additional 33.1 mg of the product. Combined yield 101.5 mg (163 μmol), 78%. White solid, poorly soluble in water, dissolves in DMSO to produce product of the displacement of aqua ligand by the solvent.

According to ^{1}H NMR, two complexes are present in solution, presumably iastereomers **4.7d'** and **4.7d'**, in ratio 1.8:1.

^{1}H NMR (D_2O, 22^0C, 400 MHz), δ: **major isomer**: 2.32 (d, J = 6.7 Hz, $^{2}J_{PtH}$ = 55 Hz, 1H), 3.99 (d, J = 6.7 Hz, 1H), 5.32 (s, 1H), 5.81 (s, 1H), 6.09 (s, 1H), 7.21-7.46 (m, 5H), 7.65 (ddd, J = 7.9, 5.5, 1.2 Hz, 1H), 7.78 (d, J = 7.9 Hz, 1H), 7.91 (d, J = 7.9 Hz, 1H), 8.05 (td, J = 7.9, 1.6 Hz, 1H), 8.13 (td, J = 7.9, 1.6 Hz, 1H), 8.74 (d, J = 5.5 Hz, 1H), 8.86 (d, J = 5.9 Hz, 1H). **Minor isomer**: 1.67 (d, J = 5.9 Hz, $^{2}J_{PtH}$ ~ 40 Hz, 1H), 5.34 (s, 1H), 5.70 (d, J = 5.9 Hz, 1H), 5.77 (s, 1H), 5.97 (s, 1H), 7.21-7.46 (m, 5H), 7.59 (ddd, J = 7.9, 5.5, 1.1 Hz, 1H), 7.76 (d, J = 7.9 Hz, 1H), 7.84 (d, J = 7.9 Hz, 1H), 8.08-8.14 (m, 2H), 8.59 (d, J = 5.5 Hz, 1H), 9.14 (d, J = 5.9 Hz, 1H).

IR (KBr), ν: 3585 (w br), 3416 (w br), 3008 (w), 2915 (w), 2869 (w), 1603 (w), 1475 (w), 1441 (w), 1358 (w), 1311 (w), 1256 (m), 1206 (s), 1172 (m), 1156 (m), 1053 (m), 1032 (s), 953 (m), 926 (m), 861 (m), 829 (s), 775 (m), 761 (s) cm^{-1}.

ESI-MS of neutral H_2O solution in the presence of small amount of Na^+ ions show peaks corresponding to an aqua complex **4.7d:** m/z 645.9 for M*Na^+, calc. for $C_{21}H_{20}N_2SO_6{}^{195}PtNa$ 646.0, and m/z 624.0 for M*H^+, calc. for $C_{21}H_{21}N_2SO_6{}^{195}Pt$ 624.1. Other peaks are also present that could be assigned to oxetane **4.5d** (M*Na^+ and M*H^+) or alternatively to the product of defragmentation of **4.7d** ((M-H_2O)*Na^+ and (M-H_2O)*H^+): m/z 627.9 for M*Na^+, calc. for $C_{21}H_{18}N_2SO_5{}^{195}PtNa$ 628.0, and m/z 606.0 for M*H^+, calc. for $C_{21}H_{19}N_2SO_5{}^{195}Pt$ 606.0. The latter two peaks become less intensive relative to peaks of **4.7d***H^+ at low cone voltages (5V) and more intensive relative to peaks of **4.7d***H^+ at high cone voltages (40V), that is consistent with these peaks as being at least in part resulting from defragmentation of **4.7d**.

Anal. Found C, 41.54; H, 3.33; N, 4.25. Calculated for aqua complex **4.7d** $C_{21}H_{20}N_2O_6PtS$, C, 40.45; H, 3.23; N, 4.49.

Preparation of (dpms)Pt($C_{10}H_9O_2$-*κC*)(dmso-d_6), 4.8d. Complex **4.8d** was generated by dissolving a complex **4.7d** in dmso-d_6 as a solvent. The formation of 1 equivalent of free water peak (3.33 ppm) was seen in ^{1}H NMR spectrum and no further changes were observed in NMR after several days at room temperature. ESI analysis showed that a peak corresponding to complex **4.8d** with dmso-d_6 as a ligand was present already after a few minutes. According to ^{1}H NMR, two complexes with similar NMR characteristics were present, presumably two diastereomers **4.8d'** and **4.8d''** in molar ratio 4.9:1.

ESI-MS: A sample of complex **4.7d** prepared in dmso-h_6, diluted with MeOH: m/z 683.9 (calc. for M*H$^+$, $C_{23}H_{25}N_2S_2O_6{}^{195}$Pt 684.0). Analogously a sample was prepared by in dmso-d_6: m/z 690.1 (calc. for M*H$^+$, $C_{23}H_{19}D_6N_2S_2O_6{}^{195}$Pt 690.1)

Major isomer: ^{1}H NMR (dmso-d_6, 22^{0}C, 400 MHz), δ: 1.80 (d, J = 6.9 Hz, $^2J_{PtH}$ = 79 Hz, 1H), 3.98 (dd, J = 6.9, 2.4 Hz, 1H), 4.58 (br s, 1H), 5.03 (s, 1H), 5.28 (d, J = 2.4 Hz, 1H, OH), 6.17 (s, 1H), 6.84-6.92 (m, 1H), 6.97-7.05 (m, 2H), 7.24-7.28 (m, 1H), 7.40-7.44 (m, 1H), 7.45-7.49 (m, 1H), 7.84 (d, J = 7.7 Hz, 1H), 7.88 (d, J = 7.7 Hz, 1H), 8.03-8.09 (m, 2H), 8.81 (d, J = 5.5 Hz, 1H), 9.88 (d, J = 5.5 Hz, 1H). **^{13}C NMR** (dmso-d_6, 22^{0}C, 500 MHz): 24.9, 75.5, 76.6, 82.8, 84.7, 116.8, 120.5, 123.4, 123.5, 125.0, 126.5, 127.7, 127.8, 139.7, 140.2, 143.5, 150.5, 152.9, 153.3, 153.4,

156.4. ($^{1}J_{PtC}$ coupling constant of a Pt-C carbon at 24.9 ppm could not be determined due to low intensity of platinum satellites and limited solubility of **4.8d**).

Major isomer:

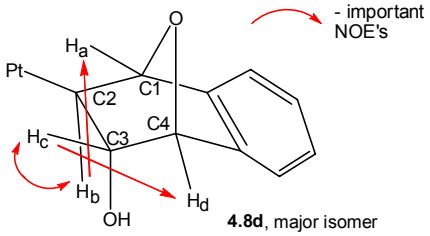

4.8d, major isomer

Selected ^{1}H assignments (from NOE and HSQC) (ppm):	
Ha	4.58
Hb	1.80
Hc	3.98
Hd	5.03
OH	5.28
CHSO3	6.17

Selected ^{13}C assignments (from HSQC) (ppm):	
C1	82.8
C2	24.9
C3	75.5
C4	84.7
CHSO3	76.6

Minor isomer: **^{1}H NMR** (dmso-d_6, 22^{0}C, 400 MHz), 2.19 (d, J = 6.9 Hz, $^{2}J_{PtH}$ = 70 Hz, 1H), 4.05 (br m, 1H), 4.41 (s, 1H), 5.09 (s, 1H), 5.63 (s, 1H, OH), 6.69 (s, 1H), 7.04-7.09 (m, 2H), 7.11-7.17 (m, 1H), 7.27-7.31 (m, 1H), 7.44-7.53 (m, 2H), 8.09-8.14 (m, 2H), 8.59 (vd, J = 7.9 Hz, 2H), 8.76 (d, J = 5.5 Hz, 1H), 9.73 (br m, 1H). Assignment of signals of the OH group was confirmed by the absence of cross peaks, corresponding to signals at 5.28 ppm (major isomer) and 5.63 ppm (minor isomer) in HSQC spectrum of **4.8**. **^{13}C NMR** (dmso-d_6, 22^{0}C, 500 MHz), 24.9, 70.3, 75.9, 83.2, 85.1, 117.7, 120.4, 123.4, 124.2, 124.8, 125.4, 126.6, 140.2, 140.6, 143.2, 149.1, 152.0, 153.7, 154.6, 154.9 (one of the meta-C peaks was not seen due to overlapping with peaks of major isomer. $^{1}J_{PtC}$ coupling constant of a Pt-C carbon at 24.9 ppm could not be determined due to low intensity of platinum satellites and limited solubility of **4.8d**).

Minor isomer:

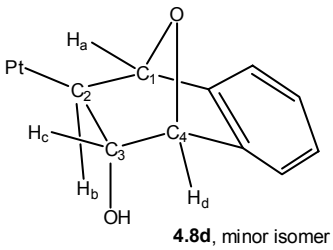

4.8d, minor isomer

Selected ^{1}H assignments (from HSQC) (ppm):	
H_b	2.19
H_c	4.05
OH	5.63
$CHSO_3$	6.69
H_a or H_d	4.41
H_a or H_d	5.09

Selected ^{13}C assignments (from HSQC) (ppm):	
C_2	24.9
C_3	75.9
$CHSO_3$	70.3
C_1 or C_4	83.2
C_1 or C_4	85.1

Generation of [(dpms)Pt^{II}($C_{10}H_9O_2$-*κC*)(OH)]$^-$, 4.10d in aqueous solution. A sample of complex **4.7d** (10 mg, 16 μmol) and 0.5 mL of deaerated D_2O were placed into a vial equipped with a magnetic stirring bar. A solution of NaOD in deaerated D_2O (0.04N, 0.5 mL, 20 μmol, 1.2 equ) was added dropwise to a stirred suspension of **4.7d** under argon. The white precipitate of complex **4.7d** dissolved after 5-10 minutes. The resulting colorless solution was transferred into an NMR Young tube and stored under argon. ^{1}H NMR spectrum recorded after ~15 minutes after preparation showed formation of two new complexes. The product was identified by ESI as anionic products of deprotonation of aqua ligand of complex **4.7d**. The product formed as a mixture of two species with similar NMR characteristics, presumably a mixture of diastereomeric **4.7d'** and **4.7d''**. Individual configurations of diastereomeric **4.7d'** and **4.7d''** were not established. The product was characterized by ^{1}H, ^{13}C, COSY and HSQC NMR. The relative molar ratio of two complexes, characterized by CHPt doublets at 2.53 and 2.33 ppm, was 1 : 1.71 respectively after ~15 minutes after preparation, according to ^{1}H NMR. The ratio of two isomers changed over time; after 3.5 hours at room temperature the ratio of isomers, characterized by CHPt doublets at 2.53 ppm ("isomer 1") and 2.33 ppm ("isomer 2"), was 1 : 0.6 respectively, and then did not change after several more hours. Slow transformation of isomeric complexes **4.10d** into a mixture of isomeric anionic oxetanes **4.4d** was observed in solution at room temperature with a half-life of ~53h: after 25 hours at room temperature: after 25 hours at room temperature, a mixture of

complexes **4.10d** and **4.4d**, characterized by CHPt doublets at 2.53 ppm, 2.33 ppm, 1.32 ppm and 0.96 ppm formed in molar ratio 6.6 : 4.0 : 1.0 : 2.1 respectively.

"Isomer 1", ^{1}H NMR (NaOD/D_2O, 22^{0}C, 400 MHz): 2.53 (d, J = 7.2 Hz, $^{2}J_{PtH}$ = 81 Hz, 1H), 4.12 (d, J = 7.2 Hz, 1H), 5.31 (s, 1H), 5.59 (s, 1H), 7.11-7.48 (m, 5H), 7.56-7.64 (m, 1H), 7.71 (d, J = 7.8 Hz, 1H), 7.86 (d, J = 7.8 Hz, 1H), 7.98 (t, J = 7.8 Hz, 1H), 8.10 (t, J = 7.8 Hz, 1H), 8.54 (d, J = 5.8 Hz, $^{3}J_{PtH}$ = 32 Hz, 1H), 8.77 (m, 1H). ($CHSO_3$ proton undergoes H/D exchange in alkaline D_2O solutions but can be seen in H_2O/D_2O mixtures using solvent suppression ^{1}H NMR as a singlet at 5.95 ppm, integrating as 1H.). **^{13}C NMR** (NaOH/H_2O/D_2O, 22^{0}C, 500 MHz), δ: 30.1, 77.4, 77.6, 87.4, 87.8, 119.4, 121.7, 126.4, 127.0, 127.1, 128.3, 129.5, 130.1, 139.2, 140.2, 142.5, 148.8, 149.8, 150.3, 152.8, 155.7. ($^{1}J_{PtC}$ coupling constant of a Pt-C carbon at 30.1 ppm could not be determined due to low intensity of platinum satellites and limited solubility of **4.10d**).

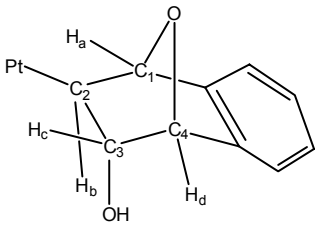

4.10d, "isomer 1"

Selected ^{1}H assignments (from COSY and HSQC) (ppm):		Selected ^{13}C assignments (from HSQC) (ppm):	
H_b	2.53	C_2	30.1
H_c	4.12	C_3	77.6
$CHSO_3$	5.95	$CHSO_3$	77.4
H_a or H_d	5.31	C_1 or C_4	87.4
H_a or H_d	5.59	C_1 or C_4	87.8

"Isomer 2", ^{1}H NMR (NaOD/D_2O, 22^{0}C, 400 MHz), δ: 2.33 (d, J = 6.8 Hz, $^{2}J_{PtH}$ = 78 Hz, 1H), 3.87 (d, J = 6.8 Hz, 1H), 5.25 (s, 1H), 5.71 (s, 1H), 7.11-7.48 (m, 5H), 7.61 (ddd, J = 7.8, 5.8, 1.5 Hz, 1H), 7.69 (d, J = 7.9 Hz, 1H), 7.84 (d, J = 7.9 Hz, 1H), 8.00 (td, J = 7.9, 1.5 Hz, 1H), 8.11 (td, J = 7.8, 1.5 Hz, 1H), 8.79 (d, J = 5.8 Hz, 1H), 8.81 (d, J = 5.8 Hz, 1H). ($CHSO_3$ proton undergoes H/D exchange in alkaline D_2O solutions but can be seen in H_2O/D_2O mixtures using solvent suppression ^{1}H NMR as

a singlet at 5.94 ppm, integrating as 1H). **^{13}C NMR** ($NaOH/H_2O/D_2O$, 22^0C, 500 MHz): 29.2, 77.4, 78.2, 86.2, 87.0, 118.8, 122.0, 126.5, 127.2, 126.9, 128.4, 129.2, 130.3, 139.3, 140.3, 142.6, 149.0, 149.5, 150.0, 153.4, 154.3. ($^1J_{PtC}$ coupling constant of a Pt-C carbon at 29.2 ppm could not be determined due to low intensity of platinum satellites and limited solubility of **4.10d**)

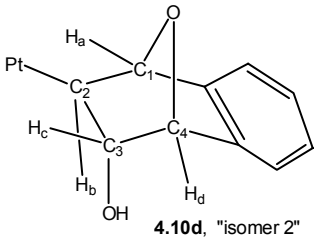

4.10d, "isomer 2"

Selected ^{1}H assignments (from COSY and HSQC) (ppm):	
H_b	2.33
H_c	3.87
$CHSO_3$	5.94
H_a or H_d	5.25
H_a or H_d	5.71

Selected ^{13}C assignments (from HSQC) (ppm):	
C_2	29.2
C_3	78.2
$CHSO_3$	77.4
C_1 or C_4	86.2
C_1 or C_4	87.0

A sample of **4.10d** for ESI-MS analysis was prepared by addition of 60 μL of 0.1 N $NaOH/H_2O$ solution to a suspension of complex **4.7d** (2.4 mg) in 1 mL of water. The resulting solution was analyzed immediately after its preparation in negative mode of ESI: m/z 622.1; calc. for $C_{21}H_{19}N_2SO_6{}^{195}Pt$ m/z 622.1. No other signals were detected

Preparation of [(dpms)Pt^{II}($C_{10}H_8O_2$-*κC,κO*)]$^-$, 4.4d. A sample of complex **4.7d** (20 mg, 32 μmol) and 0.5 mL of deaerated D_2O were placed into a vila equipped with a magnetic stirring bar. A solution of NaOD in deaerated D_2O (0.08 N, 0.5 mL, 40 μmol, 1.2 equ) was added dropwise to a stirred suspension of **4.7d** under argon. The resulting solution transferred into an NMR Young tube and heated at 60 ^{o}C. The reaction mixture was periodically monitored by 1H NMR. According to NMR, after 20 hours transformation of complexes **4.10d** into isomeric complexes **4.4d** was complete (>99%). The product was identified by ESI as anionic platinaoxetane **4.4d**. According to NMR, two isomeric forms ***cis*-4.4d** and ***trans*-4.4d** were present in 2 : 1

cis : *trans* ratio respectively; configuration of isomers was established from difference 1D-NOE experiments. The product was characterized by ^{1}H, ^{13}C, COSY and HSQC NMR.

***Cis*-4.4d, ^{1}H NMR** (D_2O, 22^0C, 400 MHz), δ: 0.96 (d, J = 5.8 Hz, $^{2}J_{PtH}$ = 60 Hz, 1H), 5.06 (s, 1H), 5.24 (s, 1H), 5.51 (d, J = 5.8 Hz, $^{3}J_{PtH}$ = 22 Hz, 1H), 7.14-7.39 (m, 5H), 7.47-7.52 (m, 1H), 7.65 (d, J = 7.9 Hz, 1H), 7.75 (d, J = 7.9 Hz, 1H), 8.03 (vtd, J = 7.9, 1.3 Hz, 2H), 8.45 (d, J = 5.9 Hz, 1H), 8.96 (d, J = 5.9 Hz, 1H). ($CHSO_3$ proton undergoes H/D exchange in alkaline D_2O solutions but can be seen in H_2O/D_2O mixtures using solvent suppression ^{1}H NMR as a singlet at 5.88 ppm, integrating as 1H). **^{13}C NMR** (H_2O/D_2O, 1:1 v/v, 22^0C, 500 MHz): -7.9, 76.3, 83.5, 85.4, 94.5, 118.9, 121.7, 126.1, 126.6, 126.8, 127.8, 129.3, 130.7, 138.4, 139.5, 141.0, 148.7, 148.9, 149.4, 151.5, 154.7. ($^{1}J_{PtC}$ coupling constant of a Pt-C carbon at -7.9 ppm could not be determined reliably due to low intensity of platinum satellites)

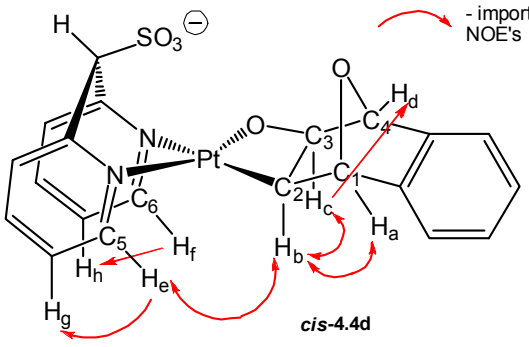

Selected ^{1}H assignments (from NOE, COSY and HSQC)

H_a	5.24
H_b	0.96
H_c	5.51
H_d	5.06
$CHSO_3$	5.88
H_e	8.96
H_f	8.45
H_g	7.24-7.34
H_h	7.47-7.52

Selected ^{13}C assignments (from HSQC) (ppm):

C_1	83.5
C_2	-7.9
C_3	94.5
C_4	85.4
$CHSO_3$	76.3
C_5	154.7
C_6	148.7

***Trans*-4.4d, ^{1}H NMR** (D_2O, 22^0C, 400 MHz), δ: 1.32 (d, J = 5.5 Hz, J_{PtH} = 71 Hz, 1H), 5.20 (s, 1H), 5.34 (d, J = 5.5 Hz, J_{PtH} = 18 Hz, 1H), 5.65 (s, 1H), 7.14-7.28 (m, 2H), 7.30-7.41 (m, 3H), 7.48-7.55 (m, 1H), 7.66 (d, J = 7.9 Hz, 1H), 7.75 (d, J = 7.9 Hz, 1H), 8.01 (vt, J = 7.9 Hz, 2H), 8.59 (d, J = 5.6 Hz, 1H), 9.09 (d, J = 5.6 Hz, 1H). ($CHSO_3$ proton undergoes H/D exchange in alkaline D_2O solutions but can be seen in

H_2O/D_2O mixtures using solvent suppression ^1H NMR as a singlet at 5.89 ppm, integrating as 1H). **^{13}C NMR** (H_2O/D_2O, 1:1 v/v, 22^0C, 500 MHz): -11.3, 76.3, 83.2, 86.1, 94.6, 118.9, 126.1, 126.6, 126.7, 127.9, 129.1, 130.6, 138.6, 139.6, 140.8, 148.5, 149.5, 149.6, 151.6, 155.4. (One of the carbon peaks cannot be seen due to overlapping with signals of major isomer. $^1J_{PtC}$ coupling constant of a Pt-C carbon at -11.3 ppm could not be determined reliably due to low intensity of platinum satellites).

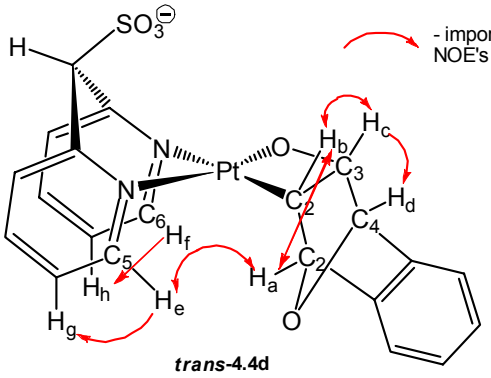

trans-4.4d

- important NOE's

Selected ^1H assignments (from NOE, COSY and HSQC)

H_a	5.65
H_b	1.32
H_c	5.34
H_d	5.20
$CHSO_3$	5.89
H_e	9.09
H_f	8.59
H_g	7.30-7.35
H_h	7.48-7.55

Selected ^{13}C assignments (from HSQC) (ppm):

C_1	83.2
C_2	-11.3
C_3	94.6
C_4	86.1
$CHSO_3$	76.3
C_5	155.4
C_6	149.5

A sample of **4.4d** for **ESI-MS** analysis was prepared by addition of 100 µL of 0.1 N NaOH/H_2O solution to a suspension of complex **4.7d** (5 mg) in 1 mL of deaerated H_2O and heating the resulting solution at 60 ^oC for 20 hours under argon. The resulting colorless solution was analyzed in a negative mode of ESI: m/z 604.1 (calc. for $C_{21}H_{17}N_2SO_5{}^{195}Pt$ 604.1); no other signals were detected.

Preparation of (dpms)Pt^{IV}($C_{10}H_9O_2$-*κC*)$(OH)_2$, 4.9d. A 10 mL flask equipped with a magnetic stirring bar was charged with 30 mg (48.1 µmol) of **4.7d** (as an isomeric mixture **4.7d'** and **4.7d''**) and 3 mL of water. 30% aqueous H_2O_2 solution (50 µL, 485 µmol) was added to the resulting suspension upon stirring. Stirring continued for 1 hour at room temperature. After 1 hour white precipitate was filtered, washed with 3 mL of water and dried under vacuum. Yield 23.4 mg (36.6 µmol), 76% (according to

^{1}H NMR, small amount of unreacted **4.7d** was present in the filtrate). The product was obtained as white fine-crystalline solid, insoluble in water, moderately soluble in methanol, DMSO. According to NMR, only one diastereomer of **4.9d** forms (>99%); configuration of the product was not established. Complex **4.9d** in DMSO solutions slowly produces **4.11d** and water with a half-life of ~6 days at 20 ^{o}C.

^{1}H NMR (dmso-d_6, 22^{0}C, 400 MHz), δ: 2.14 (br s, 1H, OH), 3.42 (br s, 1H, OH), 3.70 (d, J = 6.0 Hz, $^2J_{PtH}$ = 81 Hz, 1H), 4.22 (d, J = 6.0 Hz, 1H), 4.95 (s, 1H), 5.02 (s, 1H), 6.93 (s, 1H), 7.05-7.15 (m, 3H), 7.37 (d, J = 6.6 Hz, 1H), 7.81 (ddd, J = 7.8, 5.8,.1.3 Hz, 1H), 7.92 (ddd, J = 7.8, 5.5, 1.0 Hz, 1H), 8.05 (d, J = 7.8 Hz, 1H), 8.06 (d, J = 7.8 Hz, 1H), 8.30 (vt, J = 7.8 Hz, 2H), 8.31 (br s, 1H, OH), 8.86 (d, J = 5.5 Hz, 1H), 9.41 (d, J = 5.8 Hz, 1H). **^{13}C NMR** (dmso-d_6, 22^{0}C, 500 MHz): 35.1, 70.8, 76.9, 82.2, 86.5, 117.6, 120.8, 125.8, 126.2 (two peaks of C_5 meta protons of pyridyls overlapped, based on HSQC), 126.7, 127.1, 127.5, 141.8, 142.6, 142.8, 147.5, 148.0, 149.2, 152.4, 153.2. ($^1J_{PtC}$ coupling constant of a Pt-C carbon at 35.1 ppm could not be determined due to low intensity of platinum satellites and limited solubility of **4.9d**)

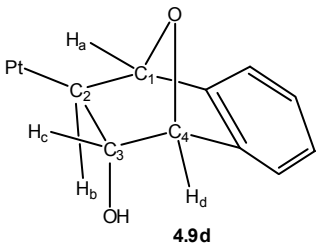

4.9d

Selected ^{1}H assignments (from HSQC) (ppm):	
H_b	3.70
H_c	4.22
$CHSO_3$	6.93
H_a or H_d	4.95
H_a or H_d	5.02
C_3-OH	8.31
PtOH	2.14
PtOH	3.42

Selected ^{13}C assignments (from HSQC) (ppm):	
C_2	35.1
C_3	76.9
$CHSO_3$	70.8
C_1 or C_4	82.2
C_1 or C_4	86.5

IR (KBr), ν: 3477 (w br), 3377 (w br), 3124 (w), 3056 (w), 2944 (w), 1603 (w), 1468 (w), 1445 (w), 1303 (s), 1204 (m), 1144 (s), 1082 (m), 1029 (w), 976 (s), 903 (w), 853 (w), 815 (w), 772 (m), 757 (s), 695 (m) cm^{-1}. **ESI-MS** of solution of **4.9d** in MeOH/H_2O (50:50 v/v), acicified with HBF_4, m/z 640.1; calc. for **4.9d***H^+

$C_{21}H_{21}N_2SO_7{}^{195}Pt$ 640.1. **Anal.** Found C, 39.55; H, 3.53; N, 4.17. Calculated for $C_{21}H_{20}N_2O_7PtS$, C, 39.44; H, 3.15; N, 4.38.

Preparation of (dpms)Pt^{IV}($C_{10}H_8O_2$-*κC*,*κO*)$(OH)_{ax}$, 4.3d. A sample of **4.7d** (41.3 mg, 66 μmol) was dissolved in a mixture of trifluoroethanol (6 mL) and water (4 mL). The solution was placed into 50 mL round-bottom flask equipped with a magnetic stirring bar. The flask was filled with oxygen and the reaction mixture was stirred vigorously under an O_2 atmosphere. Periodically samples of the reaction mixture were analyzed by ^{1}H NMR. Oxidation occurred with a half-life of ~18h and was complete after 4 days. After evaporation of the reaction mixture to dryness yellowish solid was obtained. The crude product was washed with small amount of water and dried under vacuum. Yield 35.4 mg (57 μmol), 86%. Yellowish crystalline solid, soluble in trifluoroethanol, methanol, DMSO, moderately soluble in dichloromethane. According to NMR, two isomeric oxetanes were present in ratio 10 : 1; a structure of the major isomer was assigned as ***cis*-4.3d** based on NOE experiments; the minor isomer was identical to complex **4.11d** by ^{1}H NMR.

Oxidation of **4.7d** (2 mg) in neutral aqueous solutions (20 mL) under an O_2 atmosphere (4 days, 20 ^{o}C) gives the same oxetane products, identified by ^{1}H NMR in dmso-d_6. If neat trifluoroethanol is used as a solvent without water, a complex mixture of product forms upon oxidation with O_2.

^{1}H NMR (dmso-d_6, 22^{0}C, 400 MHz), δ: 2.44 (d, J = 5.3 Hz, $^2J_{PtH}$ = 82 Hz, 1H), 3.51 (br s, $^2J_{PtH}$ ~30 Hz, 1H, OH), 4.95 (d, J = 5.3 Hz, $^3J_{PtH}$=25 Hz, 1H), 5.23 (s, 1H), 5.96 (s, 1H), 6.82 (s, 1H), 7.15-7.24 (m, 2H), 7.30-7.39 (m, 2H), 7.81 (ddd, J = 7.8, 5.6,

1.4 Hz, 1H), 7.83 (ddd, J = 7.8, 5.3, 1.2 Hz, 1H), 8.03 (d, J = 7.8 Hz, 1H), 8.05 (d, J = 7.8 Hz, 1H), 8.28 (td, J = 7.8, 1.6 Hz, 1H), 8.30 (td, J = 7.8, 1.5 Hz, 1H), 8.73 (d, J = 5.3 Hz, 1H), 9.13 (d, J = 5.6 Hz, 1H). **^{13}C NMR** (dmso-d_6, 22^{0}C, 500 MHz), δ: 2.5 ($^1J_{PtC}$ = 463 Hz), 70.5, 78.4, 83.9, 93.1 ($^2J_{PtC}$ = 80 Hz), 119.0, 121.0, 126.3, 126.4, 126.8, 127.1, 127.3, 127.8, 140.9 (C quat), 141.9, 142.5, 143.6 (C quat), 148.2, 149.7 (C quat), 151.5, 152.1 (C quat).

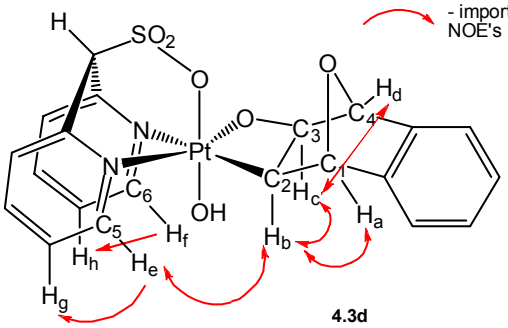

4.3d

- important NOE's

Selected ^{1}H assignments (from NOE and HSQC):	
H_a	5.96
H_b	2.44
H_c	4.95
H_d	5.23
$CHSO_3$	6.82
PtOH	3.51
H_e	9.13
H_f	8.73
H_g	7.81
H_h	7.83

Selected ^{13}C assignments (from HSQC) (ppm):	
C_1	78.4
C_2	2.5
C_3	93.1
C_4	83.9
$CHSO_3$	70.5
C_5	151.5
C_6	148.2

IR (KBr), ν: 3422 (w br), 3034 (w), 2937 (w), 2899 (w), 1603 (w), 1480 (w), 1437 (w), 1290 (m), 1201 (m), 1146 (s), 1031 (m), 1007 (w), 969 (m), 846 (w), 755 (s) cm^{-1}. **ESI-MS** of solutions of **4.3d** in MeOH/H_2O (50:50 v/v), acidified with HBF_4, m/z 622.1; calc. for **4.3d***H^+ $C_{21}H_{19}N_2SO_6{}^{195}Pt$ 622.1. **Anal.** Found C, 40.15; H, 3.06; N, 4.23. Calculated for $C_{21}H_{18}N_2O_6PtS$, C, 40.58; H, 2.92; N, 4.51.

Preparation of (dpms)Pt^{IV}($C_{10}H_8O_2$-*κC*,*κO*)$(OH)_{eq}$, 4.11d. A 50 mL round-bottom flask equipped with a magnetic stirring bar was charged with a sample of complex **4.9d** (50 mg, 78 μmol) and 10 mL of dry DMSO. The resulting suspension was heated at 80 ^{o}C under an argon atmosphere. After several hours white precipitate of complex **4.9d** dissolved; according to NMR, the reaction was complete (>99%) after 10 hours to give complex **4.11d** as the only product. DMSO was removed by vacuum

distillation, white solid residue was washed with 1-2 mL CH_2Cl_2 and dried under vacuum (100 mTorr, 65 ^oC, 2-3 days). Yield 39.0 mg (63 μmol), 80%. White solid, moderately soluble in methanol, DMSO, very slightly soluble in water.

Analogously a reaction was performed in dmso-d_6 (2 mg of complex **4.9d** in 0.7 mL of dmso-d_6) and was monitored periodically by ^{1}H NMR. No intermediates were detected in the reaction mixture during transformation; only complexes **4.9d** and **4.11d** were detected during the course of reaction. By the end of reaction one equivalent of H_2O, seen as a broad singlet at 3.33 ppm, was formed.

^{1}H NMR (dmso-d_6, 22^{0}C, 400 MHz), δ: 2.82 (d, J = 5.2 Hz, $^2J_{PtH}$ = 88 Hz, 1H), 3.90 (s, $^2J_{PtH}$ = 20 Hz, 1H, OH), 5.36 (s, 1H), 5.57 (d, J = 5.2 Hz, $^3J_{PtH}$ = 52 Hz, 1H), 5.96 (s, J_{PtH} = 27 Hz, 1H), 6.57 (s, 1H), 7.16-7.22 (m, 1H), 7.24-7.30 (m, 2H), 7.39-7.45 (m, 1H), 7.72 (ddd, J = 7.8, 5.8,. 1.3 Hz, 1H), 7.80 (ddd, J = 7.8, 5.8, 1.3 Hz, 1H), 7.99 (dd, J = 7.8, 1.3 Hz, 1H), 8.04 (dd, J = 7.8, 1.3 Hz, 1H), 8.27 (td, J = 7.8, 1.3 Hz, 1H), 8.29 (td, J = 7.8, 1.3 Hz, 1H), 8.77 (d, J = 5.8 Hz, $^3J_{PtH}$ = 20 Hz, 1H), 9.17 (dd, J = 5.8, 1.3 Hz, $^3J_{PtH}$ = 26 Hz, 1H). **^{13}C NMR** (dmso-d_6, 22^{0}C, 500 MHz): 6.8 ($^1J_{PtC}$ = 500 Hz), 71.5, 79.4, 83.4, 93.4 ($^2J_{PtC}$ = 82 Hz), 119.8, 121.3, 126.1, 126.9, 127.0, 127.4. 127.5, 128.6, 141.4 (C quat), 141.8, 142.0 (C quat), 142.1, 150.2, 150.6, 150.9 (C quat), 151.4 (C quat).

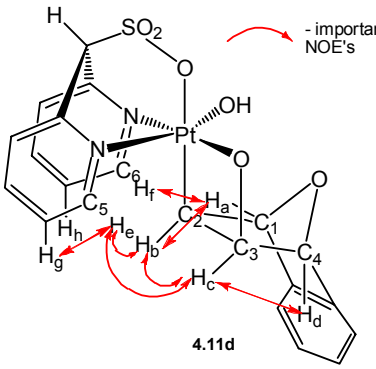

4.11d

Selected ^{1}H assignments (from NOE and HSQC):	
H_a	5.96
H_b	2.82
H_c	5.57
H_d	5.36
$CHSO_3$	6.57
PtOH	3.90
H_e	8.77
H_f	9.17
H_g	7.72
H_h	7.80

Selected ^{13}C assignments (from HSQC) (ppm):	
C_1	79.4
C_2	6.8
C_3	93.4
C_4	83.4
$CHSO_3$	71.5
C_5	150.2
C_6	150.6

IR (KBr), ν: 3449 (w br), 2902 (w), 2870 (w), 2844 (w), 1608 (w), 1479 (w), 1441 (w), 1278 (m), 1201 (m), 1144 (s), 999 (m), 970 (m), 847 (w), 815 (w), 761 (s) cm^{-1}. **ESI-MS** of solution of **4.11d** in MeOH, acidified with HBF_4: m/z 622.1; calc. for **4.11d***H^+ $C_{21}H_{19}N_2SO_6{}^{195}Pt$ 622.1. **Anal.** Found C, 40.21; H, 2.91; N, 4.27. Calculated for $C_{21}H_{18}N_2O_6PtS$, C, 40.58; H, 2.92; N, 4.51.

Preparation of (dpms)Pt^{II}(η^3-C_8H_{13}), 4.16. A sample of **4.1a** (79.8 mg, 140 μmol) was placed into 50 mL round bottom flask, equipped with a stirring bar and a reflux condenser; 20 mL of dry acetone were added. Because of the poor solubility of **4.1a** in acetone, heating was necessary to complete the reaction: the stirred suspension of **4.1a** was heated at 40 °C for 8 hours. A yellowish-white powdery precipitate formed upon heating. The precipitate was filtered, washed with water (1 mL), acetone (5 mL) and pentane (5 mL) and dried under vacuum. White solid, yield 52 mg (84 μmol), 67%. The product is soluble in DMSO, DMF and methanol, slightly soluble in acetone and CH_2Cl_2, almost insoluble in water.

According to NMR, **4.16** also forms upon dissolving (dpms)Pt(C_8H_{14})(OH) in other aprotic solvents such as DMF-d_7 and CD_2Cl_2 at room temperature with a half-life of 10-20 minutes with the release of 1 equivalent of water.

^{1}H NMR (dmso-d_6, 22 ^{o}C), δ: ***endo*-4.16**: 0.74-1.67 (m, 10H), 3.87 (m, $^2J_{195PtH}$=37 Hz, 2H), 5.22 (t, J=7.3 Hz, $^2J_{195PtH}$ =90 Hz, 1H), 5.58 (s, 1H), 7.01 (ddd, J =7.8, 5.6, 1.3 Hz, 2H), 7.50 (d, J =7.8 Hz, 2H), 7.72 (td, J =7.8, 1.3 Hz, 2H), 8.54 (d, J =5.6, $^3J_{195PtH}$ =31 Hz, 2H). ***exo*-4.16**: 0.70-1.70 (m, 8H), 2.11-2.24 (m, 2H), 3.81 (m, $^2J_{195PtH}$ =40 Hz, 2H), 4.83 (t, J =7.6 Hz, $^2J_{195PtH}$ =74 Hz, 1H), 5.51 (s, 1H), 7.10 (ddd,

J =7.9, 5.8, 1.3 Hz, 2H), 7.47 (d, *J* =7.9 Hz, 2H), 7.74 (td, *J* =7.9, 1.3 Hz, 2H), 8.65 (d, *J* =5.8 Hz, $^{3}J_{195PtH}$ =27 Hz, 2H). **IR** (KBr), ν: 3076 (w), 2924 (w), 2870 (w), 1607 (w), 1484 (m), 1249 (m), 1228 (s), 1184 (w), 1171 (w), 1038 (s), 809 (m), 767 (m), 685 (m) cm^{-1}. **ESI-MS** of the solution in trifluoroethanol acidified with HBF_4, m/z 554.1; calculated for (dpms)Pt(η^3-C_8H_{13})*H^+, $C_{19}H_{23}N_2O_3{}^{195}PtS$, 554.1.

Anal. Found: C, 40.95; H, 4.23; N, 5.07. Calculated for allyl complex (dpms)Pt(η^3-C_8H_{13}) $C_{19}H_{22}N_2O_3PtS$, C, 41.23; H, 4.01; N, 5.06.

NOE/EXSY experiments: All experiments were performed using mixing time 0.5s and delay time 4s (if not otherwise indicated).

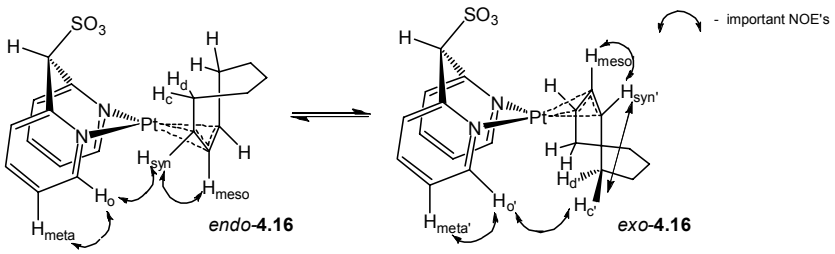

Preparation of (dpms)Pt^{II}(η^2-propylene)Cl, 4.21. Complex $KPtCl_3$(propylene) was prepared according to the literature procedure.[92] A solution of K(dpms) (0.655 g, 2.27 mmol) in 7 mL of water was added to a stirred solution of $KPtCl_3$(propylene) (0.910 g, 2.38 mmol) in 8 mL of water. White fine-crystalline precipitate formed after ~30 minutes. The reaction mixture was stirred for 12h at room temperature. The product was vacuum-filtered, washed with 10-15 mL of water and dried under vacuum to give 0.902 g (1.73 mmol) of the product; yield 76%. White crystalline solid, air-stable, poorly soluble in water and methanol. Two isomers are present according to ^{1}H NMR in ratio 3 : 1.

^{1}H NMR (CD_3OD, 22^{0}C, 400 MHz), δ: **major isomer** (CD_3OD): 1.35 (d, J = 6.1 Hz, $^2J_{PtH}$ = 27 Hz, 3H), 5.00-5.31 (m, 2H), 6.05-6.18 (m, $^2J_{PtH}$ = 43 Hz, 1H), 6.21 (s, 1H), 7.59 (ddd, J = 7.9, 5.9, 1.5 Hz, 1H), 7.72 (ddd, J = 7.9, 5.9, 1.5 Hz, 1H), 8.02 (d, J = 7.9 Hz, 1H), 8.03 (d, J = 7.9 Hz, 1H), 8.21 (td, J = 7.9, 1.5 Hz, 1H), 8.25 (td, J = 7.9, 1.5 Hz, 1H), 8.98 (d, J = 5.9 Hz, 1H), 9.04 (dd, J = 5.9, 1.5 Hz, 1H). **Minor isomer:** 1.98 (d, J = 5.5 Hz, J_{PtH} = 27 Hz, 3H), 6.27 (s, 1H), 7.60-7.63 (m, 1H), 7.69-7.72 (m, 1H), 8.50 (dd, J = 6.3, 1.0 Hz, 1H), 9.09 (dd, J = 6.0, 1.5 Hz, 1H), other peaks overlap with signals of major isomer and could not be identified. **IR** (KBr), ν: 3083 (w), 3035 (w), 2944 (w), 1607 (w), 1482 (w), 1438 (w), 1243 (m), 1225 (m), 1184 (m), 1038 (s), 853 (m), 809 (m), 757 (s), 691 (m) cm^{-1}. **ESI-MS** of solution in MeOH/water (50:50 v/v), acidified with HBF_4, m/z 522.0; calc. for M*H$^+$ $C_{14}H_{16}N_2SO_3{}^{195}Pt^{35}Cl$ 522.0. **Anal.** Found: C, 30.93; H, 2.92; N, 5.07. Calculated for allyl complex (dpms)Pt(η^3-C_3H_5) $C_{14}H_{15}ClN_2O_3PtS$, C, 32.22; H, 2.90; N, 5.37.

Preparation of (dpms)Pt(η^3-C_3H_5), 4.22. A sample of (dpms)Pt(η^2-C_3H_6)Cl (99.4 mg, 190 μmol) and 10 mL of degassed water were placed into a 100 mL Schlenk tube equipped with a magnetic stirring bar under argon. 1.94 mL (1.02 equiv) of 0.1 N NaOH solution in degassed water was added slowly to the resulting suspension upon stirring. After several minutes poorly soluble starting material dissolved to give a clear colorless solution. The resulting solution was heated under argon at 50 ^{o}C for 20 hours and periodically sampled and analyzed by ^{1}H NMR. White precipitate formed upon heating after 30-60 minutes. According to NMR, after 20 h of heating the reaction was complete. The reaction mixture was filtered from insoluble product. The

precipitate was washed with water and dried to give white fine-crystalline solid, insoluble in most organic solvents and water, presumably $(dpms)_2Pt_2(\mu\text{-}OH)_2$ resulting from the loss of propylene. The yellow filtrate was collected and evaporated to dryness under vacuum. Brownish-white solid residue formed upon evaporation of the filtrate was extracted with 2-3 mL of methanol and filtered through Celite. The resulting clear yellow methanolic solution was precipitated with ether to give yellowish-white crystals of product, yield 44 mg (91 μmol), 47%. The product is perfectly soluble in water, methanol, moderately soluble in DMSO, stable under air.

^{1}H NMR (D_2O, 22^{0}C, 400 MHz) (*exo*- and *endo*- isomers in 1.7 : 1 ratio), δ:

***Exo*-4.22**: 2.94 (d, J = 12 Hz, $^2J_{PtH}$ = 76 Hz, 2H), 3.89 (d, ^2J = 6.5 Hz, J_{PtH} = 28 Hz, 2H), 5.06 (m, $^2J_{PtH}$ = 84 Hz, 1H), 5.99 (s, 1H), 7.54 (ddd, J = 7.9, 5.6, 1.3 Hz, 2H), 7.94 (d, J = 7.9 Hz, 2H), 8.12 (td, J = 7.9, 1.5 Hz, 2H), 9.14 (d, J = 5.6 Hz, $^3J_{PtH}$ = 36 Hz, 2H) (intensity of $CHSO_3$ may be reduced due to slow H/D exchange in D_2O)

***Endo*-4.22**: 2.74 (d, J = 12 Hz, $^2J_{PtH}$ = 64 Hz, 2H), 3.83 (d, J = 6.5 Hz, $^2J_{PtH}$ = 23 Hz, 2H), 5.42 (m, $^2J_{PtH}$ = 84 Hz, 1H), 6.08 (s, 1H), 7.50 (ddd, J = 8.0, 5.6, 1.4 Hz, 2H), 7.97 (d, J = 8.0 Hz, 2H), 8.16 (td, J = 8.0, 1.7 Hz, 2H), 8.88 (d, J = 5.6 Hz, $^3J_{PtH}$ = 39 Hz, 2H) (intensity of $CHSO_3$ may be reduced due to slow H/D exchange in D_2O).

^{13}C NMR (D_2O, 22^{0}C, 400 MHz), δ: ***Exo*-4.22**: 44.7 (allyl terminal), 74.6 ($CHSO_3$), 111.1 (allyl central), 126.2 (C5 py), 129.9 (C3 py), 140.9 (C4 py), 149.5 (C1 py quat), 156.5 (C6 py). ***Endo*-4.22**: 45.4 (allyl terminal), 74.4 ($CHSO_3$), 106.2 (allyl central), 125.8 (C5 py), 129.9 (C3 py), 140.5 (C4 py), 149.7 (C1 py quat), 155.4 (C6 py). (J_{PtC} coupling constants could not be determined due to low intensity of platinum satellites and insufficient solubility of the complex). **ESI-MS** of solution of (dpms)Pt(η^3-C_3H_5)

in MeOH/water (50:50 v/v), acidified with HBF_4, m/z 496.0; calc. for M^*H^+ $C_{14}H_{15}N_2SO_3{}^{195}Pt$ 486.0.

Selective 1D-difference NOE experiments:

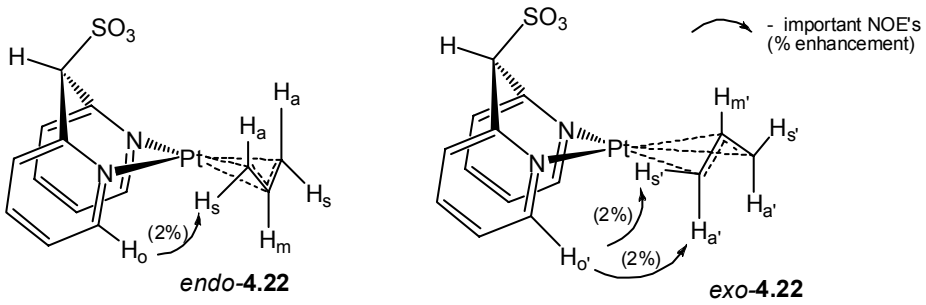

Preparation of (dpms)Pt^{II}(η^3-C_5H_7), 4.18. A solution of (dpms)Pt(C_2H_4)(OH) (102.1 mg, 209 μmol) in 3 mL of degassed H_2O and 3 mL acetone was placed into a 25 mL Schlenk tube equipped with a magnetic stirring bar under argon; 1 mL of cyclopentene was added. The reaction mixture was degassed by three freeze-pump-thaw cycles and Teflon-sealed under vacuum (50 mTorr). The resulting emulsion was stirred under vacuum for 2 days at 20 ^oC. According to ^1H NMR, no starting material was remaining after 2 days, and **4.18** was present in 60-70% yield along with other unidentified reaction products. The solution was filtered through Celite and evaporated to dryness to give 73.2 mg (143 μmol, 68%) of crude product as yellow crystalline solid. The product was purified by extraction with hot acetone; acetone solutions were collected and evaporated to dryness to give 32.4 mg (63 μmol, 30%) of product. Yellow solid, soluble in water, methanol. According to ^1H NMR, two isomers, presumably *endo*- and *exo*-**4.18**, are present in 1.1 : 1 molar ratio. Aliphatic peaks of both isomers and *syn*-protons of allylic ligand overlap and appear in the same region.

^{1}H NMR (D_2O/H_2O, 22^0C, 400 MHz), δ: **Major isomer**: 1.44 (d, *J* = 11.6 Hz, 1H), 1.65 (d, *J* = 11.6 Hz, 1H), 1.81 (d, *J* = 11.6 Hz, 1H), 2.08 (d, *J* = 11.6 Hz, 1H), 4.52 (d, $^2J_{PtH}$ = 35 Hz, 2H), 5.41 (t, *J* = 3 Hz, 1H), 5.96 (s, 1H), 7.55 (ddd, *J* = 7.8, 5.6, 1.3 Hz, 2H), 7.92 (d, *J* = 7.8 Hz, 2H), 8.16 (td, *J* = 7.8, 1.5 Hz, 2H), 9.14 (dd, *J* = 5.6, 1.5 Hz, $^3J_{PtH}$ = 34 Hz, 2H). **Minor isomer**: 1.44 (d, *J* = 11.6 Hz, 1H), 1.65 (d, *J* = 11.6 Hz, 1H), 1.81 (d, *J* = 11.6 Hz, 1H), 2.08 (d, *J* = 11.6 Hz, 1H), 4.52 (d, $^2J_{PtH}$ = 35 Hz, 2H), 5.54 (t, *J* = 3 Hz, 1H), 6.05 (s, 1H), 7.50 (ddd, *J* = 7.8, 5.6, 1.3 Hz, 2H), 7.95 (d, *J* = 7.8 Hz, 2H), 8.14 (td, *J* = 7.8, 1.5 Hz, 2H), 8.86 (dd, *J* = 5.6, 1.5 Hz, $^3J_{PtH}$ = 34 Hz, 2H) ($^2J_{PtH}$ = coupling constant of meso-protons as 5.41 ppm and 5.54 ppm could not be determined due to low intensity and broadness of platinum satellites).

IR (KBr), ν: 2955 (w), 2923 (w), 2853 (w), 1605 (w), 1478 (w), 1435 (w), 1228 (m), 1162 (m), 1033 (s), 856 (w), 811 (w), 764 (m), 689 (w) cm^{-1}. **ESI-MS** of solution of solution in H_2O acidified with HBF_4, m/z = 512.1. Calculated for $C_{16}H_{17}N_2O_3{}^{195}PtS$, 512.1.

Preparation of (dpms)Pt^{II}Cl(*cis*-butene), 4.23. Complex $KPtCl_3$(*cis*-butene)was prepared according to the literature procedure.[92] A solution of K(dpms) (68.8 mg, 238 μmol) in 0.8 mL of water was added to a stirred solution of $KPtCl_3$(*cis*-butene) (99.0 mg, 250 μmol) in 0.8 mL of water. Yellowish-white fine-crystalline precipitate formed after a few minutes. The reaction mixture was stirred for 12h at room temperature. The product was vacuum-filtered, washed with 3 mL of water and dried under vacuum to give 98.8 mg (184 μmol) of the product; yield 77%. Yellowish-white crystalline solid, air-stable, poorly soluble in water and methanol.

^{1}H NMR (CD_3OD, 22^0C, 400 MHz), δ: 1.88 (d, J = 8.5 Hz, $^3J_{PtH}$ = 42 Hz, 3H), 1.90 (d, J = 8.8 Hz, $^3J_{PtH}$ = 28 Hz, 3H), 5.35 (m, $^2J_{PtH}$ = 63 Hz, 1H), 5.85 (m, $^2J_{PtH}$ = 71 Hz, 1H), 6.25 (s, 1H), 7.56 (ddd, J = 7.8, 5.9, 1.5 Hz, 1H), 7.62 (ddd, J = 7.8, 5.9, 1.5 Hz, 1H), 7.99 (d, J = 7.8 Hz, 1H), 8.02 (dd, J = 7.8, 1.5 Hz, 1H), 8.17 (td, J = 7.8, 1.4 Hz, 2H), 8.68 (dd, J = 5.9, 1.4 Hz, $^3J_{PtH}$ = 35 Hz, 1H), 9.06 (dd, J = 5.9, 1.4 Hz, $^3J_{PtH}$ = 33 Hz, 1H). **IR** (KBr), ν: 3117 (w), 3031 (w), 2952 (w), 1604 (w), 1485 (w), 1435 (w), 1259 (m), 1220 (m), 1198 (m), 1043 (s), 954 (w), 862 (w), 812 (w), 779 (m), 765 (s), 687 (m) cm^{-1}. **ESI-MS** of solution of (dpms)Pt^{II}Cl(*cis*-butene) in MeOH/H_2O (50:50 v/v): m/z 536.0; calc. for M^*H^+ $C_{15}H_{18}N_2SO_3{}^{195}Pt^{35}Cl$ 536.0. **Anal.** Found: C, 33.93; H, 3.56; N, 4.95. Calculated for $C_{15}H_{17}ClN_2O_3PtS$, C, 33.62; H, 3.20; N, 5.23.

Chapter 5: Oxidation and Reductive Elimination Chemistry of Dpms-Supported Azaplatinacyclobutanes

5.1 Introduction

As shown in Chapter 4, some hydroxo olefin complexes of platinum(II) are selectively oxidized with O_2 to produce platina(IV)oxetanes; the latter are capable of C-O reductive elimination to produce epoxides. We thought it might be interesting to explore reactivity of the nitrogen analogues of platinaoxetanes, 1,2-azaplatinacyclobutanes, in aerobic oxidation and reductive elimination chemistry.

1,2-Azametallacyclobutanes, or 1,2-metallaazetidines have been implicated in a number of transition-metal catalyzed transformations such as hydroamination,[179] carbonylation of aziridines to form β-lactams,[180, 181] and isomerization of N-tosylaziridines into N-tosylketimines.[182]

Preparation of a number of pallada(II)- and platina(II)azetidines has been reported previosly in the literature. For example, Green,[183] Zetterberg[184] and Maresca[185, 186] described preparation of azaplalladacyclobutanes and azaplatinacyclobutanes via a nucleophilic attack of amines at the double bond of a coordinated alkene, followed by the ligand substitution at the metal center, as shown in Scheme 5.1.

Scheme 5.1

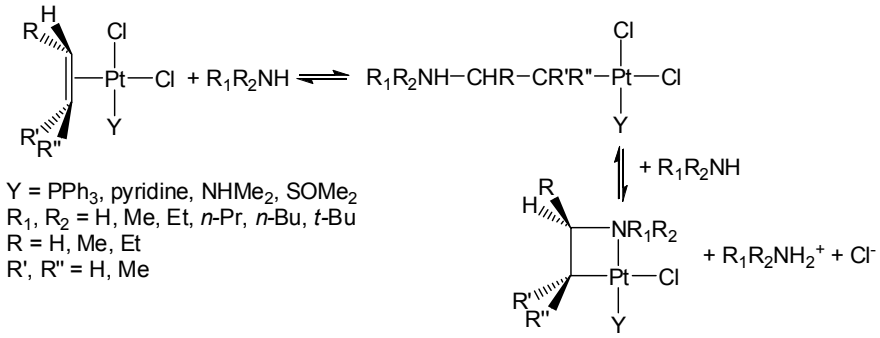

Other synthetic routes leading to the formation of azametalacyclobutanes have also been reported such as cyclometalation of amines,[129, 187] [2+2] cycloaddition of alkenes to metal imides,[188-190] and oxidative addition of aziridines.[191, 192]

Only one example of azaplatina(IV)cyclobutane complex has been reported by Mitchenko and Zamashchikov.[193] It was shown that upon addition of K_2CO_3 to the acidic aqueous solution of the acyclic β-ammonioethyl complex $[Pt^{IV}(CH_2CH_2NH_3^+)(Cl)_5]^-$ (**A**) a reductive elimination of aziridine occurs, accompanied by the parallel formation of an insoluble product **B** (Scheme 5.2). The latter was assigned a structure of an azaplatina(IV)cyclobutane $[Pt^{IV}Cl_3(CH_2CH_2NH_2\text{-}\kappa C,\kappa N)(C_2H_4N\text{-}\kappa N)]$ based on data of elemental analysis and reactivity studies. No reductive elimination was reported directly from complex **B**, which was found to be stable under basic conditions in aqueous solution. However, the azetidine ring opening takes place in acidic aqueous solutions of **B** in the presence of hydrochloric acid to produce a mixture of an acyclic $[Pt^{IV}(CH_2CH_2NH_3^+)(Cl)_5]^-$ (**A**) and a protonated aziridine.[193]

Scheme 5.2

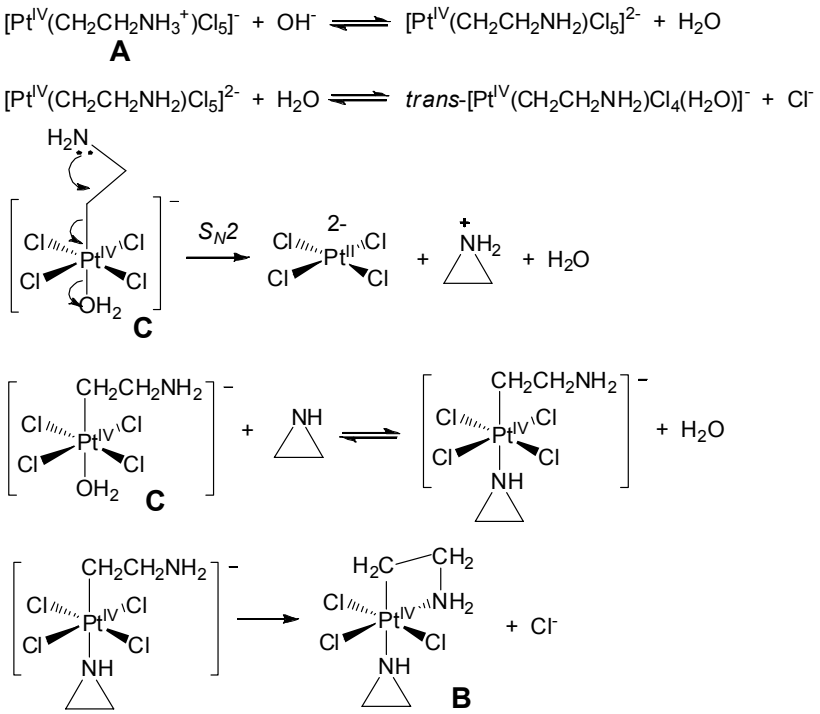

In turn, the reductive elimination of aziridine was observed from an acyclic complex **A** in alkaline aqueous solutions and was proposed to occur via an S_N2 type mechanism.[194]

To the best of our knowledge, direct (concerted) C(sp^3)-N elimination from a Pt^{IV} center has never been reported in literature. Mechanistic studies of the reductive elimination from a number of Pt(IV),[195] Pd(IV),[196] Rh(III)[197] and Ni(III)[191] complexes have implicated an S_N2 mechanism of the C(sp^3)-N reductive elimination in these systems. The direct C(sp^2)-N reductive elimination has been reported for a number of Pd(II)[198] and Ru(II),[199] however, all these examples involve sp^2- hybridized carbons of aryl or vinyl ligands.

We thought it might be interesting to examine reactivity of azaplatina(IV)cyclobutanes in C-N reductive elimination. By analogy with direct C-O reductive elimination from platina(IV)oxetanes, such reaction would produce aziridines as products.

Preparation of a number of dpms-supported azaplatinacyclobutanes and their reactivity toward oxidation and reductive elimination will be described this chapter. The azaplatina(IV)cyclobutane complexes $[LPt(CH_2CH_2NHR\text{-}\kappa C,\kappa N)(OH)]^+$ (L = dpms, R = Me, *t*-Bu) were obtained by oxidation of the corresponding azaplatina(II)cyclobutane $LPt(CH_2CH_2NHR\text{-}\kappa C,\kappa N)$ with H_2O_2 in neutral solutions or with O_2 in the presence of acids. The resulting complexes undergo reductive elimination in acidified aqueous solutions to produce *N*-alkyl ethanolammonium salts, $HOC_2H_4NH_2R^+$, and $[LPt^{II}(OH_2)_2]^+$ (**2.12**).

5.2 Results and Discussion

5.2.1 Preparation of Azaplatina(II)cyclobutane Complexes

As we have shown in Chapter 3, complex $LPt(CH_2{=}CH_2)Cl$ (L = dpms), **3.1**, reacts readily with nucleophiles to produce the corresponding β-substituted σ-ethyl complexes. Similarly, **3.1** reacts with excess aliphatic amines, *t*-$BuNH_2$ and $MeNH_2$, in methanolic solutions at room temperature to produce the corresponding zwitterionic complexes **5.1** and **5.2** respectively (Scheme 5.3). Complexes **5.1** and **5.2** were isolated in an analytically pure form by crystallization from methanol at -20 °C.

Scheme 5.3

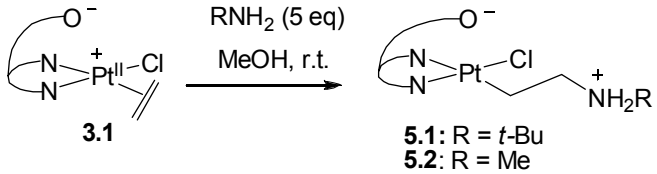

Complexes **5.1** and **5.2** were characterized by ^1H and ^{13}C NMR spectroscopy, ESI mass spectrometry and elemental analysis. In the ^1H NMR spectrum of **5.1** in dmso-d_6,

the two protons of the NH_2 group appeared as a broad singlet at 7.29 ppm with integral intensity equal to two protons relative to the singlet of the *tert*-butyl group at 1.18 ppm (9H). Similarly, the two protons of the NH_2 group in complex **5.2** produced a broad singlet at 8.29 ppm in ^{1}H NMR spectrum in dmso-d_6.

Cyclization of complexes **5.1** and **5.2** to form the corresponding platina(II)azetidines was achieved in the presence of NaOH in methanolic solutions at 50 ^{o}C (Scheme 5.4, eq. 5.1).

In the case of **5.1** a mixture of two isomeric azetidine complexes in a 6:1 ratio formed that display similar ^{1}H NMR characteristics. These complexes were assigned structures of two isomeric azaplatinacyclobutanes LPt(CH_2CH_2NH*t*-Bu-$\kappa C,\kappa N$), **5.3**, that differ by the orientation of the *tert*-butyl group with respect to the sulfonate of the dpms ligand (*cis*- and *trans*-**5.3**, Scheme 5.4). The reaction was complete after 12 hours at 50 ^{o}C to give **5.3** quantitatively by ^{1}H NMR. ESI mass spectrometry of the resulting clear solution showed the presence of only one platinum-containing peak characterized by m/z 545.1, corresponding to protonated **5.3***H^+. The product is well soluble in methanol and was not separated from inorganic salts. A mixture of complex **5.3** and one equivalent of NaCl was used in subsequent oxidation experiments targeting the preparation of Pt^{IV} azetidine as described below.

Scheme 5.4

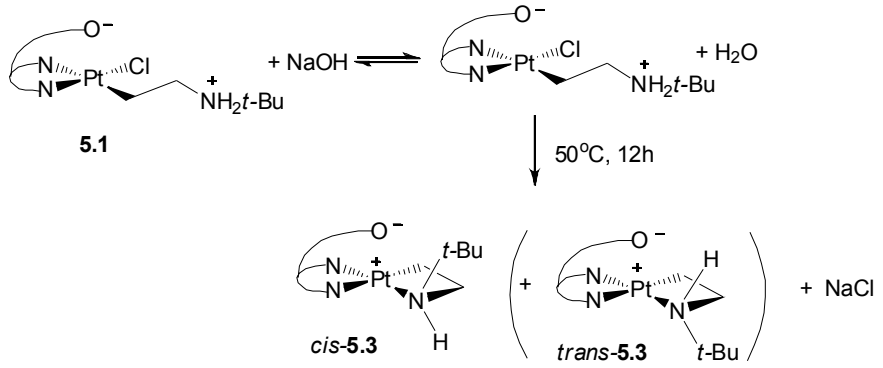

Similar to complex **5.1**, transformation of **5.2** to azaplatinacyclobutane complex **5.4** was observed in methanolic solution of **5.2** at 50 °C in the presence of 2 equivalents NaOH (eq. 5.1). The reaction was not complete if stoichiometric amount of NaOH was used, and unreacted **5.2** remained in solution even after prolonged heating. The poorly soluble product **5.4** precipitated after 24 hours from methanolic solution and was separated from excess NaOH by washing with cold methanol until neutral pH of the filtrate. The product was isolated in 76% yield and characterized by ^{1}H NMR spectroscopy and ESI mass spectrometry. The elemental analysis of a solid sample of **5.4** showed a lowered content of carbon (32.10% found, 33.47% calculated for **5.4**), presumably due to contamination with residual NaCl (~5% by weight).

$$\underset{\textbf{5.2}}{LPt(CH_2CH_2NH_2Me)Cl} + NaOH \longrightarrow \underset{\textbf{5.4}}{LPt(CH_2CH_2NHMe\text{-}\kappa C,\kappa N)} + NaCl + H_2O \qquad (5.1)$$

5.2.2 Preparation of Azaplatina(IV)cyclobutane Complexes $[LPt^{IV}(CH_2CH_2NHR\text{-}\kappa C,\kappa N)(OH)]^+$ (R = t-Bu, Me) by Oxidation with H_2O_2

Oxidation of complex **5.3** with excess H_2O_2 in the presence of 1 equivalent of NaCl in methanol produced alkaline solutions of the azaplatina(IV)cyclobutane product **5.5** quantitatively by NMR spectroscopy (eq. 5.2). The product **5.5** was isolated in an

analytically pure form in 64% yield by crystallization from methanol at -20 °C as a white crystalline solid. The solid state structure of **5.5** was established by single crystal X-ray diffraction. According to X-ray data, the product **5.5** is a cationic azaplatina(IV)cyclobutane complex with a chloride counterion that is hydrogen bound to both the NH group of the azetidine ring and the Pt-OH ligand. Crystals of **5.5** contain one molecule of methanol per one platinum center hydrogen bound to the Pt-OH group. The X-ray structure of **5.5** is given in Fig. 5.1.

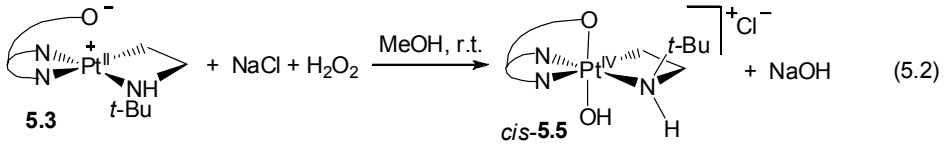

(5.2)

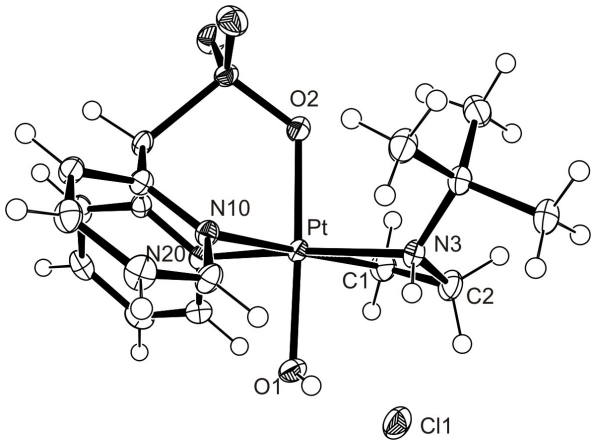

Figure 5.1. ORTEP plot (50% probability ellipsoids) for complex **5.5**. Selected bond lengths (Å) and angles (°): Pt1-C1, 2.039(3); Pt1-O1, 1.970(2); Pt1-O2, 2.066(2); Pt1-N3, 2.072(3); Pt1-N10, 2.195(3); Pt1-N20, 2.053(3); Pt1-C1-C2, 94.0(2), C1-C2-N3, 100.6(3).

Complex **5.5** was characterized by ^{1}H and ^{13}C NMR spectroscopy, ESI mass spectrometry and elemental analysis. According to NMR spectroscopy, only one isomer ***cis*-5.5** was present in solutions. The ^{1}H NMR spectrum of **5.5** in dmso-d_6 is characterized by the presence of two multiplets of the Pt-bound α-CH_2 group centered at 2.89 ppm ($^{2}J_{PtH}$ = 75 Hz) and 2.94 ppm ($^{2}J_{PtH}$ = 70 Hz) accompanied by platinum satellites, and two multiplets of the N-bound β-CH_2 group centered at 4.41 ppm ($^{3}J_{PtH}$ =

35 Hz) and 4.58 ppm ($^3J_{PtH}$ = 40 Hz), each integrating as one proton relative to the signal of the *tert*-butyl group. Two broad singlets at 4.25 ppm and 7.60 ppm were assigned to the Pt-bound OH and NH groups; the latter signal was accompanied by platinum satellites ($^1J_{PtH}$ = 58 Hz). In ^{13}C NMR spectra of ***cis*-5.5**, resonances of the carbon atoms of the azetidine ring appeared at -4.1 ppm and 54.3 ppm and were assigned to the Pt-bound carbon atom and the N-bound carbon atom respectively. These signals were characterized by ^{195}Pt-C coupling constants of 376 Hz and 114 Hz respectively.

Oxidation of complex **5.4** with 1.1 equivalent of H_2O_2 in methanolic solution cleanly produced alkaline solutions containing Pt^{IV} azetidine **5.6**, [LPt(CH_2CH_2NHMe-$\kappa C,\kappa N$)]$^+X^-$ (X^- = Cl^-, OH^-) in quantitative yield according to ^{1}H NMR spectroscopy (eq. 5.3). Complex **5.6** was characterized by ^{1}H, ^{13}C, COSY and HSQC NMR spectroscopy and ESI mass spectrometry in methanolic solutions.

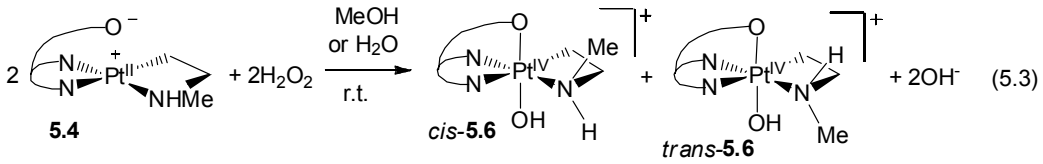

(5.3)

Two isomers of **5.6** were present in 2:1 ratio, presumably *cis*- and *trans*-**5.6** (eq. 5.3). In ^{1}H NMR spectrum of isomeric complexes **5.6**, the signals of the N-Me groups appeared as singlets at 2.87 ppm (major isomer) and 2.11 ppm (minor isomer). Both signals were accompanied by platinum satellites ($^2J_{PtH}$ is 27.5 Hz for major isomers and 33.4 Hz for minor isomer), indicating that the N-Me group is coordinated to a platinum center. In ^{13}C NMR spectra of the major isomer of **5.6**, signals of the Pt-bound carbon appeared at -2.0 ppm ($^1J_{PtC}$ = 414 Hz) and 80.3 ppm ($^2J_{PtC}$ = 115 Hz), which were assigned to the Pt-bound and N-bound carbon atoms respectively. The signal of N-Me

group of the major isomer appeared in ^{13}C NMR spectrum at 56.0 ppm and was accompanied by platinum satellites ($^2J_{PtC}$ = 22 Hz).

Only one peak corresponding to cationic complex **5.6** with m/z 519.1 was detected by ESI mass spectrometry in acidified solutions of **5.6**.

Extremely high solubility of **5.6** in alcohols and water in the presence of various counterions, such as Cl^-, BF_4^-, ClO_4^-, and SO_4^{2-}, did not allow for the isolation of the product in an analytically pure form by crystallization from these solvents. Solutions of **5.6** in solvents other than water and alcohols were unstable.

The product **5.6** was isolated in the solid state in the form of sulfate by oxidation of **5.4** in an aqueous solution with 1.1 equivalent of H_2O_2 and neutralization with dilute H_2SO_4. The resulting clear solution was evaporated to dryness to give [LPt(CH_2CH_2NHMe-*κC,κN*)]$_2$(SO_4) as a white crystalline solid in virtually quantitative yield, 90-95% pure by ^1H NMR. The product was stable in neutral solutions and in the solid state for 2-3 days at room temperature.

5.2.3 Oxidation of LPt(CH_2CH_2NH*t*-Bu-*κC,κN*) with O_2

We next examined reactivity of the Pt^{II} azetidine complexes toward O_2 in protic solvents. As shown in Chapter 2, reactivity of LPtMe(HX) complexes toward O_2 decreased in the order HX = H_2O~MeOH (half-life ~15 minutes) >> $PhNH_2$ (half-life 8-10 hours). This fact was attributed to lower acidity of the ammine ligand, compared to an aqua ligand or coordinated methanol, and, therefore, lower fraction of the anionic species [LPtMe(X)]$^-$ responsible for reaction with O_2. One could therefore expect that complex **5.3**, containing alkyl-substituted amino group, would be even less reactive toward O_2 than LPtMe(NH_2Ph). Indeed, neutral solutions of complex **5.3** in methanol or water were

stable under an O_2 atmosphere for several days at room temperature. No oxidation was observed in the presence of NaOH additives (0.2 equivalents), indicating that complex **5.3** is not acidic enough to produce anionic species [LPt(CH_2CH_2N*t*-Bu-$\kappa C,\kappa N$)]- in sufficient concentrations for reaction with O_2.

Importantly, in the presence of 1 equivalent of HBF_4, complex **5.3** reacted with O_2 in D_2O and CD_3OD solutions with a half-life of 2.5 hours to produce LPt^{IV}(CH_2CH_2N*t*-Bu-$\kappa C,\kappa N$)(OH)](BF_4), **5.5***BF_4, as the main product, as confirmed by ^1H NMR spectroscopy and ESI mass spectrometry. The oxidation of **5.3** with O_2 in CD_3OD was complete after 1 day at room temperature to produce **5.5***BF_4 in 73-80% NMR yield. The reaction is not very clean and unidentified products formed along with **5.5***BF_4 in 20-27% NMR yield.

We propose that facile oxidation of **5.3** in the presence of acid is due to the formation of an intermediate acyclic complex **5.7** with a solvent molecule, water or methanol, coordinated to the metal center. Complex **5.7** could form as a result of a reversible amino-for-solvent ligand substitution at the Pt^{II} center driven to the right by protonation of the lone electron pair of dissociated nitrogen atom (Scheme 5.5, eq. 5.4). It was shown previously that LPtMe(HX) (HX – MeOH, H_2O) and β-substituted alkyl hydroxo complex [LPt(CH_2CH_2OH)(OH)]$^-$ react readily with O_2 to produce corresponding Pt^{IV} products. Similarly, fast oxidation of complex **5.7** with O_2 in MeOH could initially produce an acyclic Pt^{IV} complex **5.8** (eq. 5.5). Subsequent proton transfer from an ammonium group to the slightly basic methoxo ligand and entropy-driven displacement of the coordinated methanol with the tethered amino group could then produce metallacyclic product **5.5***BF_4 (eq. 5.6). Similar reversible coordination of the amino

group of β-ammonioethyl Pt^{IV} complexes as a function of the solution pH was demonstrated by Mitchenko (Scheme 5.2).[193]

Scheme 5.5

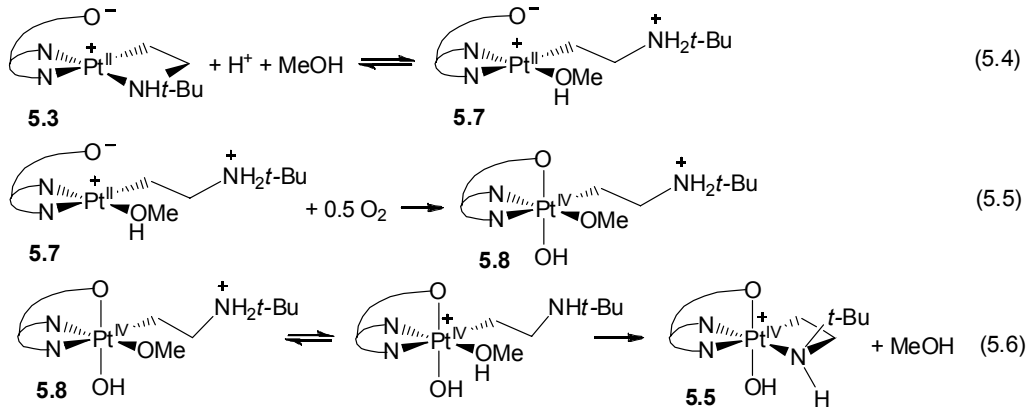

Similarly, oxidation was observed in suspensions of complex **5.4** in CD_3OD in the presence of 1 equivalent of HBF_4 and air, however, the reaction was slow due to poor solubility of **5.4** in methanol.

5.2.4 Reductive Elimination from Azaplatina(IV)butanes

By analogy with Pt^{IV} oxetane complexes, described in Chapter 4, one might expect that direct C-N elimination from azetidines **5.5** and **5.6** could produce corresponding aziridines as products. In order to examine reductive elimination from azaplatina(IV)cyclobutanes, a neutral complex with an amido arm coordinated to a Pt^{IV} center, **5.9**, was prepared and its reactivity was studied in aprotic solvents. N-*tert*-Butyl substituted complex **5.9** was used in this study due to its higher solubility in aprotic solvents, compared to an N-Me substituted analogue. The neutral complex **5.9** was prepared by deprotonation of **5.5***BAr^F_4 (BAr^F_4 = $[B(3,5\text{-}(CF_3)_2C_6H_3)_4]^-$) with *t*-BuOK in THF solution, followed by removal of *t*-BuOH by vacuum evaporation (eq. 5.8).

Complex **5.5***BAr^F_4 was obtained by the counterion exchange from the chloride salt **5.5***Cl in dry dichloromethane followed by removal of insoluble NaCl from solution of **5.5***BAr^F_4 in CH_2Cl_2 by filtration through Celite (eq. 5.7).

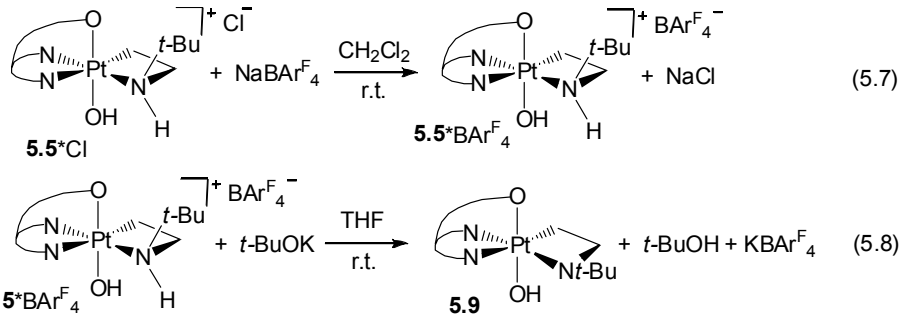

(5.7)

(5.8)

In ^{1}H NMR spectrum of **5.5***BAr^F_4 in THF-d_8, two broad singlets were present at 3.44 ppm and 5.92 ppm respectively, accompanied by platinum satellites, each integrating as one proton relative to the signal of the *tert*-butyl group. The signal at 3.44 ppm with a coupling constant $^1J_{PtH}$ of 27 Hz was assigned to the Pt-OH group, based on its characteristical chemical shift and the coupling constant value, which were similar to those for other Pt^{IV} hydroxo complexes. The more downfield shifted resonance at 5.92 ppm with a coupling constant $^1J_{PtH}$ of 74 Hz was assigned to the NH group. Although no ^{1}H NMR data are available for the (dpms)Pt^{IV} complexes with aliphatic amines for direct comparison, the NH protons of the phenylamido complexes LPtMe(NHPh)(OH) and LPtPh(NHPh)(OH) were observed in a similar region, at 4.17 ppm and 4.36 ppm respectively, in dmso-d_6 solution, downfield shifted compared to Pt-OH.

Accordingly, after deprotonation of **5.5***BAr^F_4 with *t*-BuOK, only one broad singlet was present at 3.23 ppm, integrating as one proton relative to the singlet of the *tert*-butyl group and assigned to Pt-OH. No peaks that could correspond to the NH group were present in the ^{1}H NMR spectrum of **5.9** in THF-d_8.

No aziridine product was observed upon heating complex **5.9** in THF-d_8 at 60 °C. Instead, slow decomposition of **5.9** occurred with a half-life of 22 hours at 60 °C in THF-d_8 to produce insoluble products. No evidence of isomerization of **5.9** into a corresponding "axial" isomer with a Pt-bound carbon *trans* to the sulfonate group was seen during the course of the reaction (Scheme 5.6).

Scheme 5.6

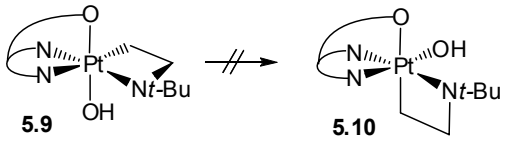

When the reaction was complete after 4 days at 60 °C, the insoluble reaction products were analyzed by ^{1}H NMR spectroscopy and ESI mass spectrometry, after dissolving in dmso-d_6 or MeOH. No products that could be identified as aziridine or Pt^{II} complex with an N-coordinated aziridine were detected among the decomposition products by ^{1}H NMR spectroscopy and ESI mass spectrometry. ^{1}H NMR spectroscopy and ESI-MS revealed the presence of the reduced species, azaplatina(II)cyclobutane **5.3**, among the other unidentified decomposition products. Although the mechanism of formation of **5.3** is currently not clear, it might presumably be due to the reduction of the Pt^{IV} center with THF solvent.[200, 201]

Reductive elimination from **5.9** was attempted in CD_2Cl_2 and C_6D_6 solutions as well. Reaction in refluxing CD_2Cl_2 was very slow and even after several days mostly unreacted starting material was present in solution. Heating solution of **5.9** in C_6D_6 at 60 °C for 25 hours lead to the formation of **5.3** in 18% yield and a mixture of unidentified product, according to ^{1}H NMR spectroscopy and ESI mass spectrometry.

One of the reasons for the lack of reactivity of **5.9** in C-N reductive elimination might be a very slow isomerization step and, therefore, unavailability of the corresponding "axial" isomer **5.10** (Scheme 5.6), necessary for the subsequent reductive elimination, so that decomposition of **5.9** via side reactions becomes the main process. Similarly, no isomerization was observed for other amido complexes, LPtMe(NHPh)(OH) and LPtPh(NHPh)(OH), in aprotic solvents, as will be described in more detail in Chapter 6.

Future direction of this work might involve optimization of the reaction conditions for preparation of the axial isomers of azaplatina(IV)cyclobutanes such as **5.10** in order to study their possible reactivity in direct C-N reductive elimination in aprotic solvents.

Attempted reductive elimination from *N*-methyl substituted **5.6** in aqueous solutions at 100 ^{o}C produced a complex mixture of products both in alkaline and neutral reaction mixtures. No aziridine or *N*-methyl ethanolamine were detected among the reaction products in alkaline aqueous solutions of **5.6**. Only trace amounts (<5%) of *N*-methyl ethanolamine were present in neutral D_2O solutions of **5.6***BF_4 after heating at 100 ^{o}C for 3 days, as detected by ^{1}H NMR spectroscopy.

Notably, in the presence of 1 equivalent of HBF_4 reductive elimination of *N*-methyl ethanolamine was observed in D_2O solution of [**5.6**]$_2(SO_4)$ with a half-life of 3.2 hours at 100 ^{o}C (eq. 5.9).

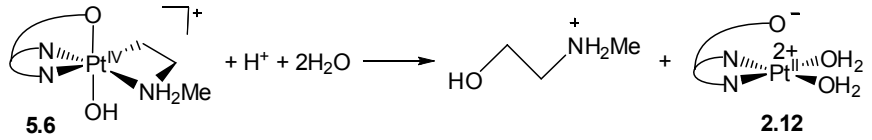

5.6 **2.12** (5.9)

The main reaction product, *N*-methyl ethanolammonium salt, $HOCH_2CH_2NH_2Me^+X^-$ (X = BF_4^-, ½SO_4^{2-}), formed in 67% yield after 33 hours at 100 ^{o}C. The product was identified by ^{1}H NMR spectroscopy and ESI mass spectrometry by comparison with an

authentic sample. The main platinum-containing product was identified by ^{1}H NMR spectroscopy as $[LPt(OH_2)_2]^+$ (**2.12**), described previously,[79] which formed in 55% yield. Insoluble crystalline precipitate, present in the reaction mixture after prolonged heating at 100 ^oC, was identified as $L_2Pt_2(\mu\text{-}OH)_2$ (**3.10**).[79] It dissolved in the presence of excess HBF_4 upon heating to produce $[LPt(OH_2)_2]^+$. Small amount of unidentified byproducts formed along with *N*-methyl ethanolammonium and $[LPt(OH_2)_2]^+$, according to ^{1}H NMR spectroscopy.

One might expect that in acidic aqueous solutions of **5.6** an acyclic complex $[LPt(CH_2CH_2NH_2Me^+)(OH)_2]^+$, **5.11**, would form (eq. 5.10-5.11, Scheme 5.7; compare with eq. 5.6) via an acid-assisted ring opening of azetidine **5.6**. For example, Mitchenko reported formation of an acyclic β-ammonioethyl complex $[Pt(CH_2CH_2NH_3^+)Cl_5]^-$ **A** via a ring-opening of azaplatina(IV)cyclobutane complex **B** (Scheme 5.2) in the presence of hydrochloric acid.[193] Subsequent isomerization of **5.11** into a corresponding "axial" isomer with *N*-methyl ammonioethyl ligand *trans* to the sulfonate, **5.12** (eq. 5.12), followed by reductive elimination, presumably via an S_N2 reaction with water,[193] would then produce *N*-methyl ethanolammonium and $[LPt(OH_2)_2]^+$ (eq. 5.13).

Scheme 5.7

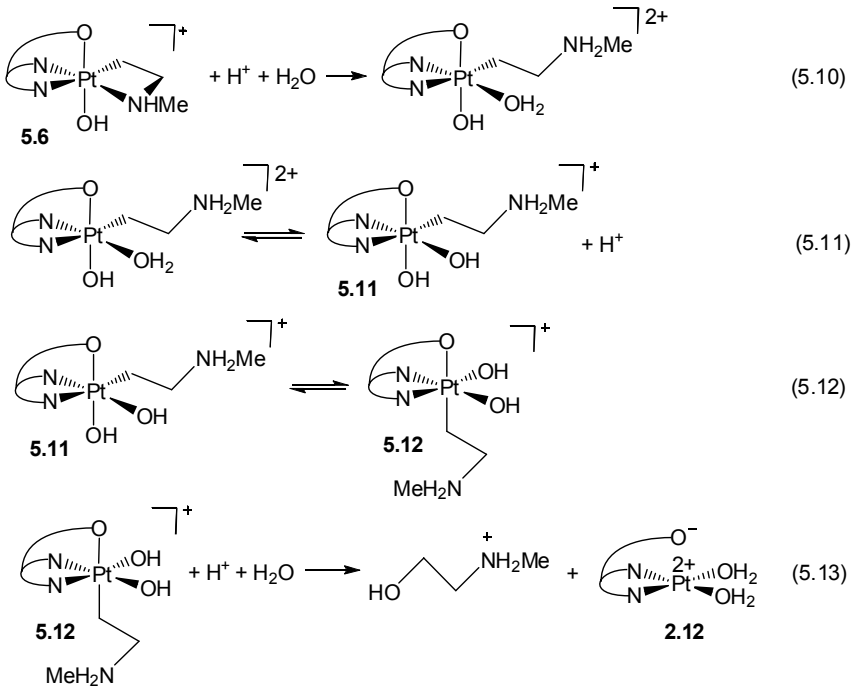

In order to detect an intermediate **5.11**, the reductive elimination from **5.6** was monitored by ^{1}H NMR spectroscopy in acidic solutions in D_2O at 100 ^oC. A new species was detected during the course of the reaction, in concentrations not exceeding 20% of the initial concentration of **5.6**. Signals of the observed intermediate grew in the initial period of reaction, reached the maximum after 6 hours at 100 ^oC and disappeared after prolonged (>30 hours) heating. The new species was characterized by the presence of multiplets at 3.86-4.06 ppm and a singlet at 2.48 ppm, integrating as 2H and 3H respectively, which could be assigned to the resonances of the N-bound β-CH_2 group, and the N-Me group respectively. The absence of platinum satellites around the signal at 2.48 ppm, assigned as N-Me, argues against the coordination of the N-Me group to the Pt center in the observed intermediate, consistent with the proposed structure of **5.11**. Two characteristically downfield shifted peaks of *ortho*-protons of pyridyls of the dpms ligand were present in the aromatic region, indicative of low C_1 symmetry of the observed

intermediate. Therefore, ^{1}H NMR characteristics of the observed species are consistent with those expected for **5.11**. Further study is necessary in order to confirm identity of the observed intermediate.

Similarly, formation of *N-tert*-butyl substituted ethanolammonium salt was observed in neutral or acidic aqueous solution of **5.5***Cl in 65% yield after 5 day at 100 ^{o}C (eq. 5.14).

$$[LPt(C_2H_4NHt\text{-}Bu)(OH)]^+ + H_2O \longrightarrow HOC_2H_4NH_2t\text{-}Bu^+ + 0.5[L_2Pt_2(\mu\text{-}OH)_2] \qquad (5.14)$$

5.3 Conclusions

The nitrogen analogues of platina(II)oxetane complexes, azaplatinacyclobutanes $LPt^{II}(CH_2CH_2NHR\text{-}\kappa C,\kappa N)$ (**5.3**, R = *t*-Bu; **5.4**, R = Me) were prepared from the corresponding zwitterionic complexes $LPt(CH_2CH_2NH_2R)Cl$ by the chloro ligand displacement in the presence of NaOH. In contrast to Pt^{II} oxetane complexes, neutral solutions of **5.3** and **5.4** in protic solvents are unreactive toward O_2. Aerobic oxidation of **5.3** and **5.4** is achieved in the presence of acids to give the cationic Pt^{IV} azetidine complexes, $[LPt(CH_2CH_2NHR\text{-}\kappa C,\kappa N)(OH)]^+$ (**5.5**, R = *t*-Bu; **5.6**, R = Me). The oxidation of **5.3** and **5.4** with O_2 occurs presumably via an acid-assisted reversible azetidine nitrogen-for-solvent substitution at the Pt^{II} center. Complex **5.5***Cl, obtained in this work, is the first X-ray structurally characterized azaplatina(IV)cyclobutane complex.

No direct C-N elimination was detected in solutions of a neutral complex $LPt(CH_2CH_2Nt\text{-}Bu\text{-}\kappa C,\kappa N)$, **5.9**, obtained by deprotonation of **5.5**, in aprotic solvents, THF-d_8, CD_2Cl_2, and C_6D_6, presumably due to the slow isomerization to the corresponding "axial" isomer, required for subsequent reductive elimination.

The reductive elimination of *N*-alkyl ethanolammonium salt, $HOCH_2CH_2NH_2R^+$ (R = Me, *t*-Bu), was observed in acidic aqueous solutions of complexes **5.5** and **5.6** at elevated temperatures.

As azaplatina(II)cyclobutanes can be obtained by a variety of methods such as CH activation of alkylamines or [2+2] cycloaddition of alkenes to metal imido complexes, the study of the aerobic oxidation and reductive elimination from azaplatinacyclobutanes could be useful in the development of novel pathways for aerobic oxidative functionalization of the azaplatina(II)cyclobutane intermediates. Further work on elucidation of the mechanism of aerobic oxidation and reductive elimination from azaplatinacyclobutane complexes is currently in progress in our laboratory.

5.4 Experimental Section

Preparation of (dpms)Pt^{II}($C_2H_4NH_2$*t*-Bu)Cl, 5.1. A 100 mL flask was charged with (dpms)Pt(C_2H_4)Cl (151 mg, 297 μmol,) and 40 mL of methanol. *Tert*-butylamine (150 μL, 1.42 mmol, 5 equ) was added dropwise to the stirred suspension at room temperature. After a few minutes all starting material dissolved. Stirring continued for 1 hour, and the resulting solution was left to crystallize overnight at -20^{0}C. White large crystals of product were filtered from cold solution, washed with several milliliters of cold methanol and dried under vacuum to give 115.7 mg of the product. An additional fraction of the product was obtained by reducing volume of the filtrate to 5 mL by vacuum evaporation. The resulting suspension was cooled down to -20^{0}C, filtered, washed with 1 mL of cold methanol and vacuum-dried to give 38.4 mg of the

pure product. Combined yield of the product 154.1 mg (265 μmol), 89%. White crystalline solid, air-stable, poorly soluble in water in methanol; soluble in DMSO. **^{1}H NMR** ^{1}H (dmso-d_6, 22^{0}C, 400 MHz), δ: 0.91-1.23 (m, 1H, $^2J_{PtH}$ could not be determined due to partial overlap with ^{t}Bu peak), 1.18 (s, 9H), 2.16-2.49 (m, 2H), 2.92-3.13 (m, $^2J_{PtH}$=50 Hz, 1H), 5.95 (s, 1H), 7.41 (ddd, J = 7.8, 5.7, 1.5 Hz, 1H), 7.50 (ddd, J = 7.8, 5.5, 1.3 Hz, 1H), 7.77 (d, J = 7.8, 1H), 7.80 (d, J = 7.8 Hz, 1H), 7.92 (br s, 2H, NH_2), 8.05 (td, J = 7.8, 1.7 Hz, 1H), 8.09 (td, J = 7.8, 1.5 Hz, 1H), 8.71 (d, J = 5.7 Hz, 1H), 9.05 (dd, J = 5.5, 1.3 Hz, 1H). **^{13}C NMR** (dmso-d_6, 22^{0}C, 500 MHz), δ: -0.77 ($^1J_{PtC}$ = 760 Hz), 25.33, 45.87, 55.34, 75.74, 124.15, 125.55, 128.22, 129.49, 137.75, 138.05, 150.46, 151.03, 152.46, 154.01. **IR** (KBr), ν: 3474 (w br), 3414 (w br), 3057 (w), 2974 (w), 2835 (w), 1604 (w), 1476 (w), 1457 (w), 1430 (w), 1376 (w), 1304 (w), 1247 (m), 1236 (m), 1211 (s), 1178 (s), 1159 (m), 1039 (s), 854 (w), 808 (w), 763 (m) cm^{-1}. **ESI-MS** of solution of **5.1** in MeOH/H_2O (50:50 v/v), m/z 581.1, calc. M*H$^+$, $C_{17}H_{25}N_3SO_3{}^{195}Pt^{35}Cl$ 581.1. **Anal**. Found C, 34.84; H, 4.28; N, 6.86. Calculated for $C_{17}H_{24}ClN_3O_3PtS$, C, 35.14; H, 4.16; N, 7.23. Complex **5.1** slowly decomposes in dmso-d_6 solutions at 20 ^{o}C with a half-life of 22 h to produce (dpms)PtCl(dmso-d_6) (identified by ^{1}H NMR), ethylene (a singlet at 5.29 ppm) and unidentified products. Complex (dpms)PtCl(dmso-d_6) was obtained independently by dissolving LPt(*cis*-cyclooctene)Cl or LPt(CH_2=CH_2)Cl in dmso-d_6. ^{1}H NMR of (dpms)PtCl(dmso-d_6) (dmso-d_6, 22^{0}C, 400 MHz), δ: 6.28 (s, 1H), 7.54 (ddd, J = 7.9, 5.9, 1.5 Hz, 1H), 7.64 (ddd, J = 7.9, 5.9, 1.5 Hz, 1H), 7.87 (d, J = 7.9 Hz, 1H), 7.94 (d, J = 7.9 Hz, 1H), 8.18 (td, J = 7.9, 1.5 Hz, 1H), 8.22 (td, J = 7.9, 1.5 Hz, 1H), 8.83 (dd, J = 5.9, 1.5 Hz, 1H), 9.06 (dd, J = 5.9, 1.5 Hz, 1H).

Preparation of (dpms)Pt^{II}($C_2H_4NH_2Me$)Cl, 5.2. 40% aqueous solution of $MeNH_2$ (85 μL, 973 μmol, 5 equ) was added to a stirred suspension of (dpms)Pt(C_2H_4)Cl (98 mg, 193 μmol) in 26 mL of MeOH at room temperature. Stirring continued for 3 hours, and the resulting suspension was stored at -20 ^oC for 4h. White fine-crystalline solid was filtered from cold solution, washed with cold methanol and dried under vacuum to give 68.9 mg of the product. The volume of the filtrate was reduced to 1 mL, the resulting suspension was cooled down to -20 ^oC, filtered and washed with cold methanol to give additional 24.7 mg of the product. Combined yield 93.6 mg (174 μmol), 90%. White crystalline solid, air-stable, poorly soluble in water and methanol, dissolves perfectly in DMSO. Solutions of **5.2** in dmso-d_6 decomposition slowly with a half-life 7 h at 20 ^oC to produce (dpms)PtCl(dmso-d_6), free ethylene (singlet at 5.29 ppm) and unidentified products.

^{1}H NMR (dmso-d_6, 22^{0}C, 400 MHz), δ: 1.02-1.41 (m, $^2J_{PtH}$ = 62 Hz, 1H), 2.10-2.41 (m, 2H), 2.33 (s, 3H), 2.59-2.84 (m, $^3J_{PtH}$ = 40 Hz, 1H), 6.00 (s, 1H), 7.41 (ddd, *J* = 7.8, 6.0, 1.5 Hz, 1H), 7.51 (ddd, *J* = 7.8, 5.6, 1.5 Hz, 1H), 7.76 (d, *J* = 7.8 Hz, 1H), 7.82 (dd, *J* = 7.8, 1.5 Hz, 1H), 8.06 (td, *J* = 7.8, 1.5 Hz, 1H), 8.12 (td, *J* = 7.8, 1.5 Hz, 1H), 8.29 (br s, 2H, NH_2), 8.87 (d, *J* = 6.0 Hz, 1H), 9.03 (dd, *J* = 5.6, 1.5 Hz, 1H).

^{13}C NMR (dmso-d_6, 22^{0}C, 500 MHz), δ: -0.7 (Pt-CH_2), 31.6 (N-CH_3), 53.6 (N-CH_2), 75.9 ($CHSO_3$), 124.1, 125.6, 128.0, 129.6, 137.9, 138.1, 150.5 (CH, py), 150.8 (C quat, py), 151.8 (CH, py), 154.0 (C quat, py) (signal assignments are from DEPT; coupling constant $^1J_{PtC}$ of a CH_2Pt signal at -0.7 ppm was not seen due to low intensity of platinum satellites). **IR** (KBr), ν: 3468 (w br), 3135 (w), 3014 (w), 2945

(w), 2907 (w), 1601 (w), 1478 (w), 1433 (w), 1407 (w), 1314 (w), 1240 (s), 1170 (s), 1034 (s), 902 (w), 860 (w), 805 (w), 758 (s) cm^{-1}. **ESI-MS** of solution of **5.2** in MeOH/H_2O (50:50 v/v): m/z 539.0; calc. M*H^+ $C_{14}H_{19}N_3SO_3{}^{195}Pt^{35}Cl$ 539.0. **Anal.** Found: C, 30.98; H, 3.63; N, 7.58. Calculated for $C_{14}H_{18}ClN_3O_3PtS$, C, 31.20; H, 3.37; N, 7.80.

Preparation of (dpms)Pt^{II}($C_2H_4NH^tBu$-*κC,κN*), 5.3. A 25 mL Schlenk flask equipped with a magnetic stirring bar was charged with 48.9 mg (84 μmol) of **5.1**, and 5 mL of 16.9 mM solution of NaOH in degassed MeOH (84 μmol, 1 equ NaOH) under an argon atmosphere. The Schlenk tube was Teflon-sealed under argon, and a stirred suspension was heated at 50^0C. The starting material dissolved after ~30 minutes, and heating continued for 12h to complete the reaction. A sample of the reaction mixture was evaporated and analyzed by ^{1}H NMR in CD_3OD. According to NMR, no starting material was present in the reaction mixture and a new product was observed, identified by ESI as azetidine complex **5.3**; two isomers of the product, *cis*- and *trans*-**5.3**, were detected in ratio 6 : 1. The product is perfectly soluble in MeOH and was not separated from NaCl. A mixture of **5.3** with 1 equivalent of NaCl was used in all oxidation experiments.

^{1}H NMR (CD_3OD, 22^0C, 400 MHz), δ: **Major isomer**: 1.00 (vtd, J = 9.2, 2.9 Hz, J_{PtH} = 78 Hz, 1H), 1.15 (s, 9H), 1.25-1.62 (m, 1H; J_{PtH} could not be determined due to low overlap with multiplets of the minor isomer), 4.36-4.56 (m, 1H; the signal is broadened at the base, but J_{PtH} could not be determined reliably due to complex multiplicity of the peak), 5.09 (ddd, J = 13.0, 9.2, 2.9 Hz, J_{PtH} = 88 Hz, 1H), 5.86 (s,

1H; slow H/D exchange of $CHSO_3$ occurs in CD_3OD), 7.30 (ddd, *J* = 7.8, 5.8, 1.6 Hz, 1H), 7.46 (ddd, *J* = 7.8, 5.8, 1.6 Hz, 1H), 7.81 (vd, *J* = 7.8 Hz, 1H), 7.84 (vd, *J* = 7.8 Hz, 1H), 8.04 (td, *J* = 7.8, 1.6 Hz, 1H), 8.05 (td, *J* = 7.8, 1.6 Hz, 1H), 8.92 (dd, *J* = 5.8, 1.6 Hz, 1H), 8.97 (d, *J* = 5.8 Hz, 1H). **Minor isomer**: 1.18 (s, 9H), 1.19-1.60 (m, 2H), 4.59-4.75 (m, 1H), 4.94-5.04 (m, 1H), 7.30-7.37 (m, 1H), 7.47-7.52 (m, 1H), 8.49-8.56 (m, 2H), 8.76 (d, *J* = 6.0 Hz, 1H), 8.86 (d, *J* = 5.6 Hz, 1H), other peaks of a minor isomer and ^{195}Pt-H coupling constants could not be determined due to overlapping with peaks of a major isomer. **ESI-MS** of solution of **5.3** in methanol, m/z 545.1; calc. for M^*H^+, $C_{17}H_{24}N_3SO_3{}^{195}Pt$ 545.1

Preparation of (dpms)Pt^{II}(C_2H_4NHMe-*κC,κN*), 5.4. A 100 mL Schlenk tube equipped with a magnetic stirring bar was charged with 91.2 mg of **5.2** (169 μmol) and 18 mL of 18.8 mM NaOH solution in degassed MeOH (338 μmol, 2 equ NaOH). If one equivalent of NaOH is used, the reaction does not reach completion. The Schlenk tube was sealed under argon and heated at 50^{0}C for 24h. The resulting suspension was cooled down to room temperature and the white precipitate was filtered, washed with methanol until a neutral pH of the filtrate and dried under vacuum to give 56.0 mg of poorly soluble **5.4**. Volume of the filtrate was reduced to 2 mL by vacuum evaporation and white crystalline product was filtered, washed with cold methanol and dried under vacuum to give 8.8 mg of the product. Yield 64.8 mg (129 μmol), 76%. White crystalline solid, poorly soluble in MeOH. The product was not obtained in an analytically pure form and was slightly contaminated with NaCl (~5% by weight, based on the results of elemental analysis).

^{1}H NMR (dmso-d_6, 22^{0}C, 400 MHz), δ: 0.98-1.12 (m, $^2J_{PtH}$ = 60 Hz, 1H), 1.18-1.34 (m, $^2J_{PtH}$ = 55 Hz, 1H), 2.30 (d, J = 5.5 Hz, $^3J_{PtH}$ ~ 20 Hz, 3H), 4.03-4.24 (m, $^3J_{PtH}$ ~ 50 Hz, 1H), 4.97-5.33 (m, 2H), 5.81 (s, 1H), 7.30 (ddd, J = 7.7, 5.6, 1.5 Hz, 1H), 7.53 (ddd, J = 7.7, 5.6, 1.5 Hz, 1H), 7.75 (d, J = 7.7 Hz, 1H), 7.78 (d, J = 7.7 Hz, 1H), 8.05 (td, J = 7.7, 1.5 Hz, 1H), 8.09 (td, J = 7.7, 1.5 Hz, 1H), 8.63 (dd, J = 5.6, 1.5 Hz, 1H), 8.72 (dd, J = 5.6, 1.5 Hz, 1H). **IR** (KBr), ν: 3480 (w), 3159 (w), 2935 (w), 2884 (w), 2817 (w), 1603 (w), 1475 (w), 1455 (w), 1433 (w), 1254 (m), 1202 (m), 1154 (m), 1031 (s), 810 (w), 762 (w) cm^{-1}. **ESI-MS** of solution of **5.4** in MeOH/H_2O (50:50 v/v): m/z 503.1; calc. $C_{14}H_{18}N_3SO_3{}^{195}Pt$, 503.0. **Anal**. Found: C, 32.10; H, 3.20; N, 7.89. Calculated for $C_{14}H_{17}N_3O_3PtS$, C, 33.47; H, 3.41; N, 8.36.

Preparation of [(dpms)Pt^{IV}(C_2H_4NH*t*-Bu-*κC,κN*)(OH)]$^+$Cl$^-$, 5.5*Cl. The solution of complex **5.3** and 1 equivalent of NaCl in MeOH was prepared by heating complex **5.1** (126 mg, 217 μmol) and 1 equivalent of NaOH in 13 mL of MeOH at 50 ^{o}C for 14h under argon as described above and was used without isolation of **5.3**. A 30% aqueous solution of H_2O_2 (282 mg, 2.49 mmol, 11 equ) was added to the stirred solution of **5.3.** The reaction mixture immediately turned bright yellow; stirring continued for 30 minutes. According to the ^{1}H NMR spectrum of the reaction mixture sample, quantitative oxidation occurred to give **5.5*Cl** as the only product; no starting material was remaining. The volume of the resulting solution was reduced by vacuum evaporation to 1 mL and was left to crystallize at -20^{0}C overnight. Large colorless crystals were filtered, washed with cold methanol and dried under vacuum to give 53.3 mg of product. The filtrate was evaporated to a volume of 0.2-0.3 mL and stored

at -20 ^{o}C overnight, crystalline product filtered and washed with small amount of cold methanol to give an additional fraction of white crystals, 34.0 mg. Combined yield 87.3 mg (139 μmol), 64%. Colorless crystalline solid, perfectly soluble in methanol, water and DMSO, slightly soluble in THF. The crystals of the product contained one molecule of MeOH per one Pt center (**5.5***Cl*MeOH), according to X-ray, which could not be removed even after drying under high vacuum (50 mTorr) for several days.

^{1}H NMR (dmso-d_6, 22^{0}C, 400 MHz), δ: 1.15 (s, 9H), 2.89 (m, $^{2}J_{PtH}$ = 75 Hz, 1H), 2.94 (m, $^{2}J_{PtH}$ = 70 Hz, 1H), 3.16 (d, J = 5.3 Hz, 3H, MeOH), 4.10 (q, J = 5.3 Hz, 1H, MeOH), 4.25 (br s, 1H, OH), 4.41 (m, $^{3}J_{PtH}$ = 35 Hz, 1H), 4.58 (m, $^{3}J_{PtH}$ = 40 Hz, 1H), 7.01 (s, 1H), 7.60 (br s, $^{2}J_{PtH}$ = 58 Hz, 1H, NH), 7.85 (ddd, J = 7.9, 5.9, 1.3 Hz, 1H), 7.91 (ddd, J = 7.9, 5.5, 1.0 Hz, 1H), 8.09 (d, J = 7.9 Hz, 1H), 8.10 (d, J = 7.9 Hz, 1H), 8.33 (td, J = 7.9, 1.4 Hz, 1H), 8.39 (td, J = 7.9, 1.2 Hz, 1H), 8.83 (d, J = 5.9 Hz, 1H), 9.48 (d, J = 5.5 Hz, 1H). **^{13}C NMR** (dmso-d_6, 22^{0}C, 500 MHz), δ: -4.1 ($^{1}J_{PtC}$ = 376 Hz, Pt-CH_2), 25.2 (C-CH_3), 48.5 (CH_3, MeOH), 54.3 ($^{2}J_{PtC}$ = 114 Hz, N-CH_2), 60.2 (C quat, *t*-Bu), 69.3 ($CHSO_3$), 126.1, 127.3, 127.4, 128.5, 142.6, 143.8 (CH, py), 149.9 (C quat, py), 150.2, 150.3 (CH, py), 150.4 (C quat, py). **IR** (KBr), ν: 3550 (w br), 3267 (w br), 3018 (w), 2971 (w), 2923 (w), 2813 (w), 1607 (w), 1477 (w), 1441 (w), 1308 (m), 1299 (m), 1204 (w), 1144 (s), 1068 (w), 1029 (w), 959 (m), 768 (m), 697 (m) cm^{-1}. **ESI-MS** of solution of **5.5*Cl** in MeOH: m/z 561.1; calc. for cationic [**5.5**]$^{+}$ $C_{17}H_{24}N_3SO_4{}^{195}Pt$ 561.1. XRD-quality crystals were obtained by slow crystallization from concentrated methanolic solution at -20 ^{o}C. **Anal**. Found: C, 34.45; H, 4.73; N, 6.36. Calculated for $C_{18}H_{28}ClN_3O_5PtS$, C, 34.37; H, 4.49; N, 6.68.

Preparation of methanolic solution of [(dpms)Pt^{IV}(C_2H_4NMe-*κC,κN*)(OH)]$^+$X (X = OH^-, Cl^-), 5.6*X, without isolation. A suspension of **5.4** (20.0 mg, 4.0 μmol) in 0.8 mL of CD_3OD (or MeOH) was placed into a 10 mL vial equipped with a magnetic stirring bar. A 30% aqueous H_2O_2 solution (4.5 μL, 4.4 μmol, 1.1 equ) was added to a stirred suspension. After a few minutes starting material completely dissolved and the solution turned yellow. Stirring continued for 1h at rt. According to ^{1}H NMR, quantitative oxidation occurred to give a strongly alkaline solution of **5.6** as a mixture of two isomers, presumably *cis*- and *trans*-**5.6**. The product was characterized by ^{1}H, ^{13}C, COSY and HSQC NMR spectroscopy.

The ratio of two isomers, characterized by signals of the NMe groups at 2.87 ppm (**5.6a**) and 2.11 ppm (**5.6b**), was 1 : 2.6 respectively after 1 hours after preparation, then slowly changed to give a 2.0 : 1 ratio of **5a** : **5b** after 10 hours at rt, which remained unchanged after 1 day. The alkaline solution of **5.6** in MeOH was used immediately after its preparation. Attempted isolation of solid **5.6** by evaporation of alkaline solutions led to its decomposition; slow decomposition of **5.6** was also observed in alkaline MeOH solutions at rt. The product was perfectly soluble in MeOH and water and could not be recrystallized in the presence of various counterions, BF_4^-, ClO_4^-, Cl^-, SO_4^{2-}.

The NOE experiment exhibited weak positive NOE's between NMe group and *ortho*-protons of pyridyl of the dpms ligand in both isomers, **5.6a** and **5.6b**, so that *cis*- or *trans*-configuraitons of **5.6a** and **5.6b** could not be assigned. Consistent with this

result, in DFT-optimized geometries of *cis*- and *trans*-**5.6**, relatively short distances between protons of NMe and *ortho*-protons of pyridyl were found in both isomers. **^{1}H NMR** (CD_3OD, 22^0C, 400 MHz), δ: **5.6a**: 2.87 (s, $^3J_{PtH}$ = 27 Hz, 3H), 2.83-2.93 (m, 1H; $^2J_{PtH}$ could not be determined due to overlap with **5.6b** signals), 3.07-3.27 (m, $^2J_{PtH}$ = 64 Hz, 1H), 4.62-4.73 (m, $^2J_{PtH}$ ~ 64, 1H), 4.86-4.98 (m, 1H), 6.61 (s; $CHSO_3$ integral intensity is diminished due to H/D exchange), 7.75 (ddd, *J* = 7.7, 5.6, 1.4 Hz, 1H), 7.88 (ddd, *J* = 7.7, 5.4, 1.4 Hz, 1H), 8.07 (d, *J* = 7.7 Hz, 1H), 8.11 (d, *J* = 7.7 Hz, 1H), 8.26-8.32 (m, 2H), 8.76 (dd, *J* = 5.6, 1.4 Hz, $^3J_{PtH}$ = 26 Hz, 1H), 9.02 (d, *J* = 5.4 Hz, $^3J_{PtH}$ = 13 Hz, 1H). **5.6b**: 2.11 (s, $^3J_{PtH}$ = 33 Hz, 3H), 2.64-2.89 (m, 1H; $^2J_{PtH}$ could not be determined due to overlap with **5.6a** signals), 2.97-3.31 (m, 1H; $^2J_{PtH}$ could not be determined due to overlap with **5.6a** signals), 4.02-4.28 (br m, 1H), 4.57-4.77 (br m, 1H), 6.70 (s; $CHSO_3$ integral intensity is diminished due to H/D exchange), 7.79 (ddd, *J* = 7.7, 5.6, 1.5 Hz, 1H), 7.91 (ddd, *J* = 7.7, 5.6, 1.1 Hz, 1H), 8.05-8.11 (m, 2H), 8.25-8.34 (m, 2H), 8.69 (d, *J* = 5.6 Hz, $^3J_{PtH}$ = 27 Hz, 1H), 8.92 (d, *J* = 5.6 Hz, $^3J_{PtH}$ = 14 Hz, 1H). **^{13}C NMR** (CD_3OD, 22^0C, 500 MHz), δ: **5.6a**: -2.0 ($^1J_{PtC}$ = 414 Hz, Pt-CH_2), 56.0 ($^2J_{PtC}$ = 22 Hz, NMe), 72.3 (m, $CDSO_3$), 80.3 ($^2J_{PtC}$ = 115 Hz, N-CH_2), 128.0, 128.4, 129.2, 130.3, 143.6, 144.4, 149.8, 151.2, 152.6, 152.9 (py). **5.6b**: -5.0 (Pt-CH_2), 39.7 (NMe), 63.8 (N-CH_2), 72.3 (m, $CDSO_3$), 128.6, 128.8, 129.4, 130.1, 144.1, 145.1, 149.7, 151.1, 151.9, 152.5 (py). (J_{PtC} could not be determined due to low intensity of platinum satellites). **ESI-MS** of solution of **5.6** in MeOH: m/z 519.1; calc. M^*H^+, $C_{14}H_{18}N_3SO_4{}^{195}Pt$ 519.1.

Preparation of [(dpms)Pt^{IV}(C_2H_4NMe-$\kappa C,\kappa N$)(OH)]$_2$(SO_4). A 50 mL round-bottom flask equipped with a magnetic stirring bar was charged with a sample of **5.4** (53.3 mg, 105 μmol) and 10 mL of H_2O. Aqueous 30% H_2O_2 solution (12 μL, 116 μmol) was added to a stirred suspension. After stirring for 1 hour at rt the resulting alkanline solution was neutralized with 1 equivalent of a standardized 1.00 N H_2SO_4 solution (105 μL). The resulting neutral (pH 7) aqueous solution of [(dpms)Pt^{IV}(C_2H_4NMe-$\kappa C,\kappa N$)(OH)]$_2$(SO_4) was evaporated to dryness under vacuum to produce white crystalline [(dpms)Pt^{IV}(C_2H_4NMe-$\kappa C,\kappa N$)(OH)]$_2$(SO_4) quantitatively, 90-95% pure by ^{1}H NMR. Solid [(dpms)Pt^{IV}(C_2H_4NMe-$\kappa C,\kappa N$)(OH)]$_2$(SO_4) was used for reductive elimination experiments immediately after its preparation. Slow decomposition of solid samples of [(dpms)Pt^{IV}(C_2H_4NMe-$\kappa C,\kappa N$)(OH)]$_2$(SO_4) occurs at room temperature.

According to ^{1}H NMR, two isomers were present in solution in D_2O, presumably *cis*- and *trans*-[**5.6**]$_2$(SO_4), in 6:1 ratio.

^{1}H NMR (D_2O, 22^{0}C, 400 MHz), δ: **major isomer**: 2.30 (s, $^3J_{PtH}$ = 33 Hz, 3H), 2.91 (m, $^2J_{PtH}$ = 62 Hz, 1H), 3.27 (m, $^2J_{PtH}$ = 80 Hz, 1H), 4.03 (m, 1H), 5.09 (m, 1H), 6.78 (s, 1H), 7.80 (ddd, J = 7.8, 5.7, 1.4 Hz, 1H), 7.92 (ddd, J = 7.8, 5.4, 1.1 Hz, 1H), 8.09 (d, J = 7.8 Hz, 1H), 8.13 (d, J = 7.8 Hz, 1H), 8.30-8.37 (m, 2H), 8.62 (d, J = 5.7 Hz, $^3J_{PtH}$ = 26 Hz, 1H), 8.85 (d, J = 5.4 Hz, $^3J_{PtH}$ = 13 Hz, 1H); **minor isomer**: 2.46 (s, $^3J_{PtH}$ = 33 Hz, 3H), 2.94-3.44 (m, 2H), 4.42-4.51 (m, 1H), 6.76 (s, 1H), 7.85-7.99 (m, 2H), 8.15-8.24 (m, 2H), 8.28-8.37 (m, 2H), 8.64 (d, J = 5.4 Hz, 1H), 8.90 (d, J = 5.4 Hz, 1H).

Preparation of [(dpms)Pt^{IV}(C_2H_4NH*t*-Bu-*κC,κN*)(OH)]BAr^F_4, 5.5*BAr^F_4. All operations were performed under an argon atmosphere in dry degassed solvents. A 50 mL flask equipped with a magnetic stirring bar was charged with **5.5***Cl*MeOH (39.0 mg, 62 μmol), $NaBAr^F_4$ (54.5 mg, 61 μmol) and 10 mL of CH_2Cl_2. The reaction mixture was stirred under for 1h at room temperature. Initially insoluble starting material **5.5***Cl*MeOH dissolved after 1 hour and NaCl precipitated from solution. The reaction mixture was filtered from NaCl through Celite, washed with small amount of CH_2Cl_2 and dried under vacuum for 1 day. The product was isolated as white solid, perfectly soluble in CH_2Cl_2 and THF. Yield 63.4 mg (44.5 μmol), 72%.

^{1}H NMR (THF-d_8, 22^{0}C, 400 MHz), δ: 1.26 (s, 9H), 2.87 (m, $^2J_{PtH}$ = 68 Hz, 1H), 3.15 (m, $^2J_{PtH}$ = 81 Hz, 1H), 3.44 (s, $^2J_{PtH}$ = 27 Hz, 1H, OH), 4.56-4.78 (m, 2H), 5.92 (br s, $^2J_{PtH}$ = 74 Hz, 1H, NH), 6.49 (s, 1H), 7.57 (s, 4H), 7.72-7.85 (m, 10H), 7.98-8.06 (m, 2H), 8.27 (td, *J* = 7.8, 1.4 Hz, 1H), 8.31 (td, *J* = 7.7, 1.4 Hz, 1H), 8.79 (dd, *J* = 6.0, 1.4 Hz, $^3J_{PtH}$ = 34 Hz, 1H), 9.16 (d, *J* = 5.4 Hz, 1H).

Preparation of (dpms)Pt^{IV}(C_2H_4NH*t*-Bu-*κC,κN*)(OH), 5.9. A 25 mL round-bottom flask equipped with a magnetic stirring bar was charged with **5.5***BAr^F_4 (63.4 mg, 44 μmol), 5.2 mg of *t*-BuOK (44 μmol, 1 equ) and 5-6 mL of dry degassed THF. The resulting solution turned yellow immediately after addition of *t*-BuOK; stirring continued for 1h. After 1h solvents were evaporated, and the yellow solid was dried under vacuum for 1 day. The product was obtained as yellow crystalline solid, 62.1 mg. The product was used as a mixture with 1 equivalent of $KBAr^F_4$ without

separation. Complex **5.9** decomposes slowly in THF-d_8 solution at room temperature with a half-life of ~17h.

^{1}H NMR (THF-d_8, 22^{0}C, 400 MHz), δ: 1.12 (s, 9H), 2.54 (m, $^2J_{PtH}$ = 67 Hz, 1H), 2.92 (m, $^2J_{PtH}$ =84 Hz, 1H), 3.23 (br s, 1H, OH), 4.17 (m, $^3J_{PtH}$ = 43 Hz, 1H), 4.35 (m, $^3J_{PtH}$ = 40 Hz, 1H), 6.32 (s, 1H), 7.62-7.71 (m, 2H), 7.91 (d, J = 7.7 Hz, 1H), 7.93 (d, J = 7.7 Hz, 1H), 8.13 (td, J = 7.7, 1.3 Hz, 1H), 8.15 (vt, J = 7.7 Hz, 1H), 8.78 (d, J = 5.6 Hz, $^3J_{PtH}$ = 23 Hz, 1H), 9.02 (d, J = 4.7 Hz, 1H). $KBAr^F_4$: 7.57 (s, 4H), 7.79 (br s, 8H).

Chapter 6: Oxidation of (dpms)Pt^{II} Aryl Complexes with O_2 and Attempted Reductive Elimination

6.1 Introduction

The previous chapters discussed aerobic conversion of (dpms)Pt alkyl- and olefin complexes, which can be considered as model systems relevant to the aerobic functionalization of alkanes and olefins, into alcohols and epoxides. We next sought to expand the scope of these aerobic transformations to aryl platinum complexes, which could provide new pathways toward aerobic Pt-mediated oxidation of arenes.

The following sequence of transformations can be envisioned leading to an overall Pt-promoted oxidation of an aromatic CH bond into an aryl-heteroatom bond (Scheme 6.1): i) aromatic CH activation of a substrate; ii) aerobic oxidation of the resulting Pt^{II}-aryl species; iii) C-heteroatom reductive elimination from the Pt^{IV}-aryl complex.

Scheme 6.1. Envivioned catalytic cycle for oxidative functionalization of arenes utilizing dioxygen as an oxidant.

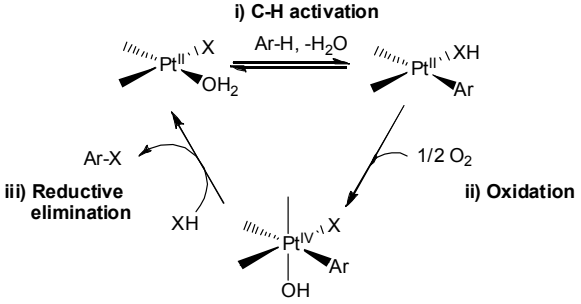

Step (i) of the envisioned catalytic cycle, aromatic CH activation by Pt^{II} complexes, is a very well documented reaction, and a number of Pt^{II} complexes capable of effective arene activation are known.[29, 165, 202] At the same time,

significantly less attention has been paid to the study of subsequent functionalization of the Pt^{II}-aryl complexes resulting from these aromatic CH activation reactions, in particular, steps (ii) and (iii) in Scheme 6.1, which will be the focus of this chapter.

We decided to examine if the dpms ligand, which proved effective in aerobic functionalization of Pt-alkyl and oxetane complexes, could also affect the reactivity of Pt^{II} aryl complexes toward dioxygen. As aromatic C-H activation by Pt^{II} complexes typically leads to the formation of mono-aryl Pt^{II} complexes as products, we chose (dpms) Pt mono-phenyl complexes as the model species in this study, and their preparation and aerobic oxidation will be discussed in this chapter. We also examined the possibility of direct aryl-O and aryl-N reductive elimination from the derived Pt^{IV}-phenyl products.

6.2 Results and Discussion

6.2.1 Preparation of (dpms)Pt^{II} Phenyl Complexes

Preparation of phenyl complex (dpms)Pt^{II}Ph(MeOH), **6.1**, was achieved through reductive elimination of benzene from diphenyl Pt^{IV} hydride (dpms)$Pt^{IV}Ph_2H$ in methanol at 50 ^oC (eq. 6.1). Complex (dpms)$Pt^{IV}Ph_2H$ was easily prepared by protonation of an anionic diphenyl precursor K[(dpms)$Pt^{II}Ph_2$] (**6.2**), reported in the literature.[29] The reductive elimination of benzene from poorly soluble complex (dpms)$Pt^{IV}Ph_2H$ occurs cleanly at 50 ^oC during the course of several hours to give colorless solution of (dpms)Pt^{II}Ph(MeOH), which was isolated by evaporation of a solvent and purified by washing with cold methanol to give the desired product in an analytically pure form in 75% yield. Complex (dpms)Pt^{II}Ph(MeOH) is a convenient

precursor for preparation of other (dpms)Pt^{II}Ph(L) complexes (L = H_2O, **6.3**; L=$PhNH_2$, **6.4**; L=Me_2SO, **6.5**) via ligand exchange (eq. 6.2). For example, complexes **6.3** and **6.5** were prepared by dissolution of precursor **6.1** in H_2O or DMSO solvents. Complex **6.4** was prepared by reacting complex **6.1** with 17 equivalents of $PhNH_2$ in methanol solution.

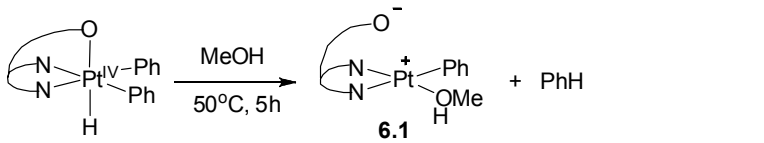

(6.1)

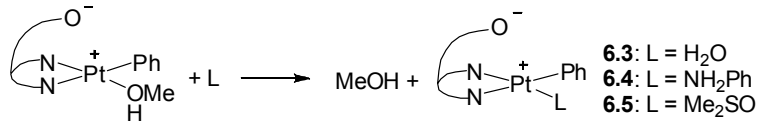

(6.2)

All complexes described in this work, **6.1, 6.3-6.5**, were isolated in an analytically pure form and characterized by ^{1}H NMR spectroscopy, ESI mass spectrometry and elemental analysis. Complex **6.4** was characterized by single crystal X-ray diffraction.

Aromatic region of ^{1}H NMR spectra of complexes **6.1** (L = MeOH), **6.3** (L = H_2O) and **6.4** (L = $PhNH_2$) was consistent with rapid rotation of Pt-Ph bond: *ortho*-protons of Pt-Ph group appeared as a doublet at 7.2-7.4 ppm integrating as two protons with characteristic platinum satellites ($^3J_{PtH}$ 32-40 Hz). In contrast, in ^{1}H NMR spectrum of complex **6.5** with a bulkier DMSO ligand two individual doublet of *ortho*-protons of the Pt-Ph group were present at 7.39 and 7.70 ppm, each integrating as one proton and characterized by coupling constants $^3J_{PtH}$=35-40 Hz, indicative of restricted rotation around Pt-Ph bond. In CD_3OD solution of **6.5** two singlets of the methyl groups of coordinated DMSO were present at 3.07 and 3.19 ppm characterized by $^3J_{PtH}$ coupling constants of 36 and 30 Hz respectively.

The IR spectrum of complex **6.5** exhibits ν(S=O) of coordinated DMSO at 1131 cm^{-1}, typical for S-bonded DMSO ligand.[147]

Single crystals of complex **6.4** suitable for an X-ray diffraction study were obtained by crystallization of **6.4** from methanolic solution at -20 ^{o}C. The X-ray analysis shows that the Pt^{II} center has an idealized square planar geometry (Figure 6.1). The Pt-N21 bond length is 2.066 Å. The Pt-N15 bond distance between Pt and the nitrogen atom of pyridyls trans to phenyl is 2.102 Å, which is longer than Pt1-N10 bond length (2.024 Å) between Pt and pyridyls *trans* to aniline, consistent with a stronger *trans*-influence of the phenyl compared to the aniline ligand.[33] The distance between oxygen of the sulfonate group, closest to Pt, and the platinum center is 3.186 Å, which is only slightly shorter that the sum of van der Walls radii of Pt and O (3.27 Å).

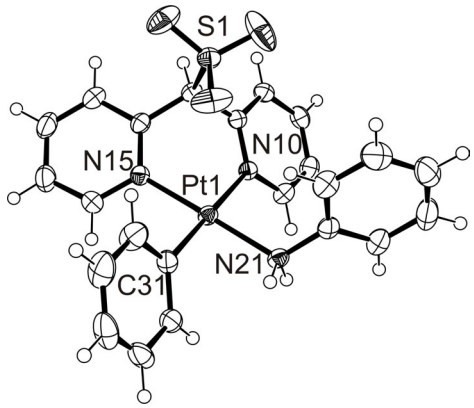

Figure 6.1. ORTEP plots (50% probability ellipsoids) for complex **6.4**. Selected bond distances, Å: Pt1-C31, 2.008(3); Pt1-N21, 2.066(3); Pt1-N10, 2.102(3); Pt1-N15, 2.024(3).

6.2.2 Oxidation of (dpms)Pt^{II}Ph complexes with O_2 or H_2O_2

An aqueous solution of an anionic diphenyl complex K[(dpms)$Pt^{II}Ph_2$] **(6.2)**, obtained according to the literature procedure,[29] undergoes fast oxidation in the

presence dioxygen or air (eq. 6.3). The reaction under 1 atm of dioxygen is complete after 2 hours at room temperature to yield poorly soluble complex *sym*-(dpms)$Pt^{IV}Ph_2(OH)$, **6.6**, which was isolated in an analytically pure form by filtration from strongly alkaline solution containing KOH and thorough washing with water. Complex **6.6** was isolated in 87% yield and characterized by ^1H, ^{13}C and HSQC NMR spectroscopy, ESI mass spectrometry and elemental analysis.

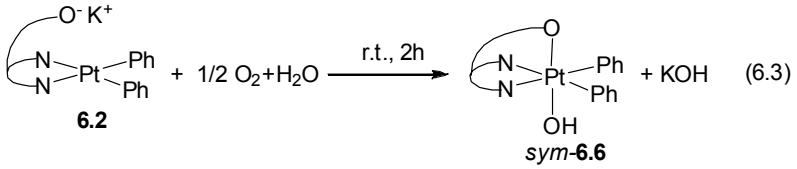

(6.3)

^1H NMR and ^{13}C NMR spectra of complex *sym*-(dpms)$Pt^{IV}Ph_2(OH)$, *sym*-**6.6**, are indicative of a mirror-symmetrical structure of the product. ^1H NMR spectrum in DMSO shows four sets of multiplets in the range of 7.65-8.30 ppm each integrating as two protons, corresponding to protons of two equivalent pyridyls of dpms ligand. A doublet of *ortho*-protons of two equivalent Pt-phenyl groups integrating as 4H, accompanied by platinum satellites ($^3J_{PtH}$ = 30 Hz), was observed at 7.34 ppm, indicative of the rapid rotation of the Pt-Ph bond on the NMR time scale. A broad singlet at 2.56 ppm with platinum satellites ($^2J_{PtH}$ = 36 Hz) integrating as one proton was assigned to Pt-OH group; accordingly, no cross peaks related to the Pt-OH signal were observed in HSQC spectrum.

The C_s symmetry of complex **6.6** implies that the geometry of the square planar Pt^{II} center is retained in the Pt^{IV} product after oxidation and that the Pt^{IV}-OH group is present in the axial position *trans* to the sulfonate ligand. The stereochemical outcome of the oxidation is therefore similar to that in K(dpms)$PtMe_2$ and (dpms)PtMe(HX) (X = OH, OMe, NHPh) complexes described in Chapter 2. Based

on these observations, we propose that the mechanism for the oxidation of diphenyl complex **6.6** is similar to that for methyl complexes previously discussed in Chapter 2.

Notably, dpms-supported diphenyl complex **6.2** is significantly more reactive toward oxidation with O_2 than Pt^{II} diphenyl complexes supported by bidentate nitrogen-donor ligands, such as *N,N,N′,N′*-tetramethylethylene diamine (tmeda) and α-diimine ligands. For example, Bercaw showed that diphenyl complexes $(NN)PtPh_2$ (NN = tmeda, CyN=HC-CH=NCy) do not react with O_2 in methanolic solutions.[43] Remarkably high reactivity of $[(dpms)Pt^{II}Ph_2]^-$ complex toward dioxygen can be explained by the presence of the pendant sulfonate group in close proximity to a Pt^{II} center, that can raise the energy of the HOMO of a Pt^{II} complex thus facilitating oxidation[30] and can stabilize the emerging octahedral Pt^{IV} center via the sulfonate oxygen coordination.

Importantly, mono-phenyl complexes $(dpms)PtPh(OH_2)$ and (dpms)PtPh(MeOH) are also reactive toward dioxygen; the products of oxidation were characterized by NMR spectroscopy, ESI mass spectrometry and elemental analysis.

Mono-phenyl aqua complex **6.3** slowly reacts with dioxygen in aqueous solutions at room temperature and atmospheric pressure to give colorless solution of *unsym*-$(dpms)Pt^{IV}Ph(OH)_2$, *unsym*-**6.7** (eq. 6.4).

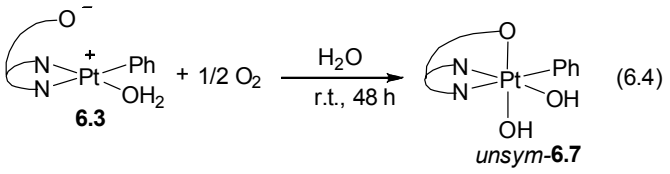

6.3 *unsym*-**6.7** (6.4)

The oxidation occurs cleanly with a half-life of 8.8 hours at 20 °C, and the product was isolated in analytically pure form in 93% yield. ^1H and ^{13}C NMR spectra of

complex *unsym*-**6.7** are evident of the low C_1 symmetry. Two non-equivalent Pt-OH groups appear in ^{1}H NMR spectrum in DMSO-d_6 as two broad singlets at 1.45 and 2.99 ppm; HSQC spectrum confirms the absence of carbon cross-peaks for these two signals.

Observed lower reactivity of (dpms)PtPh(OH_2) complex (half-life 8.8 hours) compared to K(dpms)$PtPh_2$ (half-life < 15 min) can be attributed to the neutral character of the former complex and lower concentration of its anionic form (dpms)PtPh$(OH)^-$ reactive toward O_2, compared to the anionic K[(dpms)$PtPh_2$], as the energy of HOMO is expected to be higher in anionic species.

Notably, analogous methyl complex (dpms)PtMe(OH_2) reacts much faster under the identical reaction conditions with an estimated half-life of 15 minutes, which can be explained by more electron-rich character of the methyl group.

Higher reactivity of Pt^{II} methyl complexes toward oxidation compared to analogous Pt^{II} phenyl complexes has been noted previously.[43, 203] For example, Puddephatt has found that the reactivity of diphenyl Pt complexes supported by bidentate diketimine ligands toward oxidation with methyl iodide is 50-1000 times lower than that of analogous dimethyl complexes.[203] This fact can be related to electron-poorer character of the phenyl ligand compared to Pt-methyl. Steric factor might also be important.[43]

Similar to **6.3**, (dpms)Pt^{II}Ph(MeOH) (**6.1**) is oxidized in methanol solutions under atmospheric pressure of O_2 to give (dpms)Pt^{IV}Ph(OMe)(OH) (**6.8**) (eq. 6.5) that was isolated in 91% yield in analytically pure form and characterized by NMR spectroscopy, ESI mass spectrometry and elemental analysis. ^{1}H and ^{13}C NMR

spectra are evident of low C_1 symmetry of the complex. Pt-OMe group gives rise to a singlet at 2.94 ppm integrating as 3H in ^{1}H NMR spectrum in dmso-d_6 with platinum satellites ($^3J_{PtH}$ = 33 Hz), and Pt-OH group appears as a broad singlet at 2.52 ppm integrating as 1H.

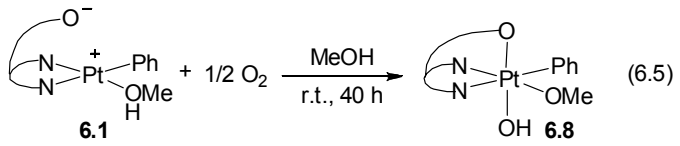

6.1 **6.8** (6.5)

Half-life of complex (dpms)PtPh(MeOH) in the presence of O_2 (1 atm) in MeOH solution was estimated to be 5.5 hours at 20 ^oC. Therefore, methanolic solutions of **6.1** are slightly more reactive than aqueous solution of (dpms)PtPh(OH_2) under the same conditions.

We propose that the mechanism of the oxidation of (dpms)Pt^{II}Ph(HX) (X = OH, OMe) complexes is the same as in (dpms)Pt^{II}Me(OH_2) complexes discussed in Chapter 2. Consistent with this mechanism, the oxidation rate is not affected in the presence of 2 equivalents of a radical inhibitor, 2,6-di-*tert*-butyl-*p*-cresol, in methanolic solution (half-life 5.5 hours).

By analogy with methyl complexes, we expected that oxidation of mono-phenyl complexes (dpms)PtPh(XH) (X = OH, OMe) involves initial deprotonation of an aqua or a methanol ligand to produce an anionic species [(dpms)PtPh(X)]$^-$, which is expected to be more reactive in subsequent electron transfer to O_2 (Scheme 6.2). Hence, aniline complex (dpms)PtPh(NH_2Ph) is expected to be less reactive toward oxidation compared to (dpms)PtPh(ROH) (R = H, Me) due to much lower acidity of aniline compared to water or MeOH. Similarly, the DMSO complex (dpms)PtPh(DMSO) may be even less reactive toward O_2.

Scheme 6.2

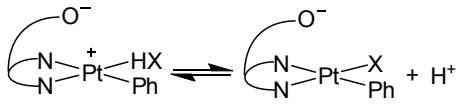

Indeed, solutions of (dpms)PtPh(NH_2Ph) (**6.4**) and (dpms)PtPh(DMSO) (**6.5**) in methanol are inert toward O_2. No changes were observed in ESI and ^{1}H NMR spectra of **6.4** solutions after 7 days of stirring under 1 atmosphere of O_2 at 20 ^oC in water or methanol.

Oxidation of (dpms)PtPh(NH_2Ph) was achieved by using a stronger oxidant, H_2O_2 (eq. 6.6). Upon addition of 2.5 equivalents of 30% aqueous H_2O_2 to methanolic solution of (dpms)PtPh(NH_2Ph) fast oxidation occurs to give a single product, (dpms)PtPh(NHPh)(OH) (**6.9**), that was isolated by precipitation with ether and isolated in an analytically pure form in 90% yield.

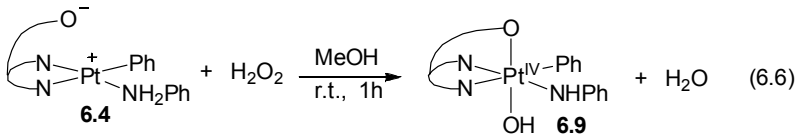

(6.6)

^{1}H NMR solution of (dpms)PtPh(NHPh)(OH) (**6.9**) in DMSO-d_6 exhibits two broad singlets at 3.01 ppm and 4.36 ppm integrating as one proton each and assigned as OH and NH respectively.

We have previously established that upon oxidation of (dpms)Pt^{II}Me(HX) (HX = MeOH, NH_2Ph) complexes with O_2 or H_2O_2 complex (dpms)Pt^{IV}Me(X)(OH) forms, in which Me and X ligands remain in the equatorial plane formed by Pt and two nitrogens of pyridyls, and the OH group is present *trans* to the sulfonate oxygen. By analogy, we expect similar retention of configuration of the equatorial ligands Ph and X in the complexes (dpms)PtPh(X)(OH) (X = OMe, NHPh).

Notably, methyl complex with aniline, (dpms)PtMe(NH_2Ph), was more reactive toward O_2, compared to **6.4**. Slow oxidation was observed in methanolic solution of (dpms)PtMe(NH_2Ph) with a half-life of 30 hours at 20 ^oC. We believe that the more electron-poor nature of the phenyl ligand is likely to be responsible for the lower reactivity of (dpms)PtPh(NH_2Ph) toward electron transfer between Pt center and O_2.

As anticipated, complex (dpms)PtPh(DMSO) (**6.5**) was completely unreactive toward oxygen consistent with its inability to produce reactive anionic intermediates.

6.2.3 Attempted Reductive Elimination from (dpms)Pt^{IV}Ph complexes

Having synthesized a series of Pt^{IV} phenyl complexes, we next set out to investigate their reactivity in C-O and C-N reductive elimination. As we have previously shown, C(sp^3)-O elimination via S_N2 or direct mechanism from (dpms)Pt^{IV} complexes requires the presence of a good leaving group *trans* to the hydrocarbyl ligand being eliminated and is preceded by isomerization into an "axial" isomer with a Pt-bound alkyl ligand in the axial position, *trans* to the sulfonate. Therefore, one could expect that the similar isomerization step might be necessary prior to reductive elimination from phenyl Pt^{IV} complexes.

Heating complex *sym*-**6.6** in DMSO-d_6 at 100 ^oC for 6 days resulted in a complete isomerization into a corresponding unsymmetrical isomer, *unsym*-**6.6**, with one of the phenyl groups in the axial position *trans* to the sulfonate (eq. 6.7). ^1H and ^{13}C NMR spectra confirmed low C_1 symmetry of complex *unsym*-**6.6**. No products of reductive elimination such as phenol or biphenyl were observed spectrum upon further heating by ^1H NMR spectroscopy.

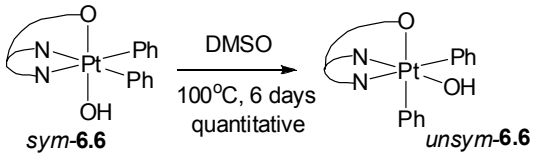

(6.7)

Similar to biphenyl complex **6.6**, the monophenyl complex *unsym*-**6.7** undergoes thermal isomerization upon heating at 100 °C for 3 days in water (half-life 12.5 hours) to produce the corresponding symmetrical isomer, *sym*-**6.7**, with a phenyl group in the axial position (eq. 6.8). Complex *sym*-**6.7** was isolated and characterized by ^{1}H, ^{13}C NMR spectroscopy and ESI mass spectrometry.

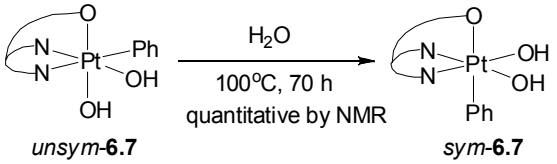

(6.8)

Reactivity of *sym*-**6.7** was probed in solutions in DMSO and water at variable pH. The solution of *sym*-**6.7** remained unchanged upon heating in neutral, acidic and alkaline aqueous solutions and in dry DMSO solution at 100 °C after 5 days, according to ^{1}H NMR spectroscopy. No phenol or other new products that could result from reductive elimination were detected. Hence, the Gibbs activation energy of direct reductive elimination from *sym*-**6.7** and *unsym*-**6.6** exceeds 30 kcal/mol.

Reactivity of methoxo and amido complexes was probed in a number of aprotic solvents. Methoxo complex (dpms)Pt^{IV}Ph(OMe)(OH) was not stable in DMSO solutions and produced a reduced complex (dpms)Pt^{II}Ph(DMSO-d_6) and free methanol upon heating at 80-100 °C. Complex (dpms)Pt^{II}Ph(DMSO-d_6) was identified by ^{1}H NMR spectroscopy and ESI mass spectrometry. No anisole or phenol was detected by ^{1}H NMR spectroscopy in the reaction mixtures. Reduction of (dpms)PtPh(OMe)(OH) presumably involves DMSO solvent as a reductant according

to eq. 6.9. Oxidation of dimethyl sulfoxides to sulfones by high-valent transition metal hydroxo- and oxo-comlpexes is precedented in literature.[25]

$$\underset{\textbf{6.8}}{(dpms)Pt^{IV}Ph(OMe)OH} + 2\ Me_2SO \longrightarrow \underset{\textbf{6.5}}{(dpms)Pt^{II}Ph(Me_2SO)} + MeOH + Me_2SO_2 \qquad (6.9)$$

We have also probed the reactivity of amido complex (dpms)Pt^{IV}(NHPh)(OH) **6.9** in aprotic solvents. Heating (dpms)Pt^{IV}Ph(NHPh)(OH) in CD_3CN resulted in its reduction into (dpms)Pt^{II}Ph(CD_3CN) complex that was identified by ^1H NMR spectroscopy and ESI mass spectrometry. No products that could result from reductive elimination, such as diphenylamine or phenol, were detected by NMR spectroscopy after heating for several hours at 80 ^oC.

Solution of (dpms)PtPh(NHPh)(OH) in DMF-d_7 were not stable upon heating at 60-80 ^oC and produced a complex mixture of products and insoluble precipitate. No diphenyl amine or phenol was detected by NMR spectroscopy. ESI-MS analysis of the reaction products revealed formation of new platinum-containing products, presumably resulting from the dimerization of amido complexes. ESI-MS spectra of the acidified reaction mixture diluted with methanol exhibited a peak of unreacted starting material, m/z 631.1, and the two new peaks characterized by m/z=1225.2 and m/z=613.1 that might be assigned to a mono- and a doubly-protonated dinuclear species $[(dpms)_2Pt^{IV}{}_2Ph_2(\mu\text{-}NPh)(\mu\text{-}NHPh)]^+$ (calcd. $C_{46}H_{39}N_6O_6{}^{195}Pt_2S_2$ 1225.1) and $[(dpms)_2Pt^{IV}{}_2Ph_2(\mu\text{-}NHPh)_2]^{2+}$ (calcd. m/z 613.1) respectively.

Since no reductive elimination was observed in all studied complexes, (dpms)$PtPh_2$(OH), (dpms)PtPh$(OH)_2$, (dpms)PtPh(OMe)(OH), and

(dpms)PtPh(NHPh)(OH), the Gibbs activation energy of reductive elimination must exceed 30 kcal/mol in all these cases.

The lack of reactivity of (dpms)Pt^{IV} phenyl complexes in C-O and C-N reductive elimination can be attributed to inaccessibility of an S_N2 reductive elimination route for an sp^2-hydridyzed carbon and the high reaction barriers for direct Ph-X (X = O, N) reductive elimination pathway.

Notably, examples of aryl-heteroatom elimination from Pt^{IV} center are exceedingly rare. A few examples of aryl-Hal (Hal = Cl, Br, I) reductive elimination from Pt^{IV} aryl complexes are known.[204-206] However, to the best of our knowledge, C(sp^2)-O or C(sp^2)-N elimination from Pt^{IV}-aryl has never been reported in the literature.

The DFT-calculated high activation barriers of direct C-O and C-N reductive elimination from Pt^{IV} phenyl complexes are in agreement with our experimental observations. For instance, the Gibbs activation energy of C-O elimination of phenol from *sym*-**6.7** calculated by DFT was found to be 29.4 kcal/mol. The same barrier of 29.4 kcal/mol was calculated for anisole elimination from (dpms)PtPh(OMe)(OH). The theoretical Gibbs activation energy of direct C-N elimination of diphenyl amine from an axial isomer of (dpms)PtPh(NHPh)(OH) with the phenyl group *trans* to the sulfonate was also high, 28.7 kcal/mol. Therefore, our theoretical results are qualitatively consistent with experimental data.

6.3 Conclusions

We have demonstrated that the dpms ligand effectively facilitates oxidation of diphenyl and monophenyl Pt^{II} complexes with O_2 to the corresponding Pt^{IV} hydroxo

complexes (dpms)Pt^{IV}Ph(X)OH with the OH ligand in the axial position *trans* to the sulfonate. Complexes (dpms)Pt^{II}Ph(L) (L = H_2O, MeOH) are first mono-phenyl platinum complexes known to be oxidized with O_2. Based on observed reactivity and stereochemistry of the reaction, we propose that mechanism of oxidation is similar to that of the methyl Pt^{II} complexes discussed in Chapter 2. Reactivity of phenyl Pt^{II} complexes (dpms)PtPh(L) depends on the nature of the ligand L. The anionic diphenyl complex is the most reactive, whereas aniline and DMSO adducts are inert. Oxidation of mono-phenyl complexes (dpms)PtPh(L) (L = MeOH, H_2O) with O_2 is at least an order of magnitude slower compared to the analogous mono-methyl complexes. To summarize, the following trends in reactivity of (dpms)Pt(R)(L) toward O_2 are observed experimentally:

$$L = Ph > MeOH \sim H_2O >> PhNH_2, DMSO;$$

$$R = Me > Ph.$$

In contrast to mono-methyl Pt^{IV} complexes discussed earlier, no C-X (X = O, N) reductive elimination of organic products was observed upon heating of diphenyl and mono-phenyl complexes **6.6-6.9** in aprotic and protic solvents at various *pH* in the temperature range of 20-100 ^{o}C.

6.4 Experimental Section

Preparation of (dpms)Pt^{II}Ph(MeOH), 6.1. (dpms)$PtPh_2H$ (184 mg, 306 μmol), prepared according to the literature procedure,[29] in MeOH (30 mL) was placed into a 100 mL Schlenk tube equipped with a stirring bar under an argon atmosphere, and a reaction mixture was stirred at 50 °C. Colorless solution formed after 5h. The solution

was filtered under argon, reduced in volume to 2-3 mL under vacuum, and the resulting suspension was cooled down to -20 °C. White precipitate of **6.1** was filtered, washed with cold methanol and dried under vacuum for 12 hours. Yield 127 mg, 75%. White solid, oxidizes in air, moderately soluble in methanol.

^{1}H NMR (CD_3OD, 22 ^oC), δ: 6.02 (s, 1H), 6.86-6.92 (m, 1H), 6.98 (vt, *J*=7.5 Hz, 2H), 7.04 (ddd, *J*=7.8, 5.7, 1.5 Hz, 1H), 7.43 (dd, *J*=7.5, 1.1 Hz, $^3J_{PtH}$=32 Hz, 2H), 7.62 (ddd, *J*=7.9, 5.4, 1.6 Hz, 1H), 7.80 (dd, *J*=7.9, 1.5 Hz, 1H), 7.94 (d, *J*=7.8 Hz, 1H), 7.98 (td, *J*=7.8, 1.6 Hz, 1H), 8.11 (td, *J*=7.9, 1.7 Hz, 1H), 8.43 (dd, *J*=5.7, 1.7 Hz, 1H), 8.81 (d, *J*=5.4 Hz, 1H). **IR** (KBr), ν: 3394 (w, br), 3046 (w), 2949 (w), 2764 (w), 1602 (w), 1572 (w), 1480 (w), 1438 (w), 1252 (m), 1168 (m), 1033 (s), 767 (m), 742 (m), 702 (m), 687 (m) cm^{-1}. **ESI-MS** of a dilute solution in methanol, m/z 554.1. Calculated for (dpms)Pt^{II}Ph(MeOH)·H^+, $C_{23}H_{21}N_3O_3{}^{195}PtS$, 554.1. **Anal.** Found: C, 39.36; H, 3.47; N, 5.19. Calcd for $C_{18}H_{19}N_2O_4PtS$, C, 39.06; H, 3.28; N, 5.06.

Preparation of (dpms)Pt^{II}Ph(OH_2), 6.3. (dpms)PtPh(MeOH) (20 mg, 36 μmol) and 20 mL of deaerated water were placed into a 50 mL round bottom flask and stirred at room temperature until complete dissolution of the starting material. ^{1}H NMR spectrum of the sample diluted with D_2O recorded after 20 minutes showed complete conversion of **6.3** into (dpms)PtPh(OH_2) and one equivalent of methanol. The mixture was evaporated to dryness and the resulting solid was dried under vacuum for 8h. Yield 19 mg, 97%. White solid, oxidizes in air, poorly soluble in water.

^{1}H NMR (D_2O, 22 ^oC), δ: 6.08 (s, 1H), 6.98-7.12 (m, 4H), 7.23 (d, *J*=7.5 Hz, 2H), 7.63 (ddd, *J*=7.7, 5.5, 1.3 Hz, 1H), 7.77 (dd, *J*=7.7, 1.5 Hz, 1H), 7.89 (d, *J*=7.9 Hz,

1H), 8.01 (td, *J*=7.7, 1.6 Hz, 1H), 8.10 (td, *J*=7.7, 1.5 Hz, 1H), 8.31 (dd, *J*=6.0, 1.5 Hz, 1H), 8.74 (vd, *J*=5.5 Hz, 1H). **ESI-MS** of aqueous solution, acidified with HBF_4, m/z 540.1. Calculated for (dpms)PtPh(OH_2)·H^+, $C_{17}H_{17}N_2O_4{}^{195}PtS$ 540.1.

Preparation of (dpms)Pt^{II}Ph(NH_2Ph), 6.4. (dpms)PtPh(MeOH) (65 mg, 117 μmol) was placed into a 10 mL vial equipped with a stirring bar. Deaerated methanol (2 mL) and 185 mg of aniline (2 mmol, 17 equivalents) were added, and a white suspension was stirred at rt (dpms)PtPh(MeOH) dissolved after 10 minutes and the target complex (dpms)PtPh(NH_2Ph) formed as large crystals. The reaction mixture was placed into a freezer at -20 ^oC for 4 hours. White precipitate of **6.4** was filtered off, washed with 0.5 mL of cold methanol and dried under vacuum for 12 hours. Yield 60 mg (97.6 μmol), 83%. White solid, poorly soluble in methanol and water.

^{1}H NMR (D_2O, 22 ^oC), δ: 6.00 (s, 1H), 6.94-7.00 (m, 1H), 7.01-7.16 (m, 6H), 7.20-7.27 (m, 3H), 7.31 (d, *J*=7.1 Hz, $^3J_{PtH}$=40 Hz, 2H), 7.77 (vd, *J*=7.8 Hz, 2H), 7.89 (td, *J*=7.8, 1.4 Hz, 1H), 7.98 (td, *J*=7.8, 1.6 Hz, 1H), 8.34 (dd, *J*=6.0, 1.4 Hz, 1H), 8.43 (dd, *J*=5.6, 1.6 Hz, 1H). **IR** (KBr), ν: 3494 (w, br), 3056 (w), 2828 (w), 1603 (w), 1573 (w), 1494 (w), 1436 (w), 1252 (m), 1222 (m) 1166 (m), 1031 (s), 757 (m), 686 (m) cm^{-1}. **ESI-MS** of solution in MeOH/H_2O (1:1 v/v), m/z 615.1. Calculated for (dpms)PtPh(NH_2Ph)·H^+, $C_{23}H_{22}N_3O_3{}^{195}PtS$, 615.1. **Anal.** Found: C, 44.63; H, 3.27; N, 6.61. Calcd for $C_{23}H_{21}N_3O_3PtS$, C, 44.95; H, 3.44; N, 6.84.

Preparation of (dpms)Pt^{II}Ph(DMSO), 6.5. (dpms)PtPh(MeOH) (55.6 mg, 100 μmol) and 5 mL of dry degassed DMSO were placed into a 25 mL Schlenk tube

under an argon atmosphere. The reaction mixture was stirred for 1 hour at rt to produce a clear solution. The solvent was removed by vacuum distillation. The resulting solid was washed with cold methanol and ether and dried under vacuum for 24 h at 65^0C. Yield 51.1 mg, 85%. White solid, soluble in methanol and DMSO. The complex is stable in MeOH solutions at rt for several days; ligand exchange occurs in dmso-d_6 solutions to give (dpms)PtPh(dmso-d_6), **6.5**-d_6 ($\tau_{1/2}$ = 1.2 h at 20 ^{o}C).

^{1}H NMR (CD_3OD, 22 ^{o}C), δ: 3.07 (s, $^3J_{195PtH}$ = 36 Hz, 3H), 3.19 (s, $^3J_{195PtH}$ = 30 Hz, 3H), 6.17 (s, 1H), 6.90 (td, J = 7.3, 1.3 Hz, 1H), 7.01 (t, J = 7.3, 1.3 Hz, 1H), 7.17-7.27 (m, 2H), 7.39 (d, J = 7.3, $^3J_{195PtH}$ = 40 Hz, 1H), 7.58 (ddd, J = 7.9, 5.5, 1.3 Hz, 1H), 7.70 (d, J = 7.3 Hz, $^3J_{195PtH}$ = 35 Hz, 1H), 7.95 (d, J = 7.9 Hz, 1H), 7.98 (d, J = 7.9 Hz, 1H), 8.04 (td, J = 7.9, 1.5 Hz, 1H), 8.12 (td, J = 7.9, 1.5 Hz, 1H), 8.30 (dd, J = 5.5, 1.5 Hz, $^3J_{195PtH}$ = 55 Hz, 1H), 9.11 (dd, J = 5.5, 1.5 Hz, $^3J_{195PtH}$ = 23 Hz, 1H).

^{13}C NMR (dmso-d_6, 22 ^{o}C), δ: 43.8 (CH_3), 44.4 (CH_3), 75.4, 124.1, 124.4, 127.3, 128.1 (C quat), 128.2, 129.3, 136.3, 137.3, 140.1, 140.8, 151.5, 152.5 (C quat), 153.2, 154.0 (C quat). **IR** (KBr), ν: 3048 (w), 2924 (w), 1606 (w), 1574 (w), 1483 (w), 1435 (w), 1231 (m), 1167 (m), 1131 (m), 1031 (s), 765 (m), 685 (m) cm^{-1}. **ESI-MS** of solution in methanol acidified with HBF_4, m/z 600.1. Calculated for (dpms)PtPh(Me_2SO)·H^+, $C_{19}H_{21}N_2S_2O_4{}^{195}Pt$, 600.1. ESI-MS of (dpms)PtPh(dmso-d_6) solution in methanol acidified with HBF_4, m/z 606.1. Calculated for (dpms)PtPh($(CD_3)_2SO$)·H^+, $C_{19}H_{15}D_6N_2S_2O_4{}^{195}Pt$, 606.1. **Anal.** Found: C, 38.42; H, 3.52; N, 4.35. Calcd for $C_{19}H_{20}N_2O_4PtS_2$, C, 38.06; H, 3.36; N, 4.67.

Preparation of *sym*-(dpms)Pt^{IV}Ph$_2$OH, *sym*-6.6. K[(dpms)PtPh$_2$][29] (**6.2**) (55.9 mg, 88 μmol) was dissolved in 2 mL of deaerated water and placed into a 10 mL vial equipped with a magnetic stirring bar. The vial was filled with O_2 and the solution was stirred at room temperature for 2 hours. No K(dpms)PtPh$_2$ was detected in solution after that time; the solution pH was ~12. White precipitate was filtered off and washed with water until neutral reaction of the filtrate. The product was dried under vacuum for 6h. Yield 47.0 mg, 87%. White solid, soluble in dichloromethane and DMSO, insoluble in water.

^{1}H NMR (dmso-d_6, 22 ^{o}C), δ: 2.56 (br s, $^2J_{195PtH}$ = 36 Hz, 1H, OH), 6.89 (s, 1H), 6.92-7.04 (m, 6H), 7.34 (dd, J = 8.0, 1.7 Hz, $^3J_{195PtH}$ = 30 Hz, 4H), 7.65 (ddd, J = 7.8, 5.5, 1.2 Hz, 2H), 8.08 (d, J = 7.8 Hz, 2H), 8.23 (td, J = 7.8, 1.5 Hz, 2H), 8.30 (dd, J = 5.5, 1.5 Hz, 2H). **^{13}C NMR** (dmso-d_6, 22 ^{o}C), δ: 70.7, 124.9, 125.9, 126.4 (C quat), 126.5, 127.3, 130.9, 141.8, 149.6, 151.4 (C quat). **IR** (KBr), ν: 3583 (w, br), 3055 (w), 2981 (w), 1604 (w), 1574 (w), 1472 (w), 1449 (w), 1294 (m), 1203 (w), 1143 (s), 1025 (m), 981 (s), 736 (m), 695 (m) cm^{-1}. **ESI-MS** of solution in MeOH/CH_2Cl_2 (1:1 v/v) acidified with HBF_4, m/z 616.1. Calculated for (dpms)PtPh$_2$(OH)·H$^+$, $C_{23}H_{21}N_2SO_4{}^{195}Pt$, 616.1. **Anal.** Found: C, 44.81; H, 3.45; N, 4.24. Calcd for $C_{23}H_{20}N_2O_4PtS$, C, 44.88; H, 3.27; N, 4.55.

Preparation of *unsym*-(dpms)Pt^{IV}Ph(OH)$_2$, *unsym*-6.7. (dpms)PtPh(MeOH) (99.1 mg, 179 μmol) and 100 mL of deaerated water were placed into 250 mL round-bottom flask. This suspension was stirred for 30 minutes under argon. Resulting clear solution was stirred under O_2 at room temperature. After 48h the solution was

reduced in volume to 1 mL under vacuum. Resulting suspension was left at 5 ^{o}C for 1h. White precipitate was filtered off, washed with 0.5 mL of cold water and dried under vacuum for 8h. Yield 92.3 mg, 93%. White solid, soluble in water, methanol, DMSO.

^{1}H NMR (dmso-d_6, 22 ^{o}C), δ: 1.45 (br s, 1H, OH), 2.99 (br s, $^{2}J_{195PtH}$ = 30 Hz, 1H, OH), 6.93 (s. 1H), 7.03-7.23 (m, 5H), 7.60 (ddd, J = 7.8, 5.5, 1.3 Hz, 1H), 7.88-8.00 (m, 2H), 8.06 (dd, J = 7.8, 1.3 Hz, 1H), 8.09 (d, J = 7.8 Hz, 1H), 8.26 (td, J = 7.8, 1.5 Hz, 1H), 8.33 (td, J = 7.8, 1.5 Hz, 1H), 8.96 (dd, J = 5.5, 1.5 Hz, 1H). **^{13}C NMR** (dmso-d_6, 22 ^{o}C), δ: 70.7, 125.6, 126.2, 126.5, 126.8, 127.1, 127.3 (C quat), 127.6, 132.2, 141.9, 142.7, 148.3, 149.5 (C quat), 151.1, 152.7 (C quat). **IR** (KBr), ν: 3548 (w, br), 3070 (w), 2928 (w), 1607 (w), 1574 (w), 1481 (w), 1445 (w), 1301 (m), 1210 (w), 1142 (s), 1027 (w), 966 (s), 737 (m), 698 (s) cm^{-1}. **ESI-MS** of solution in MeOH/H_2O (1:1 v/v) acidified with HBF_4, m/z 556.1. Calculated for (dpms)PtPh(OH)$_2$·H^{+}, $C_{17}H_{17}N_2SO_5{}^{195}Pt$, 556.1. **Anal.** Found: C, 36.48; H, 3.29; N, 4.74. Calcd for $C_{17}H_{16}N_2O_5PtS$, C, 36.76; H, 2.90; N, 5.04.

Preparation of (dpms)Pt^{IV}Ph(OMe)(OH), 6.8. (dpms)PtPh(MeOH) (98.2 mg, 177 μmol) in 75 mL of dry methanol was placed into a 250 mL round-bottom flask equipped with a magnetic stirring bar. The flask was filled with O_2 and the reaction mixture was stirred vigorously at rt. After 40h the clear solution was reduced in volume to ~0.3 mL under vacuum. Resulting suspension was left at -20^{0}C for 1h. White precipitate was filtered off, washed with small amount of cold methanol and

dried under vacuum for 12h. Yield 91.8 mg, 91%. White solid, soluble in methanol, DMSO.

^{1}H NMR (dmso-d_6, 22 ^{o}C), δ: 2.52 (br s, 1H, OH), 2.94 (s, $^3J_{195PtH}$ = 33 Hz, 3H), 6.95 (s, 1H), 7.04-7.31 (m, 5H), 7.60 (ddd, J = 7.9, 5.8, 1.5 Hz, 1H), 7.92 (dd, J = 5.8, 1.5 Hz, 1H), 7.96 (ddd, J = 7.9, 5.5, 1.2 Hz, 1H), 8.07 (dd, J = 7.9, 1.2 Hz, 1H), 8.09 (d, J = 7.9 Hz, 1H), 8.27 (td, J = 7.9, 1.5 Hz, 1H), 8.34 (td, J = 7.9, 1.5 Hz, 1H), 8.95 (dd, J = 5.5, 1.5 Hz, 1H). **^{13}C NMR** (dmso-d_6, 22 ^{o}C), δ: 57.3 (CH_3), 70.7, 125.6, 126.1, 126.3, 126.7, 127.0, 127.8, 129.3 (C quat), 131.4, 141.9, 142.7, 148.0, 149.6 (C quat), 151.5, 152.4 (C quat). **IR** (KBr), ν: 3318 (w, br), 3031 (w), 2976 (w), 2817 (w), 1606 (w), 1573 (w), 1483 (w), 1446 (w), 1298 (s), 1210 (m), 1147 (s), 1027 (m), 974 (s), 742 (s), 696 (s) cm^{-1}. **ESI-MS** of solution in MeOH acidified with HBF_4, m/z 570.1. Calculated for (dpms)PtPh(OCH_3)(OH)·H^+, $C_{18}H_{19}N_2SO_5{}^{195}Pt$, 570.1. **Anal.** Found: C, 37.79; H, 3.41; N, 4.77. Calcd for $C_{18}H_{18}N_2O_5PtS$, C, 37.96; H, 3.19; N, 4.92.

Preparation of (dpms)Pt^{IV}Ph(NHPh)(OH), 6.9. (dpms)PtPh(NH_2Ph) (53.8 mg, 87.5 μmol) and 2 mL of MeOH were placed into a 10 mL vial equipped with a stirring bar, and 25 μL of 30% aq. H_2O_2 were added slowly upon stirring. Stirring continued for 1 hour at rt. Solid (dpms)PtPh(NH_2Ph) dissolved and reddish solution formed. The yield of **6.9** is quantitative according to ^{1}H NMR spectroscopy. Ether (2 mL) was slowly added to the solution, and the resulting mixture was stored for 1 day at rt. Crystalline precipitate of **6.9** was filtered off, washed with ether and pentane; yield 36 mg. An additional fraction of the product was obtained by evaporation of the filtrate. Dry solid was washed with water (10 mL), ether (5 mL) and pentane (5 mL) and

dried under vacuum for 10 hours; yield 13.9 mg. Red crystalline solid, combined yield 50 mg (79 μmol), 90%.

^{1}H NMR (dmso-d_6, 22 ^{o}C), δ: 3.01 (br s, 1H), 4.36 (br s, 1H), 6.28-6.40 (m, 1H), 6.44-6.70 (m, 4H), 6.95 (s, 1H), 6.97-7.06 (m, 3H), 7.07-7.27 (m, 2H), 7.59 (ddd, *J*=7.8, 5.5, 1.1 Hz, 1H), 7.78-7.84 (m, 1H), 7.97 (d, *J*=5.5 Hz, 1H), 8.08 (d, *J*=7.8 Hz, 1H), 8.10 (d, *J*=7.8 Hz, 1H), 8.25 (td, *J*=7.8, 1.3 Hz, 1H), 8.29 (td, *J*=7.8, 1.3 Hz, 1H), 8.90 (d, *J*=4.3 Hz, 1H). **^{13}C NMR** (dmso-d_6, 22 ^{o}C), δ: 70.4, 115.6, 118.7, 125.4, 125.8, 126.3, 126.8, 127.2, 127.7, 127.8, 128.2 (C quat), 131.6, 141.8, 142.6, 149.0, 150.0 (C quat), 150.9, 152.1 (C quat), 155.4 (C quat). **IR** (KBr), ν: 3555 (w, br), 3050 (w), 2970 (w), 1592 (w), 1574 (w), 1489 (w), 1298 (m), 1207 (w), 1145 (s), 1026 (m), 980 (s), 760 (s), 695 (s) cm^{-1}. **ESI-MS** of solution in methanol, m/z 631.1. Calculated for (dpms)PtPh(NHPh)(OH)·H^{+}, $C_{23}H_{22}N_3O_4{}^{195}$Pt S, 631.1. **Anal.** Found: C, 43.52; H, 3.26; N, 6.33. Calcd for $C_{23}H_{21}N_3O_4PtS$, C, 43.81; H, 3.36; N, 6.66.

Chapter 7: Palladium-Catalyzed Oxidation of Ethylene to Glycol Esters Utilizing Hydrogen Peroxide as an Oxidant

7.1 Introduction: Oxidation of Alkenes Catalyzed by Pd^{II} Complexes

As shown in Chapter 3, stoichiometric oxidation of (dpms)Pt^{II}(ethylene)OH with O_2 and subsequent reductive elimination cleanly produces ethylene oxide and ethylene glycol (Scheme 3.5, 3.9). However, the Pt-containing product of the latter reaction, the hydroxo bridged dimer $L_2Pt^{II}{}_2(\mu\text{-}OH)_2$ is kinetically inert and poorly soluble in majority of solvents so rendering a catalytic version of this reaction implausible. Our experiments with a related water-soluble cationic diaqua complex, $[LPt^{II}(OH_2)_2]^+$, and an anionic dihydroxo complex $[LPt^{II}(OH)_2]^-$, showed that they both are inactive as catalysts for aerobic ethylene epoxidation in water.

Palladium complexes are many orders of magnitude more labile than analogous platinum complexes and are widely used in catalytic transformations of alkenes in a number of coordinating solvents including water.[207] In this work, the ability of palladium complexes supported by the dpms ligand and some of its analogues to serve as catalysts for oxidation of ethylene into glycol derivatives was investigated.

Oxidation of olefins catalyzed by palladium complexes typically involves a redox couple Pd^{2+}/Pd^0. For example, industrial production of acetaldehyde known as the Wacker process is based on $PdCl_2$-catalyzed oxidation of ethylene to acetaldehyde, coupled with $CuCl_2$-mediated reoxidation of Pd^0 to Pd^{II} with O_2 (eq. 7.1-7.3).[208]

$$PdCl_4^{2-} + CH_2{=}CH_2 + H_2O \longrightarrow CH_3CHO + Pd^0 + 2HCl + 2Cl^- \quad (7.1)$$

$$Pd^0 + 2CuCl_2 + 2Cl^- \longrightarrow PdCl_4^{2-} + 2CuCl \quad (7.2)$$

$$2CuCl + 0.5O_2 + 2HCl \longrightarrow 2CuCl_2 + H_2O \quad (7.3)$$

Homogeneous oxidation of ethylene in acetic acid in the presence of Pd^{II} salts yields vinyl acetate as a main product (eq. 7.4) and some ethylidene diacetate.[208]

$$CH_2{=}CH_2 + Pd^{2+} + 2OAc^- \longrightarrow CH_2{=}CHOAc + Pd^0 + HOAc \quad (7.4)$$

The proposed mechanism of this transformation involves initial acetoxypalladation, followed by β-hydride elimination from the 2-acetoxyethyl Pd^{II} intermediate (Scheme 7.1). In the presence of water, acetaldehyde forms along with vinyl acetate.[208]

Scheme 7.1

$$CH_2{=}CH_2 + Pd^{2+} + OAc^- \xrightarrow{HOAc} \left[Pd^{II}CH_2CH_2OAc\right] \xrightarrow{-HPd^{II}} CH_2{=}CHOAc$$

It is known that M^{II}/M^{IV} redox potential is noticeably higher for M=Pd rather than for M=Pt. The standard reduction potential for $[Pd^{IV}Cl_4]^{2-}/[Pd^{II}Cl_6]^{2-}$ (eq. 7.5) in acidic aqueous solution is 1.288 V compared to 0.68 V for the analogous Pt^{IV}/Pt^{II} couple (eq. 7.6).[209]

$$PdCl_6^{2-} + 2e^- \longrightarrow PdCl_4^{2-} + 2Cl^- \qquad E^o = 1.288\ V \quad (7.5)$$

$$PtCl_6^{2-} + 2e^- \longrightarrow PtCl_4^{2-} + 2Cl^- \qquad E^o = 0.68\ V \quad (7.6)$$

Accordingly, the catalytic processes involving a Pd^{II}/Pd^{IV} redox couple are rare. Strong oxidants are required in order to generate Pd^{IV} transients, such as hypervalent iodine reagents,[210] N-bromosuccinimide (NBS)[211] $Pb^{IV}(OAc)_4$, Br_2 or *m*CPBA.[36] Olefin oxidation involving Pd^{II}/Pd^{IV} redox couple typically produces products of the formal 1,2-addition across the C=C double bond, in contrast to the Pd^{II}/Pd^0 mediated processes, which typically generate carbonyl or vinyl derivatives. For example, $Pd(OAc)_2$-catalyzed oxidation of ethylene in acetic acid in the presence of

$Pb^{IV}(OAc)_2$, $K_2Cr_2O_7$, or MnO_2, produces glycol esters as main products (Scheme 7.2), whereas vinyl acetate forms in small amounts only.[212]

Scheme 7.2

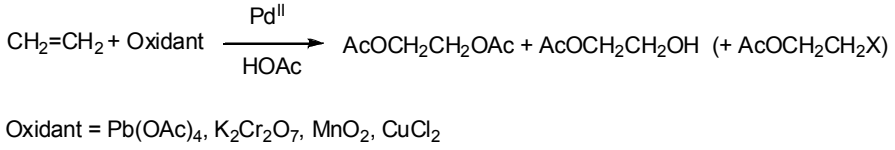

A mechanism was suggested that involves oxidation of an intermediate $Pd^{II}CH_2CH_2OAc$ with $Pb^{IV}(OAc)_2$, $K_2Cr_2O_7$, or MnO_2, to produce $Pd^{IV}CH_2CH_2OAc$ transients, followed by reductive elimination of the 1,2-addition products from the latter (Scheme 7.3).[212]

Scheme 7.3

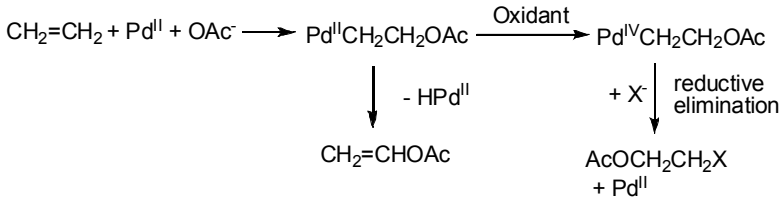

A mechanism involving a redox couple Pd^{II}/Pd^{IV}, analogous to that shown in Scheme 7.3, was often suggested for other types of 1,2-functionalization of olefins in the presence of $PhI(OAc)_2$ as an oxidant, catalyzed by Pd^{II} complexes, such as diacetoxylation,[213] aminoacetoxylation,[35] and aminoalkoxylation[78] Importantly, the mechanism shown in Scheme 7.3 implies that in order to generate the 1,2-addition products selectively, the oxidation step should be fast enough to compete with β-hydride elimination from Pd^{II} alkyl intermediates. Products of β-hydride elimination are often observed along with the 1,2-addition products even in the presence of strong oxidants, such as $PhI(OAc)_2$.[35]

At the same time, it might be important to learn how to use more readily available and environmentally benign oxidants for Pd-catalyzed oxidative 1,2-functionalization of olefins. The most advantageous oxidants for large scale practical applications would be dioxygen from air. However, in view of the difficulty of oxidation of Pd^{II} to Pd^{IV}, hydrogen peroxide might also be considered as a viable alternative to O_2. Importantly, Pd^{II}-catalyzed oxidation of olefins with H_2O_2 implies typically ketones or aldehydes as main products. An additional complication related to the use of H_2O_2 is that Pd^{II} salts catalyze decomposition of H_2O_2 so that the use of excess H_2O_2 is necessary.[214] For example, Mimoun developed Pd^{II}-catalyzed oxidation of terminal olefins into methyl ketones by aqueous H_2O_2 in HOAc (eq. 7.7). In this reaction, 5-fold excess of H_2O_2 was used in order to achieve high conversions, due to significant H_2O_2 decomposition to O_2 and water. The proposed mechanism of this reaction is shown in Scheme 7.4. In this mechanism, the ketone formation occurs via oxygen transfer and hydride shift in a cyclic intermediate resulting from olefin hydroperoxypalladation.[214]

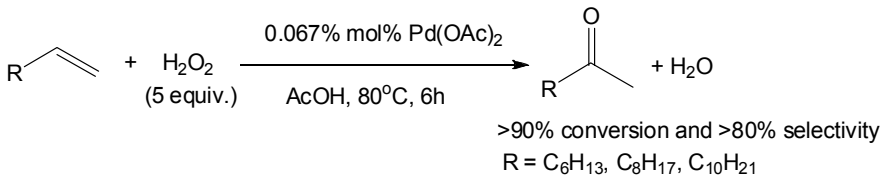

(7.7)

Scheme 7.4. Mimoun's proposed mechanism for H_2O_2-mediated olefin oxidation

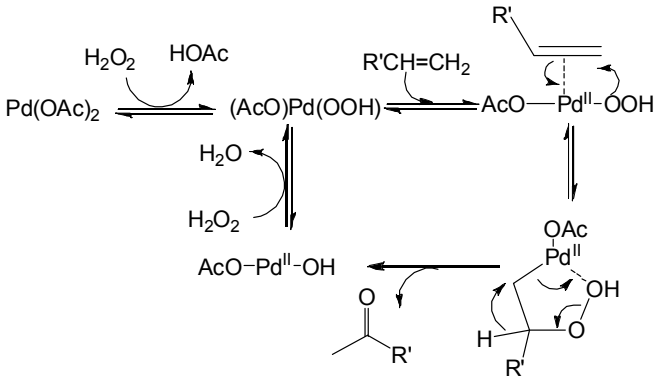

Based on our previous observations that functionalization of Pt^{II} alkyl complexes with O_2 and H_2O_2 involving Pt^{IV} intermediates is enabled by the hemilabile tridentate dpms ligand, we reasoned that similar functionalization of alkyl (dpms)Pd^{II} complexes might also be possible.

In addition to dpms, in this project we suggest to use a masked dpms-analogue, di-2-pyridyl ketone (dpk). The latter ligand forms Pd^{II} complexes that are typically more soluble in polar solvents compared to the dpms analogues.

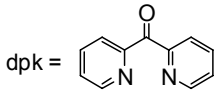

The carbonyl group of di-2-pyridyl ketone is activated towards a nucleophilic addition of water or alcohols on coordination to transition metals. For example, a reversible addition of water and methanol (eq. 7.8) was observed in solutions of (dpk)MCl_2 complexes in these solvents.[215] The ability of the deprotonated form of a hydrated dpk ligand to coordinate in a tridentate fashion to an octahedral Pt^{IV} center has been demonstrated by Puddephatt (eq. 7.9).[216]

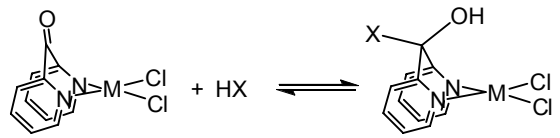

(7.8)

X = OH, OMe, OEt; M = Pt^{2+}, Pd^{2+}

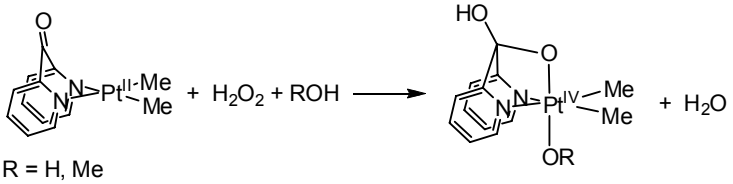

(7.9)

R = H, Me

We expected that the ability of the dpms and dpk ligands to coordinate in both bidentate and tridentate modes might facilitate oxidation of Pd^{II} complexes to Pd^{IV} with O_2 or H_2O_2 and, hence, promote selective 1,2-oxidative functionalization of ethylene. Though dioxygen proved ineffective in such transformations, H_2O_2 can effectively oxidize ethylene to glycol esters in high yield and selectivity in the presence of dpk and dpms-supported Pd^{II} complexes.

7.2 Results and Discussion

7.2.1 Complexes of $Pd(OAc)_2$ with Di-2-pyridyl Ketone (dpk) and Dpms-Type Ligands

7.2.1.1 Complexes of $Pd(OAc)_2$ with Di-2-pyridyl Ketone

a) 1 : 1 dpk : Pd^{II} ratio. Complex $(dpk)Pd(OAc)_2$, **7.1**, was prepared by reacting palladium acetate solution in acetic acid with 1 equivalent of the dpk ligand at 60 ^oC (eq. 7.10, Scheme 7.5). The resulting **7.1** was isolated in 85% yield after recrystallization.

$$dpk + 1/3\ Pd_3(OAc)_6 \longrightarrow \underset{\textbf{7.1}}{(dpk)Pd(OAc)_2} \qquad (7.10)$$

^{1}H and ^{13}C NMR spectra of the product are consistent with the mirror-symmetrical structure of **7.1**. Four multiplets of the dpk ligand are present in the aromatic region of ^{1}H NMR spectrum of **7.1**. In the ^{13}C NMR spectrum in CD_3COOD solution, two resonances are detected in the carbonyl region at 182.2 ppm and 185.2 ppm, assigned to the carbonyl groups of the Pd-bound acetate ligand and the carbonyl group of the dpk ligand respectively. ESI mass spectrometry of HOAc-H_2O solutions of **7.1** revealed the presence of a signal characterized by m/z 349.0, corresponding to a cationic product of the loss of one acetate, [**7.1**-OAc]$^{+}$.

Scheme 7.5. The 1 : 1 and 2 : 1 complexes of Pd^{II} with dpk.

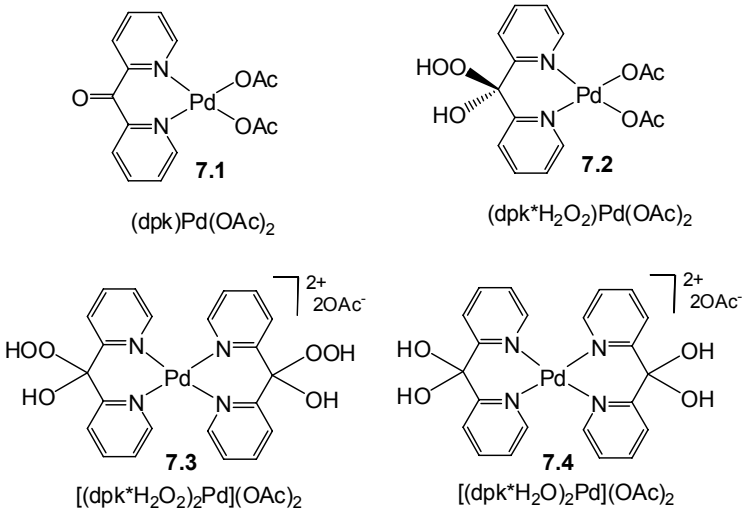

At a temperature of 20 ^{o}C the formation of **7.1** upon mixing $Pd(OAc)_2$ and dpk in 1:1 ratio in acetic acid solution is not immediate, and the reaction takes *ca* 30 hours to reach completion. A sample of the reaction mixture above picked up after less than 1 hour upon mixing the reagents was diluted with water and analyzed by ESI mass spectrometry. Four signals of comparable intensity were observed characterized by m/z 237.0, 349.0, 255.0, and 367.0. The signals were assigned to the cationic 2 : 1 and 1 : 1 dpk : Pd complexes, $[(dpk)_2Pd]^{2+}$ and $[(dpk)Pd(OAc)]^{+}$, and their adducts

with one molecule of H_2O, $[(dpk)(dpk*H_2O)Pd]^{2+}$ and $[(dpk*H_2O)Pd(OAc)]^{+}$ respectively. After equilibrating for 30 hours **7.1** was the only product present in solution. No change was observed by ^1H NMR spectroscopy after further 24 hours at 20 ^oC.

Complex **7.1** does not react with water in the presence of 0.6 M D_2O in HOAc-d_4 (50 equivalents of D_2O with respect to **7.1**), but reacted readily with excess H_2O_2 (3.5 equivalents of H_2O_2, $[H_2O_2]$ = 0.3 M) in acetic acid solution to form a product of the nucleophilic addition of H_2O_2 across the dpk carbonyl group, $(dpk*H_2O_2)Pd(OAc)_2$ **7.2** (eq. 7.11, Scheme 7.5).

$$\underset{\mathbf{7.1}}{(dpk)Pd(OAc)_2} + H_2O_2 \rightleftharpoons \underset{\mathbf{7.2}}{(dpk*H_2O_2)Pd(OAc)_2} \qquad (7.11)$$

There are precedents for formation of peroxoketals by the nucleophilic attack of H_2O_2 at the carbonyl group of ketones in literature.[217-219] The coordination of the dpk ligand to Pd^{II} center is expected to additionally increase its reactivity toward nucleophilic attack.[215]

Consistent with a mirror-symmetrical structure of **7.2**, ^1H NMR spectrum of **7.2** exhibits the presence of four multiplets of the dpk ligand in the aromatic region. In the ^{13}C NMR spectrum of **7.2** in CD_3COOD, the signal of the carbonyl group of the dpk ligand is absent. A new carbon resonance observed at 105.4 ppm was assigned to the peroxoketal carbon. Similar to **7.1**, a resonance of the coordinated acetate ligand appears at 182.7 ppm in ^{13}C NMR spectrum. ESI mass spectra of a mixture of **7.1** and H_2O_2 in HOAc-H_2O solution showed the presence of a signal of a Pd-containing species with m/z 383.0, corresponding the product of one acetate ligand loss, [**7.2**-

$OAc]^+$. Complex **7.2** is not stable in CD_3COOD solution at 20 ^oC and slowly produces **7.1**.

b) 2 : 1 dpk : Pd^{II} ratio. The reactivity of $Pd(OAc)_2$ toward 2 equivalents of dpk was examined in the absence and in the presence of water and H_2O_2. According to ^1H NMR spectroscopy, in the absence of additives a complex mixture of products forms in acetic acid solution containing $Pd(OAc)_2$ and 2 equivalents of dpk. ESI-MS analysis of a sample of the reaction mixture in acetic acid after dilution with water, showed the presence of the signals characterized by m/z 237.0, 491.0, and 509.0. These signals were assigned to a 2 : 1 complex $[(dpk)_2Pd]^{2+}$ (m/z 237.0) and its singly deprotonated adducts with water, $[(dpk)(dpk*OH)Pd]^+$ (m/z 491.0) and $[(dpk*OH_2)(dpk*OH)Pd]^+$ (m/z 509.0), respectively.

Clean quantitative formation of a 2 : 1 dpk : Pd peroxoketal complex $[(dpk*H_2O_2)_2Pd](OAc)_2$, **7.3**, was observed in the presence of 3.5 equivalents of aqueous 30 wt.% H_2O_2 (eq. 7.12, Scheme 7.5).

$$2\ dpk + 1/3\ Pd_3(OAc)_6 + 2\ H_2O_2 \longrightarrow \underset{\mathbf{7.3}}{[(dpk*H_2O_2)_2Pd](OAc)_2} \qquad (7.12)$$

NMR spectra of **7.3** are evident of a mirror-symmetrical structure of the product. Four multiplets of the dpk ligand are present in ^1H NMR spectrum of **7.3**. In ^{13}C NMR spectrum in CD_3COOD, no signals are present in the carbonyl region, and a peroxoketal carbon appears at 105.5 ppm. This is consistent with the assigned structure of $[(dpk*H_2O_2)_2Pd](OAc)_2$ with the outer-sphere acetate counterions, which undergoe fast exchange with a solvent CD_3COOD. However, no peaks corresponding to **7.3** could be detected by ESI mass spectrometry in HOAc solution of **7.3** diluted with H_2O, presumably due to low stability of **7.3** under ESI analysis conditions. ESI

mass spectrum of **7.3** in HOAc-H_2O solution showed the presence of the signals characterized by m/z 237.0 and 255.0 assigned to $[(dpk)_2Pd]^{2+}$ and its hydrated adduct $[(dpk*H_2O)_2Pd]^{2+}$, respectively.

The presence of H_2O_2 was essential for formation of **7.3**: no **7.3** was detected when the corresponding amount of water (15 equivalents of H_2O, $[H_2O]$ = 1.34 M) was used instead of hydrogen peroxide.

Formation of 2 : 1 adduct with water, **7.4**, in 83% NMR yield, was possible when large excess of water was used (80 equivalents, $[H_2O]$ = 6.2 M) under analogous reaction conditions (eq. 7.13, Scheme 7.5) and was accompanied by formation of unidentified products. Complex **7.4** was characterized by ^1H, ^{13}C NMR spectroscopy and ESI mass spectrometry without isolation.

$$2\ dpk\ +\ 1/3\ Pd_3(OAc)_6 + 2\ H_2O \longrightarrow \underset{\mathbf{7.4}}{[(dpk*H_2O)_2Pd](OAc)_2} \qquad (7.13)$$

Preferable formation of H_2O_2 adduct **7.3** in the presence of aqueous H_2O_2 in solution can be attributed to a much higher nucleophilicity of H_2O_2 compared to water.[26, 220]

7.2.1.2 Complexes of $Pd(OAc)_2$ with Me-dpms$^-$ and t-Bu-dpms$^-$

The reaction between dilute $Pd(OAc)_2$ solution and a parent dipyridylmethanesulfonate ligand, dpms, in acetic acid solvent led to the formation of insoluble products. In order to improve solubility, the alkyl substituted dpms ligands, Me-dpms[29] and *t*-Bu-dpms,[221] were utilized in further studies (Scheme 7.6).

Scheme 7.6

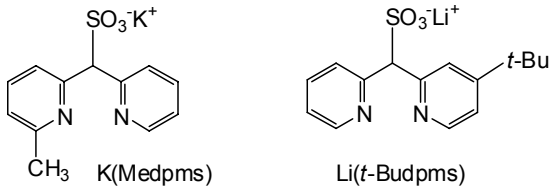

Upon mixing $Pd(OAc)_2$ solution and K(Me-dpms) in acetic acid solution at 20 ^oC, slow disappearance of signals of free Me-dpms ligand was observed in ^1H NMR spectrum. After equilibration for 24 hours resonances of free K(Me-dpms) completely disappeared and a mixture of Me-dpms-containing products formed, which remained unchanged upon further standing at 20 ^oC or after heating at 60 ^oC.

In the ESI mass spectrum of the reaction mixture in $CH_3COOH–H_2O$, two signals of comparable intensity were detected characterized by m/z 466.9 and m/z 670.9, assigned to the adducts of potassium cation with neutral 1:1 and 2:1 complexes, [(Me-dpms)Pd(OAc)]*K^+ and [(Me-dpms)$_2$Pd]*K^+ respectively.

According to ^1H NMR spectroscopy, several sets of signals of the Me-dpms ligand were observed in ^1H NMR spectrum of the mixture. Four major products were characterized by singlets of the methyl group of the Me-dpms ligand at 2.23 ppm, 2.24 ppm, 2.40 ppm and 3.25 ppm with the relative integral intensities ratio of 1.7 : 2.8 : 3.0 : 2.6 respectively. Three minor products were characterized by singlets at 2.27 ppm, 2.28 ppm, 2.49 ppm integrating as 0.53, 0.42, 0.61 respectively. The complexity of the ^1H NMR spectrum might be caused by the presence of several isomers of Me-dpms-Pd^{II} complexes (Scheme 7.7). According to previous studies in our group,[29] *exo*- and *endo*-coordination modes of the Me-dpms ligand are possible, with the sulfonate group pointing toward Pd^{II} or away from the metal center (Scheme 7.7-a). Even more options for isomerism are possible for 2 : 1 $[(Me\text{-}dpms)_2Pd]^{2+}$ (**7.6**)

complexes that differ by relative positions of the *endo*- or *exo*-sulfonate or methyl groups of the two Medpms ligands (Scheme 7.7-b).[79]

Scheme 7.7

a) 1:1 complexes

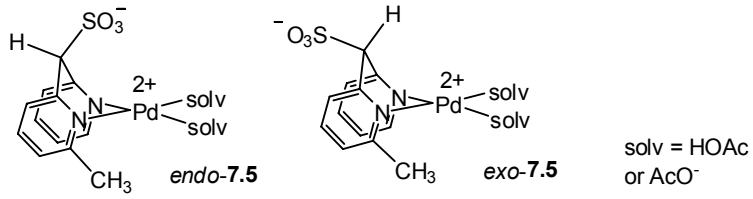

b) Some of the possible isomers of 2:1 complex **7.6** (*endo*-orientation of SO_3 is shown only)

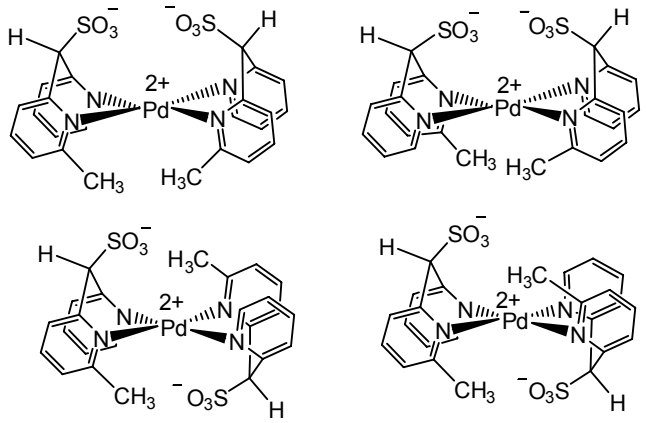

We can therefore conclude that a mixture of $[(\text{Me-dpms})\text{Pd(solv)}_2]^+$ (**7.5**, solv = HOAc or AcO^-) and $[(\text{Me-dpms})_2\text{Pd}]$ (**7.6**) complexes are present in acetic acid solutions containing equimolar amounts of Me-dpms and Pd^{II}. This mixture persists after equilibrating at 20-60 ^oC for several days. The reaction mass balance then requires that some "ligand-free" palladium acetate not coordinated to Me-dpms is present in solutions containing equimolar amounts of the Me-dpms ligand and $Pd(OAc)_2$. This is in contrast to the dpk ligand that forms a 1 : 1 complex $(\text{dpk})\text{Pd}(OAc)_2$ as the sole product after equilibrating for 30 hours at 20 ^oC.

Acetic acid solutions of $Pd(OAc)_2$ containing 2 equivalents of K(Me-dpms) produce a similar set of signals in ^1H NMR spectrum but in a different ratio of integral

intensities. Three major products are characterized by singlets of the ligand Me groups at 2.23 ppm, 2.24 ppm and 2.40 ppm, with the relative integral intensities ratio of 1.33 : 2.76 : 3.00 respectively. Four minor products are characterized by singlets at 2.27 ppm, 2.28 ppm, 2.49 ppm, 3.25 ppm integrating as 0.45, 0.24, 0.51 and 0.32 respectively. According to ESI mass spectrometry, a strong signal of [(Me-dpms)$_2$Pd]*K^+ with m/z 670.9 and a weaker signal of [(Medpms)Pd(OAc)]*K^+ with m/z 466.9 were detected.

Similarly, upon reacting palladium acetate with 1 equivalent of a lithium salt of the *tert*-butyl-substituted dpms ligand, Li(*t*-Bu-dpms), a mixture of 1:1 and 2:1 complexes was detected in acetic acid solutions by ESI mass spectrometry.

7.2.2 Catalytic Oxidation of Ethylene with H_2O_2 in Dpk – $Pd(OAc)_2$ – AcOH and Dpk – R-dpms – $Pd(OAc)_2$ – AcOH Systems (R = Me, *t*-Bu)

7.2.2.1 Catalysts Activity and Selectivity: Simple Systems

Reactivity of palladium complexes with dpk, Me-dpms and *t*-Bu-dpms ligands was probed in oxidation of ethylene in CD_3COOD solution with H_2O_2. All reactions were performed at 20 ^oC in vigorously stirred solutions in CD_3COOD under 1 atmosphere of ethylene, with H_2O_2 as the limiting reagent and the reaction time of 24 hours (Scheme 7.8). The results are given in Table 7.1.

Scheme 7.8

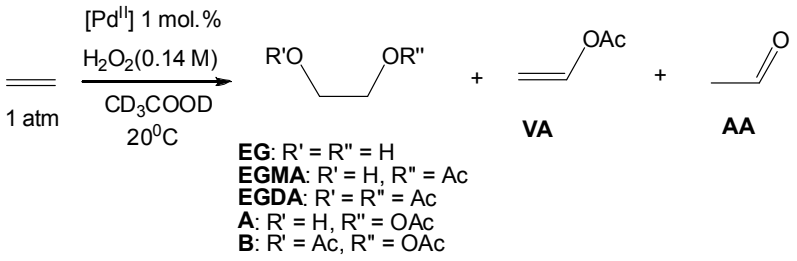

A control experiment in the absence of $Pd(OAc)_2$ showed that the yield of glycol mono- (**EGMA**) and diacetates (**EGDA**) based on H_2O_2 did not exceed 1%. No other products were observed in the reaction mixture (entry 1). These products might result from a non-catalyzed reaction between ethylene and peracetic acid. The latter forms in a reversible reaction between H_2O_2 and acetic acid (eq. 7.14).[222]

$$CH_3COOH + H_2O_2 \rightleftharpoons CH_3CO_3H + H_2O \qquad (7.14)$$

As it has been shown previously that peroxoketals are also active in olefin epoxidation.[218] A control experiment performed in the presence of H_2O_2 and 0.1 equivalent of dpk but without $Pd(OAc)_2$ showed that less than 1% of the glycol products, acetates and ethylene glycol (**EG**), formed after 12 hours (entry 2).

Reaction in the presence of palladium acetate alone produced a mixture of both glycol acetates and the Wacker-type products (entry 3) and was accompanied by formation of palladium black. Wacker-type oxidation products, vinyl acetate (**VA**) and acetaldehyde (**AA**), formed in *ca* 50% selectivity. Noticeable amounts of glycol peroxoesters, 2-hydroxyethyl peracetate (**A**) and 2-acetoxyethyl peracetate (**B**) (Scheme 7.8) were found in these reaction mixtures. The products **A** and **B** are unstable and decompose upon standing at 20 ^oC after 1-2 days or in the presence of reducing agents, such as NaI, $SnCl_2$ or $Na_2S_2O_5$, to produce equivalent amounts of ethylene glycol and 2-hydroxyethyl acetate respectively.

Oxidation of ethylene catalyzed by 1-5 mol.% $Pd(OAc)_2$ equilibrated for 2 days with 1 equivalent of K(Me-dpms) (entry 4) or Li(*t*-Bu-dpms) (entry 5) produced a mixture of the Wacker-type oxidation products and glycol acetates in low yields and low selectivity. Formation of palladium black was observed during the reaction.

Table 7.1. Yields of ethylene oxidation products in the presence of H_2O_2 and [Pd^{II}] in CD_3COOD. [$Pd(OAc)_2$] = $1.4*10^{-3}$ M; [H_2O_2] = 0.14 M; [H_2O] = 0.64 M; P(ethylene) 1 atm, 20 °C, 24 hours (if not indicated otherwise).

Entry	Catalyst (+additives)	Glycol derivatives, %[a] (**EG** : **EGMA** : **EGDA** : **A** : **B**)	TOF_{EG},[b] h^{-1}	Wacker-type products, %[a] (**VA** : **AA**)
1	none	~0.7 (0 : 0.3 : 0.4 : 0 : 0)		0
2	dpk (10 mol.%)[c]	~0.4 (0.3 : 0.1 : 0.2 : 0)		0
3	$Pd(OAc)_2$	8.0 (1.1 : 4.1 : 0.7 : 0.7 : 1.4)	0.33	8.5 (6.0 : 2.5)
4	$Pd(OAc)_2$ K(Medpms) (1 eq.)	6.7 (0.4 : 1.4 : 1.95 : 2.7 : 0.25)	0.28	8.6 (5.2 : 3.4)
5[d]	[$Pd(OAc)_2$] Li(tBudpms) (1 eq.)	16 (2.0 : 12 : 2.0 : 0 : 0)	0.13	19 (17 : 2.0)
6	(dpk)$Pd(OAc)_2$	1.1 (0 : 1.0 : 0.1 : 0 : 0)	0.05	0
7[e]	$Pd(OAc)_2$ dpk (1 equ) (freshly prepared solution)	45.9 (0.4 : 35.7 : 1.65 : 0.6 : 7.6)	1.9	4.8 (0.35 : 4.45)
8[e,f]	$Pd(OAc)_2$ dpk (1 equ)	86.8 (0.7 : 66.7 : 14.4 : 3.1 : 1.9)	2.0	4.4 (0.2 : 4.2)
9	$Pd(OAc)_2$ K(Medpms) (0.5 eq.) dpk (0.5 equ)	61.9 (1.3 : 51.3 : 9.3 : 0 : 0)	2.6	7.0 (3.9 : 3.1)
10	$Pd(OAc)_2$ K(Medpms) (0.5 eq.) dpk (0.5 equ) LiOAc (100 eq.)	87.9 (1.0 : 73.3 : 13.6 : 0 : 0)	3.7	6.1 (5.2 : 0.9)
11	$Pd(OAc)_2$ K(Medpms) (0.5 eq.) dpk (0.5 eq.) NaOAc (100 eq.)	92.8 (0.6 : 77.4 : 14.8 : 0 : 0)	3.93	7.2 (5.8 : 1.4)
12	$Pd(OAc)_2$ K(Medpms) (1 eq.) dpk (1 eq.) [D_2O] = 2.4 M	40.0 (1.3 : 32.2 : 6.5 : 0 : 0)	1.7	9.7 (5.5 : 4.2)

[a] Based on H_2O_2; yield = ([Product]/[H_2O_2])*100%, average of 2 runs. Concentrations were found from ^1H NMR integration *vs.* internal standard, hexamethyldisiloxane.

[b] TOF_{EG} is a turnover frequency of ethylene oxidation to glycol derivatives, calculated as TOF_{EG} =([**EG**]+[**EGMA**]+[**EGDA**]+[**A**]+[**B**])/([$Pd(OAc)_2$]*time)

[c] After 12 hours

[d] [$Pd(OAc)_2$] = $7.2*10^{-3}$ M; [Li(*t*-Budpms)] = $7.2*10^{-3}$ M

[e] Freshly prepared solution containing **7.2**, **7.3** and ligand-free $Pd(OAc)_2$ in av. 1.4 : 1 : 1 ratio

[f] After 43 hours

The pure complex (dpk)$Pd(OAc)_2$ (**7.1**) was inactive in Wacker-type oxidation and was very inefficient in production of glycol acetates (entry 6).

By contrast, freshly prepared solution of the dpk-containing catalyst, obtained by dissolving 1 equivalent dpk in $Pd(OAc)_2$ solution followed by immediate addition of H_2O_2 (<10 minutes after mixing dpk and $Pd(OAc)_2$), provides glycol derivatives in up to 86% yield and 90-95% selectivity depending on the reaction time (entry 7, 24 hours; entry 8, 43 hours). The major products are **EGMA** and **EGDA** in a 5:1 molar ratio; ethylene glycol was present in much smaller amounts.

7.2.2.2 Activity of Freshly Prepared Dpk – $Pd(OAc)_2$ – AcOH Systems

To understand the origin of high activity and selectivity in entries 7-8, in contrast to the catalytically inactive (dpk)$Pd(OAc)_2$ (**7.1**, entry 6), the catalytically active reaction mixtures were analyzed by means of ^{1}H NMR spectroscopy and ESI mass spectrometry. ^{1}H NMR spectrum of a freshly prepared 1.4 mM dpk / $Pd(OAc)_2$ solution in acetic acid containing 100 equivalents of H_2O_2 showed the presence of two peroxoketal-containing species, (dpk*H_2O_2)$Pd(OAc)_2$, **7.2** and [(dpk*H_2O_2)$_2$Pd]$(OAc)_2$, **7.3**, in a 1.4 : 1 molar ratio. Hence, ligand-free palladium acetate was present in solution in the same concentration as **7.3**, with a **7.2** : **7.3** : $Pd(OAc)_2$ ratio being 1.4 : 1 : 1. The **7.2** : **7.3** ratio and, hence, the fraction of $Pd(OAc)_2$ were not constant over time and varied depending on the method of preparation and concentration of the catalyst. Accordingly, catalytic activity and initial reaction rates in such reaction mixtures are not always well-reproducible.

No new complexes were detected by ^{1}H and ESI MS in reaction mixture after the catalyst solutions were exposed to ethylene atmosphere. Peroxoketal complexes **7.2** and **7.3** were the main dpk-derivatives present in solution. After all H_2O_2 was consumed, both peroxoketal complexes **7.2** and **7.3** disappeared, and catalytically inactive complex (dpk)$Pd(OAc)_2$, **7.1** formed as a major product (~80-90%) along with a small amount of the hydrated 2 : 1 complex **7.4**.

To find out which of the components of the catalytically active reaction mixture was responsible for high activity and selectivity toward glycol formation, a series of experiments were performed at various initial **7.2** : **7.3** : $Pd(OAc)_2$ ratios (Table 7.2). The catalysts were obtained by mixing solutions of **7.2**, **7.3** and $Pd(OAc)_2$ prepared independently as described above.

Table 7.2. Activity of dpk/$Pd(OAc)_2$ catalysts containing various initial molar ratios of **7.2**, **7.3** and $Pd(OAc)_2$.

$[Pd(OAc)_2]_{total} = 1.4*10^{-3}$ M; $[H_2O_2]$ =0.14 M; $[H_2O]$ = 0.64 M; P(ethylene) 1 atm; 20 °C; 3 h.

Entry	**7.2** : **7.3** : $Pd(OAc)_2$[a] ratio	Glycol derivatives, %[b] **(EG : EGMA : EGDA : A : B)**	Wacker-type products, %[b] (**VA** : **AA**)
1	0 : 0 : 100	4.2 (0.7 : 1.5 : 0.3: 1.2:0.5)	3.5 (2.5 : 1)
2	100 : 0 : 0	0.22 (0 : 0.2 : 0.02)	0
3	0 : 100 : 0	0	0
4	67 : 0 : 33	10 (0 : 5.4 : 3.0 : 1.6)	7.4 (4 : 3.4)
5	50 : 50 : 0	0.38 (0.35 : 0.03)	0
6	42 : 29 : 29	78 (0 : 67 : 11)	0.8 (0.7 : 0.5)
7	0 : 50 : 50	58 (0 : 51 : 7.3 : 0 : 0)	1.6 (1.0 : 0.6)

[a] Ratio of **7.2** : **7.3** was found by ^{1}H NMR integration; concentration of ligand-free $Pd(OAc)_2$ is calculated as $[Pd(OAc)_2] = [Pd(OAc)_2]_{total} - [\mathbf{7.2}] - [\mathbf{7.3}]$.

[b] Based on H_2O_2; yield = ($[Product]/[H_2O_2]$)*100%, average of 2 runs. Concentrations were found from ^{1}H NMR integration *vs.* internal standard, hexamethyldisiloxane.

Notably, low yield and low reaction selectivity for the glycol derivatives formation were observed when either palladium acetate or bisperoxoketal complex **7.3** were absent (entries 1-5). At the same time, **7.3** alone (entry 3), as well as $Pd(OAc)_2$ alone (entry 1) or in combination with **7.2** (entry 4) were not particularly active or selective toward formation of glycol and its derivatives. Only when both $Pd(OAc)_2$ and **7.3** were present in solution, good yield and selectivity on glycol derivatives were obtained (entries 2 and 7).

The most important limitation of the most active dpk / $Pd(OAc)_2$ catalysts is that upon consumption of H_2O_2 the fast transformation of **7.3** and $Pd(OAc)_2$ to a thermodynamically more stable and catalytically inactive **7.1** occurs so that the catalyst cannot be reused (Scheme 7.9).

Scheme 7.9

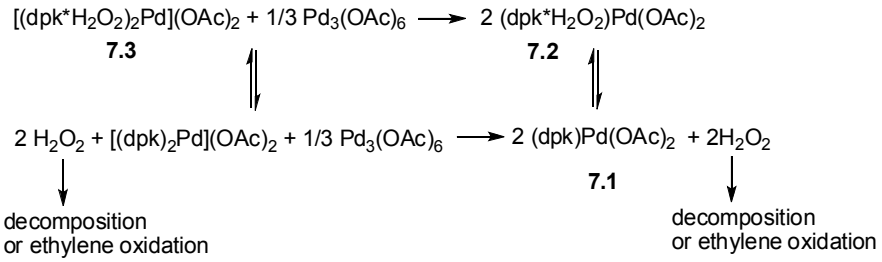

7.2.2.3 Activity of Mixed Ligand Dpk – Dpms – $Pd(OAc)_2$ – AcOH Systems

We next examined reactivity of the dpk – Medpms mixed-ligand catalytic systems, containing $Pd(OAc)_2$, dpk, and K(Me-dpms) in a 1 : 0.5 : 0.5 molar ratio. The catalyst solution was prepared by combining 0.5 equivalent of dpk and 0.5 equivalent of K(Me-dpms) with palladium acetate solution in acetic acid. The resulting mixture was then equilibrated at room temperature or heated at 60 ^{o}C until no further changes were

observed by ^{1}H NMR spectroscopy. The resulting mixed-ligand catalyst showed reproducible catalytic activity, in contrast to the dpk-solely – based system.

Analysis of the equilibrated mixed-ligand catalyst solution by means of ESI mass spectrometry showed the presence of a strong signal characterized by m/z 571.0, assigned to a heteroleptic complex $[(\text{Me-dpms})(\text{dpk*}H_2O)\text{Pd}]^+$ (**7.5**, eq. 7.15), along with the signals of the previously observed 1 : 1 dpk- and Me-dpms complexes. The presence of **7.5** implies that some ligand-free palladium acetate is present in equilibrated solution, according to eq. 7.15.

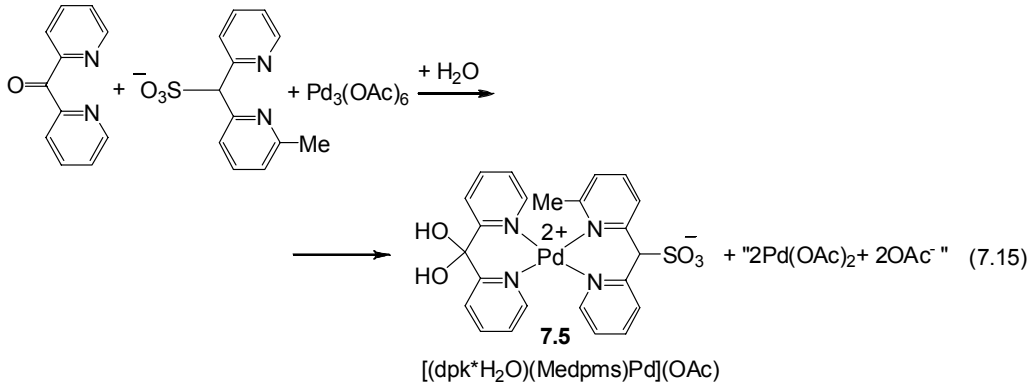

When 1 mol.% of the Me-dpms/dpk/$Pd(OAc)_2$ catalyst prepared as described above was used under typical reaction conditions listed in Table 7.1, the glycol derivatives were obtained with 90% selectivity in 62% yield (entry 9, Table 7.1). A small amount of palladium black formed at the final stages of reaction.

The yields of the glycol products were further increased in the presence of 100 equivalents of LiOAc (entry 10, 88% yield of glycol products) or NaOAc additives (entry 11, 93% yield of glycol products). The possible role of these additives will be studied in future.

When *t*-Bu-dpms ligand was used instead of Me-dpms, the catalyst activity and selectivity were similar to those of the Me-dpms/dpk/$Pd(OAc)_2$ catalyst.

In all the cases the two major reaction products are **EGMA** and **EGDA** formed in a 5 : 1 molar ratio. Ethylene glycol is present in very small amounts (~1%). The **EGMA** : **EGDA** ratio is not affected significantly in the presence of LiOAc (entry 10), NaOAc (entry 11), or water additives (entry 12).

When a Me-dpms : dpk molar ratio of more than 1 :1 was used, formation of insoluble complex was observed, presumably [$(Me\text{-}dpms)_2Pd$], which was less catalytically active and selective than the catalyst mixtures containing equal amounts of Me-dpms and dpk. In turn, decreasing a Me-dpms : dpk ratio to 1 : 2, while keeping a (dpk + Me-dpms) : Pd ratio the same (1 : 1), leads to a slightly decreased catalytic activity and selectivity of the resulting catalyst.

In summary, the mixed-ligand dpms-dpk system allows one to utilize efficiently 30% aqueous H_2O_2 as the oxidant for selective transformation of ethylene into glycol acetates without noticeable loss of the catalytic activity over time.

7.2.3 Kinetics of Glycol Esters Formation in Mixed-Ligand dpk/Me-dpms/$Pd(OAc)_2$ System

To gain insight into the mechanism of the glycol ester formation in the dpk – Me-dpms – $Pd(OAc)_2$ – AcOH system, a kinetic study of ethylene oxidation with H_2O_2 was performed. First, the reaction orders were determined by measuring the initial rates of formation of all glycol derivatives at various initial concentrations of H_2O_2, $Pd(OAc)_2$ and ethylene in a mixed-ligand system dpk : K(Medpms) : $Pd(OAc)_2$ in a 0.5 : 0.5 : 1 molar ratio. The kinetics of the reaction was well reproducible for several runs. The established rate law is given by eq. 7.16a. The second order rate constant was determined to be $(9.95 \pm 0.95)*10^{-3}$ $M^{-1}s^{-1}$.

$$\frac{d[\text{glycols}]}{dt} = V_{EG} = k[\text{Pd(OAc)}_2][\text{ethylene}] \qquad (7.16a)$$

where [glycols] = [**EG**] + [**EGMA**] + [**EGDA**] + [**A**] + [**B**]

$$\frac{d[\text{VA} + \text{AA}]}{dt} = V_W \qquad (7.16b)$$

The rate of formation of the glycol derivatives, V_{EG}, is zeroth order in H_2O_2, suggesting that the oxidation with H_2O_2 occurs after the rate-limiting step. Notably, the rate of formation of the Wacker-type products, vinyl acetate and acetaldehyde, V_W (eq. 7.16b), is 1st order in ethylene, but has a complex dependence on H_2O_2 and $Pd(OAc)_2$ concentrations.

Representative initial rates of formation of the glycol derivatives, $V_{0,EG}$, and initial rates of the Wacker products formation, $V_{0,W}$, in a mixed-ligand system and a ligand-free palladium acetate solution are given in Table 7.3.

Table 7.3. Initial rates of the formation of glycol derivatives ($V_{0,EG}$) and Wacker-type products ($V_{0,W}$). [$Pd(OAc)_2$] = 1.4*10^{-3} M, [H_2O_2] = 0.14 M, T = 20 ^{o}C, P(ethylene) 1 atm, [H_2O] = 0.64 M.

Catalyst	$V_{0,EG}$*10^{7}, M/s	$V_{0,W}$*10^{7}, M/s
K(Me-dpms) : dpk : $Pd(OAc)_2$ (in a 0.5 : 0.5 : 1 ratio)	12.2±1.2	2.00±0.26
$Pd(OAc)_2$	4.29±0.26	4.20±0.62

As can be seen from Table 7.3, formation of glycol derivatives is accelerated and formation of vinyl acetate and acetaldehyde is slightly suppressed in a mixed-ligand dpk/Me-dpms/$Pd(OAc)_2$ system, compared to the system with palladium acetate alone.

Interestingly, the selectivity of ethylene oxidation depends on concentrations of $Pd(OAc)_2$ and H_2O_2. The ratio of initial rates $V_{0,EG}$ / $V_{0,W}$ increases at higher concentrations of $Pd(OAc)_2$ and lower concentrations of H_2O_2 (Table 7.4).

Table 7.4. The ratio of the initial rates of the formation of glycol derivatives (V_{EG}) and Wacker-type products ($V_{0,W}$) at various concentrations of $Pd(OAc)_2$ and H_2O_2.[a]

$[Pd(OAc)_2]$, mM	$[H_2O_2]$, M	av. $V_{0,EG}/V_{0,W}$
1.4	0.14	6.1
2.9	0.14	10.0
4.3	0.14	11.9
1.4	0.072	11.7
1.4	0.036	10.1

[a] dpk : K(Medpms) : $Pd(OAc)_2$ = 0.5 : 0.5 : 1 (moles), 20 ^oC, P(ethylene) 1 atm, $[H_2O]$ = 0.64 M.

7.2.4 Possible Mechanisms of Ethylene Oxidation

The Wacker-type products, vinyl acetate and acetaldehyde, are observed in all reaction mixtures studied here except for these from catalysis by (dpk)$Pd(OAc)_2$, which showed marginal catalytic activity (Table 7.1, entry 6). While the formation of vinyl acetate might proceed via acetoxypalladation/β-hydride elimination route (Scheme 7.1) or, alternatively, via oxygen atom transfer from a peroxopalladium(II) complex (Scheme 7.4), acetaldehyde might result from a direct Wacker oxidation of ethylene in wet acetic acid or palladium-catalyzed hydrolysis of vinyl acetate (eq. 7.17).[208, 212]

$$H_2C{=}CHOAc + H_2O \xrightarrow{Pd^{II}} H_3C{-}CHO + HOAc \qquad (7.17)$$

Since the most active of our catalysts contains ligand-free palladium acetate, it is worth to briefly review what is known about the mechanism of ethylene oxidation in $Pd(OAc)_2$ – AcOH systems.

The mechanisms of ethylene oxidation to vinyl acetate and acetaldehyde in the presence of palladium acetate have been studied extensively over the past several decades.[208] It has been proposed that the active species responsible for ethylene activation is a dinuclear acetate complex $[Pd_2(OAc)_6]^{2-}$ (**7.6**) that forms from a less reactive trimer $Pd_3(OAc)_6$ in the presence of alkali metal acetates (eq. 7.18, Scheme 7.10).[223, 224] Henry *et al.* have found that palladium acetate dimer reacts rapidly with ethylene to produce a dinuclear product with a terminal ethylene ligand, **7.7**, which was detected spectrophotometrically (eq. 7.19).[225] An equilibrium leading to a monomeric ethylene complex **7.8** is much slower (eq. 7.20). Complex **7.7** was proposed to be the active species in ethylene acetoxypalladation leading to β-acetoxyethyl complex **7.9** (eq. 7.21).[208, 225] It has been established that β-hydride elimination from **7.9** is slower than the reversible acetoxypalladation step.[208]

Scheme 7.10

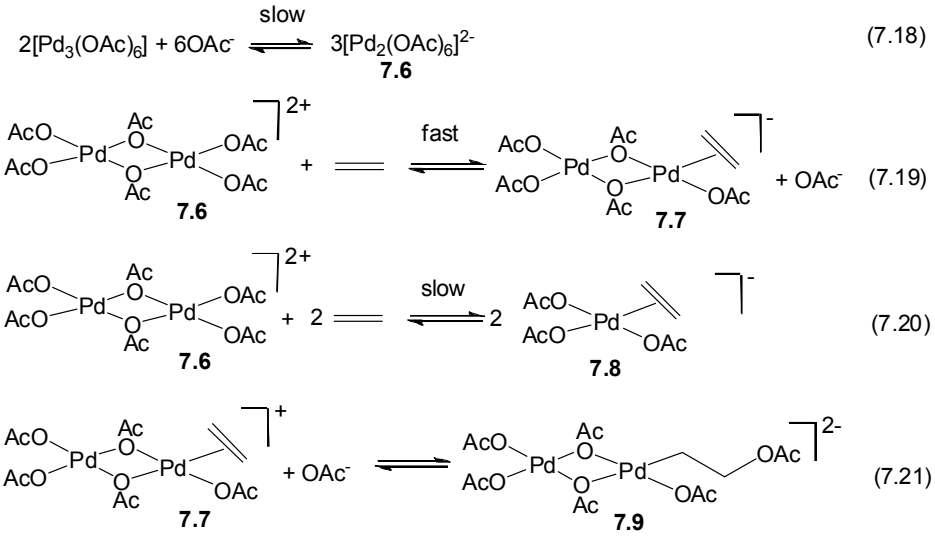

Interestingly, the rate of ethylene coordination to palladium could be qualitatively estimated in some of our systems using ^{1}H NMR spectroscopy.

A broadening of the ^{1}H NMR signal of ethylene (half-width 9.3 Hz) was observed in solutions of ligand-free palladium acetate solution in CD_3COOD. This fact suggests an existence of a ligand exchange equilibrium involving free and Pd^{II}-coordinated ethylene that is fast on the NMR time scale.

Slight broadening of the ethylene peak was also observed in solutions of catalytically active dpk- or dpk/Me-dpms-systems containing ligand-free $Pd(OAc)_2$ (half-width *ca* 2.5 Hz). By contrast, in solutions of catalytically inactive complexes **7.1**, **7.2** or **7.3** a sharp singlet of free ethylene remained unchanged compared to the ethylene solutions in the absence of palladium (half-width 0.8 Hz). No new resonances were seen that might be assigned to a metal-coordinated ethylene. All together, these observations suggest that a possible reason for negligible activity of complexes **7.1**, **7.2** and **7.3** in ethylene oxidation might be their kinetic inertness in acetate-for-ethylene ligand substitution at the metal center.

Based on these observations, we propose that in dpk/Me-dpms mixed-ligand catalytic systems initial activation of ethylene occurs via a coordination to a ligand-free palladium acetate (eq. 7.18-7.21). A subsequent substitution of acetate ligands in **7.9** for dpk or Me-dpms (or alkyl ligand transfer from **7.9** to **7.1**) might take place to give $LPd(CH_2CH_2OAc)(OAc)$, **7.10** (L = Me-dpms, dpk).[87] The source of the ligand L in the formation of **7.10** from **7.9** might be a 2:1 complex $[(dpk)_2Pd]^{2+}$ or $[(dpk*H_2O)(Medpms)Pd]^+$ **7.5**, since the catalytic activity and selectivity was low in the absence of these complexes (for example, see entries 1-2 and 4 in Table 7.2).

Based on the analogy with reactivity of $(dpms)Pt^{II}(Alkyl)$ complexes towards oxidation described in Chapters 2 and 3, we propose that the dpk and Me-dpms

ligands facilitate the oxidation of **7.10** with H_2O_2 or peracetic acid (eq. 7.14) to produce a corresponding alkyl Pd^{IV} complex **7.11** (eq. 7.22). Monoalkyl Pd^{IV} complexes are unknown and are expected to be very electrophilic.[226] Subsequent reductive elimination from **7.11** via either an S_N2[35] or direct C-O reductive elimination mechanism[78] yields glycol esters and a Pd^{II} complex (eq. 7.23).

Scheme 7.11

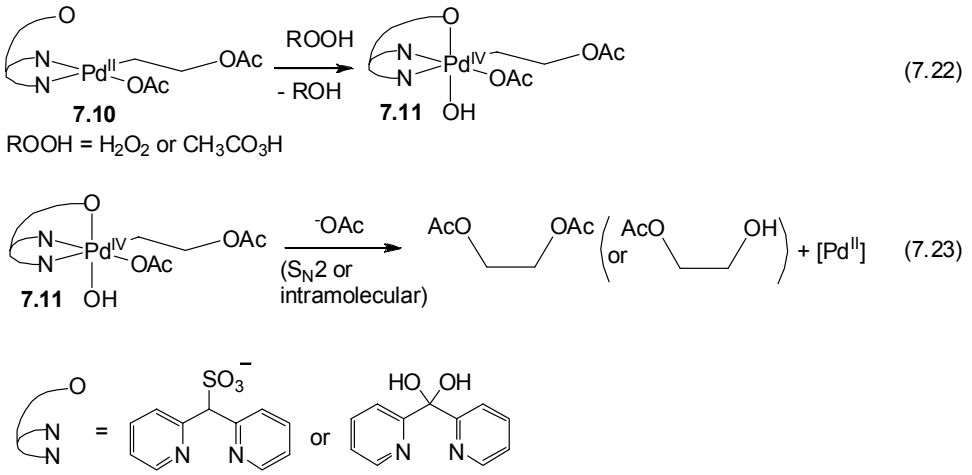

If so, the reactions in eq. 7.22-7.23 are not homolytic since the rate of ethylene oxidation catalyzed by a mixed-ligand system, dpk/Me-dpms/$Pd(OAc)_2$ (0.5 : 0.5 : 1) is not influenced by the addition of a radical inhibitor such as 2,6-di-*tert*-butyl-*p*-cresol.

Although no experimental evidence was obtained for involvement of Pd^{IV} complexes in our systems, formation of spectroscopically characterized Pd^{IV} products by oxidation of $LPd^{II}(R')(R'')$ (L = tmeda, bpy; R′=Me, R″=Tol) with benzoyl peroxide at low temperatures has been previously reported by Canty.[226] The intermediacy of Pd^{IV} species has also been proposed in some other Pd^{II}-mediated oxidative transformations utilizing H_2O_2, peroxoesters or dibenzoylperoxide as oxidants.[226-228]

The absence of detectable amounts of intermediates **7.10** or **7.11** during the course of the reaction could be explained by the virtue of the fast ligand-enabled oxidation and reductive elimination steps. This suggestion is also consistent with the observed zeroth order of the rate of glycol esters formation in H_2O_2 concentration.

The proposed reaction mechanism of the ethylene oxidation to ethylene glycol acetates in dpk – Me-dpms – $Pd(OAc)_2$ – AcOH systems is summarized in Scheme 7.12 for glycol diacetate formation; ethylene glycol monoacetate might form via a similar mechanism including a direct C-OH elimination from **7.11** or an S_N2 attack by water.

Scheme 7.12

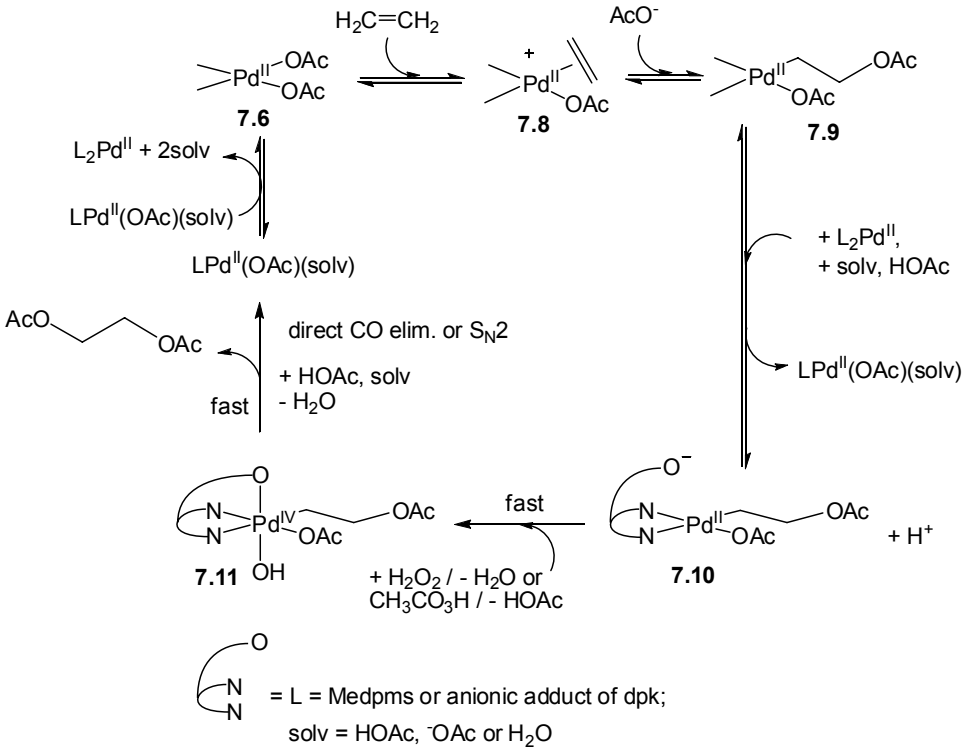

7.3 Conclusions

Efficient catalytic systems for selective oxidation of ethylene with H_2O_2 to glycol acetates were developed. The catalyst consists of a mixture of "free" palladium acetate and derived dpk and Me-dpms complexes. Glycol acetates were obtained in high yields (~90% yield based on H_2O_2) and selectivities (>90%) under mild reaction conditions (1 atmosphere of ethylene, 20^0C) with 1 mol.% catalyst loading. In the absence of ligand additives, the reaction is inefficient in terms of utilization of H_2O_2 and unselective producing mostly vinyl acetate and acetaldehyde in low yield.

By analogy with (dpms)Pt^{II}(Alkyl) complexes, we propose that high selectivity and activity of our systems in the formation of glycol acetates is due to facile dpk- or dpms enabled functionalization of Pd^{II} alkyl intermediates via Pd^{IV} species.

Future development of this work might include ligand structural modifications in order to utilize O_2 in these transformations. It would also be important to increase the scope of substrates for olefin oxidation. Preliminary studies showed that propylene is oxidized with 80% selectivity to isomeric propylene glycol acetates in the presence of dpk/Me-dpms/$Pd(OAc)_2$ catalyst under non-optimized reaction conditions. Further mechanistic studies are also necessary.

7.4 Experimental Section

Preparation of (dpk)$Pd(OAc)_2$, 7.1. In an argon atmosphere, 20 mL of degassed acetic acid was added to a 100 ml Schlenk flask equipped with a magnetic stirring bar. A sample of $Pd_3(OAc)_6$ (200 mg, 0.891 mmol of Pd^{II}) was added to the acetic acid and was allowed to stir overnight in a silicon oil bath at 60 °C. Di-2-

pyridylketone (dpk) (150.7 mg, 0.852 mmol) of was then added to the dissolved $Pd(OAc)_2$ under argon flow. The (dpk)$Pd(OAc)_2$ complex was left to stir overnight. Brown color of palladium acetate solution slowly faded away to give light yellow solution of **7.1**. The acetic acid was evaporated off, and the product was allowed to dry under vacuum. Then 10-15 ml of methylene chloride was added to the crude product. Then the same portion of ether was added causing the product to precipitate. The solution was filtered under vacuum leaving a pale yellow precipitate. The product was rinsed with ether and then pentane. The mass of the purified product was 297.4 mg giving a yield of 85%.

^{1}H NMR ($CDCl_3$, 22 ^{o}C), δ: 1.98 (s, 6H), 7.65 (ddd, *J*=7.7, 5.4, 2.0 Hz, 2H), 8.15-8.20 (m, 4H); 8.88 (d, *J*=5.4 Hz, 2H). ^{1}H NMR (CD_3COOD, 22 ^{o}C), δ: 2.10 (s, 6H), 7.82 (ddd, *J*=7.0, 5.5, 2.7 Hz, 2H), 8.26-8.31 (m, 4), 8.77(d, *J*= 5.5 Hz, 2H). **^{13}C NMR** (CD_3COOD, 22 ^{o}C), δ: 128.4, 130.5, 142.4, 149.1, 153.5, 182.2(PdOAc), 185.2(dpk C=O). **IR** (KBr), ν: 3117 (w), 3097 (w), 3050 (w), 1714 (m), 1694 (m), 1633 (m), 1577 (s), 1436 (m), 1363 (s), 1313 (s), 1302 (s), 1246 (s), 1038 (m), 1016 (m), 939 (m), 818 (m), 757 (s), 691 (s), 669 (s) cm^{-1}. **ESI- MS** of solution of **7.1** in CH_3COOH/H_2O (1:1 v/v), m/z 349.0, 367.0, corresponding to $[M\text{-}OAc]^+$ (calculated for $C_{13}H_{11}N_2O_3{}^{106}Pd$, 349.0) and $[M\text{-}OAc+H_2O]^+$ (calculated for $C_{13}H_{13}N_2O_4{}^{106}Pd$, 367.0) respectively. ESI- MS of solution of **7.1** prepared in CD_3COOH and diluted with H_2O (1:1 v/v), m/z 352.0, 370.0, corresponding to $[(dpk)Pd(CD_3COO)]^+$ and $[(dpk*H_2O)Pd(CD_3COO)]^+$ respectively.

Preparation of (dpk*H_2O_2)Pd$(OAc)_2$, 7.2, in acetic acid solution. A sample of **7.1** (28.0 mg, 0.069 mmol) prepared as described above was dissolved in 0.8 ml of acetic acid, [**7.1**]=0.086 M. Aqueous 30 wt.% solution of H_2O_2 was added by 5-10 μL portions and ^{1}H NMR spectra were recorded periodically. Complexes **7.1** and **7.2** were the only dpk-containing detected in solution by ^{1}H NMR. Concentrations of **7.1** and **7.1** as a function of added H_2O_2 are given below.

$[H_2O_2]$, M	Time, h	[**7.1**], mM	[**7.2**], mM
0.12	0.1	10	76
0.12	2.0	10	76
0.18	2.3	6.0	80
0.31	3.7	3.0	83

Complex **7.2** was characterized by NMR and ESI immediately after its preparation: **^{1}H NMR** (CD_3COOD, 22 ^{o}C), δ: 2.07 (s, 6H), 7.55 (ddd, *J*=7.8, 5.5, 1.3 Hz; 2H), 8.09 (t, *J*=7.6Hz; 2H), 8.15 (d, *J*=7.6Hz; 2H), 8.61 (d, J=5.5; 2H). **^{13}C NMR** (CD_3COOD, 22 ^{o}C), δ: 105.4, 125.5, 127.4, 141.8, 153.2, 154.9, 182.7(PdOAc). **ESI-MS** of solution of **7.2** in CH_3COOH/H_2O (1:1 v/v), m/z 383.0, corresponding to $[M\text{-}OAc]^+$ (calculated for (dpk*H_2O_2)Pd$(OAc)^+$, $C_{13}H_{11}N_2O_3{}^{106}$Pd, 383.0). ESI- MS of solution of **7.3** prepared in CD_3COOH and diluted with H_2O (1 : 1 v/v), m/z 386.0, corresponding to $[$(dpk*H_2O_2)Pd$(CD_3COO)]^+$.

Stability of acetic acid solution of (dpk*H_2O_2)Pd$(OAc)_2$, 7.2. A sample of **7.1** (28.3 mg, 0.069 mmol) was dissolved in 0.8 ml of acetic acid; 10 μL (0.098 mmol, 1.4 equiv.) of H_2O_2 was added. A mixture of **7.2** and **7.1** was detected in solution immediately after addition of H_2O_2 in 91 : 9 molar ratio. The solution was allowed to stand at 20 ^{o}C and was periodically analyzed by ^{1}H NMR. Non-1st order

decomposition of **7.2** was observed that led to disappearance of **7.2** and formation of **7.1**. The **7.2** and **7.1** were present in solution in 77 : 17 ratio after 30 days at 20 ^{o}C. After 70 hours **7.2** has completely disappeared and **7.1** was recovered in 84% yield.

Time, h	[7.2], M	[7.1], M
0	0.079	0.0075
5.3	0.073	0.0096
17.3	0.067	0.015
30.2	0.049	0.031
42.5	0.026	0.052
68.7	0.000	0.073

Preparation of [(dpk*H_2O_2)$_2$Pd](OAc)$_2$, 7.3. A solution of $Pd_3(OAc)_6$ (15.9 mg, 0.071 mmol of Pd^{II}) in 0.8 ml of CD_3COOD was prepared by heating at 80 ^{o}C in CD_3COOD. The solution was cooled down to room temperature, and then dpk was added in one portion (26.6 mg, 0.144 mmol). The resulting solution was allowed to stir for 10 minutes. Once dpk dissolved, 30 wt.% H_2O_2 solution was added (25 μL, 0.245 mmol). Brown color of palladium acetate trimer disappeared after several minutes to give a pale yellow solution of **7.3** in quantitative yield by ^{1}H NMR. The solution of **7.3** was characterized by NMR and ESI immediately after its preparation.

^{1}H NMR (CD_3COOD, 22 ^{o}C), δ: 2.07(s, 6H), 7.59 (ddd, *J*=7.9, 5.5, 1.2 Hz, 4H), 8.28 (td, *J*=7.9,1.1 Hz, 4H), 8.35(d, *J*=5.5 Hz, 4H), 8.47(dd, *J*= 7.9, 1.2 Hz, 4H).

^{13}C NMR (CD_3COOD, 22 ^{o}C), δ: 105.53, 126.73, 128.60, 143.38, 153.15, 156.10.

ESI-MS of solution of **7.3** in CH_3COOH/H_2O (1 : 1 v/v): m/z 237.0 ($[(dpk)_2Pd]^{2+}$, calc. $[C_{22}H_{16}N_4O_2{}^{106}Pd]^{2+}$ 237.0), m/z 255.0 ($[(dpk*H_2O)_2Pd]^{2+}$, calc. $[C_{22}H_{20}N_4O_4{}^{106}Pd]^{2+}$ 255.0) and m/z 509.0 $[(dpk*H_2O)(dpk*OH)Pd]^{+}$, calc.

$[C_{22}H_{19}N_4O_4{}^{106}Pd]^+$ 509.0). No ions that could correspond to $[(dpk*H_2O_2)_2Pd]^{2+}$ were detected.

Preparation of $[(dpk\text{-}D_2O)_2Pd](OAc)_2$ (7.4) in D_2O-CD_3COOD solution. The dpk (25.6 mg, 0.139 mmol) was added to a solution of palladium acetate (15.4 mg,0.069 mmol) in 0.8 mL of CD_3COOD. The solution was stirred at 20 ^oC for 10 hours, and then 100 μL (5.53 mmol) of D_2O was added. After 1-2 hours after mixing with D_2O, **7.4** formed in 83% yield by ^1H NMR. Other unidentified dpk-containing products were present.

^1H NMR (CD_3COOD, 22 ^oC), δ: 2.07(s, 6H), 7.57 (ddd, *J*=7.9, 5.5, 1.4 Hz, 4H), 8.27 (td, J=7.9,1.4 Hz; 4H), 8.34 (d, *J*=5.5 Hz; 4H); 8.36(d, *J*= 7.9 Hz, 4H).

^{13}C NMR (CD_3COOD, 22 ^oC), δ: 105.53, 126.73, 128.60, 143.38, 153.15, 156.10.

^1H NMR (CD_3COOD, 22 ^oC), δ: 2.07(s, 6H), 7.59 (ddd, *J*=7.9, 5.5, 1.2 Hz, 4H), 8.28 (td, *J*=7.9,1.1 Hz, 4H), 8.35(d, *J*=5.5 Hz, 4H), 8.47(dd, *J*= 7.9, 1.2 Hz, 4H).

^{13}C NMR (CD_3COOD, 22 ^oC), δ: 105.53, 126.73, 128.60, 143.38, 153.15, 156.10.

ESI-MS of solution of **7.4** in CH_3COOH/H_2O (1 : 1 v/v): m/z 237.0 ($[(dpk)_2Pd]^{2+}$, calc. $[C_{22}H_{16}N_4O_2{}^{106}Pd]^{2+}$ 237.0), m/z 255.0 ($[(dpk*H_2O)_2Pd]^{2+}$, calc. $[C_{22}H_{20}N_4O_4{}^{106}Pd]^{2+}$ 255.0) and m/z 509.0 $[(dpk*H_2O)(dpk*OH)Pd]^+$, calc. $[C_{22}H_{19}N_4O_4{}^{106}Pd]^+$ 509.0). No ions that could correspond to $[(dpk*H_2O_2)_2Pd]^{2+}$ were detected.

Standard procedure for oxidation of ethylene with H_2O_2 in CD_3COOD solution (Table 7.1). The catalyst solutions were equilibrated for 2-3 days at 20 ^oC before use,

if not indicated otherwise. 12 μL of 30% aq. H_2O_2 was added to 0.8 mL of the catalyst solution, and the resulting mixture was transferred with a Teflon syringe into a 25 mL Schlenk flask equipped with a magnetic stirring bar, pre-filled with ethylene and connected to an ethylene-filled Schlenk line. The reaction mixtures were thermostated at 20 ^{o}C and stirred vigorously for 24 h under an ambient pressure of ethylene. In a typical experiment the following concentrations were used: $[H_2O_2]$=0.14 M; $[H_2O]$=0.64 M; $[Pd(OAc)_2]$=1.4 mM (1 mol.%); anhydrous LiOAc or NaOAc were added if necessary. After 24h a sample of the reaction mixture was mixed with a pre-weighed amount of the standard solution (45 mM hexamethyldilisoxane in CD_3COOD). Averages of at least two runs are reported in Table 7.1.

Concentrations of vinyl acetate (**VA**), ethylene glycol diacetate (**EGDA**), 1-hydroxyethyl acetate (**EGMA**), ethylene glycol (**EG**), product **A**, product **B** and acetaldehyde were calculated based on integration of a multiplet at 4.57 ppm, singlet at 4.27 ppm, multiplet at 4.18 ppm, singlet at 4.27 ppm, multiplet at 3.87 ppm, multiplet at 4.11 ppm and quartet at 9.70 ppm respectively, using hexamethyldisiloxane peak as an internal standard.

Formation of significant amounts of palladium black was observed in the absence of ligands and in Li(*t*-Budpms) (1 equiv.)-$Pd(OAc)_2$ (entry 6, Table 7.1) and K(Medpms)(1 equiv.)-$Pd(OAc)_2$ (entry 5, Table 7.1) solutions; a small amount of palladium black was observed in the mixed-ligand catalysts K(Medpms)-dpk-$Pd(OAc)_2$ (entries 10-13, Table 7.1) and in freshly prepared dpk (1 equiv.)-$Pd(OAc)_2$

solutions (entries 8-9, Table 7.1). No palladium black was seen in the presence of $(dpk)Pd(OAc)_2$.

Ethylene glycol (EG): ^{1}H NMR (CD_3COOD, 22 ^{o}C), δ: 3.75 (s).

1-Hydroxyethyl acetate (EGMA): ^{1}H NMR (CD_3COOD, 22 ^{o}C), δ: 3.82 (m, AA' XX', 1H), 4.18 (m, AA' XX', 1H). ESI-MS of the sample of the reaction mixture dissolved in CH_3COOH, m/z 108.1. Calculated for $C_4H_6D_3O_3$, 108.1.

Ethylene glycol diacetate (EGDA): ^{1}H NMR (CD_3COOD, 22 ^{o}C), δ: 4.27 (s). ESI-MS of the sample of the reaction mixture dissolved in CH_3COOH, m/z 153.1. Calculated for $C_6H_5D_6O_4$, 153.1.

Acetaldehyde (AA): ^{1}H NMR (CD_3COOD, 22 ^{o}C), δ: 2.18 (d, *J*=3.0 Hz, 3H), 9.70 (q, *J*=3.0 Hz, 1H).

H_2O_2-adduct of acetaldehyde was observed in solutions of acetaldehyde in CD_3COOD containing H_2O_2; when H_2O_2 is not present, it converts to acetaldehyde quantitatively; conversely, upon addition of H_2O_2 to acetaldehyde solution partial conversion of acetaldehyde into H_2O_2-adduct is observed. ^{1}H NMR (CD_3COOD, 22 ^{o}C), δ: 1.27 (d, *J*=5.6 Hz, 3H), 5.30 (q, *J*=5.6 Hz, 1H). ESI-MS of the sample of the reaction mixture dissolved in CH_3COOH, m/z 79.0. Calculated for $C_2H_7O_3$, 79.0.

Vinyl acetate (VA): ^{1}H NMR (CD_3COOD, 22 ^{o}C), δ: 4.57 (dd, *J*=6.2, 1.4 Hz, 1H), 4.87 (dd, *J*=14.0, 1.4 Hz, 1H), 7.27 (dd, *J*=14.0, 6.2 Hz, 1H). ESI-MS of the sample of the reaction mixture dissolved in CH_3COOH, m/z 90.1. Calculated for $C_4H_4D_3O_2$, 90.1.

Product A was assigned as HO-CH_2-CH_2-OOAc-d_3 based on ^{1}H NMR.

^{1}H NMR (CD_3COOD, 22 ^{o}C), δ: 3.87 (m, AA' XX', 1H), 4.04 (m, AA' XX', 1H)

Product B, was assigned as AcO-CH_2-CH_2-OOAc-d_6 based on ^{1}H NMR.

^{1}H NMR (CD_3COOD, 22 ^oC), δ: 4.11 (m, AA'XX', 1H), 4.31 (m, AA' XX', 1H).

ESI-MS of the sample of the reaction mixture dissolved in CH_3COOH, m/z 169.1. Calculated for $C_6H_5D_6O_5$, 169.1.

Peroxo-products **A**, **B** and H_2O_2-adduct of acetaldehyde disappeared in the presence of peroxide-reducing additives, NaI, $SnCl_2$ and $Na_2S_2O_5$, to produce equivalent amounts of **EG**, **EGMA** and **AA**, according to ^{1}H NMR integration *vs.* HMDS as an internal standard. In the absence of reducing additives, slow decomposition occurred in the presence of Pd^{II} complexes during the course of 1-2 days at 20 ^oC.

Freshly prepared solutions of (dpk)-$Pd(OAc)_2$ used in entries 8 and 9 of Table 7.1 were prepared as follows. 14 mM palladium acetate solution in CD_3COOD (0.8 mL) was quickly combined with 12 μL H_2O_2 and 2.1 mg dpk. The resulting solution was diluted with 0.72 mL of CD_3COOD and then additional 11 μL of 30% H_2O_2 were added. According to ^{1}H NMR, complexes **7.3** and **7.2** were present in solution in ~ 1 : 1.4 average ratio respectively. ESI of the analogous solution prepared in CH_3COOH, m/z 349.0 ((dpk)Pd(OAc)$^+$), 367.0 ([(dpk*H_2O)Pd(OAc)]$^+$), 383.0 ([(dpk*H_2O_2)Pd(OAc)]$^+$), 237.0 ([$(dpk)_2Pd$]$^{2+}$), 263.0 ([(dpk*OH_2)(dpk*H_2O_2)Pd]$^{2+}$), 509.0 ((dpk*OH_2)(dpk*OH)Pd$^+$), 525.0 ((dpk*H_2O_2)(dpk*OH)Pd$^+$).

Appendix

General specifications

All manipulations were carried out under purified argon using standard Schlenk and glove box techniques. All reagents for which synthesis is not given were commercially available from Aldrich, Acros or Pressure Chemical and were used as received without further purification. Water-^{18}O with the isotopic composition of 97.9% of ^{18}O, 0.5% ^{17}O and 1.6% of ^{16}O from the Cambridge Isotope Laboratories was used as received. DMSO-d_6, CD_2Cl_2 and CD_3OD were purchased from Cambridge Isotope Laboratories were dried over CaH_2, vacuum-transferred and stored in Teflon-sealed flasks in an argon-filled glove box. K(dpms), K[(dpms)$PtMe_2$] and (dpms)$Pt^{IV}Me_2H$ were synthesized as described previously.[29] Zeise's salt $K[PtCl_3(CH_2CH_2)]\cdot H_2O$,[92] *cis*-cyclooctene oxide (**4.12a**),[229] 2,3-*exo*-epoxynorbornene (**4.12b**),[230] benzonorbornadiene-2,3-*exo*-oxide (**4.12c**)[231] and 1,4-epoxy-2,3-epoxy-1,4-dihydronaphthalene (**4.12d**)[145] were prepared according to the literature procedures. ^{1}H (400 MHz) and ^{13}C NMR (125 MHz) and 2D NMR spectra were recorded on a Bruker AVANCE 400, Bruker DRX-500 and Bruker AVANCE-600 spectrometers. Chemical shifts are reported in ppm and referenced to residual solvent resonance peaks. The assignment of proton and carbon resonances was made from NOE, DEPT, 2D ^{1}H-^{1}H COSY and 2D ^{1}H-^{13}C HSQC NMR experiments. Abbreviations for the multiplicity of NMR signals are s (singlet), d (doublet), t (triplet), q (quartet), m (multiplet), br (broad). IR spectra were recorded on a JASCO FT/IR 4100 spectrometer. Abbreviations for IR signal intensities are s (strong), m (medium), w (weak), v (very), br (broad). Elemental analyses were carried out by the Chemisar Laboratories Inc., Guelph, Canada. ESI-MS experiments were performed using the JEOL AccuTOF-CS instrument. GC/MS experiments were performed using the JEOL JMS-SX 102A instrument.

Computational details. Theoretical calculations in this work have been performed using density functional theory (DFT) method,[232] specifically functional PBE,[233] implemented in an original program package "Priroda".[234, 235] In PBE calculations relativistic Stevens-Basch-Krauss (SBK) effective core potentials (ECP)[236, 237] optimized for DFT-calculations were used. Basis set was 311-split for main group elements with one additional polarization *p*-function for hydrogen, additional two polarization *d*-functions for elements of higher periods. Full geometry optimization has been performed without constraints on symmetry. For all species under investigation frequency analysis has been carried out. All minima have been checked for the absence of imaginary frequencies.

Chapter 2

Effect of NaOH additives on the rate of oxidation of $LPt^{II}Me(OH_2)$ (2.1) by O_2 (Table 2.1).

A sample of **2.1** (99.8, 209 μmol) was dissolved in 12.14 g (10.99 mL) of deaerated D_2O under an argon atmosphere; [**2.1**]=19.0 mM. The stock solution was placed into 50 mL Schlenk tube and stored

under argon in a refrigerator. For preparation of alkaline reaction mixtures, a sample of standardized 0.100 M NaOH (200-800 mg) was slowly evaporated to dryness under vacuum and dissolved in 2.1 mL of the 19.0 mM **2.1** stock solution. ^{1}H NMR spectra were recorded before reaction with O_2 and then in regular intervals.

Three samples (0.7 mL each) of the reaction mixture were placed into 10 mL screw-cap vials equipped with magnetic stirring bars. The vials were filled with O_2 and securely capped. Each solution was stirred under an O_2 atmosphere at room temperature. After 1h, samples were placed into NMR tubes, and ^{1}H NMR spectra were recorded immediately. Yields of *unsym*-LPt^{IV}Me(OH)$_2$ and *unsym*-LPt^{IV}Me$_2$(OH) were calculated as an average of three runs by integrating the central line of the PtMe peak at 2.4 ppm and 1.7 ppm respectively (Table 2.1).

Kinetics of the C-O elimination from 2.11 in acidic aqueous solutions (Table 2.4, Fig. 2.15).

60 mM and 120 mM HBF_4 solutions were prepared by dissolving 141.9 mg and 225.2 mg of HBF_4 (50% by mass) in 13.5 mL (14.9751 g) and 10.6 mL (11.6868 g) of D_2O, respectively. The following procedure was used for all kinetic experiments. A sample of **2.11** (3.6-16.1 mg, 7.3-33 μmol) was dissolved in 0.8-1.6 mL of 60 mM or 120 mM solution of HBF_4 in D_2O. The solutions were placed in NMR Young tubes and Teflon-sealed. ^{1}H NMR spectra were recorded before heating to determine the ratio of signals of the complex to HOD used as an internal standard. The tubes were placed in an 80 ^{o}C heating bath. Periodically the tubes were removed, cooled down with ice water and ^{1}H NMR spectra were recorded. The observed rate constants of disappearance of complexes **2.11**+**2.11a**, k_{obs}, (Fig. 2.16, Table 2.4) were determined from the rates of disappearance of a central line of PtMe signal of **2.11** at 2.7-2.8 ppm.

Me$_2$O, **^{1}H NMR** (D_2O, 22 ^{o}C), δ: 3.18 (s). **ESI** mass spectrum after 100 fold dilution with H_2O, $(m+H^+)/z$ = 47.042. Calculated for C_2H_7O, 47.04969.

C-O elimination from 2.11 and 2.11-d_3 in acidic $H_2{}^{18}O$ (Tables 2.2, 2.3). A solution of complex **2.11** (17.0 mg, 34.5 μmol) and 10.0 mg of 50% HBF_4 in 987 mg of $H_2{}^{18}O$ ($[H^+]$=63 mM; [Pt]=38 mM) was placed in a NMR tube, securely capped and heated in an oil bath at 80 ^{o}C. A 0.10 mL sample was picked up with a syringe before the heating began. The mixture was periodically sampled during the reaction. The composition of the mixture was analyzed using ESI-MS to determine the Me^{18}OH/Me^{16}OH ratio and by ^{1}H NMR to determine conversion of the starting complex. No methanol was detected in the solution before the reaction.

ESI-MS, $CH_3{}^{16}OH_2^+$, m/z = 33.03176, calc 33.03404; $CH_3{}^{18}OH_2^+$, m/z = 35.03557, calc 35.03834. $CD_3{}^{16}OH_2^+$, m/z = 36.05450, calc 36.05256; $CD_3{}^{18}OH_2^+$, m/z = 38.06127, calc 38.05686.

ESI-MS conditions: a sample was introduced by syringe pumping (25 μL/min); ionization mode ESI+, needle voltage 2702 V, orifice voltage 29 V, peaks voltage 168 V.

Hydrolysis of $LPt^{IV}Me(OMe)(OH)$, 2.5, in 129 mM HBF_4 solution in $H_2{}^{18}O$. A sample of **2.5** (8.3 mg, 16 μmol) was combined with 10.2 mg (58 μmol) of 50% (mass) HBF_4 in water and 0.4947 g of $H_2{}^{18}O$ to produce a solution with [**2.5**] = 36.4 mM and [HBF_4] = 129 mM. A solution was left at 20^0C for 3.5 days and then analyzed by GC/MS (EI) and ^{1}H NMR (after dilution with D_2O). According to GC/MS, only one methanol isotopologue was present in the mixture, $CH_3{}^{16}OH$, with m/z 32.0264 (calc. for $CH_4{}^{16}O$ 32.0262). Immediately after GC/MS analysis, the reaction mixture was diluted with D_2O and analyzed by ^{1}H NMR. According to NMR, conversion of complex **2.5** was 23%, and the product of hydrolysis was identified as *unsym*-$LPt^{IV}Me(OH)_2$ (**2.4**).

GC/MS conditions: a sample was introduced by GC (HP5890, capillary column JW DB5, 30 m, internal diameter .25), temperature program from 30 ^{o}C (hold 2 min) to 150 ^{o}C at 40 ^{o}C/min; ion. mode EI+.

The $^{16}O/^{18}O$ Exchange between Complexes 2.11, 2.11-d_3 and $H_2{}^{18}O$ (Fig. 2.8). A solution of complex **2.11** or **2.11-d_3** (17.0 mg, 34.5 μmol) and 10.1 mg of 50% HBF_4 in 992 mg of $H_2{}^{18}O$ ([H^+]=63 mM; [Pt]=38 mM) placed in an NMR tube was heated in an oil bath at 80 ^{o}C. A 0.10 mL sample of the mixture was picked up with a syringe before the heating began and periodically after the reaction had started. The composition of the mixture was analyzed using ESI-MS to determine both the $Me^{18}OH/Me^{16}OH$ ratio and relative concentration of isotopomeric complexes $L^{195}PtMe(^{18}OH)_n(OH)_{2-n}$:

2.11, n=0; (m+H^+)/z = 494.070. Calc for (**2.11**·H^+), $C_{12}H_{15}{}^{16}O_5N_2{}^{195}Pt^{32}S$, 494.0349.

2.11-^{18}O, n=1; (m+H^+)/z = 496.084. Calc for (**2.11-^{18}O**·H^+), $C_{12}H_{15}{}^{16}O_4{}^{18}O_1N_2{}^{195}Pt^{32}S$, 496.0392.

2.11-$^{18}O_2$, n=2. (m+H^+)/z = 498.094. Calc for (**2.11-$^{18}O_2$**·H^+), $C_{12}H_{15}{}^{16}O_3{}^{18}O_2N_2{}^{195}Pt^{32}S$, 498.0435.

The signal at (m+H^+)/z = 492.068, which belonged to the adventitious $LPt^{IV}Me_2(OH)$ complex, inert under the reaction conditions, was used as an internal standard.

The contribution to the peak of ^{195}Pt-**2.11** coming from $L^{197}PtMe_2(OH)$ (16.1%) was taken into account when the relative concentrations of **2.11**, **2.11-^{18}O** and **2.11-$^{18}O_2$** were calculated. Similarly taken into account were the contributions to the peak of ^{195}Pt-**2.11-^{18}O** coming from ^{197}Pt-**2.11** (16.1%) and the contribution to the signal of ^{195}Pt-**2.11-$^{18}O_2$** coming from ^{197}Pt-**2.11-^{18}O** (16.1%) (Fig. 2.8).

Very weak peaks (<<1%) with (m+H^+)/z = 500, 502 and 504, which could correspond to **2.11-$^{18}O_3$**, **2.11-$^{18}O_4$**, and **2.11-$^{18}O_5$** did not change their intensity in the course of the reaction. Therefore, $^{18}O/^{16}O$-exchange in the sulfonate group did not take place. Doubly ^{18}O-labeled complex **2.12-$^{18}O_2$**, $LPt^{II}(^{18}OH_2)_2{}^+$, was only observed in the mass-spectrum of the reaction solutions.

ESI-MS of the reaction mixture composed by **2.12**, HBF_4 and $H_2{}^{18}O$, m/z = 484.044. Calculated for (**2.12**-$^{18}O_2$), $C_{11}H_{13}O_3{}^{18}O_2N_2{}^{195}Pt^{32}S$, 484.0279. Similarly, for **2.11-*d*$_3$** peaks of **2.11-*d*$_3$-^{18}O** and **2.11-*d*$_3$-^{18}O$_2$** appeared and grew in relative intensity in the course of the reaction.

2.11-*d*$_3$, n=0; $(m+H^+)/z$ = 497.081. Calc for (**2.11-*d*$_3$**$\cdot H^+$), $C_{12}H_{12}{}^2H_3{}^{16}O_5N_2{}^{195}Pt^{32}S$, 497.0534.

2.11-*d*$_3$-^{18}O, n=1; $(m+H^+)/z$ = 499.112. Calc for (**2.11-*d*$_3$-^{18}O**$\cdot H^+$), $C_{12}H_{12}{}^2H_3{}^{16}O_4{}^{18}O_1N_2{}^{195}Pt^{32}S$, 499.0577.

2.11-*d*$_3$-^{18}O$_2$, n=2. $(m+H^+)/z$ = 501.094. Calc for (**2.11-*d*$_3$-^{18}O$_2$**$\cdot H^+$), $C_{12}H_{12}{}^2H_3{}^{16}O_3{}^{18}O_2N_2{}^{195}Pt^{32}S$, 501.0620.

ESI-MS conditions: a sample was introduced by syringe pumping (25 μL/min); ionization mode ESI+, needle voltage 2702 V, orifice voltage 21 V, peaks voltage 1563 V.

Effect of one equivalent of $LPt^{II}(OH_2)_2BF_4$ additive on the kinetics of the C-O elimination from *sym*-$LPt^{IV}Me(OH)_2$ (2.11) in acidic D_2O solutions (Fig. 2.11, 2.12). A solution of complex **2.12** was prepared as follows. A sample of 4.8 mg of *sym*-$LPt^{IV}Me(OH)_2$ (**2.11**) (9.7 μmol) was dissolved in 1.3 mL of 60 mM HBF_4 solution in D_2O ([Pt] = 7.5 mM). 0.817 g of the resulting solution was placed into a NMR Young-tube and heated at 80^{0}C in a heating bath. The disappearance of *sym*-$LPt^{IV}Me(OH)_2$ was monitored by ^{1}H NMR. After heating for *ca* 190 min a complete conversion of $LPt^{IV}Me(OH)_2$ to $LPt^{II}(OH_2)_2BF_4$ and MeOH was reached.

Another sample of *sym*-$LPt^{IV}Me(OH)_2$ (**2.11**) (2.9 mg, 5.9 μmol) was placed in a vial and dissolved in the acidic solution of $LPt^{II}(OH_2)_2BF_4$ above. The resulting mixture was transferred into a NMR Young-tube. According to NMR, the *sym*-$LPt^{IV}Me(OH)_2$: $LPt^{II}(OH_2)_2BF_4$ ratio was 1.02 : 1, $LPt^{II}(OH_2)_2BF_4$=7.5 mM and *sym*-$LPt^{IV}Me(OH)_2$=7.6 mM. The solution was heated at 80^0 in a temperature controlled bath. Periodically the Young tube was removed from the bath, cooled down quickly to room temperature and NMR spectra were recorded. After heating for 5 min at 80^0 two new PtMe peaks were observed at 3.56 ppm ($^2J_{195PtH}$=64 Hz) and 3.38 ppm, corresponding to *cis*- and *trans*-$LPt^{IV}Me(\mu\text{-}OH)_2Pt^{II}LBF_4$, **2.18**, as confirmed by independent synthesis, ESI-MS and X-ray analysis. After rapid consumption of $LPt^{II}Me(OH)_2$ due to the formation of isomeric $[LPt^{IV}Me(\mu\text{-}OH)_2Pt^{II}L]BF_4$, **2.18**, which were observed during first 5 minutes, the reaction followed first order kinetics. The calculated pseudo-first order rate constant $k_{obs} = (5.82\pm0.30)\cdot10^{-4}$ s^{-1}.

Reaction of $LPt^{IV}CD_3(OH)_2$, 2.11-*d*$_3$, in the presence of 1 Equivalent of $LPt^{II}(^{18}OH_2)_2BF_4$, 2.12-^{18}O$_2$, in acidic $H_2{}^{18}O$ solutions. A 38.9 mM solution of $LPt^{II}(^{18}OH_2)_2BF_4$ was prepared by heating *sym*-$LPt^{IV}(CH_3)(OH)_2$ (**2.11**) (8.99 mg) in 119 mM HBF_4 in $H_2{}^{18}O$ (0.5149 g) for 3 hours at 80^{0}C. *sym*-$LPt^{IV}CD_3(OH)_2$ (**2.11-*d*$_3$**) (9.02 mg) was dissolved in the resulting mixture ([*sym*-$LPt^{IV}CD_3(OH)_2$] = 38.8 mM). The reaction mixture was heated at 80^{0}C in a sealed NMR Young tube for 5 min. The composition of the mixture was analyzed using ESI-MS to determine the $CD_3{}^{18}OH$/ $CD_3{}^{16}OH$ ratio

which was found to be 2.7:1. Formation of $[LPt^{IV}CD_3(\mu\text{-}^{16}OH)_2Pt^{II}L]^+$ was observed after 5 minutes of heating, m/z = 940.04649 (calculated for $C_{23}H_{20}D_3O_8N_4{}^{195}Pt_2{}^{32}S_2$, 940.04312).

Potentiometric determination of acidity of $LPt^{II}(OH_2)_2^+$, 2.12. The pH-potentiometric titrations were performed with OAKTON Waterproof pH Testr BNC pH-meter at 22^0C. To calibrate the glass-reference electrode pair, potassium biphthalate (pH 4.00, 0.05 M), potassium phosphate monobasic-NaOH (pH 7.00, 0.05 M) and potassium carbonate-potassium borate-KOH (pH 10.00, 0.05M) buffer solutions were used. For all titrations, standardized 0.1000 M NaOH solution (Acros) and 0.09702 M HNO_3 (Aldrich) were used. A solution of the protonated complex $[LPt^{II}(OH_2)_2]NO_3$ was prepared by the protonolysis of $KLPtMe_2$ complex:

$$K[LPt^{II}Me_2] + 2H_2O + 2HNO_3 \rightarrow KNO_3 + LPt^{II}(OH_2)_2NO_3 + 2MeH$$

A sample of $KLPtMe_2$ (15 mg, 30 μmol) and 1.25 mL of the standardized degassed 0.09702 M HNO_3 solution were mixed in a vial under argon atmosphere and stirred at room temperature. After 13 hours, complete protonolysis occurred and a colorless solution formed. 1.02 mL of the resulting solution was used for the titration ($[LPt(OH_2)(OH)]$=0.023 M, $[HNO_3]$=0.073 M). All titrations were performed in 3.5 mL titration cells equipped with a magnetic stirring bar. The standardized 0.1000 NaOH solution was added with a micro syringe by 10-50 μL portions. For every volume increment, the pH of the solution was read from the pH meter after stabilization (60 s).

The endpoint break is not distinct, and the protonation constant was estimated according to the following procedure. In the expression for the acid dissociation constant K_{a1}:

$$K_{a1} = \frac{[LPt(OH)(OH_2)][H^+]}{[LPt(OH_2)_2{}^+]}$$

the concentration of the protonated form $LPt(OH_2)_2{}^+$, designated as ΔH, can be calculated from the following equation:

$$[LPt(OH_2)_2{}^+] = \Delta H$$

$$\Delta H = \frac{C_{a0} \cdot V_{a0} - C_{NaOH} \cdot V_{NaOH}}{V_{a0} + V_{NaOH}} - 10^{-pH}$$

where C_{a0} is initial concentration of HNO_3, C_{NaOH} is the concentration of the titrant, V_a is initial volume of the titrated solution, and V_{NaOH} is the volume of NaOH added.

The expression for K_{a1} can be rewritten as:

$$K_{a1} = \frac{(C_{Pt} - \Delta H) \cdot 10^{-pH}}{\Delta H}$$

from which the following equation can be derived:

$$pH - pK_{a1} = \lg\left(\frac{C_{Pt}}{\Delta H} - 1\right)$$

$$pH = \lg\left(\frac{C_{Pt}}{\Delta H} - 1\right) + pK_{a1}$$

The value of pK_{a1} can be estimated by interpolation from the linear plots of pH *vs.* $\lg(C_{Pt}/\Delta H\text{-}1)$ shown below:

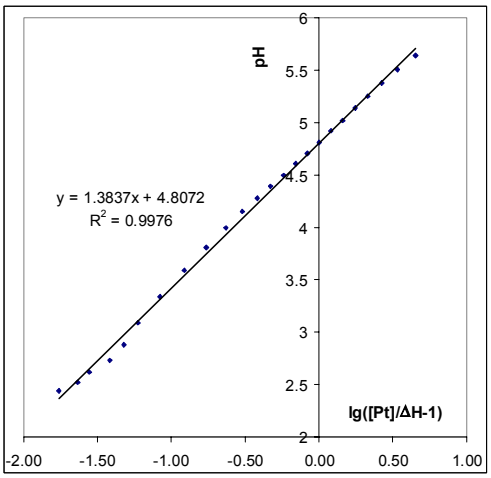

If $\lg\left(\frac{C_{Pt}}{\Delta H} - 1\right) = 0$, $pH = pK_{a1}$

The pK_{a1} of acid dissociation of $LPt(OH_2)_2^+$ was estimated to be 4.76±0.07.

Chapter 3

Effect of the NaOH additives on the rate of oxidation of $LPt^{II}(CH_2CH_2)OH$ (3.2) by O_2 (Table 3.2). A stock solution of **3.2** was prepared from $LPt^{II}(CH_2CH_2)OH$ (288 μmol) and 18.05 g (16.33 mL) of deaerated D_2O under an argon atmosphere; [**3.2**]=17.7 mM. The solution was placed into a 50 mL Schlenk tube and stored under argon for less than 2 days in a refrigerator at 7^0C. To prepare alkaline solutions of **3.2** containing 1-25 mM NaOH, a sample of standardized 0.100 M NaOH (25-595 mg) was slowly evaporated to dryness under vacuum. The residue was dissolved in 2.4 mL of the 17.7 mM stock solution of **3.2**. ^{1}H NMR spectrum was recorded before oxidation and then in regular intervals. Each reaction mixture was divided into 3 parts, 0.8 mL each, which were placed into 10 mL screw-cap vials equipped with a magnetic stirring bar. The vials were filled with O_2 and securely capped. Each sample was vigorously stirred under an O_2 atmosphere at room temperature. After 1h of stirring under O_2 samples were placed into NMR tubes, and ^{1}H NMR spectra were recorded immediately. Yields were calculated as an average of 3 runs. Results are given in Table 3.2.

Volumetric determination of the oxygen consumption in the oxidation of $LPt(CH_2CH_2)(OH)$ (3.2) in neutral solutions. The solution of complex **3.2** in H_2O was by dissolving a sample of **3.2** (28.8-30.0 mg) in 1.38-1.54 mL of deaerated H_2O. The concentration of **3.2** in the resulting solution was 42.7-40.9 mM. The 1 mL aliquots of the resulting solutions were then used for volumetric experiments. In

each run 1.00 mL of the neutral solution of **3.2** was placed into a thermostated flask equipped with a magnetic stirring bar and connected to the gas microburet. The apparatus was filled with O_2 (1 atm), and after initial volume reading was taken, the stirrer was turned on to start the run. Stirring was continued at 20 °C until no detectable changes in the amount of the consumed oxygen occurred after several hours. The reactions were stopped after 21h. Immediately after final reading was taken, the reaction mixtures were diluted with D_2O; 2 μL of dioxane was added as an internal standard and the yield of the product **3.5** was determined by ^{1}H NMR integration. According to NMR, the yield of **3.5** was found to be 43±1% (two runs), based on the integration of ortho-proton of pyridyls of dpms at 8.86 ppm using dioxane as an internal standard (delay time 20s). Volumetric measurements indicate a consumption of 0.54±0.02 equivalents of O_2 per one mole of a complex **3.2** as an average of two runs.

Transformations of $LPt^{II}(CH_2CH_2)Cl$ (3.1) in the presence of 1 equivalent of NaOH under an argon atmosphere and in the presence of O_2.

A. Preparation of stock solution containing 1 equivalent of NaOH. A sample of $LPt^{II}(CH_2CH_2)Cl$ **(3.1)** (76.4 mg, 150.4 μmol) was placed into a 10 mL vial equipped with a magnetic stirring bar and dissolved in 3.02 mL (3.3221 g) of 49.8 mM $NaOD/D_2O$ solution upon stirring for 30 min. This solution with [Pt]=49.8 mM and [NaOD]=49.8 mM was used for monitoring both the reaction under an argon atmosphere and oxidation with O_2.

B. Cl/OH exchange under an argon atmosphere (Fig. 3.3). 1.03 mL of the stock solution above was placed into a NMR Young tube under argon. A ^{1}H NMR spectrum was recorded 30 minutes after preparation of the mixture. This solution was stored under argon at room temperature and periodically analyzed by NMR.

Concentrations of complexes $LPt^{II}(CH_2CH_2)OH$ and $LPt^{II}(CH_2CH_2)Cl$ were calculated from the integral intensity of the H-C(3) proton of the dpms ligand (7.96 ppm, d) and from the multiplet of coordinated ethylene at 5.05 ppm, respectively. Concentration of $LPt^{II}(CH_2CH_2OH)Cl^-$ was calculated from the integral intensity of CH_2 signals at 1.4-2.2 ppm using residual HDO peak as an internal standard. Trace amounts (< 1 mM) of free ethylene (5.43 ppm) were detected by ^{1}H NMR in the reaction mixture in 5h.

C. Reaction under oxygen (Fig. 3.4). 1.99 mL of the stock solution above were placed into 30 mL screw-cap vial equipped with magnetic stirring bar. The vial was filled with O_2 and securely capped. The reaction mixture was vigorously stirred at room temperature. Periodically, stirring was halted and a sample of the solution was transferred into an NMR tube and analyzed by ^{1}H NMR. After recording a spectrum, the solution was returned into a vial, which was refilled with O_2 and stirring was resumed. A small amount of white precipitate of $L_2Pt^{II}_2(\mu\text{-}OH)_2$ formed by the end of reaction.

C-O reductive elimination from *unsym*-$[LPt(CH_2CH_2OH)(OH)_2]$, 3.5 (Fig. 3.5). An NMR Young tube was charged with a solution of **3.5** (11.3 mg, 21.6 μmol) in 0.8 mL D_2O; [Pt]=27.0 mM. and a ^{1}H

NMR spectrum was recorded before heating. The reaction mixture was heated in a Teflon sealed NMR Young tube in a heating bath at 80^0C and was periodically analyzed by ^{1}H NMR. Organic products were identified by ESI-MS and by comparison with ^{1}H NMR spectra of authentic samples. For quantitative measurement of ethylene oxide concentration by NMR the delay time of 50 seconds should be used due to a long relaxation time T_1 of ethylene oxide. In the course of the reaction thermal isomerization of **3.5** occurred to give **3.9,** which was unstable under reaction conditions. The complex **3.5** had a half-life of 58 minutes at 80 ^{o}C. The results are given in Fig. 3.5. The reaction was complete after 13.6h at 80 ^{o}C. NMR yields of ethylene glycol and ethylene oxide on **3.5** were 85% and 8% respectively, using residual solvent peak as an internal standard. In the course of reaction a white precipitate of complex $L_2Pt^{II}_2(\mu\text{-}OH)_2$ formed.

***sym*-LPt^{IV}(CH$_2$CH$_2$OH)(OH)$_2$ (3.9)**. ^{1}H NMR (D_2O, 22 ^{o}C), δ: 3.16 (t, *J*=5.8 Hz, $^3J_{195PtH}$=40 Hz, 2H), 3.51 (t, *J*=5.8 Hz, $^2J_{195PtH}$=80 Hz, 2H), 6.53 (s, 1H), 7.87 (ddd, *J*=7.7, 5.8, 1.3 Hz, 2H), 8.09 (dd, *J*=7.9, 1.3 Hz, 2H), 8.34 (td, *J*=7.8, 1.1 Hz, 2H), 8.75 (dd, *J*=5.8, 1.1 Hz, $^3J_{195PtH}$=26.3 Hz, 2H).

Ethylene glycol. ^{1}H NMR (D_2O, 22 ^{o}C), δ: 3.65 ppm. **ESI-MS**, solution acidified with HBF_4 and diluted 10 fold with H_2O, $(m+H^+)/z$ = 63.04890. Calculated for $C_2H_7O_2$, 63.04460.

Ethylene oxide. ^{1}H NMR (D_2O, 22 ^{o}C), δ: 2.80 ppm. **ESI-MS** in an acidified solution after 10 fold dilution with H_2O, $(m+H^+)/z$ = 45.03391. Calculated for C_2H_5O, 45.03404.

C-O reductive elimination from 3.6. A procedure similar to that described above for reductive elimination from **3.5** was used for C-O reductive elimination from **3.6** at 80 ^{o}C in D_2O ($[\mathbf{3.2}]_0$=2 mM). The reaction was complete in 10h to give a mixture of ethylene glycol (94% yield on **3.6**) and ethylene oxide (4% yield) according to ^{1}H NMR. The major Pt-containing product was $LPt^{II}Cl(OH_2)$ (NMR yield > 80%).

$LPt^{II}Cl(OH_2)$, ^{1}H NMR (D_2O, 22 ^{o}C), δ: 7.41 (m, 1H), 7.56 (m, 1H), 7.80 (vd, *J*=7.8 Hz, 1H), 7.89 (vd, *J*=7.8 Hz, 1H), 8.06 (vt, *J*=7.8 Hz, 1H), 8.14 (vt, *J*=7.8 Hz, 1H), 8.69 (m, 1H), 8.98 (m, 1H). The dpms CH bridge proton was not seen due to H/D exchange. **ESI-MS** of the acidified reaction mixture prepared under the same conditions in H_2O showed the presence of a peak belonging to $LPt^{II}Cl(OH_2)\cdot H^+$, m/z 498.001. Calculated for $LPtCl(OH_2)\cdot H^+$, $C_{11}H_{12}O_4{}^{35}ClS^{195}Pt$, 497.985.

Potentiometric determination of basicity of $LPt^{II}(C_2H_4)OH$, 3.2. The pH-potentiometric titrations were performed with OAKTON Waterproof pH Testr BNC pH-meter at 22 ^{o}C. To calibrate the glass-reference electrode pair, potassium biphthalate (pH 4.00, 0.05 M), potassium phosphate monobasic-NaOH (pH 7.00, 0.05 M) and potassium carbonate-potassium borate-KOH (pH 10.00, 0.05M) buffer solutions were used. For all titrations, standardized 0.1000 M NaOH solution (Acros) and 0.09702 M HNO_3 (Aldrich) were used.

A sample of complex **3.2** (24.5 mg, 50.1 μmol) was dissolved in 1.00 mL of deaerated aqueous 0.09702 N HNO_3. The solution was placed into a vial and was titrated with a standardized 0.1000 N

NaOH solution under argon flow at room temperature. The titration was performed in a 3.5 mL titration cell equipped with a magnetic stirring bar. The standardized NaOH solution was added with a micro syringe by 10-25 µL portions. For every volume increment, the pH of the solution was read from the pH meter after stabilization (60 s). Results of the titration are given below:

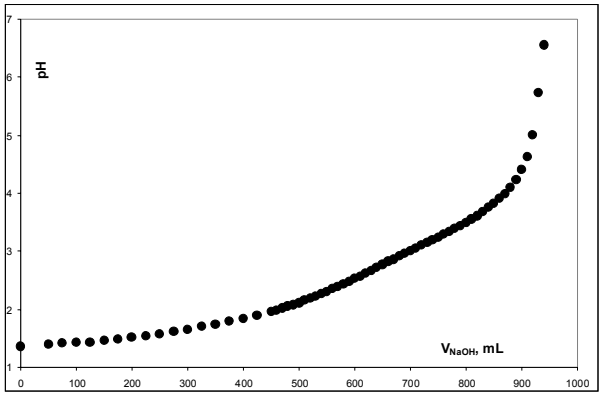

For the protonation equilibrium (eq. A1)

$$LPt(C_2H_4)OH + H^+ \rightleftharpoons LPt(C_2H_4)OH_2^+ \quad \text{(A1)}$$

We have the following expression for the protonation constant K_p (eq. A2):

$$K_p = \frac{[LPt(OH_2)^+]}{[LPt(OH)][H^+]} \quad \text{(A2)}$$

The protonation constant K_p was estimated from the plot of the solution pH versus log([Pt]/Δ[H^+]-1) as explained below.

The concentration of the protonated form $LPt(OH_2)^+$ is designated as Δ[H^+], $[LPt(OH_2)^+] = \Delta[H^+]$, and can be calculated from the following equation (eq. A3):

$$\Delta[H^+] = \frac{C_{a0} \cdot V_{a0} - C_{NaOH} \cdot V_{NaOH}}{V_{a0} + V_{NaOH}} - 10^{-pH} \quad \text{(A3)}$$

where C_{a0} is initial concentration of HNO_3, C_{NaOH} is the concentration of the titrant, V_{a0} is initial volume of the titrated solution, and V_{NaOH} is the volume of NaOH added.

The expression for K_p (eq. A2) can be rewritten as (eq. A4):

$$K_p = \frac{\Delta[H^+]}{(C_{Pt} - [H^+]) \cdot 10^{-pH}} \quad \text{(A4)}$$

where C_{Pt} is the total concentration of Pt in solution, $C_{Pt} = [LPt(OH)] + [LPt(OH_2)^+]$.

From eq. A4 we can get eq. A5 and eq. A6:

$$pK_p + pH = \lg\left(\frac{C_{Pt}}{\Delta[H^+]} - 1\right) \quad \text{(A5)}$$

$$pH = \lg\left(\frac{C_{Pt}}{\Delta[H^+]} - 1\right) - pK_p \qquad \text{(A6)}$$

The value of pK_p can be estimated by interpolation from a linear plot of pH *vs.* $\lg(C_{Pt}/\Delta[H^+]-1)$:

$$\text{at } \lg\left(\frac{C_{Pt}}{\Delta[H^+]} - 1\right) = 0 \quad pH = -pK_p$$

The value of $\lg K_p$ for complex **3.2** was estimated to be 3.00±0.01 from the linear plot of pH *vs.* $\lg([Pt]/\Delta[H^+]-1)$. Due to certain systematic error associated with conversion of the pH values to $[H^+]$ eq. A6 is the most precise when $\Delta[H^+] \sim 0.5[Pt]$, which corresponds to the plot shown below:

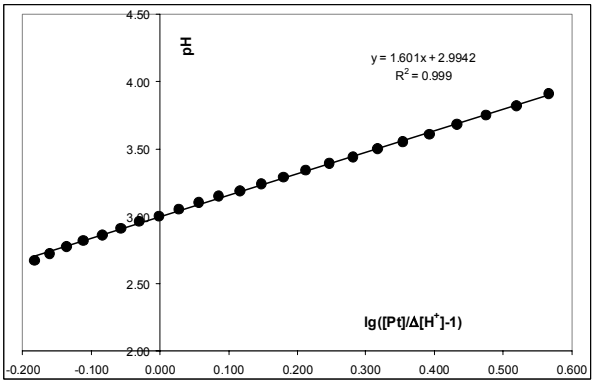

Finally, by definition, the basic hydrolysis constant of $LPt(CH_2CH_2)OH$, K_b, is the equilibrium constant for the following reaction:

$$LPt(CH_2CH_2)OH + H_2O \rightleftharpoons LPt(CH_2CH_2)OH_2^+ + OH^-$$

and can be calculated as $K_b = K_p \cdot K_w = 1.0 \cdot 10^3 \cdot 1.00 \cdot 10^{-14} = 1.0 \cdot 10^{-11}$

Determination of equilibrium constant of reaction (3.10), *K*. Potentiometric measurements of $[D^+]$ in D_2O solutions were performed with OAKTON Waterproof *pH* Testr BNC *pH*-meter equipped with a glass microelectrode and standardized for *pH* measurements at 22 °C. Potassium biphthalate (pH 4.00, 0.05 M), potassium phosphate monobasic-NaOH (*pH* 7.00, 0.05 M) and potassium carbonate-potassium borate-KOH (*pH* 10.00, 0.05M) buffer solutions were used for calibration. The determined *pH* values were converted to the *pD* scale as described,[93, 94] $pD = pH_{reading} + 0.40$; $pOD = 15 - pD$.

The concentrations of platinum-containing species **3.2** and **3.4** were determined from ^1H NMR intensities of resonances of coordinated ethylene (5.0 ppm) and CH_2 multiplet of hydroxyethyl (1.48-2.17 ppm), respectively.

A sample of **3.2** (13.4 mg, 27.3 μmol) was dissolved in deaerated D_2O (3.3689 g, 3.05 mL); variable amounts of NaOD were added. All operations were performed under an argon atmosphere.

The equilibrium constant was calculated from the plot of lg([**3.4**]/[**3.2**]) versus *pD* shown below:

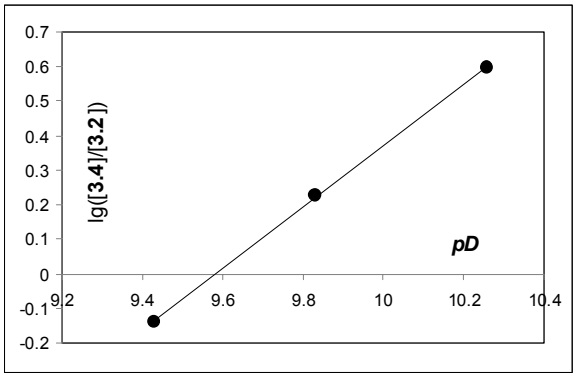

Chapter 4

Volumetric determination of the oxygen consumption in the oxidation of (dpms)Pt(η^2-C_8H_{14})(OH) (4.1a) in weakly basic solutions. The solution of complex **4.1a** in H_2O was prepared as described above. The concentration of **4.1a** was determined in a separate experiment by ^{1}H NMR in H_2O/D_2O mixture using dioxane as an internal standard, based on the integration of a multiplet at 7.50 ppm and a dioxane singlet at 3.75 ppm (delay time 20s); the concentration was found to be [**4.1a**]=29.3 mM. In each run 1.00 mL of the 29.3 mM solution of **4.1a** and 60 μL of 0.100 N NaOH/H_2O were placed into a thermostated flask equipped with a magnetic stirring bar and connected to the gas microburet. The apparatus was filled with oxygen (1 atm), and after initial volume reading was taken, the stirrer was turned on to start the run. Stirring was continued at 20 °C until no detectable changes in the amount of the consumed oxygen occurred after several hours. The reactions were stopped after 20h. Immediately after final reading was taken, the reaction mixtures were dissolved in a mixture of D_2O/acetone-d_6 (3:1 v/v), and the yield of the product was determined by ^{1}H NMR. According to NMR, the yield of the complex (dpms)Pt(*C,O*-$C_8H_{14}O$- *κC,κO*)(OH) (**4.3a**) was found to be 93±1% (two runs), and 7±1% of (dpms)Pt$(OH)_2^-$ also formed, based on the integration of multiplets at 7.82 and 7.51 ppm respectively using dioxane as an internal standard (delay time 20s); no starting material or other products were detected. Epoxide reductive elimination was negligible under these conditions (<1%). Volumetric measurements indicate a consumption of 0.51±0.04 equivalents of O_2 per one mole of a complex **4.1a** as an average of two runs.

Kinetics of C-O reductive elimination from complex 4.3a in dmso-d_6 solutions. The following representative procedure was used in all kinetic experiments. A sample of **4.3a** (4.6-9.3 mg, 7.8-15.8 μmol) was dissolved in 0.62-0.7 mL of dry degassed dmso-d_6. Hexamethyldisiloxane (HMDS, 1 μL) was added as an internal standard. The resulting yellow solutions were transferred into NMR Young tubes and Teflon-sealed. NMR spectra were recorded before heating. After that the tubes were immediately placed into a glycol thermostat with a pre-set temperature. Periodically the tubes were

removed, cooled down with ice water and ^{1}H NMR spectra were recorded. Clean formation of (dpms)Pt^{II}(OH)(dmso-d_6) complex (**4.13**-d_6) and cyclooctene oxide was observed by NMR in dmso-d_6 solutions. No other products or intermediates were detected in the amounts exceeding 2%; all components were completely soluble in dmso-d_6. The organic products were identified by ^{1}H NMR and GC-MS by comparison with authentic samples. The complex (dpms)Pt^{II}(OH)(dmso-d_6) was identified by ESI-MS. The concentrations of complex **4.3a** and cyclooctene oxide were determined by integration of CHO peak of complex **4.3a** at 5.20 ppm and CHO multiplet of epoxide at 2.78-2.86 ppm respectively using HMDS as an internal standard. The concentration of complex **8**-d_6 was determined by integration of CH multiplet of pyridyl at 7.46 ppm. The final yield of cyclooctene epoxide was determined by ^{1}H NMR after heating at 60 °C until complete disappearance of the starting material; delay time d1=100 s. Cyclooctene oxide was obtained in quantitative yields and was stable under reaction conditions (12-40h at 60 °C in dmso-d_6).

(dpms)Pt^{II}(OH)(dmso-d_6) (**4.13**-d_6). ESI-MS of dmso-d_6 solution of **4.13**-d_6 after 100-fold dilution with acetone-water mixture, m/z = 546.1. Calculated for **4.13**-d_6·H$^+$, $C_{13}H_{11}D_6N_2O_5{}^{195}PtS_2$, 546.1.

The first order rate constants k_{cot} determined for the rate law $-d([\mathbf{4.3a}]) = k_{cot}\cdot[\mathbf{4.3a}]\cdot dt$ at various temperatures were calculated to be the following:

T, °C	$k_{cot}*10^5$, s^{-1}
50	2.79±0.06
60	8.72±0.21
65	15.1±0.3
70	25.3±0.6

The rate constants determined at different concentrations of complex **4.3a** (11 and 25 mM) at 60 °C were practically the same (see below) indicating first order in complex **4.3a**; good linear graphs in first order coordinates ln([**4.3a**]$_0$/[**4.3a**]) *vs.* time were obtained up to 80% conversions of complex **4.3a**.

[**4.3a**], mM	$k_{cot}*10^5$, s^{-1} (60 °C)
11	8.72±0.21
25	8.79±0.17

The graphs of ln(C_0/C) *vs.* time for various temperatures and concentrations of complex **4.3a** in dmso-d_6 are given below.

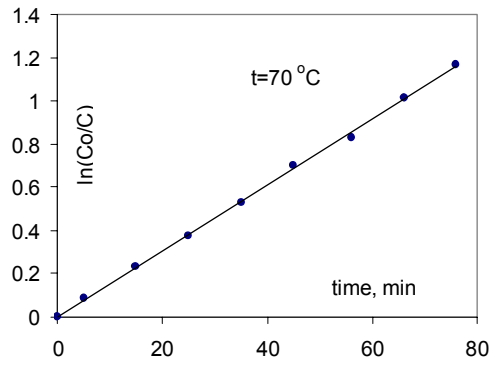

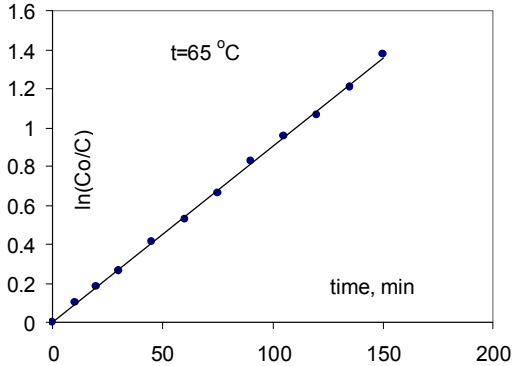

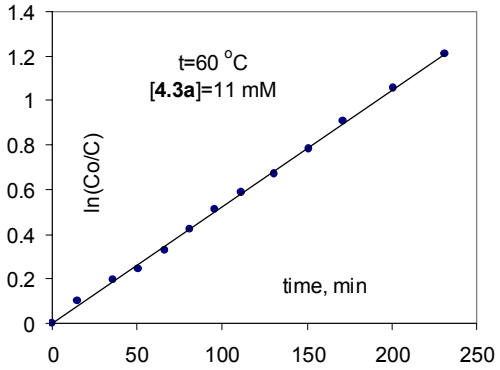

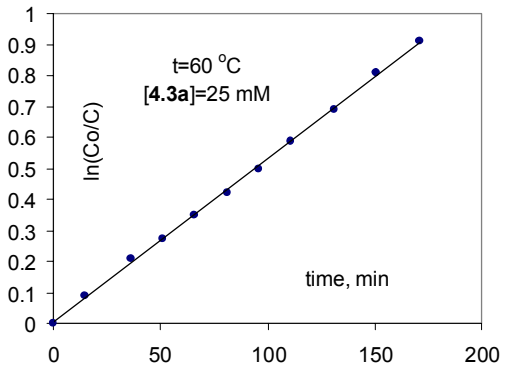

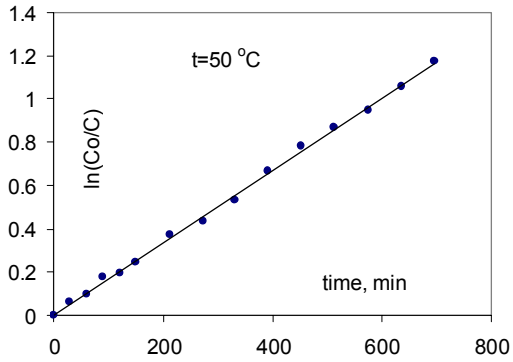

The analogous procedure was used for reductive elimination from **4.3b**. The first order rate constants k_{nb} for the rate law $-d([\textbf{\textit{cis}-4.3b}]) = k_{nb}\cdot[\textbf{\textit{cis}-4.3b}]\cdot dt$ at various temperatures were calculated to be the following:

T, °C	$k_{nb}*10^4$, s^{-1}
45	1.26±0.03
50	2.24±0.05
55	3.79±0.06
60	6.43±0.15

The graphs of $\ln(c_0/c)$ vs. time for complex **4.3b** for various temperatures are given below.

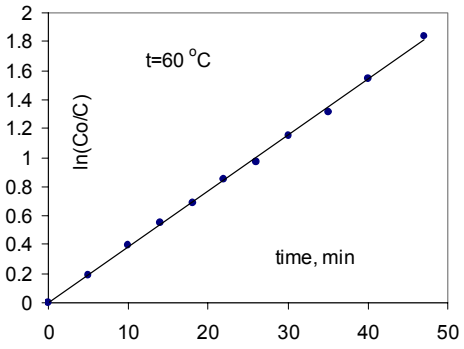

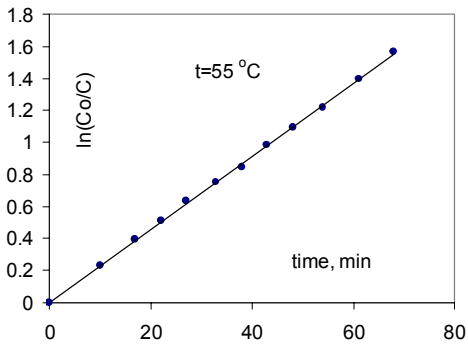

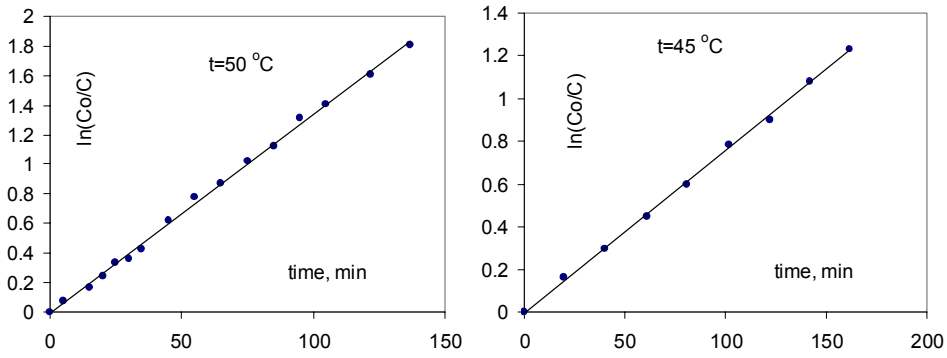

Cyclooctene oxide (9-oxabicyclo[6.1.0]nonane), 4.12a. ^{1}H NMR (dmso-d_6, 22 °C, 400 MHz), δ: 1.08-1.65 (m, 10H), 1.97-2.07 (m, 2H), 2.78-2.86 (m, 2H). **GS-MS (EI)** m/z (%) (RT=6.93 min): 111 (16), 97 (34), 83 (51), 67 (81), 55 (100), 41 (54). **GS-MS (CI)** m/z (%) (RT=6.93 min): 127 (3), 109 (39), 97 (6), 83 (10), 67 (33), 55 (100), 43 (25), 42 (33).

***Exo*-2,3-epoxybicyclo[2.2.1]heptanes (norbornene oxide), 4.12b. ^{1}H NMR** (dmso-d_6, 22 °C, 400 MHz), δ: 0.63 (d, *J*=9.4 Hz, 1H), 1.05-1.19 (m, 3H), 1.35-1.49 (m, 2H), 2.36 (s, 2H), 3.08 (s, 2H). **GS-MS (EI)** m/z (%) (RT=5.18 min): 110 (5), 109 (8), 81 (100), 67 (58), 53 (22), 39 (63). **GS-MS (CI)** m/z (%) (RT=5.18 min): 111 (88), 110 (26), 93 (100), 81 (30), 67 (37), 53 (43).

C-O reductive elimination from 4.3a and 4.3b in the solid phase. A sample of complex **4.3a** or **4.3b** (2-4 mg) was placed into a Young NMR tube under argon and Teflon-sealed. The Young NMR tube was placed into a silicon oil bath and heated at 85 ° or 60 °C respectively. After several hours an NMR tube was cooled down to room temperature, 0.7 mL of dmso-d_6 or CD_3OD and 1 μL of HMDS were transferred into and NMR tube and the contents of the tubes was shaken for several minutes. When dmso-d_6 was used as a solvent, all solids dissolved completely; starting material, epoxide and (dpms)Pt(dmso-d_6)(OH) were detected by ^{1}H NMR. When CD_3OD was used as a solvent, Pt(II)-containing product was not soluble in methanol, only starting material and epoxide could be detected; yields and conversions determined in CD_3OD were identical to those in dmso-d_6. The yields of epoxides and starting material were calculated by integration of multiplets at 2.78-2.86 and 5.20 ppm respectively using HMDS as an internal standard; half-life of the reaction was calculated as an average of 2-3 runs at conversions <50%. The complex **4.3a** undergoes reductive elimination in a solid phase with a half-life time 6h at 85 °C to produce cyclooctene oxide **4.12a**; the reaction is clean at conversions <50%; thermal decomposition of epoxide can occur at longer reaction times and leads to diminished yield of epoxide at higher conversions. Complex **4.3b** produced 10-12% of norbornene oxide **4.12b** after heating for 3.5h at 60 °C (half-life ~20h); at longer reaction times or higher temperatures a complex mixture of products forms, presumably due to low thermal stability of epoxide **4.12b**.

Kinetics of isomerization and reductive elimination from complex 4.3a in CD_2Cl_2 solution at 40 °C. A sample of complex **4.3a** (2.9 mg, 4.9 μmol) was dissolved in dry degassed CD_2Cl_2 (0.8867 g, 0.66 mL); 1 μL of hexamethyldisiloxane was added as an internal standard. The solution was transferred into the NMR Young tube, Teflon sealed and loaded into a pre-heated (40 °C) NMR probe. Temperature inside the probe was estimated (±0.5 °C) by measuring the difference in the chemical shits of an ethylene glycol sample. ^{1}H spectra were recorded periodically using automated kinetics program.

Characterization of 4.14a. *Preparation of the concentrated dmso-d_6 solution containing* **4.14a** *without isolation.* A sample of complex **4.3a** (15 mg, 25 μmol) was placed into a 50 mL Schlenk tube and dissolved in 3 mL of dry degassed CH_2Cl_2. The solution was heated under argon at 40 °C. After 8 hours the reaction mixture was filtered from white precipitate through Celite, solvent was evaporated under vacuum and the resulting yellowish solid was re-dissolved in dmso-d_6 Dmso-d_6 was chosen as it provided higher solubility and stability of **4.14a** compared to CD_2Cl_2 and other common solvents. According to ^{1}H NMR, **4.3a**, **4.14a** and **4.12a** were present in solution in a 2.6 : 1 : 2.1 molar ratio. ^{1}H, 1D-difference NOE, 2D DQF-COSY (double quantum filter correlation spectroscopy) and HSQC (gradient selection with sensitivity enhancement) NMR spectra of the resulting solution were recorded at room temperature. The concentrations of **4.3a** and **4.14a** slowly decreased over time due to reductive elimination of **4.13** and **4.12a**. Only one isomer of intermediate complex **4.14a** was detected in solution.

4.14a: ^{1}H NMR (dmso-d_6, 22 °C, 600 MHz), δ: -0.06 (br s, 1H), 0.24 (d, J=13.4 Hz, $^3J_{195PtH}$=64 Hz, 1H), 0.83-0.72 (m, 9H), 1.79-1.92 (m, 1H), 2.23-2.39 (m, 1H), 3.95 (dd, J=12.3, 7.3 Hz, $^2J_{195PtH}$=94 Hz, 1H), 5.03 (dd, J=11.2, 7.3 Hz, $^3J_{195PtH}$=34 Hz, 1H), 6.44 (s, 1H), 7.75-7.83 (m 1H), 7.88-7.96 (m, 1H), 7.98 (d, J=7.8 Hz, 1H), 8.00 (d, J=7.8, 1H), 8.29 (td, J=7.8 Hz, 1.2 Hz, 1H), 8.31 (td, J=7.8, 1.2 Hz, 1H), 8.76 (d, J=5.6 Hz, 1H), 9.38 (d, J=6.0 Hz, $^3J_{195PtH}$=26 Hz, 1H). Significantly larger coupling constant $^2J_{195PtH}$ = 94 Hz for the Pt-CH group, compared to that in complex **4.3a** ($^2J_{195PtH}$ = 70 Hz), is an indication of the presence of a ligand *trans*- to the Pt-CH with a weaker *trans*-effect (SO_3 rather than pyridyl residue).[29]

Selected ^{1}H NMR assignments from 2D DQF-COSY, HSQC and 1D-difference NOE experiments are given below. The assignment of a peak at 3.95 ppm as CHPt is based on the presence of Pt satellites with a large coupling constant (J_{195PtH}=94 Hz). The assignment of the peak at 5.03 ppm as CHO is based on its characteristically downfield shifted signal and the presence of Pt satellites with a smaller coupling constant (J_{195PtH}=34 Hz). A multiplet centered at 1.79-1.92 ppm was assigned as CH_cH-CH_bPt due to its COSY-correlation with CH_bPt peak. A multiplet at 2.23-2.39 ppm was assigned as CH_eH-CH_aO due to its COSY-correlation with CH_aO peak. The structure of **4.14a** is deduced from NOE experiments: NOE's were observed between *ortho*-proton of pyridyl H_h and CH_bPt, and *ortho*-proton H_g and two methylene protons, H_e and H_c. The structure of **4.14a** deduced from NOE-experiments is consistent with DFT-calculated short H-H distances in DFT-optimized structure of **4.14a** (DFT-

calculated distances (Å), H_h-H_b, 2.433, H_g-H_c, 2.437, H_g-H_e, 2.266; the H-H distances between H_h and H_g and other protons of the cyclooctane ring are > 3.2 Å).

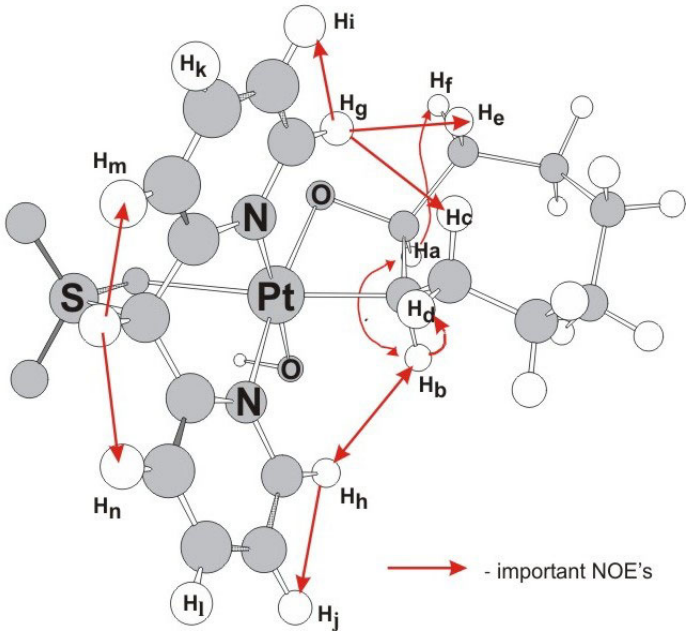

DFT-calculated structure of **4.14a** and experimentally observed NOE's.

Observed COSY peaks: H_a – H_e; H_b - H_c.

Selected ^{1}H NMR assignments from COSY, HSQC and NOE are given below:

H	δ_H (multiplicity)
H_a	5.03 (dd, *J*=11.2, 7.3 Hz, $^3J_{195PtH}$=34 Hz)
H_b	3.95 (dd, *J*=12.3, 7.3 Hz, $^2J_{195PtH}$=94 Hz)
H_c	1.79-1.92 (m)
H_d	0.24 (d, *J*=13.4 Hz, $^3J_{195PtH}$=64 Hz)
H_e	2.23-2.39 (m)
H_f	(m, 1.30-1.49)
H_g	9.38 (d, *J*=6.0 Hz, $^3J_{195PtH}$=26 Hz)
H_h	8.76 (d, *J*=5.6 Hz)
H_i	7.88-7.96 (m)
H_j	7.75-7.83 (m)
H_k	8.31 (td, *J*=7.8, 1.2 Hz)
H_l	8.29 (td, *J*=7.8 Hz, 1.2 Hz)
H_m and H_n	7.98 (d, *J*=7.8 Hz), 8.00 (d, *J*=7.8)
$CHSO_3$	6.44 (s)
OH	-0.06 (br s)

Selected ^{13}C NMR assignments of **4.14a** made from HSQC experiment are shown below.

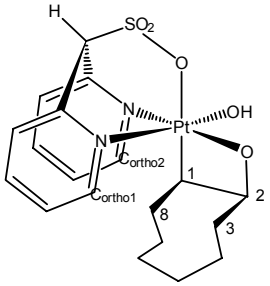

Selected ^{13}C NMR assignments
(based on HSQC; dmso-d_6, ppm):

C1: 26.5
C2: 88.5
C3: 33.5
C8: 29.9
$CHSO_3$: 71.6
C_{ortho1}: 147.3
C_{ortho2}: 148.8

Other resonances could not be determined by HSQC due to overlapping with peaks of other components of the reaction mixture.

We have also considered another possible isomer of **4.14a** with orientation of the cyclooctene ring pointing toward Pt-OH, designated below as ***endo*-4.14a**.

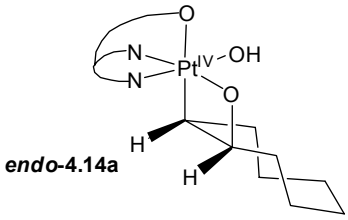

***endo*-4.14a**

The DFT-optimized structure of ***endo*-4.14a** is given below. The geometry of ***endo*-4.14a** was inconsistent with observed NOE's. The NOE between one of the *ortho*-protons of pyridine and both H_a-CO and H_b-CPt would be expected in ***endo*-4.14a,** unobserved experimentally, whereas the *ortho*-proton of another pyridine ring would show NOE to C*H*H-CHPt only, but not C*H*H-CHO.

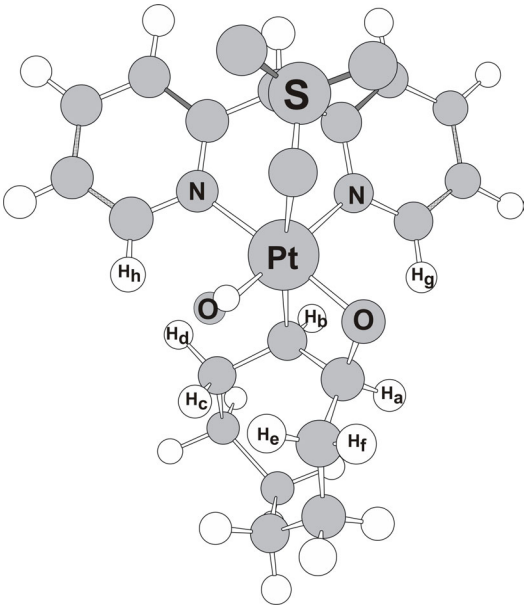

H_g-H_a, 2.335 **H_h-H_d, 2.258**

H_g-H_b, 2.352 H_h-H_c, 2.755

H_g-H_f, 3.229 H_h-H_b, 4.074

DFT-calculated structure of alternative isomer ***endo*-4.14a** (unobserved experimentally). DFT-calculated proton-proton distances are given in Å. Distances shorter than 2.5Å are shown in bold.

Attempted aerobic epoxidation of norbornene in the presence of (dpms)Pt(dmso)(OH). A sample of (dpms)Pt(dmso)(OH) (2.6 mg, 4.9 μmol) was dissolved in 0.8 mL of CF_3CD_2OD; norbornene (59 mg, 627 μmol, 128 eq) and 1 μL of hexamethyldisiloxane were added,and the resulting solution was transferred into an NMR Young tube. The Young tube was filled with O_2 and Teflon-sealed. NMR spectra were recorded before heating. After that the tube was placed into a silicon bath thermostat with a pre-set temperature and heated at 60 °C for 3 days. The reaction mixture was cooled down to room temperature, shaken carefully and analyzed by ^{1}H NMR. White precipitate of $(dpms)_2Pt_2(\mu\text{-}OH)_2$ formed in the reaction mixture upon heating. No (dpms)Pt(dmso)(OH) was present in solution by ^{1}H NMR, and free DMSO was liberated. *Exo*-2,3-epoxybicyclo[2.2.1]heptane was detected in solution and identified by comparison of its ^{1}H NMR spectrum with authentic sample. The yield of *exo*-2,3-epoxybicyclo[2.2.1]heptane was calculated based on integration of a singlet of brighehead methines at 2.45 ppm using hexamethyldisiloxane as an internal standard and was found to be 20% (1 μmol) based on (dpms)Pt(dmso)(OH).

Attempted reductive elimination from *cis*-(dpms)Pt^{IV}($C_{10}H_8O_2$-*κO,κC*)$(OH)_{ax}$ (*cis*-4.3d). Formation of complex 4.14d. A sample of complex ***cis*-4.3d** (5.6 mg) was dissolved in 0.7 mL of dry degassed dmso-d_6; 1 μL of hexamethyldisiloxane (HMDS) was added as a standard. The complex ***cis*-4.3d**, obtained by aerobic oxidation, contained 7.5% of isomeric **4.11d** initially; initial concentrations $[\mathbf{4.3d}]_0$ = 11.9 mM**;** $[\mathbf{4.11d}]_0$ = 1 mM. The resulting solution was transferred into an NMR Young tube under argon. ^{1}H NMR spectrum was recorded before heating. The reaction mixture was heated at 60 ^{o}C, periodically cooled down to room temperature and analyzed by ^{1}H NMR. The complex **4.3d** disappears with a half-life of 14.7 h at 60 ^{o}C. Dark precipitate forms in the reaction mixture after heating for more than 12 hours. Concentration of complex **4.11d** did not change significantly during the course of the reaction.

Formation of a new complex **4.14d** was detected by ^{1}H NMR whose concentration reached maximum after ~9 hours and then decreased upon further heating. The complex **4.14d** was characterized by ^{1}H, COSY and HSQC NMR without isolation from the reaction mixture.

No epoxide **4.12d** or complex (dpms)Pt^{II}(dmso-d_6)(OH) (**4.13-d_6**), expected from reductive elimination, were detected in solution by ^{1}H NMR, ESI and GC/MS. Trace amounts (<5%) of 1-naphtol and 2-naphthol were detected by ^{1}H NMR and GC/MS after 160 hours of heating.

1-Naphtol, **GC/MS (EI)** m/z (%) (RT=9.80 min): 144 (100), 116 (21), 115 (69), 89 (8), 63 (6), 39 (4). **GC/MS (CI)** m/z (%) (RT=9.80 min): 145 (66), 144 (100), 116 (30), 115 (27), 51 (22), 50 (27). **2-Naphthol**, **GC/MS (EI)** m/z (%) (RT=9.87 min): 144 (100), 116 (16), 115 (61), 89 (6), 63 (5), 39 (3). **GC/MS (CI)** m/z (%) (RT=9.87 min): 145 (59), 144 (100), 116 (14), 115 (25), 51 (20), 50 (23).

GC/MS conditions: injector temp. 250 ^{o}C, carrier gas He, temp. program from 60 ^{o}C(hold 3 min) to 280 ^{o}C (hold 2 min) at 20 ^{o}C/min for a total run time of 16 min, mass range 20-650 amu.

Characterization of complex 4.14d. Samples of the reaction mixtures containing **4.14d** (in concentrations 3-9 mM) were prepared by heating complex **4.3d** in dmso-d_6 ([**4.3d**]$_{initial}$=12-45 mM) at 60 °C for 9-11 hours. ^{1}H and ^{13}C assignments are made from selective COSY, HSQC and DEPT experiments. **^{1}H NMR** (dmso-d_6): 3.61 (s, 1H), 3.68 (d, J = 5.4 Hz, $^{2}J_{PtH}$ = 90 Hz, 1H), 4.64 (d, J = 5.4 Hz, $^{3}J_{PtH}$ = 32 Hz, 1H), 5.08 (s, 1H), 5.20 (s, 1H), 6.43 (s, 1H), 7.04-7.39 (m, 5H), 7.70-7.78 (m, 2H), 7.83 (d, J = 7.8 Hz, 1H), 7.88 (d, J = 7.8 Hz, 1H), 8.18 (td, J = 7.8, 1.6 Hz, 1H), 8.21 (td, J = 7.8, 1.6 Hz, 1H), 9.46 (dd, J = 6.0, 1.2 Hz, 1H), 9.77 (d, J = 6.0 Hz, 1H).

A doublet at 3.68 ppm was assigned as CHPt based on characteristically large Pt-H coupling constant 90 Hz and chemical shift typical for Pt^{IV}CH. 2D COSY experiment confirmed that a doublet of CHPt and a doublet at 4.64 ppm are J-coupled. Selective 1D-NOE experiments did not allow to conclusively confirm proposed structure of **4.14d**. Weak NOE was observed between one of *ortho*-protons (doublet at 9.46 ppm) and H-CO doublet at 4.64 ppm; however no NOE was detected reliably between *ortho*-protons and CHPt doublet at 3.68 ppm, expected for structure **4.14d**, which might be due to low concentration of complex **4.14d** and weak NOE.

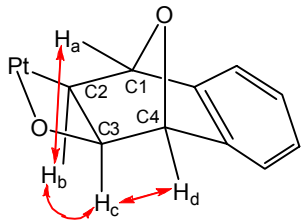

4.14d

Selected ^{1}H assignments (from NOE and HSQC) for epoxydyhydronaphthalene fragment of **4.14d**	
H_a	5.08
H_b	3.68
H_c	4.64
H_d	5.20
CHSO3	6.43
PtOH	3.61

Selected ^{13}C assignments (from HSQC) (ppm):	
C_1	80.9
C_2	6.3
C_3	91.6
C_4	83.7
$CHSO_3$	74.8

Section 4.2

H/D exchange and stability of D_2O solutions of LPt(*cis*-cyclooctene)(OH), 4.1a. The complex **4.1a** was prepared as described above. Assignment of proton resonances for **4.1a** in D_2O solution was made from NOE and described above in more detail.

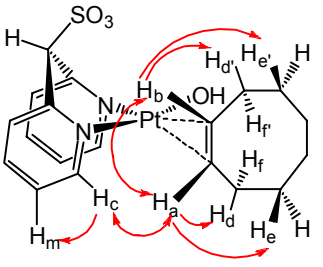

- important NOE's

Selected ^{1}H NMR assignments:	
H_a	5.67 ppm
H_b	5.11 ppm
H_c	8.50 ppm
H_d	2.28-2.39 ppm
$H_{d'}$	2.40-2.54 ppm
H_e	1.58-1.70 ppm
$H_{e'}$	1.31-1.51 ppm
H_f or $H_{f'}$	2.16-2.26 ppm
H_f or $H_{f'}$	2.00-2.22 ppm

8.9 mg (15 μmol) of **4.1a** and 5.0 μL of dioxane (internal standard) were dissolved in 0.8 mL of D_2O; initial [**4.1a**]=19.5 mM. The solution was placed into an NMR tube and stored at 20 °C under argon; NMR spectra were recorded periodically during 2 weeks. The concentration of the complex **4.1a** was calculated based on integration of the CH multiplet of the dpms ligand at 7.73 ppm; dioxane peak was used as an internal standard. Half-life of **4.1a** was estimated to be ~40 days at 20 °C. White solid precipitated during the course of the reaction. Concentration of **4.1a** decreased by 22% after 2 weeks at

20 °C (15.3 mM). Slow H/D exchange of coordinated cyclooctene protons was evident from decreasing ratio of the integral intensities of signals of cyclooctene to integral intensity of the aromatic protons dpms ligand. Four protons of coordinated cyclooctene, characterized by multiplets at 2.40-2.54 ppm, 2.28-2.39 ppm, 2.16-2.26 ppm and 2.00-2.22 ppm are 66-89% deuterated after 2 weeks at 20 ^{o}C in D_2O solution. These peaks were assigned as allylic protons based on their downfield shifted position in ^{1}H NMR spectrum and NOE experiments described above. Other peaks of coordinated cyclooctene, including vinylic positions, do not undergo significant H/D exchange (<6%). The results are given below.

H/D exchange in cyclooctene ligand in 19.5 mM solution of **4.1a** in D_2O; 20 ^{o}C:

t, h	[**4.1a**], mM	% H/D exchange in cyclooctene ligand					
		$H_{d'}$	H_d	H_f or $H_{f'}$ (2.16-2.26 ppm)	H_f or $H_{f'}$ (2.00-2.22 ppm)	multiplets at 1.23-1.93 ppm	Vinylic H_a + H_b
0	19.5	0	0	0	0	0	0
20	19.4	3	9	1	2	0	0
55	18.9	22	28	13	15	1	2
79	17.9	32	39	26	29	2	3
126	17.5	48	54	41	38	1	0
174	16.9	57	62	44	44	1	1
224	16.9	63	75	64	51	2	3
246	16.3	73	83	75	57	4	3
342	15.3	79	86	79	66	5	5

% H/D exchange was calculated from ratio of intensities of the cyclooctene resonances relative to the intensity of the non-exchangeable aromatic multiplet of dpms in **4.1a** at 7.73 ppm, related to the same ratio at the beginning of reaction (t=0).

In ^{13}C NMR spectrum after 2 weeks carbon peaks of complex **4.1a** at 29.4 and 28.8 split into two signals of comparable intensity, 29.4 and 29.3 ppm (C-D coupling was not resolved), and 28.8 and 28.7 ppm (C-D coupling was not resolved).

Formation of 4.16 in protic solvents. Identification of Pt-containing products of 4.1a decomposition in water. *1) Reaction in water at room temperature.* A solution of 50 mg (87 μmol) of (dpms)Pt^{II}(*cis*-cyclooctene)(OH) **4.1a** in 5 mL of H_2O was stored for 2 weeks at 20 ^{o}C under argon. A mixture of white microcrystalline solid and colorless crystals precipitated from solution. The larger crystals were analyzed by XRD and were identified as complex **4.16**. The precipitate was filtered, washed with water and dried; yield 4.5 mg. Dilute solution of the solid products in trifluoroethanol acidified with HBF_4 showed presence of two mass envelopes, corresponding to (dpms)Pt^{II}(η^3-C_8H_{13}) (**4.16**) and (dpms)$_2Pt^{II}{}_2$(μ-OH)$_2$ **3.10**. ESI-MS: m/z 554.1 and 923.0; calculated for (dpms)Pt^{II}(η^3-C_8H_{13})*H^+, $C_{19}H_{23}N_2O_3{}^{195}PtS$, 554.1; calculated for (dpms)$_2Pt^{II}{}_2$(μ-OH)$_2$*H^+, $C_{22}H_{21}N_4O_8{}^{195}Pt_2S_2$, 923.0.

*2) Reaction in water at 70-80 ^{o}C.*A solution of complex **4.1a** (3.3 mg) in D_2O/H_2O mixture (1:1 v/v) was placed into an NMR Young tube; dioxane (2 μL) was added as an internal standard. The solution was heated at 60-80^{0}C; NMR spectra were recorded periodically. A complex **4.1a** reacts with a half-

life of 2 hours at 70 °C to produce insoluble products; the reaction is complete after 15h at 80 °C. White precipitate was collected and dissolved in dmso-d_6 in the presence of internal standard (dioxane, 1 μL). The yield of allyl complex **4.16** was estimated to be ~30%, based on integration of doublets of *ortho*-protons of *cis*- and *trans*-**4** at 9.00 ppm and 9.18 ppm respectively using dioxane peak as an internal standard. ESI analysis showed the presence of peaks corresponding to protonated (dpms)$Pt^{II}(\eta^3\text{-}C_8H_{13})$ (**4.16**) and $(dpms)_2Pt^{II}{}_2(\mu\text{-}OH)_2$ **3.10**, m/z 554.1 and 923.0 respectively. The precipitate was analyzed elemental analysis. Anal. Found: C, 31.39; H, 2.96; N, 5.54. Calculated for allyl complex (dpms)Pt(η^3-C_8H_{13}) $C_{19}H_{22}N_2O_3PtS$, C, 41.23; H, 4.01; N, 5.06. Calculated for $(dpms)_2Pt_2(\mu\text{-}OH)_2$ $C_{22}H_{20}N_4O_8Pt_2S_2$, C, 28.64; H, 2.18; N, 6.07.

3) Reaction in methanol and water-methanol mixtures. A solution of 3.3 mg of **4.1a** in the mixture of D_2O (75 μL) and CD_3OD (615 μL) reacts at a much faster rate (half-life 12 minutes at 70 °C), compared to reaction in neat water, to produce allyl complex **4.16** with 85-90% yield after 3 hours, determined by ^{1}H NMR. The complex **4.1a** is poorly soluble in neat methanol and produces allyl complex **4.16** with a half-life of ~1.5h at 20 °C; the reaction was complete in CD_3OD after heating at 50 °C for 14 hours to give **4.16** in 80% yield, free cyclooctene (20%), determined by ^{1}H NMR, and white precipitate (presumably $(dpms)_2Pt_2(\mu\text{-}OR)_2$, R = H, Me).

Formation of 4.16 from (dpms)Pt(dmso)(OH) (4.13) and *cis*-cyclooctene

*1) Reaction in CD_3OD/D_2O (with or without NaOD).*A sample of **4.13** (5.2 mg, 10 μmol), 1 mL of CD_3OD, 20 μL of D_2O and *cis*-cyclooctene (90 μL, 690 μmol, 72 equiv.) were placed into a Young tube; 2 μL of dioxane was added to the resulting solution as an internal standard. The Young tube was Teflon-sealed and heated at 60 °C. The reaction was monitored by ^{1}H NMR. The complex **4.13** disappear with a half-life of 5h at 60 °C to produce soluble complex **4.16**, free DMSO and insoluble white precipitate, presumably $L_2Pt_2(\mu\text{-}OH)_2$. After heating for 24h at 60 °C only one soluble product was detected in solution, **4.16** (as a 1:1 mixture of *cis*- and *trans*-isomers), in 22-28% yield (2-3 μmol, 2 runs), based on integration of peaks of *ortho*-protons of pyridyls of dpms at 9.00 and 9.18 ppm relative to dioxane as an internal standard; no H/D exchange was seen in the cyclooctenyl ligand of **4.16**. An analogous reaction in the presence of 0.2 equivalent of NaOD gave **4.16** in 31% yield; no H/D exchange was seen in the cyclooctenyl ligand of **4.16**.

2) Reaction in CH_3OH/H_2O (with or without NaOH). The procedure analogous to that described above was used for the reaction in non-deuterated solvents. The reaction mixture in CH_3OH-H_2O (100 : 2 v/v) was heated at 60 °C for 24h, evaporated to dryness and redissolved in CD_3OD; 2 μL of dioxane was added as an internal standard. According to ^{1}H NMR, **4.16** formed in 22% yield in a neutral solution and 24% yield in the presence of 0.2 equivaletns of NaOH.

Attempted preparation of (dpms)Pt(η^2-cycloheptene)(OH) and (dpms)Pt(η^3-C_7H_{11}). *1) Reaction in H_2O.* A sample of (dpms)Pt(C_2H_4)(OH) (57.5 mg, 117 μmol) was dissolved in 3 mL of degassed water,

the resulting yellow solution was placed into 25 mL Schlenk tube equipped with a stirring bar. Cycloheptene (0.2 mL) was added. The reaction mixture was degassed by three freeze-pump-thaw cycles and Teflon-sealed under vacuum (50 mTorr). Stirring under vacuum continued for 2 days at rt. According to ^{1}H NMR, after 2 days 45% of the starting material is present unreacted. New products form, presumably (dpms)Pt(η^2-cycloheptene)(OH) (with characteristic multiplets of vinylic protons at 5.67 ppm and 5.10 ppm and $CHSO_3$ singlet at 6.23 ppm) and (dpms)Pt(η^3-C_7H_{11}) (characterized by triplet of *meso*-proton at 5.27 ppm, J = 5 Hz, and a singlet of $CHSO_3$ at 6.00 ppm); these new products were present in ~1:1 ratio.

2) Reaction in H_2O-acetone mixture. A solution of (dpms)Pt(C_2H_4)(OH) (49.8 mg, 102 μmol) in a mixture of H_2O (2 mL) and acetone (2 mL) was placed into 25 mL Schlenk tube equipped with a magnetic stirring bar; 0.7 mL of cycloheptene was added. Stirring continued for 2 days. According to ^{1}H NMR, after 1 days 60% of starting material in present unreacted. A new product, presumably allyl complex (dpms)Pt(η^3-C_7H_{11}), was detected in ~15% yield, characterized by a triplet at 5.27 ppm (J = 5 Hz, *meso*-H of allyl) and a singlet of $CHSO_3$ at 6.00 ppm. ESI analysis (CH_3OH-H_2O mixture) revealed the presence of the signal m/z 540.1; calculated for (dpms)Pt(η^3-C_7H_{11})*H^+ $C_{18}H_{21}N_2SO_3{}^{195}Pt$ 540.1.

Attempted preparation of (dpms)Pt(η^3-C_4H_7) by reacting (dpms)Pt(*cis*-butene)Cl (4.23) with NaOH. A suspension of 7.9 mg (15 μmol) of **4.23** in 0.7 mL D_2O was placed into a vial equipped with a magnetic stirring bar. 1 equivalent of 0.1 N NaOD/D_2O solution (150 μL) was slowly added to a stirred suspension at rt. Bubbles of gas formed immediately. Initially insoluble starting material dissolved during first few minutes. No starting material was detected in the resulting clear solution by ^{1}H NMR after 30 minutes at rt. The complex [(dpms)Pt$(OH)_2]^-$, resulting form the loss of *cis*-butene, was detected in solution and identified by ^{1}H NMR. White precipitate slowly forms in solution, presumably poorly soluble (dpms)PtCl(OH) and $(dpms)_2Pt_2(\mu\text{-}X)_2$ (X = OH, Cl).

Kinetics of allyl complex formation from 4.16 in CD_3OD/H_2O solutions at 50 °C (Table 4.2). A 19.95 mM solution of **4.1a** in H_2O was prepared as described earlier; its concentration was determined by ^{1}H NMR using dioxane as an internal standard. The reaction mixtures were prepared by mixing 50-100 μL of the above solution and CD_3OD (or H_2O if necessary); 0.5-1 equivalents of 1 N solution of HBF_4 in H_2O were added when necessary; dioxane (1 μL) was added as an internal standard. The solution was transferred into the NMR Young tube, Teflon sealed and loaded into a pre-heated (50 °C) NMR probe. Temperature inside the probe was estimated (±0.5 ^{o}C) by measuring the difference in the chemical shits of an ethylene glycol sample. ^{1}H solvent suppression spectra were recorded periodically using automated kinetics program. The concentrations of complexes **4.1a** and isomeric complexes *endo*- and *exo*-**4.16** were determined by integration of a doublet of *ortho*-protons at 8.52 ppm, doublets at 9.00 ppm and 9.18 ppm respectively using dioxane peak as an internal standard. The product **4.16**

was identified by ^{1}H NMR. No precipitate formed during the kinetic experiments on determination of initial rates of formation of **4.16** and rate constants of disappearance of **4.1a**. Upon further heating at 50 ^{o}C for several days white precipitate formed in the reaction mixtures. Formation of free *cis*-cyclooctene was detected in solution by ^{1}H NMR. The overall first order rate constant *k* of disappearance of starting material **4.1a** was determined at reaction times 0÷115 minutes.

Chapter 5

Oxidation of 5.3 with O_2 in neutral and acidic solutions

1) Oxidation in neutral solution and in the presence of 1 equivalent of HBF_4. Two samples of **5.3** (5.0-5.5 mg each, 8.3-9.0 μmol) were dissolved in 1 mL of CD_3OD each, and the resulting solutions were placed into 10 mL flasks, equipped with a magnetic stirring bar. One equivalent of HBF_4 (1.4 μL of aqueous 50% wt. HBF_4) was added to one of the solutions. The vials were filled with O_2, and the solutions were stirred under an O_2 atmosphere at rt for 2-24 hours and periodically analyzed by ^{1}H NMR. No changes were observed in ^{1}H NMR spectrum of the neutral reaction mixture after 2-24 hours under O_2, and only starting material **5.3** was present. Oxidation of **5.3** into **5.5** was observed in acidic solution with a half-life of 2h at 20 ^{o}C. After 24 hours **5.3** disappeared and **5.5** formed, along with a mixture of unidentified products. The product **5.5** was 73% pure by ^{1}H NMR, based on the integration of a singlet of *t*-Bu of **5.5** at 1.23 ppm relative to the singlets of *t*-Bu of all reaction products present in the region 1.0-1.4 ppm.

Analogous procedure was used for oxidation in D_2O in neutral solution or in the presence of 1 equivalent of HBF_4. No reaction occurred in neutral D_2O after 2-24 hours at rt. Oxidation of **5.3** was observed in the presence of 1 eq. HBF_4 in D_2O, with a half-life of 2.4 hours at 20 ^{o}C, to form **5.5** (80% pure by ^{1}H NMR, after reaction was complete).

Attempted reductive elimination from 5.9 in aprotic solvents

1) Reaction in THF-d_8. A sample of **5.9** (10 mg, 6.8 μmol, in a mixture with 1 equivalent of of $KBAr^F_4$) was dissolved in 0.7 mL of dry degassed THF-d_8, and the resulting yellow solution was placed into an NMR Young tube; [**5.9**]=9.8 mM. The reaction mixture was heated at 60 ^{o}C under an argon atmosphere and periodically analyzed by ^{1}H NMR. The signals of starting material disappear with a half-life of 22h at 60 ^{o}C to produce insoluble products. After 4 days at 60 ^{o}C no **5.9** remained in solution, and insoluble reaction products were dissolved in MeOH or dmso-d_6.

In dmso-d_6 solution of decomposition products, the complex **5.3** was detected by 1H NMR, identified by comparison with ^{1}H NMR spectrum of authentic sample of **5.3**. ESI-MS of acidified MeOH of decomposition products revealed the presence of a strong signal, characterized by m/z 545.1, corresponding to a protonated **5.3***H^+ (calc. $C_{17}H_{24}N_3SO_3{}^{195}Pt$ 545.1). Low intensity peaks were detected by ESI-MS, characterized by m/z 561.1 and 480.0.

2) Reaction in CD_2Cl_2 and C_6D_6. A solution of 15 mg of **5.9** in 0.7 mL CD_2Cl_2 ([**5.9**]=15 mM) was relatively stable at reflux temperature, and **5.9** remained in solution mostly unreacted after 3 days of heating at 60 ^oC in a sealed Young tube. The suspension of partially soluble **5.9** (8 mg, 5 μmol) in C_6D_6 was heated in a sealed Young tube at 60 ^oC for 25 hours, and the resulting reaction mixture was evaporated to dryness, redissolved in dmso-d_6 and analyzed by ^1H NMR. The presence of complex mixture of unidentified products, **5.3** (in 18% yield) and unreacted **5.9** (31%) was observed by ^1H NMR. The yields of **5.3** and **5.9** were estimated by integration of $CHSO_3$ singlets at 5.82 ppm and 6.99 ppm respectively, using BAr^F_4 peaks as an internal standard.

Reductive elimination from [5.5]Cl in neutral and acidic D_2O solutions. A solution of 3.7 mg of [*cis*-**5.5**]Cl (3.7 mg, 6 μmol) in 0.7 mL D_2O was placed into an NMR Young tube and was heated at 100 ^oC. The reaction was monitored by 1H NMR. The complex [*cis*-**5.5**]Cl disappeared with a half-life 21h. An intermediate species appeared in the beginning of reaction and eventually disappeared after prolonged heating, characterized by a multiplet at 3.87-3.97 ppm. After 5 days at 100 ^oC [*cis*-**5.5**]Cl has completely disappeared. The organic product of reaction was identified as N-*tert*-butylethanoammonium salt, by comparison of ^1H NMR spectrum with an authentic sample, which formed in 65%, yield based in integration of a multiplet at 3.83 ppm using residual solvent peak as a standard. Insoluble product formed, presumably $L_2Pt_2(\mu\text{-}OH)_2$.

$HOCH_2CH_2NH_2t\text{-}Bu^+$. ^1H NMR (D_2O, 22^0C, 400 MHz): 1.38 (s, 9H), 3.16 (m, AA'XX', 2H), 3.83 (m, AA'XX', 2H).

Reductive elimination from $[\mathbf{5.6}]_2(SO_4)$ in acidic D_2O solutions. A sample of $[\mathbf{5.6}]_2(SO_4)$ (10.8 mg, 17 μmol, isomeric *cis*-/*trans*- mixture in 6 : 1 ratio) was dissolved in 0.8 mL of D_2O, acidified with ~1 equivalent of HBF_4 (4 μL of 50% wt. aq. HBF_4, 16 μmol). The resulting solution was placed into an NMR Young tube, and ^1H NMR spectrum of the reaction solution was recorded before reaction and then in regular intervals after heating at 100 ^oC.

Formation of protonated *N*-methyl ethanolamine, $HOC_2H_4NH_2Me^+$, was detected by ^1H NMR, identified by comparison of ^1H NMR spectrum with an authentic sample. The product $[LPt^{II}(OH_2)_2]^+$, described earlier,[79] was detected by ^1H NMR as the main Pt-containing product after 33 hours at 100 ^oC.

Crystalline precipitate formed in small amounts after heating for 33h. The insoluble product was separated from solution and dissolved in 0.8 mL of D_2O the presence of 20 μL of 50 wt. % HBF_4 at 100 ^oC to give $[LPt^{II}(OH_2)_2]^+$ as the sole product, detected by ^1H NMR.

$HOCH_2CH_2NH_2Me^+$. **^1H NMR** (D_2O/HBF_4, 22^0C, 400 MHz): 2.74 (s, 3H), 3.16 (m, AA'XX', 2H), 3.83 (m, AA'XX', 2H).

The intermediate **5.11** was characterized by the following set of signals in ^1H NMR spectrum in D_2O: 2.48 (s, 3H), 2.55-2.70 (m, 1H), 3.04-3.15 (m, 1H), 3.86-3.94 (m, 1H), 3.96-4.06 (m, 1H), 8.71 (d, *J* =

6.0 Hz, *ortho*-H of py), 8.94 (d, J = 6.0 Hz, *ortho*-H of py). Other peaks could not be seen due to overlap with resonances of **5.6** and reaction products.

The graphs of concentration of **5.6** (filled circles), **5.11** (empty rhombs) and $HOC_2H_4NH_2Me^+$ (filled triangles) *vs.* time and the graph in coordinates ln([**5.6**]$_0$/[**5.6**]) *vs.* time are given below. Concentrations of **5.6**, **5.11** and $HOC_2H_4NH_2Me^+$ were calculated by integration of NMe group of isomeric complexes **5.6** at 2.46 ppm and 2.30 ppm, CH_2-multiplet of **5.11** at 3.86-4.06 ppm and a multiplet of $HOC_2H_4NH_2Me^+$ at 3.83 ppm, using residual HDO peak as an internal standard. The 1st order rate constant of disappearance of **5.6** at 100 ^oC was estimated to be (6.0±0.3)*10^{-5} s^{-1}.

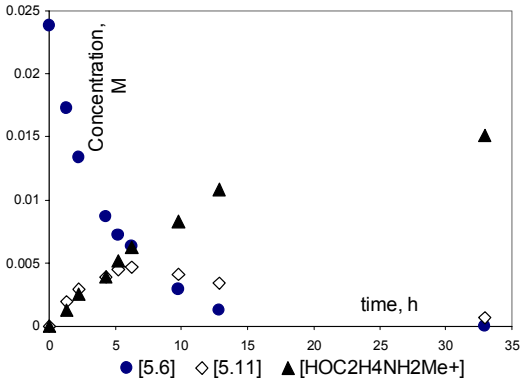

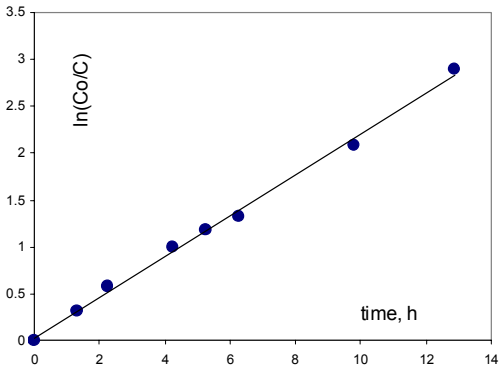

Chapter 6

Attempted reductive elimination from *sym*-(dpms)Pt^{IV}Ph$_2$(OH), *sym*-6.6 in DMSO-d_6 solution. A sample of *sym*-**6.6** (2 mg, 3.2 μmol) was dissolved in dry DMSO-d_6 (0.7 mL) and solution was placed into an NMR Young tube under an argon atmosphere. The Young tube was heated at 100^{0}C in a silicon-oil bath. The only reaction observed was isomerization of **6.6** into corresponding unsymmetrical isomer (half-life is 26h). After 6 days the isomerization was complete, yield of *unsym*-**6.6** >97% by ^{1}H NMR spectroscopy. No biphenyl or phenol were detected.

***Unsym*-6.6: ^{1}H NMR** (dmso-d_6, 22 ^oC), δ: 1.37 (br s, 1H, OH), 6.65 (d, J = 8.2 Hz, $^3J_{195PtH}$ = 44 Hz, 2H), 6.78 (s, 1H), 6.88-7.12 (m, 6H), 7.20-7.39 (m, 2H), 7.59 (ddd, J = 7.9, 5.9, 1.5 Hz, 1H), 7.65 (ddd, J = 7.9, 5.7, 1.3 Hz, 1H), 8.00 (dd, J = 5.7, 1.5 Hz, 1H), 8.08 (d, J = 7.9 Hz, 1H), 8.14 (dd, J = 7.9, 1.5 Hz, 1H), 8.20 (dd, J = 5.9, 1.5 Hz, 1H), 8.25 (td, J = 7.9, 1.5 Hz, 1H), 8.34 (td, J = 7.9, 1.5 Hz, 1H). **^{13}C NMR** (dmso-d_6, 22 ^oC), δ: 71.9, 124.3, 125.1, 125.5, 125.8, 126.9, 127.1, 127.3, 127.4, 128.4, 128.7, 132.7, 133.8, 141.6, 142.6, 148.7, 150.3, 152.7, 152.9.

Isomerization of *unsym*-(dpms)Pt^{IV}Ph(OH)$_2$, *unsym*-6.7 into *sym*-6.7. Solution of A sample of *unsym*-**6.7** (103 mg, 180 μmol) in water (30 mL) was placed into a 50 mL round bottom flask equipped with a magnetic stirring bar and a condenser. The mixture was heated at 100^{0}C. After 70h the reaction mixture was reduced in volume to ~1 mL under vacuum and left at 5^{0}C for 1h. White precipitate was filtered off and dried under vacuum for 6h. Yield 94 mg, 91%.

^{1}H NMR (dmso-d_6, 22 ^{o}C), δ: 2.32 (br s, $^2J_{195PtH}$ = 26 Hz, 2H, OH), 6.38 (d, J = 7.3 Hz, $^3J_{195PtH}$ = 35 Hz, 2H), 6.74 (s, 1H), 6.87 (vt, J = 7.3 Hz, 2H), 7.04 (vt, J = 7.3 Hz, 1H), 7.65 (ddd, J = 7.8, 5.8, 1.3 Hz, 2H), 8.06 (d, J = 5.8 Hz, 2H), 8.08 (d, J = 7.8 Hz, 2H), 8.31 (td, J = 7.8, 1.3 Hz, 2H). **^{13}C NMR** (dmso-d_6, 22 ^{o}C), δ: 72.1, 125.9, 126.3, 127.2, 127.4, 128.0, 132.5, 142.3, 149.8, 150.9. **IR** (KBr), ν: 3500 (w, br), 3062 (w), 2964 (w), 1607 (w), 1574 (w), 1475 (w), 1441 (w), 1267 (m), 1205 (m), 1146 (s), 996 (m), 736 (m), 691 (m) cm^{-1}.

Attempted reductive elimination from *sym*-(dpms)Pt^{IV}Ph(OH)$_2$, *sym*-6.7. Four samples of *sym*-**6.7** (2.5 mg each, 4.5 μmol) were dissolved in neutral D_2O (0.8 mL), 50 mM solution of HBF_4 in D_2O (0.8 mL), 11 mM NaOD/D_2O solution (0.8 mL) and DMSO-d_6 (0.8 mL) under argon. The solutions were placed into NMR Young tubes and Teflon-sealed. Residual solvent peaks were used as internal standards. The solutions were heated at 100^{0}C. According to ^{1}H NMR spectroscopy, concentration of *sym*-**6.7** remained unchanged after 5 days; no products were detected by ^{1}H NMR.

Attempted reductive elimination from (dpms)Pt^{IV}Ph(OH)(OMe), 6.8, in dmso-d_6 . A sample of **6.8** (2 mg, 3.5 μmol) was dissolved in 0.7 mL of dmso-d_6. The solution was placed into an NMR Young tube and Teflon-sealed under argon. The solution was heated at 80-100^{0}C, periodically cooled down to room temperature and analyzed by ^{1}H NMR. Slow reaction occurred at 80 °C with a half-life of ~47h. The reaction continued at 100 °C with a half-life of 4.5h; quantitative formation of (dpms)PtPh(dmso-d_6) (**6.5**-d_6) was observed. ^{1}H NMR of the product was identical to that of **6.5**-d_6 obtained by dissolving (dpms)PtPh(MeOH) in dmso-d_6; ESI of acidified solution diluted with methanol, m/z=606.1 (Calcd. For (dpms)PtPh(C_2D_6SO)·H$^+$, $C_{19}H_{15}D_6N_2S_2O_4{}^{195}$Pt, m/z 606.1). One equivalent of methanol was released into solution, according to ^{1}H NMR spectroscopy.

Attempted reductive elimination from (dpms)Pt^{IV}Ph(NHPh)(OH), 6.9.

Reaction in CD_3CN. A sample of (dpms)PtPh(NHPh)(OH) (3 mg, 5 μmol) and 0.7 mL of CD_3CN were placed into an NMR Young tube and Teflon-sealed under argon. The reaction mixture was heated at 80 °C for 5h; dark precipitate and dark-colored solution formed. The only product present in the solution after 5h was (dpms)PtPh(CD_3CN), according to ^{1}H NMR spectroscopy and ESI-MS. Characteristics of the product are identical to those of (dpms)PtPh(CD_3CN) obtained by dissolving (dpms)PtPh(MeOH) in CD_3CN:

^{1}H NMR (CD_3CN, 22 ^{o}C), δ: 5.82 (s, 1H), 6.92-7.03 (m, 4H), 7.24 (dd, J = 7.5, 1.5 Hz, $^3J_{195PtH}$=45 Hz, 2H), 7.52 (ddd, J = 7.9, 5.5, 1.5 Hz, 1H), 7.74 (dd, J = 7.9, 1.5 Hz, 1H), 7.85 (d, J = 7.9 Hz, 1H), 7.97 (td, J = 7.9, 1.5 Hz, 1H), 8.07 (td, J = 7.9, 1.5 Hz, 1H), 8.15 (dd, J = 5.7, 1.5 Hz, $^3J_{195PtH}$=63 Hz, 1H), 8.85 (dd, J = 5.5, 1.5 Hz, 1H).

ESI-MS of acidified solution diluted with methanol, m/z 566.1 (Calcd. for (dpms)^{195}PtPh(CD_3CN)·H$^+$, $C_{19}H_{15}D_3N_3O_3{}^{195}$PtS, 566.1).

The precipitate formed in the reaction mixture was dissolved in dmso-d_6; ^{1}H NMR spectrum of the resulting solution showed the presence of a complex mixture of unidentified products. No diphenylamine was detected by ^{1}H NMR.

Reaction in DMF-d_7 . Upon heating at 60 °C, the starting material slowly disappeared and an insoluble product formed. After heating the sample at 80 °C for 24h, complex mixture of product formed in DMF-d_7 solution, and a dark precipitate.

Chapter 7

^{1}H NMR and ESI-MS characterization of $Pd(OAc)_2$ – K(Medpms) solutions

Prepartion of ^{1}H NMR solutions. 7.25 mM solution of $Pd(OAc)_2$ in CD_3COOD or CH_3COOH was added to a sample of K(Medpms) (1 or 2 equivalents). The resulting orange yellow solution placed into an NMR tube and the reaction mixture was periodically analyzed by ^{1}H NMR. After 20 minutes after mixing reagents, ~50-60% of the ligand was present as free uncomplexed K(Medpms), characterized by a singlet of a Me group at 2.80 ppm and a doublet of *ortho*-proton of pyridyls at 8.77 ppm. After 24 hours a peak of free K(Medpms) disappeared completely to give a new set of signals that remained unchanged over time upon standing for 24 hours at rt and after heating at 50 ^{o}C for 15 hours. See section 7.2.1 for discussion of ^{1}H NMR spectra.

*Preparation of $Pd(OAc)_2$ – K(Medpms) solutions for ESI-MS analysis.*Samples of K(Medpms) (7.0-14.0 mg) were dissolved in 0.8 mL of 14.5 mM $Pd(OAc)_2$; the resulting solution was stored at rt for 2 days and analyzed by ESI after dilution with water (HOAc : H_2O 1:1 v/v).

ESI-MS of solution of $Pd(OAc)_2$ – K(Medpms)in 1 : 1 ratio: m/z 466.9 ((Medpms)Pd(OAc)*K^+, calc. for $C_{14}H_{14}SO_5N_2{}^{106}PdK$ m/z 466.9) and m/z 670.9 ([(Medpms)$_2$Pd]*K^+, calc. $C_{24}H_{22}S_2O_6N_4{}^{106}PdK$ m/z 671.0).

ESI-MS of solution of $Pd(OAc)_2$ – K(Medpms)in 1 : 2 ratio: a positive ion m/z 670.9 ([(Medpms)$_2$Pd]*K^+, calc. $C_{24}H_{22}S_2O_6N_4{}^{106}PdK$ m/z 671.0) was observed, and a very weak signal m/z weak 466.9 ((Medpms)Pd(OAc)*K^+, calc. for $C_{14}H_{14}SO_5N_2{}^{106}PdK$ m/z 466.9). No ions were detected in a negative mode.

^{1}H NMR and ESI-MS characterization of solution of $Pd(OAc)_2$ – K(Medpms) – dpk in 1 : 0.5 : 0.5 ratio. 0.5 equivalents of dpk and 0.5 equiv of K(Medpms) were dissolved in 7.2 mM solution of $Pd(OAc)_2$ in CD_3COOD. According to ^{1}H NMR, after 24 hours at 20 ^{o}C, signals of free K(Medpms) and dpk disappeared and a mixture of new products formed. No changes were observed in ^{1}H NMR spectrum after further standing for 48 hours at 20 ^{o}C and after heating at 50 ^{o}C for 15 hours.

According to ^{1}H NMR, two new major Medpms-containing products are formed which were not previously observed in solutions containing K(Medpms) only (in the amounts of 0.5-2 equivalents). These new products are characterized by singlets of Me group at 2.26 and 2.56 ppm, integrating as 1.48 and 3.00 respectively. Other minor Medpms-containing products were characterized by singlets of

the Me groups at 2.24 ppm, 2.40 ppm and 3.25 ppm and integrated as 0.15, 0.13 and 0.52 respectively. The latter three signals were also observed in solutions in the absence of dipyridylketone and were assigned as (2:1) and (1:1) Medpms : Pd complexes respectively. The previously characterized complex (dpk)$Pd(OAc)_2$ **7.1** was detected by ^1H and ESI-MS in mixed-ligand systems. According to ^1H NMR, 27% of all dpk ligand was present as **7.1**, based on integration of *ortho*-protons at 8.77 ppm. Other aromatic peaks could not be assigned due to the complexity of the mixture and overlapping with other signals.

ESI-MS. A solution containg K(Medpms) (5.5 μmol), dpk (5.5 μmol) and $Pd(OAc)_2$ (11 μmol) in 0.8 mL CH_3COOH was equilibrated for 3 days and then diluted with H_2O immediately before the analysis. The most intensive peak was observed at m/z 571.0, corresponding to (Medpms)(dpk*H_2O)Pd^+, and a weaker signal was observed at m/z 367.0, corresponding to (dpk*OH_2)$Pd(OAc)^+$. No anions were detected in a negative mode of ESI.

Kinetics of ethylene oxidation with H_2O_2 (Tables 7.3, 7.4)

General procedure for kinetic experiments. Mixed-ligand dpk-K(Medpms)-$Pd(OAc)_2$ catalyst solutions in CD_3COOD were equilibrated for 4-7 days before use. Aqueous 30 wt. % H_2O_2 solution (45 μL) was added with a microsyringe to 0.6 mL of the catalyst solution ([$Pd(OAc)_2$]=$1.4*10^{-3}$ M, [KMedpms]= $7.0*10^{-4}$ M; [dpk]=$7.0*10^{-4}$ M). The resulting mixture was immediately transferred with a Teflon syringe into a thermostated 50 mL Schlenk flask equipped with a magnetic stirring bar, pre-filled with ethylene and connected to an ethylene-filled Schlenk line with silicon oil-filled bubbler. The magnetic stirrer was turned on immediately after transferring of the solution into a flask; the reaction was timed from this moment. The reaction mixture was stirred vigorously under an ambient atmosphere of ethylene. Periodically a sample of the reaction mixture was collected with a Teflon syringe (0.35-0.4 mL). Each sample was mixed carefully with a pre-weight amount of a HMDS standard solution (0.4 mL) and analyzed by ^1H NMR immediately. When variable amounts of H_2O_2 were used, water concentration was kept constant (0.64 M) by adding H_2O to the reaction mixture.

Reaction order in ethylene. Ethylene solution in CD_3COOD was prepared by stirring neat CD_3COOD in a 50 mL Schlenk flask filled with ethylene under an ambient atmosphere of ethylene for 1-2 hours. A standard solution was prepared by dissolving hexamethyldisiloxane in neat CD_3COOD; [HMDS]=45 mM. The Young tube of a known volume (2.8 mL) was filled with gaseous ethylene. 100 μL of a mixed-ligand catalyst solution ([$Pd(OAc)_2$]=7.2 mM; [KMedpms]=3.1 mM, [dpk]=3.1 mM), 42 μL of 30% aq. H_2O_2 and variable amounts of the standard solution and ethylene solutions were transferred to the Young tube to the total volume 2.8 mL so that no gaseous phase was remaining when the NMR Young tube was Teflon-sealed. Variable concentrations (2 - 20 mM) of ethylene were obtained by varying the ratio of standard solution and ethylene solution in CD_3COOD. The Young tube was placed into a thermostated at 20 ^oC NMR probe. NMR spectra were recorded using automated kinetics program in regular time intervals. The standard HMDS was stable under reaction conditions.

Concentration of ethylene was determined by integration of ethylene peak at 5.38 ppm using hexamethyldisiloxane peak as an internal standard and remained practically unchanged during the period of reaction used for determining initial rate ([ethylene] > 10*[Pd]). Concentrations of palladium catalyst and hydrogen peroxide were constant in all experiments; [Pd]=$2.6*10^{-4}$ M; [H_2O_2]=0.145 M. The results of the kinetic experiments in the presence of a mixed-ligand palladium catalyst (K(Medpms) : dpk : $Pd(OAc)_2$ = 0.5 : 0.5 : 1 moles) are given below.

Mixed-ligand KMedpms (0.5 eq)-dpk (0.5 eq)-$Pd(OAc)_2$ catalyst:

Reaction order in [Pd] and H_2O_2. Reaction in the presence of 2,6-di-*tert*-butyl-*p*-cresol (BHT). T = 20 °C; P(ethylene) = 1 atm

[$Pd(OAc)_2$], mM	[H_2O_2], mM	$V_{EG}*10^6$, M/s	V_W*10^7, M/s
1.45	145	1.17±0.06	1.91±0.11
1.45	145	1.28±0.10	2.08±0.24
2.90	145	2.40±0.08	2.40±0.20
4.35	145	3.89±0.21	3.25±0.17
1.45 [BHT]=2.7 mM[a]	145	1.25±0.07	1.95±0.20
1.45	72.5	1.12±0.07	0.0953±0.122
1.45	36.2	1.10±0.08	0.109±0.0225

[a] BHT is 2,6-di-*tert*-butyl-*p*-cresol.

Reaction order in [ethylene]. [Pd]=$2.6*10^{-4}$ M; [H_2O_2]=0.145 M; T = 20 °C.

[ethylene], mM	$V_{EG}*10^6$, M/s	V_W*10^7, M/s
53.0	13.6±0.67	4.77±0.46
24.0	5.84±0.23	2.15±0.11
5.0	1.13±0.05	0.54±0.09

Crystal data and structure refinement for (dpms)$Pt^{IV}Me_{eq}(OH)$, **2.4**.

X-ray lab book No.	1320	
Empirical formula	$C_{14}H_{20}N_2O_6PtS$	
Formula weight	539.47	
Temperature	223(2) K	
Wavelength	0.71073 Å	
Crystal size	$0.095 \times 0.085 \times 0.045$ mm^3	
Crystal habit	colorless prism	
Crystal system	Monoclinic	
Space group	$P2_1/c$	
Unit cell dimensions	a = 8.457(3) Å	$\alpha = 90°$
	b = 24.941(9) Å	$\beta = 107.501(6)°$
	c = 8.718(3) Å	$\gamma = 90°$
Volume	1753.7(11) Å^3	
Z	4	
Density, ρ_{calc}	2.043 g/cm^3	
Absorption coefficient, μ	8.152 mm^{-1}	
F(000)	1040 $\bar{e}$	
Diffractometer	Bruker Smart1000 CCD area detector	
Radiation source	fine-focus sealed tube, MoK_α	
Generator power	50 kV, 20 ma	
Detector distance	4.958 cm	
Detector resolution	8.33 pixels/mm	
Total frames	1270	
Frame size	512 pixels	
Frame width	0.3 °	
Exposure per frame	53 sec	
Total measurement time	21.22 hours	
Data collection method	ω scans	
θ range for data collection	2.53 to 25.00°	
Index ranges	$-10 \le h \le 9$, $-29 \le k \le 29$, $-10 \le l \le 10$	
Reflections collected	8399	
Independent reflections	3072	
Observed reflection, I>2σ(I)	2455	
Coverage of independent reflections	99.5 %	
Variation in check reflections	0.00 %	
Absorption correction	Semi-empirical from equivalents SADABS (Sheldrick, 1996)	
Max. and min. transmission	0.693 and 0.492	
Structure solution technique	direct	
Structure solution program	SHELXS-97 (Sheldrick, 1990)	
Refinement technique	Full-matrix least-squares on F^2	
Refinement program	SHELXL-97 (Sheldrick, 1997)	
Function minimized	$\Sigma w(F_o^2 - F_c^2)^2$	
Data / restraints / parameters	3072 / 31 / 249	
Goodness-of-fit on F^2	0.996	
Δ/σ_{max}	0.001	
Final R indices: R_1, I>2σ(I)	0.0359	
wR_2, all data	0.0787	
R_{int}	0.0344	
R_{sig}	0.0428	
Weighting scheme	$w = 1/[\sigma^2(F_o^2) + (0.03P)^2 + 9.6P]$, $P = [\max(F_o^2, 0) + 2F_o^2]/3$	
Largest diff. peak and hole	2.158 and -1.082 $\bar{e}$/Å^3	

$R_1 = \Sigma||F_o|-|F_c||/\Sigma|F_o|$, $wR2 = [\Sigma w(F_o^2-F_c^2)^2/\Sigma w(F_o^2)^2]^{1/2}$

Crystal data and structure refinement for (dpms)$Pt^{IV}Me_{eq}$(OMe)(OH), **2.5**.

X-ray lab book No.	1320	
Empirical formula	$C_{14}H_{20}N_2O_6PtS$	
Formula weight	539.47	
Temperature	223(2) K	
Wavelength	0.71073 Å	
Crystal size	$0.095 \times 0.085 \times 0.045$ mm^3	
Crystal habit	colorless prism	
Crystal system	Monoclinic	
Space group	$P2_1/c$	
Unit cell dimensions	a = 8.457(3) Å	$\alpha = 90°$
	b = 24.941(9) Å	$\beta = 107.501(6)°$
	c = 8.718(3) Å	$\gamma = 90°$
Volume	1753.7(11) Å^3	
Z	4	
Density, ρ_{calc}	2.043 g/cm^3	
Absorption coefficient, μ	8.152 mm^{-1}	
F(000)	1040 $\bar{e}$	
Diffractometer	Bruker Smart1000 CCD area detector	
Radiation source	fine-focus sealed tube, MoK_α	
Generator power	50 kV, 20 ma	
Detector distance	4.958 cm	
Detector resolution	8.33 pixels/mm	
Total frames	1270	
Frame size	512 pixels	
Frame width	0.3 °	
Exposure per frame	53 sec	
Total measurement time	21.22 hours	
Data collection method	ω scans	
θ range for data collection	2.53 to 25.00°	
Index ranges	$-10 \le h \le 9$, $-29 \le k \le 29$, $-10 \le l \le 10$	
Reflections collected	8399	
Independent reflections	3072	
Observed reflection, I>2σ(I)	2455	
Coverage of independent reflections	99.5 %	
Variation in check reflections	0.00 %	
Absorption correction	Semi-empirical from equivalents SADABS (Sheldrick, 1996)	
Max. and min. transmission	0.693 and 0.492	
Structure solution technique	direct	
Structure solution program	SHELXS-97 (Sheldrick, 1990)	
Refinement technique	Full-matrix least-squares on F^2	
Refinement program	SHELXL-97 (Sheldrick, 1997)	
Function minimized	$\Sigma w(F_o^2 - F_c^2)^2$	
Data / restraints / parameters	3072 / 31 / 249	
Goodness-of-fit on F^2	0.996	
Δ/σ_{max}	0.001	
Final R indices: R_1, I>2σ(I)	0.0359	
wR_2, all data	0.0787	
R_{int}	0.0344	
R_{sig}	0.0428	
Weighting scheme	$w = 1/[\sigma^2(F_o^2) + (0.03P)^2 + 9.6P]$, $P = [\max(F_o^2, 0) + 2F_g^2]/3$	
Largest diff. peak and hole	2.158 and -1.082 $\bar{e}$/Å^3	

$R_1 = \Sigma||F_o|-|F_c||/\Sigma|F_o|$, $wR2 = [\Sigma w(F_o^2-F_c^2)^2/\Sigma w(F_o^2)^2]^{1/2}$

Crystal data and structure refinement for (dpms)Pt^{IV}Me(OH)(NHPh), **2.6**.

X-ray lab book No.	1363	
Empirical formula	$C_{18}H_{19}N_3O_4PtS$	
Formula weight	568.51	
Temperature	220(2) K	
Wavelength	0.71073 Å	
Crystal size	$0.21 \times 0.18 \times 0.17$ mm^3	
Crystal habit	dark-orange prism	
Crystal system	Monoclinic	
Space group	$P2_1/c$	
Unit cell dimensions	a = 8.530(2) Å	α = 90°
	b = 11.102(3) Å	β = 90.916(4)°
	c = 19.457(5) Å	γ = 90°
Volume	1842.4(8) Å^3	
Z	4	
Density, ρ_{calc}	2.050 g/cm^3	
Absorption coefficient, μ	7.759 mm^{-1}	
F(000)	1096 $\bar{e}$	
Diffractometer	Bruker Smart1000 CCD area detector	
Radiation source	fine-focus sealed tube, Mo*K*α	
Generator power	50 kV, 40 mA	
Detector distance	4.939 cm	
Detector resolution	8.33 pixels/mm	
Total frames	3024	
Frame size	512 pixels	
Frame width	0.3 °	
Exposure per frame	23 sec	
Total measurement time	25.33 hours	
Data collection method	ω and φ scans	
θ range for data collection	2.11 to 28.00°	
Index ranges	$-10 \le h \le 11$, $-14 \le k \le 14$, $-25 \le l \le 25$	
Reflections collected	22924	
Independent reflections	4408	
Observed reflection, I>2σ(I)	3997	
Coverage of independent reflections	98.9 %	
Variation in check reflections	0.56 %	
Absorption correction	Semi-empirical from equivalents	
	SADABS (Sheldrick, 1996)	
Max. and min. transmission	0.267 and 0.198	
Structure solution technique	direct	
Structure solution program	SHELXS-97 (Sheldrick, 1990)	
Refinement technique	Full-matrix least-squares on F^2	
Refinement program	SHELXL-97 (Sheldrick, 1997)	
Function minimized	$\Sigma w(F_o^2 - F_c^2)^2$	
Data / restraints / parameters	4408 / 1 / 267	
Goodness-of-fit on F^2	1.000	
Δ/σ_{max}	0.001	
Final R indices: R_1, I>2σ(I)	0.0231	
wR_2, all data	0.0588	
R_{int}	0.0225	
R_{sig}	0.0154	
Weighting scheme	$w = 1/[\sigma^2(F_o^2) + (0.0285P)^2 + 5.68P]$,	
	$P = [\max(F_o^2, 0) + 2F_c^2]/3$	
Largest diff. peak and hole	2.834 and -1.306 $\bar{e}$/Å^3	

$R_1 = \Sigma||F_o|-|F_c||/\Sigma|F_o|$, $wR2 = [\Sigma w(F_o^2-F_c^2)^2/\Sigma w(F_o^2)^2]^{1/2}$

Crystal data and structure refinement for (dpms)$Pt^{IV}Me_{ax}$(OMe)(OH), **2.14**.

X-ray labbook No.	1316	
Empirical formula	$C_{27.625}H_{39.50}BF_4N_4O_{11.625}Pt_2S_2$	
Formula weight	1154.74	
Temperature	223(2) K	
Wavelength	0.71073 Å	
Crystal size	$0.12 \times 0.07 \times 0.06$ mm^3	
Crystal habit	colorless prism	
Crystal system	Triclinic	
Space group	*P*-1	
Unit cell dimensions	a = 11.1100(16) Å	α = 99.996(3)°
	b = 11.5756(17) Å	β = 100.958(3)°
	c = 15.568(2) Å	γ = 109.545(2)°
Volume	1790.5(5) Å^3	
Z	2	
Density, ρ_{calc}	2.142 g/cm^3	
Absorption coefficient, μ	8.006 mm^{-1}	
F(000)	1111 ē	
Diffractometer	Bruker Smart1000 CCD area detector	
Radiation source	fine-focus sealed tube, MoKα	
Generator power	50 kV, 25 ma	
Detector distance	4.958 cm	
Detector resolution	8.33 pixels/mm	
Total frames	1631	
Frame size	512 pixels	
Frame width	0.3 °	
Exposure per frame	23 sec	
Total measurement time	14.71 hours	
Data collection method	ω scans	
θ range for data collection	2.57 to 25.00°	
Index ranges	$-13 \le h \le 13$, $-13 \le k \le 13$, $-18 \le l \le 18$	
Reflections collected	11831	
Independent reflections	6046	
Observed reflection, I>2σ(I)	4490	
Coverage of independent reflections	95.9 %	
Variation in check reflections	-1.57 %	
Absorption correction	Semi-empirical from equivalents	
	SADABS (Sheldrick, 1996)	
Max. and min. transmission	0.619 and 0.370	
Structure solution technique	direct	
Structure solution program	SHELXS-97 (Sheldrick, 1990)	
Refinement technique	Full-matrix least-squares on F^2	
Refinement program	SHELXL-97 (Sheldrick, 1997)	
Function minimized	$\Sigma w(F_o^2 - F_c^2)^2$	
Data / restraints / parameters	6046 / 62 / 520	
Goodness-of-fit on F^2	1.002	
Δ/σ_{max}	0.001	
Final R indices: R_1, I>2σ(I)	0.0321	
wR_2, all data	0.0712	
R_{int}	0.0312	
R_{sig}	0.0499	
Weighting scheme	$w = 1/[\sigma^2(F_o^2) + (0.02P)^2 + 7.25P]$,	
	$P = [\max(F_o^2, 0) + 2F_o^2]/3$	
Largest diff. peak and hole	1.638 and -0.774 ē/Å^3	

$R_1 = \Sigma||F_o|-|F_c||/\Sigma|F_o|$, $wR2 = [\Sigma w(F_o^2-F_c^2)^2/\Sigma w(F_o^2)^2]^{1/2}$

Crystal data and structure refinement for *cis*-[(dpms)Pt^{IV}Me(μ-OH)$_2$$Pt^{II}$(dpms)]$BF_4$, *cis*-**2.18**.

X-ray lab book No.	1366	
Empirical formula	$[C_{23}H_{23}N_4O_8Pt_2S_2](BF_4)\cdot 6H_2O$	
Formula weight	1132.66	
Temperature	220(2) K	
Wavelength	0.71073 Å	
Crystal size	$0.275 \times 0.175 \times 0.032$ mm^3	
Crystal habit	colorless prism	
Crystal system	Triclinic	
Space group	P1	
Unit cell dimensions	a = 11.3558(10) Å	α = 111.3060(10)°
	b = 11.5175(10) Å	β = 106.321(2)°
	c = 15.3258(14) Å	γ = 96.637(2)°
Volume	1738.3(3) Å^3	
Z	2	
Density, ρ_{calc}	2.164 g/cm^3	
Absorption coefficient, μ	8.249 mm^{-1}	
F(000)	1084 $\bar{e}$	
Diffractometer	Bruker Smart1000 CCD area detector	
Radiation source	fine-focus sealed tube, MoKα	
Generator power	50 kV, 30 mA	
Detector distance	4.939 cm	
Detector resolution	8.33 pixels/mm	
Total frames	1818	
Frame size	512 pixels	
Frame width	0.3 °	
Exposure per frame	33 sec	
Total measurement time	20.28 hours	
Data collection method	ω scans	
θ range for data collection	2.68 to 25.00°	
Index ranges	$-13 \le h \le 12$, $-13 \le k \le 12$, $0 \le l \le 18$	
Reflections collected	6752	
Independent reflections	6759	
Observed reflection, I>2σ(I)	5494	
Coverage of independent reflections	98.8 %	
Variation in check reflections	0.00 %	
Absorption correction	Semi-empirical from equivalents	
	SADABS (Sheldrick, 1996)	
Max. and min. transmission	0.768 and 0.166	
Structure solution technique	direct	
Structure solution program	SHELXS-97 (Sheldrick, 1990)	
Refinement technique	Full-matrix least-squares on F^2	
Refinement program	SHELXL-97 (Sheldrick, 1997)	
Function minimized	$\Sigma w(F_o^2 - F_c^2)^2$	
Data / restraints / parameters	6759 / 58 / 487	
Goodness-of-fit on F^2	0.999	
Δ/σ_{max}	0.000	
Final R indices: R_1, I>2σ(I)	0.0514	
wR_2, all data	0.1282	
R_{int}	0.0000	
R_{sig}	0.0265	
Weighting scheme	$w = 1/[\sigma^2(F_o^2) + (0.04P)^2 + 43.5P]$,	
	$P = [\max(F_o^2, 0) + 2F_c^2]/3$	
Largest diff. peak and hole	2.366 and -4.534 $\bar{e}$/Å^3	

$R_1 = \Sigma||F_o|-|F_c||/\Sigma|F_o|$, $wR2 = [\Sigma w(F_o^2-F_c^2)^2/\Sigma w(F_o^2)^2]^{1/2}$

Crystal data and structure refinement for (dpms)$Pt^{II}(CH_2CH_2)Cl$, **3.1**.

X-ray labbook No.	1328	
Empirical formula	$C_{13}H_{13}ClN_2O_3PtS$	
Formula weight	507.85	
Temperature	223(2) K	
Wavelength	0.71073 Å	
Crystal size	$0.39 \times 0.19 \times 0.15$ mm^3	
Crystal habit	colorless prism	
Crystal system	Orthorhombic	
Space group	$Pca2_1$	
Unit cell dimensions	a = 15.9723(5) Å	$\alpha = 90°$
	b = 9.3175(3) Å	$\beta = 90°$
	c = 19.8226(6) Å	$\gamma = 90°$
Volume	2950.04(16) Å^3	
Z	8	
Density, ρ_{calc}	2.287 g/cm^3	
Absorption coefficient, μ	9.845 mm^{-1}	
F(000)	1920 $\bar{e}$	
Diffractometer	Bruker Smart1000 CCD area detector	
Radiation source	fine-focus sealed tube, MoK_α	
Generator power	50 kV, 20 ma	
Detector distance	4.940 cm	
Detector resolution	8.33 pixels/mm	
Total frames	2992	
Frame size	512 pixels	
Frame width	0.3 °	
Exposure per frame	20 sec	
Total measurement time	22.56 hours	
Data collection method	ω and φ scans	
θ range for data collection	1.03 to 27.50°	
Index ranges	$-20 \le h \le 20$, $-12 \le k \le 12$, $-25 \le l \le 25$	
Reflections collected	37195	
Independent reflections	6619	
Observed reflection, I>2σ(I)	6091	
Coverage of independent reflections	99.8 %	
Variation in check reflections	0.00 %	
Absorption correction	Semi-empirical from equivalents SADABS (Sheldrick, 1996)	
Max. and min. transmission	0.228 and 0.117	
Structure solution technique	direct	
Structure solution program	SHELXS-97 (Sheldrick, 1990)	
Refinement technique	Full-matrix least-squares on F^2	
Refinement program	SHELXL-97 (Sheldrick, 1997)	
Function minimized	$\Sigma w(F_o^2 - F_c^2)^2$	
Data / restraints / parameters	6619 / 77 / 408	
Goodness-of-fit on F^2	0.995	
Δ/σ_{max}	0.001	
Final R indices: R_1, I>2σ(I)	0.0311	
wR_2, all data	0.0667	
R_{int}	0.0319	
R_{sig}	0.0229	
Weighting scheme	$w = 1/[\sigma^2(F_o^2) + (0.005P)^2 + 29.5P]$, $P = [\max(F_o^2, 0) + 2F_o^2]/3$	
Absolute structure parameter	0.331(13)	
Largest diff. peak and hole	2.404 and -1.058 $\bar{e}$/Å^3	

$R_1 = \Sigma||F_o|-|F_c||/\Sigma|F_o|$, $wR2 = [\Sigma w(F_o^2-F_c^2)^2/\Sigma w(F_o^2)^2]^{1/2}$

Crystal data and structure refinement for (dpms)Pt^{II}(η^2-*cis*-cyclooctene)Cl, **4.2a**.

X-ray lab book No.	1431	
Empirical formula	$2(C_{19}H_{23}N_2SO_3PtCl)\cdot CH_3OH$	
Formula weight	1212.03	
Temperature	220(2) K	
Wavelength	0.71073 Å	
Crystal size	$0.28 \times 0.24 \times 0.12$ mm^3	
Crystal habit	yellow prism	
Crystal system	Monoclinic	
Space group	C2/c	
Unit cell dimensions	a = 32.1173(15) Å	α = 90°
	b = 7.4449(3) Å	β = 104.0610(10)°
	c = 17.5732(8) Å	γ = 90°
Volume	4076.0(3) Å^3	
Z	4	
Density, ρ_{calc}	1.975 g/cm^3	
Absorption coefficient, μ	7.145 mm^{-1}	
F(000)	2360 $\bar{e}$	
Diffractometer	Bruker Smart1000 CCD area detector	
Radiation source	fine-focus sealed tube, Mo*K*α	
Generator power	50 kV, 30 mA	
Detector distance	4.939 cm	
Detector resolution	8.33 pixels/mm	
Total frames	1824	
Frame size	512 pixels	
Frame width	0.5 °	
Exposure per frame	13 sec	
Total measurement time	10.21 hours	
Data collection method	ω and φ scans	
θ range for data collection	2.62 to 27.50°	
Index ranges	$-41 \le h \le 41$, $-9 \le k \le 9$, $-22 \le l \le 22$	
Reflections collected	25159	
Independent reflections	4683	
Observed reflection, I>2σ(I)	4382	
Coverage of independent reflections	99.7 %	
Variation in check reflections	0 %	
Absorption correction	Semi-empirical from equivalents	
	SADABS (Sheldrick, 1996)	
Max. and min. transmission	0.424 and 0.153	
Structure solution technique	direct	
Structure solution program	SHELXS-97 (Sheldrick, 1990)	
Refinement technique	Full-matrix least-squares on F^2	
Refinement program	SHELXL-97 (Sheldrick, 1997)	
Function minimized	$\Sigma w(F_o^2 - F_c^2)^2$	
Data / restraints / parameters	4683 / 12 / 293	
Goodness-of-fit on F^2	1.005	
Δ/σ_{max}	0.001	
Final R indices: R_1, I>2σ(I)	0.0145	
wR_2, all data	0.0351	
R_{int}	0.0282	
R_{sig}	0.0186	
Weighting scheme	$w = 1/[\sigma^2(F_o^2) + (0.0125P)^2 + 8.9P]$,	
	$P = [\max(F_o^2, 0) + 2F_o^2]/3$	
Extinction coefficient	0.000101(10)	
Largest diff. peak and hole	1.099 and -0.769 $\bar{e}$/Å^3	

$R_1 = \Sigma||F_o|-|F_c||/\Sigma|F_o|$, $wR2 = [\Sigma w(F_o^2-F_c^2)^2/\Sigma w(F_o^2)^2]^{1/2}$

Crystal data and structure refinement for (dpms)$Pt^{IV}(C_8H_{14}O$-$\kappa C,\kappa O)$, **4.3a**.

X-ray lab book No.	1509	
Empirical formula	$C_{19}H_{24}N_2O_5PtS\cdot 3H_2O$	
Formula weight	641.60	
Temperature	220(2) K	
Wavelength	0.71073 Å	
Crystal size	$0.20 \times 0.08 \times 0.04$ mm^3	
Crystal habit	colorless needle	
Crystal system	Monoclinic	
Space group	$P2_1/c$	
Unit cell dimensions	a = 8.3017(7) Å	α = 90°
	b = 8.6291(7) Å	β = 91.2080(10)°
	c = 32.591(3) Å	γ = 90°
Volume	2334.2(3) Å^3	
Z	4	
Density, ρ_{calc}	1.826 g/cm^3	
Absorption coefficient, μ	6.147 mm^{-1}	
F(000)	1264 ē	
Diffractometer	Bruker Smart1000 CCD area detector	
Radiation source	fine-focus sealed tube, MoKα	
Generator power	50 kV, 30 mA	
Detector distance	4.950 cm	
Detector resolution	8.33 pixels/mm	
Total frames	4542	
Frame size	512 pixels	
Frame width	0.3 °	
Exposure per frame	30 sec	
Total measurement time	46.9 hours	
Data collection method	ω and φ scans	
θ range for data collection	1.25 to 27.50°	
Index ranges	$-10 \le h \le 10$, $-11 \le k \le 11$, $-42 \le l \le 42$	
Reflections collected	48404	
Independent reflections	5359	
Observed reflection, I>2σ(I)	4867	
Coverage of independent reflections	99.9 %	
Variation in check reflections	0 %	
Absorption correction	Semi-empirical from equivalents	
	SADABS (Sheldrick, 1996)	
Max. and min. transmission	0.782 and 0.501	
Structure solution technique	direct	
Structure solution program	SHELXS-97 (Sheldrick, 1990)	
Refinement technique	Full-matrix least-squares on F^2	
Refinement program	SHELXL-97 (Sheldrick, 1997)	
Function minimized	$\Sigma w(F_o^2 - F_c^2)^2$	
Data / restraints / parameters	5359 / 16 / 304	
Goodness-of-fit on F^2	0.999	
Δ/σ_{max}	0.000	
Final R indices: R_1, I>2σ(I)	0.0232	
wR_2, all data	0.0496	
R_{int}	0.0377	
R_{sig}	0.0195	
Weighting scheme	$w = 1/[\sigma^2(F_o^2) + (0.005P)^2 + 9.76P]$,	
	$P = [\max(F_o^2, 0) + 2F_c^2]/3$	
Largest diff. peak and hole	0.676 and -0.507 ē/Å^3	

$R_1 = \Sigma||F_o|-|F_c||/\Sigma|F_o|$, $wR2 = [\Sigma w(F_o^2-F_c^2)^2/\Sigma w(F_o^2)^2]^{1/2}$

Crystal data and structure refinement for (dpms)$Pt^{IV}(C_7H_{10}O$-$\kappa C,\kappa O)$, **4.3b**.

X-ray lab book No.	1523	
Empirical formula	$C_{18}H_{20}N_2O_5PtS \cdot CH_3OH \cdot 2H_2O$	
Formula weight	639.58	
Temperature	220(2) K	
Wavelength	0.71073 Å	
Crystal size	$0.27 \times 0.125 \times 0.06$ mm^3	
Crystal habit	colorless prism	
Crystal system	Monoclinic	
Space group	$P2_1$	
Unit cell dimensions	a = 8.4315(6) Å	α = 90°
	b = 8.5602(6) Å	β = 99.1130(10)°
	c = 15.7898(11) Å	γ = 90°
Volume	1125.25(14) Å^3	
Z	2	
Density, ρ_{calc}	1.888 g/cm^3	
Absorption coefficient, μ	6.375 mm^{-1}	
F(000)	628 ē	
Diffractometer	Bruker Smart1000 CCD area detector	
Radiation source	fine-focus sealed tube, MoKα	
Generator power	50 kV, 30 mA	
Detector distance	5.000 cm	
Detector resolution	8.33 pixels/mm	
Total frames	2196	
Frame size	512 pixels	
Frame width	0.5 °	
Exposure per frame	23 sec	
Total measurement time	18.4 hours	
Data collection method	ω scans	
θ range for data collection	2.58 to 27.50°	
Index ranges	$-10 \le h \le 10$, $-11 \le k \le 11$, $-20 \le l \le 20$	
Reflections collected	19852	
Independent reflections	5143	
Observed reflection, I>2σ(I)	4974	
Coverage of independent reflections	99.9 %	
Variation in check reflections	0 %	
Absorption correction	Semi-empirical from equivalents	
	SADABS (Sheldrick, 1996)	
Max. and min. transmission	0.682 and 0.404	
Structure solution technique	direct	
Structure solution program	SHELXS-97 (Sheldrick, 1990)	
Refinement technique	Full-matrix least-squares on F^2	
Refinement program	SHELXL-97 (Sheldrick, 1997)	
Function minimized	$\Sigma w(F_o^2 - F_c^2)^2$	
Data / restraints / parameters	5143 / 11 / 318	
Goodness-of-fit on F^2	0.998	
Δ/σ_{max}	0.001	
Final R indices: R_1, I>2σ(I)	0.0144	
wR_2, all data	0.0347	
R_{int}	0.0249	
R_{sig}	0.0314	
Weighting scheme	$w = 1/[\sigma^2(F_o^2) + (0.0037P)^2]$,	
	$P = [\max(F_o^2, 0) + 2F_o^2]/3$	
Absolute structure parameter	0.022(4)	
Largest diff. peak and hole	1.258 and -0.582 ē/Å^3	

$R_1 = \Sigma||F_o|-|F_c||/\Sigma|F_o|$, $wR2 = [\Sigma w(F_o^2-F_c^2)^2/\Sigma w(F_o^2)^2]^{1/2}$

Crystal data and structure refinement for (dpms)Pt(η^3-C_8H_{13}), *exo*-**4.16**.

X-ray lab book No.	1501	
Empirical formula	$C_{19}H_{22}N_2O_3PtS \cdot H_2O$	
Formula weight	571.55	
Temperature	220(2) K	
Wavelength	0.71073 Å	
Crystal size	$0.45 \times 0.21 \times 0.07$ mm^3	
Crystal habit	colorless prism	
Crystal system	Triclinic	
Space group	P-1	
Unit cell dimensions	a = 9.3702(9) Å	α = 72.504(2)°
	b = 9.5020(9) Å	β = 88.877(2)°
	c = 11.3905(11) Å	γ = 81.837(2)°
Volume	957.16(16) Å^3	
Z	2	
Density, ρ_{calc}	1.983 g/cm^3	
Absorption coefficient, μ	7.467 mm^{-1}	
F(000)	556 ē	
Diffractometer	Bruker Smart1000 CCD area detector	
Radiation source	fine-focus sealed tube, MoKα	
Generator power	50 kV, 40 mA	
Detector distance	11.950 cm	
Detector resolution	8.33 pixels/mm	
Total frames	3024	
Frame size	512 pixels	
Frame width	0.3 °	
Exposure per frame	15 sec	
Total measurement time	18.6 hours	
Data collection method	ω and φ scans	
θ range for data collection	2.85 to 27.50°	
Index ranges	$-12 \le h \le 12$, $-12 \le k \le 12$, $-14 \le l \le 14$	
Reflections collected	11602	
Independent reflections	4324	
Observed reflection, I>2σ(I)	3979	
Coverage of independent reflections	98.4 %	
Variation in check reflections	0 %	
Absorption correction	Semi-empirical from equivalents	
	SADABS (Sheldrick, 1996)	
Max. and min. transmission	0.593 and 0.150	
Structure solution technique	direct	
Structure solution program	SHELXS-97 (Sheldrick, 1990)	
Refinement technique	Full-matrix least-squares on F^2	
Refinement program	SHELXL-97 (Sheldrick, 1997)	
Function minimized	$\Sigma w(F_o^2 - F_c^2)^2$	
Data / restraints / parameters	4324 / 96 / 296	
Goodness-of-fit on F^2	1.002	
Δ/σ_{max}	0.000	
Final R indices: R_1, I>2σ(I)	0.0295	
wR_2, all data	0.0771	
R_{int}	0.0235	
R_{sig}	0.0254	
Weighting scheme	$w = 1/[\sigma^2(F_o^2) + (0.05P)^2 + 2.39P]$,	
	$P = [\max(F_o^2, 0) + 2F_c^2]/3$	
Largest diff. peak and hole	2.369 and -2.057 ē/Å^3	

$R_1 = \Sigma||F_o|-|F_c||/\Sigma|F_o|$, $wR2 = [\Sigma w(F_o^2-F_c^2)^2/\Sigma w(F_o^2)^2]^{1/2}$

Crystal data and structure refinement for (dpms)$Pt^{IV}(C_2H_4NH^tBu$-$\kappa C,\kappa N)(OH)]Cl$*MeOH, **5.5***Cl*MeOH.

X-ray lab book No.	1602	
Empirical formula	C18 H28 Cl N3 O5 Pt S	
Formula weight	629.03	
Temperature	150(2) K	
Wavelength	0.71073 Å	
Crystal size	$0.32 \times 0.15 \times 0.10$ mm^3	
Crystal habit	colourless prism	
Crystal system	Triclinic	
Space group	P-1	
Unit cell dimensions	a = 9.5764(6) Å	α = 92.272(1)°
	b = 10.0716(6) Å	β = 102.071(1)°
	c = 12.8674(8) Å	γ = 114.844(1)°
Volume	1089.87(12) $Å^3$	
Z	2	
Density, ρ_{calc}	1.917 g/cm^3	
Absorption coefficient, μ	6.690 mm^{-1}	
F(000)	616 $\bar{e}$	
Diffractometer	Bruker Smart Apex II CCD area detector	
Radiation source	fine-focus sealed tube, MoKα	
Detector distance	5.2 cm	
Detector resolution	8.33 pixels/mm	
Total frames	3030	
Frame size	512 pixels	
Frame width	0.3°	
Exposure per frame	10 sec	
Total measurement time	13.5 hours	
Data collection method	ω and φ scans	
θ range for data collection	2.25 to 27.50°	
Index ranges	$-12 \le h \le 11$, $-13 \le k \le 13$, $0 \le l \le 16$	
Reflections collected	23101	
Independent reflections	4988	
Observed reflection, I>2σ(I)	4904	
Coverage of independent reflections	99.6 %	
Variation in check reflections	0 %	
Absorption correction	Semi-empirical from equivalents SADABS (Sheldrick, 1996)	
Max. and min. transmission	0.512 and 0.250	
Structure solution technique	direct	
Structure solution program	SHELXS-97 (Sheldrick, 1990)	
Refinement technique	Full-matrix least-squares on F^2	
Refinement program	SHELXL-97 (Sheldrick, 1997)	
Function minimized	$\Sigma w(F_o^2 - F_c^2)^2$	
Data / restraints / parameters	4988 / 0 / 276	
Goodness-of-fit on F^2	1.000	
Δ/σ_{max}	0.001	
Final R indices: R_1, I>2σ(I)	0.0213	
wR_2, all data	0.0529	
R_{int}	0.0288	
R_{sig}	0.0256	
Weighting scheme	$w = 1/[\sigma^2(F_o^2)+(0.0258P)^2+2.95P]$, $P = [\max(F_o^2,0)+2F_o^2]/3$	
Largest diff. peak and hole	1.820 and -1.546 $\bar{e}/Å^3$	

$R_1 = \Sigma||F_o|-|F_c||/\Sigma|F_o|$, $wR2 = [\Sigma w(F_o^2 - F_c^2)^2/\Sigma\, w(F_o^2)^2]^{1/2}$

Crystal data and structure refinement for (dpms)$Pt^{II}Ph(NH_2Ph)$, **6.4**.

X-ray lab book No.		1474
Empirical formula		$C_{23}H_{21}N_3O_3PtS \cdot 2CH_3OH$
Formula weight		678.66
Temperature		220(2) K
Wavelength		0.71073 Å
Crystal size		$0.275 \times 0.22 \times 0.095$ mm^3
Crystal habit		colorless prism
Crystal system		Monoclinic
Space group		P2/n
Unit cell dimensions		a = 9.9681(6) Å α = 90°
		b = 8.7798(5) Å β = 90.6590(10)°
		c = 28.8445(16) Å γ = 90°
Volume		2524.2(3) Å^3
Z		4
Density, ρ_{calc}		1.786 g/cm^3
Absorption coefficient, μ		5.682 mm^{-1}
F(000)		1336 $\bar{e}$
Diffractometer		Bruker Smart1000 CCD area detector
Radiation source		fine-focus sealed tube, MoKα
Generator power		50 kV, 40 mA
Detector distance		4.950 cm
Detector resolution		8.33 pixels/mm
Total frames		3276
Frame size		512 pixels
Frame width		0.5 °
Exposure per frame		15 sec
Total measurement time		20.2 hours
Data collection method		ω and φ scans
θ range for data collection		2.42 to 27.50°
Index ranges		$-12 \le h \le 12$, $-11 \le k \le 11$, $-37 \le l \le 37$
Reflections collected		47802
Independent reflections		5791
Observed reflection, I>2σ(I)		5401
Coverage of independent reflections		99.7 %
Variation in check reflections		0 %
Absorption correction		Semi-empirical from equivalents
		SADABS (Sheldrick, 1996)
Max. and min. transmission		0.583 and 0.231
Structure solution technique		direct
Structure solution program		SHELXS-97 (Sheldrick, 1990)
Refinement technique		Full-matrix least-squares on F^2
Refinement program		SHELXL-97 (Sheldrick, 1997)
Function minimized		$\Sigma w(F_o^2 - F_c^2)^2$
Data / restraints / parameters		5791 / 31 / 336
Goodness-of-fit on F^2		1.000
Δ/σ_{max}		0.000
Final R indices:	R_1, I>2σ(I)	0.0244
	wR_2, all data	0.0583
	R_{int}	0.0321
	R_{sig}	0.0171
Weighting scheme		$w = 1/[\sigma^2(F_o^2) + (0.02P)^2 + 9.99P]$,
		$P = [\max(F_o^2, 0) + 2F_c^2]/3$
Largest diff. peak and hole		1.521 and -0.578 $\bar{e}$/Å^3

$R_1 = \Sigma||F_o|-|F_c||/\Sigma|F_o|$, $wR2 = [\Sigma w(F_o^2-F_c^2)^2/\Sigma w(F_o^2)^2]^{1/2}$

Bibliography

1. Foote, C. S.; Valentine, J. S.; Greenberg, A.; Liebman, J. F.; Editors, *Active Oxygen in Chemistry. [In: Struct. Energ. React. Chem. Ser., 1995; 2]*. 1995; 342 pp.
2. Anslyn, E. V.; Dougherty, D. A., *Modern Physical Organic Chemistry*. University Science Books: 2006; 1095 pp.
3. Mueller, M. A.; Sanderson, J. R. Preparation of tert-butyl hydroperoxide via oxidation of isobutane initiated by di-tert-butyl peroxide. US 5395980, 1995.
4. Mleczko, L.; Buchholz, S.; Munnich, C., C-H transformation in industrial processes. In *Handbook of C-H Transformations*, Dyker, G., Ed. 2005; Vol. 1, pp 11-27.
5. Weissermel, K.; Arpe, H.-J., *Industrial Organic Chemistry: Important Raw Materials and Intermediates*. Wiley-VCH: 2003; 491 pp.
6. Smith, J. V. Benzoic acid production. US 2792419, 1957.
7. Fragen, N.; Hundley, J. G. Continuous manufacture of benzoic acid from toluene. US 3210416, 1965.
8. Besmar, U. N.; Lyon, J. B.; Miller, F. J.; Musser, M. T. Preparation of cyclohexanone and cyclohexanol. US 4720592, 1988.
9. Barton, D. H. R.; Gastiger, M. J.; Motherwell, W. B., *J. Chem. Soc., Chem. Commun.* **1983**, 41-43.
10. Stavropoulos, P.; Celenligil-Cetin, R.; Tapper, A. E., *Acc. Chem. Res.* **2001,** 34, 745-752.
11. Baerns, M.; Buyevskaya, O., *Catal. Today* **1998,** 45, 13-22.
12. Yarlagadda, P. S.; Morton, L. A.; Hunter, N. R.; Gesser, H. D., *Ind. Eng. Chem. Res.* **1988,** 27, 252-256.
13. Hunter, N. R.; Gesser, H. D.; Morton, L. A.; Yarlagadda, P. S.; Fung, D. P. C., *Appl. Catal.* **1990,** 57, 45-54.
14. Wang, Y.; Otsuka, K., *J. Chem. Soc., Chem. Commun.* **1994**, 2209-10.
15. Buehler, B.; Schmid, A., Selective enzymatic hydroxylations as applied in organic synthesis. In *Handbook of C-H Transformations*, Dyker, G., Ed. 2005; Vol. 2, pp 516-529, 634-639.
16. Schmid, A.; Dordick, J. S.; Hauer, B.; Kiener, A.; Wubbolts, M.; Witholt, B., *Nature* **2001,** 409, 258-268.
17. Janowicz, A. H.; Bergman, R. G., *J. Am. Chem. Soc.* **1983,** 105, 3929-39.
18. Gol'dshleger, N. F.; Es'kova, V. V.; Shilov, A. E.; Shteinman, A. A., *Zh. Fiz. Khim.* **1972,** 46, 1353-1354.
19. Shilov, A. E., *Catalysis by Metal Complexes: Activation of Saturated Hydrocarbons by Transition Metal Complexes*. 1984; 203 pp.
20. Stahl, S.; Labinger, J. A.; Bercaw, J. E., *Angew. Chem., Int. Ed.* **1998,** 37, 2181-2192.
21. Periana, R. A.; Taube, D. J.; Gamble, S.; Taube, H.; Satoh, T.; Fujii, H., *Science* **1998,** 280, 560-564.
22. Labinger, J. A.; Bercaw, J. E., *Nature* **2002,** 417, 507-514.
23. Speight, J., *Chemical Process and Design Handbook*. 2001; 1000 pp.
24. Monnier, J. R.; Muehlbauer, P. J. Selective Monoepoxidation of Olefins. US 4897498, 1990.
25. Baeckvall, J.-E.; Editor, *Modern Oxidation Methods*. 2004; 336 pp.
26. Jones, C. W., *Applications of Hydrogen Peroxide and Derivatives: Rsc Clean Technology Monographs*. Royal Society of Chemistry: 1999; 264 pp.
27. Nijhuis, T. A.; Makkee, M.; Moulijn, J. A.; Weckhuysen, B. M., *Ind. Eng. Chem. Res.* **2006,** 45, 3447-3459.
28. Zuwei, X.; Ning, Z.; Yu, S.; Kunlan, L., *Science* **2001,** 292, 1139-1141.
29. Vedernikov, A. N.; Fettinger, J. C.; Mohr, F., *J. Am. Chem. Soc.* **2004,** 126, 11160-11161.
30. Wieghardt, K.; Koeppen, M.; Swiridoff, W.; Weiss, J., *J. Chem. Soc., Dalton Trans.* **1983**, 1869-1872.
31. Chianese, A. R.; Lee, S. J.; Gagne, M. R., *Angew. Chem., Int. Ed.* **2007,** 46, 4042-4059.
32. Hahn, C., *Chem.--Eur. J.* **2004,** 10, 5888-5899.

33. Crabtree, R., *The Organometallic Chemistry of the Transition Metals*. Wiley-IEEE: 2005; 546 pp.
34. Timokhin, V. I.; Anastasi, N. R.; Stahl, S. S., *J. Am. Chem. Soc.* **2003,** 125, 12996-12997.
35. Liu, G.; Stahl, S. S., *J. Am. Chem. Soc.* **2006,** 128, 7179-7181.
36. Baeckvall, J. E., *Acc. Chem. Res.* **1983,** 16, 335-342.
37. Vaska, L., *Science* **1963,** 140, 809-810.
38. Vaska, L., *Acc. Chem. Res.* **1976,** 9, 175-183.
39. Jones, R. D.; Summerville, D. A.; Basolo, F., *Chem. Rev.* **1979,** 79, 139-79.
40. Collman, J. P.; Gagne, R. R.; Reed, C. A.; Robinson, W. T.; Rodley, G. A., *Proc. Nat. Acad. Sci. U. S. A.* **1974,** 71, 1326-1329.
41. Valentine, J. S., *Chem. Rev.* **1973,** 73, 235-245.
42. Praetorius, J. M.; Allen, D. P.; Wang, R.; Webb, J. D.; Grein, F.; Kennepohl, P.; Crudden, C. M., *J. Am. Chem. Soc.* **2008,** 130, 3724-3725.
43. Rostovtsev, V. V.; Henling, L. M.; Labinger, J. A.; Bercaw, J. E., *Inorg. Chem.* **2002,** 41, 3608-3619.
44. Kryatov, S. V.; Rybak-Akimova, E. V.; Schindler, S., *Chem. Rev.* **2005,** 105, 2175-2226.
45. Basolo, F.; Hoffman, B. M.; Ibers, J. A., *Acc. Chem. Res.* **1975,** 8, 384-92.
46. Kieber-Emmons, M. T.; Riordan, C. G., *Acc. Chem. Res.* **2007,** 40, 618-625.
47. Mirica, L. M.; Ottenwaelder, X.; Stack, T. D. P., *Chem. Rev.* **2004,** 104, 1013-1045.
48. Lewis, E. A.; Tolman, W. B., *Chem. Rev.* **2004,** 104, 1047-1076.
49. Prigge, S. T.; Eipper, B. A.; Mains, R. E.; Amzel, L. M., *Science* **2004,** 304, 864-867.
50. Solomon, E. I.; Chen, P.; Metz, M.; Lee, S.-K.; Palmer, A. E., *Angew. Chem., Int. Ed.* **2001,** 40, 4570-4590.
51. Weitzer, M.; Schindler, S.; Brehm, G.; Schneider, S.; Hoermann, E.; Jung, B.; Kaderli, S.; Zuberbuehler, A. D., *Inorg. Chem.* **2003,** 42, 1800-1806.
52. Wuertele, C.; Gaoutchenova, E.; Harms, K.; Holthausen, M. C.; Sundermeyer, J.; Schindler, S., *Angew. Chem., Int. Ed.* **2006,** 45, 3867-3869.
53. Cheng, P. T.; Cook, C. D.; Nyburg, S. C.; Wan, K. Y., *Can. J. Chem.* **1971,** 49, 3772-3777.
54. Hayward, P. J.; Blake, D. M.; Wilkinson, G.; Nyman, C. J., *J. Amer. Chem. Soc.* **1970,** 92, 5873-5878.
55. Frech, C. M.; Shimon, L. J. W.; Milstein, D., *Helv. Chim. Acta* **2006,** 89, 1730-1739.
56. Verat, A. Y.; Fan, H.; Pink, M.; Chen, Y. S.; Caulton, K. G., *Chem.--Eur. J.* **2008,** 14, 7680-7686.
57. Landis, C. R.; Morales, C. M.; Stahl, S. S., *J. Am. Chem. Soc.* **2004,** 126, 16302-16303.
58. Kashiwagi, T.; Yasuoka, N.; Kasai, N.; Kakudo, M.; Takahashi, S.; Hagihara, N., *J. Chem. Soc. D* **1969**, 743.
59. Lawson, H. J.; Atwood, J. D., *J. Am. Chem. Soc.* **1989,** 111, 6223-6227.
60. Rostovtsev, V. V.; Labinger, J. A.; Bercaw, J. E.; Lasseter, T. L.; Goldberg, K. I., *Organometallics* **1998,** 17, 4530-4531.
61. Sarneski, J. E.; McPhail, A. T.; Onan, K. D.; Erickson, L. E.; Reilley, C. N., *J. Am. Chem. Soc.* **1977,** 99, 7376-7378.
62. Luinstra, G. A.; Wang, L.; Stahl, S. S.; Labinger, J. A.; Bercaw, J. E., *J. Organomet. Chem.* **1995,** 504, 75-91.
63. Prokopchuk, E. M.; Jenkins, H. A.; Puddephatt, R. J., *Organometallics* **1999,** 18, 2861-2866.
64. Williams, B. S.; Goldberg, K. I., *J. Am. Chem. Soc.* **2001,** 123, 2576-2587.
65. Shilov, A. E.; Shul'pin, G. B., *Chem. Rev.* **1997,** 97, 2879-2932.
66. Zhang, F.; Kirby, C. W.; Hairsine, D. W.; Jennings, M. C.; Puddephatt, R. J., *J. Am. Chem. Soc.* **2005,** 127, 14196-14197.
67. Reynolds, A. M.; Gherman, B. F.; Cramer, C. J.; Tolman, W. B., *Inorg. Chem.* **2005,** 44, 6989-6997.
68. Wick, D. D.; Goldberg, K. I., *J. Am. Chem. Soc.* **1999,** 121, 11900-11901.
69. Collman, J. P.; Hegedus, L. G.; Norton, J. R.; Finke, R. G., *Principles and Applications of Organotransition Metal Chemistry, 2nd Edition*. University Science Books: 1987; 989 pp.
70. Luinstra, G. A.; Labinger, J. A.; Bercaw, J. E., *J. Am. Chem. Soc.* **1993,** 115, 3004-3005.
71. Zamashchikov, V. V.; Kitaigorodskii, A. N.; Litvinenko, S. L.; Rudakov, E. S.; Uzhik, O. N.; Shilov, A. E., *Izv. Akad. Nauk SSSR, Ser. Khim.* **1985**, 1730-1733.

72. Zamashchikov, V. V.; Rudakov, E. S.; Mitchenko, S. A.; Pekhtereva, T. M., *Koord. Khim.* **1985,** 11, 69-72.
73. Zamashchikov, V. V.; Mitchenko, S. A., *Kinet. Katal.* **1983,** 24, 254-255.
74. Williams, B. S.; Holland, A. W.; Goldberg, K. I., *J. Am. Chem. Soc.* **1999,** 121, 252-253.
75. Thompson, J. S.; Randall, S. L.; Atwood, J. D., *Organometallics* **1991,** 10, 3906-3910.
76. Mann, G.; Hartwig, J. F., *J. Am. Chem. Soc.* **1996,** 118, 13109-13110.
77. Frech, C. M.; Milstein, D., *J. Am. Chem. Soc.* **2006,** 128, 12434-12435.
78. Desai, L. V.; Sanford, M. S., *Angew. Chem., Int. Ed.* **2007,** 46, 5737-5740.
79. Vedernikov, A. N.; Binfield, S. A.; Zavalij, P. Y.; Khusnutdinova, J. R., *J. Am. Chem. Soc.* **2006,** 128, 82-83.
80. Hill, G. S.; Puddephatt, R. J., *Organometallics* **1997,** 16, 4522-4524.
81. Ling, S. S. M.; Puddephatt, R. J.; Manojlovic-Muir, L.; Muir, K. W., *J. Organomet. Chem.* **1983,** 255, C11-C14.
82. Fulton, J. R.; Holland, A. W.; Fox, D. J.; Bergman, R. G., *Acc. Chem. Res.* **2002,** 35, 44-56.
83. Ritter, J. C. M.; Bergman, R. G., *J. Am. Chem. Soc.* **1997,** 119, 2580-2581.
84. Hellferich, F. G., *Kinetics of Multistep Reactions*. Elsevier: 2004; 488 pp.
85. Noro, K.; Ozawa, Y.; Taguchi, M.; Yagasaki, A., *Chem. Commun.* **2002**, 1770-1771.
86. Hanst, P. L.; Calvert, J. G., *J. Phys. Chem.* **1959,** 63, 104-106.
87. Benedetti, M.; Fanizzi, F. P.; Maresca, L.; Natile, G., *Chem. Commun.* **2006**, 1118-1120.
88. Halpern, J.; Jewsbury, R. A., *J. Organomet. Chem.* **1979,** 181, 223-232.
89. Matsumoto, K.; Ochiai, M., *Coord. Chem. Rev.* **2002,** 231, 229-238.
90. Matsumoto, K.; Mizuno, K.; Abe, T.; Kinoshita, J.; Shimura, H., *Chem. Lett.* **1994**, 1325-1328.
91. Lin, Y.-S.; Takeda, S.; Matsumoto, K., *Organometallics* **1999,** 18, 4897-4899.
92. Chock, P. B.; Halpern, J.; Paulik, F. E., *Inorg. Synth.* **1990,** 28, 349-351.
93. Glasoe, P. K.; Long, F. A., *J. Phys. Chem.* **1960,** 64, 188-190.
94. Fu, X.; Wayland, B. B., *J. Am. Chem. Soc.* **2006,** 128, 8947-8954.
95. Scollard, J. D.; Labinger, J. A.; Bercaw, J. E., *Helv. Chim. Acta* **2001,** 84, 3247-3268.
96. Han, Y.-Z.; Sanford, M. S.; England, M. D.; Groves, J. T., *Chem. Commun.* **2006**, 549-551.
97. Joergensen, K. A.; Schioett, B., *Chem. Rev.* **1990,** 90, 1483-506.
98. Muslehiddinoglu, J.; Vannice, M. A., *J. Catal.* **2004,** 222, 214-226.
99. Barteau, M. A., *Top. Catal.* **2003,** 22, 3-8.
100. Linic, S.; Medlin, J. W.; Barteau, M. A., *Langmuir* **2002,** 18, 5197-5204.
101. Linic, S.; Barteau, M. A., *J. Am. Chem. Soc.* **2002,** 124, 310-317.
102. Linic, S.; Piao, H.; Adib, K.; Barteau, M. A., *Angew. Chem., Int. Ed.* **2004,** 43, 2918-2921.
103. Sharpless, K. B.; Teranishi, A. Y.; Backvall, J. E., *J. Am. Chem. Soc.* **1977,** 99, 3120-3128.
104. Freeman, F., *Chem. Rev.* **1975,** 75, 439-490.
105. Cristol, S. J.; Eilar, K. R., *J. Am. Chem. Soc.* **1950,** 72, 4353-4356.
106. Stairs, R. A.; Diaper, D. G. M.; Gatzke, A. L., *Can. J. Chem.* **1963,** 41, 1059-1064.
107. Norrby, P.-O.; Becker, H.; Sharpless, K. B., *J. Am. Chem. Soc.* **1996,** 118, 35-42.
108. Pietsch, M. A.; Russo, T. V.; Murphy, R. B.; Martin, R. L.; Rappe, A. K., *Organometallics* **1998,** 17, 2716-2719.
109. Kodadek, T.; Raybuck, S. A.; Collman, J. P.; Brauman, J. I.; Papazian, L. M., *J. Am. Chem. Soc.* **1985,** 107, 4343-4345.
110. Collman, J. P.; Brauman, J. I.; Meunier, B.; Hayashi, T.; Kodadek, T.; Raybuck, S. A., *J. Am. Chem. Soc.* **1985,** 107, 2000-2005.
111. Chatterjee, D.; Basak, S.; Mitra, A.; Sengupta, A.; Le Bras, J.; Muzart, J., *Inorg. Chim. Acta* **2006,** 359, 1325-1328.
112. Hamada, T.; Fukuda, T.; Imanishi, H.; Katsuki, T., *Tetrahedron* **1996,** 52, 515-530.
113. Norrby, P.-O.; Linde, C.; Aakermark, B., *J. Am. Chem. Soc.* **1995,** 117, 11035-11036.
114. Khusnutdinova, J. R.; Newman, L. L.; Zavalij, P. Y.; Lam, Y.-F.; Vedernikov, A. N., *J. Am. Chem. Soc.* **2008,** 130, 2174-2175.
115. Cinellu, M. A.; Minghetti, G.; Cocco, F.; Stoccoro, S.; Zucca, A.; Manassero, M., *Angew. Chem., Int. Ed.* **2005,** 44, 6892-6895.
116. Flood, T. C.; Iimura, M.; Perotti, J. M.; Rheingold, A. L.; Concolino, T. E., *Chem. Commun.* **2000**, 1681-1682.
117. de Bruin, B.; Budzelaar, P. H. M.; Gal, A. W., *Angew. Chem., Int. Ed.* **2004,** 43, 4142-4157.

118. de Bruin, B.; Peters, T. P. J.; Wilting, J. B. M.; Thewissen, S.; Smits, J. M. M.; Gal, A. W., *Eur. J. Inorg. Chem.* **2002**, 2671-2680.
119. De Bruin, B.; Peters, T. P. J.; Thewissen, S.; Blok, A. N. J.; Wilting, J. B. M.; De Gelder, R.; Smits, J. M. M.; Gal, A. W., *Angew. Chem., Int. Ed.* **2002,** 41, 2135-2138.
120. De Bruin, B.; Verhagen, J. A. W.; Schouten, C. H. J.; Gal, A. W.; Feichtinger, D.; Plattner, D. A., *Chem.--Eur. J.* **2001,** 7, 416-422.
121. De Bruin, B.; Boerakker, M. J.; Verhagen, J. A. W.; De Gelder, R.; Smits, J. M. M.; Gal, A. W., *Chem.--Eur. J.* **2000,** 6, 298-312.
122. De Bruin, B.; Brands, J. A.; Donners, J. J. J. M.; Donners, M. P. J.; De Gelder, R.; Smits, J. M. M.; Gal, A. W.; Spek, A. L., *Chem.--Eur. J.* **1999,** 5, 2921-2936.
123. De Bruin, B.; Boerakker, M. J.; Donners, J. J. J. M.; Christiaans, B. E. C.; Schlebos, P. P. J.; De Gelder, R.; Smits, J. M. M.; Spek, A. L.; Gal, A. W., *Angew. Chem., Int. Ed. Engl.* **1997,** 36, 2064-2067.
124. del Rio, M. P.; Ciriano, M. A.; Tejel, C., *Angew. Chem., Int. Ed.* **2008,** 47, 2502-2505.
125. Day, V. W.; Klemperer, W. G.; Lockledge, S. P.; Main, D. J., *J. Am. Chem. Soc.* **1990,** 112, 2031-2033.
126. Budzelaar, P. H. M.; Blok, A. N. J., *Eur. J. Inorg. Chem.* **2004**, 2385-2391.
127. Calhorda, M. J.; Galvao, A. M.; Unaleroglu, C.; Zlota, A. A.; Frolow, F.; Milstein, D., *Organometallics* **1993,** 12, 3316-3325.
128. Hartwig, J. F.; Bergman, R. G.; Andersen, R. A., *Organometallics* **1991,** 10, 3344-3362.
129. Klein, D. P.; Hayes, J. C.; Bergman, R. G., *J. Am. Chem. Soc.* **1988,** 110, 3704-3706.
130. Keith, J. A.; Nielsen, R. J.; Oxgaard, J.; Goddard, I., W.A., *J. Am. Chem. Soc.* **2007,** 129, 123442-12343.
131. Henry, P. M., *J. Am. Chem. Soc.* **1966,** 88, 1595-1597.
132. Wu, J.; Sharp, P. R., *Organometallics* **2008,** 27, 1234-1241.
133. Szuromi, E.; Wu, J.; Sharp, P. R., *J. Am. Chem. Soc.* **2006,** 128, 12088-12089.
134. Szuromi, E.; Shan, H.; Sharp, P. R., *J. Am. Chem. Soc.* **2003,** 125, 10522-10523.
135. Wu, J.; Sharp, P. R., *Organometallics* **2008,** 27, 4810-4816.
136. Lenarda, M.; Ros, R.; Traverso, O.; Pitts, W. D.; Baddley, W. H.; Graziani, M., *Inorg. Chem.* **1977,** 16, 3178.
137. Schlodder, R.; Ibers, J. A.; Lenarda, M.; Graziani, M., *J. Am. Chem. Soc.* **1974,** 96, 6893-900.
138. Litvinenko, S. L.; Shologon, V. I.; Zamashchikov, V. V., *Zh. Org. Khim.* **1996,** 32, 561-566.
139. Zlota, A. A.; Frolow, F.; Milstein, D., *J. Am. Chem. Soc.* **1990,** 112, 6411-13.
140. Ohno, F.; Kawashima, T.; Okazaki, R., *Chem. Commun.* **1997**, 1671-1672.
141. Uchiyama, Y.; Kano, N.; Kawashima, T., *J. Org. Chem.* **2006,** 71, 659-670.
142. Kawashima, T.; Uchiyama, Y.; Kano, N., *Phosphorus, Sulfur Silicon Relat. Elem.* **2004,** 179, 849-852.
143. Uchiyama, Y.; Kano, N.; Kawashima, T., *J. Am. Chem. Soc.* **2003,** 125, 13346-13347.
144. Fu, X.; Li, S.; Wayland, B. B., *J. Am. Chem. Soc.* **2006,** 128, 8947-8954.
145. Sasaoka, M.; Hart, H., *J. Org. Chem.* **1979,** 44, 368-74.
146. Khusnutdinova, J. R.; Zavalij, P. Y.; Vedernikov, A. N., *Organometallics* **2007,** 26, 3466-3483.
147. Nakamoto, K., *Infrared and Raman Spectra of Inorganic and Coordination Compounds. Part B: Applications in Coordination, Organometallic, and Bioinorganic Chemistry* John Wiley: 1997; 387 pp.
148. Cramer, C. J., *Essentials of Computational Chemistry: Theories and Models*. John Wiley and Sons: 2004; 596 pp.
149. Hirshfeld, F. L., *Theor. Chim. Acta* **1977,** 44, 129-138.
150. Harvey, J. N., *Organometallics* **2001,** 20, 4887-4895.
151. Wax, M. J.; Stryker, J. M.; Buchanan, J. M.; Kovac, C. A.; Bergman, R. G., *J. Am. Chem. Soc.* **1984,** 106, 1121-1122.
152. Halpern, J., *Acc. Chem. Res.* **1982,** 15, 238-244.
153. Li, G.; Zhang, F. F.; Chen, H.; Yin, H. F.; Chen, H. L.; Zhang, S. Y., *Dalton Trans.* **2002**, 105-110.
154. Haaland, A.; Green, J. C.; McGrady, G. S.; Downs, A. J.; Gullo, E.; Lyall, M. J.; Timberlake, J.; Tutukin, A. V.; Volden, H. V.; Oestby, K.-A., *Dalton Trans.* **2003**, 4346-4356.
155. Perry, J. K.; Goddard III, W. A., *J. Am. Chem. Soc.* **1994,** 116, 5013-5014.

156. Cutler, A.; Ehtholt, D.; Lennon, P.; Nicholas, K.; Marten, D. F.; Madhavarao, M.; Raghu, S.; Rosan, A.; Rosenblum, M., *J. Am. Chem. Soc.* **1975,** 97, 3149-3157.
157. Peng, T.-S.; Gladysz, J. A., *Organometallics* **1995,** 14, 898-911.
158. Giering, W. P.; Raghu, S.; Rosenblum, M.; Cutler, A.; Ehtholt, D.; Fish, R. W., *J. Am. Chem. Soc.* **1972,** 94, 8251-8253.
159. Cutler, A.; Ehtholt, D.; Giering, W. P.; Lennon, P.; Raghu, S.; Rosan, A.; Rosenblum, M.; Tancrede, J.; Wells, D., *J. Am. Chem. Soc.* **1976,** 98, 3495-3507.
160. Lennon, P.; Rosenblum, M., *J. Am. Chem. Soc.* **1983,** 105, 1233-1241.
161. Gull, A. M.; Fanwick, P. E.; Kubiak, C. P., *Organometallics* **1993,** 12, 2121-2125.
162. Trost, B. M., *Acc. Chem. Res.* **1980,** 13, 385-393.
163. Bandoli, G.; Dolmella, A.; Di Masi, N. G.; Fanizzi, F. P.; Maresca, L.; Natile, G., *Organometallics* **2002,** 21, 4595-4603.
164. Szuromi, E.; Sharp, P. R., *Organometallics* **2006,** 25, 558-559.
165. Driver, T. G.; Williams, T. J.; Labinger, J. A.; Bercaw, J. E., *Organometallics* **2007,** 26, 294-301.
166. Williams, T. J.; Caffyn, A. J. M.; Hazari, N.; Oblad, P. F.; Labinger, J. A.; Bercaw, J. E., *J. Am. Chem. Soc.* **2008,** 130, 2418-2419.
167. Oxgaard, J.; Tenn, W. J.; Nielsen, R. J.; Periana, R. A.; Goddard III, W. A., *Organometallics* **2007,** 26, 1565-1567.
168. Muhs, M. A.; Weiss, F. T., *J. Am. Chem. Soc.* **1962,** 84, 4697-4705.
169. Roberts, J. D.; Caserio, M. C., *Basic Principles of Organic Chemistry*. W. A. Benjamin, Inc.: 1977; 1315 pp.
170. Chen, G. S.; Labinger, J. A.; Bercaw, J. E., *Proc. Natl. Acad. Sci. U. S. A.* **2007,** 104, 6915-6920.
171. Grushin, V. V.; Bensimon, C.; Alper, H., *Organometallics* **1993,** 12, 2737-2740.
172. Yoshida, T.; Okano, T.; Otsuka, S., *J. Chem. Soc., Dalton Trans.* **1976**, 993-999.
173. Klein, A.; Klinkhammer, K.-W.; Scheiring, T., *J. Organomet. Chem.* **1999,** 592, 128-135.
174. Rived, F.; Canals, I.; Bosch, E.; Roses, M., *Anal. Chim. Acta* **2001,** 439, 315-333.
175. Bercaw, J. E.; Hazari, N.; Labinger, J. A.; Oblad, P. F., *Angew. Chem., Int. Ed. Engl.* **2008,** 47, 9941-9943.
176. Anderson, J. S., *J. Chem. Soc.* **1936**, 1042-1049.
177. Otto, S.; Elding, L. I., *J. Chem. Soc., Dalton Trans.* **2002**, 2354-2360.
178. Wittig, G.; Knaus, E., *Chem. Ber.* **1958,** 91, 895-907.
179. Bender, C. F.; Widenhoefer, R. A., *J. Am. Chem. Soc.* **2005,** 127, 1070-1071.
180. Alper, H.; Urso, F.; Smith, D. J. H., *J. Am. Chem. Soc.* **1983,** 105, 6737-6738.
181. Calet, S.; Urso, F.; Alper, H., *J. Am. Chem. Soc.* **1989,** 111, 931-934.
182. Wolfe, J. P.; Ney, J. E., *Org. Lett.* **2003,** 5, 4607-4610.
183. Green, M.; Sarhan, J. K. K.; Al-Najjar, I. M., *J. Chem. Soc., Dalton Trans.* **1981**, 1565-1571.
184. Arnek, R.; Zetterberg, K., *Organometallics* **1987,** 6, 1230-1235.
185. Barone, C. R.; Benedetti, M.; Vecchio, V. M.; Fanizzi, F. P.; Maresca, L.; Natile, G., *Dalton Trans.* **2008**, 5313-5322.
186. Lorusso, G.; Barone, C. R.; Di Masi, N. G.; Pacifico, C.; Maresca, L.; Natile, G., *Eur. J. Inorg. Chem.* **2007**, 2144-2150.
187. Teuma, E.; Malbosc, F.; Pons, V.; Serra-Le Berre, C.; Jaud, J.; Etienne, M.; Kalck, P., *Dalton Trans.* **2001**, 2225-2227.
188. Casalnuovo, A. L.; Calabrese, J. C.; Milstein, D., *J. Am. Chem. Soc.* **1988,** 110, 6738-6744.
189. Walsh, P. J.; Hollander, F. J.; Bergman, R. G., *Organometallics* **1993,** 12, 3705-3723.
190. Blum, S. A.; Rivera, V. A.; Ruck, R. T.; Michael, F. E.; Bergman, R. G., *Organometallics* **2005,** 24, 1647-1659.
191. Lin, B. L.; Clough, C. R.; Hillhouse, G. L., *J. Am. Chem. Soc.* **2002,** 124, 2890-2891.
192. Ney, J. E.; Wolfe, J. P., *J. Am. Chem. Soc.* **2006,** 128, 15415-15422.
193. Mitchenko, S. A.; Zamashchikov, V. V.; Slinkin, S. M., *Zh. Obshch. Khim.* **1993,** 63, 956-957.
194. Mitchenko, S. A.; Zamashchikov, V. V.; Slinkin, S. M.; Voshchula, V. N., *Zh. Obshch. Khim.* **1991,** 61, 2127-2128.
195. Pawlikowski, A. V.; Getty, A. D.; Goldberg, K. I., *J. Am. Chem. Soc.* **2007,** 129, 10382-10393.
196. Muniz, K.; Hvelmann, C. H.; Streuff, J., *J. Am. Chem. Soc.* **2008,** 130, 763-773.
197. Sanford, M. S.; Groves, J. T., *Angew. Chem., Int. Ed. Engl.* **2004,** 43, 588-590.

198. Hartwig, J. F., *Inorg. Chem.* **2007,** 46, 1936-1947.
199. Abbenhuis, H. C. L.; Pfeffer, M.; Sutter, J. P.; de Cian, A.; Fischer, J.; Ji, H. L.; Nelson, J. H., *Organometallics* **1993,** 12, 4464-4472.
200. Cornell, C. N.; Sigman, M. S., *J. Am. Chem. Soc.* **2005,** 127, 2796-2797.
201. Cornell, C. N.; Sigman, M. S., *Inorg. Chem.* **2007,** 46, 1903-1909.
202. Lersch, M.; Tilset, M., *Chem. Rev.* **2005,** 105, 2471-2526.
203. Jawad, J. K.; Puddephatt, R. J., *J. Chem. Soc., Dalton Trans.* **1977**, 1466-1469.
204. Sanders, J. R.; Webster, D. E.; Wells, P. B., *J. Chem. Soc., Dalton Trans.* **1975**, 1191-1197.
205. Vigalok, A., *Chem. Eur. J.* **2008,** 14, 5102-5108.
206. Shul'pin, G. B.; Shilov, A. E.; Kitaigorodskii, A. N.; Krevor, J. V. Z., *J. Organomet. Chem.* **1980,** 201, 319-325.
207. Van Eldik, R.; Bertini, I., *Advances in Inorganic Chemistry: Relaxometry of Water-Metal Ion Interactions*. Academic Press: 2005; 536 pp.
208. Henry, P. M., *Palladium Catalyzed Oxidation of Hydrocarbons.* Springer Science & Business: 1980; 435 pp.
209. Day, M. C.; Selbin, J., *Theoretical Inorganic Chemistry*. Reinhold Book Corp.: 1969; 590 pp.
210. Dick, A. R.; Sanford, M. S., *Tetrahedron* **2006,** 62, 2439-2463.
211. Kalyani, D.; Dick, A. R.; Anani, W. Q.; Sanford, M. S., *Org. Lett.* **2006,** 8, 2523-2526.
212. Henry, P. M., *J. Org. Chem.* **1973,** 38, 1681-1684.
213. Li, Y.; Song, D.; Dong, V. M., *J. Am. Chem. Soc.* **2008,** 130, 2962-2964.
214. Roussel, M.; Mimoun, H., *J. Org. Chem.* **1980,** 45, 5387-5390.
215. Annibale, G.; Canovese, L.; Cattalini, L.; Natile, G.; Biagini-Cingi, M.; Manootti-Lanfredi, A.-M.; Tiripicchio, A., *J. Chem. Soc., Dalton Trans.* **1981**, 2280-2287.
216. Zhang, F.; Broczkowski, M. E.; Jennings, M. C.; Puddephatt, R. J., *Can. J. Chem.* **2005,** 83, 595-605.
217. Kharasch, M. S.; Sosnovsky, G., *J. Org. Chem.* **1958,** 23, 1322-1326.
218. Rebek, J.; McCready, R.; Wolf, S.; Mossman, A., *J. Org. Chem.* **1979,** 44, 1485-1493.
219. Bender, C.; Brauer, H.-D., *J. Chem. Soc., Perkin Trans. 2* **1999**, 2579-2587.
220. Jencks, W. P.; Carriuolo, J., *J. Am. Chem. Soc.* **1960,** 82, 1778-1786.
221. Zhang, J.; Khaskin, E.; Anderson, N. P.; Vedernikov, A. N., *Chem. Commun.* **2008**, 3625-3627.
222. Dul'neva, L. V.; Moskvin, A. V., *J. Gen. Chem.* **2005,** 75, 1125-1130.
223. Pandey, R. N.; Henry, P. M., *Can. J. Chem.* **1974,** 52, 1241-1247.
224. Kragten, D. D.; Van Santen, R. A.; Crawford, M. K.; Provine, W. D.; Lerou, J. J., *Inorg. Chem.* **1999,** 38, 331-339.
225. Pandey, R. N.; Henry, P. M., *Can. J. Chem.* **1975,** 53, 1833-1841.
226. Canty, A. J.; Denney, M. C.; Skelton, B. W.; White, A. H., *Organometallics* **2004,** 23, 1122-1131.
227. Giri, R.; Liang, J.; Lei, J.-G.; Li, J.-J.; Wang, D.-H.; Chen, X.; Naggar, I. C.; Guo, C.; Foxman, B. M.; Yu, J.-Q., *Angew. Chem., Int. Ed. Engl.* **2005,** 44, 7420-7424.
228. Yin, G.; Liu, G., *Angew. Chem., Int. Ed. Engl.* **2008,** 47, 5442-5445.
229. Fringuelli, F.; Germani, R.; Pizzo, F.; Savelli, G., *Tetrahedron Lett.* **1989,** 30, 1427-1428.
230. Walborsky, H. M.; Loncrini, D. F., *J. Am. Chem. Soc.* **1954,** 76, 5396-5399.
231. Bartlett, P. D.; Giddings, W. P., *J. Am. Chem. Soc.* **1960,** 82, 1240-1246.
232. Parr, R. G.; Yang, W., *Density-functional Theory of Atoms and Molecules*. Oxford University Press: 1989; 333 pp.
233. Perdew, J. P.; Burke, K.; Ernzerhof, M., *Phys. Rev. Lett.* **1996,** 77, 3865-3868.
234. Laikov, D. N.; Ustynyuk, Y. A., *Russ. Chem. Bull.* **2005,** 54, 820-826.
235. Laikov, D. N., *Chem. Phys. Lett.* **1997,** 281, 151-156.
236. Cundari, T. R.; Stevens, W. J., *J. Chem. Phys.* **1993,** 98, 5555-5565.
237. Stevens, W. J.; Krauss, M.; Basch, H.; Jasien, P. G., *Can. J. Chem.* **1992,** 70, 612-630.